



HEINRICH HEINE
UNIVERSITÄT DÜSSELDORF

Synthesis of Polyphenols for Potential Application in Therapy of Alzheimer's Disease

Inaugural-Dissertation

zur Erlangung des Doktorgrades
der Mathematisch-Naturwissenschaftlichen Fakultät
der Heinrich-Heine-Universität Düsseldorf

vorgelegt von

Angelika Yvonne Motzny, M. Sc.

aus Ozimek / Malapane

Düsseldorf, Mai 2018

Aus dem Institut für Organische Chemie und Makromolekulare Chemie,
Abteilung für Asymmetrische Synthese
der Heinrich-Heine-Universität Düsseldorf

Gedruckt mit der Genehmigung der
Mathematisch-Naturwissenschaftlichen Fakultät
der Heinrich-Heine-Universität Düsseldorf

Referent: Prof. Dr. C. Czekelius

Korreferent: Prof. Dr. J. Pietruszka

Tag der mündlichen Prüfung:

28. Juni 2018

Declaration

I herewith declare that I have produced this thesis without the prohibited assistance of third parties and without making use of aids other than those specified; notions taken over directly or indirectly from other sources have been identified as such. This work has not previously been presented in identical or similar form to any other German or foreign examination board. I have not previously failed a doctoral examination procedure.

The thesis work was executed from October 2014 to December 2017 under the supervision of Prof. Dr. Constantin Czekelius at Heinrich-Heine University Düsseldorf.

Place, Date

Signature

Für meine Eltern

Danksagung

Mein außerordentlicher Dank gilt meinem Doktorvater Prof. Dr. Constantin Czekelius für die Überlassung des interessanten Themas, sowie die Unterstützung durch konstruktive Gespräche, Hilfsbereitschaft, Ansprechbarkeit und sein Vertrauen in meine Person. Seine Expertise auf dem Gebiet der organischen Chemie war eine wertvolle Hilfe und Motivation bei der Anfertigung dieser Arbeit.

Herrn Prof. Dr. J. Pietruszka danke ich recht herzlich für die freundliche Übernahme des Koreferates.

Allen Mitarbeitern der Arbeitsgruppe für Asymmetrische Synthese von Prof. Dr. C. Czekelius ist mein besonderer Dank gewidmet, insbesondere Herrn K. Baumgarten (M. Sc.), Herrn A. Neuenhausen (M. Sc.), Herrn M. Spittler (M. Sc.), Herrn M. Möllemann (M. Sc.), Frau J. Reineke (M. Sc.) und Frau M. Sommer (M. Sc.), weil sie durch ihre Hilfsbereitschaft und Freundlichkeit eine angenehme Arbeitsatmosphäre schafften. Sowie für die Unterstützung bei Arbeiten in der Glovebox danke ich Herrn M. Spittler (M. Sc.) und Herrn L. Helmecke (M. Sc.).

Danken möchte ich besonders meiner Laborkollegin Frau S. Houben, die vor allem durch ihre Erfahrungen einen großen Beitrag geleistet hat. Außerdem bedanke ich mich für ihre Unterstützung im Rahmen der für mich durchgeführten Synthesen. Für die organisatorischen Angelegenheiten bedanke ich mich bei Frau V. Schürmanns.

Für die Bereitstellung der biologischen Daten der dargestellten Verbindungen und für die gute Zusammenarbeit danke ich Herrn Prof. Dr. E. Wanker und C. Secker des Max Delbrück Centers for Molecular Medicine in Berlin.

Mein zusätzlicher Dank gilt auch Frau M. Beuer, Herren P. Tommes, R. Bürgel, Frau D. Koschel für die Durchführung von analytischen Messungen an der Heinrich-Heine-Universität Düsseldorf. Und für die Aufnahme von UV und Fluoreszenzspektren bedanke ich mich bei Frau F. Merkt (M. Sc.) aus dem Lehrstuhl für Organische Chemie.

Ebenfalls möchte ich mich bei meinen Praktikumsstudent/innen Frau I. Arndt (B. Sc.), Frau V. Kemp (B. Sc.), Herrn R. Steinfurt (B. Sc.) und L. Reuss (M. Sc.) recht herzlich für die Unterstützung auf einem Forschungsgebiet bedanken.

Für die kritische Durchsicht dieser Arbeit danke ich Herrn Prof. Dr. M. Braun, Frau S. Nießing (M. Sc.) und Herrn G. Späth (M. Sc.).

An dieser Stelle möchte ich meiner Familie den allergrößten Dank aussprechen, die mich in meinem Bestreben stets unterstützten und mir den nötigen Rückhalt gegeben haben. Ohne diesen wertvollen Beitrag wäre ich nie an der Position angekommen an der ich heute stehe.

Darüber hinaus gilt mein Dank allen meinen Verwandeten, Freunden, Bahar, Betty und Dijana für die vielen gemeinsamen Stunden in der Freizeit und die große Unterstützung die mir entgegengebracht wurde.

Ganz besonders danke ich Mario für seine Geduld, die Ermutigungen und fortwährende Unterstützung.

Abstract

The main polyphenolic constituent of green tea [*Camellia sinensis* (L.) O. Kuntze (Theaceae)], (-)-epigallocatechin-3-gallate (EGCG), shows beneficial effects on many biomedical targets. To act as an effective drug, EGCG has to be administered in a relatively high dose, which is not favorable. The goal of the thesis is to develop a modified EGCG analogue that overcomes this drawback. The synthesis of EGCG derivatives linked to a fluorophore molecule and biotin moiety for various assays was successful. The key steps to reach this goal were Sharpless asymmetric dihydroxylation and subsequent stereoselective cyclization to give the *cis*-chroman-3-ol that features the naturally occurring (2*R*,3*R*)-configuration. A new approach was chosen in which the ester moiety in EGCG is replaced by a 1,2,3-triazol moiety *via* Click reaction. Besides, the remaining substituents at the **B**-ring are methylated for pharmacological application of EGCG analogues. Additionally, the substitution degree at the **D**-ring is varied.

Zusammenfassung

Die Polyphenol-basierte Hauptkomponente in grünem Tee [*Camellia sinensis* (L.) O. Kuntze (Theaceae)], (-)-Epigallocatechin-3-gallate (EGCG), zeigt positive Auswirkungen in vielen biomedizinischen Studien. Zur effektiven Wirkung als Medikament muss EGCG in hohen Dosen verabreicht werden, was nicht erwünscht ist. Das Ziel dieser Arbeit ist die Entwicklung von modifizierten EGCG-Analoga, die diese Nachteile nicht aufweisen. Die Synthese von EGCG Derivaten mit einem verbrückten Fluorophor Molekül und einer Biotin-Einheit für verschiedene Assays war erfolgreich. Die Schlüsselschritte zur Gewinnung dieser Verbindungen waren die asymmetrische Sharpless-Dihydroxylierung und anschließende Zyklisierung unter Bildung des *cis*-Chroman-3-ols mit der natürlich vorkommenden (2*R*,3*R*)-Konfiguration. Ein neuer Syntheseweg wurde gewählt, in dem die Ester-Einheit von EGCG *via* Click Reaktion durch eine 1,2,3-Triazol-Einheit ersetzt wird. Zudem wurden die weiteren Substituenten am **B**-Ring methyliert. Ferner wurde der Substitutionsgrad am **D**-Ring variiert.

Contents

Abstract	v
Contents	vii
List of Figures	xv
List of Tables	xviii
Abbreviations	xix
1. Introduction	21
1.1 Alzheimer's disease	21
1.1.1 Morbus Alzheimer	21
1.1.2 Molecular Basis of the Neurodegenerative Disorders.....	24
1.1.3 Disease Pattern.....	25
1.1.4 Pathophysiology & Amyloidosis	27
1.1.6 Therapeutic Treatment and Intervention Approach for AD.....	30
1.2 Polyphenols	33
1.2.1 Ingredients of Green Tea	33
1.2.2 Autoxidation Decomposition of (-)-EGCG	35
1.2.3 Studies in Polyphenol Chemistry and Bioactivity	37
1.2.4 Metabolism and Bioavailability of Tea Polyphenols	39
1.2.5 Antioxidative Properties of Teas	40
1.2.6 Effect of Green Tea to the Health	41
1.2.7 Novel Therapeutic Approaches for the Treatment of AD with EGCG	42
1.3 (-)-Epigallocatechin-3-gallate.....	45
1.3.1 Molecular Properties of (-)-EGCG.....	45
1.3.2 Biosynthesis of Flavan-3-ols.....	47
1.3.3 Inhibition of A β due to Amyloid Assembly Inhibitors	48
1.3.4 Epimerization of EGCG to GCG	48
1.3.5 Total Synthesis of EGCG	49
1.4 Spectrophotometric Determination of Targets in Biochemistry.....	56
1.4.1 The Avidin-Biotin Interaction.....	56
1.4.2 History and Application of the Fluorescence Assay	57
1.4.3 Binding Properties of Thioflavin-T	58
1.4.4 Spectroscopic Properties of Thioflavin-T Accumulation to Fibrils	59
1.4.5 Thioflavin-T Binding to Amyloid Fibrils	59
1.4.6 Fluorescence Imaging	60

2. Results and Discussion	63
2.1 Enantioselective Synthesis of EGCG Derivatives	63
2.1.1 Retrosynthetic Disconnection of EGCG	63
2.1.2 Synthesis of the Substituted (<i>E</i>)-Cinnamyl Alcohol Precursor	64
2.1.3 Synthetic Route to 3,5-Dibenzyloxyphenol (12)	65
2.1.4 Conversion of Diaryl-Propene 30/31 into 1,2-Diols 37/38 by Sharpless Asymmetric Dihydroxylation	66
2.1.5 Sharpless Asymmetric Dihydroxylation	67
2.1.6 Enantiomeric Excess Values of Diols 37(α) and 37(β)	70
2.1.7 Cyclization of the 1,2-Diol to <i>trans</i> -Chroman-3-ol via the <i>ortho</i> -Ester	71
2.1.8 Inversion of Konfiguration in <i>trans</i> -Chroman-3-ol to <i>cis</i> -Chroman-3-ol via Oxidation-Reduction Sequence	71
2.1.9 Synthesis of GCG Derivatives via Steglich-Esterification	73
2.1.10 Synthesis of Protected Benzoic Acids for the Steglich Esterification	76
2.1.11 Preparation of GCG and EGCG Derivatives by Catalytic Hydrogenation with Pearlman's Catalyst	76
2.1.12 Modulation of Aβ42 <i>in Vitro</i>	78
2.2 Second Approach for the Enantioselective Synthesis of EGCG Derivatives via Chalcone	84
2.2.1 Retrosynthetic Analysis of Protected (–)-Epicatechin 45	84
2.2.2 Synthesis of Acetophenone 47	85
2.2.3 Synthesis of Chalcone 46 via Claisen-Schmidt Conditions	87
2.2.4 Synthesis of Diaryl Propane 31 via Modified Luche Reduction	87
2.3 Biotin- and Dye-labeled EGCG Derivatives	88
2.3.1 Synthesis of Chain-Linker and Coupling with Biotin to Compound 56	88
2.3.2 Co-Localization of EGCG-Aβ42 in Streptavidin Assay	90
2.3.3 Synthesis of Gallate Chain Linker	91
2.3.4 Coupling of Amino-PEG-EGCG and Biotin	93
2.3.5 Click-Chemistry as Copper-Catalyzed Azide-Alkyne Cycloaddition for Labeling Targets	93
2.3.6 Fluorescence Determination in Molecular Biology	95
2.3.7 EGCG-Aβ42 <i>in Cell</i> Co-Localization	99
2.4 Development of Novel Azido-EGCG Derivatives	101
2.4.1 Synthesis of 3-Azidochromane by Common Substitution	101
2.4.2 Synthesis of Racemic 3-Aminochromane by Reductive Amination	103
2.4.3 Synthesis of the Alkyne Analogues via Corey-Fuchs Reaction	106
2.4.4 Click-Chemistry of the Alkyne Analogues with 3-Azidochromane	107

3. Conclusion and Outlook	108
4. Experimental	119
4.1 Analytics	119
4.1.1 Nuclear Magnetic Resonance Spectroscopy (NMR)	119
4.1.2 Electrospray Ionization Mass Spectrometry (ESI-MS).....	119
4.1.3 Thin-Layer Chromatography (TLC).....	119
4.1.4 High Performance Liquid Chromatography (HPLC).....	120
4.1.5 Absorption and Emission Spectroscopy.	124
4.1.6 IR Spectroscopy.....	124
4.1.7 Melting Point Determination	124
4.1.8 Specific Rotation.....	124
4.2 Methods for Biological Determination.....	125
4.2.1 A β 42 Peptide Stock Solution	125
4.2.2 Fluorescent Labeling of A β 42 Aggregates	125
4.2.3 Neuroblastoma Cell Culture and Treatment with A β 42(-TAMRA) Aggregates	125
4.2.4 Automated Fluorescence Microscopy and Quantification of Aggregate Loads.....	126
4.2.5 Screening of EGCG Derivative Library.....	126
4.2.6 Confocal Microscopy.....	127
4.2.7 Co-localization Studies of EGCG and Intracellular A β 42 Aggregates.....	127
4.3 Solvents.....	128
4.4 General Work Technique	128
4.5 Synthesis	130
4.5.1 Synthesis of Cinnamyl Alcohol 25/26	130
4.5.1.1 Methyl-3,4,5-trimethoxybenzoate (16).....	130
4.5.1.2 Benzyl-3,4,5-tris(benzyloxy)benzoate (17)	130
4.5.1.3 Methyl-3,4,5-tris(benzyloxy)benzoate (18)	131
4.5.1.4 3,4,5-Trimethoxybenzyl alcohol (19)	132
4.5.1.5 3,4,5-Tris(benzyloxy)benzyl alcohol (20).....	133
4.5.1.6 3,4,5-Trimethoxybenzaldehyde (21).....	133
4.5.1.7 3,4,5-Tris(benzyloxy)benzaldehyde (22).....	134
4.5.1.8 Ethyl-(<i>E</i>)-3,4,5-trimethoxycinnamate (23)	135
4.5.1.9 Ethyl-(<i>E</i>)-3,4,5-tris(benzyloxy)cinnamate (24)	135
4.5.1.10 (<i>E</i>)-3,4,5-Trimethoxycinnamyl alcohol (25).....	136
4.5.1.11 (<i>E</i>)-3,4,5-Tris(benzyloxy)cinnamyl alcohol (26).....	137

4.5.2.1 1,3,5-Triacetylphloroglucinol (28).....	138
4.5.2.2 1,3,5-Tris(benzyloxy)benzene (29).....	138
4.5.2.3 3,5-Bis(benzyloxy)phenol (12).....	139
4.5.3.1 (<i>E</i>)-3-(2,4-Bis(benzyloxy)-6-(<i>tert</i> -butyl-dimethyl-siloxy)phenyl)-1-(3,4,5-trimethoxyphenyl)-propane (32).....	140
4.5.3.2 (<i>E</i>)-3-[2,4-Bis(benzyloxy)-6-(<i>tert</i> -butyl-dimethyl-siloxy)phenyl]-1-[3,4,5-tris(benzyloxy)phenyl]-propane (33).....	142
4.5.4 Asymmetric Dihydroxylation of Compound 34(α) / 35(α)	143
4.5.4.1 (1 <i>S</i> ,2 <i>S</i>)-3-[2,4-Bis(benzyloxy)-6-hydroxyphenyl-1-(3,4,5-trimethoxy)phenyl]propane-1,2-diol (36(α)).....	143
4.5.4.2 (1 <i>S</i> ,2 <i>S</i>)-3-[2,4-Bis(benzyloxy)-6-hydroxyphenyl-1-(3,4,5-tris(benzyloxy)-phenyl)]propane-1,2-diol (37(α)).....	145
4.5.4.3 (<i>rac</i>)-3-(2,4-Bis(benzyloxy)-6-hydroxyphenyl)-1-(3,4,5-tris(benzyloxy)-phenyl)propane-1,2-diol (98).....	146
4.5.5 Cyclization of Compounds 36(α) / 37(β)	147
4.5.5.1 (2 <i>R</i> ,3 <i>S</i>)-5,7-Bis(benzyloxy)-2-(3,4,5-trimethoxyphenyl)chroman-3-ol (<i>trans</i> 40(α)).....	147
4.5.6 Alcohol Inversion by Oxidation-Reduction Sequence.....	149
4.5.6.1 (–)-(2 <i>R</i> ,3 <i>R</i>)- <i>cis</i> -5,7-Bis(benzyloxy)-2-(3,4,5)-tris(benzyloxy)phenylchroman-3-ol (<i>cis</i> 45(45β)).....	149
4.5.6.2 (–)-(2 <i>R</i> ,3 <i>R</i>)- <i>cis</i> -5,7-Bis(benzyloxy)-2-(3,4,5)-tri(methoxy)phenylchroman-3-ol (<i>cis</i> 44(cis 44(β))).....	150
4.5.7 Esterification of Compounds 58-61	152
4.5.7.1 (2 <i>R</i> ,3 <i>S</i>)-5,7-Bis(benzyloxy)-2-(3,4,5-trimethoxyphenyl)chroman-3-yl-(3,4,5-trimethoxy)benzoate (58a).....	152
4.5.7.2 (2 <i>R</i> ,3 <i>S</i>)-5,7-Bis(benzyloxy)-2-(3,4,5-trimethoxyphenyl)chroman-3-yl-(3,4,5-trisbenzyl)benzoate (58b).....	153
4.5.7.3 (2 <i>S</i> ,3 <i>S</i>)-5,7-Bis(benzyloxy)-2-(3,4,5-trimethoxyphenyl)chroman-3-yl-(3,4,5-trisbenzyloxy)benzoate (58c).....	153
4.5.7.4 (2 <i>S</i> ,3 <i>S</i>)-5,7-Bis(benzyloxy)-2-(3,4,5-trimethoxyphenyl)chroman-3-yl-(3,4,5-trifluoro)benzoate (58d).....	154
4.5.7.5 (2 <i>R</i> ,3 <i>S</i>)-5,7-Bis(benzyloxy)-2-(3,4,5-tribenzylphenyl)chroman-3-yl-(3,4,5-trimethoxy)benzoate (59a).....	155
4.5.7.6 (2 <i>R</i> ,3 <i>S</i>)-5,7-Bis(benzyloxy)-2-(3,4,5-tribenzylphenyl)chroman-3-yl-(3,4,5-trisbenzyloxy)benzoate (59b).....	156
4.5.7.7 (2 <i>R</i> ,3 <i>R</i>)-5,7-Bis(benzyloxy)-2-(3,4,5-trimethoxyphenyl)chroman-3-yl-(3-fluoro)benzoate (60a).....	157
4.5.7.8 (2 <i>R</i> ,3 <i>R</i>)-5,7-Bis(benzyloxy)-2-(3,4,5-trimethoxyphenyl)chroman-3-yl-(4-benzyloxy)benzoate (60b).....	158
4.5.7.9 (2 <i>R</i> ,3 <i>R</i>)-5,7-Bis(benzyloxy)-2-(3,4,5-tribenzylphenyl)chroman-3-yl-(3,4,5-trimethoxy)benzoate (61a).....	158

4.5.7.10 (2 <i>R</i> ,3 <i>R</i>)-5,7-Bis(benzyloxy)-2-(3,4,5-tribenzylphenyl)chroman-3-yl-(4-fluoro)benzoate (61b)	159
4.5.7.11 (2 <i>R</i> ,3 <i>R</i>)-5,7-Bis(benzyloxy)-2-(3,4,5-tribenzylphenyl)chroman-3-yl-(3-fluoro)benzoate (61c)	160
4.5.7.12 (2 <i>R</i> ,3 <i>R</i>)-5,7-Bis(benzyloxy)-2-(3,4,5-tribenzylphenyl)chroman-3-yl-(4-benzyloxy)benzoate (61d)	161
4.5.7.13 (2 <i>R</i> ,3 <i>R</i>)-5,7-Bis(benzyloxy)-2-(3,4,5-tribenzylphenyl)chroman-3-yl-(2,5-bisbenzyloxy)benzoate (61e)	161
4.5.7.14 (2 <i>R</i> ,3 <i>R</i>)-5,7-Bis(benzyloxy)-2-(3,4,5-tribenzylphenyl)chroman-3-yl-(2,4-bisbenzyloxy)benzoate (61f)	162
4.5.7.15 (2 <i>R</i> ,3 <i>R</i>)-5,7-Bis(benzyloxy)-2-(3,4,5-tribenzylphenyl)chroman-3-yl-(3,5-bisbenzyloxy)benzoate (61g)	163
4.5.7.16 (2 <i>R</i> ,3 <i>R</i>)-5,7-Bis(benzyloxy)-2-(3,4,5-tribenzylphenyl)chroman-3-yl-(3,4-bisbenzyloxy)benzoate (61h)	164
4.5.7.17 (2 <i>R</i> ,3 <i>R</i>)-5,7-Bis(benzyloxy)-2-(3,4,5-tribenzylphenyl)chroman-3-yl-(3-benzyloxy)benzoate (61i)	165
4.5.7.18 (2 <i>R</i> ,3 <i>R</i>)-5,7-Bis(benzyloxy)-2-(3,4,5-tribenzylphenyl)chroman-3-yl-(3,4,5-trifluoro)benzoate (61j)	166
4.5.8 Catalytic Hydrogenation of Compounds 62/65	167
4.5.8.1 (2 <i>R</i> ,3 <i>S</i>)-5,7-Dihydroxy-2-(3,4,5-trimethoxyphenyl)chroman-3-yl-(3,4,5-trimethoxy)benzoate (62a)	167
4.5.8.2 (2 <i>R</i> ,3 <i>S</i>)-5,7-Dihydroxy-2-(3,4,5-trimethoxyphenyl)chroman-3-yl-(3,4,5-trihydroxy)benzoate (62b)	168
4.5.8.3 (2 <i>R</i> ,3 <i>S</i>)-5,7-Dihydroxy-2-(3,4,5-hydroxyphenyl)chroman-3-yl-(3,4,5-trimethoxy)benzoate (63a)	168
4.5.8.4 (2 <i>S</i> ,3 <i>S</i>)-5,7-Dihydroxy-2-(3,4,5-trimethoxyphenyl)chroman-3-yl-(3,4,5-trihydroxy)benzoate (64a)	169
4.5.8.5 (2 <i>S</i> ,3 <i>S</i>)-5,7-Dihydroxy-2-(3,4,5-trimethoxyphenyl)chroman-3-yl-(3,4,5-trifluoro)benzoate (64b)	170
4.5.8.6 (2 <i>R</i> ,3 <i>R</i>)-5,7-Dihydroxy-2-(3,4,5-tris(hydroxyl)phenyl)chroman-3-yl-(4-fluoro)benzoate (65b)	171
4.5.8.7 (2 <i>R</i> ,3 <i>R</i>)-5,7-Dihydroxy-2-(3,4,5-trihydroxyphenyl)chroman-3-yl-(4-hydroxy)benzoate (65d)	171
4.5.8.8 (2 <i>R</i> ,3 <i>R</i>)-5,7-Dihydroxy-2-(3,4,5-trihydroxyphenyl)chroman-3-yl-(3,4-dihydroxy)benzoate (65h)	172
4.5.8.9 (2 <i>R</i> ,3 <i>R</i>)-5,7-Dihydroxy-2-(3,4,5-trihydroxyphenyl)chroman-3-yl-(2,5-dihydroxy)benzoate (65e)	173
4.5.8.10 (2 <i>R</i> ,3 <i>R</i>)-5,7-Dihydroxy-2-(3,4,5-trihydroxyphenyl)chroman-3-yl-(3-fluoro)benzoate (65c)	173
4.5.8.11 (2 <i>R</i> ,3 <i>R</i>)-5,7-Dihydroxy-2-(3,4,5-trihydroxyphenyl)chroman-3-yl-(3,5-dihydroxy)benzoate (65g)	174
4.5.8.12 (2 <i>R</i> ,3 <i>R</i>)-5,7-Dihydroxy-2-(3,4,5-trihydroxyphenyl)chroman-3-yl-(3,4,5-trifluoro)benzoate (65j)	175

4.5.8.13 (2 <i>R</i> ,3 <i>R</i>)-5,7-Dihydroxy-2-(3,4,5-trihydroxyphenyl)chroman-3-yl-(3-hydroxy)benzoate (65i)	176
4.5.8.14 (2 <i>R</i> ,3 <i>R</i>)-5,7-Dihydroxy-2-(3,4,5-trihydroxyphenyl)chroman-3-yl-(3,4,5-trimethoxy)benzoate (65a)	176
4.5.9 Synthesis of Acid Compounds for Steglich Esterification	177
4.5.9.1 Benzylolation of Hydroxybenzoic Acids	177
4.5.9.2 Universal Procedure of Saponification	179
4.5.10 Synthesis of Dess-Martin Periodinan	181
4.5.10.1 2-Iodoxy benzoic acid (IBX)	181
4.5.10.2 Dess-Martin Periodinane (DMP)	181
4.5.11 Synthesis of Precursor Compounds for Chalcone 46	182
4.5.11.1 2,4-Dibenzyloxy-6-hydroxyacetophenone (47)	182
4.5.11.2 (<i>E</i>)-1-(2-Bis(benzyloxy)-6-hydroxyphenyl)-3-(3,4,5-tris(benzyloxy)phenyl)prop-2-en-1-one (46)	182
4.5.11.3 (<i>E</i>)-1-[3,4,5-Tris(benzyloxy)phenyl]-3-[2,4-bis(benzyloxy)-6-hydroxyphenyl]-propene (31)	183
4.5.12 Synthesis of Biotin-PEG Linker 56	185
4.5.12.1 4-(2-(2-(2-Azidoethoxy)ethoxy)ethoxy) benzoic acid (53)	185
4.5.12.2 (2 <i>R</i> ,3 <i>R</i>)-5,7-Bis(benzyloxy)-2-(3,4,5-tris(benzyloxy)phenyl)chroman-3-yl-4-(2-(2-(2-azidoethoxy)ethoxy)ethoxy)ethoxy)benzoate (54)	185
4.5.12.3 (2 <i>R</i> ,3 <i>R</i>)-5,7-Dihydroxy-2-(3,4,5-trihydroxyphenyl)chroman-3-yl-4-(2-(2-(2-aminoethoxy)ethoxy)ethoxy)ethoxy)benzoate (55)	187
4.5.12.4 (2 <i>R</i> ,3 <i>R</i>)-5,7-Dihydroxy-2-(3,4,5-trihydroxyphenyl)chroman-3-yl-4-(2-(2-(2-(5-((3 <i>aS</i> ,4 <i>S</i> ,6 <i>aR</i>)-2-oxohexahydro-1 <i>H</i> -thieno[3,4- <i>d</i>]imidazol-4-yl)pentanamido) ethoxy)ethoxy)ethoxy)benzoate (56)	188
4.5.13 Synthesis of EGCG-PEG Linker 69	189
4.5.13.1 Methyl 7-hydroxy-2-methoxybenzo[<i>d</i>][1,3]dioxole-5-carboxylate (71)	189
4.5.13.2 Methyl-7-(2-(2-(2-azidoethoxy)ethoxy)ethoxy)-2-methoxybenzo[<i>d</i>][1,3]dioxole-5-carboxylate (73)	190
4.5.13.3 Methyl-3-(2-(2-(2-azidoethoxy)ethoxy)ethoxy)-4,5-di(hydroxy)benzoate (74)	191
4.5.13.4 Methyl-3-(2-(2-(2-azidoethoxy)ethoxy)ethoxy)-4,5-bis(benzyloxy)benzoate (75)	191
4.5.13.5 3-(2-(2-(2-azidoethoxy)ethoxy)ethoxy)-4,5-bis(benzyloxy)benzoate (76)	192
4.5.14 Steglich Esterification of <i>cis</i> -Chroman-3-ol <i>cis</i> 45 with Azido-PEG Linker 76	193
4.5.14.1 (2 <i>R</i> ,3 <i>R</i>)-5,7-Bis(benzyloxy)-2-(3,4,5-tris(benzyloxy)phenyl)chroman-3-yl-3-(2-(2-(2-azidoethoxy)ethoxy)ethoxy)-4,5-bis(benzyloxy)benzoate (77)	193
4.5.15 Synthesis of Biotin Coupled EGCG Derivatives 56/81	195
4.5.15.1 (2 <i>R</i> ,3 <i>R</i>)-5,7-Dihydroxy-2-(3,4,5-trihydroxyphenyl)chroman-3-yl-3-(2-(2-(2-aminoethoxy)ethoxy)ethoxy)-4,5-(dihydroxy)benzoate (80)	195

4.5.15.2 (2 <i>R</i> ,3 <i>R</i>)-5,7-Dihydroxy-2-(3,4,5-trihydroxyphenyl)chroman-3-yl-3,4-dihydroxy-5-(2-(2-(2-(5-((3 <i>aS</i> ,4 <i>S</i> ,6 <i>aR</i>)-2-oxohexahydro-1 <i>H</i> -thieno[3,4- <i>d</i>]imidazol-4-yl)pentanamido)ethoxy)ethoxy)ethoxy)benzoate (81).....	196
4.5.16 Synthesis of Rhodamine Dye 67	197
4.5.16.1 <i>N</i> -(6-(Diethylamino)-9-(2-(((2,5-dioxopyrrolidin-1-yl)oxy)carbonyl)phenyl)-3 <i>H</i> -xanthen-3-ylidene)- <i>N</i> -ethylethanaminium (66).....	197
4.5.16.2 <i>N</i> -(6-(Diethylamino)-9-(2-(prop-2-yn-1-ylcarbonyl)phenyl)-3 <i>H</i> -xanthen-3-ylidene)- <i>N</i> -ethylethanaminium (67).....	198
4.5.17 Click Reaction of Rhodamine Dye 67 with EGCG-PEG Linker 54/77 to Product 68/78	199
4.5.17.1 (2 <i>R</i> ,3 <i>R</i>)-5,7-Bis(benzyloxy)-2-(3,4,5-tris(benzyloxy)phenyl)chroman-3-yl-4-(2-(2-(2-(4-((2-(3-(diethyl- λ^4 azaneylidene)-3-(diethylamino)-3 <i>H</i> -xanthen-9-yl)benz-amido)methyl)-1 <i>H</i> -1,2,3-triazol-1-yl)ethoxy)ethoxy)ethoxy)benzoate (68).....	199
4.5.17.2 (2 <i>R</i> ,3 <i>R</i>)-5,7-Bis(benzyloxy)-2-(3,4,5-tris(benzyloxy)phenyl)chroman-3-yl-3,4-bis(benzyloxy)-5-(2-(2-(2-(4-((2-(3-(diethyl- λ^4 azaneylidene)-6-(diethylamino)-3 <i>H</i> -xanthen-9-yl)benzamido)methyl)-1 <i>H</i> -1,2,3-triazol-1-yl)ethoxy)ethoxy)ethoxy)benzoate (78).....	200
4.5.18 Synthesis of Blank Molecule Lacking the Catechine Moiety	201
4.5.18.1 <i>N</i> -(6-(Diethylamino)-9-(2-(((1-(2-(2-(2-(2-methoxy-6-(methoxycarbonyl)benzo[d][1,3]dioxol-4-yl)oxy)ethoxy)ethoxy)ethyl)-1 <i>H</i> -1,2,3-triazol-4-yl)methyl)carbonyl)phenyl)-3 <i>H</i> -xanthen-3-ylidene)- <i>N</i> -ethylethanaminium (72).....	201
4.5.18.2 <i>N</i> -(6-(Diethylamino)-9-(2-(((1-(2-(2-(2-(2,3-dihydroxy-5-(methoxycarbonyl)phenoxy)ethoxy)ethoxy)ethyl)-1 <i>H</i> -1,2,3-triazol-4-yl)methyl)carbonyl)phenyl)-3 <i>H</i> -xanthen-3-ylidene)- <i>N</i> -ethylethanaminium (101)	202
4.5.19 Catalytic Hydrogenation of Fluorescent Coupled Target 69/79	203
4.5.19.1 <i>N</i> -(6-(Diethylamino)-9-(2-(((1-(2-(2-(2-(4-(((2 <i>R</i> ,3 <i>R</i>)-5,7-dihydroxy-2-(3,4,5-trihydroxyphenyl)chroman-3-yl)oxy)carbonyl)phenoxy)ethoxy)ethoxy)ethyl)-1 <i>H</i> -1,2,3-triazol-4-yl)methyl (69).....	203
4.5.19.2 <i>N</i> -(6-(Diethylamino)-9-(2-(((1-(2-(2-(2-(5-(((2 <i>R</i> ,3 <i>R</i>)-5,7-dihydroxy-2-(3,4,5-trihydroxyphenyl)chroman-3-yl)oxy)carbonyl)-2,3-dihydroxyphenoxy) ethoxy)ethoxy)ethyl)-1 <i>H</i> -1,2,3-triazol-4-yl)methyl)carbonyl)phenyl)-3 <i>H</i> -xanthen-3-ylidene)- <i>N</i> -ethylethanaminium (79)	204
4.5.20 Synthesis of 3-Azidochromane 85 via Nucleophilic Substitution.....	205
4.5.20.1 (2 <i>R</i> ,3 <i>R</i>)-3-Azido-5,7-bis(benzyloxy)-2-(3,4,5-tris(benzyloxy)phenyl)-chromane (85)	205
4.5.21 Synthesis of Ethynyl Benzene Derivative via Corey Fuchs Reaction.....	207
4.5.21.1 3,4,5-Tris(benzyloxy)-2,2-(dibromovinyl)benzene (87).....	207
4.5.21.2 3,4,5-Trimethoxy-2,2-(dibromovinyl)benzene (86).....	207
4.5.21.3 3,4,5-Tris(benzyloxy)-1-ethynylbenzene (89)	208
4.5.21.4 3,4,5-Trimethoxy-1-ethynylbenzene (88)	208
4.5.22 Click Reaction of Azido-EGCG 85 and Ethynyl Benzene Derivative 89 to Compound 91	209
4.5.22.1 1-((2 <i>R</i> ,3 <i>R</i>)-5,7-Bis(benzyloxy)-2-(3,4,5-tris(benzyloxy)phenyl)chroman-3-yl)-4-(3,4,5-tris(benzyloxy)phenyl)-1 <i>H</i> -1,2,3-triazole (91)	209
4.5.23 Catalytic Hydrogenation of Click Derivative 93	210

4.5.23.1 1-((2 <i>R</i> ,3 <i>R</i>)-5,7-Dihydroxy-2-(3,4,5-trihydroxy)phenylchroman-3-yl)-4-(3,4,5-trihydroxy)phenyl)-1 <i>H</i> -1,2,3-triazole (93).....	210
4.5.24 Synthesis of Different EGCG Derivatives	211
4.5.24.1 (2 <i>R</i>)-5,7-Bis(benzyloxy)-3-((trimethylsilyl)ethynyl)-2-(3,4,5-tris(benzyloxy)phenyl)chroman-3-ol (99)	211
4.5.24.2 (2 <i>R</i> ,3 <i>R</i>)-5,7-bis(benzyloxy)-2-(3,4,5-tris(benzyloxy)phenyl)chroman-3-yl-pent-4-ynone (100)	213
List of Literature	214
Appendix	225

List of Figures

Figure 1: The psychiatrist Alois Alzheimer (1864-1915), described at first the "disease of oblivion". His teacher Emil Kraepelin suggested the name. ^[1]	21
Figure 2: Accumulation of amyloid plaques on nerve cells distinguish the characteristics of Alzheimer's disease. Chronic inflammation is caused by amyloid plaques explicit naming A β , reprinted with permission of: Creative Commons Attribution 3.0 <i>via</i> Wikimedia Common. ^[5]	22
Figure 3: Comparison of the percentage between age group and sex. ^[13]	23
Figure 4: Comparison of percentage data of causes of death between 2000 and 2015. ^[13, 16]	24
Figure 5: Characteristic transformation during AD. ^[33]	26
Figure 6: Affected brains with senile plaques containing A β (B) and neurofibrillary tangles (NFT's) constituted of hyperphosphorylated tau protein accumulated in paired helical filaments (A). Attended by extensive neuritic pathology (C), represented as accumulation in large numbers in the diseased brain (D). ^[39]	27
Figure 7: Hyperphosphorylated tau-protein caused by mutation in APP gene which leads to the formation of NFT's (in purple, right). ^[52] Function and structure of tau protein (left). ^{[53]5}	28
Figure 8: Processing of APP by cleavage through α -secretase in non-amyloidogenic pathway and through β -secretase in amyloidogenic pathway. ^[53]	30
Figure 9: Acetylcholinesterase inhibitors (AChEI), a). Donepezil (Aricept [®]), b). Galantamine (Reminly [®]), c). Rivastigmine (Exelon [®]), d). Memantine (Ebixa [®]) NMDA antagonist. ^[70]	31
Figure 10: Intervention approach for misfolding diseases: (a) monomers are not able to form aggregates, (b) disintegration of the aggregation intermediate, (c) degenerated amyloid formation, (d) increased tendency to form larger aggregates. ^[2]	32
Figure 11: Green Tea plant - <i>Camellia sinensis</i> . ^[3]	33
Figure 12: Chemical structures of the naturally occurring catechins. ^[77]	33
Figure 13: The bioavailability and metabolism of green tea catechins and processing in humans. ^[113]	40
Figure 14: Possible interaction model of EGCG on fibrils. ^[73]	43
Figure 15: Supposed neuroprotective application of EGCG. ^[140]	43
Figure 16: Structure of procyanidin B ₃ . ^[146]	45
Figure 17: Arrangement of the substituents at C2 and C3 position in the E- and A-conformer for catechin (a) and epicatechin (b). ^[148]	46
Figure 18: Ground-state energy conformations of flavanol, the hatched line displays the projection of the A-ring. ^[149]	46
Figure 19: Biosynthesis of flavonoids <i>via</i> phenylpropanoid pathway. (1) L-Tyr; (2) cinnamic acid; (3) R = H coumaric acid, R = OH caffeic acid; (4) R = H coumaroyl CoA, R = OH caffeyol CoA; (5) R = H naringenin chalcone, R = OH eriodictyol chalcone; (6) R = H naringenin, R = OH eriodictyol; (7) R = H dihydrokaempferol, R = OH dihydroquercetin (taxifolin); (8) R = H leucopelargonidin, R = OH leucocyanindin; (9) R = H (+)-afzelachin, R = H (+)-catechin. Enzymes are abbreviated as follows: tyrosine ammonia-lyase (TAL); cinnamate 4-hydroxylase (C4H); 4-coumaroyl-CoA ligase (4CL); chalcone synthase	

(CHS); chalcone isomerase (CHI); flavanone 3 β -hydroxylase (FHT); dihydroflavonol 4-reductase (DFR); leucoanthocyanidin reductase (LAR); anthocyanidin reductase (ANR). ^[152]	47
Figure 20: Illustration of scyllo-inositol as weak inhibitor (left) and tweezer CLR01 (right). ^[155, 157]	48
Figure 21: Disconnection approach for reversed polarity strategy (red curly lines) and homogeneous polarity (blue curly lines) by Ohmori <i>et al.</i> ^[173]	52
Figure 22: Schematic illustration of single-site NA/SA-HRP oligomer assay. ^[182]	56
Figure 23: Structure of ThT (right), molecular construction of ThT in its two planar segments. ^[183]	57
Figure 24: ThT binding to amyloid fibrils leads to characteristic increased excitation (left), fibril-forming peptide leads to fibrillization kinetics of increased concentrations (right). ^[183]	58
Figure 25: Amyloid fibrils with characteristic cross- β building by accumulation of laminated β -sheets (right), possible ThT binding to fibril β -sheet in a channel model by accumulation along surface side-chain parallel to long axis of β -sheet (left). ^[183, 191]	59
Figure 26: Photo induced processes in Jablonski scheme of organic fluorophores. ^[191]	60
Figure 27: HUVECs incubated with fluorescein probe imaged under fluorescence microscope. ^[192]	61
Figure 28: Illustration of FITC-EGCG. ^[194]	61
Figure 29: Visual representation by confocal microscope of suspended L-929 cells after 0 h (A), 0.5 h (B), 1 h (C), and 4 h (D) with addition of 65 μ M FITC-EGCG and after 4 h were added 50 μ M FITC-EGCG (E) (left). Visual representation by confocal microscope of cultured L-929 cells 2-4 h (A/B), 8 h (C/D), and 24 h (E) with addition of 130 μ M FITC-EGCG (right). ^[194]	62
Figure 30: Phytoestrogen mechanism of internalization into cytoplasm and nucleus. ^[196]	62
Figure 31: Retrosynthetic analysis of (-)-EGCG.	63
Figure 32: Cinchona alkaloid ligands for Sharpless asymmetric dihydroxylation. ^[209]	68
Figure 33: Simplified representation of the chair pyran rings of <i>trans</i> - and <i>cis</i> -chroman-3-ol.	72
Figure 34: NMR shift of the coupling constant during oxidation-reduction sequence.	73
Figure 35: Building blocks for the synthesis library.....	76
Figure 36: (A) Analysis of cellular A β 42 aggregate degradation promoting effect of EGCG and synthetic derivatives. The quantification of the A β 42 aggregation load was conducted by the total TAMRA fluorescence intensities per cell and normalized to DMSO treated cells. <i>The diagram depicted by means of the three individual values and the error bars are the standard deviation. One-sided ANOVA with Dunnett's post-test, *p<0.05, **p<0.002, ***p<0.001.</i> (B) <i>In vitro</i> A β 42 aggregation controlled by ThT binding, resulted in a slow-down of A β 42 aggregation though addition of EGCG and its derivatives by kinetic and reduced maximal reached ThT fluorescence intensity. (C) <i>In vitro</i> A β 42 aggregation normalized to DMSO for quantification of maximal ThT signal. Bars showed mean value derived from two individual experiments and error bars can be defined for standard deviation. (D) Promoting cellular A β degradation effect of EGCG and its derivatives in correlation analysis of <i>in cell</i> and <i>in vitro</i> potency verified by <i>Pearson's correlation coefficient</i> (r). The <i>in vitro</i> and cell assays were carried out by C. Secker and Prof. E. Wanker. For an enlarged view see appendix.....	78
Figure 37: Progression of protein aggregation represented in the beginning with individual A β proteins. After aggregation fibrils are formed until plateau is reached. ^[220]	80
Figure 38: Determination of the effectiveness of the structure relationship of EGCG derivatives.	82

Figure 39: Confocal microscopic image of compound 56 in A β 42 cells. R describes the efficiency for co-localization. The <i>in vitro</i> assays were carried out by C. Secker and Prof. E. Wanker. ¹⁸	90
Figure 40: UV and fluorescence spectra of compound 79 (left). Photophysical properties of compound 79 (recorded in MeOH at T = 293 K): $\lambda_{\text{max, abs}} [\text{nm}]^{[a]} = 276, 319$ (sh); $\lambda_{\text{max, em}} [\text{nm}]^{[b]} = 590$; Stokes shift $\Delta\tilde{\nu} [\text{cm}^{-1}]^{[a]} = 14400$; compound 79 dissolved in methanol under UV light (right).	98
Figure 41: Illustration of compound 79 (left) <i>via</i> confocal microscope, EGCG-A β 42 in cell co-localization (right). The Pearson's correlation coefficient was quantified from rhodamine B and HiLyte488 signals, the quantification was determined by normalization of the fluorescent intensity spectra to maximum intensity along illustrated white arrow. This data was provided by C. Secker and Prof. E. Wanker. ¹⁸ For an enlarged view see appendix.....	99
Figure 42: Illustration of compound 101 (left) <i>via</i> confocal microscope, EGCG-A β 42 in cell co-localization (right). The Pearson's correlation coefficient was qualified between rhodamine B and HiLyte488 signals, the quantification was determined by normalization of the fluorescent intensity spectra to maximum intensity along illustrated white arrow. The <i>in vitro</i> assays were carried out by C. Secker and Prof. E. Wanker. ¹⁸ For an enlarged view see appendix.	100
Figure 43: Investigation of compound 79 (on top) in cell-based assay <i>via</i> confocal microscope, EGCG-A β 42 in cell co-localization (below). The data was provided by C. Secker and Prof. E. Wanker. ¹⁸	112
Figure 44: Analysis of compound 101 (on top) in cell-based assay <i>via</i> confocal microscope, control compound 101 in cell co-localization (below). The data was provided by C. Secker and Prof. E. Wanker. ¹⁸	113
Figure 45: Relevant structural elements for <i>in vitro</i> and <i>in cell</i> potency of EGCG.....	116
Figure 46: Possible interaction of β -PGG galloyl group and enzyme by hydrogen-bond, G = galloyl (3,4,5-tri- <i>O</i> -benzylicgallic acid). ^[270]	117
Figure 47: EGCG on a D-glucopyranose core, R = EGCG.	118

List of Tables

Table 1: Comparison of the proportionality of people with dementia by age worldwide (cases per annum in million). ^[10]	22
Table 2: Content of catechins in green tea. ^[76]	34
Table 3: Content of catechins in tea. ^[81]	34
Table 4: Tea processing and its effect on tea polyphenol content. ^[82]	35
Table 5: Constitution of GCG- and EGCG derivatives including di- and trihydroxyphenyl variants.	75
Table 6: Illustration of desired products after deprotection.	77
Table 7: Summary of the inhibition (<i>in vitro</i> %) and the degradation (<i>in cell</i> %) effect of EGCG and its derivatives. The yellow highlighted fields show the use of purchased compounds. ¹⁸	78
Table 8: Summary of enantiomeric excess of racemic diol 53	121
Table 9: Summary of enantiomeric excess of diol 37(α)	122
Table 10: Summary of enantiomeric excess of diol 37(β)	122
Table 11: Summary of enantiomeric excess of racemat.	123
Table 12: Summary of enantiomeric excess of <i>cis</i> -chroman-3-ol <i>cis</i> 45	123

Abbreviations

*	chiral
[α]	specific rotation
A β	amyloid- β -Protein / β -Amyloid
AChEI	acetylcholinesterase inhibitor
AD	Alzheimer's disease
ADAM	A disintegrin and metalloprotease domain
AE	asymmetric epoxidation
Alox	aluminum oxide
AhR	aryl hydrocarbon receptor
ApoE	Apolipoprotein E
APP	Amyloid Precursor Protein
APP _{sa}	soluble alpha APP ectodomain
Ar	aryl
BACE	β -site of APP cleaving enzyme
C	Catechin
COMT	catechol <i>O</i> -methyltransferase
conc	concentrated
α -CTF	C-terminal fragment cleaved by α -secretase
β -CTF or C99	C-terminal fragment cleaved by β -secretase
γ -CTF or C57	C-terminal fragment cleaved by γ -secretase
<i>d</i>	doublet
<i>dd</i>	doublet of doublet
DEAD	diethylazodicarboxylate
DHQD	dihydroquinidine
DHQ	dihydroquinine
DIAD	diisopropyl azodicarboxylat
DIBAL	diisobutylaluminium hydride
dil.	diluted
DME	dimethoxyethane
DMF	dimethylformamide
DPPA	diphenylphosphoryl azide
EC	epicatechin
EDC·HCl	<i>N</i> -(3-dimethylaminopropyl)- <i>N'</i> -ethylcarbodiimide hydrochloride
<i>ee</i>	enantiomeric excess
EGC	epigallocatechin
ECG	epicatechingallate
EGCG	epigallocatechin-3-gallate
eq	equivalent
<i>et al.</i>	et alii
FAD	autosomal dominant familial AD
Fig.	Figure
FTLD	frontotemporal dementia
h	hour(s)
HIV-1	human immunodeficiency virus
HOMO	Highest Occupied Molecular Orbital
Hsp90	Heat shock protein 90
HR-MS	High Resolution Mass Spectrum
HWE	Horner-Wadsworth-Emmons reaction
I	Nuclear spin quantum number
IC ₅₀	half maximal inhibitory concentration
<i>J</i>	coupling constant
L, Lig.	ligand
LNCaP 104-R	Lymph Node Carcinoma of Prostate
LUMO	Lowest Unoccupied Molecular Orbital

m/z	mass-to-charge ratio
m	multiplet
M	molar
MCF-7	Michigan Cancer Foundation-7
min.	minute
mol%	mol per cent
MS	mass spectrometry
MSA	methanesulfonic acid
NFT	neurofibrillary tangle
NHS	<i>N</i> -hydroxysuccinimide
NMDA	<i>N</i> -methyl-D-aspartate
NMR	Nuclear Magnetic Resonance
NSAID	non-steroidal anti-inflammatory drugs
Nu	nucleophile
<i>o</i>	ortho
PDC	pyridinium dichromate
PEG	polyethylene glycol
PPO	polyphenol oxidase
RA	reductive amination
<i>R_f</i>	retention factor
PD	Parkinson's disease
PS-1	preseniline 1
PS-2	preseniline 2
<i>p</i>	para
p. a.	puriss absolute, absolute Reinheit
PPTS	pyridinium <i>p</i> -toluenesulfonate
r	Pearson's correlation
rt	room temperature
s	singlet
sat.	saturated
SOD	superoxide dismutase
sol.	solution
<i>t</i>	triplet
T	temperature
TBA	<i>tert</i> -Butyl alcohol
TBAF	tetra- <i>n</i> -butylammonium fluoride
TBSCI	<i>tert</i> -butyldimethylsilyl chloride
TBS	<i>tert</i> -butyldimethylsilyl
tert.	tertiary
TFA	trifluoroacetic acid
TLC	thin-layer chromatography
TG	trigeminal Ganglion
Thr	threonine
ThT	Thioflavin-T

1. Introduction

1.1 Alzheimer's disease

1.1.1 Morbus Alzheimer

In 1906, the psychiatrist **Alois Alzheimer** (1864-1915) (**Figure 1**)^[1] discovered a cerebral modification in a 51-year-old woman that showed a specific conduct with a speedily deteriorating memory that attended to psychiatric disturbances. She died 4 years later.^[4]

Besides behavioural as well as neuropsychiatric abnormalities and accumulation of plaque causing the damage of nerve cells, the woman's brain also showed neurofibrillary tangles (NFT) (**Figure 2**).^[4-5] In 1910, this disease pattern, called Alzheimer's disease (AD) was declared a new nosologic entity, which was endorsed by Emil Kraepelin.^[6] AD is ranked as a disease very difficult to treat. Accounting for an estimated 60% to 80% of cases are identified, compared to other causes of dementia like vascular dementia, dementia with Lewy bodies, Parkinson's disease (PD) with dementia, frontotemporal dementia (FTLD) and reversible dementias.^[7]

The symptoms of Morbus Alzheimer represent a clinical and neuropathological disease pattern, which can differentiate between the categories of familiarly, presenile type and the senile, sporadic disease. The clinical symptoms in the latter case are characteristic for the age of ca 65 years. In contrast, the rare familial form becomes manifest before the age of 50 years.^[8] Alzheimer's disease is a neurodegenerative disorder that represents the most common case of dementia worldwide. In 2015, the estimated number of people living with dementia is 46 million, whereas in 2030 it will be an increasing number of 75 million people and reaching 132 million in

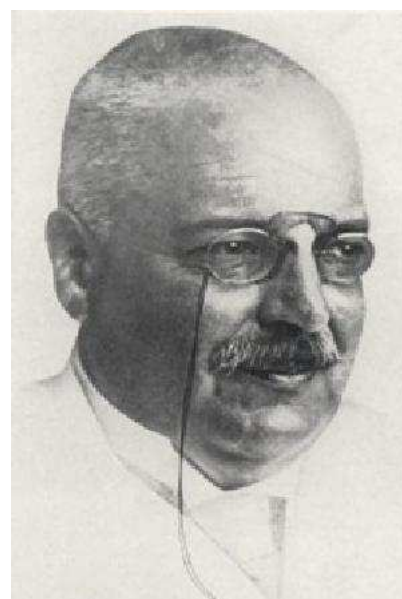


Figure 1: The psychiatrist Alois Alzheimer (1864-1915), described at first the "disease of oblivion". His teacher Emil Kraepelin suggested the name.^[1]

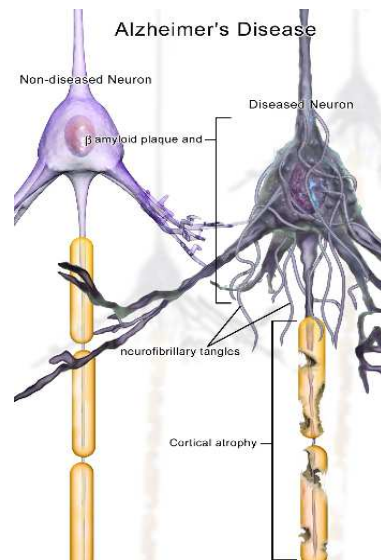


Figure 2: Accumulation of amyloid plaques on nerve cells distinguish the characteristics of Alzheimer's disease. Chronic inflammation is caused by amyloid plaques explicit naming $A\beta$, reprinted with permission of: Creative Commons Attribution 3.0 *via* Wikimedia Common.^{[5]1}

2050.^[9] Consequently, from 2015 to 2050 the number of people suffering from dementia will have increased twofold in Europe, about twofold in North America, threefold in Asia and fourfold in Latin America and Africa. Presently, 37% of the people that are afflicted with dementia are in high-income countries, whereas 63% can be associated to low and middle-income countries.^[10]

Table 1: Comparison of the proportionality of people with dementia by age worldwide (cases per annum in million).^[10]

Region	Age group (years)							Total
	60-64	65-68	70-74	75-79	80-84	85-89	90+	
Asia	0.39	0.48	0.62	0.72	0.66	0.44	0.26	3.56
Europe	0.13	0.18	0.32	0.43	0.54	0.44	0.29	2.34
America	0.10	0.13	0.17	0.21	0.25	0.23	0.17	1.25
Africa	0.07	0.09	0.10	0.11	0.09	0.04	0.53	0.53
World total	0.69	0.88	1.22	1.46	1.54	1.15	0.74	7.68

In addition, it is apparent that the prevalence rate rises with age. There is also a correlation between the incidence of AD and the sex, - more women are affected by AD and other

¹ "Blausen 0017 AlzheimersDisease" by BruceBlaus - Own work. Licensed under Creative Commons Attribution 3.0 *via* Wikimedia Commons - http://commons.wikimedia.org/wiki/File:Blausen_0017_AlzheimersDisease.png#mediaviewer/File:Blausen_0017_AlzheimersDisease.png

dementias than men. In consequence, 3.2 million out of the 5 million people afflicted aged 65 and older are women, 1.8 million are men. At the age of 71 and above 16% of women suffer from AD compared to 11% of men.^[11] In regards to age these facts result from the higher life expectancy of women and older age is the most harmful risk factor of AD (**Figure 3**).^[12]

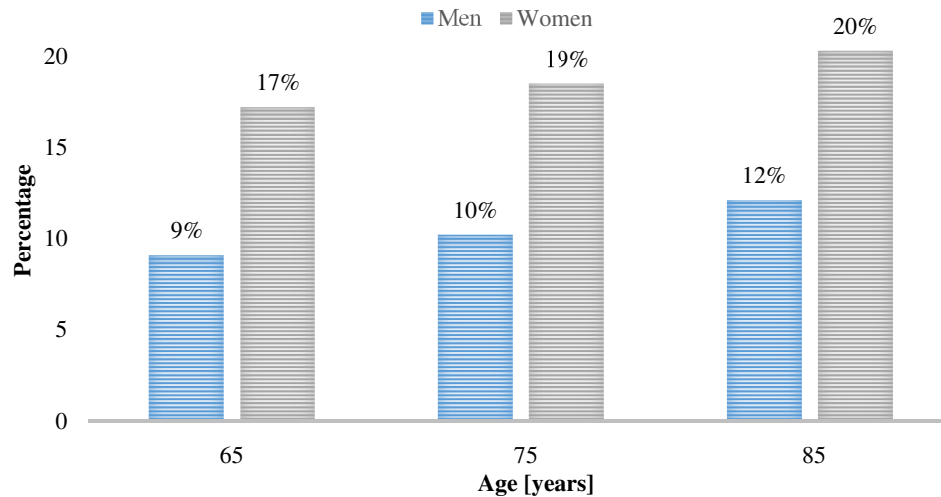


Figure 3: Comparison of the percentage between age group and sex.^[13]

Apart from age, there are various other risk factors for the formation of AD such as high blood pressure and diabetes. Additionally, an increased risk of becoming affected originates from lower levels of education and other socioeconomic factors.^[14]

Due to the increase of dementia incidence, there is a need to promote its prevention and therapy. In the United States, AD is officially listed as the sixth most frequent cause of death. For elderly, the disease has developed as the most common cause of death.^[15] Over a period of 15 years there was an increase of death due to AD by 123%, compared to other causes of death, like, for example, heart disease which was reduced to 11%.^[16] This fact implies that over the next 5 years, 5% to 15% of all deaths in elderly people will be the underlying Alzheimer's disease (**Figure 4**).^[17]

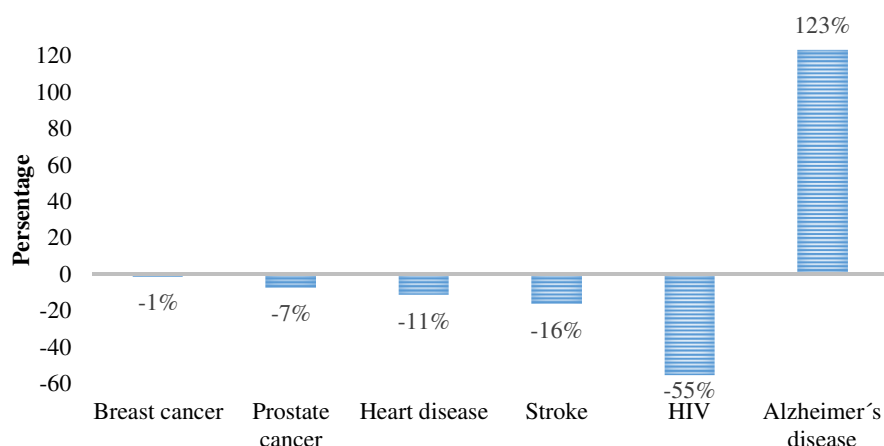


Figure 4: Comparison of percentage data of causes of death between 2000 and 2015.^[13, 16]

In high-income countries, the demographic transition shows other significant shifts to low- or middle-income countries: in combination with improved health conditions this causes an increase in this kind of diseases (epidemiologic transition).^[18] Due to the fact of an increasing number of deaths attributed to AD, the emphasis should be on its prevention and therapy. Currently, Alzheimer's disease is not curable. However, modern medication facilitates an enhanced survival rate of dementia patients, especially a higher life expectancy. Nonetheless, it is necessary to prevent dementia disease or to inhibit the progression of disease. The research in medicinal therapy aims at detecting preclinical Alzheimer's disease with suitable biomarker tests, so that it will be possible to detect it before symptoms develop.^[19] Right now, Alzheimer is associated with the most cost-intensive diseases; furthermore it requires the most intensive medical care. In the United States, nursing accounts for up to 43.000 US\$ per patient per year.^[20] If there is no success in new neuroprotective and neurodegenerative therapy strategies, there will be a higher socioeconomic force caused by a successively increasing number of Alzheimer's patients.^[21]

1.1.2 Molecular Basis of the Neurodegenerative Disorders

The characteristic properties of neurodegenerative disorders are selective and symmetric loss of neurons in motoric, sensoric, or cognitive systems. These containments of the patterns could support the nosologic classification, which consists of senile plaques, neurofibrillary tangles, neuronal loss and acetylcholine deficiency which define Alzheimer's disease.^[22] Lewy bodies and depletion of dopamine characterize Parkinson's

disease.^[23] Amyotrophic lateral sclerosis is embossed by cellular inclusions and swollen motor axons,^[24] and γ -aminobutyric acid containing neurons of the neostriatum are damaged in Huntington's disease.^[25] Some of these diseases follow the inheritance according to Mendelian, while Alzheimer's disease,^[26] Parkinson's disease,^[27] and amyotrophic lateral sclerosis^[24] are inherited by about 1 – 10% as an autosomal dominant inheritance. In 1980, people were intensively searching for the gene which is responsible for Huntington's disease^[28] and about 50 disorders of the central nervous system are by mutant genes.^[29] Neurodegenerative diseases, caused by genetic anomalies, are very diverse and complex. Not only the presence of one gene is responsible for the development of disorders. Exemplified by Alzheimer's disease, some genes lead to clinical and pathological syndromes dependent on age at onset or rate of progression.^[22, 27] Errors in DNA replication cause other diseases due to the increased number of trinucleotides. An increased sequence of amino acids of CAG is caused by elongation of glutamine, which affects heterozygotes as well as homozygotes. Biochemical change caused by mutation leads to altered function, which is toxic to the cell. Friedreich's ataxia, an autosomal recessive disorder, induced by incorrect protein production, leads to cellular loss of function.^[29] Neurodegenerative diseases are induced by abnormalities in the transport, degradation, and aggregation of proteins. These conditions influence the cell environment and initiate neuronal death by apoptosis.^[30]

1.1.3 Disease Pattern

AD is a progressive, neurodegenerative disease that is dependent on age. The hippocampus and neocortical regions of the human brain are affected by severe neurodegeneration.^[31] The pathophysiological characteristic of dementia is a successive cognitive decline initiated by progressive degeneration of neurons and synapses in the cerebral cortex and subcortical regions, e.g. cholinergic neurons, which are responsible for the regulation of the neurotransmitter acetylcholine (**Figure 5**).^[32]

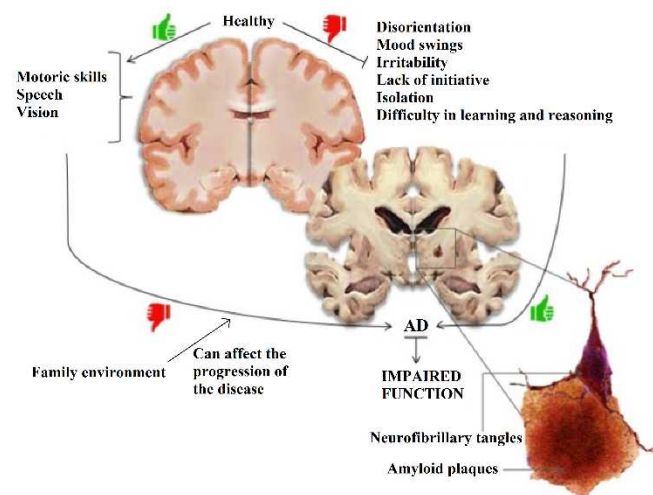


Figure 5: Characteristic transformation during AD.^[33]

Representative AD brains exhibit neuronal and dendritic loss, neuropil threads, dystrophic neuritis, granulovacuolar degeneration,² Hirano bodies,³ and cerebrovascular⁴ amyloid.^[34] Evidence for the formation of AD is not well-known,^[35] but genetic predisposition is included which leads to an heredity with autosomal dominant inheritance in 5 – 10%.^[36] The disease pattern, as clinical evidence manifests, becomes apparent by an irreversibly advancing damage to cognitive skills. Consequently, people are affected by degeneration of memory, orientation as well as personality and the navigation of bodily function (apraxia). These symptoms are accompanied by cognitive inclination to aggression, hallucination, depression, dysfunction of the motor function and deteriorating speech. Accordingly, after 8 years on average the disease results in death.^[37] The principle feature for AD are the degeneration in the temporal and parietal lobe, including parts of the frontal cortex as well as cingulated gyrus, so that the affected regions are atrophied.^[38] The brain shows abnormalities like ubiquitous shrinkage of brain cells with characteristic slots of cerebral sulcus and progress of the cerebral ventricle. The neuropathology involves the deposit of extracellular β -amyloid protein ($A\beta_{42}$) in the brain parenchyma and cerebral blood vessels originating from non-adaptive cleavage of the amyloid precursor protein (APP), also bearing tau-protein dependent neurofibrillary tangles (**Figure 6**).^[14]

² Injury of hippocampal brain cells in old people.

³ Intracellular aggregates of actin in nerve cells.

⁴ Affected the blood vessels and blood supply of the cerebrum or brain.

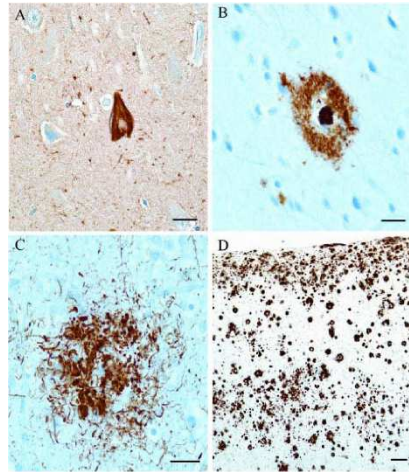


Figure 6: Affected brains with senile plaques containing A β (B) and neurofibrillary tangles (NFT's) constituted of hyperphosphorylated tau protein accumulated in paired helical filaments (A). Attended by extensive neuritic pathology (C), represented as accumulation in large numbers in the diseased brain (D).^[39]

1.1.4 Pathophysiology & Amyloidosis

The hallmarks of AD are extracellular A β and intracellular aggregates called neurofibrillary tangles (NFT's), initially triggered by accumulation of hyperphosphorylated tau-protein. The former tends to be constituted of long linear or fibrillary aggregations of misfolded proteins, which are characterized by its insolubility.^[40] There is a distinction between extracellular amyloid plaques in human brains: neuritic (*senile*) and non-neuritic (*diffuse*) plaques. Senile plaques originate from extracellular A β 42 protein depositions, while diffuse plaques consist of rather diffuse-defined partial amyloid plaques without a central core.^[41] Commonly, the occurrence of both senile, and diffuse plaques is observed in brains of older people without any dementia apparition. The AD pathophysiology implicates the post-translational proteolytic cleavage of the APP (amyloid precursor protein) to form A β 42 peptides, ranging from 39 – 42 amino acids, induced by β - and γ -secretases.^[42] The delegation of the intracellular A β 42 cleavage byproduct into the extracellular milieu leads to an aggregation of toxic A β 42 peptides, which indicates resistance in respect of proteolytic depletion processes. This extracellular deposition of amyloid plaques results in secondary inflammatory consequently, irreversible nerve degradation and destruction of nerve cells.^[43] Outside and around the neurons an accumulation of dense, mostly insoluble deposits of protein and cellular material plaques are located, whereas inside the nerve cells insoluble twisted fibers are accumulated.^[44] The occurrence of pathological oligomers and

the occurrence of this soluble A β origins (ADDL) is attributed to a destruction of the neuronal communication and synaptic plasticity.^[45] The appearance of the AD pathology and Down's syndrome is associated with the amyloid cascade hypothesis. Whereas the APP is localized on chromosome 21, Down's syndrome originates from an extra copy of chromosome 21 (trisomy 21).^[46] Mutations in the APP lead to an autosomal dominant familial AD (FAD), in addition to presenilin 1 (PS-1), and presenilin 2 (PS-2) genes, localized on chromosomes 14 and 1, respectively.^[47] The presenilins belong to transmembrane proteins, assumed to be part of the γ -secretase complex. In the case of mutation, the cleavage of presenilin 1 would result in an increasing loss of protein function.^[48] Familial early-onset AD is connected to mutations in the presenilin protein encoding genes and causes a deposit of A β in the brain, as well as white matter and also extensively within blood vessels.^[48] The development of AD is manifested by the presence of ϵ 4 allele of ApoE, a serum cholesterol transport protein, which can lead to a cholesterol imbalance^[39] and variations in the amyloid cascade^[49] by accelerate deposition of A β 42.^[50]

As mentioned above, a second pathological characteristic of AD is the presence of intracellular fibrillous inclusion in neurons, the neurofibrillary tangles (NFT's). NFT's consist of matched helical filaments (paired helical filaments) which are elongated to 10 – 12 nm (**Figure 7**).^[51]

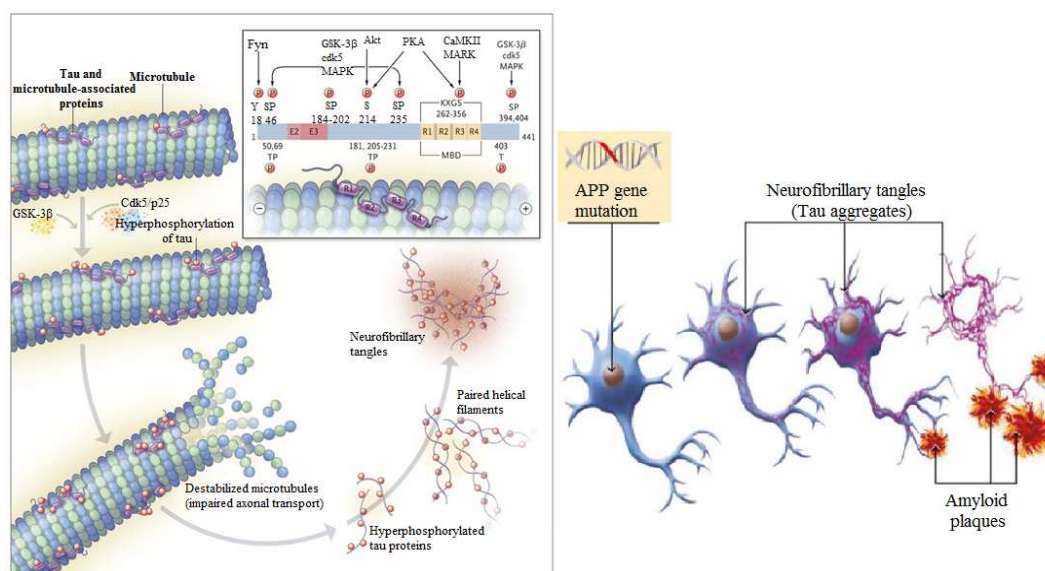


Figure 7: Hyperphosphorylated tau-protein caused by mutation in APP gene which leads to the formation of NFT's (in purple, right).^[52] Function and structure of tau protein (left).^[53]

⁵ Reproduced with permission from (scientific reference citation: Review Article "Alzheimer's Disease, Henry W. Querfurth, M.D., Ph.D., Frank M. LaFerla, Ph.D., *N Engl J Med* **2010**; 362:329-344, January 28, 2010, DOI: 10.1056/NEJMra0909142), Copyright Massachusetts Medical Society.

Tau-proteins constitute microtubule-binding proteins, closed to be involved in microtubulus stabilization and the regulation of axonal transport in the brain.^[54] The tau-protein occupies six isoforms which are dependent on the involvement of *N*-terminal exon 2,3 and a microtubule binding in exon 10. A mutation of this tau-protein affects splicing and microtubule binding efficiency.^[54] The function of the proven abnormal phosphorylation seems to be dissociated in microtubular systems with resultant destabilization of the cell skeleton and finally to cell-declination (**Figure 7**).^[55]

1.1.5 APP Metabolism

The neurogenesis and neuronal regeneration is caused by the transmembrane protein, called APP. The large *N*-terminal extracellular region is equipped with a heparin-binding and copper-binding site, a short hydrophobic transmembrane domain, and additionally, a short intracellular domain integrative *C*-terminus. The cysteine-rich *N*-terminus consists of a heparin-binding side and functions as a cell surface receptor which is responsible for the neurite growth, neuronal adhesion, axonogenesis, and cell mobility.^[56] The intracellular *C*-terminus domain is part of transcription regulation as a result of protein-protein interactions.^[57] In the case of usual conditions the sequential proteolytic cleavage, dominated by α - and γ -secretase, generates soluble fragments (**Figure 8**).^[55] With its tendency to cleave the APP in its transmembrane region α -Secretase appertains to the family of proteolytic enzymes.^[58] The α -secretase pathway is ascribable to the predominant APP processing pathway. The emergence of the non-amyloidogenic pathway in APP processing caused by the α -secretase leads to the cleavage without the formation of A β . The APP metabolism is initiated firstly by α -secretase, which generates, by cleavage of APP, a soluble *N*-terminal ectodomain (sAPP- α), called α -CTF or C83, that seems to be neuro protective and a membrane-bound *C*-terminal fragment (**Figure 8**).^[59] The formation of sAPP α promotes a decreased production of toxic A β peptides.^[60] Moreover, an alternative amyloidogenic pathway subsists in cases of illness: β -secretase (BACE = *β -site of APP cleaving enzyme*) generates A β peptides by cleavage, containing *C*-terminal fragment (CFT) identified as β -CTF or C99 and a soluble, extracellular *N*-terminal fragment declared as an AP- β (sAPP- β) fragment.^[61] Subsequently, the β -CTF fragment is clefted intracellularly by γ -secretase complex terminating in toxic A β -peptides and a minor γ -CTF (C57), but much larger than the p3 fragment.^[62] So far, no biological role is

attributed to the p3 fragment generated by cleavage by α - and β -secretases. After cleavage these fragments are emitted in the extracellular space of the brain where they are able to accumulate and form amyloid plaques, respectively.^[63]

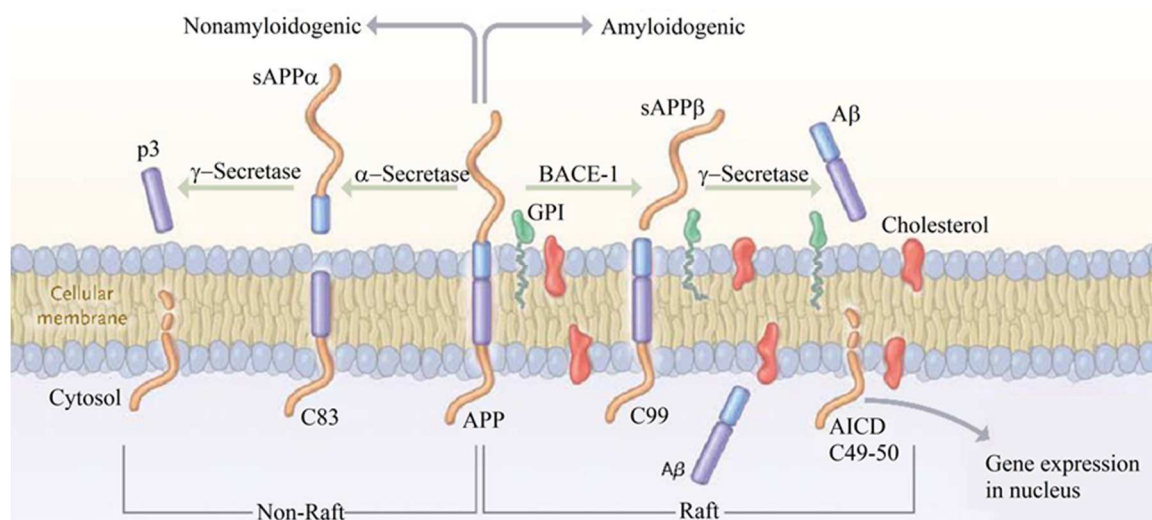


Figure 8: Processing of APP by cleavage through α -secretase in non-amyloidogenic pathway and through β -secretase in amyloidogenic pathway.^{[53]6}

Consequently, plaques exert a deleterious effect on neuronal and synaptic function, as a result of neuronal cell death. The accumulation leads to microscopic plaques, followed by a multi-step polymerization mechanism to oligomers. These A β peptides are able to form fibrils by aggregation with a regular β -sheet structure, and clump together to build plaques. A β induces deleterious effects accompanied by disrupting brain cells by clogging points of cell-cell communications, whereas they activate immune cells which trigger inflammation, followed by cell lethality.^[63]

1.1.6 Therapeutic Treatment and Intervention Approach for AD

The extraordinary percentage of people with AD underscore the urgency of new and more effective therapeutic interventions. Patients are not only afflicted by cognitive and memory deterioration, but rather restricted in the activities of daily living and therefore diminished in their livability.^[50] AD is an amnesic type of memory impairment,^[64] accompanied by decline of language,^[65] and visuospatial deficits in attention/processing.^[66] Until the late

⁶ Reproduced with permission from (scientific reference citation: Review Article "Alzheimer's Disease, Henry W. Querfurth, Frank M. LaFerla, *N Engl J Med* **2010**; 362:329-344, January 28, 2010, DOI: 10.1056/NEJMra0909142), Copyright Massachusetts Medical Society.

phases of the disease, patients are more and more limited in the basic activities of daily life, with symptoms of psychosis and agitation, while mood changes and apathy occur in early stages of the disease and continue for its duration.^[67] Nowadays, an effective therapeutic strategy includes the neuroprotection against deleterious varieties of A β as well as the suppression of processes, which cause neuronal dysfunction and degeneration. Complicated mechanisms underlay these processes,^[68] the onset and progression of AD consist of a fundamental interaction, like excessive accumulation of A β , oxidative stress, tau phosphorylation, leading to excitotoxicity, damage of synapses, neurites and neurons and substantial loss of neurotransmitter function. Currently, some clinically available drugs are approved for the treatment of AD, but the capabilities of these agents have to be studied to see if there is a delaying effect on onset or slowing disease progression.^[69] Donepezil (**a**), Galantamine (**b**), and Rivastigmine (**c**)^[70] are acetylcholinesterase inhibitors (AChEI)^[71] that may induce the symptomatic improvement of the cognitive conditions.^[70] Memantine (**Figure 9**), an adamantane derivative, causes the obstruction of NMDA (*N*-methyl-D-aspartate)^[72] receptor activity without the impairment of current receptor activity, and furthermore, it is accredited to block excitotoxicity by neuroprotective properties.^[71] In the case of neurodegenerative disorders the NMDA receptors of the neurotransmitter glutamate are over-activated by glutamatergic release which leads to excitotoxicity through high levels of Calcium ions (Ca²⁺). Memantine (**d**) prevents the high stimulation of NMDA receptor activity without affecting the common glutamate synaptic transfer.^[70]

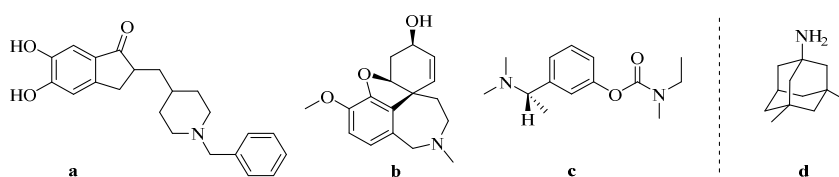


Figure 9: Acetylcholinesterase inhibitors (AChEI), **a**). Donepezil (Aricept[®]), **b**). Galantamine (Reminyl[®]), **c**). Rivastigmine (Exelon[®]), **d**). Memantine (Ebixa[®]) NMDA antagonist.^[70]

Nowadays, there are several possible therapeutic strategies for intervention of misfolding diseases established (**Figure 10**):^[2, 73]

- (1) the prevention in an early-onset phase by inhibition of β -secretase to prevent harmful deposits of monomeric proteins,
- (2) prevention of aggregation by drugs,

- (3) redirection of amyloid cascade in direction of non-toxic aggregates,
- (4) stabilization of larger aggregates,
- (5) the prevention in a mid-phase by inhibition of generation of neurofibrillary tangles,
- (6) the suppression of inflammation in a late-phase to decelerate disease processes.^[2, 73]

The main source of toxicity are the oligomeric deposits in the brain. The mechanistic properties enable the investigation of new targets and treatment strategies for a therapy of neurodegenerative diseases, e.g. AD and Parkinson's diseases. In this context, natural compounds, the polyphenols present in green tea, provide a potential approach for treatment for these diseases and give rise to new intervention strategies.^[2, 73]

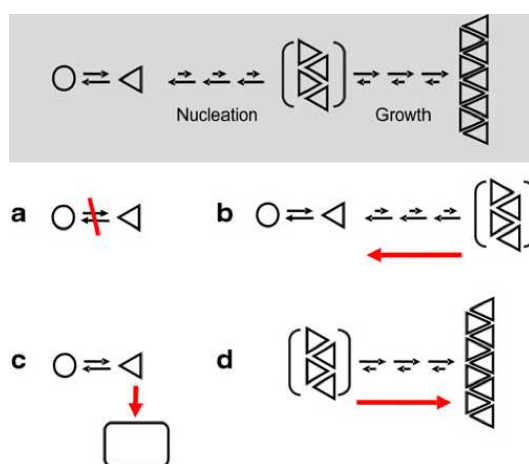


Figure 10: Intervention approach for misfolding diseases: **(a)** monomers are not able to form aggregates, **(b)** disintegration of the aggregation intermediate, **(c)** degenerated amyloid formation, **(d)** increased tendency to form larger aggregates.^[2]

1.2 Polyphenols

1.2.1 Ingredients of Green Tea

In 1753, Carl von Linné initially classified the tea plant, *Camellia sinensis* (**Figure 11**), to the camellia family (Theaceae), and in 1887 Carl Otto L. Kuntze, a German botanist, integrated it in to the genus *Camellia*. Both subspecies are characterized as *Camellia sinensis* var. *sinensis* (*chinatea*) or var. *assamica* (*assamtea*).^[74]



Figure 11: Green Tea plant - *Camellia sinensis*.^[3]

Green and white teas are rich in polyphenols mostly catechin (C), epicatechin (EC), epigallocatechin (EGC), epicatechingallate (ECG), and especially epigallocatechin-3-gallate (EGCG) (**Figure 12**). These catechins, belonging to tea-polyphenols, particular to a subcategory of the flavonoids, are called flavonoles.^[75] Dried green tea leaves contain many other ingredients, like the flavonoids kaempferol, quercetin, and myricetin. In addition, the amino acid derivative theanine, the xanthine alkaloids caffeine, theophylline, theobromine, and saponins etc.^[76]

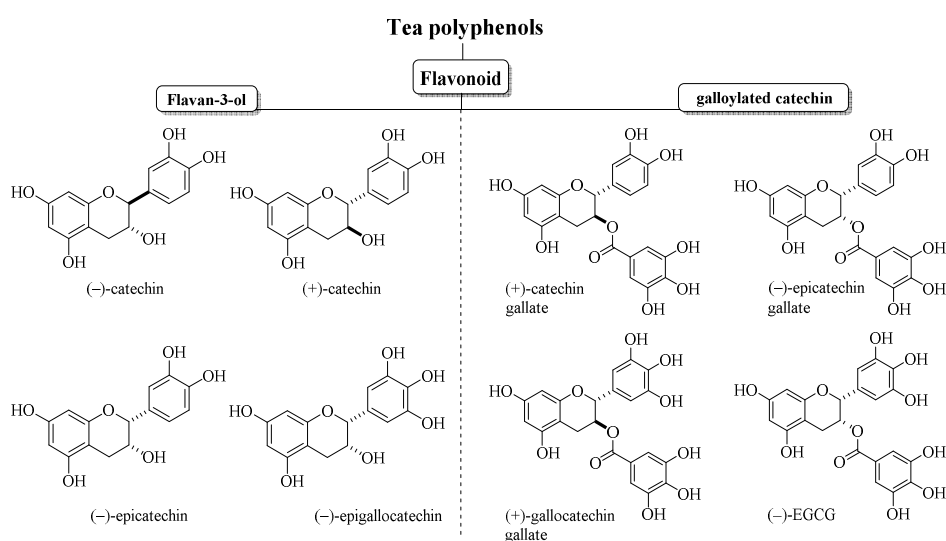


Figure 12: Chemical structures of the naturally occurring catechins.^[77]

Especially, the degree of the fermentation leads to variable composition of polyphenols as

well as a different oxidation level in the tea production. The fermentation process leads to the deactivation of the enzymes in green tea, mainly polyphenol oxidase (PPO), so that the oxidation and polymerization of primary polyphenols is inhibited completely. Black tea, in comparison, is completely oxidized. In freshly-harvested leaves the primary polyphenols are located in the vacuoles of the cells, where they are separated from the enzymes which are present in the chloroplast.^[78] It is interesting, that the fermentation does not influence the total amount of the polyphenols in green tea, but rather the structural conditions of catechins, which have a ratio of 10 – 20% or, accordingly, 35% dry weight.^[79]

Table 2: Content of catechins in green tea.^[75]

Green Tea					
Content of Catechins (dry weight)	C	EC	EGC	ECG	EGCG
Arithmetic mean	0.2%	0.8%	2.4%	2.0%	6.8%
Minimum value	0.1%	0.3%	0.7%	0.9%	3.1%
Maximum value	0.9%	3.2%	4.3%	5.6%	10.9%

Source: Hilal, 34 grüne Tees aus Indien, China und Japan, S. 37, 2010.^[75]

During the manufacturing process the enzymes (**Table 4**) will be fermented and the polyphenols become affected by each other, resulting in oxidation and polymerization to form dimers. The comparison of the levels of catechins in green tea shows that the concentration of EGCG is the largest ratio with slightly more than 50% among these catechins (**Table 3**).^[75] According to another study, the comparison of the ratio of different catechins after extraction revealed a higher content of EGCG than of EGC (**Table 3**).^[80]

Table 3: Content of catechins in tea.^[80]

Green Tea		
Content	Dry extract	mg/cup
EC	1.98%	15
ECG	5.20%	39
EGC	8.42%	63
EGCG	20.30%	152

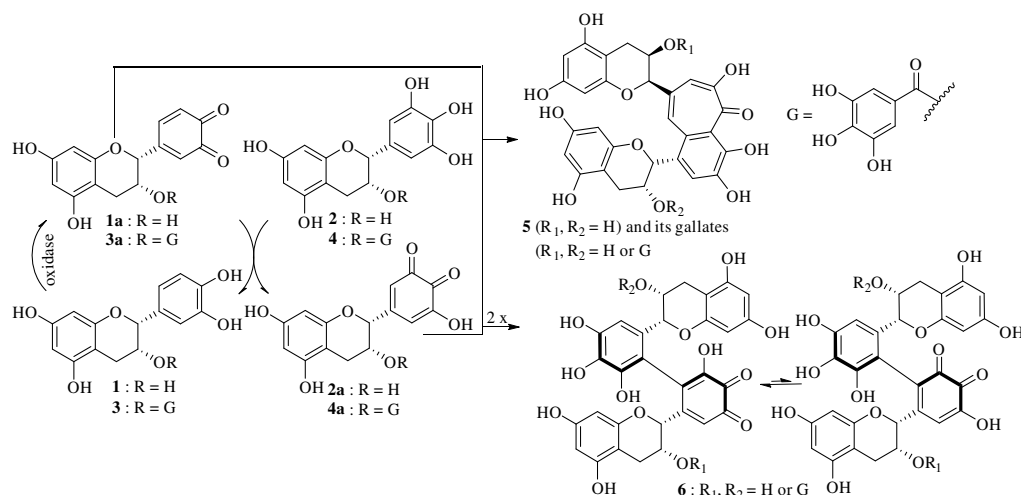
Source: R. Schneider, T. Lüdde, S. Töpfer, P. Imming: After infusion of 2.3 g tea leaves with 150 mL of water (750 mg dry extract).

Table 4: Tea processing and its effect on tea polyphenol content.^[81]

catechins	process						theaflavin & thearubigin
	→						
↑	white tea ⁷	steamed ⁸				dried	↓
	green tea ⁹	withered	steamed or panfired ⁸			dried	
	oolong tea ⁹	withered	bruised	partially fermented	panfired	dried	
	black tea ⁹	withered	rolled	fully fermented	fried	dried	

1.2.2 Autoxidation Decomposition of (-)-EGCG

EGCG is prone to sensitivity against oxidation processes as consequence of the low bond dissociation energy of the phenolic O–H bond (in gas phase: 87 – 90 kcal/mol and in polar aprotic solvents to 95 kcal/mol).^[82] The abstraction of H-atoms leads to a phenoxy radical which enables the formation of more complex oligomeric or polymeric polyphenols.^[83] Due to the degradation of EGCG through autoxidation by radical chain reactions the dimeric products theaflavins and quinones are formed as main products which are responsible for browning of EGCG (Scheme 1).^[83]



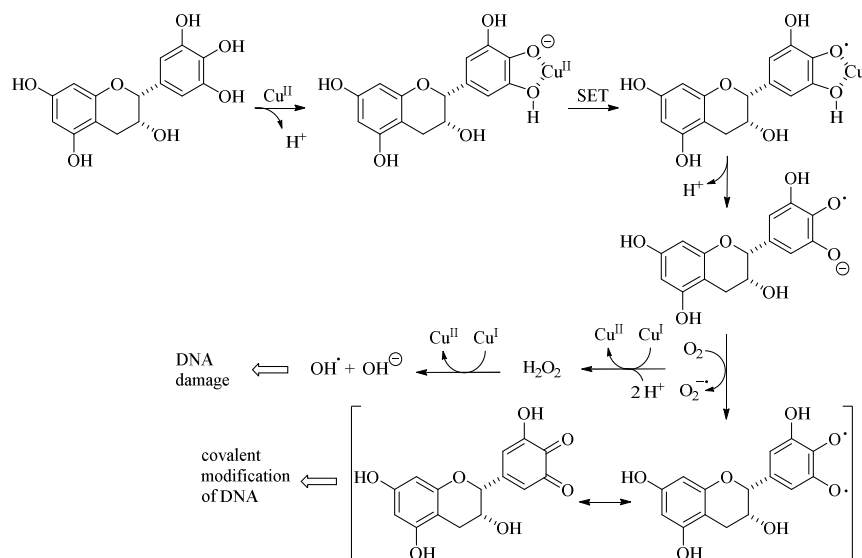
Scheme 1: Oxidation process of tea catechins and the constitution of theaflavins and epigallocatechin dimer quinones.^[77]

⁷ buds or young leaves

⁸ oxidase inactivation

⁹ mature leaves

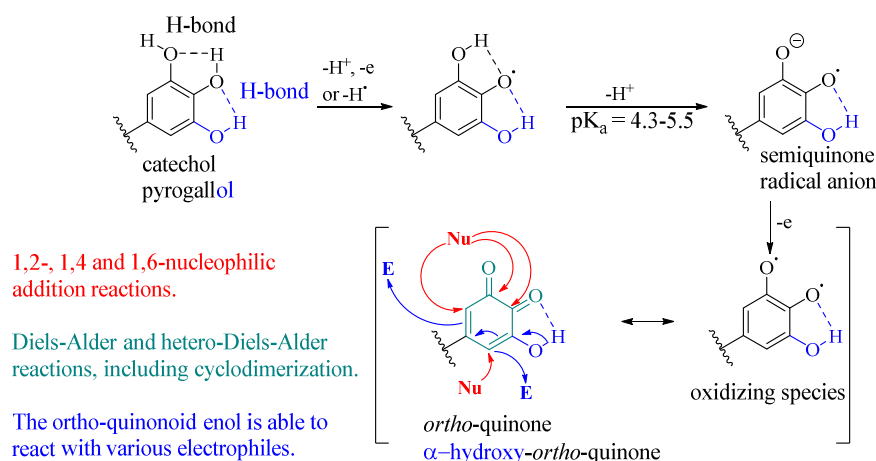
Tanaka *et al.* introduced an alternative mechanism (**Scheme 2**) by an initial intermolecular C–C bond formation between **1** (or **3**) and **2a** (or **4a**), realized by an intermolecular π - π complex formation between an electron-rich catechol ring **1** and an electron-poor hydroxyl *ortho*-quinone **2a** prior to the C–C bond formation.^[79]



Scheme 2: Proposed mechanism that emphasizes the role of oxygen.^[83-84]

Especially, EGCG is a weak acid with pK_a of 7.99. During an enzymatic oxidation in the neutral or slightly alkaline pH in the cell culture medium, molecular oxygen is able to oxidize EGCG due to its low redox potential by transferring two electrons to form superoxide radical (O₂^{•-}) and an EGCG radical (EGCG[•]) probably by catalysis with a metal ion such as Cu²⁺ (E^0 : Cu²⁺/Cu⁺ = 0.15 V) (**Scheme 2**).^[85] The reactive species O₂^{•-}, a stronger oxidant than molecular oxygen, is able to react with another EGCG molecule to form radicals. Both EGCG radicals may recombine together forming an EGCG dimer. The formation of superoxide radical can initiate a chain reaction and is also able to be converted to H₂O₂ in presence of superoxide dismutase.^[84, 86] Under certain circumstances, H₂O₂ is transformed into HO• under Cu(II) mediation by a Fenton-type reaction, which encourages DNA damage.^[87]

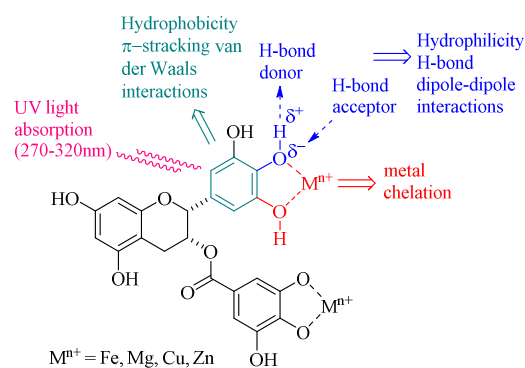
Another possibility of the formation of *ortho*-quinones and α -hydroxy-*ortho*-quinones is a result of an one-electron oxidation process of catechol- and pyrogallol phenols, leading to an electrophilic and a nucleophilic species and also possible (hetero)dienes and dienophiles in Diels-Alder type cycloaddition reactions (**Scheme 3**).^[83]



Scheme 3: Oxidative formation of pyrogallol to reactive quinone species and possible side reactions.^[83]

1.2.3 Studies in Polyphenol Chemistry and Bioactivity

Polyphenols are widely spread in the world of plants and represent an important class of natural products.^[88] They are available in human diet^[89] and are applied in traditional herbal medicines.^[90] Due to their multiple polar functionalities, polyphenols exhibit a strong interaction with proteins in an unselective way, which brings about precipitation of insoluble protein-polyphenol complexes.^[91] This principle is utilized in the tanning process of leather through the application of certain classes of polyphenols as tannins. Especially proanthocyanidins, condensed polyphenols (tannins), are responsible for astringency – a feeling of mouth puckering and dryness by consumption of oligoflavanol-rich food as wine or black tea.^[92] In addition, two adjacent hydroxy groups on the phenyl ring enable the metal chelation.^[93] A ubiquitous characteristic of polyphenols is the intense free-radical scavenging (antioxidant) effect, which is attributed to the reaction with one-electron oxidants^[94] and the formation of Fe^{2+} -complexes. These complexes act as inhibitors for radical formation by influencing autoxidative degradation.^[95] Mainly copper, iron, magnesium, and zinc hinder the decomposition of EGCG by complexation and subsequent reduction of pK_a value (**Scheme 4**).^[96] Another characteristic of polyphenols is the secondary (π - π^*) absorption maximum at 270 nm to red shifted, whereas an additional hydroxy group in *para*-position or an electron-withdrawing group shifts the absorption to 280 – 320 nm. The reason for the absorption in this region is that UV-B (280 – 315 nm) emits low wavelength but has the highest energy and flavonoids perform as UV filters for protecting the underlying photosynthetic process from damage.^[97] Furthermore, the polyphenols promote plant protection against fungi, bacteria and insects.^[92, 98]



Scheme 4: Possible metal complexation and reactivities of EGCG, including physicochemical features.^[83]

The beneficial effects of catechins against iron-induced lipid peroxidation in synaptosomes is manifested by the interference effect of catechin decrease in the order of EGCG>ECG>EGC>EC.^[99] Indeed, under certain conditions, some polyphenols indicate the opposite (pro-oxidant) effect.^[100] Actually, cell damage caused by free radicals is an important aspect of various diseases.^[101] In addition, polyphenols exhibit several significant biological activities, like the inhibition of viral reverse transcriptase,^[102] the inhibition of the replication of HIV 1 *in vitro*,^[103] of the reduction of the risk of heart disease^[103b] and the suppression of ulcer formation.^[104] Animal experiments with nude mice verified that EGCG prevents the growth of human PC-3 and LNCaP 104-R prostate tumor cells and of human MCF-7 mammary cancer cells. In contrast, the structurally related catechins ECG and EGC do not exhibit any biological activities.^[105] Furthermore, EGC and EGCG are attributed to the inhibition of leukemia cell growth. The latter hinders urokinase, which is responsible for cancer development^[106] and they are able to induce apoptosis.^[107] Based on these studies, polyphenols are gaining more attention. Due to the structural conditions with an increasing degree of oligomerization, the isolation of the pure compounds from natural sources is fraught with difficulties. Which further increases with the chain length as a consequence of altered hydroxylation arrangement and C3 configuration in the monomer units and also various stereochemical problems.^[101]

1.2.4 Metabolism and Bioavailability of Tea Polyphenols

The effect mechanism of the tea polyphenols leads to a better understanding of the bioavailability and biotransformation of the processes in the liver and intestine. Initially, the metabolism of polyphenols begins in the mouth, where the microbial catechins esterase leads to a conversion of EGCG to EGC and eventually of EGC to EC.^[108] Whereas other galloyl groups are separated in the small intestine the hydroxy groups are conjugated with glucuronic acid, sulfate, glycine or *O*-methylated in jejunum and small intestine. The derivatized catechins reach the liver. This derivatization with glucuronides and sulfate groups paves the way for urinary and biliary excretion, which conducts rapid elimination. These derivatized compounds are dispersed by the blood stream from the liver to all organs and are secreted to the duodenum.^[109] After the consumption of green tea, substantial amounts of EGC and EC were detected in the esophagus, large intestine, kidney, bladder, lung and prostate, whereas smaller amounts were observed in liver, spleen, heart and thyroid.^[110] Animal studies with mice indicate higher lung concentrations of EGCG than EGC and equivalent liver concentrations of both the before mentioned. By these results, it can be assumed, that mice have a higher bioavailability of EGCG than rats.^[110a] Studies with rats show that EGCG and EGC concentrations in serum were close to the concentrations in the applied green tea and demonstrate a corresponding mechanism.^[111] Bacterial enzymes in the colon have to metabolize polyphenols to ensure the absorption through the small intestine.^[110b] Catechins or conjugated catechins are hydrolyzed into more simple compounds, which leads, in the EGCG case, to 4-hydroxybenzoic acid, 3,4-dihydroxybenzoic acid, 3-methoxy-4-hydroxy-hippuric acid and vanillic acid. The mechanism could be verified by marked EGCG. The disintegration of catechins by microorganisms in the human and animal intestinal leads to the buildup of 5-(3',4'-dihydroxyphenyl)- γ -valerolactone and 5-(3',4',5'-trihydroxyphenyl)- γ -valerolactone. Both are metabolites of the ring fusion of EGC and EC, respectively, and consequently, are metabolized like catechins which was proven by detection in human urine and plasma. Surprisingly, in some probands higher concentrations of these compounds were identified compared to their respective precursor.^[111] It was also discovered in some studies that in humans and rats, EGCG is mainly excreted through the bile while EGC and EC are released through urine and bile,^[110b] which is in line with the observation of EGC and EC, but no EGCG was identified in human urine samples.^[110a] Overall, 47 – 58% of the initial amount of green tea catechins are removed from the body *via* the urine, only

0.1 – 2% of catechins remains unchanged.^[111] When compared to black tea, it has been shown, that the share of corresponding catechins in plasma and urine constitute about 1.68% of the total content of catechins. Inferentially, it can be surmised, that catechins of black tea are not well absorbed in human organism or faster metabolized. Consequently, free catechins are more readily available in human organism in the form of their respective gallates (**Figure 13**).^[112]

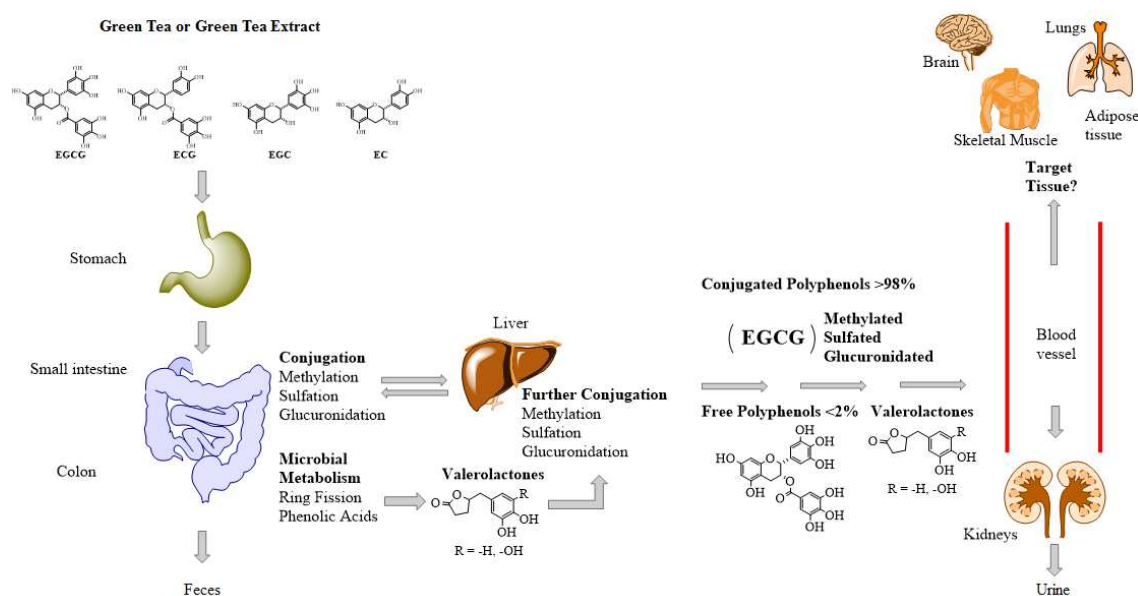


Figure 13: The bioavailability and metabolism of green tea catechins and processing in humans.^[113]

1.2.5 Antioxidative Properties of Teas

According to a current hypothesis, the health benefits of tea are linked to the antioxidant properties of the ingredients – polyphenols.^[114] The correlation between the antioxidant activity of tea polyphenols and their chemical structure is verified in many studies.^[115] A fundamental correlation consists of the availability of many hydroxy groups and the greatest antioxidant activity. The antioxidant potential of catechins to inhibit radicals in aqueous layer was observed to follow the order of decreasing affectivities as ECG~EGCG>EGC>gallic acid>EC>C.^[116] Additionally, the antioxidative effect of catechins can be intensified by addition of vitamin C or vitamin E.^[117] The green tea polyphenol extract (44% of dry weight of the green tea preparation) is responsible for 90% of the antioxidant activity.^[118] Thus, ECGC is the strongest antioxidant. The comparison between catechins and theaflavin, as dimer of catechins, theaflavin is expected to be a

stronger antioxidant.^[119] Crucial for the scavenger ability is the galloyl moiety of catechins and theaflavins.^[116] Moreover, the galloyl unit in both compounds increases the number of phenolic hydroxy groups which leads to an additional stabilization of the anion formed upon the oxidation process by hydrogen bonding. To act as scavenger for free radicals is a consequence of the standard one-electron reduction potential (E°). Coherently lower reduction potentials of catechins need less energy for hydrogen or electron donation and resulted in its potent scavenging properties ((-)-EGCG: $E^\circ = 430 \text{ mV}$).^[120]¹⁰ With respect to the structural construction of the catechins, the presence of 3,4,5-trihydroxybenzoate on the **D**-ring and gallate moiety correlate with the increased antioxidant activity. In addition, 3,4,5-trihydroxyphenyl **B**-ring substitution pattern is associated to increased activity.^[121]

1.2.6 Effect of Green Tea to the Health

In Asia, green tea has been consumed for hundreds of years. Traditional medicine in Japan and China uses green tea to promote digestive health, regulation of blood sugar and wound healing by the presence of the potent antioxidants and free-iron scavenging activities of phenolic ingredients.^[122] In recent years, these positive features of green tea have attracted attention. These ingredients are said to stop neurodegenerative diseases in common with Alzheimer's and Parkinson's disease,^[73] cholesterol disorders, weight reduction,^[73] therapy of cancer and cardiovascular diseases, especially coronary heart disease and strokes.^[123] These benefits have been proven in many different animal models^[124] in which EGCG indicates biological actions, including antioxidant, free radical-scavenging,^[125] anti-atherosclerotic, cardioprotective,^[126]¹¹ neuroprotective,^[127] anti-inflammatory,^[128] and antimutagenic^{12/} anticarcinogenic^[129]¹³ relevance. In addition, oxidative stress appears into the pathology of various chronic diseases as already mentioned: cancer, cardiovascular and neurodegenerative diseases.^[129] The antioxidant properties of catechins in green tea are especially suitable for a therapy in which these catechins are biologically active in terms of modulating cellular signaling pathways. Catechins decrease inflammation and platelet aggregation, and reduce vascular reactivity.^[130] The characteristic fat-burning properties enable weight loss^[131] by the intervention of the catechol *O*-methyltransferase (COMT)

¹⁰ E° measured at pH 7.0, 20 °C.

¹¹ Inhibition of hearts attacks by protection of the heart.

¹² Compounds that counteract the mutagenic following by reduced mutation.

¹³ Drugs or agents which counteract the effects to build up cancer.

which decreases the energy expenditure and fat-oxidation.^[132] This process leads to decreased hydrophilicity of the catechins by methylation, secondary sulfation and excretion in urine and bile.^[133] The application of catechins in neurodegenerative disease plays a pivotal role by performing as an iron chelator to bind and remove iron, which influences the production of free radicals.^[133a] The decrease of the damage produced by free radicals is facilitated by EGCG which promotes the activity of two antioxidant enzymes, the superoxide dismutase (SOD) and catalase.^[133b]

1.2.7 Novel Therapeutic Approaches for the Treatment of AD with EGCG

In recent years, EGCG showed promising results in the prevention and treatment of AD, as well as protective effects against neuronal damage in general. For example, the traditional consumption of green tea in Asia was connected with a reduction of the incidence of Parkinson's disease by a factor of five to ten with respect to Western countries where green tea is not consumed as regularly.^[134] The antioxidative activity of polyphenols allows their therapeutic application performs in misfolding related diseases. It became apparent that the mechanistic consideration of EGCG in treatment of AD was confirmed by many *in vivo* studies: In the case of neurodegenerative disorders, (-)-EGCG is supposedly involved in the inhibition of fibrillogenesis of A β 42 by direct binding to the natively unfolded polypeptides to the random-coil structures. The conversion into toxic, on-pathway aggregation intermediates is prevented by the transition of large A β -fibrils into smaller, amorphous non-toxic protein aggregates.^[122, 135] Besides the anti-oxidative impact of EGCG as a drug, it shows promising results in cell models, as well as the reduction of the toxicity of A β 42 in pheochromocytoma and neuroblastoma models.^[136] In experimental studies Rezai-Zadeh *et al.* could prove that EGCG reduces the formation of amyloid deposits.^[137] In the past, the mechanistic impact to reduce the amyloid toxicity by EGCG was not well-known. Furthermore, Ehrenhofer and Bieschke *et al.* showed in 2008, that EGCG is able to bind to the protein and prevents aggregation of amyloid fibrils.^[73] This examination was confirmed by NMR in which EGCG bound to α -synuclein (α S), a natively unstructured protein, by reduced resonance of 30%. It is therefore plausible that the hydroxy groups of EGCG stabilized the α S protein by hydrogen bonds in form of spherical oligomers (**Figure 14**).^[73]

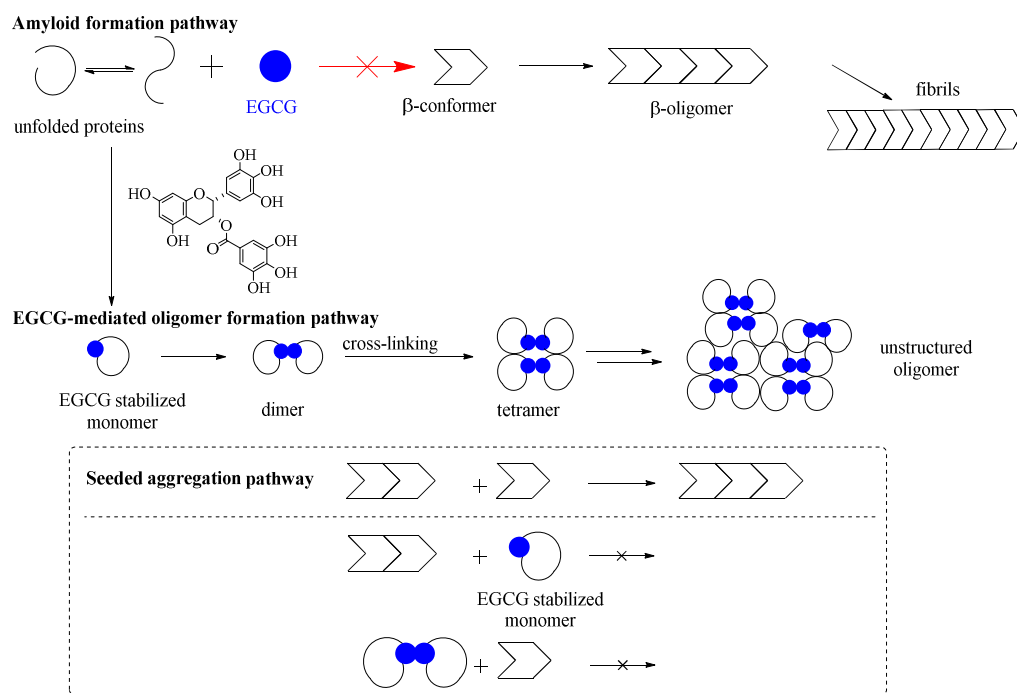


Figure 14: Possible interaction model of EGCG on fibrils.^[73]

In 2010, Fernandez and Rezai-Zadeh *et al.* reported the increased cleavage of APP in the presence of EGCG into non-amyloidogenic peptides by an high occurrence of α -secretase,^[138] as well as a suppression of β -secretase by EGCG (**Figure 14**).^[139] In the light of these properties, EGCG is able to intervene in the processes of amyloid formation, to change it from fibrils to spherical aggregates. The conversion has to be proven in detail, but it can be assumed, that EGCG could weaken the cross- β structure of fibrils by binding to A β 42, while the aggregation is supported by hydrophobic interactions simultaneously, π - π -stacking interactions or covalent cross-linking (**Figure 15**).^[73, 122, 135]

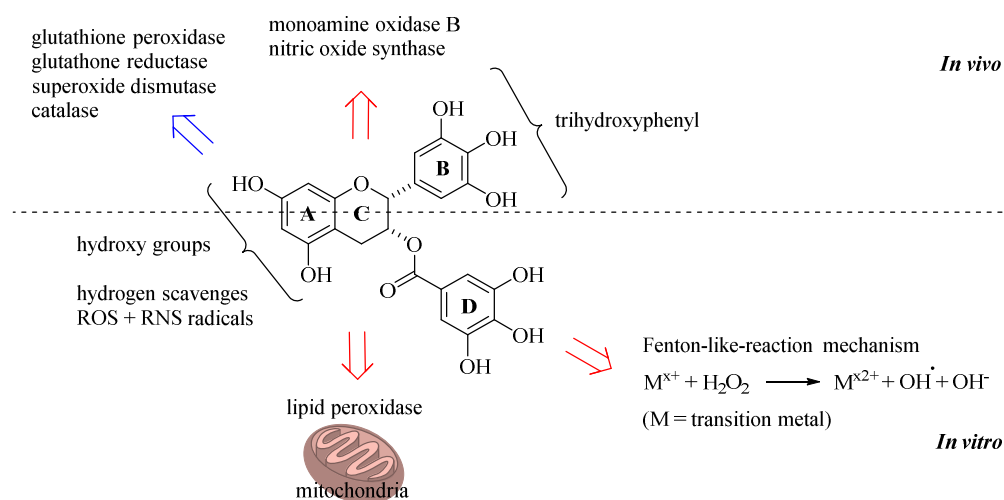


Figure 15: Supposed neuroprotective application of EGCG.^[140]

Nevertheless, several challenges of studies that verified the activity of EGCG on *in vitro* molecular targets, display an inhibition of A β 42 but the scope of applications takes place at relatively high concentrations of about 10 to 100 μ M, which leads to apoptosis of the cells.^[141] Rezai-Zadeh *et al.* showed the impact of reduced A β 42 deposition in transgenic mice by oral administration of EGCG in drinking water (50 mg/kg). The immunohistochemical analysis exemplified the successive degradation in the cingulate cortex by 54%, in the hippocampus by 43%, and in the entorhinal cortex by 51%.^[142] An important consideration is the pharmacokinetic property for the development of drugs in treatment of diseases. The bioavailability of EGCG in therapeutic application upon oral administration represented problems by its high susceptibility to oxygen, just like the affinity to casein in the digestive tract by conjugation. The fast metabolism limits the ability of the efficacy of EGCG in decreased bioavailability as well.^[143] This becomes particularly obvious in the suppressed crossing of EGCG (10 – 20%) through the blood-brain barrier.^[144] Some investigations of Peters and Green *et al.*^[145] have shown that the oral intake of catechins by consumption of green tea can be enhanced by additional supply of vitamin C. Thereby, the absorption of catechins is ensured due to intestinal stability and transport.^[145] In conclusion, EGCG is suitable for a therapeutic medication of amyloidogenesis in AD, which have been indicated by extensive studies. This provides a good foundation for the development of novel targets with identical mechanistic action in treatment of detoxification of A β 42 and other misfolding diseases.^[2]

1.3 (-)-Epigallocatechin-3-gallate

1.3.1 Molecular Properties of (-)-EGCG

The electronic nature of catechin-class polyphenols is determined by the lone pairs of the contiguous three oxygen atoms, which have an electron-donating effect on C6 and C8 (**Scheme 5 A**). Attempts to synthesize C4–C6-linked catechins by an inherent nucleophilic behavior failed due to preferred connection at the C8 position. In nature, the C4–C8 connection can be found in procyanidin B₃ (**Figure 16**).^[146]

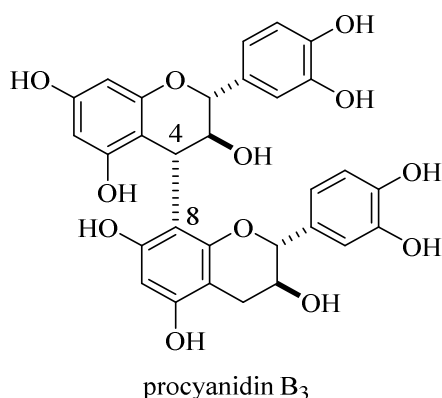
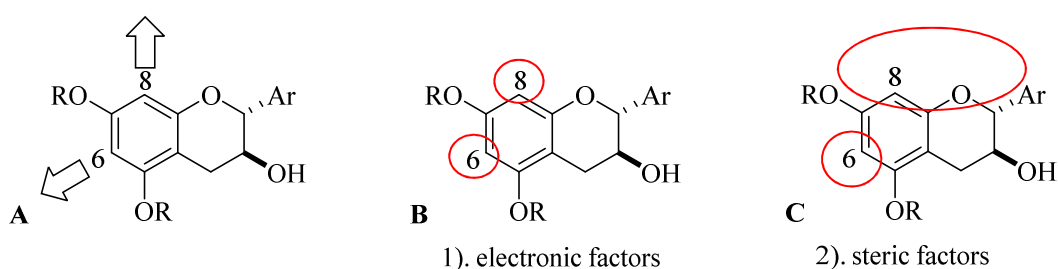


Figure 16: Structure of procyanidin B₃.^[146]

The decisive reason is not the electronic effect (**Scheme 5 B**) but rather the steric nature, which is caused by the pyran oxygen O1. The embedded oxygen in the ring blocks the adjacent C8 position from its substituents. Due to this limitation the C6 position is affected by steric crowding by the free rotation of its substituents (**Scheme 5 C**).^[146]



Scheme 5: Ground state consideration of chromane.^[146]

Clark-Lewis *et al.*^[147] suggested a half-chair conformation for the pyran C-ring, whereas the B-ring occupies to an equatorial position for flavan-ring systems with protected phenolic groups (**Figure 17**).

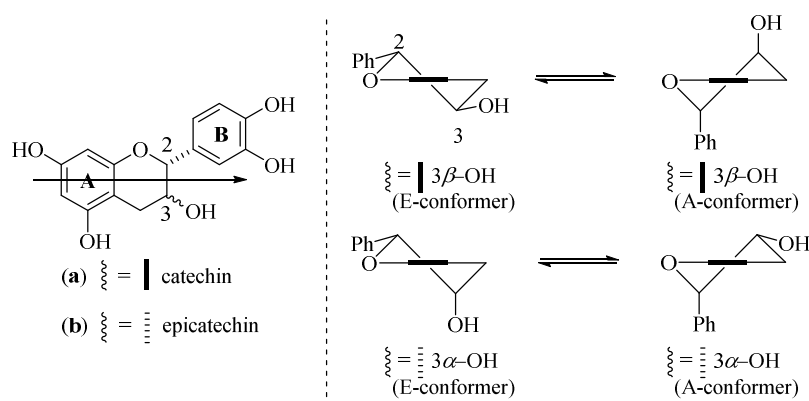


Figure 17: Arrangement of the substituents at C2 and C3 position in the **E**- and **A**-conformer for catechin (a) and epicatechin (b).^[148]

The conformational properties of the substituents in flavan-3-ols are apparent from a dynamic equilibrium between **E**(quatorial) and **A**(axial) conformation through various orientations of the substituents at C2 and C3 (**Figure 17**).^[148] Porter, Mattice *et al.*^[149] observed the equilibrium of the **C**-ring of flavanols (**Figure 18**) in which the **B**-ring adapts its equatorial or axial orientation respectively.

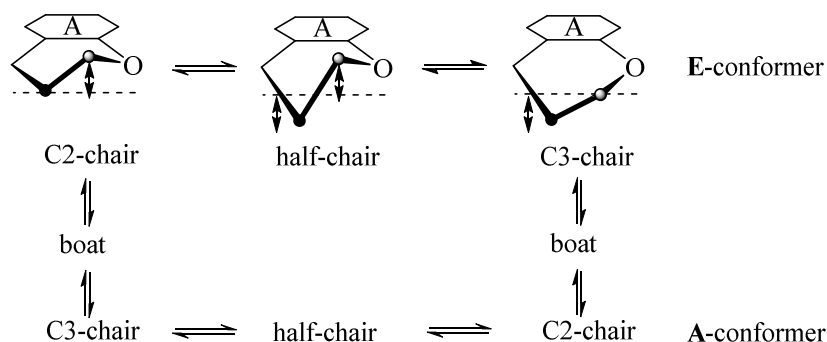


Figure 18: Ground-state energy conformations of flavanol, the hatched line displays the projection of the **A**-ring.^[149]

Theoretical calculations supported the high-energy transition state of the boat conformation between the **E**- and **A**-conformers and leads to an **E:A** ratio for (+)-catechin (a) and (-)-epicatechin (b) of 62:38 and 86:14, respectively. Furthermore, an acylation of the available hydroxy group at C3 demonstrated a stabilization of the **A**-conformation by reduced *pseudo*-allylic or A(1,3)-strain effect manifested by the ratio of 48:52.^[149]

1.3.2 Biosynthesis of Flavan-3-ols

The shikimic acid pathway opens the possibility to biosynthesis of plant compounds like important aromatic amino acids e.g. phenylalanine (Phe), tyrosine (Tyr) and tryptophan (Trp). These initial starter units enable the synthesis of plant flavones and the anthocyanidine flower pigments.^[150] The transformation of tyrosine into secondary products is represented by the phenylpropanoid metabolism (**Figure 19**).^[151]

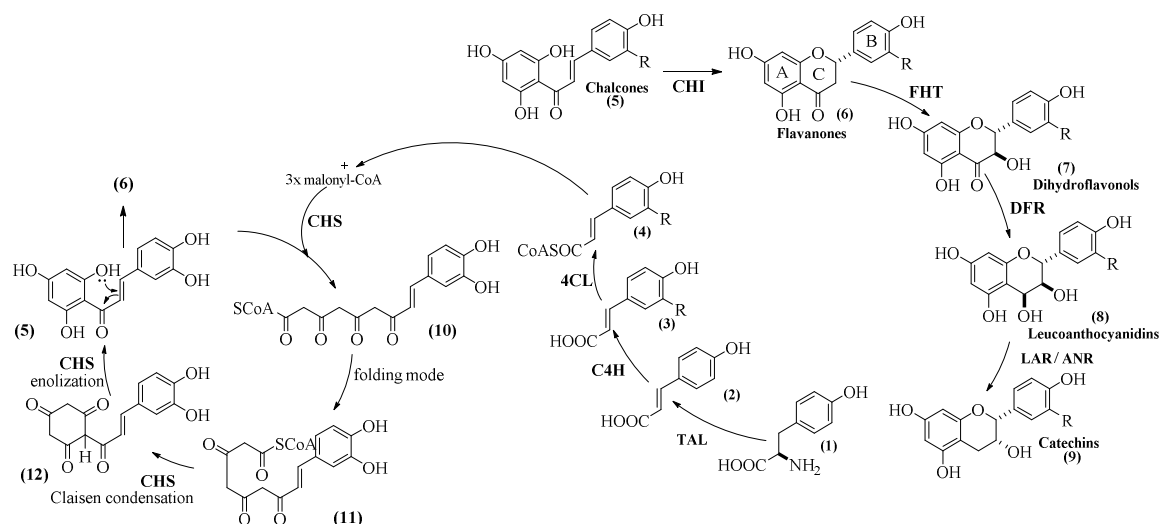


Figure 19: Biosynthesis of flavonoids *via* phenylpropanoid pathway. (1) L-Tyr; (2) cinnamic acid; (3) R = H coumaric acid, R = OH caffeic acid; (4) R = H coumaroyl CoA, R = OH caffeoyl CoA; (5) R = H naringenin chalcone, R = OH eriodictyol chalcone; (6) R = H naringenin, R = OH eriodictyol; (7) R = H dihydrokaempferol, R = OH dihydroquercetin (taxifolin); (8) R = H leucopelargonidin, R = OH leucocyanidin; (9) R = H (+)-afzelachin, R = H (+)-catechin. Enzymes are abbreviated as follows: tyrosine ammonia-lyase (**TAL**); cinnamate 4-hydroxylase (**C4H**); 4-coumaroyl-CoA ligase (**4CL**); chalcone synthase (**CHS**); chalcone isomerase (**CHI**); flavanone 3 β -hydroxylase (**FHT**); dihydroflavonol 4-reductase (**DFR**); leucoanthocyanidin reductase (**LAR**); anthocyanidin reductase (**ANR**).^[152]

Tyr (**1**) is reduced by tyrosine ammonia lyase (**TAL**) to cinnamic acid **2**. Cinnamate 4-hydroxylase is able to incorporate oxygen in *meta*-position to the propene-chain in the presence of O₂ and NADPH as cofactor to give rise to caffeic acid (**3**). The available carboxy group is linked by 4-coumaroyl-CoA ligase (**4CL**) *via* a carbon-sulfur bond to caffeoyl-CoA (**4**). Furthermore, the need of a cinnamoyl-CoA precursor (**4**) engineered for chain extension requires three molecules of malonyl-CoA in existence of chalcone synthase (**CHS**) giving stilbenes **10**. The cyclization of the stable enol from the 1,3-diketone **11** implements series of reactions e.g. chain extension, Claisen condensation, and cyclization by enolization. The flavanone **6** is built up by aromatization of the oxygen heterocycle of chalcone **5**.^[152-153] The final steps depend on the species and on various enzymes for modifying the flavonoid scaffold to its altered flavonoid subclasses.^[154]

1.3.3 Inhibition of A β due to Amyloid Assembly Inhibitors

Klärner and Schrader *et al.*^[155] investigated the inhibition or modulation of A β of three amyloid assembly inhibitors: Scyllo-inositol (left), EGCG and a Lys-specific molecular tweezer (right, **Figure 20**). The letter is able to protect neurons from synaptotoxicity by toxic A β deposition in brains of transgenic AD mice.^[156]

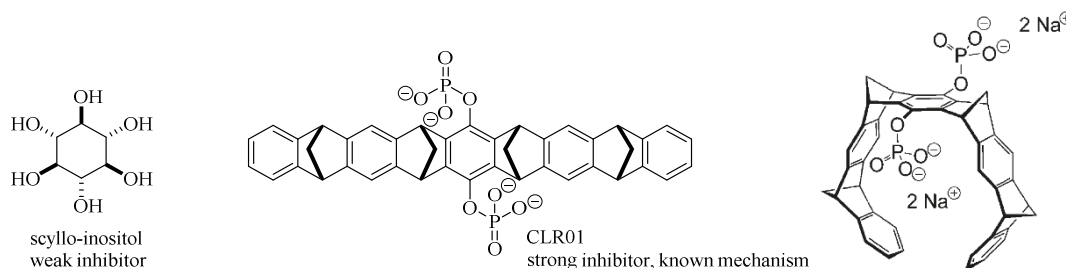


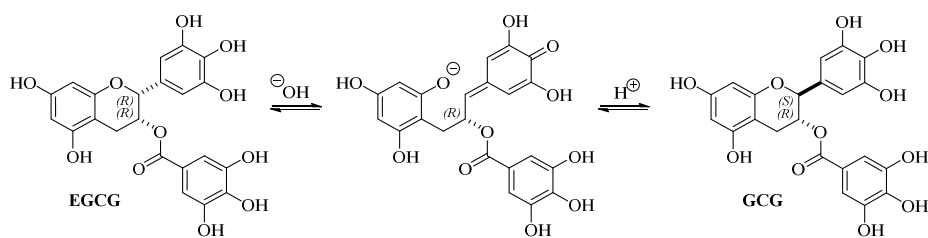
Figure 20: Illustration of scyllo-inositol as weak inhibitor (left) and tweezer CLR01 (right).^[155, 157]

The Lys-specific molecular tweezer is well known to bind specifically to Lys and deform A β into nontoxic oligomers by a process-specific mechanism whereas the binding mechanism of EGCG is not understood^[157] and it is undergoing phase II clinical testing in combination with AD.^[158] This prevents the development of compounds due to the mode of synergy of mechanistic action by inhibition of A β and tau oligomerization. Whereas the process specific mechanism of CLR01 is declared to bind to Lys with micromolar affinity^[157] and expresses by means of hydrophobic and electrostatic interactions in combination with A β ^[159] and tau.^[160] These studies evidence the inhibition of the toxic A β 42 oligomers by EGCG and CLR01 with polyclonal antibody A11 and A β 42 β -sheet formation. Consequently, CLR01 binds to A β monomers, whereas EGCG interactions lead at late degree of the assembly process by less well defined binding sites. It can be concluded that EGCG develop interaction with alternative targets than with A β in cases of its protective effect of cells as antioxidant.^[155]

1.3.4 Epimerization of EGCG to GCG

Naturally occurring catechins, like EGCG, are able to undergo C2 epimerization leading in lower biological effectivity (**Scheme 6**).^[161] This epimerization is caused by deprotonation of the *para*-hydroxy group on the **B**-ring.^[162] Mehta and Whalley *et al.* suggested a quinone intermediate formed by *retro*-1,6 addition of the pyran oxygen atom.^[163] The equilibrium under basic conditions preferentially leads to the formation of the catechin structure (2,3-

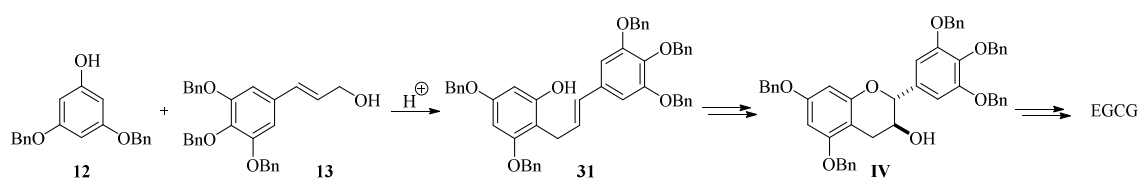
trans) instead of the epicatechin (2,3-*cis*).^[164]



Scheme 6: C2 epimerization of EGCG to GCG.^[161]

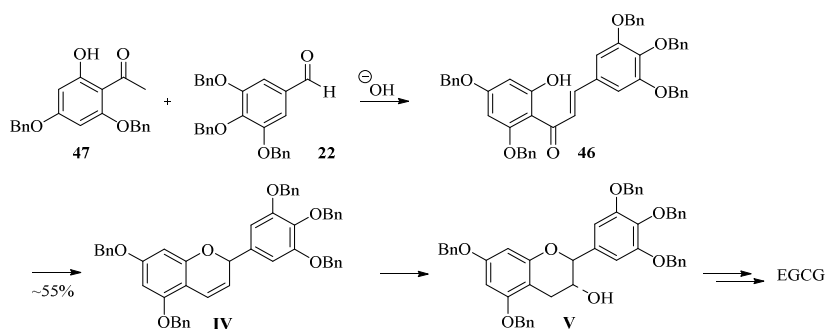
1.3.5 Total Synthesis of EGCG

Generally, the synthesis of EGCG follows two approaches: first, the synthesis of flavan-3-ols by cyclization leads to C2–O1 formation all giving the thermodynamically more stable *trans*-flavanol, followed by inversion of configuration at C3.^[165] Second, the synthesis to the desired 3-flavene *via* cyclization of chalcone.^[165a, 166] The first enantioselective synthesis of EGCG was described 2001 by Li and Chan employing a Friedel-Crafts alkylation of phenol **12** with cinnamyl alcohol **13** under acidic conditions, followed by a Sharpless asymmetric dihydroxylation of cinnamyl phenol **31**.^[165b, 167] The cyclization was realized by conversion of the dihydroxylated product *via* an *ortho*-ester. A subsequent oxidation-reduction sequence led to the stereochemical inversion at C3 to the epicatechin with 2,3-*cis*-configuration. The esterification with gallic acid furnished the desired (-)-EGCG product (**Scheme 7**).



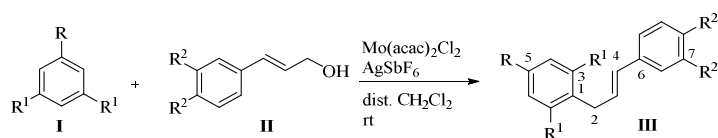
Scheme 7: Total synthesis of (-)-epigallocatechin-3-gallate by Li and Chan.^[165b]

A second synthesis providing natural EGCG was reported by Zaveri in 2001 by reductive isomerization of enones to alkenes.^[165a] The key step was the formation of chalcone **46** by condensation of aldehyde **22** and acetophenone **47**. The direct cyclization to 3-flavene **IV** was realized using NaBH_4 by a method of Clark-Lewis and Skingle.^[168] Compound **IV** was transformed to the *trans*-3-flavanol (2,3-*trans* catechin) by a hydroboration/oxidation process with BH_3/THF followed by H_2O_2 treatment under basic conditions (**Scheme 8**). The next steps were similar to the synthesis as mentioned above.



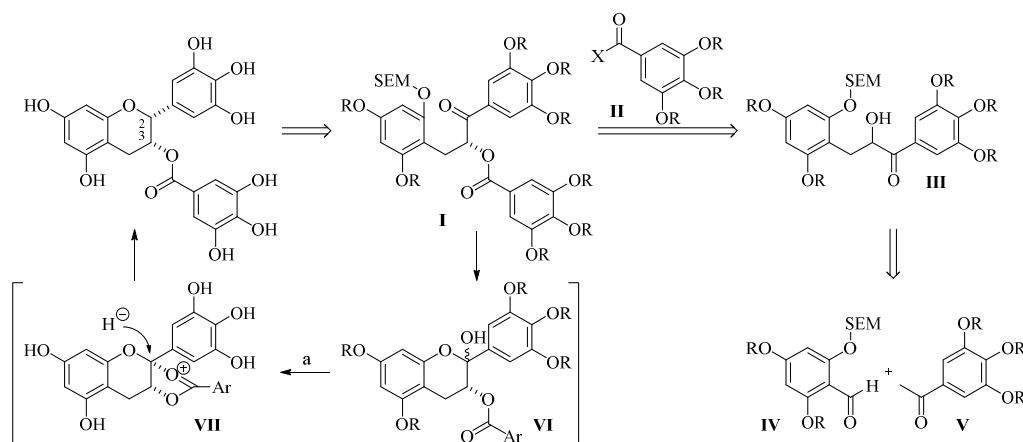
Scheme 8: Synthesis of EGCG by cyclization of chalcone **46** to 3-flavene **IV** by Zaveri.^[165a]

In 2002, Nay *et al.*^[169] developed a new entry for the formation of propene **III** as a precursor to natural flavonoids by a transition-metal catalyzed allylic substitution with styrenes.^[170] This method employs a molybdenum(IV)-catalyzed C–C coupling of phenols **I** with cinammyl alcohols **II** to the corresponding cinnamyl phenols **III** (**Scheme 9**).^[171]



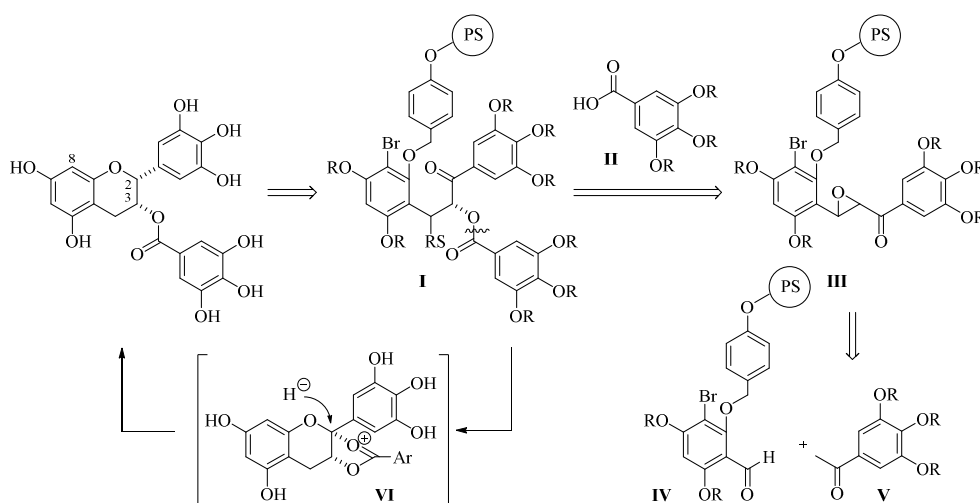
Scheme 9: Synthesis of molybdenum(IV)-catalyzed coupling to cinnamyl phenol derivatives.^[171]

In 2006, Kitade *et al.* introduced a synthesis of EGCG by reductive cyclization of an α -acyloxy ketone to *cis*-benzopyran (**Scheme 10**). Ketone **I** formed the consecutive hemiacetal **VI** under acidic conditions by deprotection, which underwent a reductive cyclization *via* oxonium cation **VII** to the EGCG derivative. Moreover, the hydride attack is hindered by the acyloxy group at the same side through the neighboring group effect to provide *cis*-substituted benzopyran. Precursor **III** was formed as well by aldol condensation of aldehyde **IV** with ketone **V** and oxidation with dimethyldioxirane in acetone of the enone.^[172]



Scheme 10: Approach of the synthesis of EGCG by reductive intramolecular etherification. Reagents and conditions: 10% triethylsilane, 25% trifluoroacetic acid, CH_2Cl_2 , $0\text{ }^\circ\text{C}$.^[172]

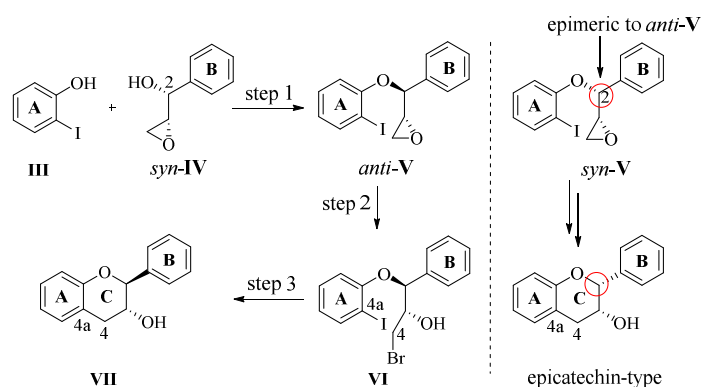
In 2007, Tanaka *et al.*^[166] elaborated an efficient method for the construction of epicatechin based on a solid-phase synthesis. The solid-supported aldehyde **IV** equipped with an acid-labile Wang linker at the hydroxy group, was coupled with the ketone **V** and carboxy acid **II** to the corresponding catechin skeleton. The bromine substitution in position C8 complicated the Friedel-Crafts alkylation with the Wang linker after cleavage (**Scheme 11**).^[166] The C8 protection ensures the reduction of nucleophilicity and prevents multiple undesired reactions.^[173] After cleavage of the Wang linker and reductive etherification of the α -acyloxy ketone assisted by the neighboring group provided the *cis*-substituted benzopyran.^[166]



Scheme 11: Approach of the solid-phase synthesis of EGCG.^[166]

In 2010, Ohmori *et al.*^[173] developed a route of several epicatechins based on a reversed polarity strategy (see **Figure 21**). The synthesis comprises three key steps:

- I. At first the Mitsunobu-type C–O bond formation^[174] between iodophenol **III** and epoxy alcohol *syn*-**IV** was generated *via* Sharpless asymmetric dihydroxylation and;^[175]
- II. opening of the oxirane ring to give bromohydrin **VI**, and
- III. pyran ring-closing reaction by selective iodine-metal exchange to afford the catechin skeleton **VII** (**Scheme 12**).^[173]



Scheme 12: Stereocontrolled approach to catechin skeleton **VII** published by Ohmori *et al.*^[173]

As presented in retrosynthetic **Figure 21**, the focus lies on the reversed polarity approach chosen here in the disconnection of the Ar–O and Ar–C bonds (red curly lines), which provides the fragments **a** and **b** with reversed polarity without affecting the C2-stereochemistry (red circle). Previous work focused on the dissection of the C-ring forming fragments **c** and **d** (blue curly lines).^[173]

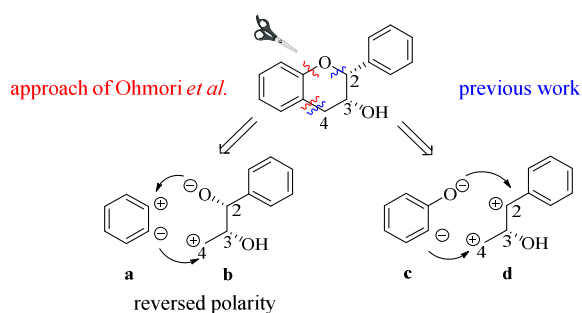
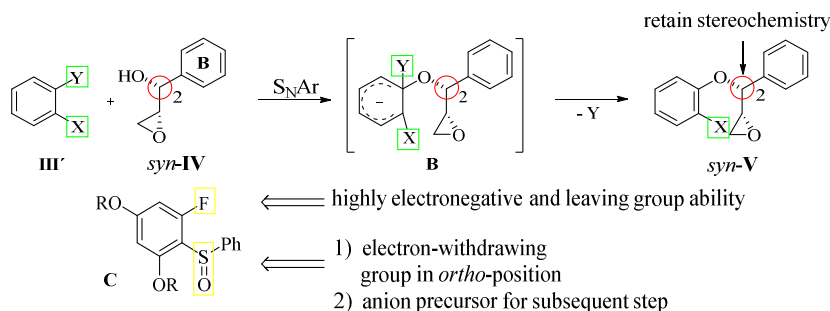


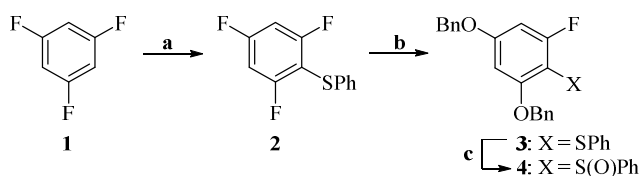
Figure 21: Disconnection approach for reversed polarity strategy (red curly lines) and homogeneous polarity (blue curly lines) by Ohmori *et al.*^[173]

In terms of synthetic equivalents, synthons **a** can be represented by an electrophilic unit **III'** and an alkoxide unit *syn-IV* as suitable reagents for an aromatic nucleophilic substitution (S_NAr) (**Scheme 13**).^[176]



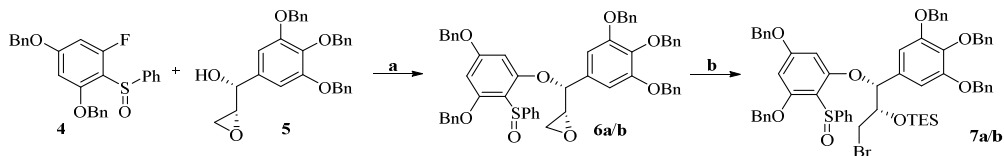
Scheme 13: S_NAr as a possible scenario for the reversed polarity strategy by Ohmori *et al.*^[173]

Compound **III** is linked with the Y-group which directs the attack of a nucleophile by its highly electronegative nature to form Meisenheimer complex **B**. The X-group should act as a π -electron acceptor to facilitate the conjugate attack, and secondly as an anion precursor that is required for the subsequent step of pyran ring building. As a synthetic equivalent to structure **III**, arylsulfoxide **4** was prepared starting from 1,3,5-trifluorobenzene **1** by lithiation with *n*-BuLi and subsequent treatment with PhSSO₂Ph to afford sulfide **2** in 87% yield (**Scheme 14**).^[177] Treatment of **2** with sodium benzyloxide leads to the substitution of two fluorine atoms with high regioselectivity, giving 2,4-bis-benzyl ether **3**. Final oxidation to the sulfoxide by *m*CPBA furnishes **4** in 85% yield (**Scheme 14**).



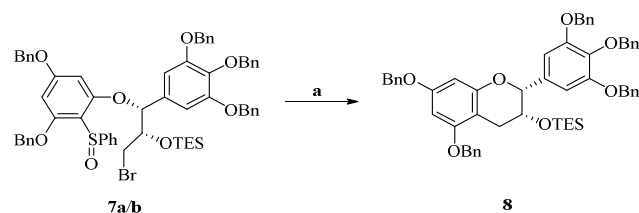
Scheme 14: Synthesis of arylsulfoxide **4** from 1,3,5-trifluorobenzene. Reagents and conditions: (a) *n*-BuLi, PhSSO₂Ph, Et₂O, -78 °C, 87%; (b) BnOH, NaH, DMF, 0 °C; (c) *m*CPBA, CH₂Cl₂, 0 °C, 2 steps, 85%.^[173]

Next, with the synthetic equivalent for **III** in hand, nucleophilic aromatic substitution of **4** and 2,3-epoxy alcohol **5** smoothly affords substitution product **6** in 76% as a mixture of diastereomers without any side products from Payne rearrangement. After column-chromatography the epimere epoxy ethers **6a** (39%) and **6b** (37%), differing in the configuration of the sulfoxide are obtained. Subsequently, oxirane opening with Li₂NiBr₄ and silylation with triethylsilyl triflate results in the corresponding diastereomeric bromides **7a** and **b** (97%; **7a** from **6a**, 91%; **7b** from **6b**) (**Scheme 15**).^[173]



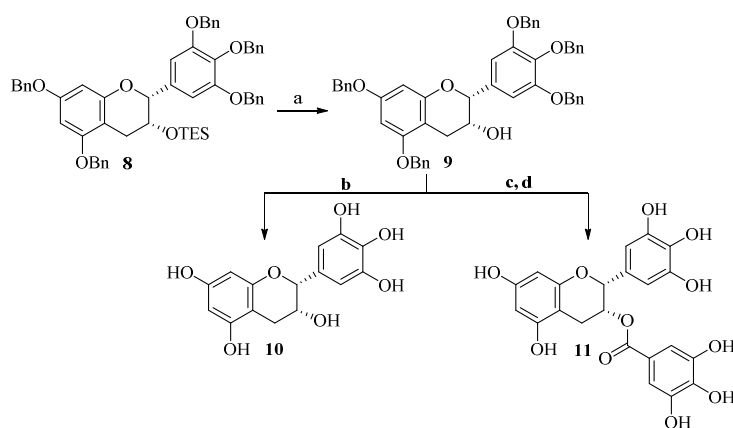
Scheme 15: Aromatic nucleophilic substitution of fluoro-sulfoxide **4** and epoxide **5** to compound **6**. Reagents and conditions: (a) NaH, toluene, DMPU, rt, 39% for **6a**, 37% for **6b**; (b) Li₂NiBr₄, THF, 0 °C; (c) TESOTf, 2,6-lutidine, CH₂Cl₂, 0 °C, 2 steps, 97% for **7a**, 91% for **7b**.^[173]

The cyclization is realized by a sulfinyl-metal exchange of **7a/b** and intramolecular nucleophilic substitution of the resulting aryl lithium species from treatment with PhLi, giving dihydrofuran **8** (81% from **7a** and 62% from **7b**) (**Scheme 16**).^[173]



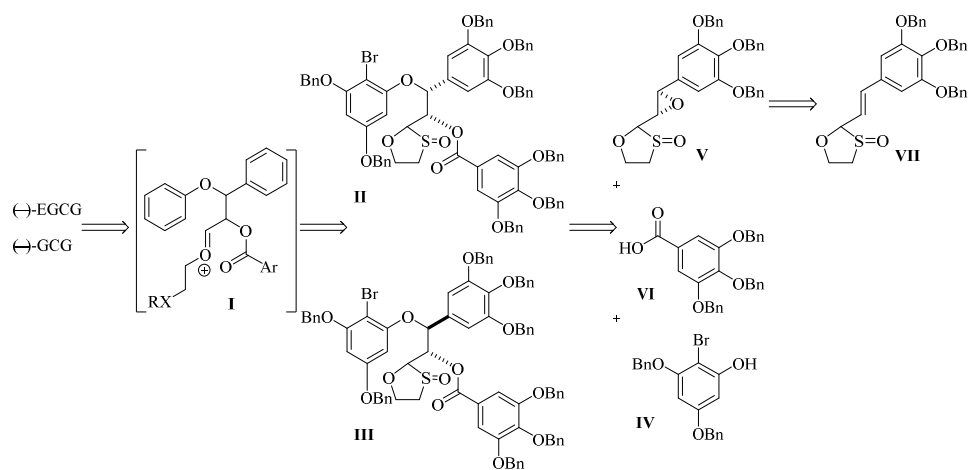
Scheme 16: Cyclization of **7a/b** by sulfinyl-metal exchange and intramolecular nucleophilic substitution forming the *cis*-chroman-3-ol precursor **8**. Reagents and conditions: (a) PhLi, THF, 1 h, rt.^[173]

The last step in this route to chroman-3-ol **9** is the removal of the TES protecting group by $n\text{-Bu}_4\text{NF}$. Hydrogenolysis with Pearlman's catalyst affords (–)-ECG (**10**). Furthermore, (–)-EGCG (**11**) was prepared from **9** by Steglich esterification with 3,4,5-tri-*O*-benzylgallic acid, followed by hydrogenolytic removal of all benzyl protecting groups (**Scheme 17**).



Scheme 17: Synthesis of (–)-ECG **10** and (–)-EGCG **11**. Reagents and conditions: (a) $n\text{-Bu}_4\text{NF}$, THF, 0 °C, 99%; (b) H_2 , Pd(OH)₂/C, THF, MeOH, H₂O (4:4:1), rt, 71%; (c) 3,4,5-tri-*O*-benzylgallic acid, EDC·HCl, DMAP, Et₃N, CH₂Cl₂, rt; (d) H_2 , Pd(OH)₂/C, THF, MeOH, H₂O (4:4:1), rt, 68% (2 steps).^[173]

Another approach of Tanaka *et al.*^[178] in 2012 was based on the synthesis of racemic EGCG and GCG derivatives by C4–Ar bond formation. The key step included the intramolecular electrophilic cyclization of acetal **II** and the previous reagent-controlled *anti*- and *syn*-epoxide opening of compound **V** (**Scheme 18**). The oxonium cation **I** precursor enabled the electrophilic cyclization of the 1,3-oxathiolane 3-oxide intermediates **II/III**. A measure to be taken in order to prevent self-condensation was the introduction of the bromide in position 8 for decreased reactivity of the aromatic moiety. Deprotection led to racemic GCG and EGCG products in 45% and 47%, respectively.^[178]



Scheme 18: Approach of the synthesis of racemic EGCG and GCG.^[178]

1.4 Spectrophotometric Determination of Targets in Biochemistry

1.4.1 The Avidin-Biotin Interaction

The mechanistic elucidation of biochemical processes is possible by the application of a biotin-assay. For this assay, compounds are functionalized with a biotin moiety, which enables the interaction with biotin-binding sites on immobilized proteins, like avidin for example: Natural occurrence of avidin, a protein, in the chicken egg white and its bacterial counterpart streptavidin (bacterium *Streptomyces avidinii*) show high affinity for biotin, which is commonly available in all cells as vitamin H/vitamin B₇.^[179] Streptavidin, as tetramer, is able to bind four biotin molecules and exhibits the highest affinity (dissociation constant of $\sim 10^{-14}$ M)^[180] in biological systems between ligand and protein and this is of great common interest in diagnostic purpose, e.g. imaging, pre-targeted cancer immunotherapy, and nano-assembly.^[181] Thus, some studies illustrate the use of biotin for screening assays and it is applied in a single-site neutravidin (NA) capture/labeled streptavidin (SA-HRP) detection. It is by far the strongest noncovalent interaction in biological systems. The monomeric occurrence of bio-A42 connects to immobilized NA by its biotin moiety. Thereby, biotin forms an amide-bond to the *N*-terminal aspartate of A β (1 – 42), these positions are not available for SA-HRP. Unlike the oligomeric, bio-A42 also fixes to immobilized NA, whereby the biotin moiety binds to SA-HRP and leads to a signal (**Figure 22**).^[182]

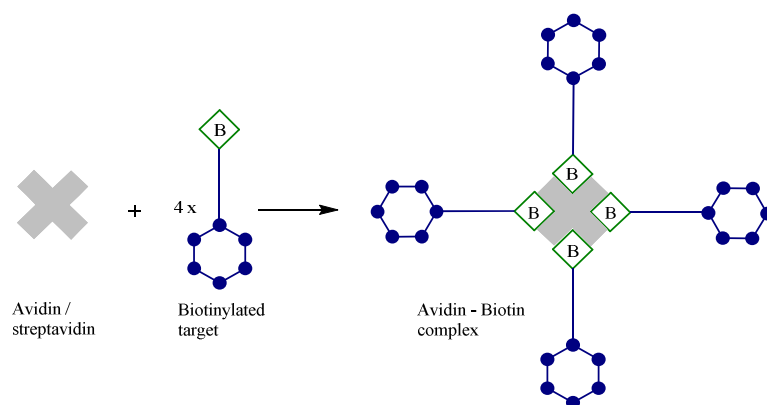


Figure 22: Schematic illustration of single-site NA/SA-HRP oligomer assay.^[182]

1.4.2 History and Application of the Fluorescence Assay

The interest in the understanding of mechanistic bases on the molecular level for the exploitation of therapeutic drugs and methods for the inhibition and reversal of amyloidogenesis is of great importance.^[183] In 1853, Virchow first reported the staining method of infected cells by iodine-sulphuric acid treatment.^[184] Afterwards, in the 20th century the detection of amyloid was performed by Congo red, based on different affinities to fibrils, but this staining process led to insufficient reproducibility. In 1959, the fluorescent dye Thioflavin-T (ThT) (**Figure 23**) was introduced as an efficient method for the identification of amyloid fibrils both *in vivo* and *in vitro* analysis.^[183]

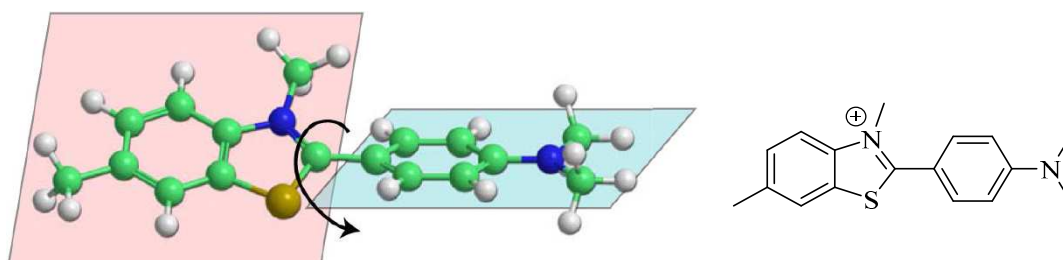


Figure 23: Structure of ThT (right), molecular construction of ThT in its two planar segments.^[183]

Thereby, the enhanced fluorescence emission due to the binding to amyloid fibrils is exploited and extends ThT to an agreeable and efficacious device by interactions at an atomic level. Vasser and Culling found the amyloid-specific, fluorescent stains for amyloid fibril diagnosis in which ThT operated as a potent fluorescence marker by localizing amyloid deposits and finally resulted in increased fluorescence brightness.^[185]

1.4.3 Binding Properties of Thioflavin-T

Naiki *et al.* and LeVine characterized the fluorescence spectra and the binding properties of ThT. The connection of fibrils to the fluorescence marker ThT results in an enormous shift of the excitation maximum from 385 nm to 450 nm and the emission maximum from 445 nm to 482 nm (**Figure 24**).^[186]

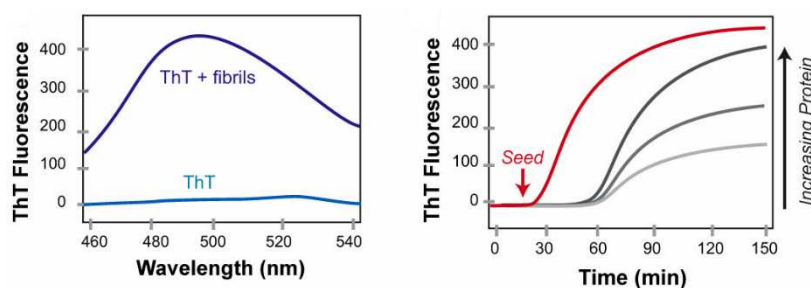


Figure 24: ThT binding to amyloid fibrils leads to characteristic increased excitation (left), fibril-forming peptide leads to fibrillization kinetics of increased concentrations (right).^[183]

The properties of being soluble in water, as well as the moderate affinity to fibrils (K_d^{14} in the sub- and low- μM range) binds ThT to many experimental systems. Significantly, ThT is characterized by the equal bond to biological and synthetic sources.^[186-187] The application as an *in vitro* marker of amyloid formation permits a prediction about the mechanism of ThT binding – in particular which structures are recognized by ThT and how the interaction affects fluorescence (**Figure 25**).^[188]

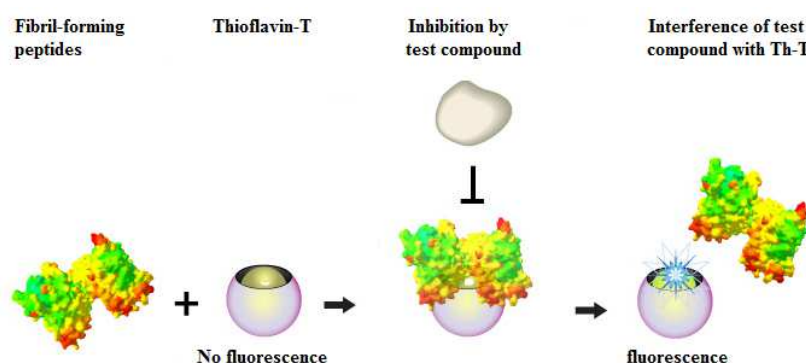


Figure 25: Principle of ThT binding process.^[188]

¹⁴ K_d = dissociation constant, the higher the affinity of a protein to its ligand, the lower the dissociation constant of the complex.

1.4.4 Spectroscopic Properties of Thioflavin-T Accumulation to Fibrils

The advantage of fluorescence in biological and medical processes is of great importance especially, in the making of the bond relation of toxic fibrills in combination with ThT evidence. Presumably, an increased ThT fluorescence is a consequence of a selective immobilization of a subset of ThT conformers,^[189] whereas ThT acts as a “molecular rotor”.^[190] As shown in **Figure 23**, a low energy barrier allows the C–C bond between the benzylamine moiety and the benzothiole ring of ThT to rotate freely in soluble conditions. Excited states which are caused by photon excitation are rapidly quenched by this rotation and consequently, low fluorescence emission for free ThT is detected (**Figure 24**, left).^[183] A high quantum yield of fluorescence is brought about by rotational immobilization of ThT to conserve the excited state. Continuing this, amyloid fibrils will usually demonstrate a ThT-binding site that sterically binds the trapped dye which leads to an increased ThT fluorescence.^[183]

1.4.5 Thioflavin-T Binding to Amyloid Fibrils

ThT is able to bind to diverse fibrils on the amino acid sequence by identification of structural attribute. It is constituted by the cross- β architecture of the amyloid fibrils (**Figure 26**, right) whose surfaces of cross- β framework create the ThT-binding site. The fibrils consist of a specific arrangement called “cross-stand ladders” in which the side-chain’s interactions run parallel to a long axis of the β -sheet and form channel-like motifs (**Figure 26**, left) where linear dyes can bind.^[191] ThT connects to the β -sheet surface along these channels which leads to many peptide self-assemblies.^[183, 192]

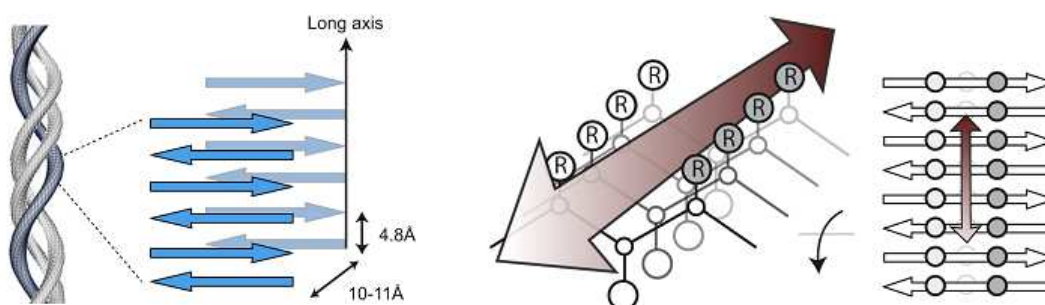


Figure 26: Amyloid fibrils with characteristic cross- β building by accumulation of laminated β -sheets (right), possible ThT binding to fibril β -sheet in a channel model by accumulation along surface side-chain parallel to long axis of β -sheet (left).^[183, 192]

1.4.6 Fluorescence Imaging

The visualization of targets in biochemical probes is a common technique which enables researchers to identify rapidly the positions of concerning areas in cells or dynamic intercellular processes in living cells in the clinical laboratory by specific determining of fluorescent dyes. Fluorescent labeled probes coupled with the target can be visualized *via* microscopy.^[193]

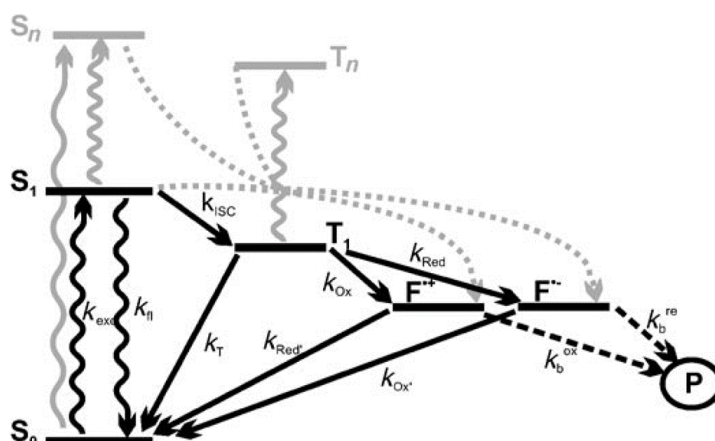
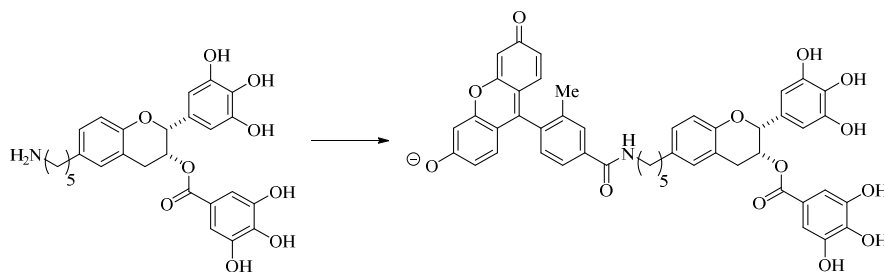


Figure 27: Photo induced processes in Jablonski scheme of organic fluorophores.^[192]

Photo-induced processes are explained by a three-state model (Jablonski scheme) in which excitation of the ground state S_0 to the first excited singlet state S_1 leads to absorption while emission results in fluorescence k_{fl} . A second process, the intersystem crossing, is in competition with the fluorescence to emit at rate k_{ISC} to the lowest triplet state T_1 , awarding long lifetime and a photochemically most active state (**Figure 27**).^[192]

In 2011, Kan *et al.* developed a new EGCG derivative combined with a Tokyo Green photophore, which was introduced at the A-ring in position C6 of the chroman-3-ol moiety acting as possible anti-influenza drug (**Scheme 19**).^[193]



Scheme 19: EGCG derivative with Tokyo Green coupled fluorophore.^[193]

The results hardly provide the biological activity in comparison to the natural EGCG due to the attachment of the linker group. In combination with HUVECs (human umbilical vein endothelial cells)^[194] for imaging studies this method is used for elucidation of dynamics in EGCG cellular uptake, intracellular mechanism and transport (**Figure 28**).^[193] Further areas of application can be reached by binding of fluorescein-4-isothiocyanate (FITC, **Figure 29**) on EGCG which was successfully described by Han *et al.*^[195] Thereby, FITC-EGCG was incorporated into cytoplasm of L-929 cells, thenceforth the molecule continue to go into the nucleus to elucidate the working process as target, as well as the exact mechanism in cancer cells.^[195]

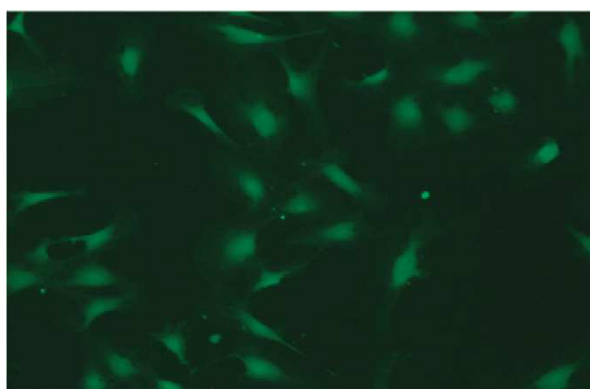


Figure 28: HUVECs incubated with fluorescein probe imaged under fluorescence microscope.^[193]

Furthermore, it has to be clarified how FITC bound to hydroxy group in the gallate ring **D** influences the receptor binding of EGCG while one hydroxy group is not available (**Figure 29**), consequently reduced activity or no impact.^[195]

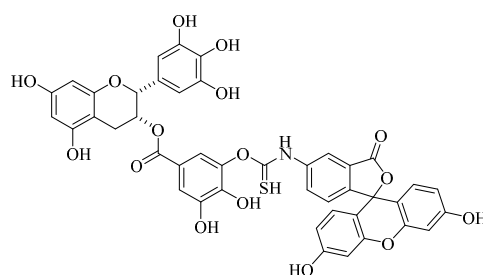


Figure 29: Illustration of FITC-EGCG.^[195]

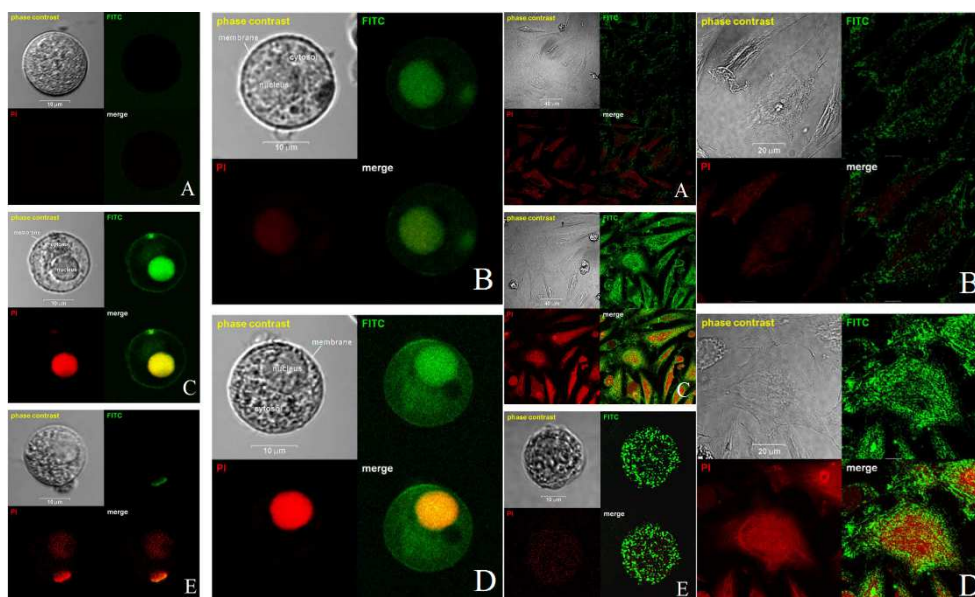


Figure 30: Visual representation by confocal microscope of suspended L-929 cells after 0 h (A), 0.5 h (B), 1 h (C), and 4 h (D) with addition of 65 μM FITC-EGCG and after 4 h were added 50 μM FITC-EGCG (E) (left). Visual representation by confocal microscope of cultured L-929 cells 2 – 4 h (A/B), 8 h (C/D), and 24 h (E) with addition of 130 μM FITC-EGCG (right).^[195]

Due to the visualization, it is possible to image the process by which the EGCG binds to membrane receptors in cells by forming an EGCG-receptor complex, followed by internalization into cytoplasm through previously unidentified mechanism.^[195] The successive translocation in the nucleus can be evidenced by a structurally related molecule to catechins, the phytoestrogen, which enables the connectivity to an estrogen receptor and arises by migration to the nucleus through nuclear pores. Inside the nucleus, it regulates and controls various gene processes (Figure 31).^[196]

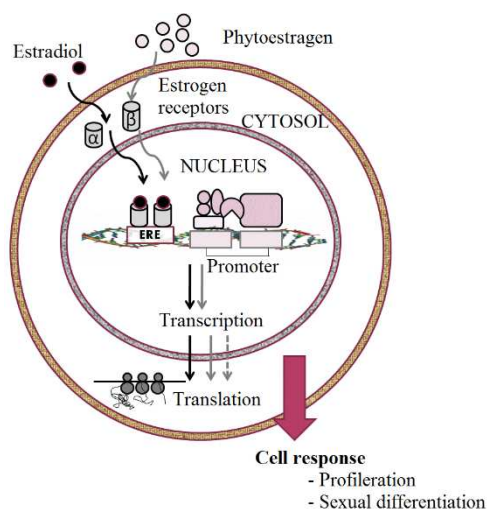


Figure 31: Phytoestrogen mechanism of internalization into cytoplasm and nucleus.^[197]

2. Results and Discussion

2.1 Enantioselective Synthesis of EGCG Derivatives

2.1.1 Retrosynthetic Disconnection of EGCG

The first synthesis of EGCG in this work was performed according to the report by Li and Chan^[165b], and Ding *et al.*^[198] The *cis*-chroman-3-ol was formed by the coupling between cinnamyl alcohol and phenol by Friedel-Crafts alkylation. Thus, this method enables the synthesis of **A**, **B** and **D**-ring (–)-EGCG analogues.

The retrosynthetic analysis leads to three aromatic compounds: a substituted phenolic compound **12**, a cinnamyl alcohol **13** and a substituted carboxylic acid **14** (**Figure 32**):^[165b]

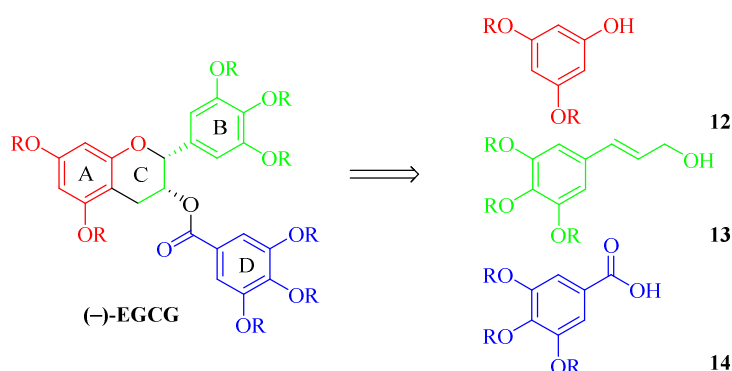
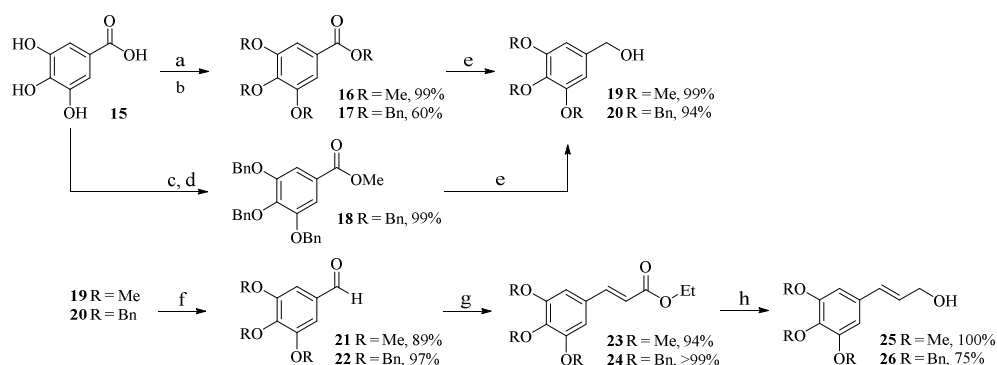


Figure 32: Retrosynthetic analysis of (–)-EGCG.^[165b]

A synthesis following the shown retrosynthetic analysis would rely on the selective formation of the thermodynamically less stable *cis*-di-substituted benzopyran^[165b] or chroman-3-ol. The formation of the *cis*-chroman-3-ol was made possible by means of a reduction-oxidation sequence.

2.1.2 Synthesis of the Substituted (*E*)-Cinnamyl Alcohol Precursor

The synthesis of the (*E*)-cinnamyl alcohol fragment started with the protection of the free hydroxy groups of gallic acid (**15**). Two differently substituted substrates were addressed: Both methylated and benzylated analogs were synthesized under concomitant formation of methyl ester **16** and benzylester **17**. Alam *et al.*^[199] described a method for the methylation by treatment with K₂CO₃ and methyl iodide in DMF in 99% isolated yield of **16**, that is essentially a Williamson ether synthesis, involving deprotonation of the phenol groups and subsequent reaction with alkylating agent such as methyl iodide or benzyl chloride. According to the procedure of Kawamoto *et al.*,^[200] gallic acid (**15**) was treated with benzyl chloride and 60% sodium hydride (NaH) in DMF to deliver **17** in 36% yield. A modified approach was performed in order to overcome the low yield of the benzylation: For this purpose, gallic acid (**15**) was first converted into the corresponding methyl ester using catalytic amounts of sulfuric acid to give methyl ester in 81% yield.^[167] The subsequent benzylation was described previously and led to **18** in 99% yield. Both precursors were used in the next four steps according to the literature of Li *et al.* (Scheme 20).^[165b]

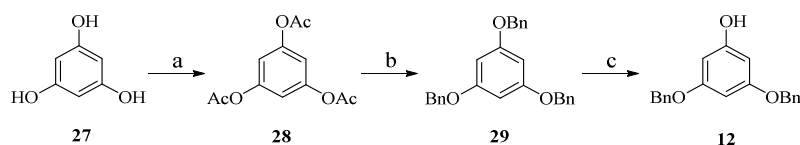


Scheme 20: Synthesis of cinnamyl alcohol derivatives **25/26**. Reagents and conditions: (a) MeI, K₂CO₃, DMF for **16**; (b) benzyl chloride, 60% NaH, H₂O, for **17**; (c) conc. H₂SO₄, MeOH; (d) benzyl chloride, 60% NaH, H₂O; (e) LiAlH₄, THF, 0 °C, NH₄HF₂; (f) PDC, CH₂Cl₂, rt; (g) triethyl phosphonoacetate, 60% NaH, THF; (h) DIBAL, THF, -78 °C.

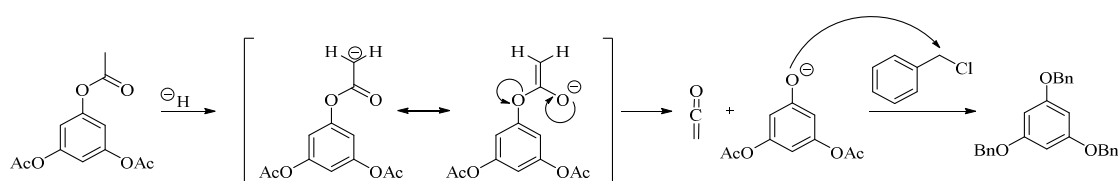
Reduction of the ester functionality **18** with lithium aluminum hydride and work-up with NH₄HF₂ gave the alcohols **19** and **20** in 99% and 94% yield, respectively. The alcohols were then oxidized by PDC to the corresponding aldehydes that underwent a Horner-Wadsworth-Emmons reaction (HWE) with triethyl phosphonoacetate to generate the cinnamates **23** and **24**. Reduction of the esters with diisobutyl aluminium hydride and work-up with NH₄HF₂ resulted in the formation of cinnamyl alcohol **25** in 100% and **26b** in 75% yield.

2.1.3 Synthetic Route to 3,5-Dibenzyloxyphenol (**12**)

The synthesis of 3,5-dibenzyloxyphenol (**12**) as the second coupling compound (**Scheme 21**) was performed according to a literature procedure by Kawamoto *et al.*^[200] The first step was the acylation of the hydroxy groups of phloroglucinol (**27**) to decrease the electron density in the aromatic system. During a direct benzylation of the electron-rich phenol *C*-benzylation would compete with *O*-benzylation. Phloroglucinol (**27**) was treated with sulfamic acid as catalyst and acetic anhydride for about five hours at 70 °C to afford the triacetate **28** in >99% yield. The subsequent benzylation is conducted using a mixture of benzyl chloride and 60% NaH in DMF as solvent. Dropwise addition of water converts product **28** into phloroglucinol tribenzyl ether (**29**) in 80% yield. Analogous alkylation with benzyl bromide as reported in the literature led to lower yields.^[201] Other modified conditions enable the benzylation by using BnBr, K₂CO₃, DMF^[202] or NaH, BnBr and DMF^[203] (**Scheme 21/22**). In a final step the mono-debenzylation by hydrogenation of compound **29** afforded **12** in 71% yield.^[204]



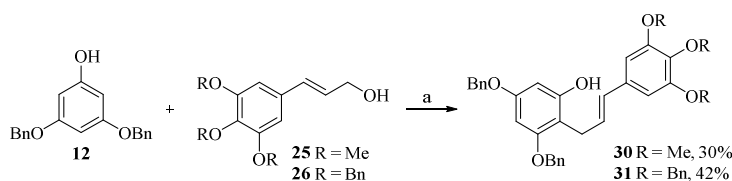
Scheme 21: Synthesis of 3,5-dibenzyloxy phenol (**12**). Reagents and conditions: (a) sulfamic acid, acetic anhydride, 4 h, 70 °C, >99%; (b) benzyl chloride, 60% NaH, H₂O, 80%; (c) 10% Pd/C, 1 atm H₂, 71%.



Scheme 22: Potential mechanism for the benzylation of **28** with BnCl/NaH, H₂O.

2.1.4 Conversion of Diaryl-Propene **30/31** into 1,2-Diols **37/38** by Sharpless Asymmetric Dihydroxylation

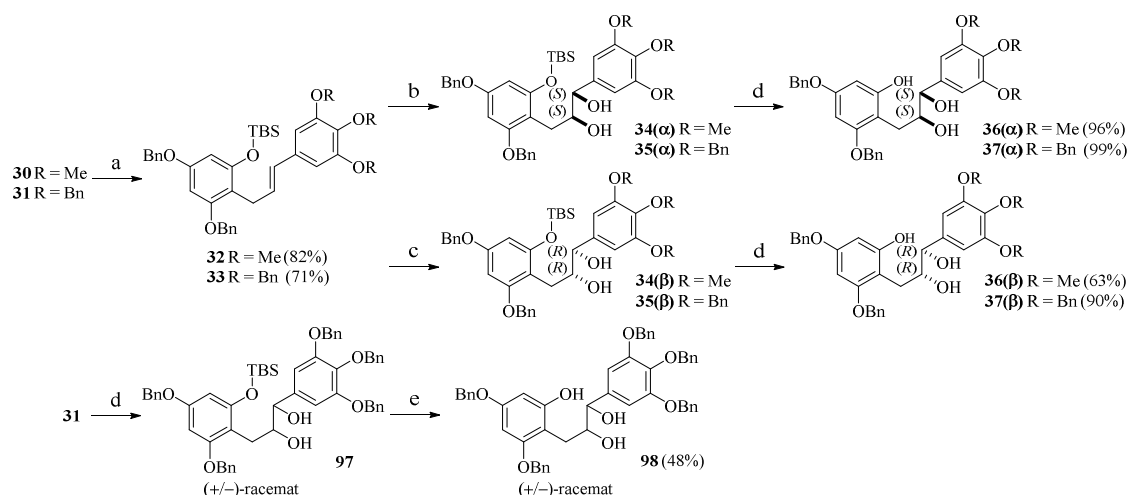
First, the Friedel-Crafts alkylation of phenol **12** with cinnamyl alcohol **25/26** under acidic conditions with methanesulfonic acid was chosen according to the report of Ding *et al.*^[167] These conditions prevented the application of highly toxic CS₂ as solvent (**Scheme 23**). The procedure required the sufficiently slow addition of substituted cinnamyl alcohol **25/26** and a solution of methanesulfonic acid in CH₂Cl₂ to the solution of phenol **12** in CH₂Cl₂ at 0 °C. In the further course of the reaction, the color of the reaction mixture changed to red-pink and gave the products **30/31** in moderate isolated yield (30/42%).^[167] An attempt to improve the yields by using a new sample of methanesulfonic acid failed. Li *et al.*^[165b] described an alternative procedure by the use of H₂SO₄/SiO₂ as catalyst in CH₂Cl₂/CS₂. This approach was not successful, either. The alcohol was protected by TBSCl and imidazole in DMF (**Scheme 24**).



Scheme 23: Synthesis of (*E*)-alkenes **30/31** via Friedel-Crafts reaction. Reagents and conditions: (a) MeSO₃H, CH₂Cl₂, 4 h, 0 °C.^[167]

The Sharpless asymmetric dihydroxylation was realized by using AD-mix- α and methane sulfonamide in a solvent mixture of *tert*-BuOH and water. Five portions of AD-mix- α and methane sulfonamide were added, each one over a period of 24 h. The reaction time could be reduced by the application of a KPG-stirrer by vigorous mixing. During the reaction the lightly yellow color of the aqueous phase turned to maroon as a consequence of the phase-transfer of the osmium catalyst from the organic into the aqueous phase.^[205] The isolated product contained two stereocenters with *1S,2S* configuration, which was obtained from AD by “ α -face” attack in agreement with previous observations in enantioselective EGCG syntheses. After successful dihydroxylation, deprotection with TBAF gave the optically active products (+)-**36/37** with a free phenolic hydroxy group (**Scheme 24**). By using the same procedure with AD-mix- β , the enantiomer was prepared with identical NMR spectra as the (+)-isomer. The racemic diol was synthesized by the use of potassium osmate dihydrate and *N*-methylmorpholine *N*-oxide (NMO) in an Upjohn dihydroxylation in 48% yield and showed identical NMR spectra as the enantioenriched samples **98**. For a detailed

mechanistic description, see next chapter.



Scheme 24: Synthesis of 1,2-diol derivatives **36/37** according to the literature of Ding *et al.*^[167] and racemic diol **53** was prepared by Upjohn dihydroxylation. Reagents and conditions: (a) TBSCl, imidazole, DMF, rt; (b) AD-mix- α , MeSO₂NH₂, *tert*-BuOH/H₂O/CH₂Cl₂ (1:1:1), 0 °C (on top); (c) AD-mix- β , MeSO₂NH₂, *tert*-BuOH/H₂O/CH₂Cl₂ (1:1:1), 0 °C, (centred); (d) TBAF, THF, rt; (e) K₂OsO₄·2 H₂O, NMO, acetone/H₂O, rt, (below).^[165b]

2.1.5 Sharpless Asymmetric Dihydroxylation

The Sharpless asymmetric dihydroxylation is a practical and reliable catalytic asymmetric reaction which allows the enantioselective preparation of 1,2-diols from olefins. In contrast to the Sharpless epoxidation that requires the presence of directing functional groups, the Sharpless asymmetric dihydroxylation is less restricted in the selection of substrates^[206] AD-mix- α / β , a commercially available composite for Sharpless asymmetric dihydroxylation, consists of catalytic amounts of potassium osmate K₂OsO₂(OH)₄ as an osmium tetroxide source and a cinchona-derived asymmetric ligand. Minato, Yamamoto and Tsuji studied the influence of potassium ferricyanide K₃Fe(CN)₆ as inorganic co-oxidant in combination with K₂CO₃ as agent for an excellent composition for the Sharpless asymmetric dihydroxylation.^[207] In addition, the co-oxidant reduces the amount of highly toxic and expensive osmium tetroxide species. Only small amounts of the osmium catalyst are required due to the ligand acceleration effect (LAE).^[208] Besides, the introduction of chirality is realized by ligands derived from quinine and quinidine, which are readily available and behave as pseudoenantiomers. AD-mix- α contains phthalazine-linked dihydroquinine (DHQ)₂PHAL while in AD-mix- β dihydroquinidine-derived (DHQD)₂PHAL is used (Figure 33).^[209]

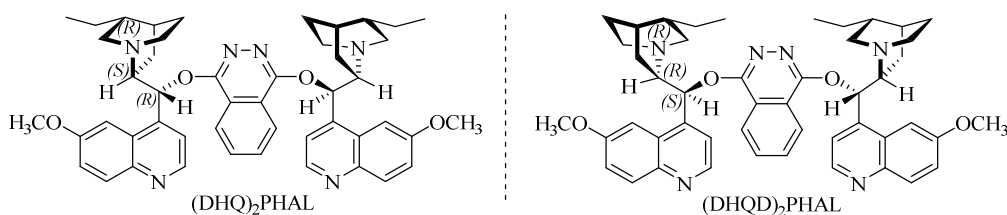
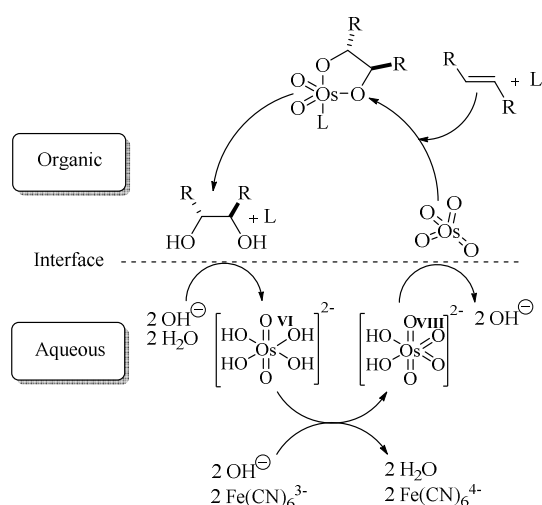


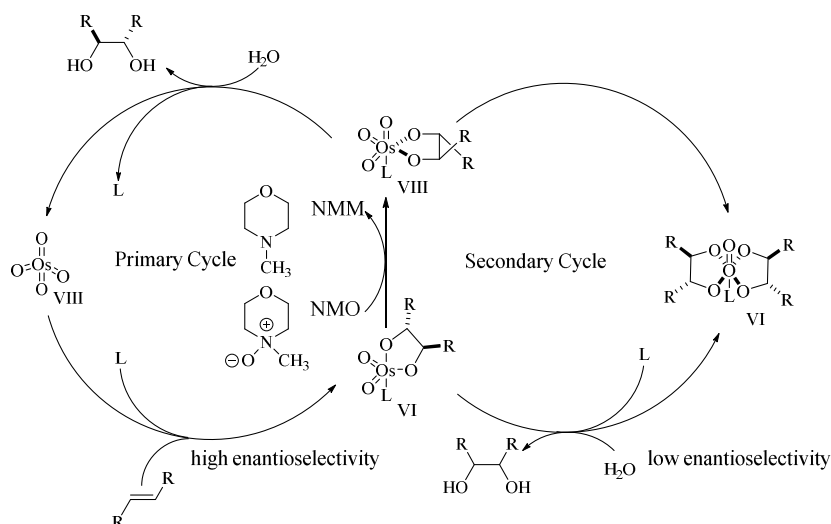
Figure 33: Cinchona alkaloid ligands for Sharpless asymmetric dihydroxylation.^[210]

It is common practice to perform this reaction using methanesulfonamide (MeSO_2NH_2) for satisfyingly shorter reaction times in a solvent mixture of TBA and water. MeSO_2NH_2 represents a co-reactant for the phase-transfer of hydroxide ions from the aqueous into the organic phase.^[209b]



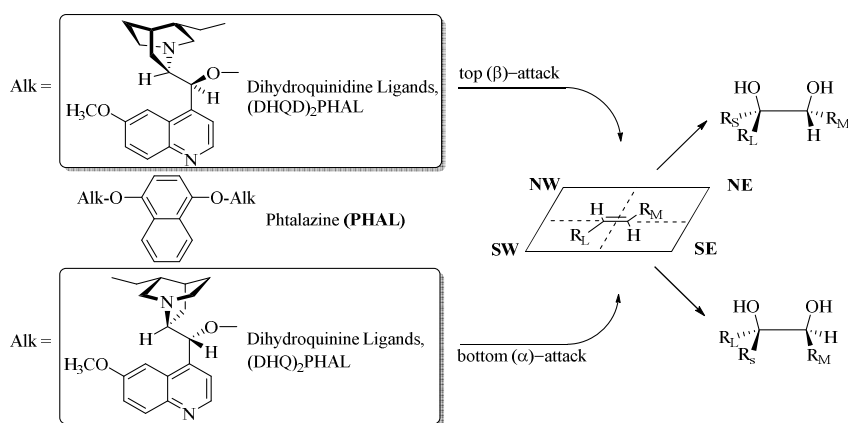
Scheme 25: Possible catalytic cycle of the Sharpless asymmetric dihydroxylation with $\text{K}_3\text{Fe}(\text{CN})_6$ as co-oxidant.^[205]

The catalytic cycle (**Scheme 25**) of the Sharpless asymmetric dihydroxylation contains the coordination of osmium tetroxide to the ligand, followed by the formation of a monoglycolate ester in a reaction between the alkene and the osmium tetroxide-ligand complex, which was proposed by Böseken and Criegee to occur as a concerted [3+2]-cycloaddition.^[211] The monoglycolate ester is cleaved by hydrolysis releasing the diol and the ligand to the organic phase. The oxidation of the $\text{OsO}_2(\text{OH})_4^{2-}$ species by $\text{Fe}(\text{CN})_6^{3-}$ leads to regeneration of OsO_4 .^[205] Furthermore, the reaction is performed in a two-phase medium, which allows the suppression of a secondary (less selective) oxidation cycle as it might occur under Upjohn conditions (one-phase medium, NMO as oxidant, **Scheme 26**). The re-oxidation of osmium takes place in the aqueous layer by $\text{K}_3\text{Fe}(\text{CN})_6$, so that the Os(VI) glycolate ester does not get in touch with the oxidizing agent before its hydrolysis in the organic layer.^[212]



Scheme 26: Possible secondary oxidation cycle of an asymmetric dihydroxylation using Upjohn conditions.^[206]

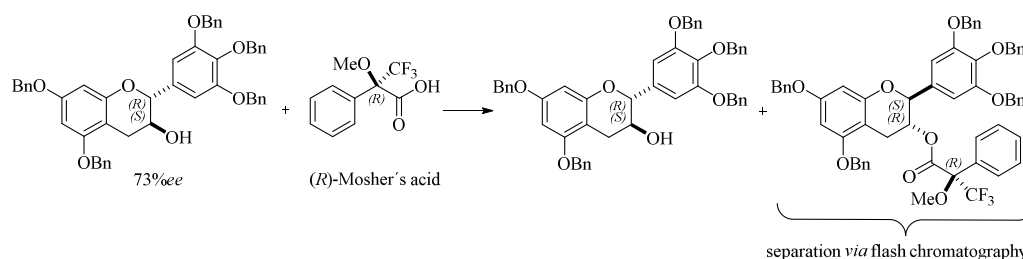
An explanation for the enantiofacial selectivity of the Sharpless asymmetric dihydroxylation reaction may be that the NW and SE quadrant serve as steric barriers, the SW quadrant presents an open area to olefin substituents of moderate size (**Scheme 27**). The NE quadrant allows the attack of flat, aromatic substituents and “large” aliphatic groups. Consequently, the use of dihydroquinidine (DHQD) enables the attack from the top face (β -face), while the presence of the dihydroquinine (DHQ) favors the bottom face attack (α -face).^[212]



Scheme 27: Enantiofacial selectivity of AD-mix- α and AD-mix- β .^[212]

2.1.6 Enantiomeric Excess Values of Diols **37**(α) and **37**(β)

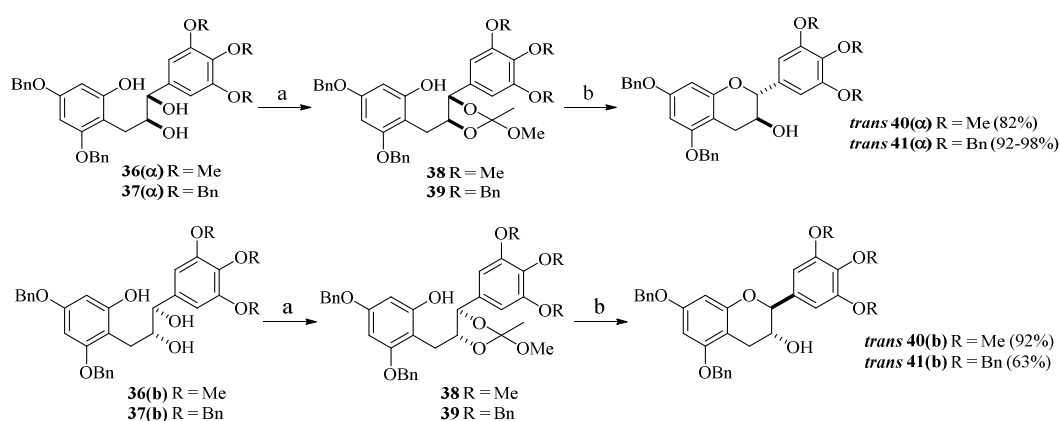
The evaluation of the enantiomeric purity was performed by chiral HPLC analysis. First, the retention times for the enantiomers were determined on racemic dihydroxylated product. The naturally occurring EGCG was prepared by the use of AD-mix- α . After enantioselective Sharpless dihydroxylation the diol **37** showed an enantiomeric ratio of 73% *ee* for **37**(α) (*2S,3S*) and 71% *ee* for **37**(β) (*2R,3R*), demonstrated in diagrams/tables 1 – 3 (experimental). The purity of the optically active diol with AD-mix- α of the olefins was lower than assumed. The reduced enantioselectivity could be a result of long reaction times. Usually, the reaction showed completion after 5 to 7 days. This may be the case due to an excessive use of MeSO₂NH₂ which was added after 24 h with the half of amount at the beginning, may cause the reduced *ee*. Regarding this, it could be an improvement to perform this reaction without using MeSO₂NH₂. To improve enantiomeric excess, the diols were recrystallized from hexane for an enrichment of the major enantiomer. Additionally, the *ee* values of *trans*-catechins could be enhanced by esterification *via* kinetic resolution with 12 – 18% of (*R*)-(+)- α -methoxy- α -trifluoromethyl-phenylacetic acid (Mosher's acid) by treatment with EDC·HCl and DMAP. This method was not applied in the further synthesis but is a possible approach of an enrichment of one enantiomer described by Zhang *et al.*^[213] This is based on the consideration that the minor enantiomer (*2S,3R*) reacts faster (3 – 7 fold) with the (*R*)-Mosher's acid to the corresponding ester than the major enantiomer,^[213] shown in **Scheme 28**.



Scheme 28: Resolution of *trans*-catechin with Mosher's acid by Zhang *et al.*^[213] Reagents and conditions: EDC·HCl, DMAP, CH₂Cl₂, 0 °C.

2.1.7 Cyclization of the 1,2-Diol to *trans*-Chroman-3-ol via the *ortho*-Ester

Krohn *et al.*^[214] reported the successful cyclization using S_N2-type Mitsunobu conditions for the synthesis of enantiomerically pure flavan-3-ol. The first attempt to receive the chroman-3-ol *via* intramolecular Mitsunobu reaction by the addition of triphenylphosphine (PPh₃) and diisopropyl azodicarboxylate (DIAD) in THF, following a protocol of Ding *et al.*,^[167] was not successful. The cyclization was realized *via* an alternative route by treatment with trimethyl orthoacetate and catalytic amounts of pyridinium *p*-toluenesulfonate (PPTS) to the *ortho*-ester. The addition of boron trifluoride etherate as Lewis acid, and the following methanolysis with K₂CO₃ led to *trans*-chroman-3-ol **40/41** (Scheme 29). Since the methanolysis did not show completion, the purification *via* column chromatography was difficult. Thus, to achieve full conversion, the *ortho*-ester was dissolved in methanol at 50 °C and was treated as described previously.

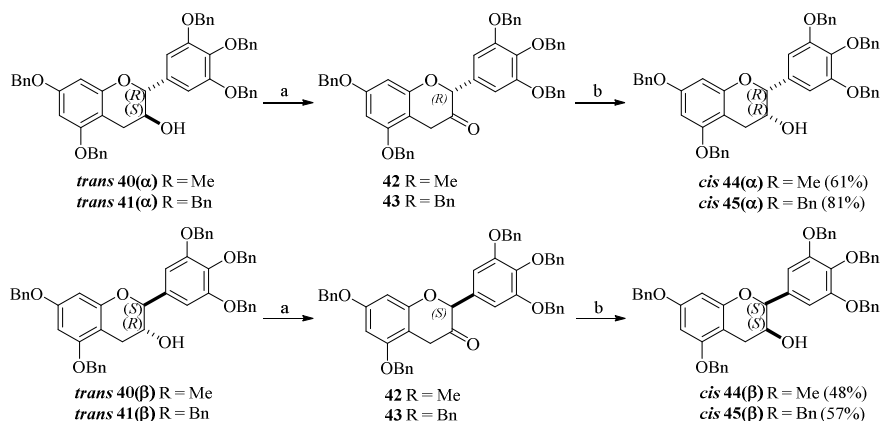


Scheme 29: Cyclization of 1,2-diol to *trans*-chroman-3-ol. Reagents and conditions: (a) trimethyl orthoacetate, PPTS, rt \rightarrow 0 °C, BF₃·OEt₂, acetone; (b) MeOH, K₂CO₃, rt.^[215]

2.1.8 Inversion of Configuration in *trans*-Chroman-3-ol to *cis*-Chroman-3-ol via Oxidation-Reduction Sequence

Since the Mitsunobu reaction failed, an oxidation-reduction sequence by Tückmantel *et al.*^[101] was considered. The reduction of the ketone with L-Selectride[®] in the presence of 6 eq. LiBr, followed by oxidative workup afforded the C3 inversion in a reasonable 81% yield. The oxidation with Dess-Martin periodinane of *trans* **40/41** in CH₂Cl₂ gave yields of 80% of the corresponding ketones **42/43** with 2*R* configuration. The application of a bulky hydride source like lithium tri-*sec*-butylborohydride (L-Selectride[®]) should

exhibit a selectivity that favors an attack from the less hindered β -face to give the epimers *cis* 44/45 with 2*R*,3*R* stereochemistry after column chromatography with aluminum oxide (Scheme 30).



Scheme 30: Synthesis of *cis*-chroman-3-ol via Dess-Martin oxidation and reduction by L-Selectride®. Reagents and conditions: (a) DMP, CH₂Cl₂, rt, 2 h; (b) L-Selectride®, LiBr, THF, -78 °C.^[101]

Worth mentioning the spectroscopic evaluation showed a significant change in the coupling constant during the oxidation-reduction process (Figure 34). The protons of the cyclohexane ring are present in the energetically favorable half chair conformation in which they are pseudo-axially (a) or pseudo-equatorially (e) orientated to the plane of the ring.^[216] In this case, conformers with equatorially oriented substituents are preferred. The *cis*-chroman-3-ol contains the hydroxy group in the unfavorable axial and the aryl ring in equatorial orientation which leads to a dynamic equilibrium (isomerization) of the substituents in the opposite orientation (Figure 33). The fast rotation of the pyran ring between the half-chair conformations results in a merged signal in the NMR spectrum as well in a mean value for the ³*J* coupling. The relationship between the substituents in the pyran ring results in maximal coupling of vicinal H atoms, when these show dihedral angles of 180° or 0°. The relationship of coupling in chair cyclohexane for ³*J*_{aa} is much larger ~7–12 Hz ($\phi = 180^\circ$), shown in *trans*-chroman-3-ol, than ³*J*_{ee} or ³*J*_{ea} ~2–5 Hz ($\phi = 60^\circ$), in *cis*-chroman-3-ol.^[217]

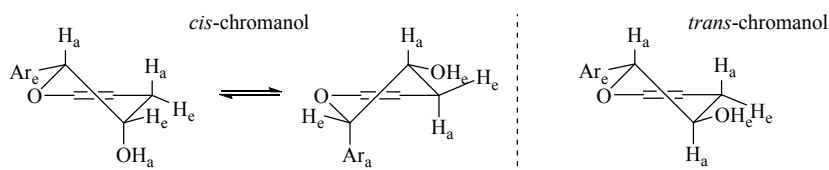


Figure 34: Simplified representation of the chair pyran rings of *trans*- and *cis*-chroman-3-ol.

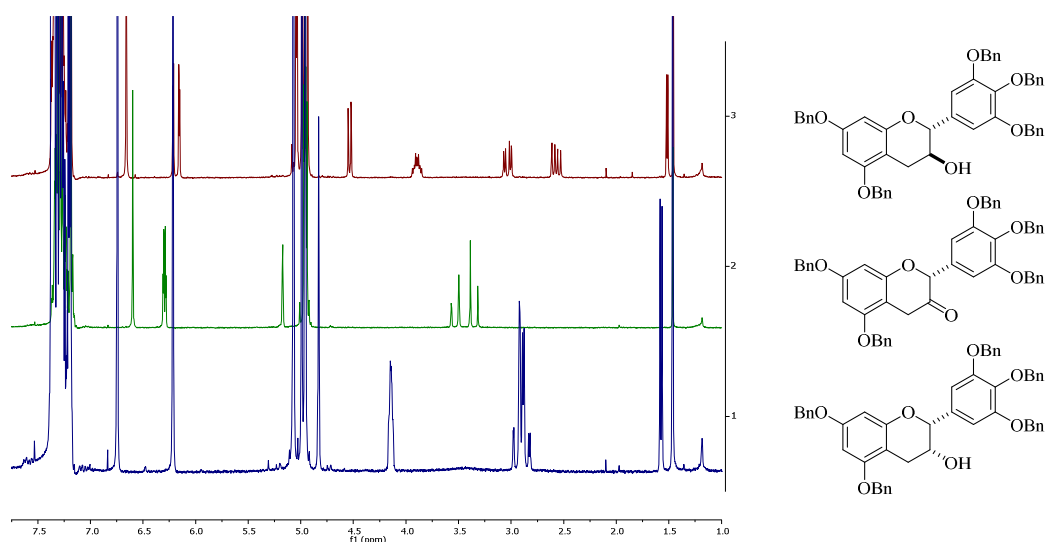
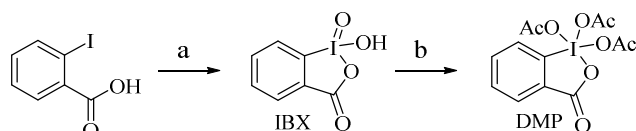


Figure 35: NMR shift of the coupling constant during oxidation-reduction sequence.

The enantiomeric excess after the oxidation-reduction sequence was determined to amount to 98% *ee*. The *ee* value was increased by crystallization in each process of the reaction sequence (see experimental part).

The Dess-Martin periodinane was synthesized from 2-iodobenzoic acid, potassium bromate and sulfuric acid to afford IBX in 93% yield according to the literature of Ireland *et al.* IBX was acylated using a catalytic amount of *para*-toluenesulfonic acid monohydrate in 57% yield (**Scheme 31**).^[218]

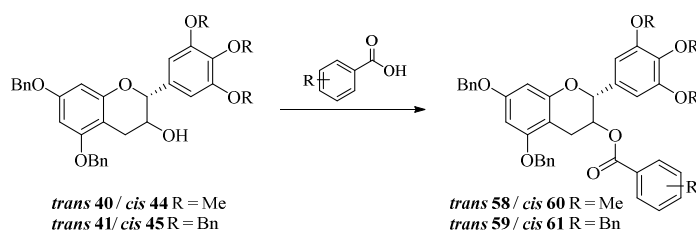


Scheme 31: Synthesis of DMP *via* 2-iodobenzoic acid, reagents and conditions: (a) KBrO_3 , H_2SO_4 , 93%; (b) *p*-TsOH· H_2O , acetic anhydride, 57%.^[218]

2.1.9 Synthesis of GCG Derivatives *via* Steglich-Esterification

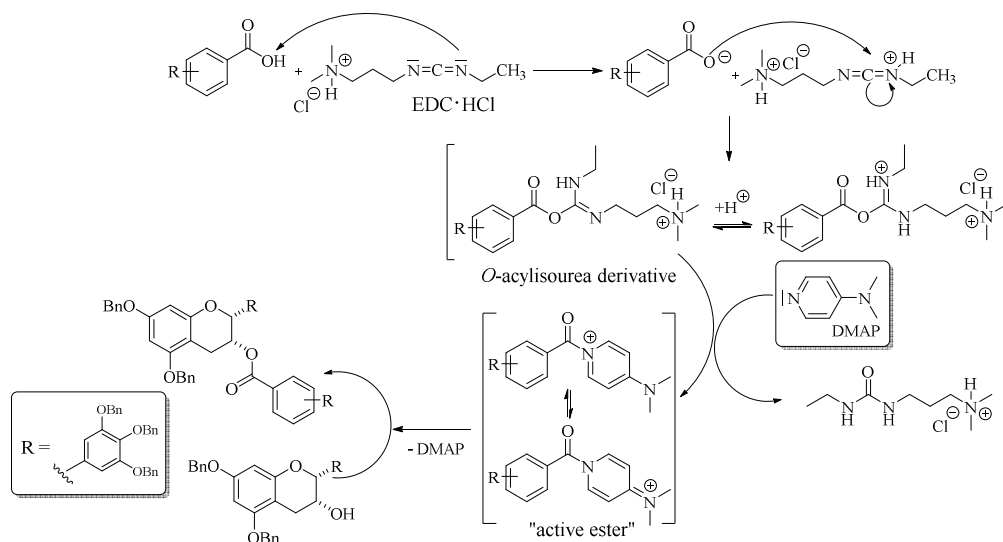
In addition, the effect of hydroxy groups on the **D**-ring was explored by esterification with various substituted benzoic acids. The chroman-3-ol moieties **40/41** with *anti*-configuration served as late-stage intermediates to incorporate additional substituents onto the **D**-ring. The acids used (**Table 5**) which were chosen as replacements for the metabolically labile gallic ester moiety of GCG were synthesized. Li *et al.*^[165b] described the esterification with 3,4,5-tri-*O*-benzylgallic acid, which was refluxed with COCl_2 to gain the acid chloride. Followed by reaction with DMAP in CH_2Cl_2 offered the ECGC

derivatives. Khandelwal *et al.*^[215] illustrated the coupling of the alcohols with aromatic acids using 1-ethyl-3-(3-dimethylaminopropyl)carbodiimide hydrochloride (EDC·HCl), as soluble alternative for DCC, and DMAP gave the corresponding esters (**Scheme 32**). The *syn*-configured chroman-3-ol derivatives were used for the same procedure.

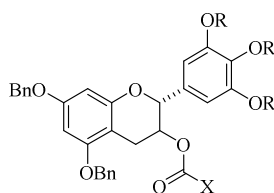


Scheme 32: Synthesis of GCG and EGCG derivatives *via* Steglich esterification. Reagents and conditions: 2.00 eq EDC·HCl, 1.00 eq DMAP, CH₂Cl₂, 0 °C.^[215]

In the beginning of the reaction, the carboxylic acid and the carbodiimide form an *O*-acylisourea intermediate (**Scheme 33**). This mixed anhydride is able to react with DMAP as catalyst leading to an acyl pyridinium species (“active ester”) which forms the desired ester with the alcohol. Due to its ammonium group the urea byproduct, which is the driving force of this reaction, can be removed by slightly acidic workup.^[219] The following table represents the synthesized compounds, as well as the substitution level and the stereochemical information.



Scheme 33: Illustration of Steglich esterification.^[219a, 220]



The following **Table 5** shows the preparation of **B**- and **D**-ring modified EGCG derivatives. The yellow shaded fields indicate the use of AD-mix- β during dihydroxylation.

Table 5: Constitution of GCG and EGCG derivatives including di- and trihydroxyphenyl variants.

Compound / No.	<i>cis</i> / <i>trans</i>	R	X ¹⁵
58a	<i>trans</i>	Me	Methoxygallate
58b	<i>trans</i>	Me	Bn-oxygallate
58c	<i>cis</i>	Me	Bn-oxygallate ¹⁶
58d	<i>cis</i>	Me	C / 3,4,5-F-C ₆ H ₅ ¹⁶
60a	<i>cis</i>	Me	A / 3-F-C ₆ H ₅
60b	<i>cis</i>	Me	J / 4-Bn-C ₆ H ₅
59a	<i>trans</i>	Bn	Methoxygallate
59b	<i>trans</i>	Bn	Bn-oxygallate
61a	<i>cis</i>	Bn	Methoxygallate
61b	<i>cis</i>	Bn	B / 4-F-C ₆ H ₅
61c	<i>cis</i>	Bn	A / 3-F-C ₆ H ₅
61d	<i>cis</i>	Bn	J / 4-Bn-C ₆ H ₅
61e	<i>cis</i>	Bn	H / 2,5-Dibn-C ₆ H ₅
61f	<i>cis</i>	Bn	D / 2,4-Dibn-C ₆ H ₅
61g	<i>cis</i>	Bn	F / 3,5-Dibn-C ₆ H ₅
61h	<i>cis</i>	Bn	G / 3,4-Dibn-C ₆ H ₅
61i	<i>cis</i>	Bn	I / 3-Bn-C ₆ H ₅
61j	<i>cis</i>	Bn	C / 3,4,5-F-C ₆ H ₅
61j	<i>cis</i>	Bn	E / 2,6-Dibn-C ₆ H ₅ ¹⁷

¹⁵ **Figure 36:** Illustration of available benzoic acids (*chapter 2.2.10*).

¹⁶ Dihydroxylation was performed with AD-mix- β (stereochemistry *S,S*).

¹⁷ No reaction was observed.

2.1.10 Synthesis of Protected Benzoic Acids for the Steglich Esterification

The benzoic acid derivatives were introduced in their benzylated or methylated analogues for the formation of EGCG derivatives (**Figure 35**). The benzylation was realized by the use of benzyl bromide, DMF and K_2CO_3 , since the synthesis was described in *chapter 2.1.2*. The methylation was realized as described previously. The following saponification of the ester to the corresponding acid could be completed by the use of potassium hydroxide in a mixture of ethanol and water. All benzoic acids could be coupled with the chroman-3-ol, but the 2,6-dibenzylated benzoic acid showed no reaction caused by steric hindrance.

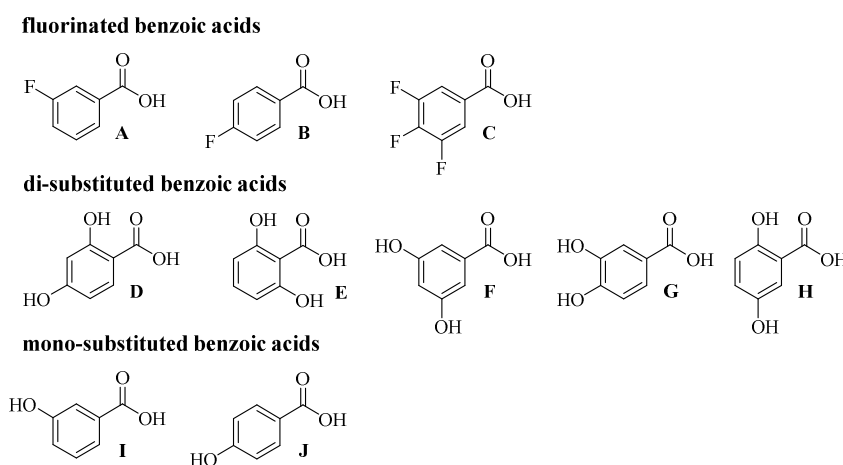
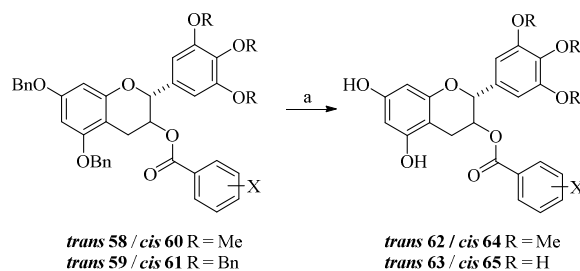


Figure 36: Building blocks for the synthesis library.

2.1.11 Preparation of GCG and EGCG Derivatives by Catalytic

Hydrogenation with Pearlman's Catalyst

Hydrogenolysis of *cis/trans*-chroman-3-ols with $Pd(OH)_2/C$ in a solvent mixture of degassed THF/methanol (1:1) afforded the compounds **63/65a-d** (**Scheme 34**). Due to its sensitivity to oxidation the reaction has to be handled very carefully under exclusion of oxygen by use of argon, also the molecular polarity necessitated the application of reversed phase chromatography. All deprotected compounds were handled in the glove box.



Scheme 34: Catalytic debenzoylation with Pearlman's catalyst. Reagents and conditions: (a) Pd(OH)₂/C, THF/MeOH (1:1, v:v), rt, 1 atm H₂.^[165b]

The following **Table 6** sets out the synthesized deprotected EGCG derivatives. The yellow shaded fields indicate the use of AD-mix-β during dihydroxylation.

Table 6: Illustration of desired products after deprotection.

Compound/No.	<i>cis/trans</i>	R	X ¹⁵
62a	<i>trans</i>	Me	Methoxygallate
62b	<i>trans</i>	Me	OH-oxygallate
64a	<i>cis</i>	Me	OH-oxygallate ¹⁶
64b	<i>cis</i>	Me	C / 3,4,5-F-C ₆ H ₅ ¹⁶
64c	<i>cis</i>	Me	A / 3-F-C ₆ H ₅
64d	<i>cis</i>	Me	J / 4-OH-C ₆ H ₅
63a	<i>trans</i>	H	Methoxygallate
63b	<i>trans</i>	H	OH-oxygallate
65 a	<i>cis</i>	H	Methoxygallate
65b	<i>cis</i>	H	B / 4-F-C ₆ H ₅
65c	<i>cis</i>	H	A / 3-F-C ₆ H ₅
65d	<i>cis</i>	H	J / 4-OH-C ₆ H ₅
65e	<i>cis</i>	H	H / 2,5-DiOH-C ₆ H ₅
65f	<i>cis</i>	H	D / 2,4-DiOH-C ₆ H ₅
65g	<i>cis</i>	H	F / 3,5-DiOH-C ₆ H ₅
65h	<i>cis</i>	H	G / 3,4-DiOH-C ₆ H ₅
65i	<i>cis</i>	H	I / 3-OH-C ₆ H ₅
65j	<i>cis</i>	H	C / 3,4,5-F-C ₆ H ₅

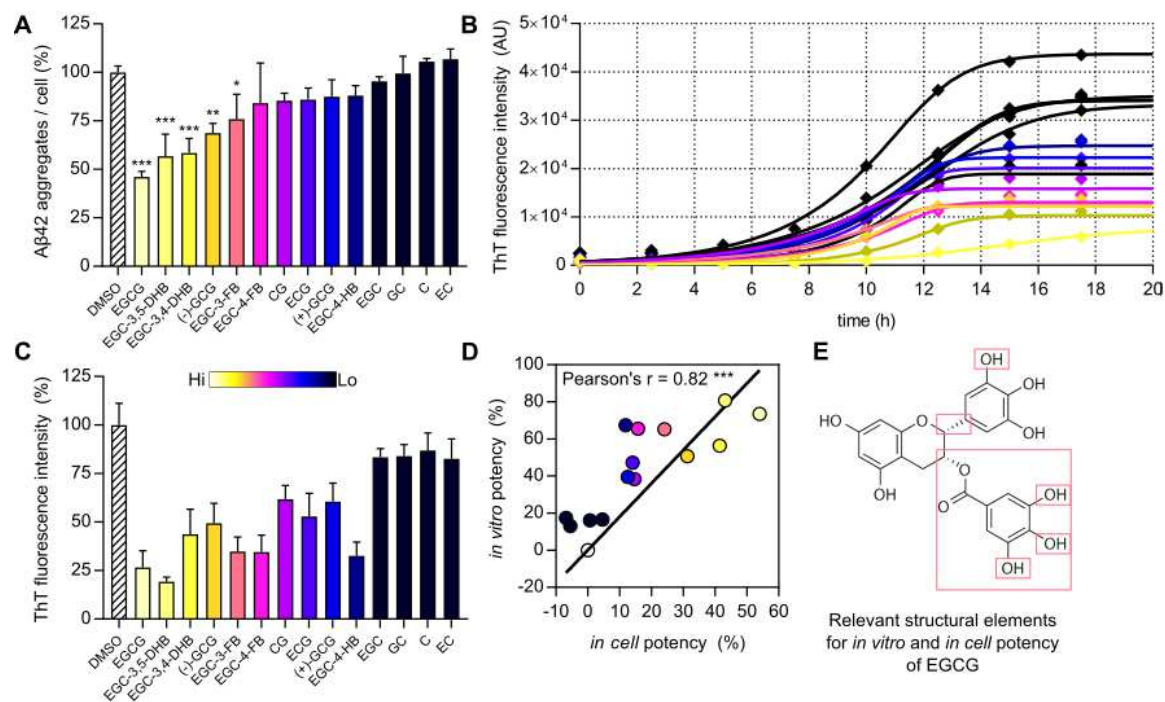
2.1.12 Modulation of A β 42 *in Vitro*

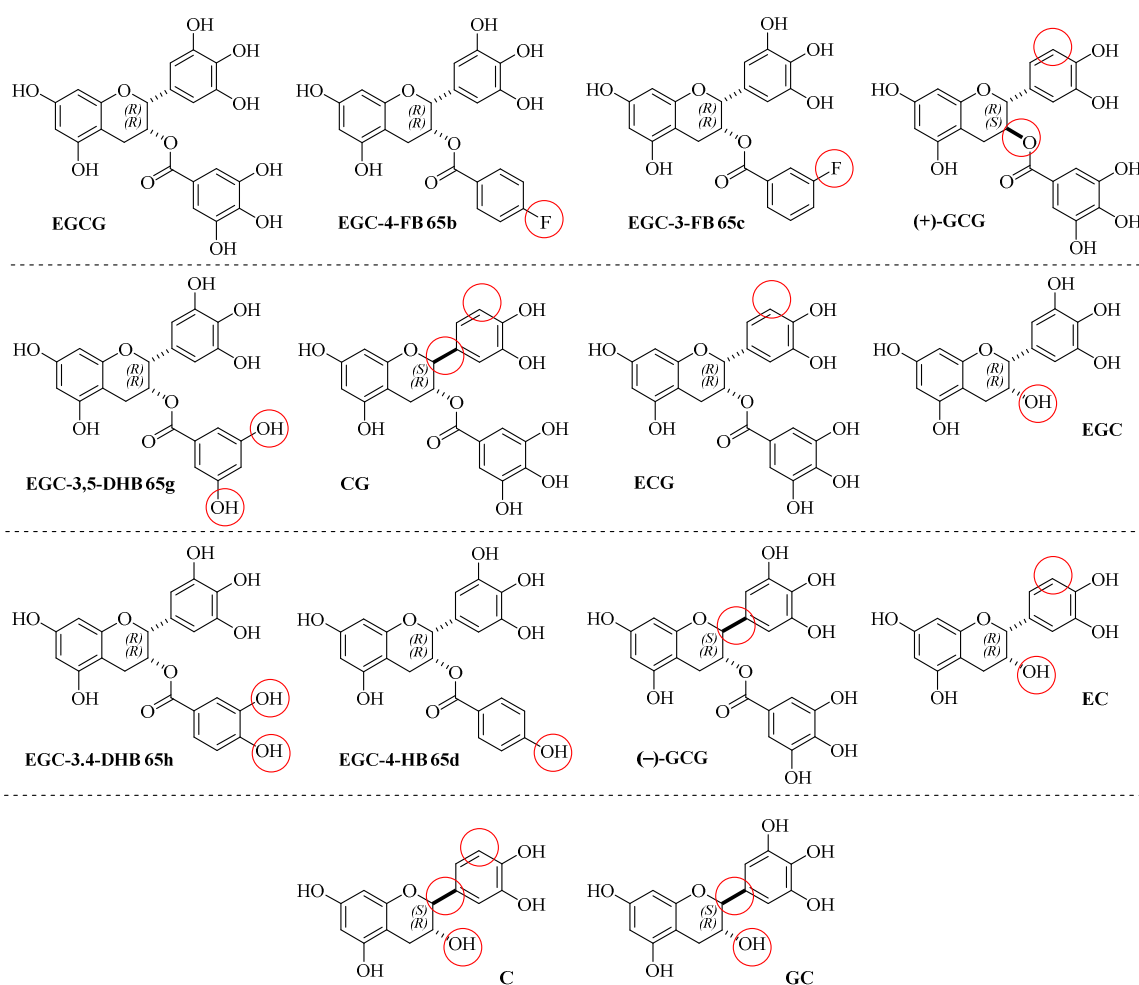
Figure 37: (A) Analysis of cellular A β 42 aggregate degradation promoting effect of EGCG and synthetic derivatives. The quantification of the A β 42 aggregation load was conducted by the total TAMRA fluorescence intensities per cell and normalized to DMSO treated cells. The diagram depicted by means of the three individual values and the error bars are the standard deviation. One-sided ANOVA with Dunnett's post-test, * $p < 0.05$, ** $p < 0.002$, *** $p < 0.001$. (B) *In vitro* A β 42 aggregation controlled by ThT binding, resulted in a slow-down of A β 42 aggregation though addition of EGCG and its derivatives by kinetic and reduced maximal reached ThT fluorescence intensity. (C) *In vitro* A β 42 aggregation normalized to DMSO for quantification of maximal ThT signal. Bars showed mean value derived from two individual experiments and error bars can be defined for standard deviation. (D) Promoting cellular A β degradation effect of EGCG and its derivatives in correlation analysis of *in cell* and *in vitro* potency verified by Pearson's correlation coefficient (r). The *in vitro* and cell assays were carried out by Prof. E. Wanker and C. Secker.¹⁸ For an enlarged view see appendix.

Table 7: Summary of the inhibition (*in vitro* %) and the degradation (*in cell* %) effect of EGCG and its derivatives. The yellow highlighted fields show the use of purchased compounds.¹⁸

Abbreviation	Derivative name	Inhibition <i>in vitro</i> (%)	Degradation <i>in cell</i> (%)
EGCG	(-)-Epigallocatechin-3-gallate	73.4 ± 8.6	54.0 ± 3.0
EGC-3,5-DHB	(-)-Epigallocatechin-3,5-dihydroxybenzoate	80.8 ± 2.4	43.2 ± 11.4

¹⁸ Prof. E. Wanker and C. Secker, Proteomics and Molecular Mechanisms of Neurodegenerative Diseases, Max Delbrück Center for Molecular Medicine, Robert-Rössle Strasse 10, 13125 Berlin, Germany.

EGC-3,4-DHB	(-)-Epigallocatechin-3,4-dihydroxybenzoate	56.4 ± 13.0	41.5 ± 7.5
(-)-GCG	(-)-Gallocatechin-3-gallate	50.6 ± 10.3	31.3 ± 5.0
EGC-3-FB	(-)-Epigallocatechin-3-fluorobenzoate	65.2 ± 7.5	24.1 ± 12.8
EGC-4-FB	(-)-Epigallocatechin-4-fluorobenzoate	65.5 ± 8.8	15.8 ± 20.6
CG	(-)-Catechin-3-gallate	38.3 ± 7.2	14.7 ± 3.9
ECG	(-)-Epicatechin-3-gallate	47.1 ± 12.0	14.1 ± 6.0
(+)-GCG	(+)-Gallocatechin-3-gallate	39.5 ± 9.6	12.6 ± 8.9
EGC-4-HB	(-)-Epigallocatechin-4-hydroxybenzoate	67.4 ± 7.0	11.9 ± 5.1
EGC	(-)-Epigallocatechin	16.6 ± 4.4	4.6 ± 2.3
GC	(-)-Gallocatechin	16.1 ± 6.0	0.7 ± 8.9
C	(-)-Catechin	13.1 ± 8.9	-5.5 ± 1.5
EC	(-)-Epicatechin	17.5 ± 10.4	-6.8 ± 5.3



E. Wanker *et al.* developed an assay which allows the measurement of the degradation of intracellular A β 42 aggregates in cells. For monitoring A β 42 aggregation Thioflavin T was used in the *in vitro* amyloid fibril formation assays (**Figure 36 B**) (for assay description see *chapter 1.4.2*). Binding of ThT to beta-sheet rich structures results in a typical fluorescence spectrum shift and increase of its fluorescence intensity at a specific wavelength. This can be exploited to monitor the kinetic of spontaneous A β 42 aggregate formation, which is characterized by different phases: in the lag phase only individual A β peptides are available and low fluorescence intensities are detected from soluble peptide solutions. After incubation and aggregation to A β fibrils the amount ThT fluorescence increases until a plateau is reached (**Figure 37**).^[221]

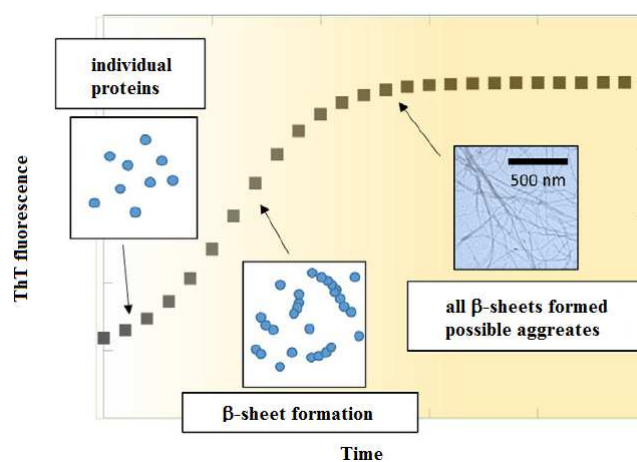


Figure 38: Progression of protein aggregation represented in the beginning with individual A β proteins. After aggregation fibrils are formed until plateau is reached.^[221]

Using the developed cell-assay, a library of 20 compounds, including EGCG, was tested. Hereby, EGCG was the most potent compound in promoting cellular A β 42 degradation. Furthermore, addition of EGCG to spontaneous A β 42 aggregation *in vitro* resulted in a slowdown of the A β 42 aggregation kinetic and EGCG and its derivatives strongly reduced maximal reached ThT fluorescence intensities. **Table 7** shows the *in vitro* inhibition and *in cell* potency of EGCG and derivatives. Compounds containing an ester-bond (EGC-3,5-DHB **65g**, EGC-3,4-DHB **65h**, EGC-3-FB **65c**, EGC-4-FB **65b**) and the presence of the 3,4,5-trihydroxyphenyl **B**-ring led to promotion of cellular A β 42 aggregates and similar derivatives were able to slow down A β 42 aggregation *in vitro*. The hydroxy substitution pattern on the **D**-ring was apparently irrelevant. The results indicate that the presence of the 3,4,5-trihydroxyphenyl **B**-ring represents the most influential factor for binding to amyloid; nevertheless the non-identical activity was consistent with the

trans-configuration, which does not differ significantly from EGCG. This can be demonstrated by the (–)-GCG diastereomer. The flavanols GC, C, EC were even less active than flavanols containing the galloyl moiety. The *in vitro* assay allows the conclusion that the examined derivatives show a significant effect on the A β 42 aggregate ThT binding. Diagram C shows the quantification of the maximal reached ThT intensity of *in vitro* A β 42 aggregation reactions in presence of EGCG and derivatives normalized to DMSO (Figure 36 C). The values of ThT intensity reduction are summarized in Table 6. EGC-3,5-DHB 65g and EGCG were the most potent compounds in reducing A β 42 aggregation *in vitro*. The cell-based assay (Figure 36 A) shows the effect of EGCG and its derivatives on A β 42 aggregates in mammalian cells. This assay give insight into the ability of EGCG to increase degradation of A β 42 aggregates in neuroblastoma cells. Quantification of the A β 42 aggregation load was conducted by the total TAMRA fluorescence intensities *per cell* and normalized to DMSO-treated cells. Compared to the *in vitro* ThT assay, all compounds showed less degradation promoting effects in cells (Table 6). This may be due to the fact that the very polar compounds have to diffuse through the lipid bilayer of the cells, which correlates with the diminished passage of EGCG through the blood-brain barrier (chapter 1.2.7). In addition, possible interactions with cellular components could arise, which could lead to a diminished effect. As the same derivatives, which stimulate cellular A β 42 degradation also inhibit A β 42 aggregation *in vitro* (ThT Assay) (Figure 36 D), it was supposed that the cellular effect arises through a direct effect on A β 42 aggregates in cells. The correlation analysis of *in cell* and *in vitro* potency of EGCG and its derivatives was verified by *Person's correlation coefficient* (**r**). It is a measure of the linear correlation between the *in vitro* (%) and the *in cell* potency (%). EGCG and its derivatives, which stimulates cellular A β 42 degradation inhibit A β 42 aggregation in the *in vitro* assay. However, it is interesting to note that the fluorinated derivatives (EGC-3-FB 65c and EGC-4-FB 65b) were more effective *in vitro* than in the cellular experiments. Usually, the introduction of fluorine in drugs changes the lipophilicity, which could influence the solubility, permeability and the protein binding.^[222]

These diagrams A-D (Figure 36) showed the effectiveness of the structure connections and relevant characteristics of commercially available EGCG derivatives and synthesized EGCG derivatives in this work. The antioxidant potential was a result of the availability of many hydroxy groups at the B-/D-ring and led to a higher effectiveness in aggregation inhibition of A β 42. The higher the degree of hydroxy groups, the higher the activity.

3,4,5-Trihydroxyphenyl **B**-ring led to increased activity and was responsible for antioxidant activity (**Figure 38**). In addition, the (–)-GCG diastereomer shows a reduced effectiveness in the stimulation of the cellular A β 42 degradation in terms of the presence of the *trans*-configuration. Moreover, the essential prerequisite was the presence of the galloyl moiety of catechins. In conclusion, the synthesized molecules were effective A β 42 aggregation inhibitors *in vitro* assays and – in part – promoters of cellular A β 42 degradation.

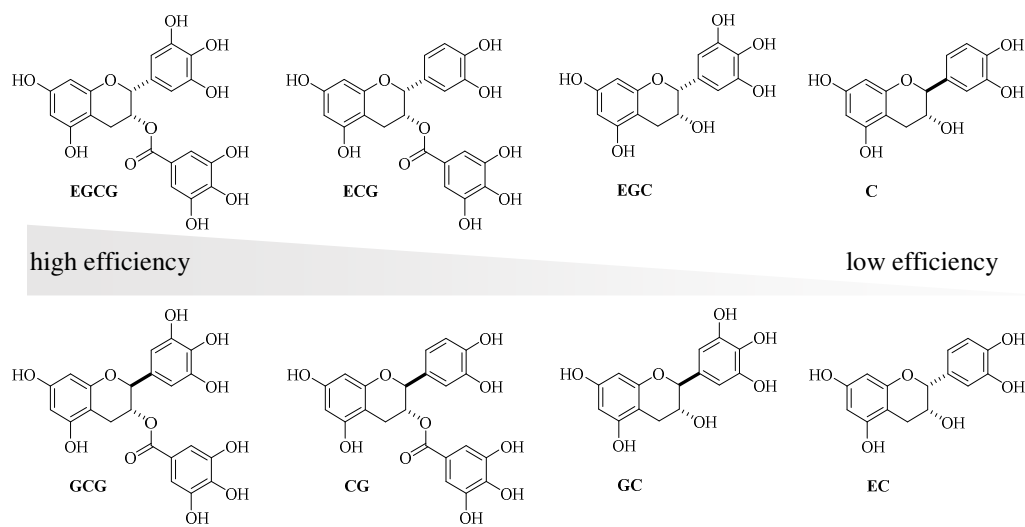


Figure 39: Determination of the effectiveness of the structure relationship of EGCG derivatives.

Finally, this study was performed with the intention to investigate a valuable therapeutic strategy for AD in which EGCG and its derivatives lead to the inhibition of A β 42 aggregation and furthermore, to an increase of cellular A β 42 degradation. The investigation of a new therapeutic strategy has emerged in recent years by an off-pathway in which EGCG redirects A β 42 into unstructured oligomers. Thereby, stabilization of toxic oligomers into non-toxic, soluble proteins leads to an inhibition of amyloidogenic proteins.^[2] The results of the fluorescence assay implicate that EGCG and its derivatives could prevent the formation of A β in neurodegenerative disorders. Additionally, the result of an increase in ThT fluorescence does not agree with a loss of amyloid-like structures.^[223] For the explanation how EGCG shows an effect on ThT fluorescence, various hypothesis are possible:

- I. EGCG enables the displacement of ThT without altering aggregation of A β -42;
- II. EGCG enables a new pathway of aggregation products which have no affinity for ThT;

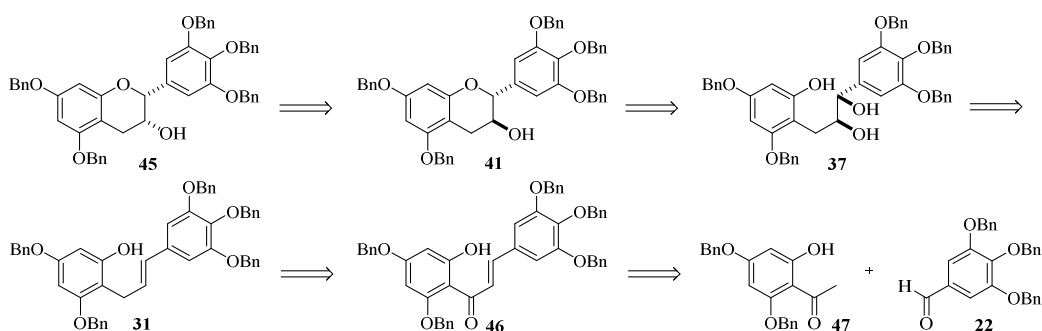
- III. EGCG enables a polymerization of A β so that the protein left in its unfolded monomeric form. These results may indicate that the effect of EGC on A β , in addition a conclusive mechanism of protein-binding to increase the formation of non-toxic peptides, resulting in a possible off-pathway.^[223]

2.2 Second Approach for the Enantioselective Synthesis of EGCG Derivatives *via* Chalcone

2.2.1 Retrosynthetic Analysis of Protected (-)-Epicatechin **45**

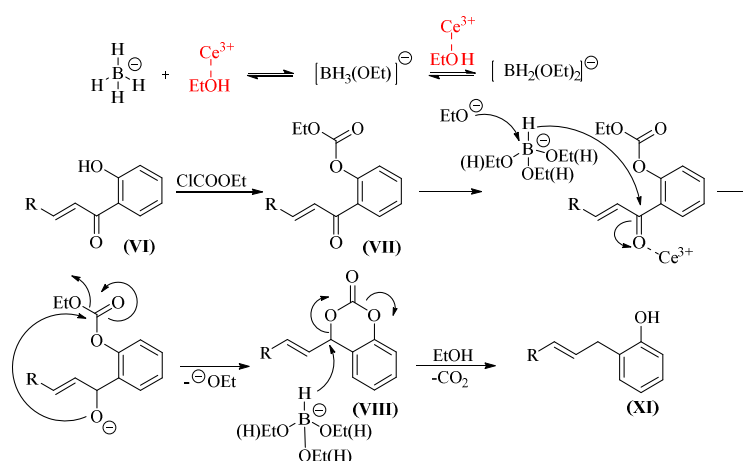
The synthesis of (*E*)-olefin **31** in this work was performed according to the report by Krohn *et al.*^[214] The (*E*)-olefin **31** was synthesized by Claisen-Schmidt condensation between acetophenone and aldehyde.

A second approach was used for the formation of catechins, because the Friedel-Crafts alkylation during the first synthesis led to disappointment. Therefore, the synthesis was repeated several times to acquire sufficient amounts of the desired product which furthermore had to be separated from its regioisomer. In the second approach the (*E*)-olefin **31** was traced back to chalcone **46**, as key intermediate for setting the desired protected catechin by an efficient and convenient strategy. Chalcone **46** can be build up from acetophenone **47** and benzaldehyde **22** (Scheme 35).^[224]



Scheme 35: Retrosynthetic analysis of catechin **45**.^[214]

The reaction to alkene **31** was realized by reduction with NaBH₄. In 1978, Luche described the selective conversion of α,β -unsaturated carbonyl groups to allylic alcohols in presence of lanthanide chlorides and NaBH₄.^[225] This reaction is significantly influenced by the solvent. Mainly EtOH or MeOH are used and on the contrary, dipolar aprotic solvents like acetonitrile and THF lead to inferior results by the formation of over-reduced product.^[226] A possible mechanism explaining the conversion of the enone to the alkene is illustrated in

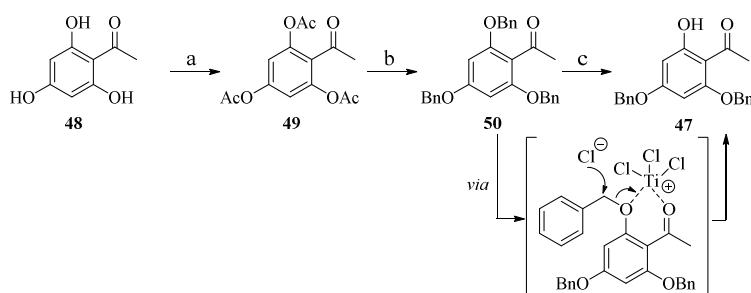
Scheme 36 by Yuan *et al.*^[226]**Scheme 36:** Possible mechanism of modified Luche reduction.^[226]

The mechanism of this reaction can be described as a two-step sequence including rapid alcohol formation and a much slower deoxygenation leading to the desired product. Based on the theory of hard and soft acids and bases (HSAB), it can be concluded that the substitution of hydrides in BH_4^- increases the hardness of the species by alkoxy groups, so the nucleophilic attack on the conjugate enone system is favored at the hard side (1,2-addition). During this process it is assumed that the alkoxy borohydride^[227] is the active species based on a modified Luche reduction. Cerium acts as catalyst of the reaction to form the alkoxy borohydrides, and increases the electrophilicity of the carbonyl carbon atom. The hard cerium cation coordinates to the alkoxy borohydride, which functions as hard reducing agent.^[228] The α,β -unsaturated acylphenol **VI** is treated with TEA and ClCOOEt to form the carbonate **VII**. This is able to react with the alkoxy borohydride generated *in situ* of EtOH and NaBH_4 , supported by coordination of the solvent molecule to oxygen. The Lewis acid activation of the carbonyl group and the improvement of the acidity of the medium and activation of the carbonyl of the enone, leads to the intermediate **VIII**. The last steps are the decarboxylation and finally protonation leading to the (E) -configured product **XI**.^[226]

2.2.2 Synthesis of Acetophenone **47**

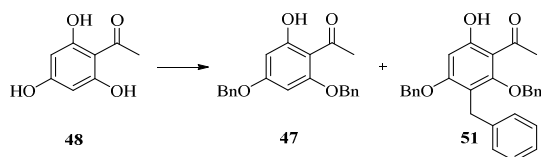
For the construction of the chalcone **46** a second component - the acetophenone **47** - was additionally required, whose synthesis is described below. The first approach to synthesize the protected acetophenone **47** was realized by the acylation of 2,4,6-trihydroxyacetophenone (**48**) in order to decrease the electron density as already

described in *chapter 2.1.3*,^[229] affording product **49** in 68% yield. The following benzylation with benzylchloride in the presence of K_2CO_3 in DMF leads to protected product **50** as yellow oil in 62% yield. The mono-debenzylation was realized by the use of conc. titanium tetrachloride in CH_2Cl_2 at $-5\text{ }^\circ\text{C}$ for 1.5 h following a procedure by Bazin *et al.*^[230] affording product **47** in 18% yield. In a second attempt, a 1 M titanium tetrachloride solution in CH_2Cl_2 was used which led to reasonable 62% yield of **47**. The mechanism of the reaction could be explained by the simultaneous chelation by the titanium to the oxygen atoms, consequentially chloride could attack the benzyl group nucleophilically (**Scheme 37**).



Scheme 37: Synthesis of 2,4-dibenzyloxy-6-hydroxyacetophenone (**47**). Reagents and conditions: (a) acetic anhydride, sulfamic acid, 68%; (b) benzyl chloride, K_2CO_3 , DMF, 62%; (c) $TiCl_4$, CH_2Cl_2 , $-5\text{ }^\circ\text{C}$, 18%.^[230]

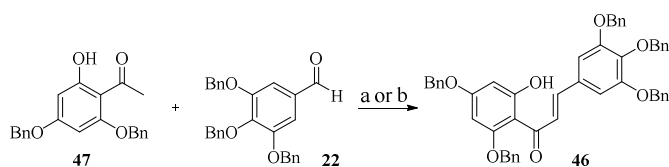
A second approach to build up compound **47** was based on the direct benzylation of **48** following a procedure by Huang *et al.*^[231] As already explained above **48**, was reacted under the same conditions. The application of 2.00 eq benzyl chloride and 2.20 eq K_2CO_3 in DMF for 2 h at $70\text{ }^\circ\text{C}$ was successful (**Scheme 38**).^[213] The brown oil was then purified by column chromatography affording **47** as a slightly yellow solid in 66 – 78% yield. This benzylation occurred in a regioselective manner due to an intramolecular hydrogen-bonding between the carbonyl group and one neighbouring phenolic hydroxy group (e.g. tautomerism). The application of basic conditions in this reaction led to nucleophilic substitution with benzyl chloride in position 3 to form the non-desired C-benzylated byproduct **51** (**Scheme 38**).^[200]



Scheme 38: Direct benzylation of 2,4,6-trihydroxyacetophenone (**47**). Reagents and conditions: 2.00 eq benzyl chloride, 2.2 eq K_2CO_3 , DMF, $70\text{ }^\circ\text{C}$, 2 h, 72%.^[231]

2.2.3 Synthesis of Chalcone **46** via Claisen-Schmidt Conditions

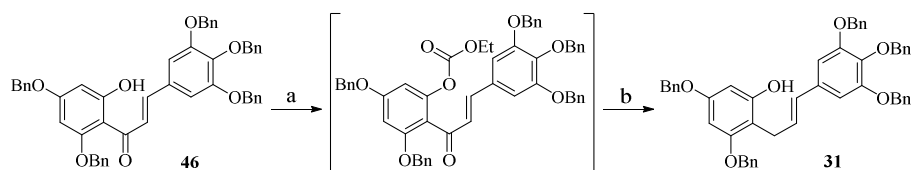
Chalcone **46** was formed by base-catalyzed aldol condensation of the previously synthesized acetophenone **47** and benzylaldehyde **22**, the synthesis of which is described above in *chapter 2.2.1*. Several possibilities to prepare the chalcone **46** were available following a procedure by Krohn *et al.*:^[214] the first was the condensation of **47** and **22** with sodium hydride dispersed in mineral oil in DMF at rt for 2 h.^[213] After completion of the reaction a recrystallization from ethanol gives **46** in yellow crystals in 38% yield. A second alternative protocol was performed using 50 wt% KOH in refluxing EtOH.^[232] After stirring for 2-3 h a precipitation formed, the precipitate was filtered off and extracted to give the crude product of **46** (**Scheme 39**). The recrystallization from methanol resulted in chalcone **46** as yellow crystals in 55% yield.



Scheme 39: Formation of chalcone **46** via Claisen-Schmidt conditions. Reagents and conditions: (a) 60% NaH, DMF, 0 °C, 38%; (b) 40 wt% KOH (aq.), EtOH, reflux, 55%.^[214]

2.2.4 Synthesis of Diaryl Propene **31** via Modified Luche Reduction

The deoxygenation of chalcone **46** was realized by employing cerium chloride heptahydrate/sodium borohydride and ethyl chloroformate.^[214, 226] The compound was prepared according to the literature following a procedure by Yuan *et al.*^[226] Chalcone **46** was treated with triethylamine in anhydrous THF to deprotonate the hydroxy group. The dropwise addition of ethyl chloroformate led to a carbonate. The mechanistic pathway is described in *chapter 2.2.1*. The two-step sequence was performed by treatment with NaBH₄ in combination with cerium chloride heptahydrate to form the (*E*)-configured product **31**, starting from the α,β -unsaturated ketone **46**. Purification by flash chromatography led to the product **31** in 74% yield (**Scheme 40**).

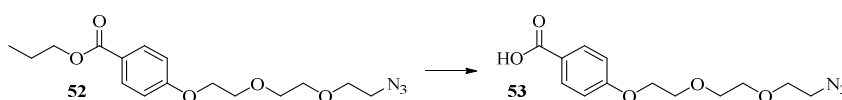


Scheme 40: Deoxygenation of chalcone **46** to the corresponding (*E*)-configured propene **31**. Reagents and conditions: (a) TEA, ClCOOEt, THF, 0 °C; (b) NaBH₄, EtOH, CeCl₃·7 H₂O, 74%.^[226]

2.3 Biotin- and Dye-labeled EGCG Derivatives

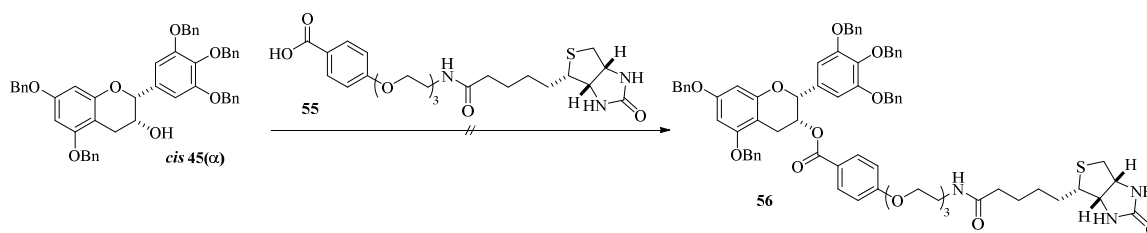
2.3.1 Synthesis of Chain-Linker and Coupling with Biotin to Compound **56**

The biotin- and dye labeled EGCG derivatives were prepared on the basis of the Steglich esterification. The reaction conditions were optimized based on my own knowledge. The elucidation of the dynamics of EGCG in cellular uptake, the metabolism as well as the intracellular transport are highly relevant for the investigations of future drug development for medicinal use.^[193] In principle, a biotin-EGCG conjugate is designed and prepared mainly for evaluating its efficacy in Alzheimer-targeting drug delivery. The motivation for this work is to develop novel EGCG derivatives with a spacer arm incorporated between EGCG and the biotin, to provide additional flexibility and a reduced conjugate aggregation. A further advantage of a long spacer is a minimized steric hindrance upon binding. Meanwhile, the biological activity of EGCG has to be maintained by the presence of the gallate-ester moiety. The azido-linker **52** and biotin-PEG-linker **55** were prepared as described previously by L. Reus.^[233] In this investigation, *cis*-chroman-3-ol *cis* **45(a)** was attached to an azido-linker **53** by Steglich esterification. First, the azido linker must be saponified to generate the corresponding carboxylic acid by treatment with 40 wt% potassium hydroxide in ethanol (**Scheme 41**).



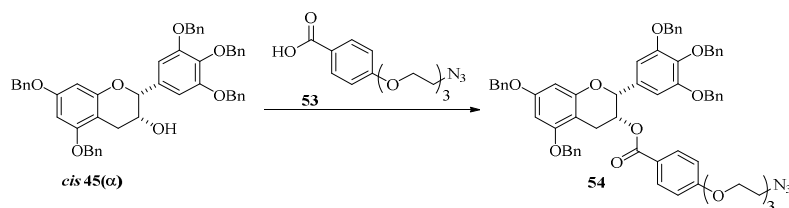
Scheme 41: Saponification of *n*-propyl ester **52** to free acid **53**. Reagents and conditions: 40 wt% KOH, EtOH, 90%.

The first attempt to build up the highly functionalized EGCG-linked biotin **56** by direct coupling of *cis*-chroman-3-ol *cis* **45(a)** with the biotin-PEG linker **55** failed (**Scheme 42**). The biotin-PEG linker **55** was poorly soluble. Therefore, the esterification had to be performed in DMF instead of CH₂Cl₂. A second approach was investigated in which the biotin moiety is tethered finally.



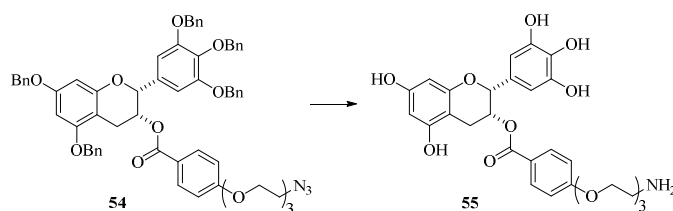
Scheme 42: Coupling of *cis*-chroman-3-ol **45(a)** with biotinylated acid to compound **56**. Reagents and conditions: 1.00 eq **55**, EDC·HCl, DMAP, CH₂Cl₂, 0 °C → rt.

Furthermore, it has to be considered that the sulfur atom of the biotin moiety might poison the heterogenous catalyst during a late-stage hydrogenation. The lone pair of the sulfur atom is strongly attracted to metal surfaces, in this case to palladium. Consequently, the initial approach featured the incooperation of an azido precursor without a biotin unit. The coupling of the *cis*-chroman-3-ol **45(a)** with the aromatic azido acid **53** was realized by Steglich esterification making us of EDC·HCl and DMAP to give the corresponding ester **54** in 89% yield (**Scheme 43**). The first approach to the coupling product **54** was conducted as described above in *chapter 2.1.9*, but complete conversion was not observed.



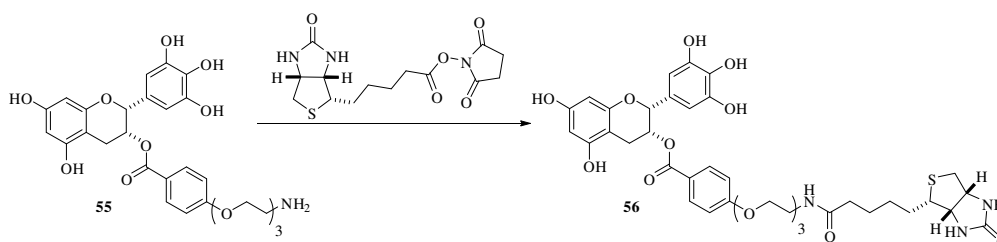
Scheme 43: Steglich esterification of *cis*-chroman-3-ol **45(a)** to compound **54**. Reagents and conditions: 2.00 eq **53**, 2.00 eq EDC·HCl, 1.00 eq DMAP, CH₂Cl₂, 0 °C → rt, 89%.

The next step consists of the hydrogenation of **54** with Pearlman's catalyst to remove the benzyl protective groups and to reduce the azide functionality to the primary amine **55**. Due to the high sensitivity of the deprotected product **55** to oxygen, the workup has to be done very carefully and under an oxygen-free atmosphere. The high polarity of the product requires the use of reversed phase rather than silica gel for chromatography. Therefore, compound **55** was used for the next step without purification (**Scheme 44**).



Scheme 44: Hydrogenolytic cleavage of compound **54** to free amine **55**. Reagents and conditions: Pd(OH)₂/C, THF/MeOH (1:1, v:v), 1 atm H₂, 90%.^[165b]

The last step comprised the coupling of the EGCG-PEG-NH₂ **55** compound with commercially available (+)-biotin *N*-hydroxysuccinimide ester (biotin-NHS) as activated carboxylic acid. In general, succinimidyl esters form stable peptide bonds. Consequently, these compounds are reliable tools for amine modification.^[234] The coupling reaction takes place in anhydrous DMF in approximately equimolar quantities at rt overnight. *N*-hydroxysuccinimide is the only byproduct of the reaction. The solvent is evaporated by heating to 45 °C under reduced pressure (**Scheme 45**).



Scheme 45: Coupling of compound **55** with biotin-NHS to **56**. Reagents and conditions: 1.00 eq biotin-NHS, DMF, rt, 79%.

2.3.2 Co-Localization of EGCG-A β 42 in Streptavidin Assay

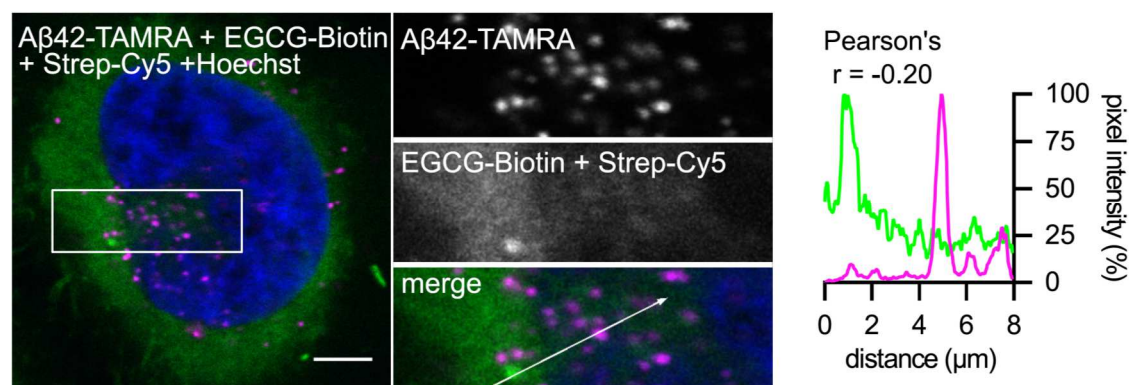
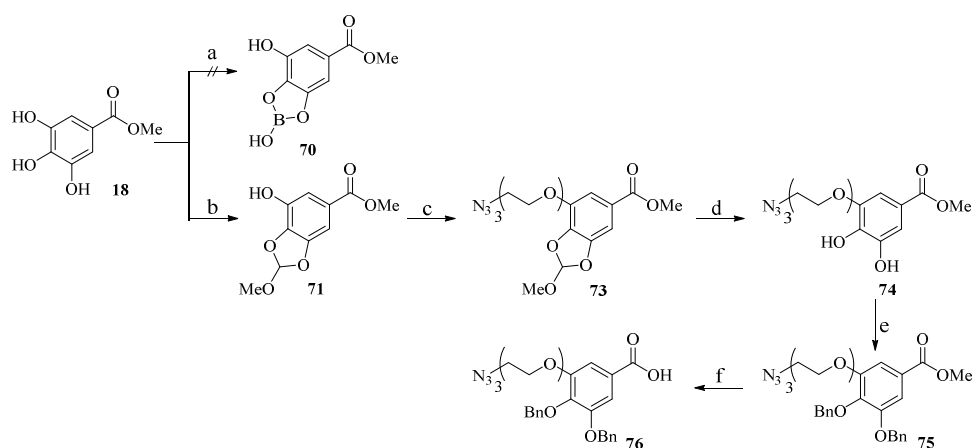


Figure 40: Confocal microscopic image of compound **56** in A β 42 cells. **R** describes the efficiency for co-localization. The *in vitro* assays were carried out by C. Secker and Prof. E. Wanker.¹⁸

Due to the results in **Figure 39** the biotin-labeled EGCG derivative **56** showed no specific co-localization with TAMRA-labeled A β 42 aggregates. For visualization of the biotin labeled EGCG derivative the cells were stained with Streptavidin-Cy5. For an enlarged view see appendix.

2.3.3 Synthesis of Gallate Chain Linker

Previous investigations verified the beneficial effect of a high degree of substitution by hydroxy groups at the **B**- and **D**-ring system. So, in order to maintain a high level of activation of the EGCG-moiety, the synthesis is performed with a highly substituted **D**-ring. This synthesis differs from the second approach, described in *chapter 2.3.1*, in as much as two out of three hydroxy groups having to be protected *via* boronate ester **70** (**Scheme 46**). The compound was prepared by R. Steinfort.¹⁹



Scheme 46: Synthesis of gallic acid to azido-linked gallic acid **76**. Reagents and conditions: (a) 5 wt% Borax; (b) $\text{HC}(\text{OCH}_3)_3$, IR-120 plus, toluene, 4 h, 150 °C, 76%;^[235] (c) **72**, Cs_2CO_3 , DMF, 78%;^[236] (d) *p*-TsOH, MeOH, 24 h, rt, 31%;^[235] (e) benzyl chloride, K_2CO_3 , DMF, 7 h, 80 °C, 88%;^[237] (f) 40 wt% KOH, EtOH, 1 h, 80 °C, 90%.

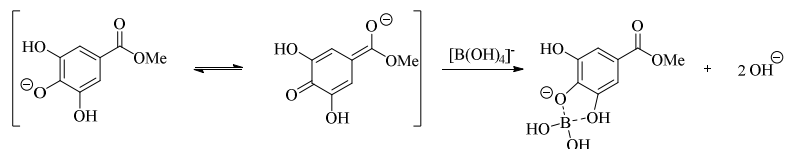
This synthesis was described by Schelie *et al.*^[238] and was performed by R. Steinfort using an aqueous borax solution to mask two vicinal hydroxyl groups of gallic acid. Gallic ester **18** was treated with a 5 wt% borax solution overnight in base-catalyzed conditions, but compound **70** could not be isolated. Boric acid forms $\text{B}(\text{OH})_4^-$ -ions in aqueous solution, acting as weak acid (ionization equilibrium of boric acid (pK_a 9.0) in water).



Vicinal 1,2-diols e.g. in catechols feature higher Lewis acidic character due to the phenolic hydroxy groups and the benzene ring.^[239] The formation of the boronic esters can affect the binding affinity between the boric acid moiety and the diol by the solvent, pH, buffer and ionic states. In aqueous solution, the tetra coordinated hydroxyborate anion ($\text{B}(\text{OH})_4^-$) is

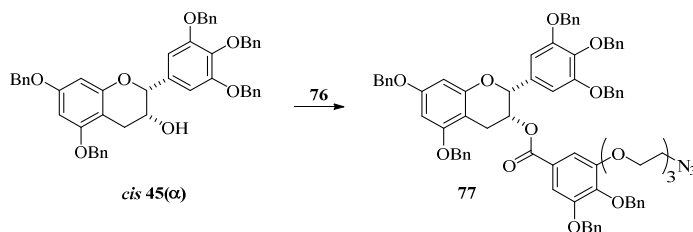
¹⁹ R. Steinfort, Synthese eines Azido-PEGylierten Gallussäure-Derivates, bachelor thesis, 2017, Heinrich-Heine Universität.

10^3 to 10^4 times more reactive in contrast to the trigonal neutral boronic acid.^[240] A nucleophilic attack by the phenolates at the electron deficient boron should form the cyclic borate (**Scheme 47**). One of the possible consequences is an insufficient concentration of acid and base which forms by borates and led to a suppression of the formation of product **70** (**Scheme 46**).



Scheme 47: Possible formation of boronic esters.

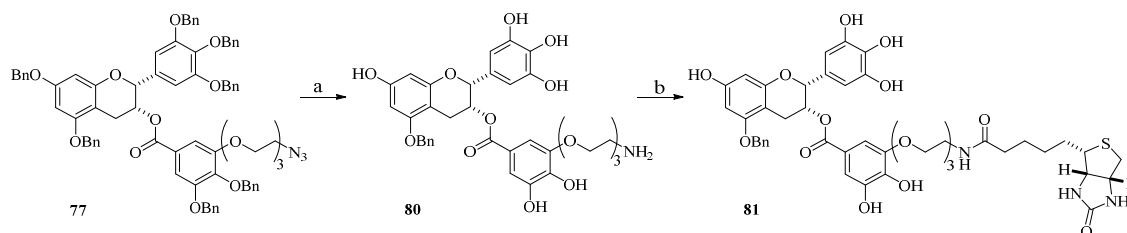
An alternative selective 1,2-diol protection was realized by the reaction of gallic acid methylester (**18**) with trimethyl orthoformate for the introduction of an acetal **71** in 76% yield. This reaction was carried out in the presence of ion-exchange resin IR-120 plus in toluene at 150 °C (**Scheme 46**), according to a protocol of Merz *et al.*^[235] The available hydroxy group is coupled with the azido-PEG linker **72** in 78% yield to form compound **73** in the presence of Cs_2CO_3 . The carbonate functions as base for alkylation reactions (cesium effect): Due to its position in the periodic table, cesium cations are larger compared to the smaller alkali metals like lithium, sodium or potassium. In addition, it might be expected that the salt dissociates in a polar solvent like DMF to a higher extent than smaller cations. In cases where the nucleophilicity of the cesium phenolate is higher instead of the ion pair, the bromide will be displaced.^[236] The next step involved deprotection of the acetal by treatment with *p*-TsOH which led to the 1,2-diol in 31% of **74**. The two available hydroxy groups had to be protected a second time with benzyl chloride to obtain the benzylated product **75** in 88% yield. The last reaction served to ensure the methyl ester saponification to the carboxylic acid by treatment with 40 wt% potassium hydroxide in refluxing ethanol for 1 h to gain compound **76** in 90% yield (**Scheme 46**). With the acid **76** in hand coupling with *cis*-chroman-3-ol **cis 45(a)** was performed by Steglich conditions, yielding 75% of compound **77** (**Scheme 48**).



Scheme 48: Steglich esterification of *cis* **45(a)** with azido linked gallic acid **76** to compound **77**. Reagents and conditions: 2.00 eq **76**, EDC·HCl, DMAP, 0 °C → rt, 75%.^[215]

2.3.4 Coupling of Amino-PEG-EGCG and Biotin

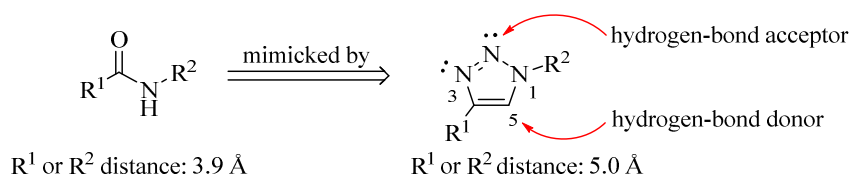
One possible option for connecting azido-PEG-linked EGCG **77** and biotin is presented in **Scheme 49**: First, the benzyl protecting groups were removed and the azide was concomitantly reduced by hydrogenation. The amine was then coupled with biotin-NHS to form the amide bond in compound **81**. The procedure was performed as already mentioned in *chapter 2.3.1*.



Scheme 49: Hydrogenolytic cleavage of **77** and coupling of amine **80** with biotin-NHS. Reagents and conditions: (a) Pd(OH)₂/C, THF/MeOH (1:1, v:v), 1 atm H₂, 79%; (b) biotin-NHS, DMF, rt 57%.

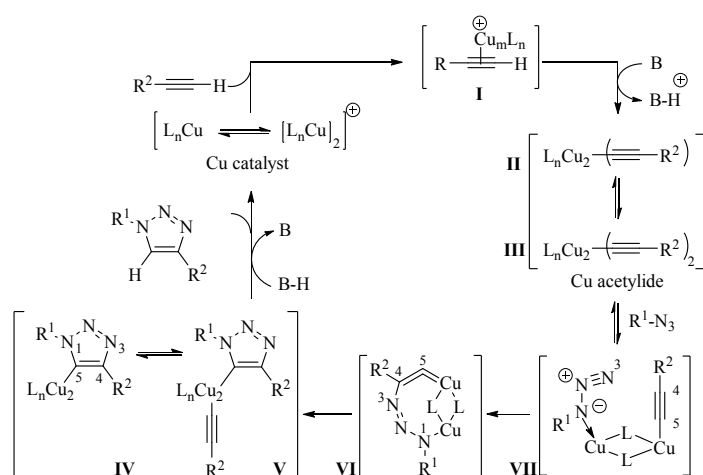
2.3.5 Click-Chemistry as Copper-Catalyzed Azide-Alkyne Cycloaddition for Labeling Targets

Sharpless^[241] and Meldal^[242] reported a copper(I)-catalyzed reaction of terminal alkynes and azides that leads to 1,4-disubstituted 1,2,3-triazoles and provides a large variety of applications in organic and bioorganic chemistry. Furthermore, the high-yielding reaction can be performed in many solvent systems, allows a wide temperature range, is insensitive to pH and shows a high degree of tolerance to functional groups.^[243] Generally, formation of the heterocycle is supported by the presence of polar solvents, assisted by the solubility of the substrate and catalyst. However, solvents with coordinating properties impair the metal-substrate coordination.^[244] Of great interest with respect to the issue of biological activity is the 1,2,3-triazole heterocycle as rigid linkage with the ability to mimic a peptide bond and shows, due to the atomic constitution and electronic properties no tendency to hydrolytic cleavage (concept of bioisosterism) (**Scheme 50**).^[243]



Scheme 50: Comparison between amides and 1,2,3-triazoles.^[243]

The additional *N* atom in 1,2,3-triazoles has the effect of an increase of R^1 – R^2 -distance by 1.1 Å, which arises from the stronger dipole moment and leads to a polarization of the C5 proton, which will accomplish as hydrogen-bond donor. Finally, the N2 and N3 atoms can act as hydrogen-bond acceptors.^[243] Not only the chemical properties of 1,2,3-triazoles are worth mentioning: compounds with a 1,2,3-triazol unit display attractive biological activity by its ability to mimic a peptide bond, like the *anti*-HIV effect,^[245] selective β_3 adrenergic receptor inhibition,^[246] *anti*-bacterial activity,^[247] and many more. Some EGCG derivatives with an amide bond instead of gallate ester were synthesized by Bhat *et al.* as potential Hsp90 inhibitors.^[248] In recognition of these results, it can be of great interest to examine the 1,2,3-triazoles for replacement of the gallate ester in EGCG since no information is available in this respect at the moment.



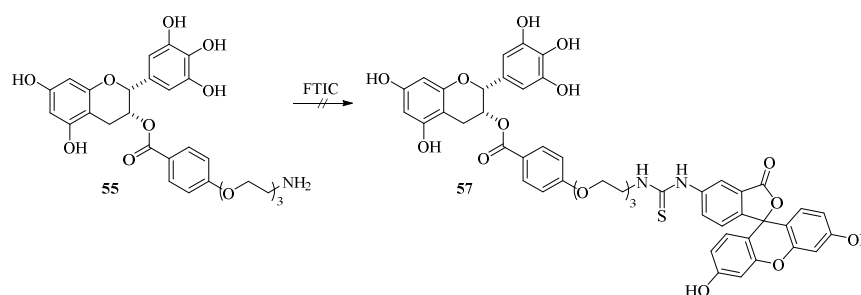
Scheme 51: Illustration of Mendal-Sharpley Click mechanism with proposed species involved in cycle.^[243]

The mechanistic outline occurs as a stepwise reaction as already manifested by DFT calculations (**Scheme 51**). Experiments showed evidence that internal alkynes do not react,^[241] underlining that the first step in the proposed cycle is the formation of a Cu^I acetylide species *via* a π -complex **I**. Due to the copper coordination to the alkyne bond, the pK_a of the alkyne C–H decreases up to 9.8 pK_a units, which enables deprotonation in aqueous medium without any additional base.^[249] Furthermore, kinetic studies showed that the kinetic of this reaction is second order in copper.^[250] The second copper atom is assumed to play a role in the activation of the azide function like in dimer **VII** by reducing the alkyne electron density, so that the acetylide is prone to cyclization.^[242] Additionally, the Cu acetylide-azide complex **VII** is formed by azide exchange of one ligand. The activation of the azide by complexation leads to a nucleophilic attack of the acetylide carbon C4 to N3 and furnished species **VI**. Thereby electron-withdrawing substituents on

the alkyne promote Cu^I-catalyzed alkyne-azide coupling.^[242] Finally, the metallacycle enables a ring contraction between the N1 and the C5–Cu π^* orbital to **V**. Product generation arises out of the deprotonation of triazole-copper derivative **IV** by external base or solvent and subsequent regeneration of the catalyst and protodecupration.^[243]

2.3.6 Fluorescence Determination in Molecular Biology

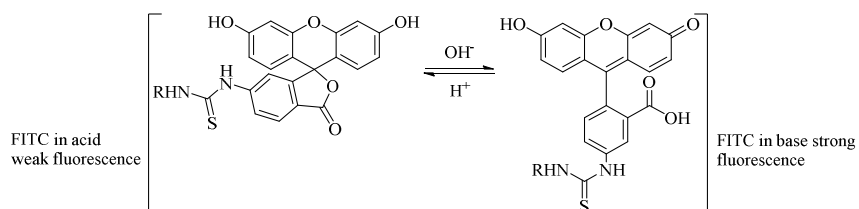
A common method for the visualization of intracellular processes in living cells is the imaging with dyes in fluorescence microscopy. Biomolecules equipped with a conventional fluorophore may become visible this way and enable detection of complex structures with excellent sensitivity, allowing the utilization in imaging processes involving antibodies, peptides, proteins, and DNA etc. One of the fluorescence dyes is fluorescein, it became more important after its development in the 19th century as a very efficient fluorescent marker, as it is emitting light at the range of over 500 nm.^[251] This approach was used to design an EGCG derivative with an incorporated fluorophore. The initial idea was to combine the EGCG-PEG-NH₂ **55** with a fluorescein molecule in the same way like the analogous with biotin as described above for the biotinylated molecule **81** (*chapter 2.3.3*). Additionally, a fluorescein isothiocyanate (FITC) molecule was incorporated instead of the biotin moiety for a fluorescence assay in which the compound **57** can be visualized under a fluorescence microscope (**Scheme 52**). The resulting fluorescence in cells indicates an effective fluorescence-labelled molecule which will be suitable for illustrating the dynamics of EGCG in active brain cells. Furthermore, the bright EGCG target is vital when working out the localization on the cellular and organ scale, respectively.



Scheme 52: Coupling of compound **55** with fluorescein. Reagents and conditions: (a) Fluorescein, DMF, 25 °C.

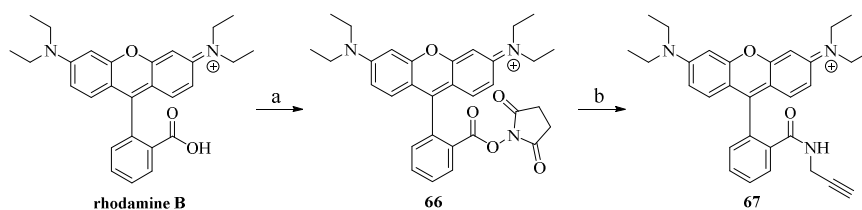
The amino-EGCG-PEG linker **55** should have been coupled with the fluorescein isothiocyanate Isomer I (**Scheme 52**) but there was no reaction to compound **57**. Due to the

very high sensitivity against oxygen after removal of the benzyl groups, oxidation or decomposition of the product may result. It is well-known that certain dye molecules lead to photobleaching and show pH dependent fluorescence. FITC ($\lambda_{em} = 517$ nm) shows a high selectivity towards H^+ in environmental conditions, on the basis of fluorescence shift caused by changing pH by the formation of a lactone in equilibrium between the lactone and a carboxylic acid (**Scheme 53**).^[251]



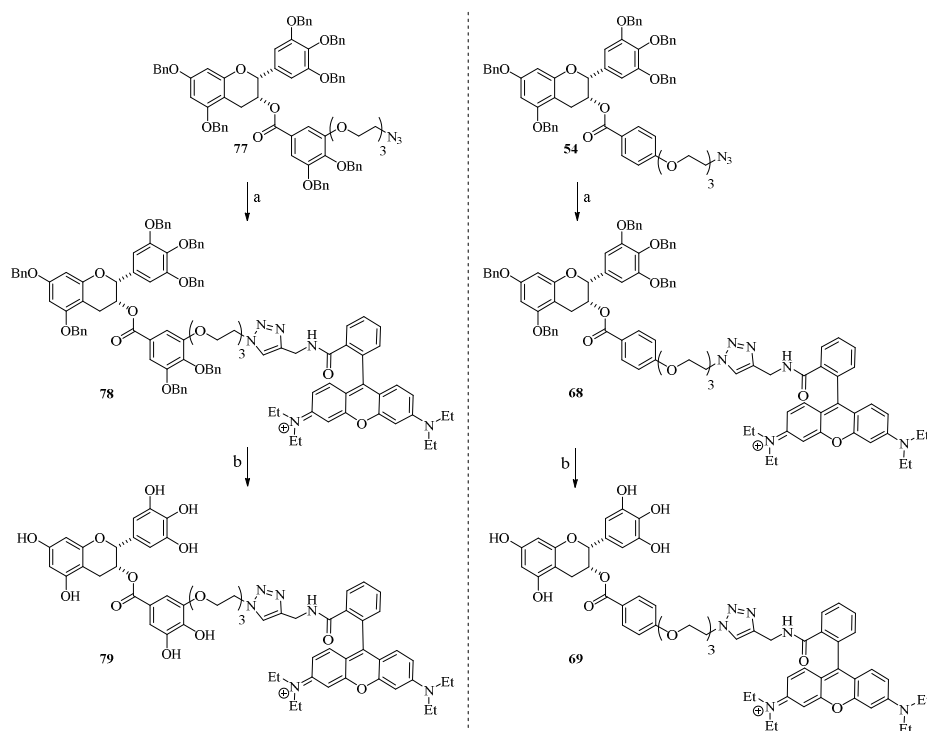
Scheme 53: pH Dependence of fluorescein isothiocyanate I (FITC) (right), fluorescein divided into benzene section and the Fluorophore (left).^[251]

A second approach was carried out with the idea of avoiding a pH-dependent equilibrium. In this synthesis, alkyne functionalized rhodamine B was used for the coupling with the azido-linked EGCG molecule. Rhodamine B contains a free carboxylic acid that was converted into the active ester **66** with *N*-hydroxysuccinimid in 88% yield followed by treatment with propargyl amine to obtain alkyne derivative **67** in 68% yield (**Scheme 54**).



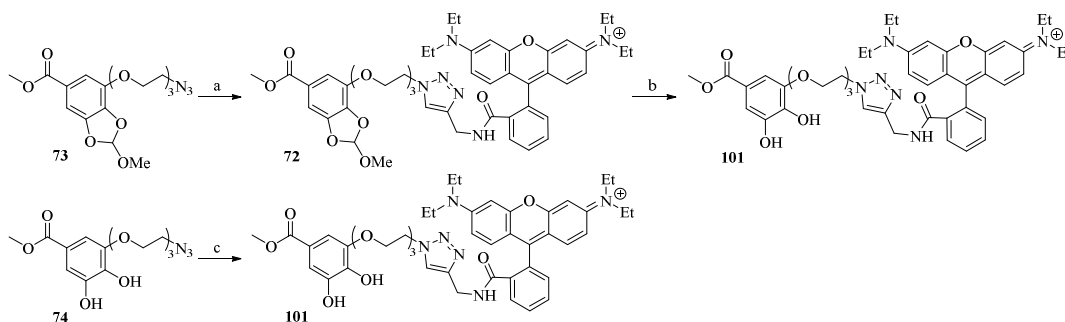
Scheme 54: Synthesis of alkyne-coupled rhodamine **67** from rhodamine B. Reagents and conditions: (a) DCC, HOSu, DMF, rt, 88%; (b) NEt_3 , propargylamine, DMF, rt, 68%.

Subsequently, the connecting of the alkyne-rhodamine derivative **67** and the azido-PEG-EGCG derivative **55** was performed *via* click-reaction in the presence of 10 mol% sodium ascorbate and 5 mol% copper sulfate in DMSO^[252] afforded product **68** in 83% and product **78** in 87% yields. For detailed explanation see *chapter 2.3.5*. The crucial, final step included the deprotection of the benzylated hydroxy groups to obtain **69** in 89% yield and **79** in 87% yield, respectively (**Scheme 55**). It was very important to degas all solvents used by the method “Freeze-Pump-Thaw”.



Scheme 55: Click reaction between azido EGCG **54/77** and rhodamine-alkyne **67** to the dye products **68** (right) and **78** (left), followed by hydrogenolytic cleavage to product **69** and **79**. Reagents and conditions: (a) **67**, 5 mol% CuSO₄, 10 mol% sodium ascorbate, DMSO, 65 °C, **68** (83%), **78** (87%); (b) Pd(OH)₂/C, THF/MeOH (1:1, v:v), 1 atm H₂, **69** (89%), **79** (87%).

For a more detailed study of the accumulation of dye-labelled EGCG **69/79** to A β 42, a negative control substrate **101** was designed lacking the *cis*-chroman-3-ol moiety shown in **Scheme 56**. Two synthetic pathways were possible: starting with the *ortho*-ester **73** coupling with dye **67** led to compound **72**. The following deprotection by the use of PPTS yielded compound **101** missing *cis*-chroman-3-ol moiety in 77% yield, respectively. The alternative synthesis route starts directly with deprotected compound **74** by following linking with dye **67** to compound **101** in 52% yield.



Scheme 56: Synthesis of negative control substrate **101**. Reagents and conditions: (a/c) **67**, 5 mol% CuSO₄, 10 mol% sodium ascorbate, DMSO, 65 °C, 77%; (b) *p*-TsOH, MeOH, 24 h, rt, 52%.^[235]

The determination of the spectral properties of compound **79** were examined in ethanol and indicated that dye-labeled EGCG **79** is a good fluorescent molecule (**Figure 43**). By comparison with pure EGCG, the absorption peak is approximately at 275 nm and a weak absorption at wavelengths ≥ 325 nm,^[253] the emission maxima are at 350 and 400 nm.^[254] The EGCG derivative functionalized with rhodamine (compound **79**) shows the main peak slightly blue shifted to 276 nm and a small tail up to 319 nm. Moreover, the fluorescence emission bands of compound **79** appear at approximately 590 nm. Rhodamine B exhibits a broad fluorescence emission at 510 nm as free carboxylic acid dissolved in ethanol.^[255] The new rhodamine EGCG dye shows a large Stokes shift of 14400 cm^{-1} .

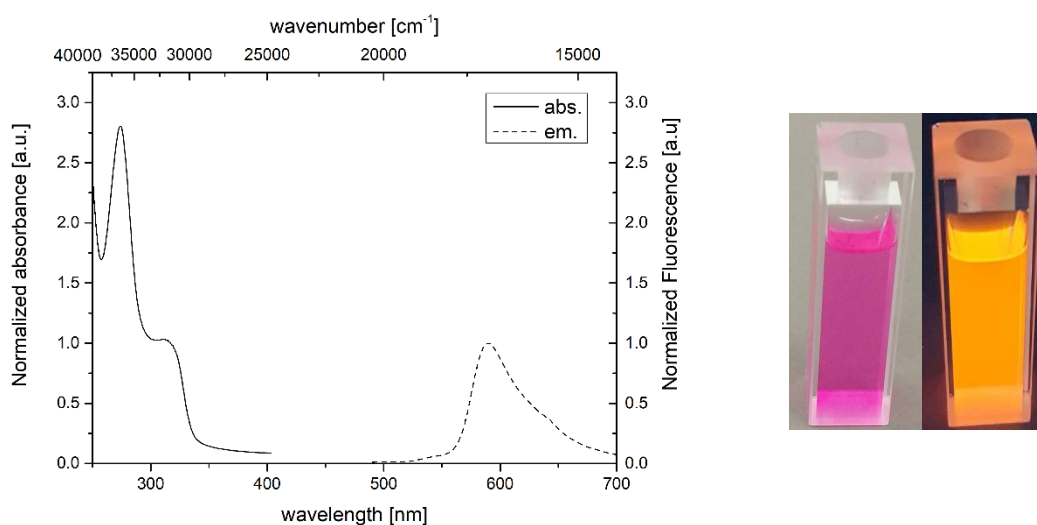


Figure 41: UV and fluorescence spectra of compound **79** (left). Photophysical properties of compound **79** (recorded in MeOH at $T = 293\text{ K}$): $\lambda_{\text{max, abs}} [\text{nm}]^{[a]} = 276, 319$ (sh); $\lambda_{\text{max, em}} [\text{nm}]^{[b]} = 590$; Stokes shift $\Delta\tilde{\nu} [\text{cm}^{-1}]^{[a]} = 14400$; compound **79** dissolved in methanol under UV light (right).

2.3.7 EGCG-A β 42 in Cell Co-Localization

The histogram (**Figure 41**, right) is an analysis of the co-localization for determining cellular processes of EGCG in cells.¹⁸

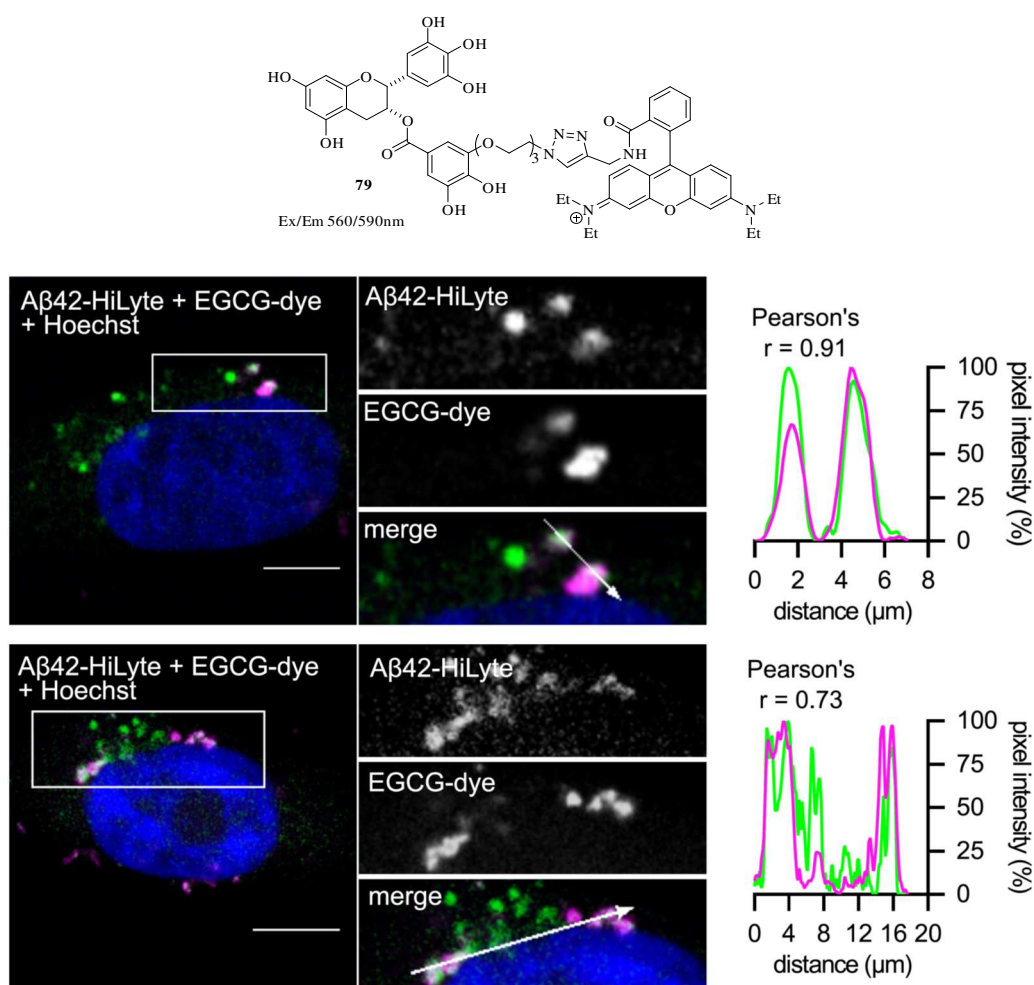


Figure 42: Illustration of compound **79** (left) via confocal microscope, EGCG-A β 42 in cell co-localization (right). The Pearson's correlation coefficient was quantified from rhodamine B and HiLyte488 signals, the quantification was determined by normalization of the fluorescent intensity spectra to maximum intensity along illustrated white arrow. This data was provided by C. Secker and Prof. E. Wanker.¹⁸ For an enlarged view see appendix.

Moreover, r (Pearson's correlation coefficient) describes the efficiency for that co-localization. The relevant section of the graph shows the same curve progression with $r = 0.91$ for co-localization. Thus compound **79** showed clear co-localization with intracellular, HiLyte488-labeled A β 42 aggregates. With this results, it can be shown that EGCG directly targets A β 42 aggregates the cells (**Figure 41 left**). This strongly suggests that the cellular degradation mechanism is mediated by direct effect and not by an effect of

the compound on other cellular compounds. In contrast, control compound **101** lacking the *cis*-chroman-3-ol moiety showed no co-localization with HiLyte488-labeled A β 42 aggregates with $r = 0.27$ (**Figure 42**). Rhodamine B has a very similar spectra as TAMRA, so A β 42 aggregates labeled with HiLyte488 were prepared and used for this experiment (see *chapter 4.2*).

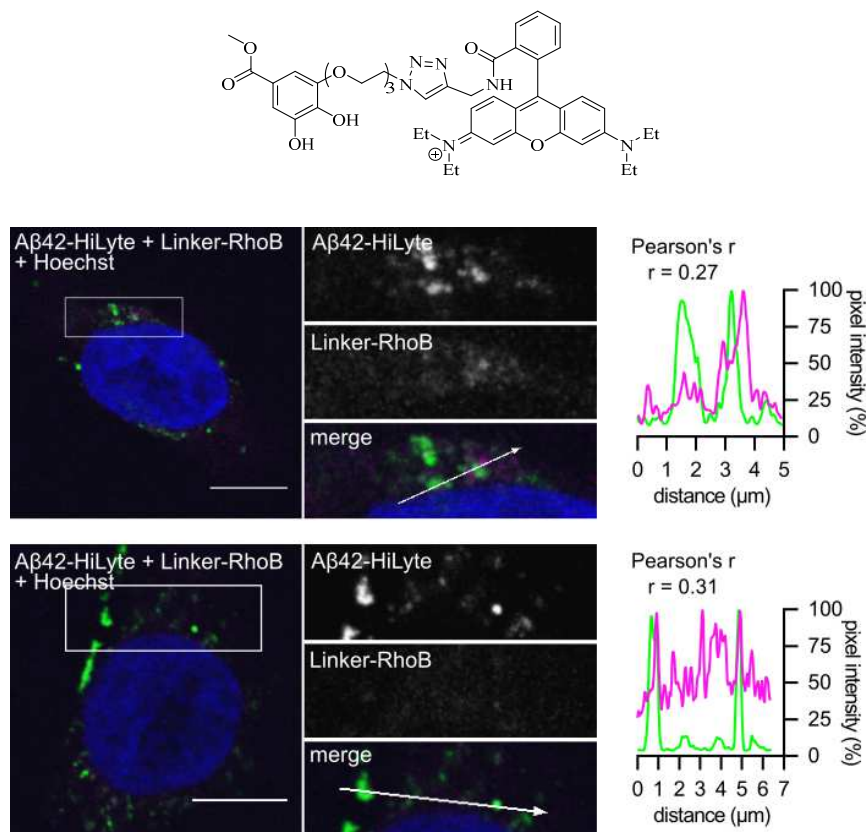
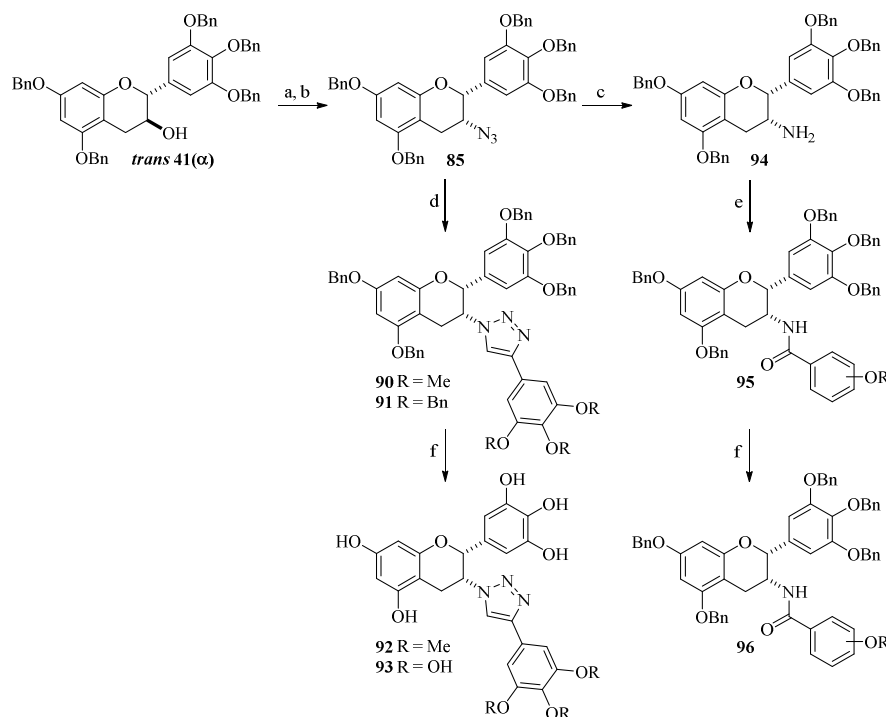


Figure 43: Illustration of compound **101** (left) via confocal microscope, EGCG-A β 42 in cell co-localization (right). The Pearson's correlation coefficient was qualified between rhodamine B and HiLyte488 signals, the quantification was determined by normalization of the fluorescent intensity spectra to maximum intensity along illustrated white arrow. The *in vitro* assays were carried out by C. Secker and Prof. E. Wanker.¹⁸ For an enlarged view see appendix.

2.4 Development of Novel Azido-EGCG Derivatives

2.4.1 Synthesis of 3-Azidochromane by Common Substitution

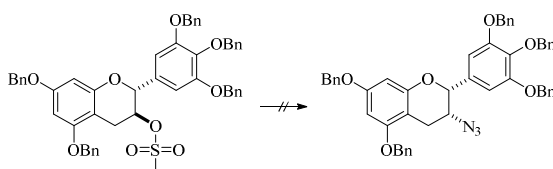
The 3-azidochromane was prepared on the basis of a S_N2 reaction and opens the synthesis of new EGCG derivatives linked by a 1,2,3-triazol unit or by an amide bond. It was obtained to prepare synthetic EGCG derivatives by replacement of the metabolically labile ester group by a 1,2,3-triazole moiety shown in **Scheme 57**. The reaction conditions were optimized based on my own knowledge.



Scheme 57: Illustration of the possible reaction pathways of 3-azidochromane. Reagents and conditions: (a) *trans* **41(a)**, NEt_3 , methanesulfonic anhydride, CH_2Cl_2 , $0\text{ }^\circ\text{C} \rightarrow \text{rt}$; (b) 10.0 eq NaN_3 , DMSO, $60\text{ }^\circ\text{C}$; (c) Staudinger reaction; (d) Click reaction, **85**, 5 mol% CuSO_4 , 10 mol% sodium ascorbate, DMSO $65\text{ }^\circ\text{C}$; (e) Steglich esterification, available benzoic acids illustrated in **Figure 36**; (f) $\text{Pd}(\text{OH})_2/\text{C}$, THF/MeOH (1:1, v/v), rt, 1 atm H_2 .

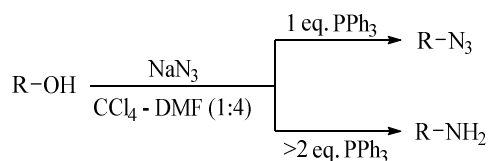
These amide-based analogues can be prepared from previously synthesized *trans*-chroman-3-ol *trans* **41(a)** by substitution with sodium azide in DMF.^[256] A previously performed synthesis using methoxy-chroman-3-ol *cis* **44** with 20.0 eq NaN_3

over 7 days at 140 °C led to a moderate yield of the 3-azidochromane. However, the benzylated product *trans* **41(a)** did not lead to any azido substituted product (**Scheme 58**). Furthermore, the solubility of NaN₃ in DMF was very poor resulting maybe in a decreased reaction. Supported by the high temperature which may lead to a thermally decomposition to give CO and dimethyl amine of DMF. Even after the addition of 15-Krone-5 ether no reaction was observed.



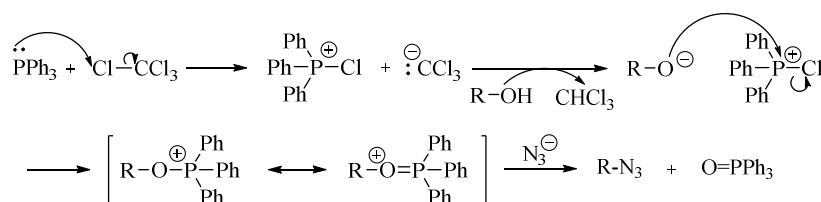
Scheme 58: Nucleophilic substitution with sodium azide. Reagents and conditions: 20.0 eq. NaN₃, DMF, 140 °C.

A modified protocol for the conversion of alcohols to azides/amines was reported by Reddy *et al.*^[257] as an Appel-reaction. Treatment of the alcohol with one equivalent of PPh₃ and NaN₃ in a mixture of CCl₄-DMF (1:4) delivers the azide product, whereas more than two molar equivalents PPh₃ affords the amine (**Scheme 59**).



Scheme 59: Procedure to convert alcohols to azides or amines.^[257]

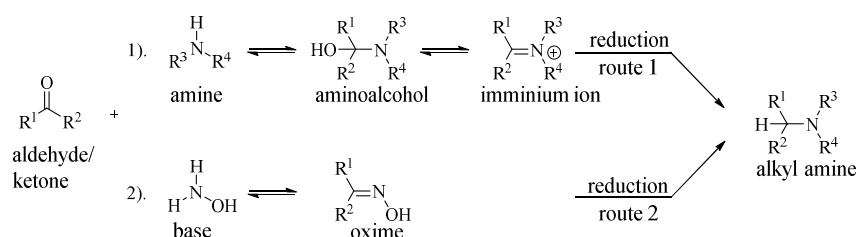
The mechanism of the Appel reaction proceeds *via* the activation of triphenylphosphine with tetrahalomethane. The following attack of the alkoxide generates an oxyphosphonium ion, an intermediate that provides a good leaving group. The S_N2 displacement by azide leads to the inversion of configuration. The driving force of the reaction is the formation of triphenylphosphine oxide (**Scheme 60**).^[258]



Scheme 60: Mechanism of Appel reaction in the presence of NaN₃.^[258]

2.4.2 Synthesis of Racemic 3-Aminochromane by Reductive Amination

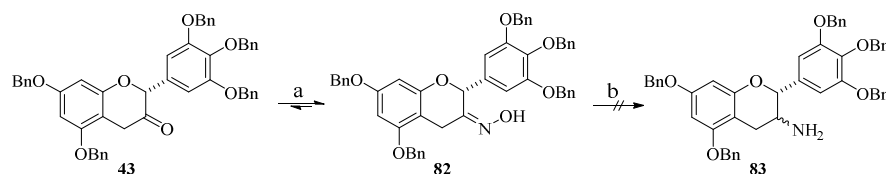
A further attempt to develop nitrogen-containing chromanone derivatives is based on the reductive amination to convert amines to azides: The reductive amination of aldehydes or ketones is a versatile method to prepare amines in biological and chemical systems. The reaction takes place with ammonia or primary-/secondary amines and the relevant aldehyde or ketone in presence of a reducing agent, mostly NaBH_3CN to gain primary, secondary or tertiary amines.^[259]



Scheme 61: General procedures of reductive amination of aldehyde/ketone to amine.^[259-260]

Route 1 (Scheme 61) allows the formation of primary imine intermediates, which are unstable, so the reaction conditions provide secondary and tertiary amines in an unselective way. The second route undergoes a stable oxime intermediate, which can be reduced by hydride sources such as LiAlH_4 , $\text{NaBH}_3(\text{CN})$, or NaBH_4 .^[259]

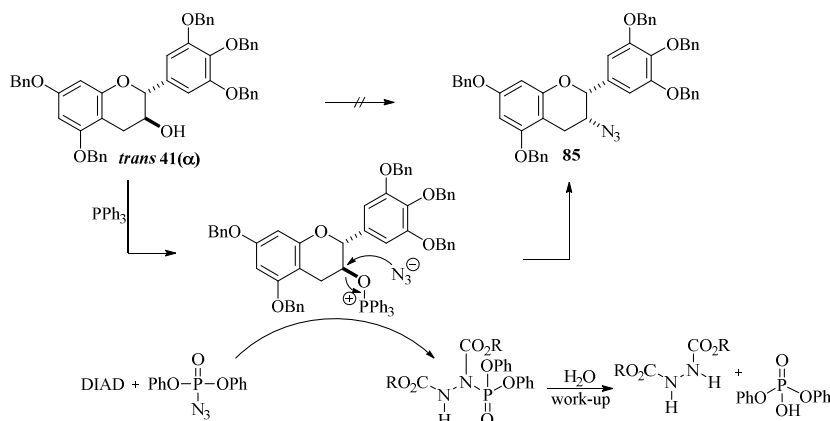
Ayedi *et al.*^[259] described a one-pot reductive amination by the use of hydroxylammonium chloride ($\text{H}_2\text{NOH}\cdot\text{HCl}$) and a subsequent reducing step with zinc in hydrochloric acid. The authors assumed the formation of a complex between the resulting primary amine and Zn^{2+} . Treatment with ammonia in the presence of sodium hydroxide releases the amine. The same procedure was applied to chromanone **43** by treatment with $\text{H}_2\text{NOH}\cdot\text{HCl}$ to convert it into oxime **82**. Subsequent reduction of the oxime by zinc and HCl without isolation did not lead to the desired product (**Scheme 62**).



Scheme 62: Reaction sequence of reductive amination. Reagents and conditions: (a) 1.20 eq $\text{H}_2\text{NOH}\cdot\text{HCl}$, EtOH, rt; (b) 2.50 eq. Zn, 4.00 eq. conc. HCl, EtOH, rt.^[259]

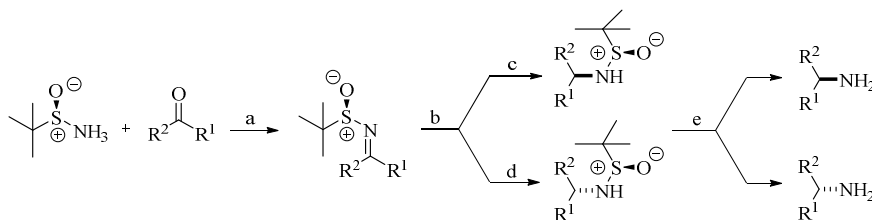
Considering the desired amine was not isolated and it turned out that, due to the smooth reaction condition, the oxime was generated, but the conversion with Zn/HCl was not

successful. Due to the stability of the oxime much more vigorous reagents would be required. A. Feher-Voelger *et al.*^[261] described another approach to convert the alcohol functionality to an azide *via* Mitsunobu conditions:



Scheme 63: Reaction of *trans*-chroman-3-ol *via* Mitsunobu conditions. Reagents and conditions: 1.50 eq DIAD = diisopropyl azodicarboxylate, 1.50 eq DPPA = diphenyl phosphorazidate, 1.50 eq PPh₃.^[261]

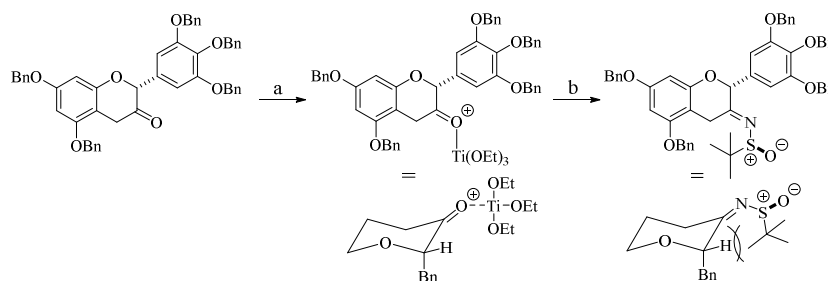
The Mitsunobu reaction showed no transformation of *trans* **41(α)** to the compound **85**, which may be due to the fact that the hydroxy group was not sufficiently transformed to a leaving group for the formation of oxyphosphonium ion with PPh₃. After deprotection of the available hydroxy group the alkoxide could form the key oxyphosphonium ion by the oxophilicity of the phosphor. The oxophosphetane is a very stable species which can be attacked by the nucleophile, but the reaction did not lead to product formation (**Scheme 63**). In 1997, Ellman *et al.*^[262] disclosed the enantioselective synthesis of (*S*)- or (*R*)-*tert*-butanesulfinamide as an auxiliary for the preparation of enantioenriched amines *via* a sulfinyl imine followed by reduction with NaBH₄ or L-Selectride[®] to form the sulfinyl amine product (**Scheme 64**).



Scheme 64: Possible reaction using Ellman's auxiliary.^[262] Reagents and conditions: (a) 2.00 eq Ti(OEt)₄, 1.10 eq ketone, THF, rt; (b) -78°C; (c) 4.00 eq DIBAL-H; (d) 3.00 eq L-Selectride[®]; (e) 4 M HCl.^[263]

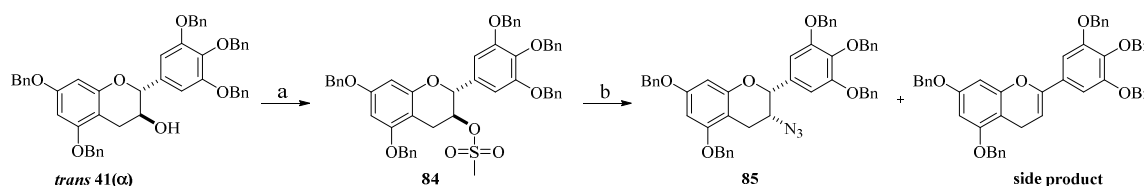
The ketimine synthesis was performed by using 2.00 eq Ti(OEt)₄ as strong Lewis acid for activation of the carbonyl functionality by coordination. However, in the case of

chromanone **43** the formation of the *N*-sulfinyl imine was not observed (**Scheme 65**). This result might be explained by non-binding interactions between the *tert*-butyl group and the equatorially oriented benzyl groups in α -position of the ketimine.



Scheme 65: Reaction of chroman-3-one with Ellman's auxiliary. Reagents and conditions: (a) $\text{Ti}(\text{OEt})_4$, THF, $0\text{ }^\circ\text{C}$; (b) Ellman's auxiliary, THF, $0\text{ }^\circ\text{C} \rightarrow \text{rt}$.^[262]

The last attempt following this strategy was a second nucleophilic substitution based on the reaction presented in **Scheme 66**. *trans*-Chroman-3-ol **trans 41(a)** was first converted to the corresponding methane sulfonate yielding product **84** in 93% without further purification. Subsequent nucleophilic substitution with sodium azide in DMSO affords *cis*-azido chromane **85** in 33% yield with the appropriate *cis*-configuration.^[264] DMSO allowed the strong binding of cations, forming complexes with enhanced solubility. The competition between substitution and elimination should be expected. As byproduct an alkene was obtained by the elimination of the mesylate group. It can be assumed that the large excess of NaN_3 , which served as weak base and the slight temperature of $60\text{ }^\circ\text{C}$ were consistent with obtaining the $\text{S}_\text{N}2$ product, despite the presence of a secondary alcohol.

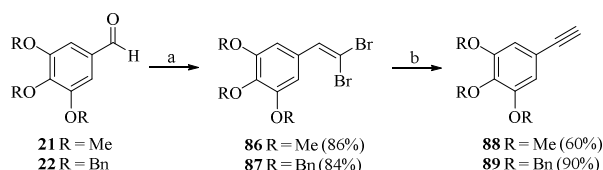


Scheme 66: Synthesis of 3-azidochromane *via* mesylate formation. Reagents and conditions: (a) TEA, methanesulfonyl chloride, CH_2Cl_2 , $0\text{ }^\circ\text{C} \rightarrow \text{rt}$, 93%; (b) 10.0 eq NaN_3 , DMSO, $60\text{ }^\circ\text{C}$, 33%.

Due to the low yield of the desired azide, it was tried to improve the results by the application of crown-15-ether in combination with NaN_3 but no reaction was observed. TMS-N_3 (trimethylsilyl azide) could also be used as possible azide source for halides in azidation.^[265]

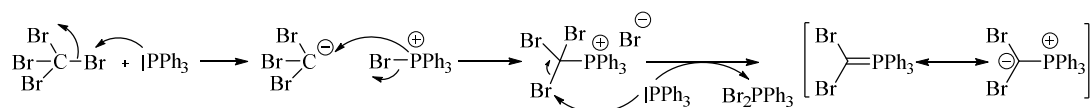
2.4.3 Synthesis of the Alkyne Analogues *via* Corey-Fuchs Reaction

The alkyne analogues **88/89** were synthesized from **21/22** *via* Corey-Fuchs reaction.



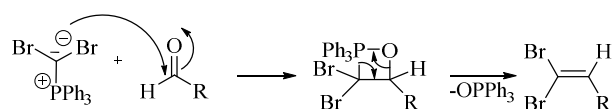
Scheme 67: Corey-Fuchs reaction of aldehydes **21/22** to corresponding alkynes.^[266] Reagents and conditions: (a) CBr_4 , PPh_3 , CH_2Cl_2 ; (b) 2.00 eq *n*-BuLi, THF, -78°C .

In the first step, aldehydes **21/22** were treated with tetrabromomethane in the presence of PPh_3 according to Corey and Fuchs.^[266] Subsequently, dibromo-olefins **86/87** were transformed into the corresponding alkynes **88/89** with 2.00 eq *n*-BuLi.

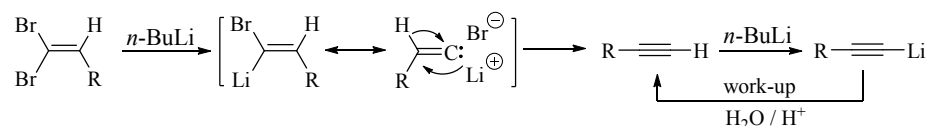


Scheme 68: Mechanism of Corey-Fuchs reaction.^[267]

The Corey-Fuchs reaction is a special variant of the Wittig reaction and allows the preparation of terminal alkynes (**Scheme 68**). The first step was the *in situ* formation of a phosphonium ylide that formed a 1,1-dibromo alkene by reaction with an aldehyde (**Scheme 69**).^[267]



Scheme 69: Formation of 1,1-dibromo alkene. Reagents and conditions: 1.00 eq aldehyde, PPh_3 , CBr_4 , CH_2Cl_2 , rt, **86** (86%), **87** (82%).^[267]

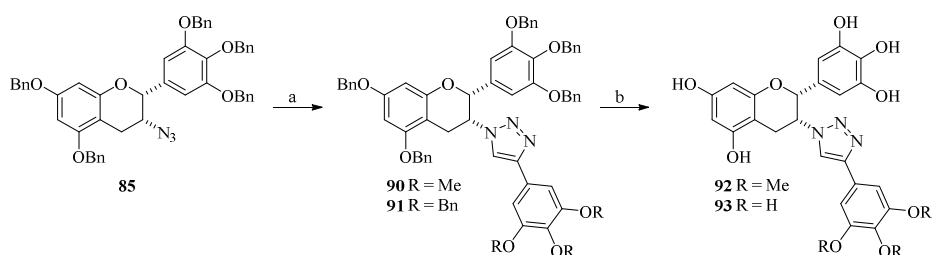


Scheme 70: Formation of alkyne *via* 1,1-dibromo alkene. Reagents and conditions: 2.00 eq *n*-BuLi, -78°C , **88** (60%), **89** (60%).^[267]

Finally, the 1,1-dibromo alkene was treated with 2.00 eq of a strong base such as *n*-BuLi or lithium diisopropylamide to form a vinyl carbenoid, which undergoes [1,2]-rearrangement constituting the alkyne. The second equivalent *n*-BuLi completed the Li-acetylide formation from the alkyne. Aqueous work-up led to the desired alkyne (**Scheme 70**).^[267]

2.4.4 Click-Chemistry of the Alkyne Analogues with 3-Azidochromane

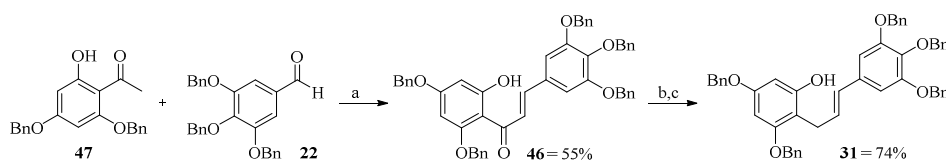
The selective introduction of the azido functionality into the chromane led to a versatile tool suitable for a click reaction with the alkynes **88/89** to give the 1,2,3-triazole moiety as illustrated in **Scheme 71**. The reaction is best performed in DMSO at 65 °C, with the addition of 10 mol% sodium ascorbate as reducing agent and 5 mol% copper sulfate as mentioned in the preceding *chapter 2.3.6* and provided the products **90** in 14% and **91** in 92% yields. The last step was the hydrogenolytic cleavage of the protecting groups which led to the product **93** in 58% yield.



Scheme 71: Click reaction of 3-azidochromane with alkynyl derivatives **88/89** to 1,2,3-triazol compounds **90/91**. Reagents and conditions: (a) 1.00 eq **85**, 5 mol % CuSO₄, 10 mol% sodium ascorbate, DMSO, 65 °C; (b) Pd(OH)₂/C, THF/MeOH (1:1, v:v), 1 atm H₂, rt, **93** (58%).

3. Conclusion and Outlook

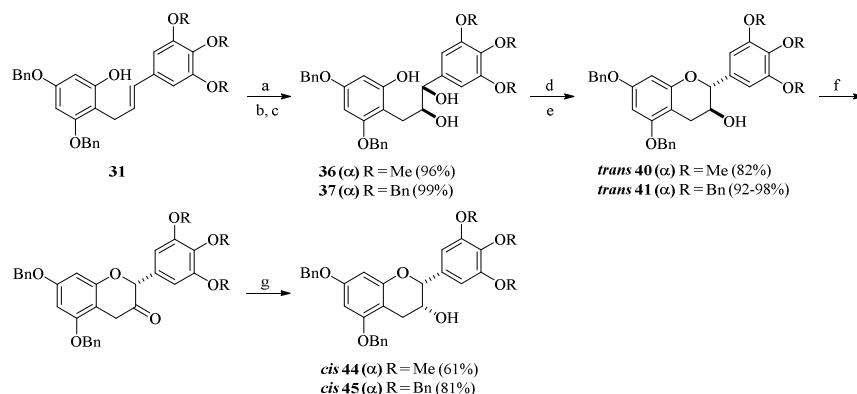
Within the scope of this work, a synthesis of modified EGCG derivatives as well as EGCG derivatives with linked biotin moiety and a fluorescence dye was developed. These compounds were provided for biological testing. A synthesis of the *cis*-chroman-3-ol core using Friedel-Crafts alkylation was feasible but not efficient enough. Therefore, a different strategy was employed, which uses a Claisen-Schmidt condensation for the construction of a chalcone.



Scheme 72: Synthesis of chalcone **46** and desoxygenation to *(E)*-alkene **31**.^[214, 226] Reagents and conditions: (a) 40 wt% KOH (aq.), EtOH, reflux, 55%; (b) TEA, ClCOOEt, THF, 0 °C; (c) NaBH₄, EtOH, CeCl₃·7 H₂O, 74%.

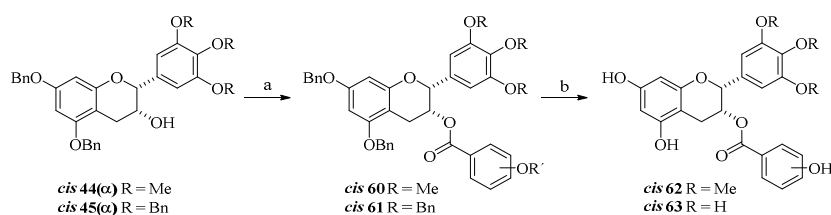
The *(E)*-olefin **31** was synthesized *via* Claisen-Schmidt condensation between aldehyde **22** and acetophenone **47** to chalcone **46** in 55% yield. This was then reduced based on a modified Luche reduction in the presence of cerium chloride to provide *(E)*-olefin in good yield of 74% (**Scheme 72**).

After successful dihydroxylation to compounds **36(a)**/**37(a)**, the cyclization was realized by the reaction of the 1,2-diol with trimethyl orthoacetate forming an *ortho*-ester, followed by methanolysis yielding the desired product *trans* **41(a)** in 92 – 98%. The oxidation-reduction sequence led to the *cis*-chroman-3-ol *cis* **45** by use of L-Selectride[®] and LiBr (**Scheme 73**) in 81% yield.



Scheme 73: Dihydroxylation of (*E*)-alkene followed by cyclization to *cis*-chroman-3-ol.^[165b, 215, 268] Reagents and conditions: (a) TBSCl, imidazole, DMF, rt; (b) AD-mix- α , MeSO₂NH₂, *tert*-BuOH/H₂O/CH₂Cl₂ (1:1:1), 0 °C; (c) TBAF, THF, rt; (d) trimethyl orthoacetate, PPTS, rt \rightarrow 0 °C, BF₃·OEt₂, acetone; (e) MeOH, K₂CO₃, rt; (f) DMP, CH₂Cl₂, rt, 2 h; (g) L-Selectride®, LiBr, THF, -78 °C.

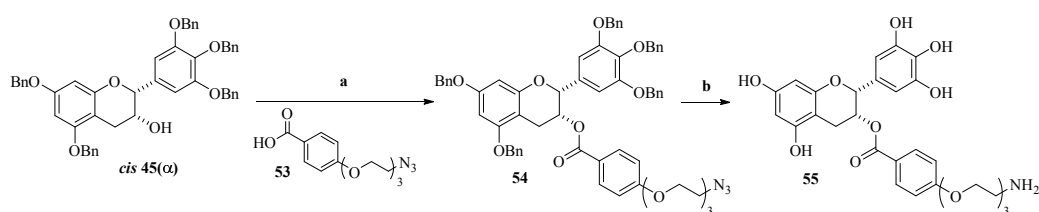
cis-Chroman-3-ol **cis 45**(α) was then transformed into the protected EGCG derivatives **59a-b/60a-b/61a-j** by Steglich esterification with the corresponding carboxylic acids. Finally, the hydrogenolytic cleavage of the protecting groups of the EGCG derivatives led to the unprotected compounds that feature a varying degree of hydroxy substitution at the galloyl ester **D**-ring **62/63** (Scheme 74).



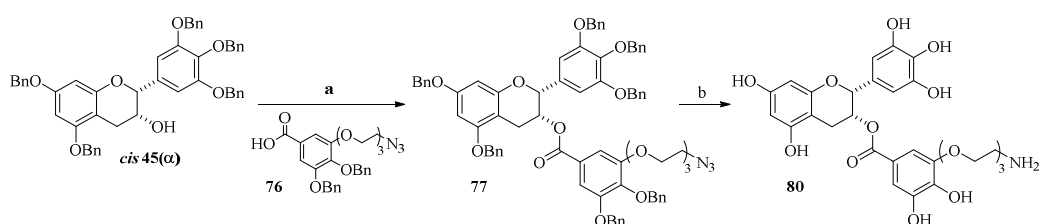
Scheme 74: Steglich esterification and hydrogenolytic cleavage to EGCG derivatives.^[165b, 215] Reagents and conditions: (a) 2.00 eq EDC·HCl, 1.00 eq DMAP, CH₂Cl₂, 0 °C; (b) Pd(OH)₂/C, THF/MeOH (1:1, v:v), rt, 1 atm H₂.

The focus in this work was the synthesis of EGCG analogues lacking phenolic hydroxy groups at the **D**-ring and the modification of the **A**-ring by methoxy groups for a possible higher stability. Our collaborators Prof. E. Wanker and C. Secker *et al.*¹⁸ developed a specific *in cell* assay to identify enhancers of cellular A β 42 degradation as potential candidates for Alzheimer's disease therapy. Using this assay, the potency of different structural EGCG derivatives was examined using this cell-based assay. It is well known that EGCG affects molecular targets, as well as pathways in neurodegenerative disorders. The molecular mechanism of EGCG can be enlightened by structure activity studies to verify structural motives of EGCG, which are necessary for a possible action: in

this assay, a focused library of 20 compounds including EGCG was tested and it was demonstrated that EGCG was most active in reducing intracellular A β 42 aggregates. The next step was the comparison of purchased (Sigma) and synthesized derivatives on increasing cellular A β 42 degradation (*chapter 2.1.12*). It has been suggested that this cellular effect, which induces A β 42 degradation, is caused by a direct effect on the aggregates and not by an effect on a specific pathway in the cells. The conclusion is that the derivatives which stimulate cellular A β 42 degradation are also potent inhibitors of *in vitro* A β 42 aggregation. To further support this, it was of tremendous interest whether EGCG is able to directly target intracellular A β 42 aggregates. As the presence of the 3,4,5-trihydroxyphenyl **B**-ring and the ester-bond were essential for biological activity, synthesis of fluorophore labeled derivatives focused on the modification at the **D**-ring. Following this strategy, two carboxylic acids – one derived from *p*-hydroxybenzoic acid **53** (**Scheme 75**), and the other from gallic acid **77** (**Scheme 76**) – were synthesized incorporating a PEG-linker and an azide functionality.

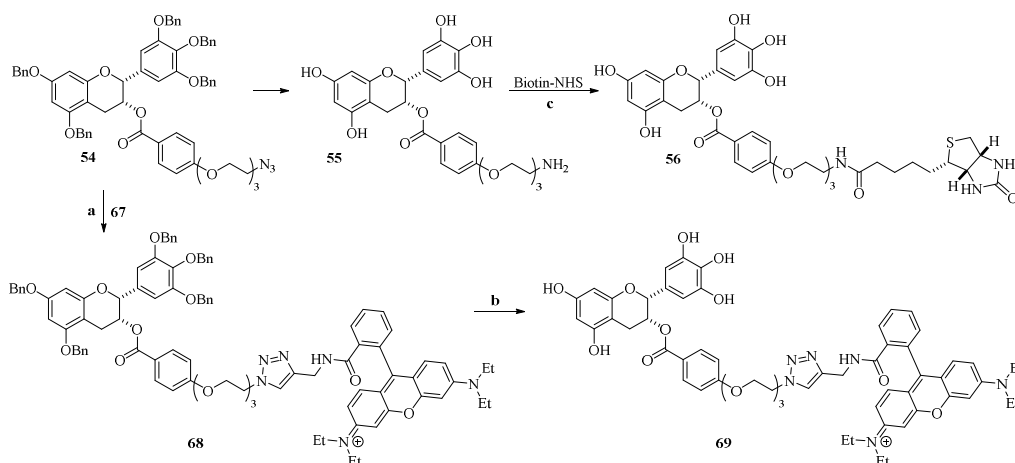


Scheme 75: Synthesis of compound **55** by Steglich esterification of *cis*-chroman-3-ol *cis* **45(α)** and *p*-hydroxybenzoic acid **53**. Reagents and conditions: (a) 2.00 eq **53**, 2.00 eq EDC·HCl, 1.00 eq DMAP, CH₂Cl₂, 0 °C → rt, 89%; (b) Pd(OH)₂/C, THF/MeOH (1:1, v:v), 1 atm H₂, 90%.

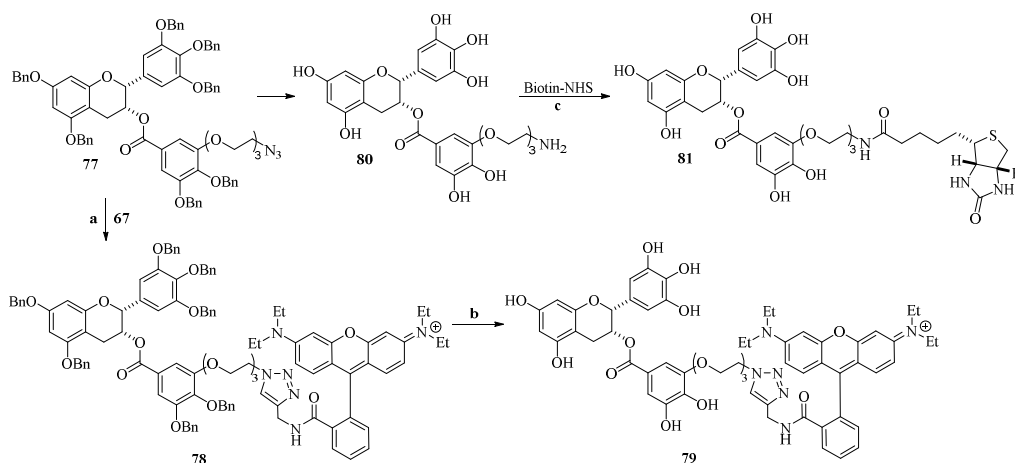


Scheme 76: Synthesis of EGCG derivative **80** by Steglich esterification of *cis*-chroman-3-ol *cis* **45(α)** and a linker functionalized gallic acid. Reagents and conditions: (a) 2.00 eq **76**, EDC·HCl, DMAP, 0 °C → rt, 75%; (b) Pd(OH)₂/C, THF/MeOH (1:1, v:v), 1 atm H₂, 79%.

The first approach towards these compounds involved the coupling with a rhodamine dye *via* Click reaction to products **69/79**, the second was based on hydrogenolytic cleavage of the azide that provided the amine for coupling with biotin to products **56/81** (**Scheme 77/78**).



Scheme 77: Synthesis of dye-EGCG **69** and biotin coupled EGCG derivatives **56**. Reagents and conditions: (a) **67**, 5 mol% CuSO₄, 10 mol% sodium ascorbate, DMSO, 65 °C, **68** (83%); (b) Pd(OH)₂/C, THF/MeOH (1:1, v:v), 1 atm H₂, **69** (89%); (c) 1.00 eq biotin-NHS, DMF, rt, **56** (79%).



Scheme 78: Dye-linked EGCG **79** and biotin-coupled EGCG derivatives **81** with gallic acid. Reagents and conditions: (a) **67**, 5 mol% CuSO₄, 10 mol% sodium ascorbate, DMSO, 65 °C, **78** (87%); (b) Pd(OH)₂/C, THF/MeOH (1:1, v:v), 1 atm H₂, **79** (87%); (c) biotin-NHS, DMF, rt, **81** (57%).

According to the biological results in **Figure 44**, the rhodamine labeled EGCG derivative **79** showed clear co-localization with intracellular HiLyte488-labeled A β 42 aggregates with $r = 0.91$ (Pearson's correlation coefficient). In contrast, the control compound **101** lacking the *cis*-chroman-3-ol moiety showed no significant aggregation (**Figure 50**).

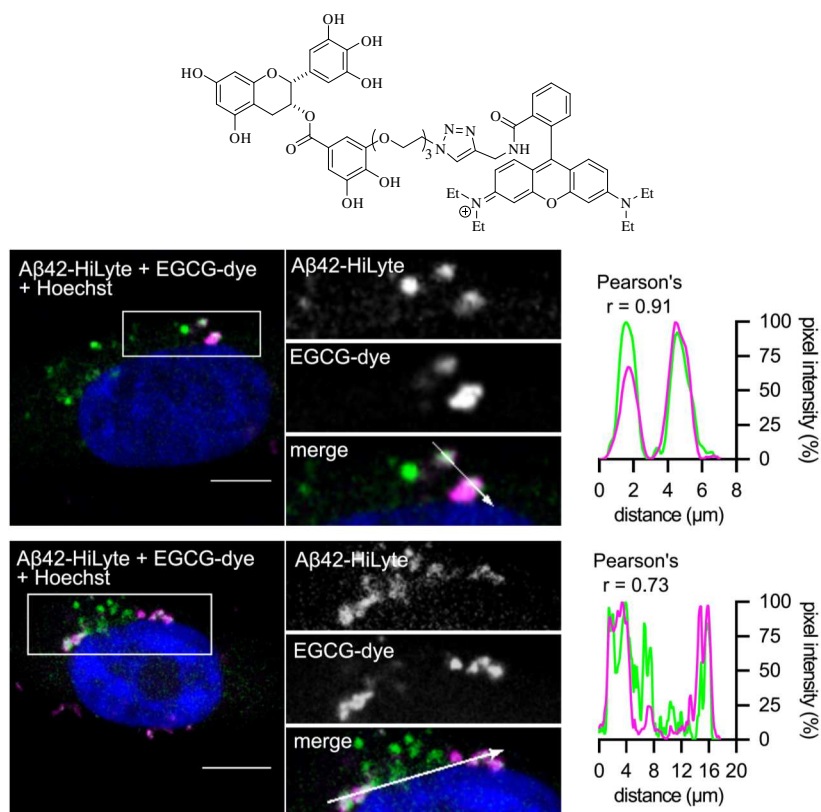


Figure 44: Investigation of compound **79** (on top) in cell-based assay *via* confocal microscope, EGCG-Aβ42 in cell co-localization (below). The data was provided by C. Secker and Prof. E. Wanker.¹⁸

The rhodamine-coupled derivatives showed direct binding of EGCG to the Aβ42 aggregates in the cells. All this strongly suggests that the cellular degradation mechanism is mediated by direct binding and not by an effect of the compound on other cellular components.

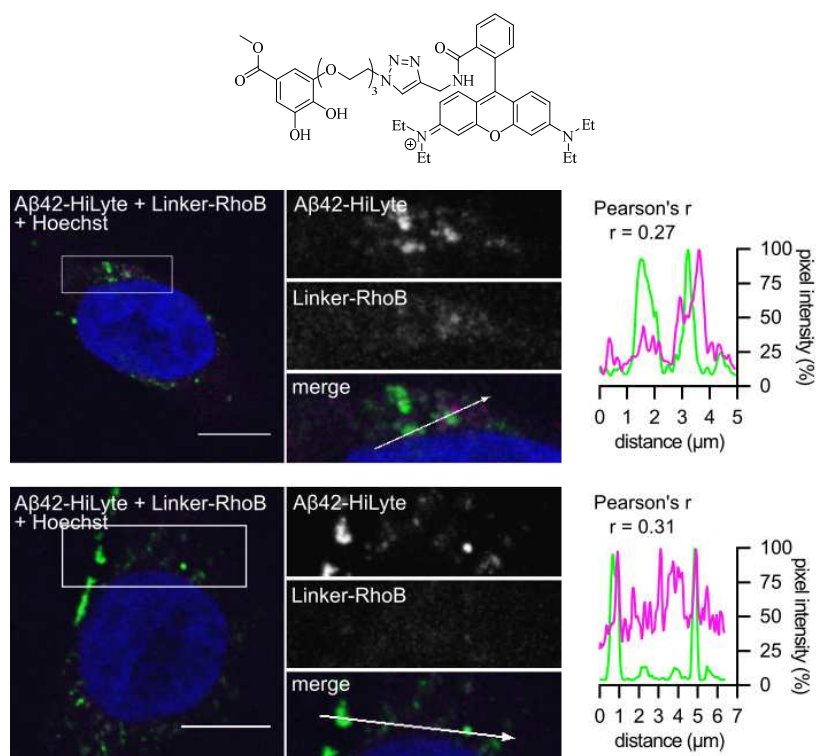
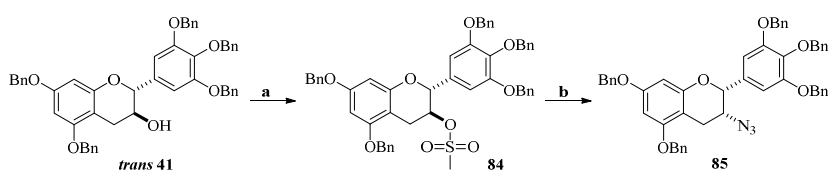
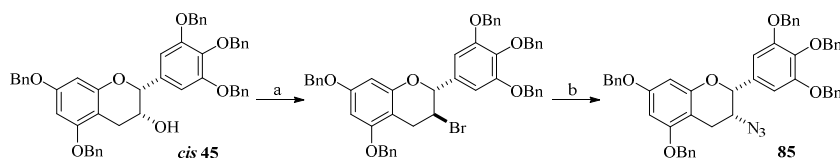


Figure 45: Analysis of compound **101** (on top) in cell-based assay *via* confocal microscope, control compound **101** in cell co-localization (below). The data was provided by Prof. E. Wanker and C. Secker.¹⁸

The work performed within this thesis opened a route to EGCG analogues containing an azide linker – a novel approach that has not yet been reported in literature. The azide analog was prepared from the alcohol *via* a mesylate **84** (Scheme 79), followed by nucleophilic displacement with NaN_3 in DMSO in 33% yield.



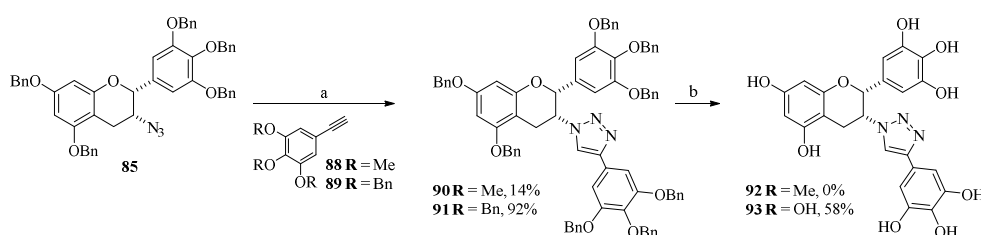
Scheme 79: Synthesis of novel azido-EGCG derivatives **85**. Reagents and conditions: (a) TEA, methanesulfonyl anhydride, CH_2Cl_2 , $0\text{ }^\circ\text{C} \rightarrow \text{rt}$, 93%; (b) 10.0 eq NaN_3 , DMSO, $60\text{ }^\circ\text{C}$, 33%.



Scheme 80: Possible Appel reaction for the synthesis of azide **85**. Reagents and conditions: (a) CBr_4 , PPh_3 ; (b) NaN_3 , DMSO.

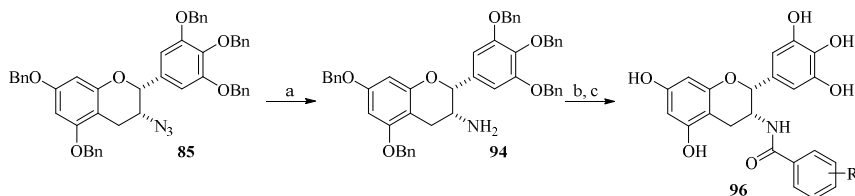
Additionally, future attempts could be performed by the conversion of the alcohol to the corresponding alkyl halide and followed by azidation, according to an Appel reaction to obtain an increased yield (**Scheme 80**).

The alkynes **88/89** were successfully synthesized both in 60% yield *via* Corey-Fuchs reaction starting from aldehyde **21/22**. The desired azide **85** was used for the Click reaction with the alkyne derivatives **88/89** to build up 1,2,3-triazols **90/91**. Compound **91** was obtained in 92% yield. The final hydrogenolytic cleavage led to 58% of unprotected EGCG derivative **93** (**Scheme 81**). The biological data of compound **93** is pending at the time.



Scheme 81: Synthesis of compound **93** with substituted ester moiety. (a) 1.00 eq **89**, 5 mol % CuSO_4 , 10 mol% sodium ascorbate, DMSO, 65 °C, **91** (92%); (b) $\text{Pd}(\text{OH})_2/\text{C}$, THF/MeOH (1:1, v:v), 1 atm H_2 , rt, **93** (58%).

Future attempts of azide **85** would include the Staudinger reaction, which converts azides to amines by mild reduction with PPh_3 and aqueous work up to amine **94**.

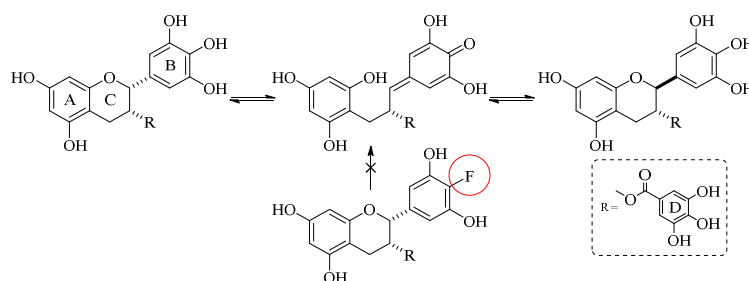


Scheme 82: Synthesis of amines **94** by Staudinger reaction of azide **85**. Reagents and conditions: (a) Staudinger reaction, PPh_3 , THF; (b) Steglich esterification, compounds illustrated in **Figure 57**; (c) $\text{Pd}(\text{OH})_2/\text{C}$, THF/MeOH (1:1, v/v), rt, 1 atm H_2 .

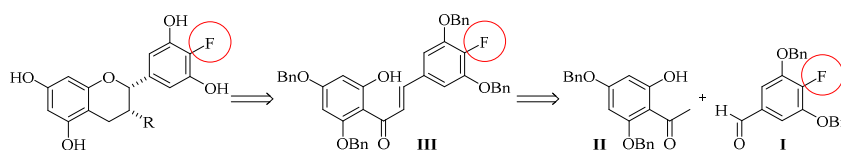
The following Steglich esterification with protected benzoic acids (**Figure 36**) would allow the formation of EGCG analogues containing an amide bond after successful cleavage of the benzylated groups.

All these compounds will have to be investigated with respect to their effectiveness based on the elucidation of the molecular mechanistic properties of EGCG in AD. In addition, it needs to be investigated whether the beneficial effects of compounds with a triazol moiety leads to more satisfactory results than the ester moiety in the natural compound. Many

in vitro studies demonstrated effects of EGCG as potential therapeutic target but problems occur with the oral administration of EGCG: while in clinical trials (NCT00951834)²⁰ daily doses of 800 mg EGCG were given without disadvantageous effects,^[269] the inherent properties of EGCG relating to the bioavailability, the oxidation sensitivity and the very fast metabolism complicated the successful and potential therapeutic application.^[2, 143] It would be interesting to examine the possible suppression of the epimerization which is caused by deprotonation of the *para*-hydroxy group on the **B**-ring (**Equation 1**) and leads to the disadvantages mentioned above. The *para*-hydroxy group would be replaced by a fluorine, which could be introduced by the chalcone formation **III** of acetophenone **II** and aldehyde **I** (**Equation 2**).



Equation 1



Equation 2

Treatment of dye-labeled EGCG with A β 42 indicated an EGCG binding direct to A β 42 (**Figure 42**). It has to be examined how these interactions between EGCG and the protein become apparent. According to the reduced ThT fluorescence impact, it is to be assumed that the 3,4,5-trihydroxyphenyl **B**-ring was essential for the aggregation with A β 42, so the binding could occur by hydrogen bonding between hydroxy groups and A β 42. However, studies with EGCG analogues containing 3-fluoro groups on the **B**-ring have not yet been tested and allow a new approach.

²⁰ Clinical trial Sunphenon EGCg (Epigallocatechin-Gallate) in the Early Stage of Alzheimer's Disease (SUN-AK). 2013 (Accessed at <http://clinicaltrials.gov/show/NCT00951834>).

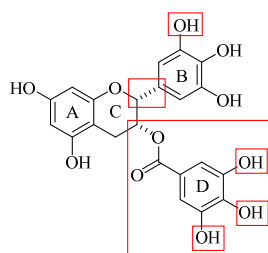
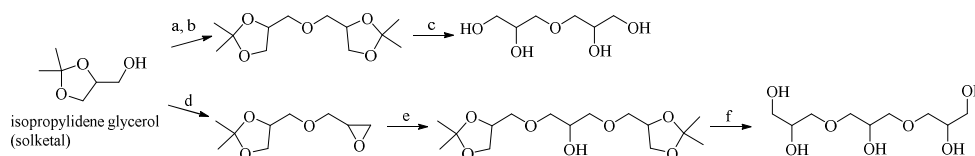


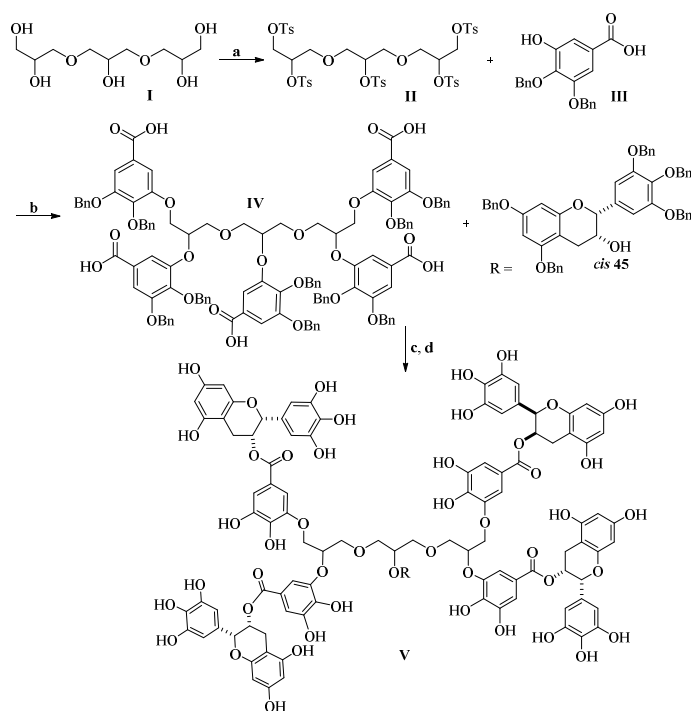
Figure 46: Relevant structural elements for *in vitro* and *in cell* potency of EGCG.

Future investigations could focus on the synthesis of multivalent EGCG targets tethered by a flexible polyether spacer. Iaych *et al.*^[270] investigated a polymerization method of glycerol carbonate to form an ether- or carbonate linkage by nucleophilic attack of the hydroxy group of glycerol carbonate (**Scheme 83**).



Scheme 83: Microwave-assisted synthesis of linear di- or tri-glycerols. Reagents and conditions: (a) NaH, DMF; (b) isopropylidene glycerol tosylate; (c) Dowex 50WX8, MeOH; (d) aq. 50% NaOH, hexane, Bu₄NBr (cat.); (e) isopropylidene glycerol, aq. 50% NaOH, hexane, Bu₄NBr (cat); Dowex 50WX8, MeOH.^[270]

The hyperbranched polymeric material is equipped with many hydroxy groups, which could be converted to tosylate **II**. The gallic acid **III** (for synthesis see *chapter 2.3.3*) contains one available hydroxy group for the coupling with tosylated polyether spacer **II**. After successful coupling to product **IV**, the following esterification would be performed with protected *cis*-chroman-3-ol **cis 45(α)**. Finally, the protecting groups should be removed to gain a highly functionalized EGCG target with flexible spacer.



Scheme 84: Synthesis of hyperbranched EGCG derivative. Reagents and conditions: (a) *p*-Toluenesulfonyl chloride, KOH, CH₂Cl₂; (b) Cs₂CO₃, DMF; (c) 2.00 eq EDC·HCl, 1.00 eq DMAP, CH₂Cl₂, 0 °C; (d) Pd(OH)₂/C, THF/MeOH (1:1, v/v), rt, 1 atm H₂.

In 1974, Haslam examined the enzymatic activity of galloylated D-glucoses with standard protein bovine serum albumin (BSA).^[271] This exemplified a hydrogen bond development between the ketoamide moiety of β -pleated sheet fragment of the enzyme and the gallotannic β -PGG structure (**Figure 46**). It was also verified, that polyphenols developed strong interactions to proline-rich proteins (PRPs).^[272]

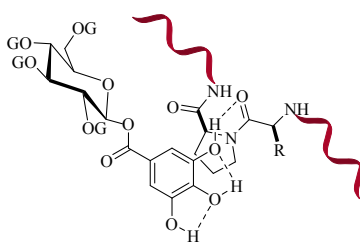


Figure 47: Possible interaction of β -PGG galloyl group and enzyme by hydrogen-bond, G = galloyl (3,4,5-tri-*O*-benzylgallic acid).^[271]

In this case, a high number of galloyl groups on a D-glucopyranose would encourage the protein-binding capacity after complete saturation of the β -PGG structure.^[271] On this basis, future investigations could be established on the substitution of the galloyl groups by EGCG of the β -D-glucopyranose to examine the interaction. This synthesis would start from the tosylated β -D-glucopyranose which would be coupled with the available hydroxy

group of protected gallic acid. Followed by Steglich esterification with the *cis*-chroman-3-ol **45(a)** to the corresponding ester. The hydrogenolytic cleavage would yield the completely deprotected sugar (**Figure 47**). This highly functionalized molecule would exemplify the optimal construction for protein binding. It could be of great interest to explore the mechanism of inhibition or interactions in pathways to amyloidogenesis as therapeutic agents for the treatment of neurodegenerative diseases.

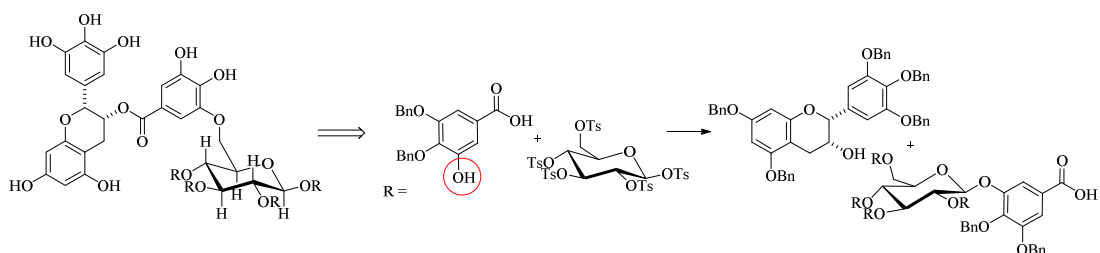


Figure 48: EGCG on a D-glucopyranose core, R = EGCG.

4. Experimental

4.1 Analytics

4.1.1 Nuclear Magnetic Resonance Spectroscopy (NMR)

¹H- and ¹³C-NMR-spectra were measured at room temperature using a Bruker Avance III – 300 (300 MHz) or Bruker Avance III – 600 (600 MHz) and decoupled. The chemical shifts were referenced to residual chloroform (¹H 7.26 ppm, ¹³C 77.16 ppm), dimethyl sulfoxide (¹H 2.50 ppm, ¹³C 39.7 ppm) or methanol (¹H 3.35 or 4.78 ppm, ¹³C 3.35 or 49.3 ppm) peaks. The order of citation in parentheses is a) multiplicity (s = singlet, d = doublet, t = triplet, q = quartet, ABq = AB quartet, dd = doublet of doublet, td = triplet of doublet, m = multiplet, br = broad), b) coupling constants in Hertz (Hz), c) number of protons, and d) assignment.

4.1.2 Electrospray Ionization Mass Spectrometry (ESI-MS)

ESI is a method which is called electrospray ionization mass spectrometry (ESI-MS). ESI allows very little fragmentation by soft ionization. All ESI-MS were measured on UHR-QTOF maXis 4 G (Bruker Daltonics) and HRMS (ESI) on Ion-Trap-API-mass spectrometer Finnigan LCQ Deca (Thermo Quest). Sample inlet was performed *via* over syringe pump.

Mass area to m/z 2000; expandable to m/z 4000

Data system: Xcalibur

4.1.3 Thin-Layer Chromatography (TLC)

Thin-layer chromatography (TLC) is a chromatographic technique, which allows the purification of mixtures of compounds and for fast control of reactions. TLC was performed on a sheet of aluminium foil that is laminated with a thin layer of silica gel 60 Å (stationary phase). The TLC was performed in an eluent enriched atmosphere inside a TLC chamber. The samples that are dissolved in the mobile phase were applied to the TLC plates by

spotting with the help of a capillary. Reactions were monitored by thin-layer chromatography using aluminum foil backed silica gel from Macherey-Nagel (ALUGRAM® Xtra SIL G/U254) with fluorescence indicator or thin-layer chromatography using aluminum foil backed silica gel 60 RP-18 F254s from Merck. Finally, TLC-separations were controlled using a UV lamp with a wavelength of 254 nm. For preparative TLC the following equipment was used: Chromatography sheet TLC 20 x 20 cm, aluminium sheets precoated with silica gel 60 F254 from Merck. For purification by column chromatography silica gel 60 from Fischer Scientific (Acros Organics, ultrapure, 40 – 60 µm, 60 Å) and aluminum oxide (Brockmann act. III) from Macherey-Nagel (50 – 200 µm) were used. Or aluminum oxide activated, neutral Brockmann activity I. Visualization was achieved by the quenching of UV fluorescence ($\lambda_{\text{max}} = 254 \text{ nm}$) or by staining with potassium permanganate solution.

4.1.4 High Performance Liquid Chromatography (HPLC)

For purifications by high performance liquid chromatography, an HPLC system equipped with a Merck column (LiChrospher® Si 60 (5 µm)), a HITACHI L-4000 UV detector and a gradient pump (L-6250 Intelligent Pump) with fraction collector (L-7650 Fraction Collector) were used. All samples were filtered with syringe filters (13 mm, 0.2 µm PTFE membrane). Enantiomeric excess was determined using a Hitachi LaChrom® High Performance Liquid Chromatography (HPLC) system equipped with Daicel CHIRALPAK® IA, IB or IC prepacked chiral columns (0.46 cm x 25 cm) and all samples were dissolved in HPLCgrade *n*-hexane (5 mg/mL) and filtered before measuring through VWR 13 mm syringe filters (0.2 µm PTFE membrane).

HPLC column: LiChrospher® Si 60 (5 µm) from Merck
 Maximum pressure 4350 PSI

HPLC equipment: Merck HITACHI L-4000 UV Detector
 L-6250 Intelligent Pump
 L-7650 Fraction Collector

HPLC for analytical samples

HPLC column: Si 60, 25 cm, 4.6 mm diameter from Merck

HPLC chiral column: Chiralpak® IB 0.46 cm Ø x 25 cm, DAIC 81325
 Chiralpak® IC 0.46 cm Ø x 25 cm, DAIC 83325

HPLC equipment: VWR HITACHI, Elite LaChrom, UV-Detector L-2490
 VWR HITACHI, Elite LaChrom, UV-Detector L-2400
 VWR HITACHI, Elite LaChrom, Autosampler L-2200
 VWR HITACHI, Elite LaChrom, Pump L-2130

HPLC conditions for compounds **37(α)** and **37(β)** (dihydroxylation):

Retention times for the enantiomers were first determined on racemic mixtures.

Retention time for enantiomers: **37(α)** = 17.773 min, **37(β)** = 16.690 min

Column: CHIRALPAK® IB, *n*-hexane (0.1 % isopropyl alcohol):EtOAc, 85:15, flow rate: 0.85 mL/min.

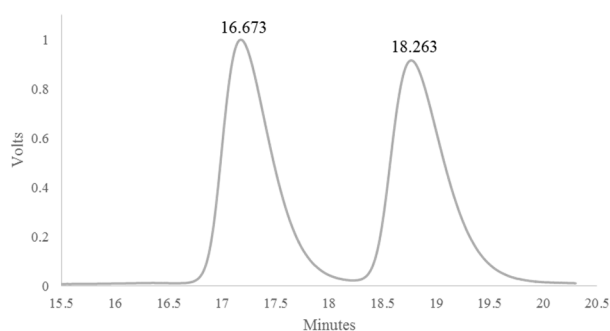


Diagram 1: HPLC trace (UV detection) of racemic diol **53**.²¹

Table 8: Summary of enantiomeric excess of racemic diol **53**.

Retention Time [min]	Area	Area %	Height	Height %
16.673	20396527	49.74	630527	52.20
18.263	20608475	50.26	577465	47.80
Total	41005002	100.0	718463	100.0

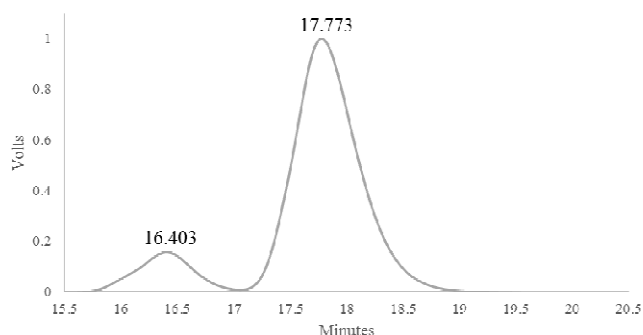


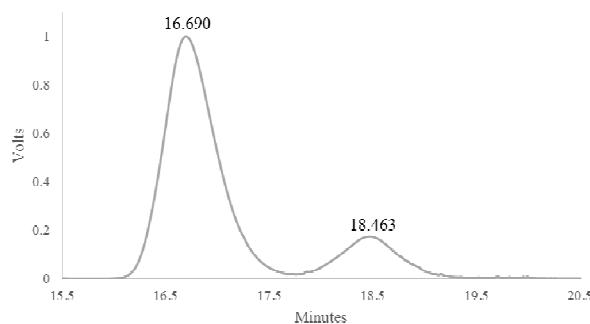
Diagram 2: HPLC diagram of enantiomeric excess of AD-mix- α product.²²

²¹ Method: *n*-hexane (0.1 % isopropyl alcohol):EtOAc, 85:15, flow rate: 0.85 mL/min, CHIRALPAK® IB.

²² HPLC conditions: *n*-hexane (0.1 % isopropyl alcohol):EtOAc, 85:15, flow rate: 0.85 mL/min, CHIRALPAK® IB.

Table 9: Summary of enantiomeric excess of diol **37(α)** (the dihydroxylation was performed with AD-mix- α).

Retention Time [min]	Area	Area %	Height	Height %
16.400	3618056	12.57	98512	13.71
17.773	25174617	87.43	619951	86.29
Total	28792673	100.0	718463	100.0

**Diagram 3:** HPLC diagram of dihydroxylated product with AD-mix- β .²³**Table 10:** Summary of enantiomeric excess of diol **37(β)** (the dihydroxylation was performed with AD-mix- β).

Retention Time [min]	Area	Area %	Height	Height %
16.690	22668819	83.53	618861	85.25
18.463	4471311	16.47	107059	14.75
Total	28792673	100.0	718463	100.0

HPLC conditions for compounds *cis*-chroman-3-ol **cis 45:**

Retention times for the enantiomers were first determined on racemic mixtures.

Retention time for enantiomers: **cis 45** (2*S*,3*S*)-configuration = 10.640 min, **cis 45(α)** (2*R*,3*R*)-configuration = 13.943 min.²⁴

Retention time for product **cis 45(α)** (2*R*,3*R*)-configuration = 14.130 min.²⁴

²³ **HPLC conditions:** *n*-hexane (0.1 % isopropyl alcohol):EtOAc, 85:15, flow rate: 0.85 mL/min, CHIRALPAK® IB.

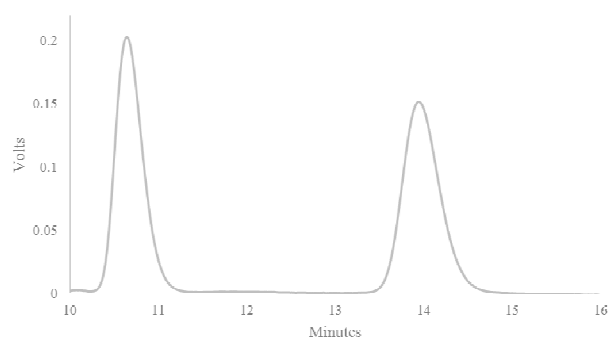


Diagram 4: HPLC chromatogram of racemic chroman-3-ol.²⁴

Table 11: Summary of enantiomeric excess of racemat.

Retention Time [min]	Area	Area %	Height	Height %
10.640	8364521	49.10	382668	57.07
13.943	8671166	50.90	287853	42.93
Total	17035687	100.0	670521	100.0

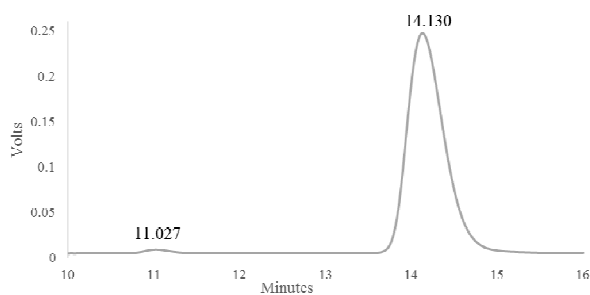


Diagram 2: HPLC chromatogram of *cis*-chroman-3-ol *cis* **45**.²⁴

Table 12: Summary of enantiomeric excess of *cis*-chroman-3-ol *cis* **45** (*2R,3R*)-configuration (the dihydroxylation was performed with AD-mix- α).

Retention Time [min]	Area	Area %	Height	Height %
11.027	387427	1.10	19266	1.63
14.130	34868988	98.90	1160136	98.37
Total	35256415	100.0	1179402	100.0

²⁴ HPLC conditions: *n*-hexane:EtOAc, 75:25, flow rate: 0.6 mL/min, 247 nm, CHIRALPAK® IC.

4.1.5 Absorption and Emission Spectroscopy.

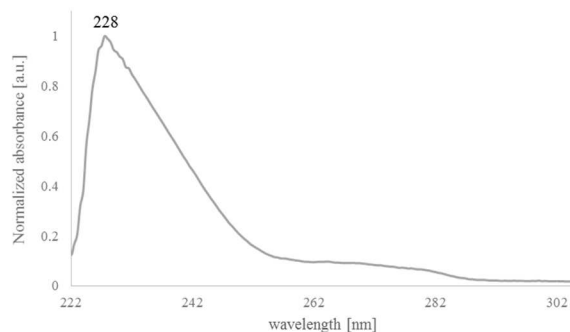


Diagram 5: Absorbance of *cis*-chroman-3-ol.

The absorption spectra were recorded on a Lambda 19 from Perkin Elmer and the emission spectra on an LS55 from Perkin Elmer. The solvents used corresponded to the purity grades HPLC grade or p.a.

$$[a]_v = \frac{1}{\lambda_{\max \text{ abs.}}} - \frac{1}{\lambda_{\max \text{ em.}}}$$

4.1.6 IR Spectroscopy

IR spectra were recorded using a Jasco FT/IR-6200 spectrometer for probes, which were applied as films on a NaCl single crystal. Evaluation was done using the supplementary software. IR spectra for probes, which were measured as solid were recorded using a Shimadzu IR Affinity-1 (Fourier Transform infrared spectrophotometer). The absorption bands are given in wave numbers (cm^{-1}) and intensities are reported as follows: s: strong, m: medium, w: weak, br: broad band.

4.1.7 Melting Point Determination

Melting points were determined using a Büchi Melting Point B-540 apparatus and were not corrected.

4.1.8 Specific Rotation

Specific rotations were measured on a Perkin Elmer 341 polarimeter at the indicated concentration, temperature, and with the specified solvent using a sodium lamp (589 nm).

4.2 Methods for Biological Determination

The biological results were recorded and evaluated at Max Delbrück Center for Molecular Medicine by Prof. E. Wanker and C. Secker in Berlin.¹⁸

4.2.1 A β 42 Peptide Stock Solution

Synthetic A β 42 peptides were formed *via* solid-state peptide synthesis (Bachem, H-1368) and dissolved in (1,1,1,3,3,3)-Hexafluoroisopropanol (HFIP) overnight. After sonication for 30 min, the peptides were aliquoted and lyophilized with a vacuum concentrator (Savant SpeedVac Plus, SC110A). A monomeric A β solutions (200 μ M) were produced from HFIP treated peptides due to the dissolution of the lyophilized peptides in 10mM NaOH, followed by water bath sonication (Bandelin SONOREX Digitec) for 5 min and dilution in low salt buffer (NSP) to relevant assay concentration. The processing, including the lyophilization and the handling of A β 42 solutions were done in Protein Lobind tubes (Eppendorf) for minimized binding of peptides to plastic surfaces.

4.2.2 Fluorescent Labeling of A β 42 Aggregates

A 20 μ M A β 42 peptide stock solution was diluted in NSP buffer and mixed with 5% A β 42 peptides, for fluorophore labeled A β 42 aggregates which have been equipped at the *N*-terminus with the fluorophore 5-Carboxytetramethylrhodamine (TAMRA) (Bachem, H-7448) or HiLyteTM Fluor 488 (HiLyte) (AnaSpec, AS-60479-01) in solid-state peptide synthesis. The desired A β 42 peptide solutions aggregated at 37 °C for 18 h under constant agitation (300 rpm) and by subsequent tip sonication (Branson Ultrasonicator 450) at lowest intensity for 1 min.

4.2.3 Neuroblastoma Cell Culture and Treatment with A β 42(-TAMRA) Aggregates

SH-EP cells (RRID: CVCL_0524) were cultivated in Dulbecco's modified eagle medium (DMEM) consisting of 10% FCS (fatal calf serum), 5% D-glucose, 100 units/mL penicillin and streptomycin. Incubation was performed at 37 °C with 5% (v/v) CO₂. For A β 42

aggregation, the cells were dealt with 600 nM or 1 μ M unlabeled or A β 42-TAMRA aggregates by direct infusion into the cell culture medium.

4.2.4 Automated Fluorescence Microscopy and Quantification of Aggregate Loads

For indicated timeframes, cells were mixed with A β 42-TAMRA aggregates. A β 42 consisting medium was aspirated for removal of non-incorporated and surface-bound aggregates. These cells were washed with PBS (phosphate buffered saline), trypsinized and collected in fresh medium. The cells were plated into 96-well cell culture plates (BD Flacon, 353219) at an initial density of 4.5×10^4 cells per cm^2 . After adhesion for 3 h, the cells were fasten in 2% paraformaldehyde (PFA) for 20 min at rt and nuclei staining with Hoechst 33342 (1:2500, Life Technologies). The cells were washed twice with PBS before fluorescent microscopy in a high-content screening system (HCS) by usage of an objective with 20-fold magnification (CellomicsTM ArrayScan VTI HCS, ThermoFisher Scientific). After image completion, an automated data analysis – the HCS analysis software – (ThermoFisher Scientific) was used. The quantification was performed by detection of individual cells from Hoechst fluorescent signals (Ex/Em 353/483 nm) and total TAMRA fluorescent areas per cell (Ex/Em 555/580 nm) were measured and calculated from technical triplicates.

4.2.5 Screening of EGCG Derivative Library

The commercially available EGCG compound was purchased from Sigma-Aldrich. Compounds **65 b**, **65 c**, **65 d**, **65 g**, **65 h**, **56**, **69**, **79**, **81** and **101** were synthesized at the Heinrich-Heine University Düsseldorf by own knowledge in the work group of Prof. Dr. Constantin Czekelius. The compounds were used at analytical grade (> 95% purity or higher) and dissolved in DMSO at 20 mM or 60 mM and stored at -20 °C or -80 °C. For testing of the cellular A β 42 degradation promoting effect of the compounds, the cells were treated at first with A β 42-TAMRA for 6 h as mentioned above, then washed with PBS, trypsinized and collected. Cells with stocked A β 42-TAMRA aggregate were seeded onto 10 μ M compound dilution or DMSO as control. Finally, incubation was done for 20 h. For data analysis determination of cellular A β 42 aggregates loads and previously automated fluorescent microscopy were carried out as already mentioned in *chapter 4.2.4*. For kinetic determination of A β 42 *in vitro*, 20 μ M A β 42 peptide solutions were treated as mentioned

before and equimolar amounts of Thioflavin T (ThT) (Sigma-Aldrich, T3516) in 384-well microtiter plates (BD Falcon, 353962) were added. For testing compounds equimolar amounts of EGCG, compounds or DMSO, as control were mixed to the in vitro A β 42 aggregation reactions (total volume 40 μ L). The fluorescence intensities (Ex/Em 420/485 nm) were recorded at intervals of 20 min in a fluorescence microplate reader (Tecan M1000).

4.2.6 Confocal Microscopy

For determination on confocal microscope, 9.0×10^4 SH-EP cells per well were plated on fibronectin coated (1:100) cover slips in 24-well cell culture plates (Greiner, 662160). After cell adhesion for 3 h, the cover slips were relocated to conventional microscope slides by the use of fluorescence mounting medium then image acquisition with a Leica SP5 confocal microscope was recorded (Advanced Light Microscopy Facility, MDC). The cells were analyzed form Hoechst fluorescent signals, the co-localization analysis was performed by an ImageJ software (Fiji, RGB Profiles Tool).

4.2.7 Co-localization Studies of EGCG and Intracellular A β 42 Aggregates

SH-EP cells were mixed with 600 nM A β 42-TAMRA or A β 42-HiLyte aggregates for 6 h as mentioned above, followed by trypsinization and washing for removal of extracellular and surface-bound aggregates. 9.0×10^4 cells per well were plated onto fibronectin (1:100) and poly-L-lysine (1:100) coated cover slips in 24-well cell culture plates. The cells were mixed with 30 μ M of biotin- **56/81** or rhodamine-labeled EGCG derivatives **69/79** and DMSO or control compound **101**. SH-EP cells were located in 2% PFA after 3 h of incubation and arranged for confocal microscopy. The fixed biotin-labeled EGCG derivatives were treated with 0.1% Triton X-100 and stained with Streptavidin-Cy5 (Molecular Probes/ThermoFisher Scientific, SA1011). Fluorescence signals were detected by Hoechst (Ex/Em 555/580 nm), HiLyte (Ex/Em 488/528 nm), Cy5 (Ex/Em 649/670 nm) and Rhodamine B (Ex/Em 553/627 nm) at the appropriate wavelength.

4.3 Solvents

The used solvents were purely or purified and/or dried by conventional methods. To dry dimethyl sulfoxide, *N,N*-dimethylformamide 4 Å molecular sieves were used. Methanol was distilled over magnesium and stored over 3 Å molecular sieves. The solvents diethyl ether, tetrahydrofuran, dichloromethane, toluene, and pentane were purchased from Sigma-Aldrich and were dried by a MBraun (MB-SPS-800) solvent purification system (residual water ± 5 ppm). THF and methanol as well as deuterated methanol were degassed by using the method “freeze-pump-thaw”. Acetonitrile and water (HPLC quality) were degassed in an ultrasound bath. Other solvents were used in technical grade. Ethyl acetate and *n*-hexane were used for column chromatography and were distilled in vacuum on rotary evaporator before use.

4.4 General Work Technique

The reactions, unless otherwise stated, were performed under exclusion of oxygen and moisture by Schlenk technique. These are used on a laboratory scale by using a combined vacuum and laboratory-nitrogen line connected to a vacuum pump or to a nitrogen circular pipeline. The nitrogen was passed through a bubbler, which was filled with silicone oil and then through a U-shaped tube filled with orange gel for drying. To prevent enter of liquid and oxygen, and to ensure optimum overpressure, a pressure relief valve was downstream of the line. In addition, one cooling trap immersed in liquid nitrogen was mounted between the nitrogen-vacuum line and vacuum pump. Before the reactions were started the glass ware were heated-out three times, evacuated and purged with nitrogen. The reaction vessels were equipped with a magnetic stirring bar and sealed with a septum. This ensures that liquids could be added *via* cannules under inert conditions, whereas solids are previously filled and can be dried on the vacuum line for some time. Room temperature (rt) referred to ambient temperature. Temperatures of 0 °C were maintained using an ice-water bath and temperatures of -78 °C were maintained using an acetone-dry ice bath. Full spectral data for all novel compounds are given below, all previously characterized compounds gave spectra consistent with the literature. The first synthesis of EGCG in this work was

performed according to the report by Li and Chan^[165b], and Ding *et al.*^[167] The *cis*-chroman-3-ol was synthesized by Friedel-Crafts alkylation between cinnamyl alcohol and phenol. This synthesis of (*E*)-olefin **31** in this work was performed according to the report by Krohn *et al.*^[214] The (*E*)-olefin **31** was performed by Claisen-Schmidt condensation between acetophenone and aldehyde. The biotin- and dye labeled EGCG derivatives were prepared on the basis of the Steglich esterification and designed according to the coupling with the biotin and rhodamine moiety. The reaction conditions were optimized based on my own knowledge. The 3-azidochromane **85** was prepared on the basis of a S_N2 reaction and opens the synthesis of new EGCG derivatives linked by a 1,2,3-triazol unit or by an amide bond. The reaction conditions were optimized based on my own knowledge. The biological results were recorded and evaluated at Max Delbrück Center for Molecular Medicine by C. Secker and Prof. E. Wanker in Berlin.¹⁸ *n*-Propyl ester **52** was made available by L. Reus.^[233] Compound **76** was prepared *via ortho*-ester by R. Steinfort.²⁵

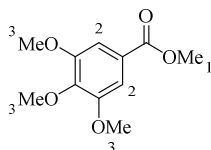
²⁵ R. Steinfort, Synthese eines Azido-PEGylierten Gallussäure-Derivates, bachelor thesis, **2017**, Heinrich-Heine Universität.

4.5 Synthesis

4.5.1 Synthesis of Cinnamyl Alcohol **25/26**

4.5.1.1 Methyl-3,4,5-trimethoxybenzoate (**16**)

The compound was prepared according to literature following a procedure by Alam *et al.*^[273] A 1000-mL, round-bottomed flask equipped with a magnetic stirring bar and with an air condenser was sequentially charged at rt with gallic acid (**15**) (10.0 g, 5.88 mmol, 1.00 eq), potassium carbonate (40.6 g, 0.294 mol, 5.00 eq). DMF (130 mL) and methyl iodide (18.3 mL, 0.294 mol, 5.00 eq) were added. The resulting beige mixture was heated up to 55 °C for 20 h. When TLC (SiO₂, *n*-hexane/EtOAc; 3:1, R_f = 0.45) showed full consumption of the starting material, the mixture was poured into water (300 mL) giving white deposition formed in the dark green solution. The precipitate was filtered through a fritted glass funnel, and the residue was dissolved in EtOAc (100 mL). The organic layer was washed water (3 x 50 mL), the combined organic layers were washed with brine (50 mL) and dried (MgSO₄). The drying agent was filtered off and the organic layer was concentrated under reduced pressure, the product **16** (13.2 g, 5.83 mmol, 99%) was obtained as a white yellow, crystalline solid. The spectroscopic data were in accordance with those described in the literature.^[273]

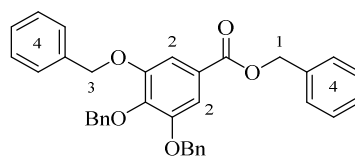


¹H NMR (300 MHz, CDCl₃): δ [ppm] = 7.30 (s, 2H, H-2), 3.91 (s, 12H, H-1, H-3).

4.5.1.2 Benzyl-3,4,5-tris(benzyloxy)benzoate (**17**)

The compound was prepared according to literature following a procedure by Kawamoto *et al.*^[200] A 1000-mL, round-bottomed flask equipped with a magnetic stirring bar was sequentially charged at rt with gallic acid (**15**) (15.0 g, 0.088 mol, 1.00 eq) and benzyl chloride (41.0 mL, 0.353 mol, 4.00 eq) dissolved in DMF (125 mL). To the resulting, yellow solution was added in 10 batches 60 % NaH in mineral oil (16.9 g, 0.705 mol,

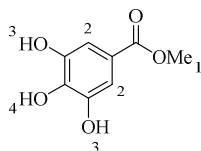
8.00 eq) and cooled to 0 °C. Water (13 mL, 0.705 mol) was added dropwise to the stirred mixture over a period of 1 h. A strong gas evolution and foam solid occurred. The mixture were then stirred until the water has been completely consumed over two days at rt until TLC (SiO₂, *n*-hexane/EtOAc; 4:1, R_f = 0.56) showed full consumption of the starting material. The mixture was poured into ice-water (500 mL). A red deposition was formed in the brown-green solution. The precipitate was filtrated through a glass frit (pore 2) and washed with methanol (80 mL). The aqueous layer was extracted with EtOAc (3 x 80 mL, and with dil. NaHCO₃ (80 mL) solution, the combined organic layers were concentrated under reduced pressure. The red residue was recrystallized from methanol and filtrated hot. The precipitate was filtered through a glass frit and the product **17** (28.2 g, 53.1 mmol, 60%) obtained as a white, crystalline solid. The reaction was done 4 times, 83.0 g of **17** were received. The spectroscopic data were in accordance with those described in the literature.^[200]



¹H NMR (300 MHz, CDCl₃): δ [ppm] = 7.44 – 7.34 (m, 20H, 4-H), 7.27 – 7.25 (m, 2H, 2-H), 5.33 (s, 2H, 1-H), 5.13 – 5.12 (d, *J* = 2.3 Hz, 6H, 3-H).

4.5.1.3 Methyl-3,4,5-tris(benzyloxy)benzoate (**18**)

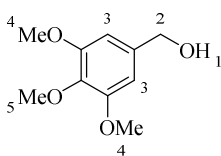
The compound was prepared according to literature following a procedure by Ding *et al.*^[167] A 500-mL, round-bottomed flask equipped with a magnetic stirring bar was sequentially charged at rt with gallic acid **5** (15.0 g, 88.2 mmol, 1.00 eq) dissolved in methanol (200 mL). To the resulting solution was added conc. sulfuric acid (9.0 mL) and the mixture heated up to 70 °C for 8 h. After TLC (SiO₂, EtOAc, R_f = 0.83) showed complete conversion, the mixture was hydrolyzed with water (200 mL) and solid potassium carbonate was added (vigorous evolution of gas and foaming). The formed alcohol was removed under reduced pressure. To the solution, sat. NaHCO₃-solution (100 mL) was added. The solution was extracted with EtOAc (3 x 100 mL). The combined organic layers were washed with brine (100 mL) and dried (Na₂SO₄). The drying agent was filtered off and the organic layer was concentrated under reduced pressure. The product **18** was obtained (16.5 g, 0.896 mol, 99%) as a slightly beige, crystalline solid. The spectroscopic data were in accordance with those described in the literature.^[167]



$^1\text{H NMR}$ (300 MHz, DMSO): δ [ppm] = 9.30 (s, 2H, 3-H), 8.95 (s, 1H, 4-H), 6.94 (s, 2H, 2-H), 3.74 (s, 3H, 1-H).

4.5.1.4 3,4,5-Trimethoxybenzyl alcohol (**19**)

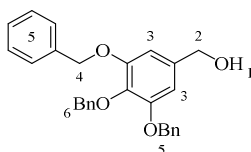
The compound was prepared according to literature following a procedure by Li *et al.*^[165b] A 2-L, two-necked round-bottomed flask equipped with a magnetic stirring bar and a plug valve to ensure nitrogen supply was charged at rt with methyl benzoate **16** (50.0 g, 0.221 mol, 1.00 eq) dissolved in dry THF (500 mL) and cooled to 0 °C. LiAlH_4 (8.39 g, 0.221 mol, 1.00 eq) was added in ten batches under a N_2 -atmosphere to the mixture. The flask was capped with a rubber septum, and the reaction was kept under N_2 -atmosphere for two hours at rt monitored by TLC (SiO_2 , *n*-hexane/EtOAc, 1:1, $R_f = 0.27$). Then *n*-hexane (500 mL) was added and a saturated solution of ammonium hydrogen fluoride (26 mL) was added dropwise. The solution was stirred at rt for one hour and then the white residue was filtered through a glass frit and washed with EtOAc. The filtrate was dried (MgSO_4). The drying agent was filtered off and the organic layer was concentrated under reduced pressure. The product **19** (43.8 g, 0.221 mol, 99%) was obtained as a lightly yellow oil. The spectroscopic data were in accordance with those described in the literature.^[215]



$^1\text{H NMR}$ (300 MHz, CDCl_3): δ [ppm] = 6.59 (s, 2H, 3-H), 4.63 (s, 2H, 2-H), 3.86 (s, 6H, 4-H), 3.83 (s, 3H, 5-H), 1.80 (s, 1H, 1-H).

4.5.1.5 3,4,5-Tris(benzyloxy)benzyl alcohol (**20**)

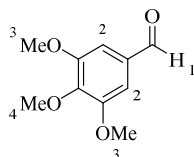
The compound was prepared according to literature following a procedure by Li *et al.*^[165b] A 500-mL, two-necked, round-bottomed flask equipped with a magnetic stirring bar and a plug valve, to ensure nitrogen supply, was charged at rt with methyl benzoate (**18**) (31.2 g, 69.5 mmol, 1.00 eq) dissolved in dry THF (290 mL) and cooled to 0 °C. LiAlH₄ (2.64 g, 69.5 mmol, 1.00 eq) was added in ten batches under a N₂-atmosphere to the mixture. The flask was capped with a rubber septum, and the reaction was kept under N₂-atmosphere for two hours at rt monitored by TLC (SiO₂, *n*-hexane/EtOAc, 1:1, R_f = 0.28). Then *n*-hexane (90 mL) were added and a saturated solution of ammonium hydrogen fluoride (4 mL) were added dropwise. The solution was again stirred at rt for one hour and, then the white residue was filtered through a glass frit and washed with EtOAc. The filtrate was dried (MgSO₄). The drying agent was filtered off and the organic layer was concentrated under reduced pressure. The product **20** was offered (27.7 g, 65.0 mmol, 94%) as a white solid. The spectroscopic data were in accordance with those described in the literature.^[165b]



¹H NMR (300 MHz, CDCl₃): δ [ppm] = 7.45 – 7.27 (m, 15H, 5-H), 6.68 (s, 2H, 3-H), 5.12 (s, 4H, 4-H), 5.05 (s, 2H, 6-H), 4.59 (s, 2H, 2-H).

4.5.1.6 3,4,5-Trimethoxybenzaldehyde (**21**)

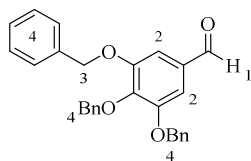
The compound was prepared according to literature following a procedure by Li *et al.*^[165b] A 1-L, two-necked round-bottomed flask equipped with a magnetic stirring bar and plug valve, to ensure nitrogen supply, was sequentially charged at rt with alcohol **19** (49.0 g, 0.247 mol, 1.00 eq) and CH₂Cl₂ (600 mL). PDC (65.1 g, 0.173 mol, 0.500 eq) was added to the flask, which was capped with a rubber septum, and the reaction was kept under N₂-atmosphere. The resulting mixture was then stirred at rt overnight. The reaction was quenched by adding Et₂O (750 mL) and the mixture filtered through a layer of silica gel. The residue was washed with Et₂O. The solvent was concentrated under reduced pressure, and the solid was dried in high vacuum overnight to yield the product **21** (43.0 g, 0.219 mol, 89%) as a lightly yellow solid. This material was used without further purification for the next step. The spectroscopic data were in accordance with those described in the literature.^[215]



$^1\text{H NMR}$ (300 MHz, CDCl_3): δ [ppm] = 9.87 (s, 1H, 1-H), 7.13 (s, 2H, 2-H), 3.94 (d, J = 2.3 Hz, 9H, 4-H, 3-H).

4.5.1.7 3,4,5-Tris(benzyloxy)benzaldehyde (**22**)

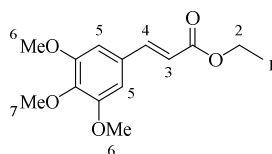
The compound was prepared according to literature following a procedure by Li *et al.*^[165b] A 500-mL, two-necked, round-bottomed flask equipped with a magnetic stirring bar and a plug valve, to ensure nitrogen supply, was sequentially charged at rt with alcohol **20** (11.0 g, 25.8 mmol, 1.00 eq) and CH_2Cl_2 (100 mL). PDC (9.70 g, 25.8 mmol, 1.00 eq) was added to the flask, which was capped with a rubber septum, and the reaction was kept under N_2 -atmosphere. The resulting mixture was then stirred at rt overnight. The reaction was quenched by addition of Et_2O (100 mL) and the mixture filtered through a layer of silica gel. The residue was washed with Et_2O . The solvent was concentrated under reduced pressure, and the solid was dried in high vacuum overnight to yield the product **22** (18.8 g, 44.3 mmol, 97%) as a slightly yellow solid. This material was used without further purification for the next step. The spectroscopic data were in accordance with those described in the literature.^[165b]



$^1\text{H NMR}$ (300 MHz, CDCl_3): δ [ppm] = 9.80 (s, 1H, 1-H), 7.44 – 7.34 (m, 15H, 4-H), 7.19 (s, 2H, 2-H), 5.17 (s, 6H, 3-H).

4.5.1.8 Ethyl-(*E*)-3,4,5-trimethoxycinnamate (**23**)

The compound was prepared according to literature following a procedure by Li *et al.*^[165b] A 2-L, three-necked, round-bottomed flask equipped with a magnetic stirring bar was charged at rt with aldehyde **21** (35.9 g, 0.183 mol, 1.00 eq) dissolved in THF (540 mL). Triethyl phosphonoacetate (28.6 mL, 0.144 mol, 1.20 eq) was added to the solution and the mixture was cooled to 0 °C. NaH (60 %) in mineral oil (5.21 g, 0.217 mmol, 1.20 eq) was added in ten batches into the flask and the reaction was allowed to proceed at rt for two hours. The mixture was quenched with sat. NaHCO₃ solution (150 mL), which was transferred into a 1 L separatory funnel and the organic layer was separated. The aqueous layer was extracted with EtOAc (3 x 100 mL). The combined organic layers were washed with brine (100 mL), dried (MgSO₄), the drying agent was filtered off, and concentrated under reduced pressure to afford a solid. The product was washed with *n*-hexane to remove the mineral oil and the excess of triethyl phosphonoacetate, the product **23** (45.7 g, 0.171 mol, 94%) was obtained as a lightly yellow solid. The spectroscopic data were in accordance with those described in the literature.^[215]

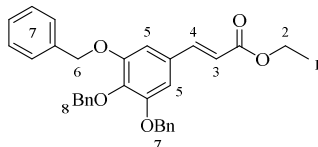


¹H NMR (300 MHz, CDCl₃): δ [ppm] = 7.60 (d, *J* = 15.9 Hz, 1H, 4-H), 6.75 (s, 2H, 5-H), 6.34 (d, *J* = 15.9 Hz, 1H, 3-H), 4.26 (q, *J* = 7.2 Hz, 2H, 2-H), 3.88 (d, *J* = 2.1 Hz, 9H, 7-H, 6-H), 1.38 – 1.30 (m, 3H, 1-H).

4.5.1.9 Ethyl-(*E*)-3,4,5-tris(benzyloxy)cinnamate (**24**)

The compound was prepared according to literature following a procedure by Li *et al.*^[165b] A 1-L, three-necked, round-bottomed flask equipped with a magnetic stirring bar was charged at rt with aldehyde **22** (26.3 g, 62.0 mmol, 1.00 eq) dissolved in THF (500 mL). Triethyl phosphonoacetate (14.8 mL, 74.5 mmol, 1.20 eq) was added to the solution and cooled to 0 °C. NaH (60 %) in mineral oil (2.97 g, 74.4 mmol, 1.20 eq) was added in ten batches to the flask and the reaction was allowed to proceed at rt for two hours. The mixture was quenched with sat. NaHCO₃ solution (100 mL), which was transferred into a 1 L separatory funnel and the organic layer was separated. The aqueous layer was extracted with EtOAc (3 x 100 mL). The combined organic layers were washed with brine (100 mL), dried (MgSO₄), the drying agent was filtered off and concentrated under reduced pressure.

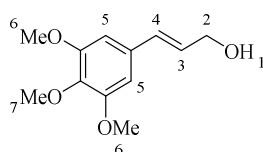
The product was washed with *n*-hexane to remove the mineral oil and the excess of triethyl phosphonoacetate. The product **24** was offered (32.8 g, 66.4 mmol, > 99%) as lightly yellow solid. The spectroscopic data were in accordance with those described in the literature.^[165b]



¹H NMR (300 MHz, CDCl₃): δ [ppm] = 7.54 (d, *J* = 15.9 Hz, 1H, 4-H), 7.44 – 7.27 (m, 15H, 8-H, 7-H), 6.82 (s, 2H, 5-H), 6.27 (d, *J* = 15.9 Hz, 1H), 5.11 (d, *J* = 7.5 Hz, 6H), 4.26 (q, *J* = 7.2 Hz, 2H), 1.38 – 1.30 (m, 3H, 1-H).

4.5.1.10 (*E*)-3,4,5-Trimethoxycinnamyl alcohol (**25**)

The compound was prepared according to literature following a procedure by Li *et al.*^[165b] A 1-L, three-necked, round-bottomed flask equipped with a magnetic stirring bar and a plug valve, to ensure nitrogen supply, was charged at rt with cinnamate **23** (20.0 g, 75.1 mmol, 1.00 eq) dissolved in dry THF (300 mL) and cooled to –78 °C with an acetone dry ice bath. To the pre-cooled solution, 1 M solution diisobutylaluminium hydride in toluene (165 mL, 2.20 eq) was dropwise added over a period of two hours to the colorless solution *via* a double cannula. The mixture was then stirred for one hour at –78 °C and afterwards stirred for one hour at rt. The warm-up caused the solution to become slightly yellow and was monitored by TLC (SiO₂, *n*-hexane/EtOAc, 2:1, *R_f* = 0.12). The solution was cooled to 0 °C and the mixture poured into a mixture of *n*-hexane (250 mL) and sat. NH₄HF₂ solution (15 mL). The stirring was continued until a large quantity of solid had formed. After one hour the mixture was filtered through a frit, and washed with EtOAc. The combined organic layers were dried (MgSO₄), the drying agent was filtered off and the solution was concentrated under reduced pressure. The residue was washed with *n*-hexane and was purified by flash chromatography (SiO₂, *n*-hexane/EtOAc, 2:1, *R_f* = 0.12). The desired product **25** was obtained (18.8 g, 83.3 mmol, 100%) as slightly yellow, clear oil. The spectroscopic data were in accordance with those described in the literature.^[215]

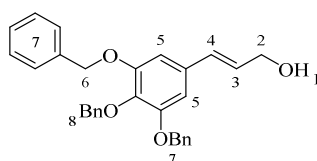


¹H NMR (300 MHz, CDCl₃): δ [ppm] = 6.60 (s, 2H, 5-H), 6.53 (dt, *J* = 15.8, 1.5 Hz, 1H,

4-H), 6.27 (dt, $J = 15.8, 5.7$ Hz, 1H, 3-H), 4.31 (dd, $J = 5.7, 1.5$ Hz, 2H, 2-H), 3.85 (d, $J = 6.5$ Hz, 9H, 7-H, 6-H), 1.70 (br s, 1H, 1-H).

4.5.1.11 (*E*)-3,4,5-Tris(benzyloxy)cinnamyl alcohol (**26**)

The compound was prepared according to literature following a procedure by Li *et al.*^[165b] A 500-mL, three-necked bottomed flask equipped with a magnetic stirring bar and a plug valve, to ensure N₂-supply, was charged at rt with cinnamate **24** (11.7 g, 23.7 mmol, 1.00 eq) dissolved in dry THF (150 mL) and the solution cooled to -78 °C with an acetone dry ice bath. To the pre-cooled solution, 1 M diisobutylaluminium hydride solution in toluene (89 ml, 2.20 eq) was added dropwise in a period of two hours to the colorless solution *via* a double cannule. The mixture was then stirred for one hour at -78 °C. Afterwards stirred for one hour at rt and was monitored by TLC (SiO₂, *n*-hexane/EtOAc, 1:1, $R_f = 0.54$). The solution was cooled to 0 °C with an ice bath and the mixture poured into a mixture of *n*-hexane (200 mL) and sat. NH₄HF₂ solution (13 mL). The mixture was stirred until a large quantity of solid had formed. After one hour the mixture was filtered through a frit, and washed with EtOAc. The combined organic layers were dried (MgSO₄), the drying agent was filtered off and the solution was concentrated under reduced pressure. The residue was recrystallized from *n*-hexane/EtOAc 5:1 to yield **26** (8.04 g, 17.8 mmol, 75%) as a white solid. The spectroscopic data were in accordance with those described in the literature.^[165b]

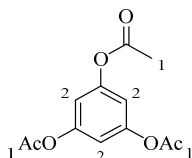


¹H NMR (300 MHz, CDCl₃): δ [ppm] = 7.45 – 7.27 (m, 15H, 8-H, 7-H), 6.69 (s, 2H, 5-H), 6.48 (dt, $J = 15.8, 1.5$ Hz, 1H, 4-H), 6.21 (dt, $J = 15.8, 5.7$ Hz, 1H, 3-H), 5.11 (s, 4H, 6-H), 5.06 (s, 2H, 8-H), 4.30 (td, $J = 5.8, 1.5$ Hz, 2H, 2-H).

4.5.2 Synthesis of 3,5-Bis(benzyloxy)-phenol (**12**)

4.5.2.1 1,3,5-Triacetylphloroglucinol (**28**)

The compound was prepared according to literature following a procedure by Kawamoto *et al.*^[200] A 1-L, round-bottomed flask equipped with a magnetic stirring bar was charged at rt with phloroglucinol (**27**) (26.0 g, 0.206 mol, 1.00 eq). Chloroform (100 mL) was added to the flask. Then, acetic anhydride (116 mL, 1.24 mol, 6.00 eq) and amidosulfonic acid (4.00 g, 41.3 mmol, 0.200 eq) were added to the suspension. The flask was equipped with a water-cooled condenser. The resulting mixture was heated up to 70 °C and stirred for 24 h. The reaction was cooled down to rt over a period of one day. Et₂O (200 mL) was added, the mixture was stirred vigorously for 5 min and any solids were removed by filtration. The filtrate was poured into a 1-L separatory funnel and the layers were separated. The organic layer was washed with HCl (5%, 100 mL), followed by NaHCO₃ solution (5wt%, 100 mL) and finally with brine (3 x 100 mL). The combined organic layers were dried (Na₂SO₄), the drying agent was filtered off, and concentrated under reduced pressure. The product **28** was obtained (54.1 g, 0.214 mol, > 99%) as a white solid. The spectroscopic data were in accordance with those described in the literature.^[200]

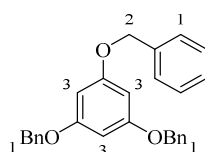


¹H NMR (300 MHz, CDCl₃): δ [ppm] = 7.17 (s, 3H, 2-H), 2.61 (s, 9H, 1-H).

4.5.2.2 1,3,5-Tris(benzyloxy)benzene (**29**)

The compound was prepared according to literature following a procedure by Kawamoto *et al.*^[200] A 1-L, round-bottomed flask equipped with a magnetic stirring bar was charged at rt with acylated phloroglucinol **28** (17.0 g, 67.4 mmol, 1.00 eq). DMF (340 mL) and benzyl chloride (31.0 mL, 0.268 mol, 4.00 eq) were added. To the resulting solution NaH (60 %) in mineral oil (21.4 g, 0.893 mol, 8.00 eq) was added in ten batches and the mixture cooled to 0 °C. Then, water (3.6 mL) was added dropwise to the stirred mixture in the flask over a period of one hour. A strong gas evolution and foam was formed: besides, a yellow-green color was observed. The mixture was stirred until the water had been completely consumed over 24 h at rt. The mixture was poured into water (1.6 L). A brown solid arose in the darkly colored solution. The residue was filtered through a glass frit (pore 2) and

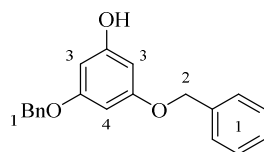
washed with methanol (90 mL). The brown residue was dissolved with EtOAc (130 mL) and the solution was poured to a 1-L separatory funnel and the layers were separated. The aqueous layer was extracted with EtOAc (3 x 100 mL). The combined organic layers were washed with distilled water (6 x 100 mL) and brine (100 mL), dried (MgSO₄), and the drying agent filtered off. The filtrate was concentrated under reduced pressure. The solid was recrystallized from methanol. The flask was allowed to cool to rt and then, cooled to -5 °C in a fridge. The product was isolated by vacuum filtration. The crystals were washed with ice cold *n*-hexane (100 mL) and dried under vacuum. The product **29** was obtained (21.4 g, 54.0 mmol, 80%) as a brown solid. The spectroscopic data were in accordance with those described in the literature.^[200]



¹H NMR (300 MHz, CDCl₃): δ [ppm] = 7.43 – 7.32 (m, 15H, 1-H), 6.27 (s, 3H, 3-H), 5.00 (s, 6H, 2-H).

4.5.2.3 3,5-Bis(benzyloxy)phenol (**12**)

The compound was prepared according to literature following a procedure by Curtis *et al.*^[204] A 1-L, three-necked, round-bottomed flask equipped with a magnetic stirring bar, sealed with a septum and an adapter with tap to the N₂-vacuum line, was charged with benzylated product **29** (5.00 g, 12.6 mmol, 1.00 eq) at rt, evacuated and purged with nitrogen. Dry methanol (300 mL) and dioxan (150 mL) were added *via* cannula through the septum. After complete dissolution sodium methoxide (0.980 g, 18.1 mmol, 1.40 eq) and 10 % Pd/C (0.15 g) were added. After 1.5 h the reaction mixture was filtered through a pad of celite. This pad was suspended several times with methanol, the filtrate was acidified with 2 M HCl, and concentrated under reduced pressure to a brown oil. The residue was dissolved in CH₂Cl₂ and extracted with sat. NaHCO₃ (100 mL), washed with brine (100 mL), and dried (MgSO₄). The drying agent was filtered off and concentrated under reduced pressure. The residue was purified by flash chromatography on silica gel (*n*-hexane/EtOAc, 5:1, R_f = 0.30). The product **12** was obtained (2.73 g, 8.91 mmol, 71%) as a slightly yellow solid. The spectroscopic data were in accordance with those described in the literature.^[200]



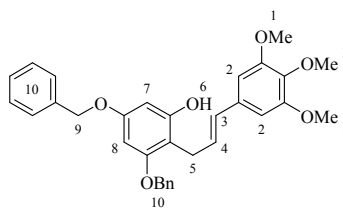
$^1\text{H NMR}$ (300 MHz, CDCl_3): δ [ppm] = 7.37 – 7.22 (m, 11H, 1-H), 6.17 (t, J = 2.2 Hz, 1H, 4-H), 6.11 (d, J = 2.1 Hz, 2H, 3-H), 5.00 (s, 4H, 2-H).

4.5.3 Synthesis of (*E*)-3-(2,4-Bis(benzyloxy)-6-(*TBS*)phenyl)-1-(3,4,5-trimethoxyphenyl)-propane (**32**) and (*E*)-3-(2,4-Bis(benzyloxy)-6-(*TBS*)phenyl)-1-(3,4,5-tris(benzyloxy)phenyl)-propane **33** via **30/31**

4.5.3.1 (*E*)-3-(2,4-Bis(benzyloxy)-6-(*tert*-butyl-dimethyl-siloxy)phenyl)-1-(3,4,5-trimethoxyphenyl)-propane (**32**)

The compound was prepared according to literature following a procedure by Ding *et al.*^[167] A 250-mL, three-necked, round-bottomed flask equipped with a magnetic stirring bar, sealed with a septum and an adapter with tap to the N_2 /vacuum line, was charged with phenol **12** (3.05 g, 10.0 mmol, 1.00 eq) at rt, evacuated and purged with nitrogen. Dry CH_2Cl_2 (100 mL) was added *via* cannula through the septum and the solution was cooled down to 0 °C. A 25-mL round-bottomed flask equipped with a magnetic stirring bar and sealed with a septum was filled with cinnamyl alcohol **25** (2.27 g, 10.0 mmol, 1.00 eq). The flask was evacuated and purged with nitrogen three times. Then dry CH_2Cl_2 (10 mL) was poured *via* cannula to dissolve **25**. A third 25 -mL flask equally was prepared and charged with methane sulfonic acid (0.657 mL, 10.0 mmol, 1.00 eq) dissolved in CH_2Cl_2 (10 mL). To the well-stirred solution of **12**, the solution of compound **25**, and the solution of methane sulfonic acid were respectively added slowly at 0 °C *via* syringe pumps under N_2 -atmosphere. The solution became purple colored. After stirring for 24 h at rt the solution was quenched with sat. NaHCO_3 solution (100 mL). The mixture was transferred into a 500 mL separatory funnel and the organic layer was separated. The aqueous layer was extracted with EtOAc (3 x 90 mL) and the combined organic layers were washed with brine (90 mL), dried (MgSO_4), the drying agent was filtered off, and concentrated under reduced pressure. The residue was purified by flash chromatography on silica gel (*n*-hexane/EtOAc, 3:1, R_f = 0.57). The product **30** (2.12 g, 4.15 mmol, 30%) was obtained as white solid. The reaction was done several times. The spectroscopic data were in accordance with those

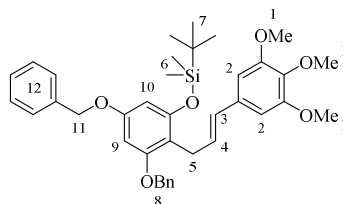
described in the literature.^[215]



$^1\text{H NMR}$ (300 MHz, CDCl_3): δ [ppm] = 7.44 – 7.31 (m, 10H, 10-H), 6.53 (s, 2H, 2-H), 6.29 (d, J = 2.3 Hz, 1H, 4-H), 6.18 (d, J = 2.3 Hz, 1H, 3-H), 5.05 – 4.99 (m, 5H, 9-H), 3.83 (d, J = 5.2 Hz, 9H, 1-H).

$^{13}\text{C NMR}$ (75 MHz, CDCl_3): δ [ppm] = 158.96, 158.10, 155.80, 153.34, 137.50, 137.22, 136.97, 133.28, 130.50, 128.75, 128.64, 128.17, 128.01, 127.98, 127.66, 127.41, 106.99, 103.30, 95.23, 93.79, 70.46, 70.27, 61.06, 56.18, 26.47.

A 100-mL, round-bottomed flask equipped with a magnetic stirring bar was charged with propene **30** (9.30 g, 18.1 mmol, 1.00 eq) dissolved in dry DMF (115 mL) rt. To this solution imidazole (3.71 g, 54.4 mmol, 3.00 eq) and *tert*-butyldimethylsilyl chloride (5.47 g, 36.3 mmol, 2.00 eq) were added. The resulting mixture was stirred at rt overnight monitored by TLC (SiO_2 , *n*-hexane/EtOAc, 7:1, R_f = 0.39). The mixture was quenched by the addition of sat. Na_2CO_3 solution and transferred into a 500 mL separatory funnel. The solution was extracted with EtOAc (3 x 100 mL). The combined organic layers were washed with brine (100 mL), dried (MgSO_4), the drying agent was filtered off, and finally evaporated under reduced pressure. The residue was purified by flash chromatography on silica gel (*n*-hexane/EtOAc, 7:1). The product **32** (9.31 g, 14.9 mmol, 82%) was obtained as a colorless oil. The spectroscopic data were in accordance with those described in the literature.^[215]



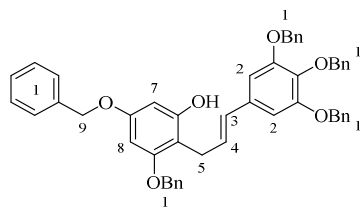
$^1\text{H NMR}$ (300 MHz, CDCl_3): δ [ppm] = 7.43 – 7.22 (m, 10H, 12-H), 6.48 (s, 2H, 2-H), 6.30 (d, J = 2.3 Hz, 1H, 4-H), 6.22 (d, J = 2.3 Hz, 2H, 9-H, 10-H), 6.12 (d, J = 2.3 Hz, 1H, 3-H), 5.02 (d, J = 7.2 Hz, 4H, 11-H), 3.82 (d, J = 2.2 Hz, 9H, 1-H), 3.56 – 3.44 (m, 2H, 5-H), 1.01 (s, 9H, 7-H), 0.20 (s, 6H, 6-H).

$^{13}\text{C NMR}$ (75 MHz, CDCl_3): δ [ppm] = 171.26, 158.46, 158.25, 154.87, 153.25, 137.44,

137.16, 137.12, 134.15, 129.50, 129.11, 128.76, 128.58, 128.11, 127.85, 127.51, 127.39, 112.17, 103.08, 98.54, 93.97, 70.30, 70.25, 61.03, 60.52, 56.12, 31.73, 26.95, 25.96, 25.79, 22.80, 21.19, 18.44, 14.34, 14.26, -3.94.

4.5.3.2 (*E*)-3-[2,4-Bis(benzyloxy)-6-(*tert*-butyl-dimethyl-siloxy)phenyl]-1-[3,4,5-tris(benzyloxy)phenyl]-propane (**33**)

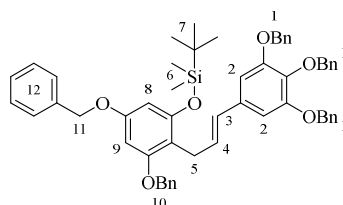
The compound was prepared according to literature following a procedure by Ding *et al.*^[167] A 250-mL, three-necked, round-bottomed flask equipped with a magnetic stirring bar, sealed with a septum, and adapter with tap to N₂-vacuum line, was charged with phenol **12** (2.00 g, 6.53 mmol, 1.00 eq) at rt, evacuated and purged with nitrogen. Dry CH₂Cl₂ (100 mL) was added *via* a cannula through the septum and the solution was cooled to 0 °C. A 25 mL round-bottomed flask equipped with a magnetic stirring bar and sealed with a septum was filled with cinnamyl alcohol **31** (2.95 g, 6.53 mmol, 1.00 eq). The flask was evacuated and purged with N₂ three times, respectively. Then dry CH₂Cl₂ (15 mL) was poured *via* a cannula to dissolve **31**. A third 25 mL flask was equally prepared and charged with methane sulfonic acid (0.424 mL, 6.53 mmol, 1.00 eq) and dry CH₂Cl₂ (15 mL). To the well-stirred solution of **12**, the solution of compound **31** and the solution of methane sulfonic acid were added slowly at 0 °C *via* a syringe pumps under N₂-atmosphere. The solution became purple colored. After stirring for 4 h the solution was quenched with sat. NaHCO₃ solution. The mixture was transferred into a 500 mL separatory funnel and the organic layer separated. The aqueous layer was extracted with EtOAc (3 x 50 mL) and the combined organic layer was washed with brine (50 mL), dried (MgSO₄), the drying agent was filtered off, and concentrated under reduced pressure. The residue was purified by column chromatography on silica gel (*n*-hexane/EtOAc 3:1, R_f = 0.42) to afford **31** (2.00 g, 2.73 mmol, 42%) as a lightly yellow solid. The spectroscopic data were in accordance with those described in the literature.^[167]



¹H NMR (300 MHz, CDCl₃): δ [ppm] = 7.43 – 7.29 (m, 30H, 1-H), 6.63 (s, 2H, 2-H), 6.32 – 6.16 (m, 4H, 8-H, 7-H, 4-H, 3-H), 5.10 – 4.97 (m, 10H, 9-H), 3.56 (d, *J* = 6.2 Hz, 2H, 5-H).

^{13}C NMR (75 MHz, CDCl_3): δ [ppm] = 171.35, 158.93, 158.10, 155.78, 153.02, 137.96, 137.93, 137.28, 137.25, 137.22, 136.99, 133.37, 130.33, 128.73, 128.70, 128.65, 128.59, 128.36, 128.24, 128.16, 128.09, 127.97, 127.95, 127.88, 127.66, 127.63, 127.58, 127.40, 107.06, 106.09, 106.06, 95.24, 93.76, 75.39, 71.38, 70.44, 70.26, 60.56, 26.46, 21.19, 14.34.

A 100-mL, round-bottomed flask equipped with a magnetic stirring bar was sequentially charged with propene **31** (2.00 g, 2.70 mmol, 1.00 eq) dissolved in dry DMF (40 mL) at rt. To the solution imidazole (0.551 g, 8.10 mmol, 3.00 eq) and *tert*-butyldimethylsilyl chloride (0.81 g, 5.40 mmol, 2.00 eq) were added. The resulting mixture was stirred at rt overnight, monitored by TLC (SiO_2 , *n*-hexane/EtOAc, 7:1, R_f = 0.6). The mixture was quenched by the addition of sat. Na_2CO_3 solution and transferred into a 250 mL separatory funnel. The solution was extracted with EtOAc (6 x 50 mL). The combined organic layers were washed with brine (50 mL), dried (MgSO_4), the drying agent was filtered off, and finally evaporated under reduced pressure. The residue was purified by flash chromatography on silica gel (*n*-hexane/EtOAc, 7:1) to afford the desired product **33** (1.64 g, 1.92 mmol, 71%) as a white solid. The spectroscopic data were in accordance with those described in the literature.^[167]



^1H NMR (300 MHz, CDCl_3): δ [ppm] = 7.43 – 7.28 (m, 24H, 1-H, 10-H), 6.57 (s, 2H, 2-H), 6.30 (d, J = 2.3 Hz, 1H, 9-H), 6.18 (t, J = 1.6 Hz, 2H, 4-H, 3-H), 6.11 (d, J = 2.3 Hz, 1H, 8-H), 5.06 (s, 4H, 11-H), 5.02-5.01 (d, 6H, 1-H), 3.49 (d, J = 4.6 Hz, 2H, 5-H), 1.00 (s, 9H, 7-H), 0.19 (s, 6H, 6-H).

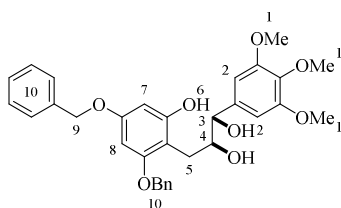
4.5.4 Asymmetric Dihydroxylation of Compound **34**(α)/**35**(α)

4.5.4.1 (1*S*,2*S*)-3-[2,4-Bis(benzyloxy)-6-hydroxyphenyl-1-(3,4,5-trimethoxy)phenyl]propane-1,2-diol (**36**(α))

The compound was prepared according to literature following a procedure by Li *et al.*^[165b]

A 500-mL, two-necked, round-bottomed flask equipped with a KPG stirrer was

sequentially charged with AD-mix- α (22.5 g), methane sulfonamide (1.51 g, 15.9 mmol, 1.00 eq) and was dissolved in a mixture of *tert*-butylalcohol (90 mL) and H₂O (90 mL) at rt. This orange colored mixture was stirred at rt for five minutes and was cooled down to 0 °C using a thermostat and a solution of compound **32** (5.00 g, 7.98 mmol, 1.00 eq) in CH₂Cl₂ (90 mL) was added. This reaction was allowed to stir overnight. A total of four batches of each methane sulfonamide (755 mg, 7.94 mmol) and each of AD-mix- α (11.3 g) were added within 24 h intervals. The mixture was then stirred at 0 °C overnight until the starting material has been completely consumed as monitored by TLC (SiO₂, *n*-hexane/EtOAc, 4:1, R_f = 0.29). After the reaction had completed the mixture was quenched with Na₂S₂O₃ (100 mL, 10% wt) solution. The mixture was filtered through a layer of celite and washed with EtOAc. The filtrate was transferred into a separatory funnel and the organic layer was separated. The aqueous layer was extracted with EtOAc (3 x 80 mL), the combined organic layer was dried (MgSO₄), the drying agent was filtered off, and concentrated under reduced pressure. The product **34**(α) (6.13 g, 9.28 mmol) was obtained as a brown oil. The same procedure was prepared with AD-mix- β to get the EGCG isomer **34**(β). A 50-mL, round-bottomed flask equipped with a magnetic stirring bar, was sequentially charged with dihydroxylated compound **34**(α) (6.13 g, 9.28 mmol) dissolved in THF (50 mL). 1 M *tetra*-butylammonium fluoride in THF (3.24 g, 10.27 mmol) was added. The resulting mixture was stirred at rt for 4 h until TLC (SiO₂, *n*-hexane/EtOAc, 1:1, R_f = 0.19) showed complete reaction. The mixture was quenched with sat. NaHCO₃ solution and transferred into a separatory funnel. The solution was then extracted with (3 x 40 mL) EtOAc. The organic layers were combined, dried (MgSO₄), the drying agent was filtered off, and concentrated under reduced pressure. The residue was purified by flash chromatography on silica gel (*n*-hexane/EtOAc, 1:1), the product **36**(α) (4.17 g, 7.63 mmol, 96%) was obtained as a white solid. The specific rotation for **36**(α) is $[\alpha]_D^{25} = +1.85$ ($c = 1.0$ mol/L, CHCl₃). For **36**(β) (63%) a value of $[\alpha]_D^{25} = +6.3$ ($c = 1.0$ mol/L, CHCl₃) was found. The spectroscopic data were in accordance with those described in the literature.^[215]

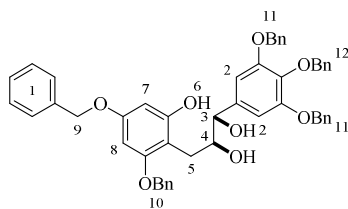


¹H NMR (300 MHz, CDCl₃): δ [ppm] = 7.43 – 7.11 (m, 10H, 10-H), 6.52 (s, 2H, 2-H), 6.23

(dd, $J = 17.3, 2.4$ Hz, 2H, 8-H, 7-H), 4.98 (s, 2H, 9-H), 4.90 (s, 2H, 9-H), 4.49 (d, $J = 5.9$ Hz, 1H, 3-H), 4.05 – 3.93 (m, 1H, 4-H), 3.76 (s, 9H, 1-H), 2.97 (dd, $J = 14.6, 3.9$ Hz, 1H, 5-H), 2.81 (dd, $J = 14.6, 8.3$ Hz, 1H, 5-H).

4.5.4.2 (1*S*,2*S*)-3-[2,4-Bis(benzyloxy)-6-hydroxyphenyl-1-(3,4,5-tris(benzyloxy)-phenyl)]propane-1,2-diol (**37**(α))

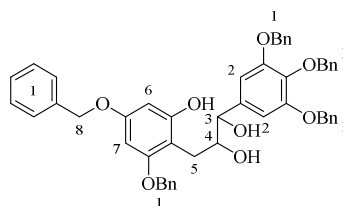
The compound was prepared according to literature following a procedure by Li *et al.*^[165b] A 100-mL, two-necked, round-bottomed flask equipped with a magnetic stirring bar was sequentially charged with AD-mix- α (8.82 g), methane sulfonamide (890 mg, 9.36 mmol) dissolved in a mixture of *tert*-butylalcohol (28 mL) and H₂O (28 mL) at rt. This orange colored mixture was stirred at rt for five min. The mixture was cooled to 0 °C using a thermostat and a solution of compound **33** (8.00 g, 9.36 mmol, 1.00 eq) in CH₂Cl₂ (28 mL) was added. This reaction was allowed to stir overnight. The mixture was then stirred at rt overnight until the starting material has been completely consumed as shown by TLC (SiO₂, *n*-hexane/EtOAc, 4:1, $R_f = 0.25$). On completeness of the reaction, the mixture was quenched with Na₂S₂O₃ solution (80 mL, 10 %wt) and washed with EtOAc. The filtrate was transferred into a separatory funnel and the organic layer was separated. The aqueous layer was extracted with EtOAc (3 x 50 mL), dried (MgSO₄), the drying agent was filtered off, and concentrated under reduced pressure to yield the product **35**(α) (314 mg, 0.353 mmol) as a slightly yellow oil. A 25-mL, round-bottomed flask equipped with a magnetic stirring bar, was charged with dihydroxylated product **35**(α) (13.9 g, 15.6 mmol) dissolved in THF (80 mL). 1 M tetra-*n*-butylammonium fluoride solution (5.42 g, 1 M solution in THF) was added. The resulting mixture was stirred at rt for four hours until TLC (SiO₂, *n*-hexane/EtOAc, 2:1, $R_f = 0.14$) showed a complete reaction. The mixture was quenched with sat. NaHCO₃ solution and transferred into a separatory funnel. The solution was then extracted with EtOAc (3 x 50 mL). The organic layer was combined, dried (MgSO₄), the drying agent was filtered off, and concentrated under reduced. The residue was purified by flash chromatography on silica gel (acetone/CH₂Cl₂, 1:10), the desired product **37**(α) (7.15 g, 9.23 mmol, 99%) was obtained as a beige solid. By using the same procedure as described above, **37**(β) (90%) was prepared with identical NMR spectra as the **37**(α) (–)-isomer $[\alpha]_D^{25} = -5.7$ ($c = 1.0$ mol/L, CHCl₃). The spectroscopic data were in accordance with those described in the literature.^[165b]



$^1\text{H NMR}$ (300 MHz, CDCl_3): δ [ppm] = 7.84 (br s, 1H, 6-H), 7.43 – 7.14 (m, 27H, 12-H, 11-H, 10-H, 1-H), 6.61 (s, 2H, 2-H), 6.24 (dd, $J = 18.9, 2.3$ Hz, 2H, 8-H, 7-H), 5.06 – 4.86 (m, 10H, 12-H, 11-H, 10-H, 9-H), 4.46 (t, $J = 5.0$ Hz, 1H, 3-H), 3.94 (br s, 1H, 4-H), 2.91 (dd, $J = 14.7, 3.7$ Hz, 1H, 5-H), 2.76 (dd, $J = 14.6, 8.2$ Hz, 1H, 5-H).

4.5.4.3 (*rac*)-3-(2,4-Bis(benzyloxy)-6-hydroxyphenyl)-1-(3,4,5-tris(benzyloxy)-phenyl)propane-1,2-diol (**98**)

The compound was prepared according to literature following a procedure by Sharpless *et al.*^[165b] A 100-mL, two-necked, round-bottomed flask equipped with a magnetic stirring bar was sequentially charged with $\text{K}_2\text{OsO}_4 \cdot 2 \text{H}_2\text{O}$ (0.2 mol%, 259 mg, $0.702 \cdot 10^{-3}$ mmol) and NMO (123 mg, 1.05 mmol, 3.00 eq) and then in a mixture of acetone (3 mL) and H_2O (3 mL) added at rt. This mixture was stirred at rt for five min. Then a solution of compound **31** (300 mg, 0.351 mmol, 1.00 eq) in CH_2Cl_2 (25 mL) was added. This reaction was allowed to stir overnight. On completeness of the reaction the mixture was quenched with $\text{Na}_2\text{S}_2\text{O}_3$ solution (50 mL, 10 %wt). The mixture was filtered through a layer of celite and washed with EtOAc. The filtrate was transferred into a separatory funnel and the organic layer was separated. The aqueous layer was extracted with EtOAc (3 x 15 mL), dried (MgSO_4), the drying agent was filtered off and concentrated under reduced pressure to yield the product **97** (231 mg, 0.260 mmol) as a lightly yellow oil. A 25-mL round-bottomed flask equipped with a magnetic stirring bar, was charged with dihydroxylated product **97** (231 mg, 0.260 mmol) dissolved in THF (10 mL). 1 M *tetra-n*-butylammonium fluoride solution (0.390 mL) was added. The resulting mixture was stirred at rt for four hours until TLC (SiO_2 , *n*-hexane/EtOAc, 2:1, $R_f = 0.14$) showed a complete reaction. The mixture was quenched with sat. NaHCO_3 solution and transferred into a separatory funnel. The solution was then extracted with EtOAc (3 x 10 mL). The organic layer was combined, dried (MgSO_4), the drying agent was filtered off and concentrated under reduced. The residue was purified by flash chromatography on silica gel (acetone: CH_2Cl_2 , 1:10), the desired product **98** (130 mg, 0.168 mmol, 48%) was obtained as a white beige solid.



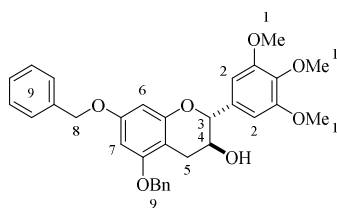
$^1\text{H NMR}$ (300 MHz, CDCl_3): δ [ppm] = 7.93 – 7.13 (m, 25H, 1-H), 6.59 (s, 2H, 2-H), 6.22 (dd, $J = 16.4, 2.3$ Hz, 1H, 7-H, 6-H), 4.99 – 4.94 (m, 8H, 9-H), 4.88 (s, 2H, 9-H), 4.42 (br s, 1H, 3-H), 3.91 (bs, 1H, 4-H), 2.90 (dd, $J = 14.6, 3.8$ Hz, 1H, 5-H), 2.75 (t, $J = 7.1$ Hz, 1H, 5-H).

4.5.5 Cyclization of Compounds **36**(α)/**37**(β)

4.5.5.1 (2*R*,3*S*)-5,7-Bis(benzyloxy)-2-(3,4,5-trimethoxyphenyl)chroman-3-ol (*trans* **40**(α))

The compound was prepared according to literature following a procedure by Khandelwal *et al.*^[215] A 250-mL, round-bottomed flask equipped with a magnetic stirring bar was charged with dihydroxylated product **36**(α) (2.40 g, 4.39 mmol, 1.00 eq) dissolved in CH_2Cl_2 (100 mL). Trimethyl orthoacetate (633.05 mg, 5.27 mmol, 1.20 eq) and pyridinium *p*-toluenesulfonate (2.21 mg, 0.00878 mmol, 0.2 mol%) were added to the solution at rt. This mixture was stirred for 30 min at rt. After the mixture was cooled down to 0 °C, then borontrifluoride etherate (53.9 μL , 0.437 mmol, 0.100 eq) was added dropwise. The reaction was warmed up to rt and stirred for another 15 min until the mixture became a clear, slightly yellow solution. Then the reaction mixture was quenched with aqueous acetone (50 mL). The solvent was removed under reduced pressure and the yellow oil was diluted in methanol (50 mL). To afford complete dissolution, the solvent was heated up to 50 °C. Then, potassium carbonate (641 mg, 4.64 mmol, 1.20 eq) was added and the mixture was stirred overnight at rt (white suspension). Methanol was removed under reduced pressure, water (60 mL) was added and the solution was transferred into a separatory funnel. The suspension was extracted with (3 x 15 mL) EtOAc, the combined organic layers were washed with brine (15 mL), dried (Na_2SO_4), the drying agent was filtered off, and the solvent was removed under reduced pressure. The product *trans* **40**(α) (1.90 g, 3.59 mmol, 82%) was obtained as a white solid. By using the same procedure as described above, (+)-*trans* **40**(β) (92%) was prepared with identical NMR spectra as the (–)-isomer.

The spectroscopic data were in accordance with those described in the literature.^[215]

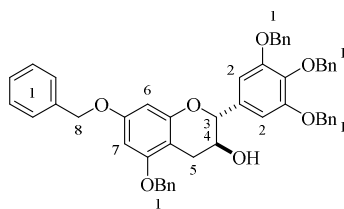


$^1\text{H NMR}$ (300 MHz, CDCl_3): δ [ppm] = 7.35 – 7.26 (m, 10H, 9-H), 6.60 (s, 2H 2-H), 6.20 – 6.14 (m, 2H, 7-H, 6-H), 4.94 (d, $J = 12.1$ Hz, 4H, 8-H), 4.58 (d, $J = 8.2$ Hz, 1H, 3-H), 3.99 (td, $J = 8.5, 5.6$ Hz, 1H, 4-H), 3.76 (dd, $J = 7.8, 1.0$ Hz, 9H, 1-H), 3.05 (dd, $J = 16.4, 5.7$ Hz, 1H, 5-H), 2.57 (dd, $J = 16.4, 9.0$ Hz, 1H, 5-H).

$^{13}\text{C NMR}$ (75 MHz, MeOD): δ [ppm] = 158.68, 157.67, 155.17, 153.23, 137.70, 136.87, 136.79, 134.09, 128.52, 128.45, 127.93, 127.82, 127.44, 127.08, 104.24, 102.50, 94.43, 93.84, 82.06, 70.10, 69.94, 67.69, 60.72, 56.03, 27.99.

4.5.5.2 (–)-(2*R*,3*S*)-5,7-Bis(benzyloxy)-2-(3,4,5-tris(benzyloxy)phenyl)chroman-3-ol (*trans* **41(a)**)

A more efficient method was used for subsequent compounds according to literature following a general procedure by Khandelwal *et al.*^[215] To a solution of dihydroxylated product **37(a)** (1.00 eq) in CH_2Cl_2 (3 mL). Trimethyl orthoacetate (1.20 eq) and pyridinium *p*-toluenesulfonate (0.0205 eq) were added and was stirred 30 min at rt. The mixture was cooled to 0 °C and borontrifluoride diethyletherate (0.12 eq) was added dropwise, then the solution was warmed to rt and was stirred 15 min at rt. The reaction was quenched with aqueous acetone (5 mL) and the solvent was evaporated. The residue was dissolved in methanol (5 mL) and potassium carbonate (1.10 eq) was added and stirred overnight (TLC = SiO_2 , *n*-hexane/EtOAc, 3:1, $R_f = 0.24$). The solvent was removed under reduced pressure and the residue was dissolved in CH_2Cl_2 . The aqueous layer was extracted (3 x 5 mL) with CH_2Cl_2 , the combined organic layers were washed with brine (10 mL), dried (Na_2SO_4), the drying agent was filtered off and the solvent was evaporated. The spectroscopic data were in accordance with those described in the literature.^[215]

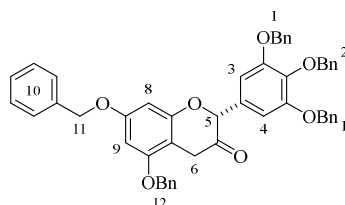


$^1\text{H NMR}$ (300 MHz, CDCl_3): δ [ppm] = 7.45 – 7.40 (m, 25H, 1-H), 6.73 (s, 2H, 2-H), 6.26 (dd, J = 17.5, 2.3 Hz, 2H, 7-H, 6-H), 5.14 – 4.98 (m, 10H, 8-H), 4.61 (d, J = 8.1 Hz, 1H, 3-H), 4.02 – 3.91 (m, 1H, 4-H), 3.11 (dd, J = 16.4, 5.7 Hz, 1H, 5-H), 2.64 (dd, J = 16.4, 9.0 Hz, 1H, 5-H).

4.5.6 Alcohol Inversion by Oxidation-Reduction Sequence

4.5.6.1 (–)-(2*R*,3*R*)-*cis*-5,7-Bis(benzyloxy)-2-(3,4,5)-tris(benzyloxy)phenylchroman-3-ol (*cis* **45** (**45 β**))

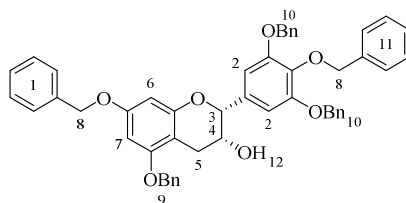
The compound was prepared according to literature following a procedure by Tückmantel *et al.*^[268] A 100 -mL, round-bottomed flask equipped with a magnetic stirring bar was sequentially charged with *cis*-chroman-3-ol **trans** **41** (867 mg, 1.15 mmol, 1.00 eq) dissolved in CH_2Cl_2 (35 mL) at rt, resulting in a clear solution. Dess-Martin periodinane (583 mg, 1.37 mmol, 1.20 eq) was added in one batch to the stirred solution at rt under N_2 -atmosphere for 2 h, until TLC (SiO_2 , *n*-hexane/EtOAc, 3:1, R_f = 0.65) showed full consumption of the starting material. The reaction was quenched by addition of sat. NaHCO_3 (20 mL) solution and $\text{Na}_2\text{S}_2\text{O}_3$ (20 mL, 10 wt%) solution. This mixture was allowed to stir until a clear two phase solution was formed. The organic layer was separated, and the aqueous layer was extracted with CH_2Cl_2 (3 x 10 mL). The combined organic layers were washed with brine (10 mL), dried (Na_2SO_4), the drying agent was filtered off and the solvent was removed under reduced pressure. The residue was recrystallized from *n*-hexane/EtOAc 5:1 to yield **43** (753 mg, 0.999 mmol, 87%) as a white solid. The spectroscopic data were in accordance with those described in the literature.^[165b]



$^1\text{H NMR}$ (300 MHz, CDCl_3): δ [ppm] = 7.46 – 7.24 (m, 25H, 12-H, 10-H, 2-H, 1-H), 6.68 (s, 2H, 4-H, 3-H), 6.40 – 6.35 (m, 2H, 9-H, 8-H), 5.25 (s, 1H, 5-H), 3.68 – 3.34 (m, 2H, 6-H).

The residue (643 g, 0.852 mmol, 1.00 eq) was dissolved in THF (10 mL), and the solution was cooled to -78 °C, then L-Selectride[®] (1.00 mL, 1 M solution in THF, 0.100 mmol) and

(444 mg, 5.11 mmol, 6.00 eq) LiBr were added under N₂-atmosphere. The resulting solution was stirred at -78 °C for 6 h at rt overnight. The reaction was quenched by addition of aqueous NaOH (5 mL) and of 35% aqueous H₂O₂ (3 mL). The organic layer was separated, and the aqueous layer was extracted with EtOAc (3 x 5mL). The combined organic layers were washed with brine (5 mL), dried (Na₂SO₄), the drying agent was filtered off and the solvent was removed under reduced pressure to yield a brown oil. The residue was purified by flash chromatography on aluminum oxide (activation level III, *n*-hexane/EtOAc + 1% THF, 4:1, R_f = 0.44) and product *cis* **45** (519 mg, 0.686 mmol, 81%) was obtained as white solid. The same procedure was performed for its (-)-isomer *cis* **45**(β) (*n*-hexane/EtOAc, 5:1 + 1% THF, R_f = 0.33) to afford the product *cis* **45**(β) (0.47 g 0.62 mmol, 57%) as white solid. The spectroscopic data were in accordance with those described in the literature.^[165b]



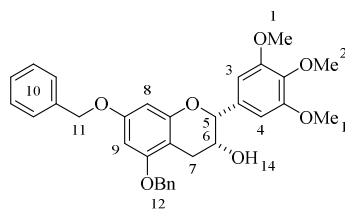
¹H NMR (300 MHz, CDCl₃): δ [ppm] = 7.55 – 7.27 (m, 25H, 11-H, 10-H, 9-H, 1-H), 6.82 (s, 2H, 2-H), 6.29 (s, 2H, 7-H, 6-H), 5.18 – 4.99 (m, 10H, 10-H, 9-H, 8-H), 4.90 (br s, 1H, 3-H), 4.22 (br s, 1H, 4-H), 3.08 – 2.85 (m, 2H, 5-H).

¹³C NMR (151 MHz, CDCl₃): δ [ppm] = 171.21, 158.87, 158.38, 155.20, 153.08, 138.40, 137.92, 137.07, 137.01, 136.56, 133.87, 128.67, 128.64, 128.61, 128.60, 128.56, 128.25, 128.06, 127.98, 127.96, 127.89, 127.64, 127.60, 127.29, 127.13, 127.02, 106.22, 101.10, 94.81, 94.21, 78.64, 75.31, 71.39, 70.65, 70.22, 70.04, 66.47, 60.47, 53.54, 28.21, 21.12, 14.29.

$[\alpha]_D^{25} = -16.9$ (*c* = 1.00 mol/L, CHCl₃).

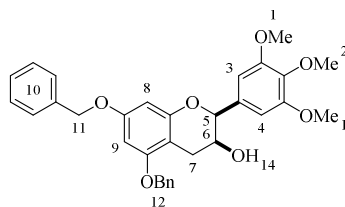
4.5.6.2 (-)-(2*R*,3*R*)-*cis*-5,7-Bis(benzyloxy)-2-(3,4,5)-tri(methoxy)phenylchroman-3-ol (*cis* **44** (*cis* **44**(β)))

The compound was prepared according to literature following a procedure by Tückmantel *et al.*^[268] The spectroscopic data were in accordance with those described in the literature.^[215] *cis* **44** was obtained as white solid in 61% yield.



^1H NMR (300 MHz, CDCl_3): δ [ppm] = 7.47 – 7.29 (m, 10H, 12-H, 10-H), 6.75 (d, J = 0.6 Hz, 2H, 4-H, 3-H), 6.34 – 6.23 (m, 2H, 9-H, 8-H), 5.03 (d, J = 4.7 Hz, 12-H, 11-H), 4.96 (s, 1H, 5-H), 4.31 – 4.28 (m, 1H, 6-H), 3.90 (s, 6H, 1-H), 3.87 (s, 3H, 2-H), 3.18 – 2.86 (m, 2H, 7-H).

^{13}C NMR (75 MHz, CDCl_3): δ [ppm] = 158.95, 158.48, 155.25, 153.64, 137.88, 137.10, 137.03, 134.02, 128.73, 128.67, 128.13, 128.03, 127.67, 127.62, 127.35, 103.44, 101.09, 94.90, 94.34, 78.86, 70.30, 70.13, 66.68, 60.99, 56.37, 28.42.



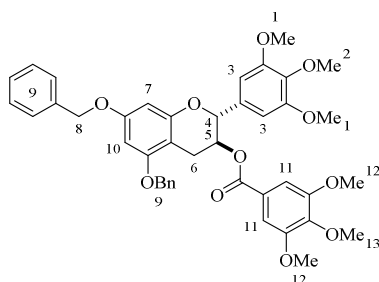
cis **44(β)** was obtained as white solid in 57% yield.

^1H NMR (300 MHz, CDCl_3): δ [ppm] = 7.44 – 7.31 (m, 10H, 12-H, 10-H), 6.75 (d, J = 0.6 Hz, 2H, 4-H, 3-H), 6.35 – 6.25 (m, 2H, 9-H, 8-H), 5.03 (d, J = 4.8 Hz, 4H, 12-H, 11-H), 4.96 (s, 1H, 5-H), 4.29 (br s, 1H, 6-H), 3.88 (d, J = 11.6 Hz, 9H, 2-H, 1-H), 3.15 – 2.83 (m, 2H, 7-H).

^{13}C NMR (75 MHz, CDCl_3): δ [ppm]: 170.26, 159.04, 157.79, 154.85, 153.38, 137.94, 136.96, 136.90, 133.43, 128.72, 128.68, 128.13, 128.08, 127.61, 127.40, 103.75, 101.50, 94.49, 94.01, 78.59, 70.24, 70.12, 69.06, 60.96, 56.26, 24.27, 21.26.

4.5.7 Esterification of Compounds **58-61**4.5.7.1 (2*R*,3*S*)-5,7-Bis(benzyloxy)-2-(3,4,5-trimethoxyphenyl)chroman-3-yl-(3,4,5-trimethoxy)benzoate (**58a**)

The compound was prepared according to literature following a procedure by Khandelwal *et al.*^[215] A 100-mL, two necked, round-bottomed flask equipped with a magnetic stirring bar was sequentially charged with substituted acids **22a/b** (2.00 eq), EDC·HCl (2.00 eq), and DMAP (2.00 eq) in dry CH₂Cl₂ (8 mL) at 0 °C under N₂-atmosphere. To this mixture a solution of *cis*-chroman-3-ol *cis* **44/cis** **45** (1.00 eq) in dry CH₂Cl₂ (2 mL) was added at 0 °C under N₂-atmosphere. The resulting mixture was stirred overnight at rt. Then the reaction was diluted with CH₂Cl₂ (5 mL) and washed with HCl (2 mL, 2.5 M) and, sat. NaHCO₃ (10 mL) solution. The organic layer was washed with brine (10 mL) and dried (Na₂SO₄), the drying agent was filtered off, and concentrated under reduced pressure. The residue was purified *via* flash chromatography (Alox III, *n*-hexane/EtOAc, 1:5) to give the desired ester **58a** (69.8 mg, 0.0966 mmol, 78%) as white solid. By using the same procedure as described above, EDCG-derivative were prepared with identical NMR spectra as the (–)-isomer.



¹H NMR (300 MHz, CDCl₃): δ [ppm] = 7.44 – 7.30 (m, 11H, 9-H), 7.12 (s, 2H, 11-H), 6.66 (s, 2H, 3-H), 6.30 (s, 2H, 10-H, 7-H), 5.59 – 5.52 (m, 1H, 5-H), 5.13 – 5.10 (m, 1H, 4-H), 3.88 – 3.70 (m, 19H, 13-H, 1-H, 2-H, 1-H), 3.23 – 2.85 (m, 2H, 6-H).

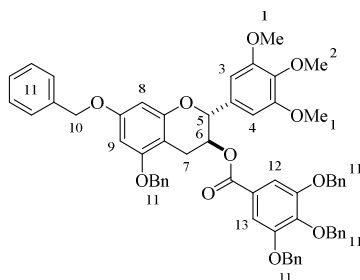
¹³C NMR (75 MHz, CDCl₃): δ [ppm] = 171.25, 165.35, 159.06, 157.81, 155.12, 153.45, 153.01, 142.59, 138.15, 136.93, 133.40, 128.73, 128.67, 128.14, 128.07, 127.59, 127.35, 125.07, 107.07, 104.02, 101.67, 94.53, 94.08, 79.09, 70.25, 70.12, 61.04, 60.93, 60.51, 56.37, 56.23, 25.11, 21.18, 14.33.

IR (Film): ν [cm⁻¹] = 2963 (b), 2837 (m), 2251 (s), 1715 (m), 1619 (s), 1591 (m), 1504 (m), 1462 (m), 1416 (s), 1333 (m), 1222 (m), 1175 (m), 1127 (b), 1038 (s), 1013 (b), 912 (m), 863 (s), 809 (b), 739 (b), 699 (m), 647 (s), 526 (s), 511 (s).

HRMS (ESI+) *m/z*: [M+H⁺] Calc C₄₂H₄₃O₁₁ 723.2800; found 723.2800.

4.5.7.2 (2*R*,3*S*)-5,7-Bis(benzyloxy)-2-(3,4,5-trimethoxyphenyl)chroman-3-yl-(3,4,5-trisbenzyl)benzoate (**58b**)

The compound was prepared according to the procedure described in *chapter 4.5.7.1*.



$^1\text{H NMR}$ (300 MHz, CDCl_3): δ [ppm] = 7.32 – 7.18 (m, 25H, 11-H), 7.15 (s, 2H, 12-H, 13-H), 6.53 (s, 2H, 4-H, 3-H), 6.25 (d, $J = 4.1$ Hz, 2H, 9-H, 8-H), 5.46 (q, $J = 6.7$ Hz, 1H, 6-H), 5.06 – 5.04 (m, 1H, 5-H), 5.00 – 4.97 (m, 10H, 10-H), 3.72 (s, 3H, 2-H), 3.65 (s, 6H, 1-H), 3.05 – 2.98 (m, 1H, 7-H), 2.84 – 2.76 (m, 1H, 7-H).

$^{13}\text{C NMR}$ (75 MHz, CDCl_3): δ [ppm] = 164.05, 157.92, 156.67, 153.87, 152.28, 151.41, 141.63, 136.31, 135.75, 135.71, 127.56, 127.52, 127.50, 127.48, 127.16, 127.02, 126.60, 126.46, 126.21, 123.91, 108.21, 102.63, 100.43, 93.36, 92.88, 77.61, 74.50, 70.22, 69.10, 68.97, 68.81, 59.79, 55.08, 23.40.

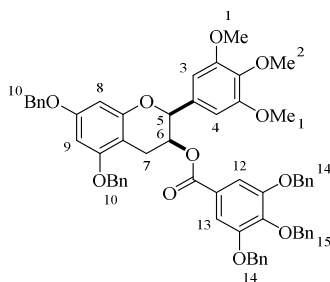
IR (Film): ν [cm^{-1}] = 3031 (s), 2961 (b), 2250 (m), 1953 (s), 1714 (m), 1619 (s), 1591 (m), 1502 (m), 1455 (s), 1428 (m), 1373 (m), 1330 (m), 1259 (m), 1101 (b), 1026 (b), 911 (s), 810 (s), 741 (b), 697 (s), 647 (s).

HRMS (ESI+) m/z : $[\text{M}+\text{H}^+]$ Calc $\text{C}_{60}\text{H}_{55}\text{O}_{11}$ 951.3739; found 951.3741.

58b (66.3 mg, 0.0698 mmol, 37%) was obtained as a white solid.

4.5.7.3 (2*S*,3*S*)-5,7-Bis(benzyloxy)-2-(3,4,5-trimethoxyphenyl)chroman-3-yl-(3,4,5-trisbenzyloxy)benzoate (**58c**)

The compound was prepared according to the procedure described in *chapter 4.5.7.1*.



$^1\text{H NMR}$ (300 MHz, CDCl_3): δ [ppm] = 7.46 – 7.20 (m, 25H, 15-H, 14-H, 10-H), 6.63 (s, 2H, 4-H, 3-H), 6.37 – 6.31 (m, 2H, 9-H, 8-H), 5.61 – 5.54 (m, 1H, 6-H), 5.25 (s, 1H, 5-H), 5.31 – 4.91 (m, 12H, 15-H, 14-H, 10-H), 3.82 (s, 3H, 2-H), 3.74 (s, 6H, 1-H), 3.16 – 2.87 (m, 2H, 7-H).

$^{13}\text{C NMR}$ (75 MHz, CDCl_3): δ [ppm] = 171.13, 165.13, 159.03, 157.77, 154.99, 153.38, 152.51, 142.71, 138.02, 137.42, 136.87, 136.81, 136.62, 133.42, 128.64, 128.61, 128.59, 128.57, 128.26, 128.19, 128.11, 128.06, 128.03, 127.84, 127.70, 127.59, 127.54, 127.31, 125.02, 109.29, 103.77, 101.53, 94.48, 93.99, 78.71, 75.19, 71.29, 70.17, 70.05, 69.93, 60.86, 60.42, 56.16, 53.50, 24.53, 21.09, 14.27.

IR (Film): ν [cm^{-1}] = 2961 (b), 2250 (s), 1952 (s), 1876 (s), 1714 (m), 1591 (m), 1501(m), 1455 (m), 1428 (m), 1373 (m), 1331 (m), 1239 (m), 1124 (b), 1026 (b), 910, (s), 813 (s), 738 (b), 697 (s).

HRMS (ESI+) m/z : $[\text{M}+\text{H}^+]$ Calc $\text{C}_{60}\text{H}_{55}\text{O}_{11}$ 951.3739; found 951.3739.

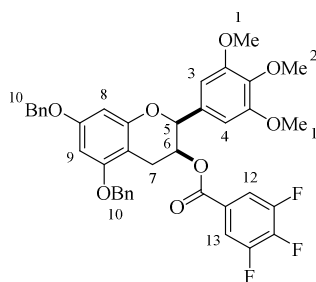
58c (139 mg, $0.146 \cdot 10^{-3}$ mol, 98%) was obtained as a slightly yellow oil.

TLC = SiO_2 , *n*-hexane/EtOAc, 3:1, R_f = 0.58.

Specific rotation: $[\alpha]_D^{25} = -6.7$ ($c = 1.57$ mol/L, CHCl_3).

4.5.7.4 (2*S*,3*S*)-5,7-Bis(benzyloxy)-2-(3,4,5-trimethoxyphenyl)chroman-3-yl-(3,4,5-trifluoro)benzoate (**58d**)

The compound was prepared according to the procedure described in *chapter 4.5.7.1*.



$^1\text{H NMR}$ (300 MHz, CDCl_3): δ [ppm] = 7.53 – 7.40 (m, 2H, 13-H, 12-H), 7.37 – 7.19 (m, 10H, 10-H), 6.53 (s, 2H, 4-H, 3-H), 6.22 (s, 2H, 9-H, 8-H), 5.50 – 4.48 (m, 1H, 6-H), 5.05 – 4.92 (m, 5H, 10-H), 3.71 (d, $J = 7.6$ Hz, 9H, 2-H, 1-H), 3.11 – 2.60 (m, 2H, 7-H).

$^{13}\text{C NMR}$ (75 MHz, CDCl_3): δ [ppm] = 171.14, 162.84, 159.12, 157.74, 154.82, 153.44, 138.07, 136.86, 136.76, 133.05, 128.65, 128.60, 128.07, 128.04, 127.63, 127.54, 127.34,

125.92, 125.86, 114.43, 114.33, 114.23, 114.13, 103.66, 101.08, 94.55, 94.13, 78.51, 71.02, 70.17, 70.09, 60.85, 60.42, 56.14, 24.53, 21.07, 14.26.

^{19}F NMR (300 MHz, CDCl_3): δ [ppm] = -132.50, -152.11.

IR (Film): ν [cm^{-1}] = 3066 (s), 2938 (b), 2839 (s), 2251 (s), 1955 (s), 1729 (s), 1620 (s), 1593 (s), 1529 (s), 1503 (s), 1441 (m), 1422 (s), 1371 (m), 1222 (m), 1182 (s), 1147 (s), 1128 (m), 1097 (s), 1048 (s), 911 (s), 886 (s), 812 (m), 740 (m), 698 (s), 647 (s), 530 (s).

HRMS (ESI+) m/z : $[\text{M}+\text{H}^+]$ Calc $\text{C}_{39}\text{H}_{34}\text{F}_3\text{O}_8$ 687.2206; found 687.2196.

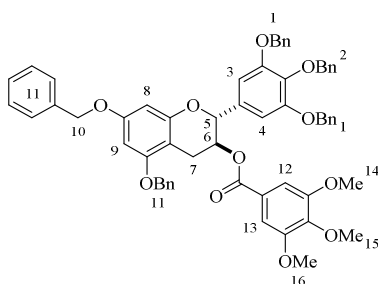
58 d (96 mg, $0.140 \cdot 10^{-3}$ mol, 94%) was obtained as a lightly yellow oil.

TLC = SiO_2 , *n*-hexane/EtOAc, 3:1, R_f = 0.50.

Specific rotation: $[\alpha]_D^{25} = -6.1$ ($c = 1.07$ mol/L, CHCl_3).

4.5.7.5 (2*R*,3*S*)-5,7-Bis(benzyloxy)-2-(3,4,5-tribenzylphenyl)chroman-3-yl-(3,4,5-trimethoxy)benzoate (**59a**)

The compound was prepared according to the procedure described in *chapter 4.5.7.1*.



^1H NMR (300 MHz, CDCl_3): δ [ppm] = 7.48 – 7.31 (m, 25H, 11-H, 2-H, 1-H), 7.18 (s, 2H, 13-H, 12-H), 6.79 (s, 2H, 4-H, 3-H), 6.34 (s, 2H, 9-H, 8-H), 5.53 (td, $J = 7.1, 5.4$ Hz, 1H, 6-H), 5.15 (d, $J = 7.0$ Hz, 1H, 5-H), 5.09 – 4.99 (m, 10H, 10-H, 2-H, 1-H), 3.89 (s, 3H, 15-H), 3.84 (s, 6H, 16-H, 14-H), 3.13 (dd, $J = 16.7, 5.4$ Hz, 1H, 7-H), 2.91 (dd, $J = 16.7, 7.2$ Hz, 1H, 7-H).

^{13}C NMR (75 MHz, CDCl_3): δ [ppm] = 171.17, 165.25, 159.03, 157.75, 154.99, 152.99, 152.97, 142.53, 138.62, 137.78, 136.92, 136.85, 133.47, 128.69, 128.62, 128.56, 128.51, 128.18, 128.11, 128.01, 127.95, 127.85, 127.56, 127.29, 125.03, 107.04, 106.64, 101.52, 94.48, 93.97, 78.74, 75.22, 71.40, 70.20, 70.02, 60.94, 60.44, 56.30, 24.64, 21.11, 14.28.

IR (Film): ν [cm^{-1}] = 3089 (b), 3031 (b), 2939 (b), 2838 (b), 2251 (m), 1953 (m), 1875 (m),

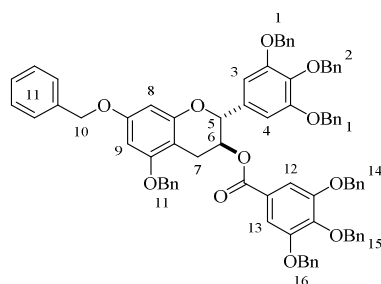
1808 (m), 1714 (b), 1620 (b), 1591 (b), 1504 (m), 1455 (m), 1416 (m), 1372 (m), 1334 (m), 1223 (b), 1128 (b), 1012 (b), 911 (m), 813 (m), 740 (b), 697 (s), 647 (s).

HRMS (ESI+) m/z : $[M+H]^+$ Calc $C_{60}H_{55}O_{11}$ 951.3739; found 951.3740.

59a (118 mg, 0.124 mmol, 94%) was obtained as a colorless oil.

4.5.7.6 (2*R*,3*S*)-5,7-Bis(benzyloxy)-2-(3,4,5-tribenzylphenyl)chroman-3-yl-(3,4,5-trisbenzyloxy)benzoate (**59b**)

The compound was prepared according to the procedure described in *chapter 4.5.7.1*.



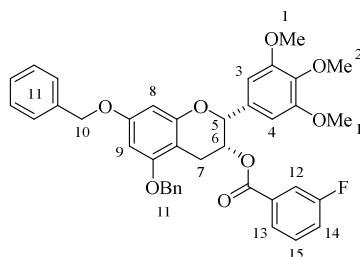
$^1\text{H NMR}$ (300 MHz, CDCl_3): δ [ppm] = 7.50 – 7.18 (m, 45H, 16-H, 15-H, 14-H, 11-H, 2-H, 1-H), 6.71 (s, 2H, 4-H, 3-H), 6.32 (s, 2H, 9-H, 8-H), 5.53 – 5.43 (m, 1H, 6-H), 5.14 – 5.11 (m, 4H, 5-H), 5.07 – 4.93 (m, 16H, 16-H, 15-H, 14-H, 10-H, 2-H, 1-H), 3.05 – 2.72 (m, 2H, 7-H).

$^{13}\text{C NMR}$ (75 MHz, CDCl_3): δ [ppm] = 171.25, 165.20, 159.10, 157.81, 154.95, 153.04, 152.67, 152.56, 142.77, 138.59, 137.86, 137.52, 136.95, 136.89, 136.77, 136.65, 133.55, 128.73, 128.68, 128.65, 128.63, 128.61, 128.57, 128.54, 128.29, 128.23, 128.16, 128.13, 128.08, 128.04, 127.96, 127.88, 127.77, 127.64, 127.36, 125.11, 109.29, 109.18, 106.47, 101.49, 94.49, 93.97, 78.58, 75.27, 71.43, 71.33, 60.51, 53.55, 21.17, 14.33.

59b (132.8 mg, 0.113 mmol, 85%) was obtained as a white solid.

4.5.7.7 (2*R*,3*R*)-5,7-Bis(benzyloxy)-2-(3,4,5-trimethoxyphenyl)chroman-3-yl-(3-fluorobenzoate) (**60a**)

The compound was prepared according to the procedure described in *chapter 4.5.7.1*.



$^1\text{H NMR}$ (300 MHz, CDCl_3): δ [ppm] = 7.67 – 7.64 (m, 1H, 13-H), 7.56 – 7.52 (m, 1H, 12-H), 7.40 – 7.06 (m, 12H, 15-H, 14-H, 11-H), 6.61 (s, 2H, 4-H, 3-H), 6.25 (dd, $J = 21.3$, 2.3 Hz, 2H, 9-H, 8-H), 5.58 (br s, 1H, 6-H), 5.03 – 4.89 (m, 5H, 10-H, 5-H), 3.70 (s, 3H, 2-H), 3.64 (s, 2H, 6-H), 3.04 (d, $J = 3.5$ Hz, 2H, 7-H).

$^{13}\text{C NMR}$ (75 MHz, CDCl_3): δ [ppm] = 164.46, 164.42, 164.13, 160.85, 158.93, 158.05, 155.60, 153.26, 137.89, 136.94, 136.87, 133.29, 132.29, 132.19, 130.14, 130.04, 128.70, 128.63, 128.12, 128.02, 127.68, 127.35, 127.29, 125.60, 125.56, 120.41, 120.13, 116.80, 116.49, 103.79, 100.79, 94.97, 94.14, 77.94, 70.26, 70.09, 69.15, 60.89, 56.04, 26.32.

$^{19}\text{F NMR}$ (300 MHz, CDCl_3): δ [ppm] = -112.23.

IR (Film): ν [cm^{-1}] = 3066 (s), 2938 (b), 2839 (s), 2250 (s), 1724 (m), 1619 (s), 1592 (m), 1500 (m), 1455 (m), 1420 (s), 1358 (m), 1296 (m), 1236 (m), 1202 (m), 1151 (m), 1129 (m), 1029 (s), 1004 (s), 910 (s), 812 (s), 754 (s), 734 (m), 698 (s).

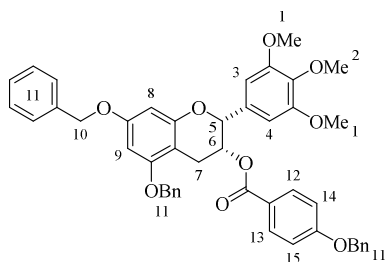
HRMS (ESI+) m/z : $[\text{M}+\text{H}^+]$ Calc $\text{C}_{39}\text{H}_{36}\text{FO}_8$ 651.2389; found 651.2396.

60a (67.3 mg, $7.66 \cdot 10^{-2}$ mmol, 97%) was obtained as a colorless oil.

TLC = SiO_2 , *n*-hexane/EtOAc, 3:1, $R_f = 0.32$.

4.5.7.8 (2*R*,3*R*)-5,7-Bis(benzyloxy)-2-(3,4,5-trimethoxyphenyl)chroman-3-yl-(4-benzyloxy)benzoate (**60b**)

The compound was prepared according to the procedure described in *chapter 4.5.7.1*.



$^1\text{H NMR}$ (300 MHz, CDCl_3): δ [ppm] = 7.82 – 7.76 (m, 2H, 13-H, 12-H), 7.33 – 7.15 (m, 15H, 11-H), 6.81 – 6.74 (m, 2H, 15-H, 14-H), 6.57 (s, 2H, 4-H, 3-H), 6.20 (dd, $J = 39.1, 2.3$ Hz, 2H, 9-H, 8-H), 5.56 – 5.51 (m, 1H, 6-H), 5.14 (s, 1H, 5-H), 4.99 – 4.84 (m, 7H, 10-H), 3.66 (s, 3H, 2-H), 3.56 (s, 6H, 1-H), 3.01 – 2.95 (m, 2H, 7-H).

$^{13}\text{C NMR}$ (151 MHz, CDCl_3): δ [ppm] = 171.40, 165.43, 162.86, 159.04, 158.29, 155.93, 153.39, 138.07, 137.20, 137.12, 136.44, 133.64, 132.10, 128.97, 128.89, 128.82, 128.51, 128.30, 128.19, 127.86, 127.67, 127.48, 122.89, 114.76, 104.24, 101.33, 95.14, 94.23, 78.39, 70.44, 70.34, 70.27, 68.36, 61.07, 60.67, 56.24, 53.74, 26.64, 21.33, 14.50, 14.43.

IR (Film): ν [cm^{-1}] = (2950 (b), 1714 (m), 1592 (b), 1508 (s), 1455 (m), 1359 (m), 1251 (m), 1150 (s), 1127 (m), 1008 (b), 771 (m), 696 (s).

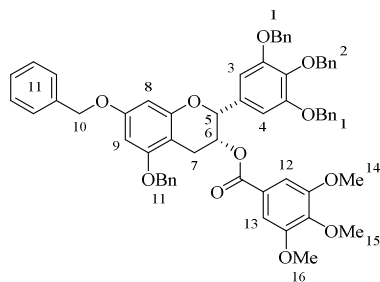
HRMS (ESI+) m/z : $[\text{M}+\text{H}^+]$ Calc $\text{C}_{46}\text{H}_{43}\text{O}_9$ 739.2902; found 739.2898.

60a (66.2 mg, 0.090 mmol, 95%) was obtained as a yellowish oil.

TLC = SiO_2 , *n*-hexane/EtOAc, 3:1, $R_f = 0.35$.

4.5.7.9 (2*R*,3*R*)-5,7-Bis(benzyloxy)-2-(3,4,5-tribenzylphenyl)chroman-3-yl-(3,4,5-trimethoxy)benzoate (**61a**)

The compound was prepared according to the procedure described in *chapter 4.5.7.1*.



$^1\text{H NMR}$ (300 MHz, CDCl_3): δ [ppm] = 7.36 – 7.22 (m, 25H, 11-H, 2-H, 1-H), 7.13 (m,

2H, 12-H, 13-H), 7.11 (s, 2H, 3-H, 4-H), 6.31 – 6.21 (m, 2H, 9-H, 8-H), 5.60 (dt, $J = 4.1$, 1.9 Hz, 1H, 6-H), 5.05 – 4.72 (m, 11H, 10-H, 5-H, 2-H, 1-H), 3.72 (d, $J = 3.6$ Hz, 9H, 16-H, 15-H, 14-H), 3.11 – 3.01 (m, 2H, 7-H).

^{13}C NMR (75 MHz, CDCl_3): δ [ppm] = 165.18, 158.92, 158.03, 155.64, 153.00, 142.61, 138.61, 137.82, 136.98, 133.48, 128.71, 128.64, 128.60, 128.52, 128.13, 128.02, 127.96, 127.86, 127.57, 127.51, 127.29, 125.14, 107.28, 106.91, 100.98, 94.71, 94.02, 75.26, 71.49, 70.23, 70.06, 68.71, 60.91, 56.36, 26.10.

IR (Film): ν [cm^{-1}] = 2924 (b), 2357 (s), 1716 (s), 1219 (s), 1125 (b), 1027 (b), 772 (s).

HRMS (ESI+) m/z : $[\text{M}+\text{H}^+]$ Calc $\text{C}_{60}\text{H}_{58}\text{NO}_{11}$ 968.4004; found 968.4003.

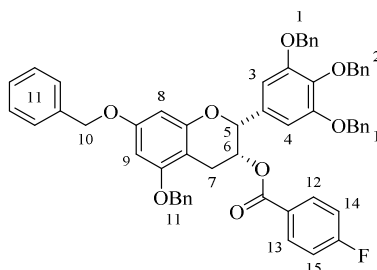
61a (104.1 mg, 0.110 mmol, 92%) was obtained as a colorless oil.

TLC = SiO_2 , *n*-hexane/EtOAc, 3:1, $R_f = 0.28$.

Specific rotation: $[\alpha]_D^{25} = -55.6$ ($c = 3.31$ mol/L, CHCl_3).

4.5.7.10 (2*R*,3*R*)-5,7-Bis(benzyloxy)-2-(3,4,5-tribenzylphenyl)chroman-3-yl-(4-fluoro)benzoate (**61b**)

The compound was prepared according to the procedure described in *chapter 4.5.7.1*.



^1H NMR (300 MHz, CDCl_3): δ [ppm] = 7.91 – 7.83 (m, 2H, 12-H, 13-H), 7.33 – 7.06 (m, 27H, 11-H, 1-H, 2-H), 6.97 – 6.87 (m, 2H, 3-H, 4-H), 6.69 (s, 2H, 8-H, 9-H), 6.26 – 6.14 (m, 2H, 6-H), 5.58 (s, 1H, 5-H), 5.00 – 4.81 (m, 9H, 1-H, 2-H), 4.74 – 4.70 (m, 2H, 10-H), 3.00 (m, 2H, 7-H).

^{13}C NMR (300 MHz, CDCl_3): δ [ppm] = 167.58, 164.52, 164.21, 158.92, 158.06, 155.59, 152.96, 138.40, 137.84, 137.01, 136.95, 136.88, 133.35, 132.50, 132.37, 131.00, 128.72, 128.64, 128.62, 128.53, 128.32, 128.18, 128.14, 128.03, 127.95, 127.83, 127.74, 127.67, 127.57, 127.51, 127.29, 126.40, 126.36, 115.77, 115.48, 106.62, 100.90, 94.90, 94.09, 75.21, 71.37, 70.25, 70.08, 68.65, 26.24.

^{19}F NMR (300 MHz, CDCl_3): δ [ppm] = -105.01.

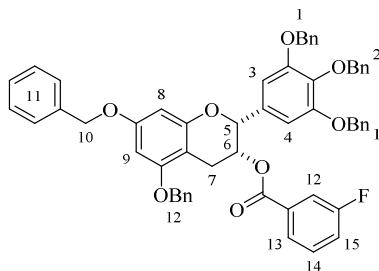
HRMS (ESI+) m/z : $[M+H^+]$ Calc $C_{57}H_{48}FO_8$ 879.3328; found 879.3328.

61b (95 mg, 0.107 mmol, 90%) was obtained as a colorless oil.

TLC = SiO_2 , *n*-hexane/EtOAc, 3:1, R_f = 0.50.

4.5.7.11 (2*R*,3*R*)-5,7-Bis(benzyloxy)-2-(3,4,5-tribenzylphenyl)chroman-3-yl-(3-fluorobenzoate) (**61c**)

The compound was prepared according to the procedure described in *chapter 4.5.7.1*.



1H NMR (300 MHz, $CDCl_3$): δ [ppm] = 7.97 (dd, J = 8.8, 5.4 Hz, 3H, 13-H), 7.49 – 7.29 (m, 25H, 11-H, 2-H, 1-H), 7.22 – 7.18 (m, 2H, 15-H, 12-H), 7.04 (t, J = 8.6 Hz, 1H, 14-H), 6.78 (s, 2H, 4-H, 3-H), 6.36 – 6.27 (m, 2H, 9-H, 8-H), 5.67 (br s, 1H, 6-H), 5.08 – 4.74 (m, 11H, 12-H, 10-H, 5-H, 2-H, 1-H), 3.12 – 3.10 (m, 2H, 7-H).

^{13}C NMR (75 MHz, $CDCl_3$): δ [ppm] = 167.60, 164.54, 164.23, 158.93, 158.06, 155.59, 152.97, 138.41, 137.85, 137.02, 136.89, 133.36, 132.51, 132.38, 130.99, 128.73, 128.65, 128.63, 128.54, 128.19, 128.15, 128.04, 127.96, 127.84, 127.68, 127.52, 127.30, 126.41, 115.78, 115.49, 106.63, 100.90, 94.90, 94.09, 75.22, 71.38, 70.27, 70.09, 68.66, 26.25.

^{19}F NMR (300 MHz, $CDCl_3$): δ [ppm] = -105.04.

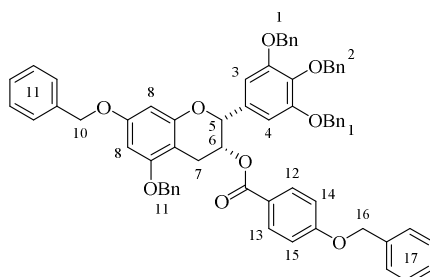
HRMS (ESI+) m/z : $[M+H^+]$ Calc $C_{57}H_{48}FO_8$ 879.3328; found 879.3324.

61b (64.7 mg, 0.0737 mmol, 93%) was obtained as a colorless oil.

TLC = SiO_2 , *n*-hexane/EtOAc, 4:1, R_f = 0.38.

4.5.7.12 (2*R*,3*R*)-5,7-Bis(benzyloxy)-2-(3,4,5-tribenzylphenyl)chroman-3-yl-(4-benzyloxy)benzoate (**61d**)

The compound was prepared according to the procedure described in *chapter 4.5.7.1*.



$^1\text{H NMR}$ (300 MHz, CDCl_3): δ [ppm] = 7.94 – 7.83 (m, 2H, 13-H, 12-H), 7.45 – 7.09 (m, 30H, 17-H, 11-H, 2-H, 1-H), 6.90 – 6.81 (m, 2H, 15-H, 14-H), 6.74 (s, 2H, 4-H, 3-H), 6.31 – 6.20 (m, 2H, 9-H, 8-H), 5.64 – 5.55 (m, 1H, 6-H), 5.02 – 4.83 (m, 11H, 10-H, 5-H), 4.72 (d, $J = 11.5$ Hz, 1H), 3.04 (s, 2H, 7-H).

$^{13}\text{C NMR}$ (300 MHz, CDCl_3): δ [ppm] = 165.18, 162.79, 158.88, 158.09, 155.68, 152.93, 138.38, 137.92, 137.14, 137.01, 136.94, 136.22, 133.48, 132.01, 128.78, 128.73, 128.65, 128.60, 128.51, 128.33, 128.19, 128.14, 128.02, 127.91, 127.82, 127.70, 127.58, 127.53, 127.32, 122.76, 114.60, 106.78, 101.11, 94.89, 94.04, 78.02, 75.23, 71.31, 70.28, 70.19, 70.09, 68.10, 26.27.

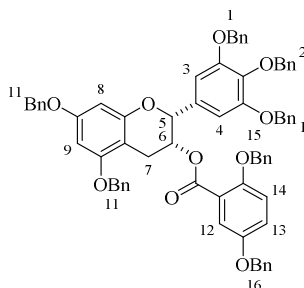
HRMS (ESI+) m/z : $[\text{M}+\text{H}^+]$ Calc $\text{C}_{64}\text{H}_{55}\text{O}_9 = 967.3841$; found 967.3824.

61c (51.8 mg, 0.054 mmol, 58%) was obtained as a colorless oil.

TLC = SiO_2 , n -hexane/EtOAc 3:1, $R_f = 0.80$.

4.5.7.13 (2*R*,3*R*)-5,7-Bis(benzyloxy)-2-(3,4,5-tribenzylphenyl)chroman-3-yl-(2,5-bisbenzyloxy)benzoate (**61e**)

The compound was prepared according to the procedure described in *chapter 4.5.7.1*.



$^1\text{H NMR}$ (300 MHz, CDCl_3): δ [ppm] = 7.49 – 7.11 (m, 39H, 16-H, 15-H, 11-H, 2-H, 1-H), 6.94 – 6.68 (m, 5H, 14-H, 13-H, 12-H, 4-H, 3-H), 6.30 – 6.20 (m, 2H, 9-H, 8-H),

5.69 – 5.68 (br s, 1H, 6-H), 5.30 (s, 1H, 5-H), 5.14 – 4.66 (m, 16H, 16-H, 15-H, 11-H, 2-H, 1-H), 3.26 – 2.98 (m, 2H, 7-H).

^{13}C NMR (300 MHz, CDCl_3): δ [ppm] = 164.74, 158.87, 158.04, 155.61, 152.90, 152.85, 152.60, 152.48, 138.38, 137.97, 137.15, 137.12, 136.93, 136.63, 133.49, 128.68, 128.65, 128.63, 128.57, 128.54, 128.44, 128.32, 128.16, 128.13, 128.09, 128.06, 127.97, 127.82, 127.80, 127.76, 127.71, 127.61, 127.57, 127.31, 127.25, 127.21, 127.06, 121.27, 120.46, 117.38, 116.68, 106.78, 101.12, 94.80, 94.04, 77.89, 75.21, 71.73, 71.25, 70.78, 70.53, 70.17, 70.00, 68.34, 29.81, 26.16.

IR (Film): ν [cm^{-1}] = 3853 (b), 2925 (m), 1497 (s), 1455 (s), 1435 (m), 1375 (s), 1219 (s), 1148 (s), 1113 (s), 1075 (s), 1026 (s), 909 (s), 772 (s), 696 (s).

HRMS (ESI+) m/z [$\text{M}+\text{H}^+$] Calc $\text{C}_{71}\text{H}_{64}\text{NO}_{10}$ 1090.4525; found 1090.4525.

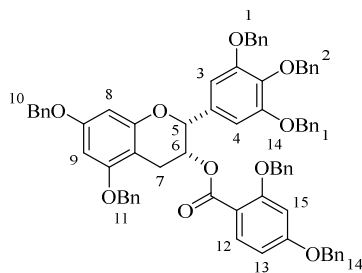
61e (64.2 mg, 0.0599 mmol, 91%) was obtained as colorless oil.

TLC = SiO_2 , *n*-hexane/EtOAc 3:1, R_f = 0.30.

Specific rotation: $[\alpha]_D^{25} = -45.4$ ($c = 3.81$ mol/L, CHCl_3).

4.5.7.14 (2*R*,3*R*)-5,7-Bis(benzyloxy)-2-(3,4,5-tribenzylphenyl)chroman-3-yl-(2,4-bisbenzyloxy)benzoate (**61f**)

The compound was prepared according to the procedure described in *chapter 4.5.7.1*.



^1H NMR (300 MHz, CDCl_3): δ [ppm] = 7.57 – 7.54 (m, 2H, 13-H, 12-H), 7.40 – 7.03 (m, 35H, 15-H, 14-H, 11-H, 10-H, 2-H, 1-H), 6.74 (s, 2H, 3-H, 4-H), 6.29 (dd, $J = 14.2, 2.3$ Hz, 2H, 9-H, 8-H), 5.62 (br s, 1H, 6-H), 5.04 – 4.67 (m, 15H, 14-H, 11-H, 10-H, 5-H, 2-H, 1-H), 3.14 – 3.00 (m, 2H, 7-H).

^{13}C NMR (75 MHz, CDCl_3): δ [ppm] = 165.33, 158.93, 158.79, 158.09, 155.66, 152.96, 138.40, 137.91, 137.12, 136.99, 136.94, 136.43, 133.40, 131.49, 129.59, 128.75, 128.73, 128.67, 128.65, 128.50, 128.26, 128.19, 128.14, 128.04, 127.91, 127.83, 127.70, 127.61,

127.34, 122.51, 120.07, 115.75, 106.71, 100.99, 94.92, 94.12, 77.96, 75.23, 71.31, 70.30, 70.26, 70.11, 68.66, 26.24.

IR (Film): ν [cm^{-1}] = 3066 (m), 3032 (b), 2938 (b), 2839 (s), 2251 (s), 1955 (s), 1729 (m), 1620 (m), 1592 (s), 1529 (s), 1503 (m), 1441 (b), 1371 (b), 1222 (b), 1147 (m), 1128 (m), 1048 (m), 1010 (m), 740 (m), 698 (s), 647 (s), 530 (s).

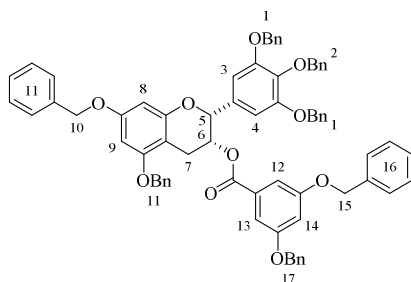
HRMS (ESI+) m/z : $[\text{M}+\text{NH}_4^+]$ Calc $\text{C}_{71}\text{H}_{61}\text{NO}_{10}$ 1090.4525; found 1090.4525.

61f (49.4 mg, 0.046 mmol, 70%) was obtained as colorless oil.

Specific rotation: $[\alpha]_D^{25} = -45.4$ ($c = 3.81$ mol/L, CHCl_3).

4.5.7.15 (2*R*,3*R*)-5,7-Bis(benzyloxy)-2-(3,4,5-tribenzylphenyl)chroman-3-yl-(3,5-bisbenzyloxy)benzoate (**61g**)

The compound was prepared according to the procedure described in *chapter 4.5.7.1*.



$^1\text{H NMR}$ (600 MHz, CDCl_3): δ [ppm] = 7.39 – 7.22 (m, 35H, 17-H, 16-H, 11-H, 2-H, 1-H), 7.18 – 7.13 (m, 3H, 13-H, 12-H), 6.73 (s, 2H, 3-H, 4-H), 6.67 (t, $J = 2.4$ Hz, 1H, 14-H), 6.29 (dd, $J = 26.3, 2.3$ Hz, 2H, 9-H, 8-H), 5.60 (br s, 1H, 6-H), 5.03 – 4.71 (m, 15H, 17-H, 15-H, 10-H, 5-H, 2-H, 1-H), 3.14 – 2.99 (m, 2H, 7-H).

$^{13}\text{C NMR}$ (151 MHz, CDCl_3): δ [ppm] = 165.01, 159.66, 158.73, 157.88, 155.45, 152.76, 138.20, 137.73, 136.95, 136.77, 136.75, 136.12, 133.16, 131.84, 128.55, 128.51, 128.47, 128.44, 128.28, 128.10, 127.99, 127.93, 127.84, 127.70, 127.68, 127.62, 127.50, 127.43, 127.14, 108.58, 106.75, 106.51, 100.76, 94.76, 93.96, 77.81, 75.03, 71.10, 70.21, 70.11, 69.92, 68.59, 26.03.

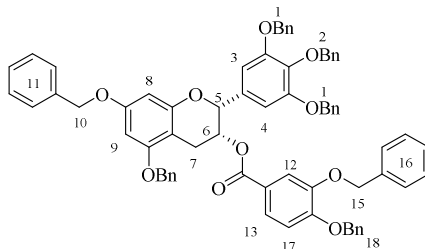
IR (Film): ν [cm^{-1}] = 3064 (s), 3031 (s), 2961 (m), 2871 (s), 2250 (s), 1951 (s), 1875 (s), 1809 (s), 1718 (m), 1592 (m), 1497 (m), 1442 (m), 1374 (m), 1295 (m), 1260 (m), 1220 (m), 1150 (s), 1102 (m), 1027 (m), 910 (s), 809 (m), 746 (m), 696 (m).

HRMS (ESI+) m/z : $[\text{M}+\text{H}^+]$ Calc $\text{C}_{71}\text{H}_{61}\text{O}_{10}$ 1073.4259; found 1073.4252.

61g (61.5 mg, 0.057 mmol, 72%) was obtained as a colorless oil.

4.5.7.16 (2*R*,3*R*)-5,7-Bis(benzyloxy)-2-(3,4,5-tribenzyloxyphenyl)chroman-3-yl-(3,4-bisbenzyloxy)benzoate (**61h**)

The compound was prepared according to the procedure described in *chapter 4.5.7.1*.



$^1\text{H NMR}$ (600 MHz, CDCl_3): δ [ppm] = 7.59 – 7.49 (m, 2H, 13-H, 17-H), 7.45 – 7.14 (m, 38H, 18-H, 16-H, 11-H, 2-H, 1-H), 6.77 (dd, $J = 8.5, 1.4$ Hz, 1H, 12-H), 6.73 (s, 2H, 4-H, 3-H), 6.32 (dt, $J = 30.6, 2.4$ Hz, 2H, 6-H), 5.63 (br s, 1H, 6-H), 5.13 – 4.90 (m, 12H, 10-H, 5-H, 2-H, 1-H), 4.75 (ddd, $J = 89.5, 11.5, 1.6$ Hz, 4H, 18-H, 15-H), 3.11 – 3.01 (m, 2H, 7-H).

$^{13}\text{C NMR}$ (151 MHz, CDCl_3): δ [ppm] = 164.84, 158.69, 157.90, 155.49, 152.92, 152.70, 148.05, 138.22, 137.70, 136.90, 136.76, 136.71, 136.47, 136.32, 133.20, 128.50, 128.47, 128.43, 128.40, 128.26, 127.97, 127.90, 127.88, 127.86, 127.81, 127.65, 127.59, 127.57, 127.42, 127.31, 127.10, 126.86, 124.02, 122.68, 115.30, 112.92, 106.61, 100.90, 94.62, 93.85, 77.84, 75.00, 71.02, 70.88, 70.62, 70.05, 69.88, 67.92, 26.09.

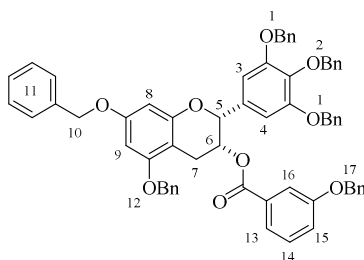
IR (Film): ν [cm^{-1}] = 3064 (s), 3031 (s), 2961 (b), 2870 (b), 2249 (m), 1952 (m), 1876 (m), 1809 (m), 1714 (m), 1619 (s), 1592 (m), 1504 (m), 1428 (m), 1373 (m), 1263 (b), 1206 (b), 1104 (b), 911 (m), 813 (m), 740 (m), 696 (m).

HRMS (ESI+) m/z : [$\text{M}+\text{NH}_4^+$] Calc $\text{C}_{71}\text{H}_{61}\text{NO}_{10}$ 1090.4525; found 1090.4525.

61h (133.5 mg, 0.124 mmol, 76%) was obtained as a colorless oil.

4.5.7.17 (2*R*,3*R*)-5,7-Bis(benzyloxy)-2-(3,4,5-tribenzyloxyphenyl)chroman-3-yl-(3-benzyloxy)benzoate (**61i**)

The compound was prepared according to the procedure described in *chapter 4.5.7.1*.



$^1\text{H NMR}$ (300 MHz, CDCl_3): δ [ppm] = 7.64 – 7.53 (m, 3H, 15-H, 14-H, 13-H), 7.43 – 7.03 (m, 36H, 17-H, 11-H, 12-H, 2-H, 1-H), 6.75 (s, 2H, 4-H, 3-H), 6.29 (dd, $J = 28.5, 2.3$ Hz, 2H, 9-H, 8-H), 5.63 – 5.62 (m, 1H, 6-H), 5.07 – 4.69 (m, 15H, 17-H, 12-H, 10-H, 5-H, 2-H, 1-H), 3.12 – 3.01 (m, 2H, 7-H).

$^{13}\text{C NMR}$ (75 MHz, CDCl_3): δ [ppm] = 167.03, 165.33, 158.93, 158.84, 158.78, 158.08, 155.65, 152.95, 138.39, 137.91, 137.12, 136.99, 136.94, 136.67, 136.43, 133.40, 131.60, 131.49, 129.59, 129.57, 128.74, 128.72, 128.66, 128.64, 128.60, 128.49, 128.29, 128.25, 128.22, 128.19, 128.14, 128.04, 128.01, 127.90, 127.82, 127.69, 127.67, 127.64, 127.60, 127.33, 122.50, 122.37, 120.33, 120.06, 115.75, 115.21, 106.71, 100.99, 94.92, 94.11, 77.95, 75.22, 71.46, 71.31, 70.28, 70.25, 70.11, 68.66, 52.31, 26.24.

IR (Film): ν [cm^{-1}] = 3031 (s), 2931 (b), 2870 (b), 2249 (s), 1951 (s), 1876 (s), 1809 (s), 1720 (s), 1618 (s), 1592 (s), 1498 (s), 1454 (s), 1440 (s), 1374 (s), 1354 (m), 1271 (m), 1216 (s), 1149 (s), 1114 (m), 1027 (m), 909 (s), 811 (m), 734 (b), 696 (m).

HRMS (ESI+) m/z : $[\text{M}+\text{NH}_4^+]$ Calc $\text{C}_{64}\text{H}_{58}\text{NO}_9$ 984.4106; found 984.4107.

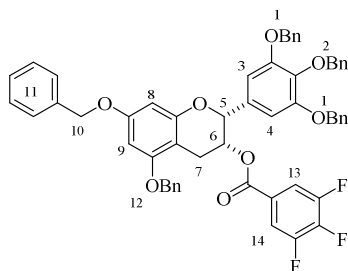
61h (46.9 mg, $4.85 \cdot 10^{-5}$ mol, 61%) was obtained as a colorless oil.

TLC = SiO_2 , *n*-hexane/EtOAc, 3:1, $R_f = 0.30$.

Specific rotation: $[\alpha]_D^{25} = -63.3$ ($c = 2.35$ mol/L, CHCl_3).

4.5.7.18 (2*R*,3*R*)-5,7-Bis(benzyloxy)-2-(3,4,5-tribenzylphenyl)chroman-3-yl-(3,4,5-trifluorobenzoate) (**61j**)

The compound was prepared according to the procedure described in *chapter 4.5.7.1*.



$^1\text{H NMR}$ (600 MHz, CDCl_3): δ [ppm] = 7.46 (t, $J = 6.9$ Hz, 2H, 14-H, 13-H), 7.39 – 7.03 (m, 25H, 11-H, 2-H, 1-H), 6.69 (s, 2H, 4-H, 3-H), 6.24 (dd, $J = 26.5, 2.3$ Hz, 2H, 9-H, 8-H), 5.56 – 5.50 (m, 1H, 6-H), 5.03 – 4.78 (m, 12H, 10-H, 5-H, 2-H, 1-H), 3.10 – 2.92 (m, 2H, 7-H).

$^{13}\text{C NMR}$ (151 MHz, CDCl_3): δ [ppm] = 162.85, 159.03, 158.04, 155.42, 153.06, 138.38, 137.80, 136.96, 136.91, 136.84, 133.17, 128.74, 128.67, 128.63, 128.58, 128.20, 128.19, 128.12, 128.09, 128.01, 127.88, 127.69, 127.46, 127.33, 126.04, 114.47, 114.43, 114.35, 114.32, 106.27, 100.51, 94.97, 94.24, 75.23, 71.44, 70.30, 70.14, 69.89, 53.55, 26.14, 24.80.

$^{19}\text{F NMR}$ (600 MHz, CDCl_3): δ [ppm] = -132.31, -152.06.

IR (Film): ν [cm^{-1}] = 3031 (b), 2869 (b), 2358 (b), 1728 (s), 1619 (m), 1592 (s), 1527 (s), 1498 (s), 1439 (s), 1372 (s), 1345 (s), 1220 (s), 1149 (s), 1115 (s), 1048 (s), 1028 (s), 912 (s), 811 (m), 742 (m), 696 (s).

HRMS (ESI+) m/z : $[\text{M}+\text{H}^+]$ Calc $\text{C}_{57}\text{H}_{46}\text{F}_3\text{O}_8$ 915.3139; found 915.3139.

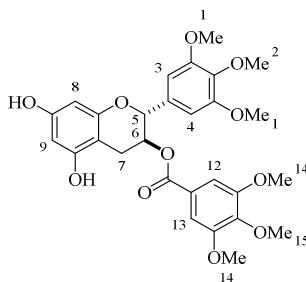
61j (45.2 mg, 0.0494 mmol, 75%) was obtained as a colorless oil.

Specific rotation: $[\alpha]_D^{25} = -44.1$ ($c = 2.56$ mol/L, CHCl_3).

4.5.8 Catalytic Hydrogenation of Compounds **62/65**

The compounds were prepared according to literature following a procedure by Li *et al.*^[165b] A 100-mL, two necked round-bottomed flask equipped with a magnetic stirring bar and three-way-cock, equipped with a balloon filled with hydrogen, was charged with ester **58-61** (0.100 mmol, 1.00 eq) in a mixture of THF/methanol (5 mL, 1:1, v/v). The space was purged with N₂, then Pd(OH)₂ (0.82 eq, 20 % on carbon) was added in one batch to the solution. The resulting mixture was stirred at rt under H₂-atmosphere until TLC (RP 18, acetonitrile/H₂O, 3:2) showed full consumption of the starting material. The black solution was filtered through a syringe filters (0.2 μm PTFE)) and the filtrate was evaporated.

4.5.8.1 (2*R*,3*S*)-5,7-Dihydroxy-2-(3,4,5-trimethoxyphenyl)chroman-3-yl-(3,4,5-trimethoxy)benzoate (**62a**)



¹H NMR (300 MHz, CDCl₃): δ [ppm] = 7.02 (s, 2H, 8-H, 9-H), 6.58 (s, 2H, 3-H, 4-H), 6.03 (s, 1H, 8-H, 9-H), 5.87 (s, 2H, 13-H, 12-H), 5.43 (q, *J* = 7.7 Hz, 1H, 5-H), 4.96 (d, *J* = 7.6 Hz, 1H, 6-H), 3.79 – 3.66 (m, 18H, 1-H, 2-H, 14-H, 15-H), 3.06 (dd, *J* = 16.1, 5.5 Hz, 1H, 7-H), 2.75 (dd, *J* = 16.1, 8.0 Hz, 1H, 7-H)

¹³C NMR (75 MHz, CDCl₃): δ [ppm] = 165.73, 155.85, 155.32, 155.29, 155.26, 153.18, 152.85, 142.46, 137.69, 133.50, 124.73, 106.94, 104.06, 99.36, 95.61, 78.91, 70.58, 60.94, 60.87, 56.21, 56.07, 24.89.

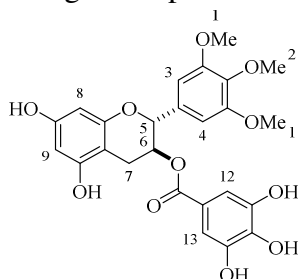
IR (Film): ν [cm⁻¹] = 3423 (b), 2839 (m), 225 (s), 1714 (m), 1626 (m), 1593 (m), 1505 (m), 1462 (m), 1357 (m), 1334 (m), 1177 (m), 1037 (m), 863 (s), 759 (s), 633 (m).

HRMS (ESI+) *m/z*: [M+H⁺] Calc C₂₆H₃₁O₁₁ 543.1861; found 543.1862.

62a (16.7 mg, 0.0308 mmol, 24%) was obtained as a colorless oil.

4.5.8.2 (2*R*,3*S*)-5,7-Dihydroxy-2-(3,4,5-trimethoxyphenyl)chroman-3-yl-(3,4,5-trihydroxy)benzoate (**62b**)

The compound was prepared according to the procedure described in *chapter 4.5.8*.



$^1\text{H NMR}$ (300 MHz, CD_3OD): δ [ppm] = 6.88 (s, 2H, 8-H, 9-H), 6.61 (s, 2H, 3-H, 4-H), 5.91 – 5.85 (m, 2H, 8-H, 9-H), 5.32 – 5.24 (m, 1H, 5-H), 4.97 (d, $J = 6.9$ Hz, 2H, 6-H), 3.64 (s, 3H, 11-H), 3.61 (s, 6H, 1-H), 2.79 (dd, $J = 16.4, 5.5$ Hz, 2H, 7-H), 2.61 (dd, $J = 16.4, 7.1$ Hz, 2H, 7-H).

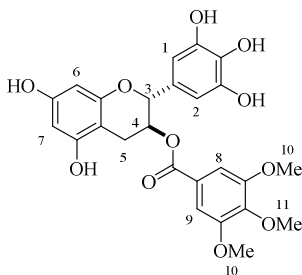
$^{13}\text{C NMR}$ (300 MHz, CD_3OD): δ [ppm] = 167.24, 158.30, 157.71, 156.45, 154.39, 146.48, 135.75, 121.27, 110.15, 105.01, 99.82, 96.70, 79.57, 71.18, 61.12, 56.57, 30.68.

IR (Solid): ν [cm^{-1}] = 3418 (b), 2940 (m), 2839 (s), 2252 (s), 1714 (m), 1625 (s), 1593 (m), 1505 (m), 1462 (m), 1417 (m), 1334 (m), 1230 (m), 1176 (s), 1128 (m), 1002 (m), 912 (m), 821 (s), 757 (s), 732 (s), 647 (s).

HRMS (ESI+) m/z : $[\text{M}+\text{H}^+]$ Calc $\text{C}_{25}\text{H}_{25}\text{O}_{11}$ 501.1391; found 501.1380.

4.5.8.3 (2*R*,3*S*)-5,7-Dihydroxy-2-(3,4,5-hydroxyphenyl)chroman-3-yl-(3,4,5-trimethoxy)benzoate (**63a**)

The compound was prepared according to the procedure described in *chapter 4.5.8*.



$^1\text{H NMR}$ (300 MHz, CD_3OD): δ [ppm] = 7.01 (s, 2H, 8-H, 9-H), 6.36 (s, 2H, 1-H, 2-H), 5.85 (d, $J = 9.1$ Hz, 1H, 6-H, 7-H), 5.24 – 5.08 (m, 1H, 3-H), 4.84 (d, $J = 7.1$ Hz, 1H, 4-H), 3.70 (s, 6H, 10-H), 3.68 (s, 3H, 11-H), 2.93 (dd, $J = 16.2, 5.2$ Hz, 1H, 5-H), 2.61 (dd, $J = 16.2, 7.4$ Hz, 1H, 5-H).

^{13}C NMR (75 MHz, CD_3OD): δ [ppm] = 166.92, 158.21, 157.67, 156.75, 154.24, 147.04, 143.43, 134.17, 130.64, 126.62, 107.83, 106.84, 99.80, 96.51, 95.54, 80.05, 72.51, 61.10, 56.65, 25.61.

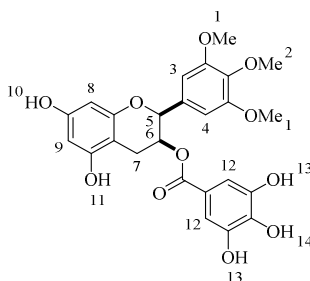
IR (Solid): ν [cm^{-1}] = 2920 (m), 1507 (s), 1456 (s), 1260 (s), 1017 (s), 913 (s), 745 (s).

HRMS (ESI+) m/z : $[\text{M}+\text{H}^+]$ Calc $\text{C}_{25}\text{H}_{25}\text{O}_{11}$ 501.1386; found 501.1391.

63a (29.8 mg, 0.0596 mmol, 43%) was obtained as a slightly yellow oil.

4.5.8.4 (2*S*,3*S*)-5,7-Dihydroxy-2-(3,4,5-trimethoxyphenyl)chroman-3-yl-(3,4,5-trihydroxy)benzoate (**64a**)

The compound was prepared according to the procedure described in *chapter 4.5.8*.



^1H NMR (600 MHz, CD_3OD): δ [ppm] = 7.01 (s, 2H, 12-H), 6.72 (s, 2H, 3-H, 4-H), 6.04 – 5.97 (m, 2H, 8-H, 9-H), 5.42 – 5.39 (m, 1H, 6-H), 5.08 (d, J = 6.9 Hz, 1H, 5-H), 3.75 (s, 6H, 1-H), 3.72 (s, 3H, 2-H), 2.92 – 2.75 (m, 2H, 7-H).

^{13}C -NMR (151 MHz, CD_3OD): δ [ppm] = 167.21, 158.20, 157.63, 156.39, 154.31, 146.41, 139.90, 138.63, 135.68, 121.24, 110.14, 104.95, 99.82, 96.68, 95.57, 79.55, 71.15, 61.11, 56.48, 49.85, 25.30.

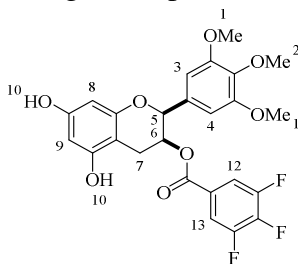
HRMS (ESI+) m/z : $[\text{M}+\text{H}^+]$ Calc $\text{C}_{25}\text{H}_{25}\text{O}_{11}$ 501.1391; found 501.1380.

64a (62.1 mg, 0.124 mmol, 75%) was obtained as a colorless oil.

Specific rotation: $[\alpha]_D^{25} = -6.7$ (c = 1.57 mol/L, CHCl_3).

4.5.8.5 (2*S*,3*S*)-5,7-Dihydroxy-2-(3,4,5-trimethoxyphenyl)chroman-3-yl-(3,4,5-trifluorobenzoate) (**64b**)

The compound was prepared according to the procedure described in *chapter 4.5.8*.



$^1\text{H NMR}$ (600 MHz, CD_3OD): δ [ppm] = 7.69 – 7.60 (m, 2H, 13-H, 12-H), 6.74 (d, $J = 2.3$ Hz, 2H, 4-H, 3-H), 6.04 – 5.96 (m, 2H, 9-H, 8-H), 5.47 – 5.43 (m, 1H, 6-H), 5.09 (dd, $J = 7.2, 1.5$ Hz, 2H, 5-H), 3.75 (d, $J = 25.1$ Hz, 11H, 2-H, 1-H), 3.01 – 2.76 (m, 2H, 7-H).

$^{13}\text{C NMR}$ (151 MHz, CD_3OD): δ [ppm] = 157.00, 156.33, 155.01, 153.07, 137.48, 133.98, 113.92, 113.77, 103.75, 98.16, 95.40, 94.20, 78.07, 71.56, 67.46, 59.68, 55.14, 25.09, 24.04.

$^{19}\text{F NMR}$ (600 MHz, CD_3OD): δ [ppm] = -136.20, -155.84.

IR (solid): ν [cm^{-1}] = 2972 (m), 2493 (m), 1728 (m), 1625 (s), 1593 (s), 1525 (8s), 1504 (s), 1440 (m), 1371 (m), 1220 (m), 1120 (m), 1045 (m), 1004 (s), 883 (s), 819 (m), 761 (s), 742 (s), 711 (s), 634 (s).

HRMS (ESI+) m/z : [$\text{M}+\text{H}^+$] Calc $\text{C}_{25}\text{H}_{22}\text{F}_3\text{O}_8$ 507.1267; found 507.1257.

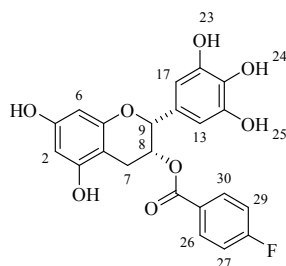
TLC = RP 18, acetonitrile/ H_2O , 3:2, $R_f = 0.48$.

Specific rotation: $[\alpha]_D^{25} = -6.1$ ($c = 1.08$ mol/L, CHCl_3).

64b (66.7 mg, 0.132 mmol, 83%) was obtained as colorless oil.

4.5.8.6 (2*R*,3*R*)-5,7-Dihydroxy-2-(3,4,5-tris(hydroxyl)phenyl)chroman-3-yl-(4-fluoro)benzoate (**65b**)

The compound was prepared according to the procedure described in *chapter 4.5.8*.



$^1\text{H NMR}$ (600 MHz, CD_3OD): δ [ppm] = 7.96 – 7.92 (m, 2H, 12-H, 14-H), 7.17 – 7.11(m, 2H, 15-H, 13-H), 6.52 (s, 2H, 3-H, 4-H), 6.00 – 5.96 (m, 2H, 9-H, 8-H), 5.57 (br s, 1H, 6-H), 5.02 (s, 1H, 5-H), 3.03 (dd, $J = 17.5, 4.4$ Hz, 1H, 7-H), 2.95 – 2.89 (m, 1H, 7-H).

$^{13}\text{C NMR}$ (151 MHz, CD_3OD): δ [ppm] = 168.01, 166.34, 166.29, 158.00, 157.95, 157.86, 157.14, 146.78, 143.79, 133.73, 133.41, 133.35, 130.71, 127.85, 127.83, 116.52, 116.37, 106.61, 99.13, 96.54, 95.77, 78.41, 70.89, 30.67, 26.66.

$^{19}\text{F NMR}$ (300 MHz, CDCl_3): δ [ppm] = -108.09.

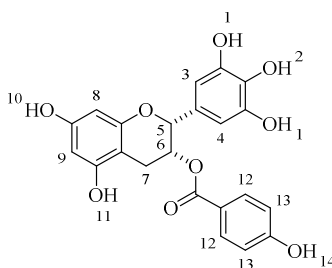
IR (film): ν [cm^{-1}] = 3176 (b), 2465 (b), 2416 (b), 2225 (s), 1695 (s), 1595 (s), 1525 (m), 1485 (m), 1444 (s), 1359 (m), 1284 (s), 1269 (s), 1205 (s), 1145 (s), 1093 (s), 1070 (s), 1031 (s), 1016 (s), 968 (s), 937 (m), 889 (s), 815 (m), 781 (s), 754 (s).

HRMS (ESI+) m/z : [$\text{M}+\text{H}^+$] Calc $\text{C}_{22}\text{H}_{18}\text{FO}_8$ 429.0980; found 429.0977.

65b (23.0 mg, 0.0537 mmol, 48%) was obtained as colorless oil.

4.5.8.7 (2*R*,3*R*)-5,7-Dihydroxy-2-(3,4,5-trihydroxyphenyl)chroman-3-yl-(4-hydroxy)benzoate (**65d**)

The compound was prepared according to the procedure described in *chapter 4.5.8*.



$^1\text{H NMR}$ (600 MHz, CD_3OD): δ [ppm] = 7.79 – 7.74 (m, 2H, 12-H), 6.80 – 6.74 (m, 2H,

13-H), 6.54 (s, 2H, 4-H, 3-H), 6.03 – 5.97 (m, 2H, 9-H, 8-H), 5.55 – 5.49 (m, 1H, 6-H), 5.02 (s, 1H, 5-H), 3.02 (dd, $J = 17.3, 4.6$ Hz, 1H, 7-H), 2.90 (dd, $J = 17.4, 2.8$ Hz, 1H, 7-H).

^{13}C NMR (151 MHz, CD_3OD): δ [ppm] = 167.49, 163.37, 157.88, 157.84, 157.79, 157.77, 157.72, 157.16, 157.12, 157.10, 146.68, 133.66, 132.90, 132.83, 130.83, 122.27, 118.14, 116.06, 106.73, 99.34, 96.51, 95.77, 78.51, 70.21, 26.67.

IR (solid): ν [cm^{-1}] = 3275 (b), 2478 (b), 2073 (s), 1681 (m), 1600 (m), 1512 (s), 1423 (s), 1357 (s), 1265 (m), 1205 (m), 1165 (m), 1101 (b), 1043 (m), 966 (m), 850 (s), 813 (s), 769 (s), 694 (s).

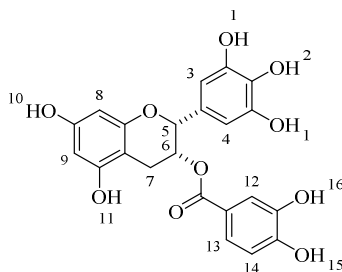
HRMS (ESI+) m/z : $[\text{M}+\text{H}^+]$ Calc $\text{C}_{22}\text{H}_{19}\text{O}_9$ 427.1024; found 427.016.

65d (32.4 mg, 0.07609 mmol, 79%) was obtained as a white solid.

TLC = RP 18, acetonitrile/ H_2O , 3:2, $R_f = 0.82$.

4.5.8.8 (2*R*,3*R*)-5,7-Dihydroxy-2-(3,4,5-trihydroxyphenyl)chroman-3-yl-(3,4-dihydroxy)benzoate (**65h**)

The compound was prepared according to the procedure described in *chapter 4.5.8*.



^1H NMR (600 MHz, CD_3OD): δ [ppm] = 7.31 – 7.25 (m, 2H, 14-H, 13-H), 6.72 – 6.65 (m, 1H, 12-H), 6.47 (s, 2H, 4-H, 3-H), 5.96 – 5.85 (m, 2H, 9-H, 8-H), 5.48 (br s, 1H, 6-H), 4.94 (s, 1H, 5-H), 3.00 – 2.77 (m, 2H, 7-H).

^{13}C NMR (600 MHz, CD_3OD): δ [ppm] = 167.27, 157.56, 156.89, 151.36, 146.38, 145.59, 133.42, 130.52, 123.66, 122.34, 117.21, 115.54, 106.52, 99.10, 96.23, 95.54, 78.26, 69.77, 26.46.

IR (solid): ν [cm^{-1}] = 3313 (b), 2941 (s), 2463 (b), 2237 (s), 2071 (s), 1689 (b), 1593 (m), 1504 (m), 1440 (m), 1421 (s), 1371 (m), 1336 (s), 1224 (m), 1116 (m), 1035 (s), 968 (s), 871 (s), 819 (s), 763 (s), 630 (s).

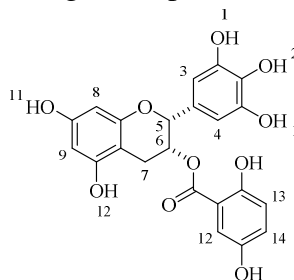
HRMS (ESI+) m/z : $[M+H^+]$ Calcd $C_{22}H_{19}O_{10}$ 443.0973; found 443.0971.

65h (50.7 mg, 0.115 mmol, 91%) was obtained as a slightly grey solid offered.

TLC = RP 18, acetonitrile/ H_2O , 3:2) R_f = 0.77.

4.5.8.9 (2*R*,3*R*)-5,7-Dihydroxy-2-(3,4,5-trihydroxyphenyl)chroman-3-yl-(2,5-dihydroxy)benzoate (**65e**)

The compound was prepared according to the procedure described in *chapter 4.5.8*.



1H NMR (600 MHz, CD_3OD): δ [ppm] = 7.13 (d, J = 3.0 Hz, 1H, 12-H), 6.95 – 6.90 (m, 1H, 14-H), 6.74 (dd, J = 9.0, 2.9 Hz, 1H, 13-H), 6.53 (s, 2H, 4-H, 3-H), 5.99 (s, 2H, 9-H, 8-H), 5.69 – 5.66 (m, 1H, 6-H), 5.04 – 5.01 (m, 1H, 5-H), 3.09 – 2.87 (m, 2H, 7-H).

^{13}C NMR (75 MHz, CD_3OD): δ [ppm] = 170.08, 157.98, 157.83, 157.07, 156.15, 156.03, 150.43, 146.78, 133.79, 130.52, 125.07, 118.93, 118.31, 116.29, 115.54, 113.28, 106.63, 106.27, 99.05, 96.63, 95.89, 78.28, 70.82, 70.31, 67.85, 54.77, 33.04, 28.61, 26.76, 24.29.

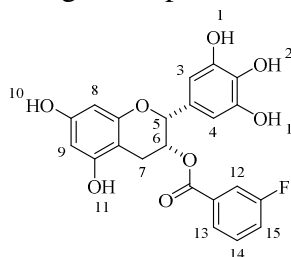
IR (solid): ν [cm^{-1}] = 2924 (s), 2459 (b), 1666 (m), 1614 (m), 1485 (s), 1444 (s), 1367 (m), 1282 (s), 1209 (m), 1080 (s), 1016 (m), 968 (m), 821 (s), 786 (s), 729 (s).

65e (25 mg, 0.0565 mmol, 81%) was obtained as a slightly grey solid offered.

TLC = RP 18, acetonitrile/ H_2O , 3:2) R_f = 0.69.

4.5.8.10 (2*R*,3*R*)-5,7-Dihydroxy-2-(3,4,5-trihydroxyphenyl)chroman-3-yl-(3-fluoro)benzoate (**65c**)

The compound was prepared according to the procedure described in *chapter 4.5.8*.



1H NMR (300 MHz, CD_3OD): δ [ppm] = 7.69 (m, 1H, 13-H), 7.53 (m, 1H, 12-H), 7.42 (m,

^1H NMR (600 MHz, CD_3OD): δ [ppm] = 7.28 (m, 1H, 15-H), 6.51 (s, 2H, 4-H, 3-H), 6.05 – 5.91 (m, 2H, 9-H, 8-H), 5.98 (br s, 1H, 6-H), 5.02 (s, 1H, 5-H), 3.03 (dd, J = 17.4, 4.4 Hz, 1H, 7-H), 2.91 (dd, J = 17.6, 2.7 Hz, 1H, 7-H).

^{13}C NMR (75 MHz, CD_3OD): δ [ppm] = 210.11, 166.06, 166.02, 165.50, 162.25, 158.01, 157.85, 157.12, 146.80, 133.77, 133.73, 133.67, 131.51, 131.41, 130.65, 126.56, 126.52, 121.13, 120.84, 117.23, 116.92, 106.55, 99.08, 96.58, 95.78, 78.33, 71.18, 30.67, 26.63.

^{19}F NMR (600 MHz, CD_3OD): δ [ppm] = -110.55.

IR (solid): ν [cm^{-1}] = 3176 (b), 2465 (b), 1695 (m), 1593 (m), 1525 (s), 1444 (m), 1359 (m), 1284 (m), 1269 (m), 1205 (s), 1145 (s), 1093 (s), 1070 (s), 1016 (s), 968 (s), 937 (s), 889 (s), 815 (m), 781 (s), 754 (s), 671 (s).

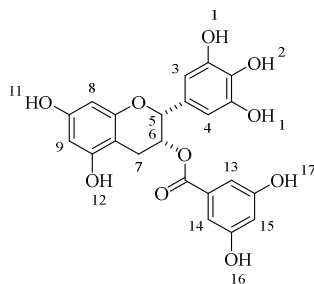
HRMS (ESI+) m/z : $[\text{M}+\text{H}^+]$ Calc $\text{C}_{22}\text{H}_{18}\text{FO}_8$ 429.0980; found 429.0979.

65c (20.8 mg, 0.0486 mmol, 66%) was obtained as a lightly grey solid.

TLC = RP 18, acetonitrile/ H_2O , 3:2, R_f = 0.85.

4.5.8.11 (2*R*,3*R*)-5,7-Dihydroxy-2-(3,4,5-trihydroxyphenyl)chroman-3-yl-(3,5-dihydroxy)benzoate (**65g**)

The compound was prepared according to the procedure described in *chapter 4.5.8*.



^1H NMR (600 MHz, CD_3OD): δ [ppm] = 6.85 (dd, J = 2.4, 0.8 Hz, 2H, 14-H, 13-H), 6.54 (s, 2H, 3-H, 4-H), 6.44 (td, J = 2.3, 0.8 Hz, 1H, 15-H), 6.00 (s, 2H, 9-H, 8-H), 5.60 – 5.98 (br s, 1H, 6-H), 5.05 – 4.98 (m, 1H, 5-H), 3.03 (dd, J = 17.3, 4.7 Hz, 1H, 7-H), 2.90 (dd, J = 17.5, 2.6 Hz, 1H, 7-H).

^{13}C NMR (151 MHz, CD_3OD): δ [ppm] = 167.28, 159.62, 159.50, 157.85, 157.78, 157.15, 146.66, 133.72, 133.09, 132.88, 130.72, 128.51, 118.14, 116.05, 108.95, 108.86, 108.29, 106.76, 106.34, 99.28, 96.52, 95.86, 78.44, 70.36, 70.19, 26.74, 26.44.

IR (solid): ν [cm^{-1}] = 3296 (b), 2474 (b), 1697 (m), 1597 (m), 1448 (m), 1363 (m), 1332

(m), 1238 (m), 1163 (m), 1109 (m), 1033 (s), 997 (s), 964 (m), 848 (s), 763 (s), 731 (s), 673 (s).

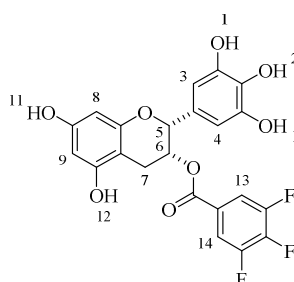
HRMS (ESI+) m/z : $[M+H^+]$ Calc $C_{22}H_{19}O_{10}$ 433.0973; found 443.0971.

TLC = RP 18, acetonitrile/ H_2O , 3:2, R_f = 0.84.

65g (22 mg, 0.0498 mmol, 88%) was obtained as a lightly grey solid.

4.5.8.12 (2*R*,3*R*)-5,7-Dihydroxy-2-(3,4,5-trihydroxyphenyl)chroman-3-yl-(3,4,5-trifluoro)benzoate (**65j**)

The compound was prepared according to the procedure described in *chapter 4.5.8*.



1H NMR (600 MHz, CD_3OD): δ [ppm] = 7.62 – 7.54 (m, 2H, 14-H, 13-H), 6.51 (s, 2H, 4-H, 3-H), 6.00 (dd, J = 14.7, 2.2 Hz, 2H, 9-H, 8-H), 5.60 – 5.58 (m, 1H, 6-H), 5.02 (s, 1H, 5-H), 3.05 (dd, J = 17.5, 4.6 Hz, 1H, 7-H), 2.94 (dd, J = 17.6, 2.4 Hz, 1H, 7-H).

^{13}C NMR (151 MHz, CD_3OD): δ [ppm] = 158.05, 157.03, 146.82, 133.73, 130.51, 115.25, 115.10, 106.40, 98.91, 96.62, 95.75, 78.16, 71.84, 68.85, 26.52, 26.47.

^{19}F NMR (600 MHz, CD_3OD): δ [ppm] = -135.48, -156.51.

IR (solid): ν [cm^{-1}] = 3223 (b), 2927 (s), 2476 (b), 1720 (m), 1712 (m), 1600 (m), 1525 (s), 1440 (s), 1371 (s), 1344 (m), 1251 (s), 1220 (m), 1147 (s), 1085 (s), 1045 (s), 966 (m), 916 (s), 885 (s), 83 (s), 763 (s), 731 (m), 711 (s), 630 (s).

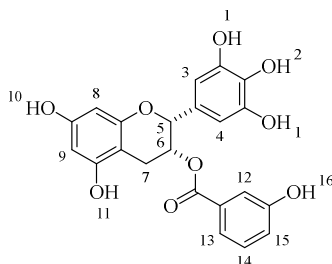
HRMS (ESI+) m/z : $[M+H^+]$ Calc $C_{22}H_{16}F_3O_8$ 465.0792; found 465.0790.

65j (25.7 mg, 0.0553 mmol, 87%) was obtained as beige solid.

The enantiomer (2*S*,3*R*) was obtained with identical spectroscopically data.

4.5.8.13 (2*R*,3*R*)-5,7-Dihydroxy-2-(3,4,5-trihydroxyphenyl)chroman-3-yl-(3-hydroxy)benzoate (**65i**)

The compound was prepared according to the procedure described in *chapter 4.5.8*.



$^1\text{H NMR}$ (600 MHz, CD_3OD): δ [ppm] = 7.50 – 6.92 (m, 6H, 15-H, 14-H, 13-H, 12-H), 6.53 (s, 2H, 4-H, 3-H), 6.01 – 5.94 (m, 2H, 9-H, 8-H), 5.98 – 5.57 (m, 1H, 6-H), 5.01 (s, 1H, 5-H), 3.02 (dd, $J = 17.3, 4.6$ Hz, 1H, 7-H), 2.90 (dd, $J = 17.6, 2.7$ Hz, 1H, 7-H).

$^{13}\text{C NMR}$ (151 MHz, CD_3OD): δ [ppm] = 168.63, 167.36, 158.79, 158.51, 157.92, 157.81, 157.77, 157.17, 157.15, 146.72, 133.72, 132.60, 132.53, 130.75, 130.58, 130.50, 121.90, 121.83, 121.57, 121.22, 117.02, 116.98, 106.73, 99.26, 96.55, 95.85, 78.46, 70.56, 68.85, 52.57, 26.72, 26.48.

IR (solid): ν [cm^{-1}] = 3234 (b), 2465 (b), 2073 (s), 1697 (m), 1589 (m), 1489 (s), 1446 (s), 1421 (s), 1359 (s), 1284 (m), 1222 (b), 1147 (m), 1107 (m), 1033 (m), 968 (m), 885 (s), 808 (s), 754 (s) 680 (s).

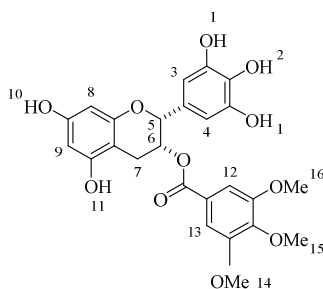
(ESI+) m/z : $[\text{M}+\text{H}^+]$ Calc $\text{C}_{22}\text{H}_{19}\text{O}_9 = 427.1$; found 426.1.

65i (11.8 mg, 0.0277 mmol, 79%) was obtained as a lightly grey solid.

TLC = RP 18, acetonitrile/ H_2O , 3:2, $R_f = 0.75$.

4.5.8.14 (2*R*,3*R*)-5,7-Dihydroxy-2-(3,4,5-trihydroxyphenyl)chroman-3-yl-(3,4,5-trimethoxy)benzoate (**65a**)

The compound was prepared according to the procedure described in *chapter 4.5.8*.



$^1\text{H NMR}$ (600 MHz, CD_3OD): δ [ppm] = 7.15 (s, 2H, 12-H, 13-H), 6.55 (s, 2H, 3-H, 4-H),

3.04 (dd, $J = 17.3, 4.4$ Hz, 1H), 2.96 (dd, $J = 17.4, 3.3$ Hz, 1H), 5.51 (br s, 1H, 5-H), 5.06 (br s, 1H, 6-H), 3.81 (s, 6H, 14-H, 16-H), 3.78 (3H, 15-H), 3.04 (dd, $J = 17.3, 4.4$ Hz, 1H, 7-H), 2.96 (dd, $J = 17.4, 3.3$ Hz, 1H, 7-H).

^{13}C NMR (151 MHz, CD_3OD): δ [ppm] = 167.11, 158.03, 157.05, 154.18, 146.83, 143.30, 133.68, 130.91, 126.72, 107.89, 106.55, 99.17, 96.49, 95.61, 78.25, 71.19, 67.85, 61.07, 56.62, 54.76, 33.05, 26.25, 24.30.

IR (solid): ν [cm^{-1}] = 2474 (b), 2358 (s), 1683 (m), 1593 (m), 1502 (s), 1448 (m), 1415 (s), 1363 (s), 1327 (s), 1255 (s), 1222 (s), 1184 (s), 1174 (s), 1147 (s), 1122 (m), 1016 (s), 993 (s), 958 (s), 819 (s), 761 (s), 731 (s).

HRMS (ESI+) m/z : $[\text{M}+\text{H}^+]$ Calc $\text{C}_{25}\text{H}_{25}\text{O}_{11}$ 501.1391; found 501.1391.

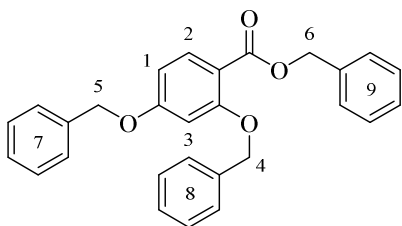
65a (53.3 mg, 0.107 mmol, 97%) was obtained as a white solid.

TLC = RP 18, acetonitrile/ H_2O , 3:2, $R_f = 0.75$.

4.5.9 Synthesis of Acid Compounds for Steglich Esterfication

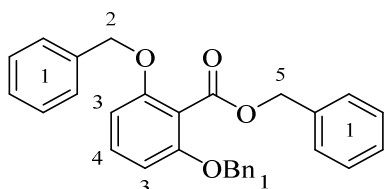
4.5.9.1 Benzylation of Hydroxybenzoic Acids

The corresponding compounds were prepared according to literature following a procedure by Kawamoto *et al.*^[200] A 50-mL, round-bottomed flask equipped with a magnetic stirring bar, was sequentially charged with substituted hydroxybenzoic acid (1.00 g, 1.00 eq) which was dissolved in 20 mL DMF at rt. To the solution was added potassium carbonate (3.00 eq) and benzyl bromide dropwise (3.00 eq) for di-hydroxy benzoic acid. For mono-hydroxy benzoic acid potassium carbonate (2.00 eq) and benzyl bromide (2.00 eq) were necessary. This suspension was allowed to stir overnight at rt under N_2 -atmosphere until TLC showed completeness of the reaction. The solid was filtered through a glass frit and washed with Et_2O . The filtrate was poured into ice-cooled water and extracted with Et_2O (3 x 10mL). The combined organic layers were washed with brine (10 mL), dried (MgSO_4), the drying agent was filtered off and concentrated under reduced pressure.



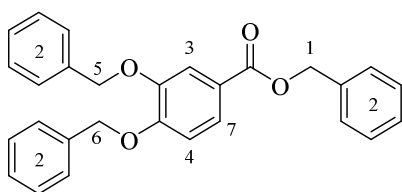
$^1\text{H NMR}$ (300 MHz, CDCl_3): δ [ppm] = 7.92 (d, J = 8.6 Hz, 1H, 3-H), 7.46 – 7.29 (m, 15H, 9-H, 8-H, 7-H), 6.63 – 6.55 (m, 2H, 2-H, 1-H), 5.33 (s, 2H, 6-H), 5.13 (s, 2H, 4-H), 5.07 (s, 2H, 4-H).

TLC (SiO_2 , n -hexane/EtOAc 4:1, R_f = 0.58), 2.62 g (6.18 mmol, 95%) yellowish solid.



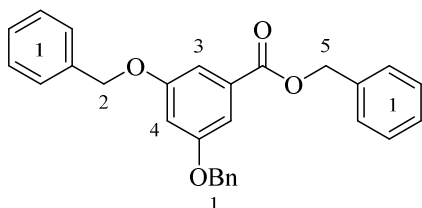
$^1\text{H NMR}$ (300 MHz, CDCl_3): δ [ppm] = 7.30 – 7.10 (m, 18H, 1-H, 3-H, 4-H), 6.51 (s, 1H, 3-H), 5.27 (s, 2H, 5-H), 5.03 (s, 4H, 2-H).

TLC (SiO_2 , n -hexane/EtOAc 4:1, R_f = 0.51), 3.13 g (7.38 mmol, 99%) brown oil.



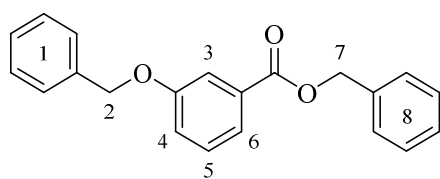
$^1\text{H NMR}$ (300 MHz, CDCl_3): δ [ppm] = 7.61 – 7.23 (m, 18H, 2-H, 3-H, 4-H, 7-H), 5.24 (s, 2H, 1-H), 5.15 (s, 2H, 5-H), 5.12 (s, 2H, 6-H).

TLC (SiO_2 , n -hexane/EtOAc 4:1, R_f = 0.54), 2.72 g (6.41 mmol, 98%) white solid.



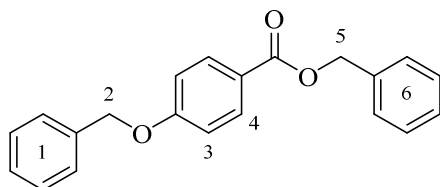
$^1\text{H NMR}$ (300 MHz, CDCl_3): δ [ppm] = 7.36 – 7.24 (m, 18H, 1-H), 6.73 (t, J = 2.4 Hz, 1H, 4-H), 5.27 (s, 2H, 5-H), 4.99 (s, 4H, 2-H).

TLC (SiO_2 , n -hexane/EtOAc 4:1, R_f = 0.67), 2.53 g (5.96 mmol, 92%) white solid.



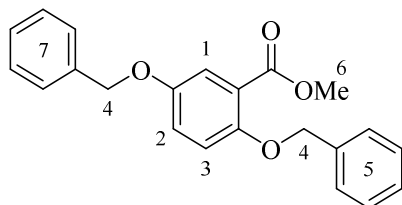
$^1\text{H NMR}$ (300 MHz, CDCl_3): δ [ppm] = 7.63 – 7.60 (m, 2H, 3-H, 6-H, 8-H), 7.35 – 7.25 (m, 11H, 1-H, 5-H), 7.12 (s, 1H, 4-H), 7.10 – 7.07 (m, 1H, 4-H), 5.28 (s, 2H, 7-H), 5.03 (s, 2H, 2-H).

TLC (SiO_2 , n -hexane/EtOAc 4:1, R_f = 0.75), 2.33 g (7.32 mmol, 100%) colorless oil.



$^1\text{H NMR}$ (300 MHz, CDCl_3): δ [ppm] = 7.98 – 7.94 (m, 2H, 4-H), 7.35 – 7.28 (m, 11H, 1-H, 6-H), 6.94 – 6.89 (m, 2H, 3-H), 5.26 (2, 2H, 2-H), 5.04 (s, 2H, 5-H).

TLC (SiO_2 , n -hexane/EtOAc 4:1, R_f = 0.63), 2.09 g (6.57 mmol, 91%) white solid.

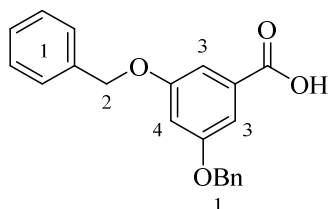


$^1\text{H NMR}$ (300 MHz, CDCl_3): δ [ppm] = 7.88 (dd, J = 8.4, 0.6 Hz, 1H, 1-H), 7.50 (ddt, J = 7.4, 1.4, 0.7 Hz, 2H, 3-H, 2-H), 7.43 – 7.29 (m, 11H, 7-H, 5-H), 5.15 (s, 2H, 4-H), 5.07 (s, 2H, 4-H), 3.88 (s, 3H, 6-H).

TLC (SiO_2 , *n*-hexane/EtOAc 4:1, R_f = 0.79), 2.01 g (5.77 mmol, 99%) white solid.

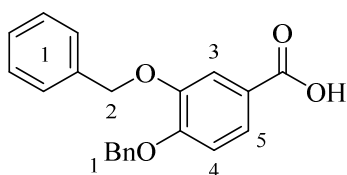
4.5.9.2 Universal Procedure of Saponification

A 25-mL, round-bottomed flask equipped with a magnetic stirring bar and with a water condenser was sequentially charged with benzylated product (1.00 eq) dissolved in EtOH (10 mL) and aq. KOH solution (5 mL, 40 wt%) was added at rt. The solution was heated to reflux for one hour. The reaction was cooled down to rt and water (50 mL) was added. 1 M hydrochloric acid was added dropwise until a precipitate occurred. The organic layer was extracted with CH_2Cl_2 (3 x 10 mL), washed with brine (10 mL), dried (MgSO_4) and the drying agent was filtrated off. The residue was recrystallized from EtOH. The product was dried under vacuum to afford benzylated acids.



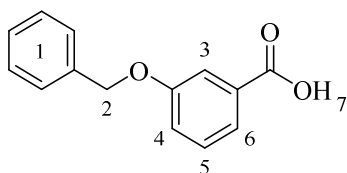
$^1\text{H NMR}$ (300 MHz, CDCl_3): δ [ppm] = 7.38 – 7.28 (m, 13H, 4-H, 3-H, 1-H), 6.78 (t, J = 2.4 Hz, 1H, 4-H), 5.02 (s, 2H, 3-H).

1.30 g (3.88 mmol, 65%) white solid.



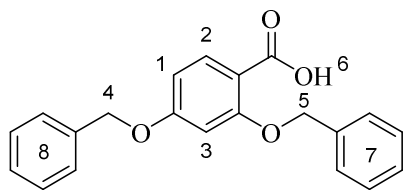
$^1\text{H NMR}$ (300 MHz, DMSO-d_6): δ [ppm] = 7.56 – 7.53 (m, 2H, 5-H, 4-H), 7.48 – 7.29 (m, 10-H, 1-H), 7.19 – 7.12 (m, 1H, 3-H), 5.22 (s, 2H, 2-H), 5.18 (s, 2H, 1-H).

1.79 g (5.36 mmol, 84%) white solid.



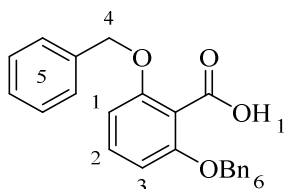
$^1\text{H NMR}$ (300 MHz, DMSO-d_6): δ [ppm] = 13.01 (br s, 1H, 7-H), 7.59 – 7.24 (m, 9H, 6-H, 5-H, 4-H, 3-H), 5.17 (d, J = 2.8 Hz, 2H, 2-H).

3.27 g (9.78 mmol, 119%) yellowish solid.



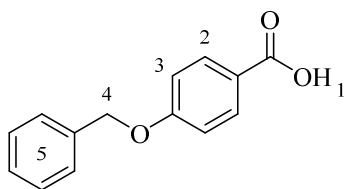
$^1\text{H NMR}$ (300 MHz, DMSO-d_6): δ [ppm] = 12.23 (br s, 1H, 6-H), 7.72 (d, J = 8.6 Hz, 1H, 2-H), 7.55 – 7.29 (m, 11H, 9-H, 8-H, 1-H), 6.82 (d, J = 2.3 Hz, 1H, 3-H), 6.68 (dd, J = 8.7, 2.3 Hz, 1H, 1-H), 5.20 (s, 2H, 5-H), 5.16 (s, 2H, 4-H).

1.38 g (4.13 mmol, 67%) white solid.



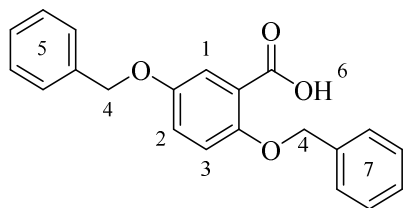
$^1\text{H NMR}$ (300 MHz, DMSO-d_6): δ [ppm] = 7.37 – 7.17 (m, 11H, 6-H, 5-H, 2-H), 6.70 (dd, J = 12.0, 8.4 Hz, 2H, 3-H, 1-H), 5.07 (d, J = 2.2 Hz, 4-H).

1.67 g (4.99 mmol, 68%) white solid.



$^1\text{H NMR}$ (300 MHz, CD_3OD): δ [ppm] = 8.02 – 7.93 (m, 2H, 2-H), 7.50 – 7.27 (m, 5H, 5-H), 7.10 – 7.02 (m, 2H, 3-H), 5.17 (s, 2H, 4-H).

1.30 g (5.70 mmol, 90%) white solid.



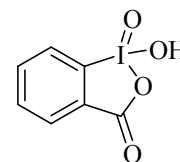
$^1\text{H NMR}$ (300 MHz, DMSO-d_6): δ [ppm] = 12.23 (br s, 1H, 6-H), 7.72 (d, J = 8.6 Hz, 1H, 1-H), 7.54 – 7.26 (m, 10H, 7-H, 5-H), 6.82 (d, J = 2.3 Hz, 1H, 3-H), 6.68 (dd, J = 8.7, 2.3 Hz, 1H, 2-H), 5.20 (s, 2H, 4-H), 5.16 (s, 2H, 4-H).

1.58 g (4.73 mmol, 82%) grey solid.

4.5.10 Synthesis of Dess-Martin Periodinan

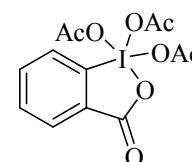
4.5.10.1 2-Iodoxy benzoic acid (IBX)

The compound was prepared according to literature following a procedure by Ireland *et al.*^[218] A 250-mL, three necked, round-bottomed flask equipped with a magnetic stirring bar, water cooler and adapter with tap to N₂-line was sequentially charged at rt with sulphuric acid (85 mL, 0.75 M), 2-iodobenzoic acid (10.0 g, 40.3 mmol, 1.00 eq) and the suspension was heated up to 55-57 °C. To the resulting yellow solution (8.96 g, 53.6 mmol, 1.3 eq) potassium bromate was added in batches within 20 min. The temperature was not allowed to exceed over 57 °C. During this reaction bromine gas was developed. After the addition of the KBrO₃ was completed, the reaction was heated up to 67-72 °C. After 2 h no bromine gas was evolved. The mixture was cooled to 0 °C and the precipitated solid was filtered. The solid was washed with water (3 x 20 mL), with cooled EtOH (2 x 10 mL) and with (3 x 10 mL) EtO₂. The product was isolated by vacuum filtration and dried under vacuum to afford IBX (10.6 g, 37.9 mmol, 93%) as white solid.



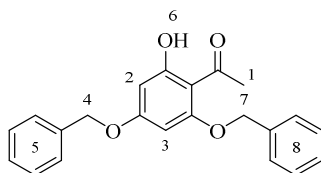
4.5.10.2 Dess-Martin Periodinane (DMP)

The compound was prepared according to the literature following a procedure by Ireland *et al.*^[218] A 250-mL, two-necked, round bottom flask equipped with a magnetic stirring bar, and adapter with tap to N₂-line was charged at rt with IBX (10 g, 35.7 mol), acetic anhydride (40 mL, 0.424 mol), and *p*-toluene sulfonic acid monohydrate (50.0 mg, 0.263 mmol) under N₂-atmosphere. The resulting mixture was heated up to 90 °C. After dissolution stirring was continued for 30 min at 90 °C. Then the mixture was allowed to cool to 0 °C and dried Et₂O (80 ml) was added to the precipitated solid, which was filtered quickly and washed with dried Et₂O (2 x 20 mL). The product was isolated by vacuum filtration and dried under vacuum to afford DMP (8.94 g, 21.1 mmol, 59%) as white solid.



4.5.11 Synthesis of Precursor Compounds for Chalcone **46**4.5.11.1 2,4-Dibenzyloxy-6-hydroxyacetophenone (**47**)

The compound was prepared according to literature following a procedure by Huang *et al.*^[231] A 250-mL, round-bottomed flask equipped with a magnetic stirring bar, was sequentially charged with 2,4,6-trihydroxy acetophenone (**48**) (10.0 g, 59.5 mmol, 1.00 eq) dissolved in DMF (100 mL) at rt. Potassium carbonate (18.1 g, 0.131 mol, 2.20 eq) and (15.1 mL, 0.130 mol, 2.20 eq) benzyl chloride were added to the solution. This suspension was allowed to stir for 2 h at 70 °C and was monitored by TLC (SiO₂, petroleum ether/EtOAc, 3:1, R_f = 0.67) and cooled to rt. The solid was filtered off, washed with methylene chloride and the solvent was evaporated under reduced pressure. The residue was dissolved in EtOAc and washed with water (5 x 100 mL). The combined organic layers were washed with sat. NH₄Cl solution (100 mL), brine (100 mL) and dried (NaSO₄). The drying agent was filtered off and the organic layer was concentrated under reduced pressure to give 19.7 g of a brown oil. After purification by column chromatography (SiO₂, petroleum ether/EtOAc, 5:1) the product acetophenone **47** was obtained (16.2 g, 46.5 mmol, 66-78%) as lightly yellowish crystals. The purified compound **47** is also recrystallized from *n*-hexane. The spectroscopic data were in accordance with those described in the literature.^[231]

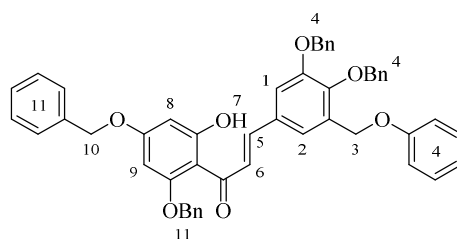


¹H NMR (300 MHz, CDCl₃): δ [ppm] = 13.95 (s, 1H, 6-H), 7.33 – 7.18 (m, 10H, 5-H, 8-H), 6.09 (d, *J* = 2.3 Hz, 1H, 2-H), 6.02 (d, *J* = 2.4 Hz, 1H, 3-H), 4.99 (s, 4H, 4-H, 7-H), 2.48 (s, 3H, 1-H).

4.5.11.2 (*E*)-1-(2-Bis(benzyloxy)-6-hydroxyphenyl)-3-(3,4,5-tris(benzyloxy)phenyl)prop-2-en-1-one (**46**)

The compound was prepared according to literature following a procedure by Krohn *et al.*^[214] A 250-mL, round-bottomed flask equipped with a magnetic stirring bar, was sequentially charged with equimolar amounts of acetophenone **47** (1.00 g, 2.87 mmol, 1.00 eq) and aldehyde **22** (1.22 g, 2.87 mmol, 1.00 eq) dissolved in ethanol (100 mL). This

lightly yellow mixture was warmed up to 50 °C. To this solution was added dropwise NaOH (1.30 mL, 50 wt%, 2.00 eq). The mixture was further stirred for 2-3 h at 100 °C and was monitored by TLC (SiO₂, *n*-hexane/EtAOc, 3:1, R_f = 0.67). EtOH (50 mL) was distilled off and fresh EtOH (50 mL) was added and heated up for 3 h at 100 °C. This procedure was performed three times, while in later progress a yellow-orange precipitate occurred which was filtered off and dissolved in CH₂Cl₂. The suspension was poured into ice water and acidified by addition of HCl (1 M). The residue was filtered off and dissolved in CH₂Cl₂ (50 mL). The organic layer was poured to a 500-mL separatory funnel and washed with (5 x 50 mL) water. The combined organic layers were washed with brine (50 mL) and dried (Na₂SO₄). The drying agent was filtered off and the organic layer was concentrated under reduced pressure. Crystallization from *n*-hexane gave chalcone **46** (1.78 g, 2.36 mmol, 46%) as yellow crystals. The spectroscopic data were in accordance with those described in the literature.^[165b]



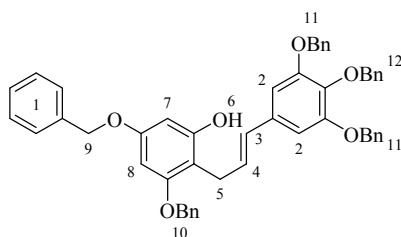
¹H NMR (300 MHz, CDCl₃): δ [ppm] = 14.10 (s, 1H, 7-H), 7.71 – 7.49 (m, 2H, 5-H, 6-H), 7.38 – 7.05 (m, 25H, 11-H, 4-H), 6.58 (s, 2H, 2-H, 1-H), 6.10 (dd, *J* = 21.9, 2.3 Hz, 2H, 9-H, 8-H), 5.01 – 4.97 (m, 6H, 3-H), 4.75 (s, 4H, 10-H).

¹³C NMR (75 MHz, CDCl₃): δ [ppm] = 192.73, 168.29, 165.33, 161.61, 152.97, 142.61, 140.42, 137.71, 136.94, 135.97, 135.87, 130.88, 128.95, 128.88, 128.73, 128.63, 128.54, 128.42, 128.31, 128.06, 127.83, 127.56, 127.27, 127.18, 108.32, 106.96, 95.20, 93.12, 77.58, 77.36, 77.16, 76.74, 75.35, 71.17, 70.49.

4.5.11.3 (*E*)-1-[3,4,5-Tris(benzyloxy)phenyl]-3-[2,4-bis(benzyloxy)-6-hydroxyphenyl]-propene (**31**)

The compound was prepared according to literature following a procedure by Yuan *et al.*^[226] A 250-mL, two-necked, round-bottomed flask, equipped with a magnetic stirring bar, was sequentially charged with chalcone **46** (3.00 g, 3.97 mmol, 1.00 eq) dissolved in anhydrous THF (80 mL). To this solution, trimethylamine (0.716 mL, 5.17 mmol, 1.30 eq)

was added dropwise and allowed to stir for 5 min at rt. This yellow mixture was cooled to 0 °C and ethyl chloroformate (454 μ L, 4.77 mmol, 1.20 eq) was added dropwise over a period of 10 min, whereas a discoloration was observed. After stirring at 0 °C for 1.5 h, a mixture of cerium chloride heptahydrate (1.77 g, 4.76 mmol, 1.20 eq) in anhydrous EtOH (80 mL) was admitted to the solution. NaBH₄ (571 mg, 15.1 mmol, 3.80 eq) was added in portions at 0 °C. After stirring for 2 h, the reaction was monitored by TLC (SiO₂, *n*-hexane/EtAOc, 3:1, R_f = 0.41) and diluted with HCl (0.5 M) and water. The aqueous layer was washed with CH₂Cl₂ (3 x 50 mL). The combined organic layers were washed with brine (50 mL) and dried (Na₂SO₄). The drying agent was filtered off and the organic layer was concentrated under reduced pressure to give an orange-brown oil. Purification by column chromatography (SiO₂, *n*-hexane/EtOAc, 5:1) provided allyl product **31** (2.17 g, 2.93 mmol, 74%) as white crystals. The spectroscopic data were in accordance with those described in the literature.^[165b]



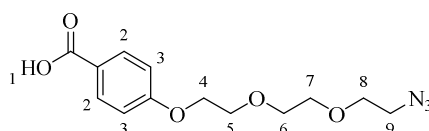
¹H NMR (600 MHz, CDCl₃): δ [ppm] = 7.34 – 7.08 (m, 25H, 12-H, 11-H, 10-H, 1-H), 6.53 (s, 2H, 2-H), 6.25 – 6.06 (m, 4H, 8-H, 7-H, 4-H, 3-H), 5.02 – 4.82 (m, 12H, 12-H, 11-H, 10-H, 9-H), 3.46 (dd, *J* = 6.4, 1.6 Hz, 2H, 5-H).

¹³C NMR (151 MHz, CDCl₃) δ [ppm] = 158.73, 157.87, 155.54, 152.81, 137.73, 137.06, 136.99, 136.76, 133.11, 130.21, 130.17, 128.75, 128.62, 128.59, 128.57, 128.53, 128.51, 128.47, 128.45, 128.44, 128.37, 128.32, 128.06, 128.03, 127.95, 127.82, 127.77, 127.74, 127.68, 127.66, 127.46, 127.37, 127.34, 127.31, 127.19, 127.15, 127.11, 127.06, 126.98, 106.79, 105.85, 95.02, 93.61, 75.18, 75.16, 71.16, 70.24, 70.05, 70.02, 26.25.

4.5.12 Synthesis of Biotin-PEG Linker **56**

4.5.12.1 4-(2-(2-(2-Azidoethoxy)ethoxy)ethoxy) benzoic acid (**53**)

The compound **52** was prepared by L. Reus^[233] according to literature following a procedure by Hanson *et al.*^[274] A 25-mL, round-bottomed flask equipped with a magnetic stirring bar and with a water condenser was charged with propyl benzoate **52** (100 mg, 0.296 mmol, 1.00 eq) dissolved in EtOH (5 mL, 96%) at rt and aq. KOH solution (0.5 mL, 40 wt%) was added. The solution was heated to reflux for one hour. The reaction was cooled down to rt and HCl (1 mL, 1 M) was added. The precipitated residue was dissolved in water (10 mL) and washed with EtOAc (3 x 20 mL). The combined organic layers were washed with brine (10 mL) and dried (Na₂SO₄). The drying agent was filtered and the organic layer was concentrated under reduced pressure. The product was isolated and dried under vacuum to afford **53** (78.9 mg, 0.267 mmol, 90%) as beige solid.



¹H NMR (300 MHz, CDCl₃): δ [ppm] = 11.75 (br s 1H, 1-H), 8.01 (d, J = 8.7 Hz, 2H, 2-H), 6.93 (d, J = 8.6 Hz, 2H, 3-H), 4.17 (t, J = 4.7 Hz, 2H, 4-H), 3.87 (t, J = 4.7 Hz, 2H, 5-H), 3.78 – 3.62 (m, 6H, 8-H, 7-H, 6-H), 3.36 (t, J = 5.0 Hz, 6H, 9-H).

¹³C NMR (75 MHz, CD₃OD): δ [ppm] = 171.53, 163.21, 132.29, 121.87, 114.30, 70.93, 70.75, 70.32, 69.62, 67.61, 50.67.

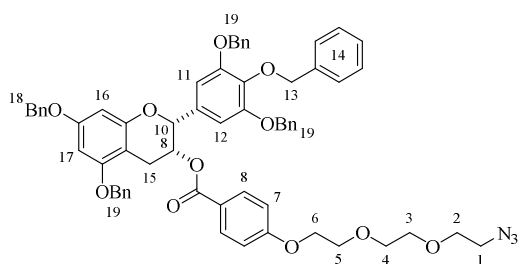
IR (Film): ν [cm⁻¹] = 2902 (w), 2105 (s), 1681 (s), 1606 (s), 1513 (s), 1494 (s), 1428 (w), 1256 (s), 1172 (s), 1127 (w), 915 (w), 852 (s), 772 (s), 733 (s), 649 (s), 551 (s).

HRMS (ESI) m/z : [M+H⁺] Calc C₁₃H₁₈N₃O₅ 296.1241; found 296.1241.

4.5.12.2 (2*R*,3*R*)-5,7-Bis(benzyloxy)-2-(3,4,5-tris(benzyloxy)phenyl)chroman-3-yl-4-(2-(2-(2-azidoethoxy)ethoxy)ethoxy)benzoate (**54**)

The compound was prepared according to literature following a procedure by Khandelwal *et al.*^[215] A 25-mL, two necked, round-bottomed flask equipped with a magnetic stirring bar was sequentially charged with acid **53** (82.7 mg, 0.280 mmol, 2.00 eq), DMAP

(17.1 mg, 0.140 mmol, 1.00 eq) and EDC·HCl (53.5 mg, 0.280 mmol, 2.00 eq) in CH₂Cl₂ (8 mL) at rt under N₂-atmosphere. The mixture was cooled down to 0 °C and a solution of **cis 45** (106 mg, 0.140 mmol, 1.00 eq) dissolved in CH₂Cl₂ (2 mL) was added under N₂-atmosphere. The resulting mixture was stirred over night at rt. Then the reaction was diluted with CH₂Cl₂ (5 mL) and washed with HCl (1 mL, 0.5 M) and sat. NaHCO₃ solution (3 mL). The organic layer was washed with brine (3 mL) and dried (Na₂SO₄), the drying agent was filtered off, and concentrated under reduced pressure. The residue was purified *via* flash chromatography (Alox, activity level III, *n*-hexane/EtOAc, 1:5, R_f = 0.18) to give the desired ester **54** in 149 mg (0.144 mmol, 80%) as lightly yellow oil.



¹H NMR (300 MHz, CDCl₃): δ [ppm] = 7.92 – 7.85 (m, 2H, 8-H), 7.42 – 7.21 (m, 25H, 19-H, 18-H, 14-H), 6.84 – 6.77 (m, 2H, 7-H), 6.74 (s, 2H, 12-H, 11-H), 6.32 – 6.23 (m, 2H, 17-H, 16-H), 5.65 – 5.58 (s, 1H, 9-H), 5.09 – 4.66 (m, 11H, 19-H, 18-H, 13-H, 10-H), 4.03 – 3.95 (m, 2H, 6-H), 3.78 – 3.72 (s, 2H, 5-H), 3.68 – 3.55 (m, 6H, 4-H, 3-H, 2-H), 3.32 – 3.25 (m, 2H, 1-H), 3.10 – 2.98 (m, 2H, 15-H).

¹³C NMR (75 MHz, CDCl₃): δ [ppm] = 165.12, 162.77, 158.79, 158.00, 155.60, 152.83, 138.27, 137.83, 137.04, 136.92, 136.85, 133.39, 131.87, 128.64, 128.56, 128.41, 128.10, 128.06, 127.93, 127.80, 127.73, 127.61, 127.48, 127.22, 125.59, 114.24, 106.67, 101.04, 94.80, 93.95, 75.13, 71.2, 70.75, 70.14, 70.00, 68.01, 67.55, 50.68, 26.18.

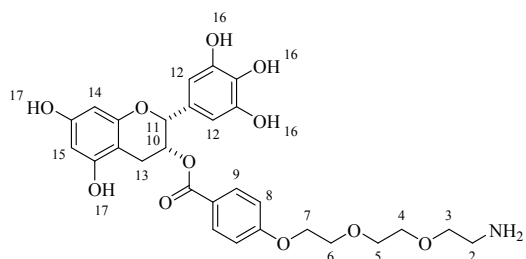
IR (Film): ν [cm⁻¹] = 3063 (s), 3031 (s), 2925 (s), 2870 (s), 1953 (s), 2102 (s), 1714 (m), 1618 (s), 1592 (m), 1498 (m), 1454 (s), 1439 (w), 1373 (m), 1355 (w), 1307 (w), 1255 (s), 1186 (s), 1167 (s), 1148 (w), 1114 (w), 1028 (s), 911 (s), 848 (s), 813 (s), 736 (s), 697 (s), 647 (s), 506 (s).

HRMS (ESI): m/z: [M+NH₄⁺] Calc C₆₃H₆₃N₄O₁₁ 1051.4488; found 1051.4487.

Specific rotation: [α]_D²⁵ = -49.5 (c = 0.845 mol/L, CHCl₃).

4.5.12.3 (2*R*,3*R*)-5,7-Dihydroxy-2-(3,4,5-trihydroxyphenyl)chroman-3-yl-4-(2-(2-(2-aminoethoxy)ethoxy)ethoxy)benzoate (**55**)

The compound was prepared according to literature following a procedure by Li *et al.*^[165b] An oven-dried 25-mL, two necked, round-bottomed flask, equipped with a magnetic stirring bar, connected to an Ar-line, was charged with **54** (47.4 mg, 0.0459 mmol, 1.00 eq) in dry THF/MeOH (10 mL, 1:1, v/v) at rt under Ar-atmosphere. To this solution a spatula tip of 20% Pd(OH)₂/C was added in one batch and stirred for 5 min under Ar-atmosphere. The argon tap was removed, and a balloon of hydrogen gas was connected to the flask. The resulting mixture was stirred at rt under H₂-atmosphere until TLC (RP 18, acetonitrile/H₂O 3:2, R_f = 0.4) showed full consumption of the starting material. The black solution was filtered through a syringe filter (0.2 μm PTFE) and the solvent was evaporated. The residue was purified by flash chromatography on RP 18 with acetonitrile to afford the desired compound **55** (12.6 mg, 0.0226 mmol, 49%) as lightly grey solid.



¹H NMR (300 MHz, CD₃OD): δ [ppm] = 7.87 – 7.79 (m, 2H, 9-H), 6.95 – 6.88 (m, 2H, 8-H), 6.54 (s, 2H, 12-H), 5.55 – 5.49 (m, 1H, 10-H), 5.02 (br s, 1H, 11-H), 4.18 – 4.11 (m, 2H, 7-H), 3.84 – 3.77 (m, 2H, 6-H), 3.73 – 3.51 (m, 8H, 5-H, 4-H, 3-H), 3.12 – 3.06 (m, 2H, 2-H), 3.00 (d, *J* = 4.5 Hz, 1H, 13-H), 2.90 (dd, *J* = 17.4, .2.8 Hz, 1H, 13-H).

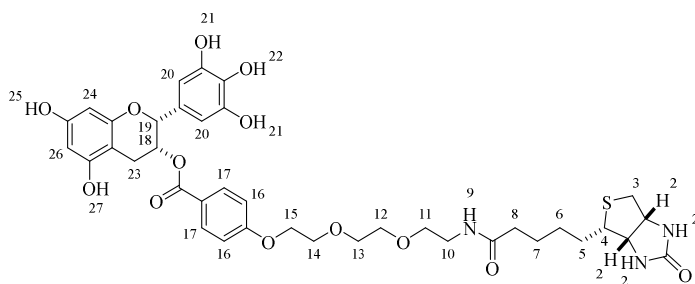
¹³C NMR (75 MHz, CD₃OD): δ [ppm] = 167.18, 164.13, 157.96, 157.85, 157.18, 146.72, 133.66, 132.78, 130.86, 123.86, 115.30, 106.70, 99.26, 96.53, 96.79, 78.45, 71.73, 71.24, 70.68, 70.46, 68.87, 40.67, 26.50.

IR (Solid): ν [cm⁻¹] = 3225 (w), 3031 (s), 2920 (s), 2852 (s), 1693 (w), 1604 (s), 1510 (s), 1452 (w), 1255 (s), 1099 (w), 1035 (s), 914 (s), 844 (s), 828 (s), 767 (s), 732 (s), 696 (s).

HRMS (ESI) m/z: [M+2·OCH₃] Calc C₃₀H₃₈NO₁₃ 620.2342; found 620.2338.

4.5.12.4 (2*R*,3*R*)-5,7-Dihydroxy-2-(3,4,5-trihydroxyphenyl)chroman-3-yl-4-(2-(2-(2-(5-((3*aS*,4*S*,6*aR*)-2-oxohexahydro-1*H*-thieno[3,4-*d*]imidazol-4-yl)pentanamido)ethoxy)ethoxy)ethoxy)benzoate (**56**)

A 25-mL, two necked pointed flask equipped with a magnetic stirring bar, connected to an argon line, was sequentially charged with **55** (34.7 mg, 0.0623 mmol, 1.00 eq) in dry DMF (0.2 mL) at rt under Ar-atmosphere. To this solution, commercial available biotin-NHS (21.2 mg, 0.0621 mmol, 1.00 eq) was added in one batch under Ar-atmosphere. The lightly brown solution was stirred at rt for two days (TLC = RP 18, acetonitrile/H₂O 3:2, $R_f = 0.57$). After removal of the solvent under reduced pressure, the solution was purified by flash chromatography on RP 18 with degassed H₂O/acetonitrile in a solvent gradient. The product fraction was transferred into a Schlenk-flask and the solvent was evaporated at 70 °C by vacuum pump yielding the product **56** (42 mg, 0.0536 mmol, 79%) as white solid.



¹H NMR (600 MHz, CD₃OD): δ [ppm] = 7.99 (s, 2H, 26-H, 24-H), 7.88 – 7.83 (m, 1H, 17-H), 6.98 – 6.93 (m, 1H, 16-H), 6.57 – 6.52 (m, 2H, 20-H), 5.55 (br s, 1H, 18-H), 5.02 (br s, 1H, 19-H), 4.52 and 4.50 (dd, $J = 5.0, 1.0$ Hz, 1H, 2-H), 4.33 (dd, $J = 7.9, 4.4$ Hz, 1H, 2-H), 4.21 – 4.18 (m, 2H, 15-H), 3.88 – 3.85 (m, 2H, 14-H), 3.79 – 3.67 (m, 8H, 13-H, 12-H, 11-H, 10-H), 3.26 – 3.2 (m, 2H, 4-H), 3.12 – 3.06 (m, 2H, 3-H), 2.98 – 2.92 (m, 2H, 23-H), 2.77 – 2.62 (m, 4H, 11-H, 10-H), 1.92 – 1.85 (m, 2H, 8-H), 1.67 – 1.53 (m, 4H, 7-H, 6-H), 1.37 – 1.28 (m, 2H, 5-H).

¹³C NMR (75 MHz, CD₃OD): δ [ppm] = 171.93, 170.22, 167.16, 164.85, 164.12, 157.87, 157.78, 151.85, 146.72, 132.78, 130.85, 123.90, 115.29, 106.69, 99.25, 78.45, 71.75, 71.25, 70.69, 70.45, 68.86, 68.66, 67.85, 63.29, 61.65, 56.84, 41.05, 40.66, 36.95, 31.65, 31.42, 29.28, 26.70, 26.50, 26.29, 25.67.

IR (Solid): ν [cm⁻¹] = 3388 (w), 3309 (b), 3294 (b), 3273 (s), 3176 (b), 2358 (b), 2341 (s), 2331 (w), 1818 (s), 1728 (s), 1683 (b), 1604 (b), 1456 (s), 1354 (s), 1313 (w), 1253 (b),

1209 (m), 1197 (s), 1168 (s), 1143 (s), 1101 (s), 1070 (m), 1037 (s), 1016 (s), 858 (s), 846 (s), 825 (s), 790 (s), 767 (s), 650 (b).

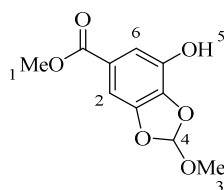
HRMS (ESI) m/z : $[M+H^+]$ Calc $C_{38}H_{46}N_3O_{13}S$ 784.2746; found 784.2736.

TLC = RP 18, acetonitrile/ H_2O , 3:2, R_f = 0.57.

4.5.13 Synthesis of EGCG-PEG Linker **69**

4.5.13.1 Methyl 7-hydroxy-2-methoxybenzo[*d*][1,3]dioxole-5-carboxylate (**71**)

The compound was prepared by R. Steinfort²⁶ according to literature following a procedure by Merz *et al.*^[235] A 100-mL, round-bottomed flask equipped with a magnetic stirring bar and with a water condenser was charged with gallic acid **18** (3.00 g, 16.3 mmol, 1.00 eq) dissolved in toluene (54 mL) at rt. Trimethyl orthoformate (2.59 g, 24.4 mmol, 1.50 eq) and Amberlite® IR-120 plus (0.15 g) were added. The suspension was heated up to 150 °C using an oil bath for four hours until methanol was distilled off. The purple colored reaction was cooled down to rt and *n*-hexane (20 mL) and EtOAc (10 mL) were added, and was heated to 80 °C for 3 h. The precipitated residue was mixed with *n*-hexane (20 mL) and cooled down to rt. The drying agent was filtered off and the organic layer was concentrated under reduced pressure. The product was isolated and dried under vacuum to afford the product **71** (2.81 g, 12.4 mmol, 76%) as purple solid.



1H NMR (300 MHz, $CDCl_3$): δ [ppm] = 7.40 (d, J = 1.5 Hz, 1H, 2-H), 7.21 (d, J = 1.5 Hz, 1H, 6-H), 6.95 (s, 1H, 4-H), 3.89 (s, 3H, 1-H), 3.44 (s, 3H, 3-H).

^{13}C NMR (75 MHz, DMSO): δ [ppm] = 165.53, 146.80, 140.24, 136.58, 123.52, 119.68, 113.22, 100.63, 52.01, 50.38.

IR (Film): ν [cm^{-1}] = 3364 (b), 2953 (b), 2849 (b), 2347 (b), 1697 (m), 1644 (s), 1617 (m), 1518 (m), 1506 (m), 1441 (s), 1376 (m), 1338 (m), 1285 (m), 1250 (m), 1204 (m), 1146(m),

²⁶ R. Steinfort, Synthese eines Azido-PEGylierten Gallussäure-Derivates, bachelor thesis, 2017, Heinrich-Heine Universität.

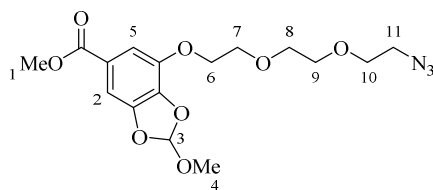
1077 (s), 1031 (s), 993 (b), 913 (b), 876 (b), 820 (bw), 768 (m), 748 (m), 726 (b), 665 (b), 614 (b), 524 (b).

HRMS (ESI) m/z : $[M+H^+]$ Calc $C_{10}H_{11}O_6$ 227.0556; found 227.0555.

Melting point: 128.9 °C.

4.5.13.2 Methyl-7-(2-(2-(2-azidoethoxy)ethoxy)ethoxy)-2-methoxybenzo[*d*][1,3]dioxole-5-carboxylate (**73**)

The compound was prepared by R. Steinfort²⁶ according to literature following a procedure by Ueno *et al.*^[275] A 25-mL, round-bottomed flask equipped with a magnetic stirring bar was sequentially charged with carbonate **71** (211 mg, 0.932 mmol, 1.00 eq) dissolved in DMF (12 mL) at rt. Linker **72** (307 mg, 0.932 mmol, 1.00 eq) and caesium carbonate (304 mg, 0.932 mmol, 1.00 eq) were added. The suspension was stirred at rt under N_2 -atmosphere about two days. The residue was dissolved in water (150 mL), poured into a 250-mL separatory funnel and washed with (5 x 10 mL) CH_2Cl_2 . The combined organic layers were washed with water (4 x 10 mL) and with brine (10 mL) and dried (Na_2SO_4). The drying agent was filtered and the organic layer was concentrated under reduced pressure. After purification of the residue by column chromatography (SiO_2 , *n*-hexane/EtOAc, 2:1) provided product **73** (280 mg, 0.731 mmol, 78%) as lightly yellowish oil.



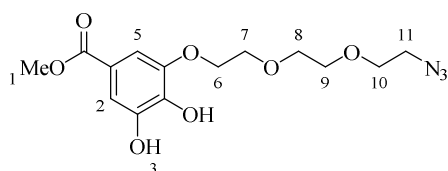
1H NMR (300 MHz, $CDCl_3$): δ [ppm] = 7.36 (d, $J = 1.5$ Hz, 1H, 2-H), 7.24 (d, $J = 1.5$ Hz, 1H, 5-H), 6.91 (s, 1H, 3-H), 4.32 – 4.27 (m, 2H, 6-H), 3.89 – 3.84 (m, 5H, 4-H, 7-H), 3.76 – 3.70 (m, 2H, 10-H), 3.70 – 3.64 (m, 4H, 8-H, 9-H), 3.42 (s, 3H, 1-H), 3.40 – 3.34 (m, 2H, 11-H).

^{13}C NMR (75 MHz, $CDCl_3$): δ [ppm] = 166.28, 147.21, 141.72, 138.21, 124.33, 120.24, 111.69, 103.49, 70.96, 70.71, 70.09, 69.69, 69.17, 52.19, 50.69, 50.17.

HRMS (ESI) m/z : $[M+NH_4^+]$ Calc $C_{16}H_{25}N_4O_8$ 401.1672; found 401.1672.

4.5.13.3 Methyl-3-(2-(2-(2-azidoethoxy)ethoxy)ethoxy)-4,5-di(hydroxy)benzoate (**74**)

The compound was prepared by R. Steinfort²⁶ according to literature following a procedure by Merz *et al.*^[235] A 10-mL, round-bottomed flask equipped with a magnetic stirring bar was charged with carbonate **73** (280 mg, 0.731 mmol, 1.00 eq) and *p*-toluene sulfonic acid (5.04 mg, 0.0292 mmol, 0.04 eq) dissolved in methanol (4 mL) at rt. The suspension was stirred at rt under N₂-atmosphere overnight. To the reaction mixture, 4 drops con. HCl were added and was diluted with water (10 mL), poured into a 50 -mL separatory funnel and washed with Et₂O (8 x 5 mL). The combined organic layers were washed with brine (10 mL) and dried (Na₂SO₄). The drying agent was filtered off and the organic layer was concentrated under reduced pressure. Purification of the residue by column chromatography (SiO₂, *n*-hexane/EtOAc, 2:1, R_f = 0.22) provided product **74** (77.1 mg, 0.226 mmol, 31%) as colorless oil.



¹H NMR (300 MHz, CDCl₃): δ [ppm] = 7.37 (d, *J* = 1.9 Hz, 1H, 5-H), 7.27 (d, *J* = 1.9 Hz, 1H, 10-H), 4.23 – 4.18 (m, 2H, 6-H), 3.86 (s, 3H, 1-H), 3.85 – 3.81 (m, 2H, 7-H), 3.79 – 3.75 (m, 2H, 10-H), 3.74 – 3.66 (m, 4H, 8-H, 9-H), 3.45 – 3.39 (m, 2H, 11-H).

¹³C NMR (75 MHz, CDCl₃): δ [ppm] = 166.90, 145.86, 144.73, 139.53, 121.65, 111.94, 110.48, 70.9, 70.71, 70.57, 70.21, 69.68, 52.16, 50.91.

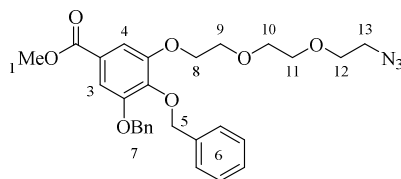
IR (Film): ν [cm⁻¹] = 3375 (b), 2927 (b), 2110 (m), 1713 (s), 1607 (s), 1516 (s), 1438 (s), 1345 (m), 1318 (m), 1227 (m), 1090 (m), 1008 (b), 916 (b), 876 (b), 806 (b), 768 (b), 657 (b), 557 (b), 505 (b).

HRMS (ESI): *m/z*: [M+H⁺] Calc C₁₄H₂₀N₃O₇ 342.1301; found 342.1300.

4.5.13.4 Methyl-3-(2-(2-(2-azidoethoxy)ethoxy)ethoxy)-4,5-bis(benzyloxy)benzoate (**75**)

The compound was prepared by R. Steinfort²⁶ according to literature following a procedure by Percec *et al.*^[237] A 10-mL, round-bottomed flask equipped with a magnetic stirring bar was charged with diol **74** (76.5 mg, 0.224 mmol, 1.00 eq) dissolved in DMF (5 mL) at rt. To this solution, benzyl chloride (77.0 μL, 0.672 mmol, 3.00 eq) and potassium carbonate

(83.6 mg, 0.605 mmol, 2.70 eq) were added. The suspension was stirred at 80 °C for eight hours. The reaction mixture was poured into ice water and extracted with (4 x 10 mL) EtOAc and with water (6 x 10mL). The combined organic layers were washed with brine (30 mL) and dried (Na₂SO₄). The drying agent was filtered and the organic layer was concentrated under reduced pressure. Purification of the residue by column chromatography (SiO₂, *n*-hexane/EtOAc, 3:1, R_f = 0.29) provided product **75** (103 mg, 0.197 mmol, 88%) as colorless oil.



¹H NMR (300 MHz, CDCl₃): δ [ppm] = 7.51 – 7.27 (m, 12H, 10-H, 7-H, 6-H, 4-H, 3-H), 5.14 (s, 2H, 5-H), 5.13 (s, 2H, 7-H), 4.24 – 4.19 (m, 2H, 8-H), 3.92 – 3.86 (m, 5H, 9-H, 1-H), 3.76 – 3.71 (m, 2H, 12-H), 3.68 – 3.61 (m, 4H, 11-H, 10-H), 3.36 – 3.30 (m, 2H, 13-H).

¹³C NMR (75 MHz, CDCl₃): δ [ppm] = 166.60, 152.62, 152.48, 142.21, 137.64, 136.69, 128.53, 128.45, 128.18, 128.00, 127.93, 127.52, 125.20, 109.00, 108.74, 77.56, 77.14, 76.71, 74.97, 71.19, 70.94, 70.74, 70.06, 69.75, 68.81, 52.2, 50.64.

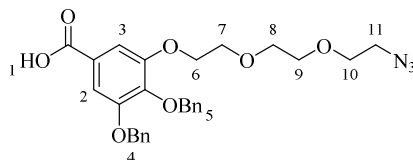
IR (Film): ν [cm⁻¹] = 3648 (b), 3032 (b), 2961 (s), 2360 (s), 2341 (m), 2104 (m), 1716 (s), 1589 (s), 1499 (s), 1455 (m), 1429 (s), 1335 (s), 1259 (s), 1110 (m), 1014 (m), 912 (b), 865 (b), 800 (m), 759 (m), 698 (s), 560 (b).

HRMS (ESI) m/z: [M+NH₄⁺] Calc C₂₈H₃₅N₄O₇ 539.2506; found 539.2502.

4.5.13.5 3-(2-(2-(2-azidoethoxy)ethoxy)ethoxy)-4,5-bis(benzyloxy)benzoate (**76**)

The compound was prepared by R. Steinfort.²⁶ A 10-mL, round-bottomed flask equipped with a magnetic stirring bar was charged with ester **75** (103 mg, 0.197 mmol, 1.00 eq) dissolved in EtOH (7 mL) at rt. To this mixture, a KOH solution (2.70 mL, 40 wt%) was added. The solution was stirred at 100 °C for three hours until TLC (SiO₂, *n*-hexane/EtOAc, 3:1, R_f = 0.29) showed full consumption of the starting material. After cooling down to rt, a precipitate was formed by acidifying with HCl (1 mL, 1 M), which was extracted with EtOAc (4 x 10mL) and with water (2 x 10 mL). The combined organic

layers were washed with brine (30 mL) and dried (Na_2SO_4). The drying agent was filtered off and the organic layer was concentrated under reduced pressure, yielding in product **76** (90.2 mg, 0.178 mmol, 90%) as brown oil.



$^1\text{H NMR}$ (300 MHz, CDCl_3): δ [ppm] = 11.13 (br s, 1H, 1-H), 7.51 – 7.27 (m, 12-H, 4-H, 5-H, 3-H, 2-H), 5.16 (s, 2H, 5-H), 5.14 (s, 2H, 4-H), 4.27 – 4.19 (m, 2H, 7-H), 3.94 – 3.86 (m, 2H, 8-H), 3.77 – 3.70 (m, 2H, 11-H), 3.69 – 3.61 (m, 4H, 9-H, 10-H), 3.38 – 3.30 (m, 2H, 12-H).

$^{13}\text{C NMR}$ (75 MHz, CDCl_3): δ [ppm] = 171.50, 152.78, 152.61, 143.10, 137.65, 136.68, 128.67, 128.56, 128.32, 128.16, 128.09, 127.65, 124.27, 109.68, 109.48, 75.13, 71.32, 71.07, 70.86, 70.19, 69.88, 68.98, 50.77.

IR (Film): ν [cm^{-1}] = 3089 (b), 3064 (m), 3032 (m), 2927 (b), 2871 (b), 2552 (b), 2352 (b), 2318 (b), 2104 (s), 1954 (b), 1812 (b), 1683 (s), 1584 (m), 1503 (s), 1454 (m), 1428 (s), 1371 (m), 1327 (m), 1221 (m), 1120 (m), 1048 (b), 1029 (b), 987 (b), 915 (b), 870 (b), 853 (b), 770 (m), 736 (m), 697 (s), 678 (b), 641 (b), 607 (b), 556 (b).

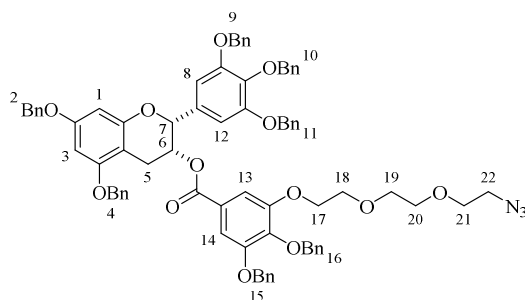
HRMS (ESI) m/z : $[\text{M}+\text{NH}_4^+]$ Calc $\text{C}_{27}\text{H}_{33}\text{N}_4\text{O}_7$ 525.2349; found 525.2362.

4.5.14 Steglich Esterification of *cis*-Chroman-3-ol *cis* **45** with Azido-PEG Linker **76**

4.5.14.1 (2*R*,3*R*)-5,7-Bis(benzyloxy)-2-(3,4,5-tris(benzyloxy)phenyl)chroman-3-yl-3-(2-(2-azidoethoxy)ethoxy)ethoxy)-4,5-bis(benzyloxy)benzoate (**77**)

The compound was prepared according to literature following a procedure by Khandelwal *et al.*^[215] A 25-mL, two necked, round-bottomed flask equipped with a magnetic stirring bar was charged with linker **76** (0.211 g, 0.416 mmol, 2.00 eq), DMAP (25.0 mg, 0.208 mmol, 1.00 eq) and EDC·HCl (79.5 mg, 0.416 mmol, 2.00 eq) dissolved in CH_2Cl_2 (8 mL) at rt under N_2 -atmosphere. The mixture was cooled down to 0 °C and a solution of *cis* **45** (157 mg, 0.207 mmol, 1.00 eq) in CH_2Cl_2 (2 mL) was added under N_2 -atmosphere. The resulting mixture was stirred overnight at rt. Then the reaction was diluted with CH_2Cl_2

(5 mL) and washed with HCl (1 mL, 0.5 M) and with sat. NaHCO₃ (5 mL) solution. The organic layer was washed with brine (5 mL), dried (Na₂SO₄), the drying agent was filtered off, and concentrated under reduced pressure. The residue was purified *via* flash chromatography (Alox, activity level III, *n*-hexane/EtOAc, 1:3, R_f = 0.20) to give the desired ester **77** (0.218 g, 0.174 mmol, 84%) as lightly yellow oil.



¹H NMR (300 MHz, CDCl₃): δ [ppm] = 7.43 – 7.13 (m, 35H, 16-H, 15-H, 11-H, 10-H, 9-H, 4-H, 2-H), 6.73 (s, 2H, 12-H, 8-H), 6.35 (d, *J* = 2.2 Hz, 2H 3-H, 1-H), 5.66 – 5.60 (m, 1H, 6-H), 5.12 – 4.90 (m, 12H, 11-H, 10-H, 9-H, 4-H, 2-H, 7-H), 4.84 (d, *J* = 11.5 Hz, 2H, 16-H), 4.71 (m, 2H, 15-H), 4.08 – 4.01 (m, 2H, 17-H), 3.75 – 3.69 (m, 2H, 18-H), 3.61 – 3.58 (m, 2H, 21-H), 3.62 – 3.56 (m, 4H, 20-H, 19-H), 3.25 – 3.19 (m, 2H, 22-H), 3.15 – 2.99 (m, 2H, 5-H).

¹³C NMR (151 MHz, CDCl₃): δ [ppm] = 165.01, 158.96, 158.09, 155.69, 152.96, 152.74, 152.33, 142.78, 138.54, 137.87, 137.74, 137.01, 136.92, 136.54, 133.40, 128.71, 128.66, 128.65, 128.59, 128.49, 128.31, 128.28, 128.14, 128.13, 128.05, 127.96, 127.91, 127.83, 75.23, 75.01, 71.36, 71.16, 70.93, 70.74, 70.27, 70.08, 69.75, 69.03, 68.53, 50.69, 26.22.

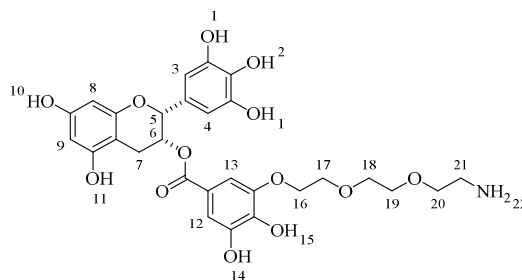
IR (Film): ν [cm⁻¹] = 2929(b), 2869 (b), 2102 (m), 1715 (s), 1618 (s), 1590 (s), 1498 (s), 1372 (m), 1327 (m), 1214 (w), 1147 (m), 1114 (m), 1028 (s), 739 (w), 697 (s).

HRMS (ESI) *m/z*: [M+NH₄⁺] Calc C₇₇H₇₅N₄O₁₃ 1263.5331; found 1263.5325.

Specific rotation: [α]_D²⁵ = -55.8 (*c* = 0.35 mol/L, CHCl₃).

4.5.15 Synthesis of Biotin Coupled EGCG Derivatives **56/81**4.5.15.1 (2*R*,3*R*)-5,7-Dihydroxy-2-(3,4,5-trihydroxyphenyl)chroman-3-yl-3-(2-(2-(2-aminoethoxy)ethoxy)ethoxy)ethoxy)-4,5-(dihydroxy)benzoate (**80**)

The compounds were prepared according to literature following a procedure by Li *et al.*^[165b] and was performed according to *chapter 4.6.2.3*.



¹H NMR (300 MHz, CD₃OD): δ [ppm] = 7.10 – 7.00 (m, 2H, 12-H, 13-H), 6.57 – 6.49 (m, 2H, 3-H, 4-H), 6.00 – 5.93 (m, 2H, 8-H, 9-H), 5.50 – 5.45 (m, 1H, 6-H), 5.00 (br s, 1H, 5-H), 4.20 – 4.00 (m, 2H, 16-H), 3.89 – 3.80 (m, 2H, 17-H), 3.75 – 3.60 (m, 4H, 18-H, 19-H), 3.56 – 3.43 (m, 2H, 20-H), 3.03 (d, $J = 14.2$ Hz, 2H, 21-H), 2.89 (qd, $J = 17.5, 3.5$ Hz, 2H, 7-H).

¹³C NMR (75 MHz, CD₃OD): δ [ppm] = 217.38, 200.76, 174.40, 162.32, 157.85, 157.14, 148.23, 147.12, 146.76, 133.74, 130.95, 129.92, 129.21, 112.09, 111.80, 108.65, 106.77, 99.36, 96.50, 95.76, 84.73, 81.50, 78.47, 72.95, 71.07, 70.63, 70.33, 69.55, 69.50, 68.86, 26.49.

IR (Solid): ν [cm⁻¹] = 3346 (b), 3253 (b), 2985 (b), 2922 (m), 2900 (b), 1705 (m), 1695 (m), 1604 (s), 1589 (m), 1516 (s), 1448 (m), 1328 (b), 1217 (b), 1193 (m), 1141 (s), 1082 (m), 1037 (s), 1016 (s), 970 (s), 879 (m), 821 (s), 761 (s), 734 (s), 717 (s), 657 (s), 650 (s), 630 (s).

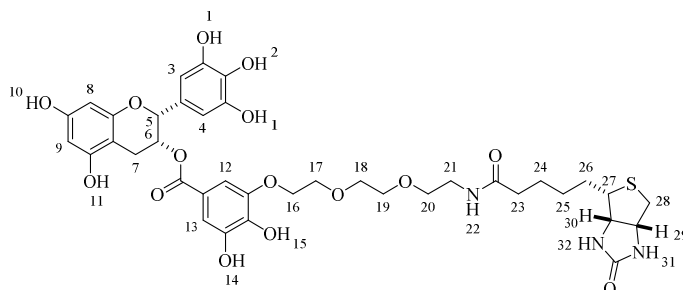
HRMS (ESI) m/z: [M+NH₄⁺] Calc C₂₈H₃₂NO₁₃ 590.1868; found 590.1870.

TLC = RP 18, acetonitrile/H₂O, 3:2, R_f = 0.52).

80 (42 mg, 0.071 mmol, 79%) was obtained as a lightly beige solid.

4.5.15.2 (2*R*,3*R*)-5,7-Dihydroxy-2-(3,4,5-trihydroxyphenyl)chroman-3-yl-3,4-dihydroxy-5-(2-(2-(2-(5-((3*aS*,4*S*,6*aR*)-2-oxohexahydro-1*H*-thieno[3,4-*d*]imidazol-4-yl)pentanamido)ethoxy)ethoxy)ethoxy)benzoate (**81**)

This synthesis was performed according to *chapter 4.5.12.4*.



¹H NMR (600 MHz, CD₃OD): δ [ppm] = 7.08 (d, $J = 1.9$ Hz, 1H, 13-H), 7.03 (d, $J = 1.9$ Hz, 1H, 12-H), 6.55 – 6.51 (s, 2H, 4-H, 3-H), 5.98 (d, $J = 2.3$ Hz, 1H, 9-H), 5.96 (d, $J = 2.3$ Hz, 1H, 8-H), 5.50 – 5.46 (m, 1H, 6-H), 5.01 (s, 1H, 5-H), 4.62 – 4.54 (m, 1H, 30-H), 4.51 – 4.45 (m, 1H, 29-H), 4.37 (dd, $J = 7.9, 4.9$ Hz, 1H, 27-H), 4.34 – 4.27 (m, 1H, 25-H), 4.17 – 4.09 (m, 2H, 16-H), 3.88 -3.85 (m, 2H, 17-H), 3.74 – 3.70 (m, 2H, 18-H), 3.66 – 3.62 (m, 2H, 19-H), 3.54 (t, $J = 5.3$ Hz, 2H, 20-H), 3.36 (t, $J = 5.3$ Hz, 2H, 21-H), 3.23 – 3.16 (m, 1H), 3.03 – 2.96 (m, 2H), 2.95 – 2.90 (m, 2H), 2.84 – 2.79 (m, 2H, 7-H), 2.73 – 2.68 (m, 2H, 27-H), 2.67 – 2.62 (m, 2H), 2.17 – 2.11 (m, 2H), 1.81 – 1.75 (m, 2H, 23-H), 1.83 – 1.41 (m, 4H, 25-H, 24-H), 1.38 – 1.25 (m, 2H, 26-H).

¹³C NMR (151 MHz, CD₃OD): δ [ppm] = 176.26, 174.87, 171.95, 170.26, 167.50, 166.06, 157.97, 157.14, 147.97, 146.79, 146.47, 141.15, 133.71, 130.99, 121.67, 112.31, 108.77, 108.22, 106.77, 99.31, 96.58, 95.82, 78.39, 71.51, 71.06, 70.58, 69.71, 68.87, 63.30, 62.08, 61.58, 56.96, 56.87, 41.09, 40.31, 36.84, 31.45, 30.42, 29.71, 29.43, 29.30, 26.85, 26.54, 26.32, 25.70.

IR (Solid): ν [cm⁻¹] = 2989 (s), 2912 (s), 2382 (b), 2322 (b), 1809 (s), 1780 (s), 1735 (s), 1705 (b), 1589 (b), 1514 (s), 1435 (s), 1367 (b), 1336 (b), 1217 (m), 1014 (b), 950 (s), 877 (s), 763 (s), 705 (s), 650 (s).

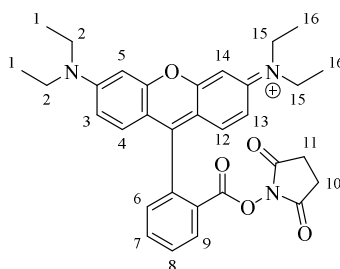
HRMS (ESI) m/z: [M+NH₄⁺] Calc C₃₈H₄₆N₃O₁₅S 816.2644; found 816.2599.

TLC = RP 18, acetonitrile/H₂O 3:2, R_f = 0.52.

81 (18 mg, 0.0220 mmol, 54%) was obtained as a lightly beige solid.

4.5.16 Synthesis of Rhodamine Dye **67**4.5.16.1 *N*-(6-(Diethylamino)-9-(2-(((2,5-dioxopyrrolidin-1-yl)oxy)carbonyl)phenyl)-3*H*-xanthen-3-ylidene)-*N*-ethylethanaminium (**66**)

The compound was prepared according to literature following a procedure by Fujisaki *et al.*^[276] A 100-mL, round-bottomed flask equipped with a magnetic stirring bar was charged with rhodamine B (500 mg, 1.04 mmol, 1.00 eq) dissolved in DMF (15 mL) at rt. To this solution EDC·HCl (259 mg, 1.36 mmol, 1.30 eq) and *N*-hydroxysuccinimide (156 mg 1.36 mmol, 1.30 eq) were added. The solution was stirred at rt for 24 hours until TLC (SiO₂, MeOH/CH₂Cl₂, 95:5, *R_f* = 0.43) showed complete consumption of starting material. The red solution was extracted with EtOAc (8 x 10 mL) and with water (8 x 10mL). The combined organic layers were washed with brine (30 mL) and dried (Na₂SO₄). The drying agent was filtered off and the organic layer was concentrated under reduced pressure, yielding product **66** without purification (602 mg, 1.11 mmol, 88%) as pink solid.

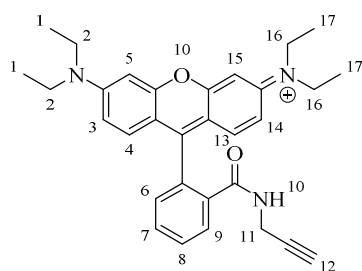


¹H NMR (300 MHz, CDCl₃): δ [ppm] = 8.41 – 8.38 (dd, *J* = 9.0, 8.0 Hz, 1H, 9-H), 7.99 – 7.94 (m, 1H, 6-H), 7.80 (td, *J* = 7.8, 1.3 Hz, 1H, 7-H), 7.61 (td, *J* = 7.4, 1.4 Hz, 1H, 8-H), 7.48 – 7.42 (m, 1H, 3-H), 7.20 – 7.17 (d, *J* = 9.5 Hz, 1H, 14-H), 7.06 (d, *J* = 9.4 Hz, 1H, 5-H), 6.85 (dd, *J* = 9.5, 2.5 Hz, 2H, 13-H, 12-H), 6.80 (d, *J* = 2.4 Hz, 1H, 3-H), 2.79 – 2.71 (m, 4H, 11-H, 10-H), 3.64 (q, *J* = 7.2 Hz, 8H, 15-H, 2-H), 1.32 (t, *J* = 7.1 Hz, 12H, 16-H, 1-H).

¹³C NMR (75 MHz, CDCl₃): δ [ppm] = 169.76, 168.74, 160.82, 157.90, 155.81, 155.73, 153.73, 149.94, 135.04, 134.59, 134.30, 131.87, 131.16, 131.06, 130.80, 129.29, 129.23, 128.36, 125.48, 125.23, 124.59, 114.56, 113.53, 108.45, 106.56, 97.60, 96.70, 46.34, 44.67, 36.61, 31.55, 25.72, 12.79, 12.66.

4.5.16.2 *N*-(6-(Diethylamino)-9-(2-(prop-2-yn-1-ylcarbamoyl)phenyl)-3*H*-xanthen-3-ylidene)-*N*-ethylethanaminium (**67**)

The compound was prepared according to literature following a procedure by Andrade *et al.*^[277] A 100-mL, round-bottomed flask equipped with a magnetic stirring bar was charged with propargyl amine (71.4 μ L, 1.11 mmol, 1.00 eq) and triethyl amine (311 μ L, 2.22 mmol, 2.00 eq) in DMF (45 mL) and cooled down to 0 °C. To this cooled mixture a solution of **66** (602 mg, 1.11 mmol, 1.00 eq) in DMF (5 mL) was slowly added dropwise, followed by stirring for 30 min at 0 °C. The ice bath was removed and the resulting solution was stirred overnight at rt. The solution was extracted with ethyl acetate (8 x 20mL) and with water (8 x mL). The combined organic layers were washed with brine (30 mL) and dried (Na_2SO_4). The drying agent was filtered off and the organic layer was concentrated under reduced pressure. Purification by column chromatography (SiO_2 , MeOH/ CH_2Cl_2 , 1:99, $R_f = 0.31$) provided product **76** (246 mg, 0.511 mmol, 68%) as pink solid.

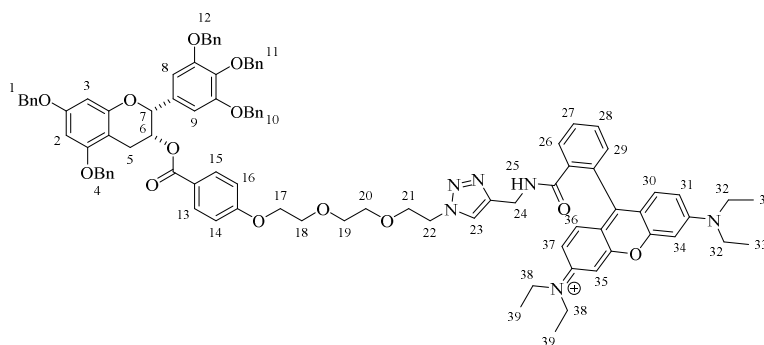


^1H NMR (300 MHz, CDCl_3): δ [ppm] = 7.96 – 7.98 (m, 1H, 9-H), 7.47 – 7.38 (m, 2H, 8-H, 7-H), 7.14 – 7.06 (m, 1H, 6-H), 6.48 (s, 1H, 15-H), 6.45 (s, 1H, 5-H), 6.39 (d, $J = 2.5$ Hz, 2H, 4-H, 3-H), 6.27 (dd, $J = 8.9, 2.6$ Hz, 2H, 14-H, 13-H), 3.95 (d, $J = 2.5$ Hz, 2H, 11-H), 3.33 (q, $J = 7.0$ Hz, 8H, 16-H, 2-H), 1.76 (t, $J = 2.5$ Hz, 1H, 12-H), 1.16 (t, $J = 7.0$ Hz, 12H, 17-H, 1-H).

4.5.17 Click Reaction of Rhodamine Dye **67** with EGCG-PEG Linker **54/77** to Product **68/78**

4.5.17.1 (2*R*,3*R*)-5,7-Bis(benzyloxy)-2-(3,4,5-tris(benzyloxy)phenyl)chroman-3-yl-4-(2-(2-(4-((2-(3-(diethyl- λ^4 azaneylidene)-3-(diethylamino)-3*H*-xanthen-9-yl)benz-amido)methyl)-1*H*-1,2,3-triazol-1-yl)ethoxy)ethoxy)ethoxy)benzoate (**68**)

The compound was prepared according to literature following a procedure by Kolarovic *et al.*^[278] A 10-mL, round-bottomed flask equipped with a magnetic stirring bar was sequentially charged with copper sulfate (0.257 mg, $1.03 \cdot 10^{-2}$ mmol, 5 mol%) and sodium ascorbate (0.408 mg, 0.00206 mmol, 0.10 mol%) in DMSO (100 μ L). To this green mixture a solution of **54** (21.3 mg, 0.0206 mmol, 1.10 eq) in DMSO (100 μ L) followed by a solution of **67** (9.00 mg, 0.0187 mmol, 1.00 eq) in DMSO (100 μ L) were added. The brown solution was stirred at 65 °C overnight until TLC (SiO₂, MeOH/CH₂Cl₂, 5:95, R_f = 0.43) showed complete consumption of starting material. The solvent was evaporated and the residue was purified by column chromatography (Alox, activity level III, MeOH/CH₂Cl₂, 5:95), providing product **68** (21.1 mg, 0.0139 mmol, 68%) as pink oil.



¹H NMR (300 MHz, CDCl₃): δ [ppm] = 7.95 – 7.86 (m, 2H, 15-H, 13-H), 7.42 – 7.24 (m, 25H, 12-H, 11-H, 10-H, 4-H, 1-H), 7.23 – 7.10 (m, 4H, 29-H, 28-H, 27-H, 26-H), 7.07 – 6.99 (m, 1H, 23-H), 6.90 – 6.86 (m, 2H, 16-H, 14-H), 6.79 (s, 2H, 9-H, 8-H), 6.35 – 6.25 (m, 4H, 37-H, 36-H, 31-H, 30-H), 6.14 – 6.06 (m, 2H, 35-H, 34-H), 5.69 – 5.63 (m, 1H, 6-H), 5.07 – 4.90 (m, 11H, 12-H, 11-H, 10-H, 4-H, 1-H), 4.76 (d, $J = 11.5$ Hz, 2H, 22-H) 4.47 (s, 2H, 24-H), 4.16 – 4.09 (m, 2H, 17-H), 4.02 – 3.96 (m, 2H, 18-H), 3.76 – 3.66 (m, 4H, 20-H, 19-H), 3.64 – 3.55 (m, 2H, 21-H), 3.54 – 3.49 (m, 2H, 22-H), 3.28 (q, $J = 7.0$ Hz, 8H, 38-H, 32-H), 3.18 – 3.01 (m, 2H, 5-H), 1.12 (t, $J = 7.0$ Hz, 12H, 39-H, 33-H).

¹³C NMR (75 MHz, CDCl₃): δ [ppm] = 167.84, 166.09, 162.71, 158.76, 157.97, 155.57,

153.41, 152.79, 148.65, 144.17, 138.23, 137.01, 133.36, 132.53, 131.85, 130.93, 128.74, 128.62, 128.54, 128.39, 128.07, 128.03, 127.91, 127.78, 127.71, 127.59, 127.46, 127.20, 123.89, 123.29, 122.81, 122.55, 114.19, 107.77, 106.63, 106.33, 101.01, 97.86, 94.78, 93.92, 75.10, 71.18, 70.72, 70.58, 70.17, 69.98, 69.43, 67.97, 67.53, 64.99, 53.45, 49.65, 44.33, 41.02, 35.35, 12.63.

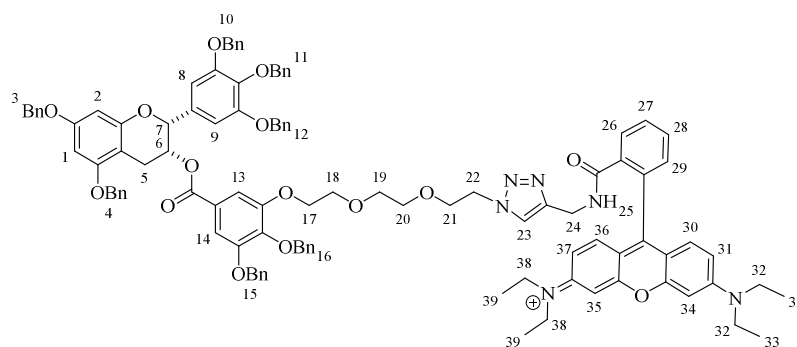
IR (Film): ν [cm^{-1}] = 2918 (w), 1687 (m), 1633 (s), 1604 (m), 1593 (s), 1548 (s), 1512 (m), 1467 (s), 1427 (s), 1375 (s), 1355 (s), 1328 (s), 1305 (s), 1253 (s), 1219 (s), 1166 (s), 1145 (s), 1114 (m), 1045 (m), 1028 (s), 912 (m), 815 (s), 786 (s), 734 (m), 696 (s).

HRMS (ESI) m/z : [M^+] Calc $\text{C}_{94}\text{H}_{93}\text{N}_6\text{O}_{13}$ 1513.6795; found 1513.6786.

Specific rotation: $[\alpha]_D^{25} = -30.2$ ($c = 0.48$ mol/L, CHCl_3).

4.5.17.2 (2*R*,3*R*)-5,7-Bis(benzyloxy)-2-(3,4,5-tris(benzyloxy)phenyl)chroman-3-yl-3,4-bis(benzyloxy)-5-(2-(2-(2-(4-((2-(3-(diethyl- λ^4 azaneylidene)-6-(diethylamino)-3*H*-xanthen-9-yl)benzamido)methyl)-1*H*-1,2,3-triazol-1-yl)ethoxy)ethoxy)ethoxy)benzoate (**78**)

The compound was prepared according to literature following a procedure by Kolarovic *et al.*^[278] and was synthesized according to *chapter 4.5.17.2*.



^1H NMR (600 MHz, CDCl_3): δ [ppm] = 7.91 – 7.86 (m, 2H, 14-H, 13-H), 7.45 – 7.14 (m, 45H, 29-H, 28-H, 27-H, 26-H, 16-H, 15-H, 12-H, 11-H, 10-H, 4-H, 3-H), 7.10 – 7.01 (m, 1H, 23-H), 6.74 (s, 2H, 9-H, 8-H), 6.38 (d, $J = 2.0$ Hz, 2H, 2-H, 1-H), 6.33 (d, $J = 2.2$ Hz, 2H, 30-H, 31-H), 6.28 (d, $J = 8.7$ Hz, 2H, 37-H, 36-H), 6.12 (d, $J = 8.1$ Hz, 2H, 35-H, 34-H), 5.67 (s, 1H, 6-H), 5.07 – 4.94 (m, 10H, 12-H, 11-H, 10-H, 4-H, 3-H), 4.92 (s, 1H, 7-H), 4.84 (d, $J = 11.5$ Hz, 2H, 16-H), 4.74 (d, $J = 11.5$ Hz, 2H, 15-H), 4.46 (s, 2H, 24-H), 4.16 – 4.09 (m, 2H, 17-H), 4.05 – 3.99 (m, 2H, 18-H), 3.70 – 3.64 (m, 2H, 21-H),

3.61 – 3.55 (m, 2H, 19-H), 3.54 – 3.49 (m, 2H, 20-H), 3.43 – 3.38 (m, 2H, 22-H), 3.32 – 3.20 (m, 8H, 38-H, 32-H), 3.14 – 3.01 (m, 1H, 5-H), 1.14 – 1.06 (m, 12H, 39-H, 33-H).

^{13}C NMR (151 MHz, CDCl_3): δ [ppm] = 167.81, 164.89, 158.87, 158.00, 155.60, 153.40, 152.86, 152.64, 152.21, 148.64, 142.65, 138.42, 137.77, 136.90, 136.41, 133.32, 132.50, 128.76, 128.62, 128.57, 128.49, 128.40, 128.19, 128.17, 128.10, 128.07, 128.04, 127.96, 127.90, 127.83, 127.75, 127.51, 127.49, 127.22, 125.03, 123.87, 123.20, 122.85, 109.23, 109.08, 107.78, 106.72, 105.36, 100.97, 97.86, 94.73, 94.00, 77.84, 75.14, 74.89, 71.25, 71.06, 70.67, 70.51, 70.18, 70.02, 69.59, 69.36, 68.94, 68.44, 44.33, 41.05, 12.63.

IR (Film): ν [cm^{-1}] = 2968 (w), 1683 (w), 1614 (s), 1589 (s), 1516 (s), 1427 (s), 1373 (s), 1328 (w), 1307 (s), 1263 (s), 1219 (w), 1120 (w), 910 (w), 813 (s), 734 (s), 696 (s).

HRMS (ESI) m/z : [M^+] Calc $\text{C}_{108}\text{H}_{105}\text{N}_6\text{O}_{15}$ 1725.7632; found 1725.7618.

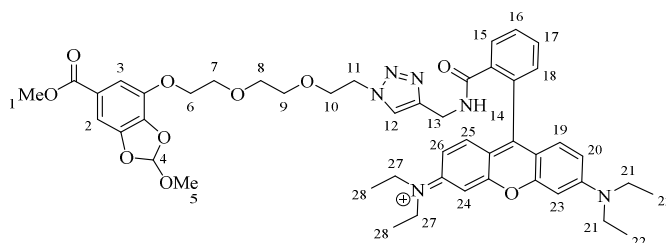
78 (37.7 mg, 0.0218 mmol, 78%) was obtained as a pink oil.

Specific rotation: $[\alpha]_D^{25} = -42.7$ ($c = 0.845$ mol/L, CHCl_3).

4.5.18 Synthesis of Blank Molecule Lacking the Catechine Moiety

4.5.18.1 *N*-(6-(Diethylamino)-9-(2-(((1-(2-(2-(2-((2-methoxy-6-(methoxycarbonyl)benzo[d][1,3]dioxol-4-yl)oxy)ethoxy)ethoxy)ethyl)-1H-1,2,3-triazol-4-yl)methyl)carbamoyl)phenyl)-3H-xanthen-3-ylidene)-*N*-ethylethanaminium (**72**)

The compound was prepared according to literature following a procedure by Kolarovic *et al.*^[278]



^1H NMR (300 MHz, CDCl_3): δ [ppm] = 7.92 – 7.86 (m, 1H, 15-H), 7.43 – 7.37 (m, 2H, 17-H, 16-H), 7.32 (d, $J = 1.5$ Hz, 1H, 2-H), 7.21 (d, $J = 1.5$ Hz, 1H, 3-H), 7.15 (s, 1H, 4-H), 7.09 – 7.01 (m, 1H, 18-H), 6.87 (s, 1H, 12-H), 6.35 – 6.22 (m, 4H, 24-H, 23-H, 20-H, 19-H), 6.12 (dd, $J = 8.9, 2.6$ Hz, 2H, 26-H, 25-H), 4.45 (s, 2H, 13-H), 4.27 – 4.18

(m, 4H, 7-H, 6-H), 3.83 (s, 3H, 1-H), 3.80 – 3.74 (m, 2H, 8-H), 3.70 (t, $J = 5.4$ Hz, 2H, 9-H), 3.65 – 3.59 (m, 2H, 10-H), 3.55 – 3.52 (m, 2H, 11-H), 3.37 (s, 3H, 5-H), 3.27 (q, $J = 7.1, 6.3$ Hz, 8H, 27-H, 21-H), 1.11 (t, $J = 7.0$ Hz, 12H, 28-H, 22-H).

^{13}C NMR (75 MHz, CDCl_3): δ [ppm] = 167.69, 166.13, 153.45, 153.28, 148.54, 147.11, 144.01, 141.61, 138.10, 132.42, 130.82, 129.77, 128.67, 127.93, 127.81, 124.23, 123.76, 123.16, 122.71, 120.16, 111.59, 107.68, 105.24, 103.40, 97.72, 70.70, 70.49, 69.54, 69.34, 69.11, 64.84, 52.11, 50.17, 49.56, 44.24, 40.94, 35.19, 12.54.

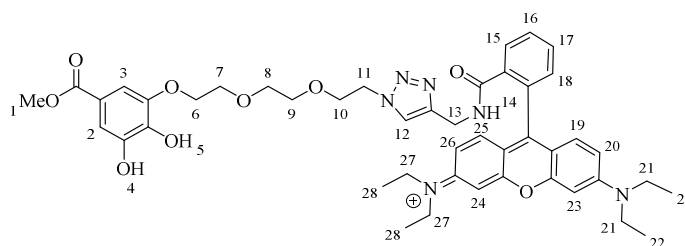
IR (Film): ν [cm^{-1}] = 3443 (b), 2971 (m), 2872 (m), 1690 (m), 1634 (s), 1615 (m), 1547 (s), 1514 (m), 1467 (s), 1434 (m), 1375 (s), 1358 (s), 1324 (s), 1265 (s), 1219 (m), 1118 (m), 1044 (m), 915 (m), 820 (m), 757 (m), 701 (s), 666 (s).

HRMS (ESI) m/z : $[\text{M}^+]$ Calc $\text{C}_{47}\text{H}_{55}\text{N}_6\text{O}_{10}$ 863.3974; found 863.3978.

72 (152.2 mg, 0.176 mmol, 77%) was obtained as a pink oil.

TLC = SiO_2 , $\text{CH}_2\text{Cl}_2/\text{MeOH}$, 98:2, $R_f = 0.2$.

4.5.18.2 *N*-(6-(Diethylamino)-9-(2-(((1-(2-(2-(2-(2,3-dihydroxy-5-(methoxycarbonyl)phenoxy)ethoxy)ethoxy)ethyl)-1*H*-1,2,3-triazol-4-yl)methyl)carbamoyl)phenyl)-3*H*-xanthen-3-ylidene)-*N*-ethylethanaminiumm (**101**)



^1H NMR (300 MHz, CDCl_3): δ [ppm] = 8.85 (br s, 1H, 5-H), 7.96 – 7.90 (m, 1H, 15-H), 7.46 – 7.39 (m, 3H, 18-H, 17-H, 16-H), 7.35 (d, $J = 1.9$ Hz, 1H, 2-H), 7.18 (d, $J = 2.0$ Hz, 1H, 3-H), 7.11 – 7.05 (m, 1H, 12-H), 6.87 (br s, 1H, 4-H), 6.34 (d, $J = 2.5$ Hz, 2H, 20-H, 19-H), 6.26 (d, $J = 8.8$ Hz, 2H, 24-H, 23-H), 6.11 (dd, $J = 8.9, 2.6$ Hz, 2H, 26-H, 25-H), 4.46 (s, 2H, 13-H), 4.28 (t, $J = 5.1$ Hz, 2H, 6-H), 4.14 – 4.08 (m, 2H, 7-H), 3.84 (s, 3H, 1-H), 3.75 (t, $J = 5.1$ Hz, 2H, 8-H), 3.68 – 3.63 (m, 2H, 9-H), 3.60 – 3.53 (m, 4H, 11-H, 10-H), 3.29 (q, $J = 7.0$ Hz, 8H, 27-H, 21-H), 1.13 (t, $J = 7.0$ Hz, 12H, 28-H, 22-H).

^{13}C NMR (75 MHz, CDCl_3): δ [ppm] = 168.34, 167.08, 153.73, 153.53, 148.83, 146.26, 145.21, 144.10, 139.72, 132.81, 130.75, 128.67, 128.22, 124.01, 123.04, 121.04, 111.73,

108.69, 107.88, 104.96, 98.06, 70.63, 70.44, 69.77, 69.46, 65.52, 49.92, 44.44, 41.08, 12.67.

IR (Film): ν [cm^{-1}] = 2970 (s), 2929 (s), 2871 (s), 2358 (s), 2337 (s), 2244 (s), 1687 (b), 1633 (s), 1614 (s), 1547 (s), 1515 (m), 1433 (m), 1331 (b), 1266 (s), 1220 (m), 1118 (s), 1090 (s), 1016 (m), 913 (m), 819 (s), 788 (m), 731 (m).

HRMS (ESI) m/z : [M^+] Calc $C_{45}H_{53}N_6O_9$ 821.3869; found 821.3861.

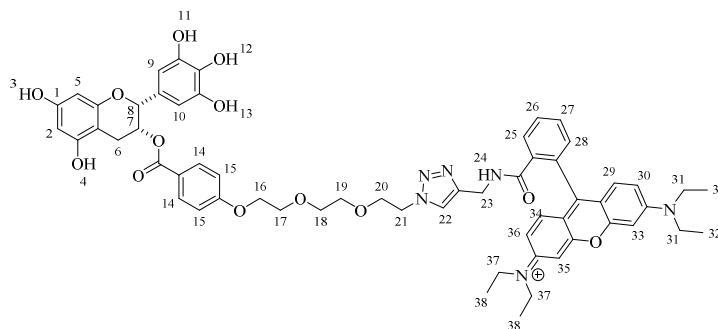
101 (57.7 mg, 0.0702 mmol, 52%) was obtained as a pink oil.

TLC = SiO_2 , $\text{CH}_2\text{Cl}_2/\text{MeOH}$, 98:2, R_f = 0.11.

4.5.19 Catalytic Hydrogenation of Fluorescent Coupled Target **69/79**

4.5.19.1 *N*-(6-(Diethylamino)-9-(2-(((1-(2-(2-(2-(4-(((2*R*,3*R*)-5,7-dihydroxy-2-(3,4,5-trihydroxyphenylchroman-3-yl)oxy)carbonyl)phenoxy)ethoxy)ethoxy)ethyl)-1*H*-1,2,3-triazol-4-yl)methyl (**69**))

The compounds were prepared according to literature following a procedure by Li *et al.*^[165b] A 25-mL, two necked round-bottomed flask equipped with a magnetic stirring bar and three way cock, which was equipped with a balloon filled with hydrogen, was sequentially charged with **68** (21.1 mg, 0.0139 mmol, 1.00 eq) in a mixture of THF/methanol (2 mL, 1:1, v/v). The flask was flowed with argon when one lightly heaped spatula $\text{Pd}(\text{OH})_2$ (20% on carbon) was added in one batch to the solution. The resulting mixture was stirred at rt under H_2 -atmosphere until TLC (RP 18, acetonitrile/ H_2O , 1:1) showed complete consumption of the starting material. The black suspension was filtered through a syringe filter (0.20 μm PTFE) and the filtrate was evaporated. The residue was purified by flash chromatography on RP with ACN to afford the desired compound.



^1H NMR (600 MHz, CD_3OD): δ [ppm] = 7.90 (d, J = 6.8 Hz, 1H, 25-H), 7.81 – 7.73

(m, 2H, 14-H), 7.56 – 7.43 (m, 2H, 26-H, 27-H), 7.25 (s, 1H, 22-H), 7.06 – 6.99 (m, 1H, 28-H), 6.82 – 6.74 (m, 2H, 15-H), 6.54 (s, 2H, 10-H, 9-H), 6.36 – 6.31 (m, 2H, 34-H, 33-H), 6.24 – 6.15 (m, 2H, 5-H, 2-H), 5.97 (q, $J = 2.3$ Hz, 2H, 30-H, 29-H), 5.55 – 5.50 (m, 1H, 7-H), 5.01 (s, 1H, 8-H), 4.36 (s, 1H, 23-H), 4.25 (t, $J = 5.0$ Hz, 2H, 16-H), 4.05 – 3.99 (m, 2H, 17-H), 3.73 – 3.64 (m, 4H, 19-H, 18-H), 3.62 – 3.50 (m, 4H, 21-H, 20-H), 3.32 (q, $J = 1.6$ Hz, 8H, 31-H, 37-H), 3.07 – 2.83 (m, 1H, 6-H), 1.14 – 1.05 (m, 12H, 38-H, 32-H).

^{13}C NMR (151 MHz, CD_3OD): δ [ppm] = 168.40, 165.74, 162.68, 156.53, 155.82, 128.39, 128.08, 127.82, 127.43, 127.20, 126.88, 123.91, 123.63, 122.51, 122.30, 120.80, 113.87, 111.76, 105.33, 97.89, 95.18, 94.46, 77.09, 70.30, 70.06, 69.18, 69.05, 68.68, 67.46, 65.17, 55.01, 49.67, 34.31, 25.42, 25.09, 11.23.

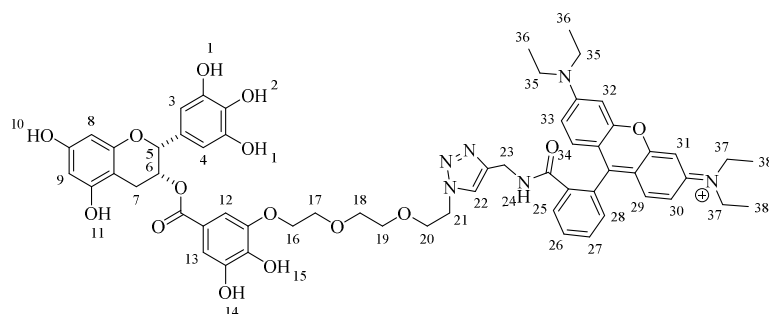
IR (Film): ν [cm^{-1}] = 2985 (s), 2970 (m), 2900 (s), 1514 (s), 1253 (m), 1220 (s), 1143 (s), 1076 (m), 1053 (m), 1028 (s).

HRMS (ESI) m/z : [M^+] Calc $\text{C}_{59}\text{H}_{63}\text{N}_6\text{O}_{13}$ 1063.4448; found 1063.4438.

69 (28.5 mg, 0.0268 mmol, 89%) was obtained as a pink solid.

4.5.19.2 *N*-(6-(Diethylamino)-9-(2-(((1-(2-(2-(2-(5-(((2*R*,3*R*)-5,7-dihydroxy-2-(3,4,5-trihydroxyphenyl)chroman-3-yl)oxy)carbonyl)-2,3-dihydroxyphenoxy)ethoxy)ethoxy)ethyl)-1*H*-1,2,3-triazol-4-yl)methyl)carbamoyl)phenyl)-3*H*-xanthen-3-ylidene)-*N*-ethylethanaminium (**79**)

The compounds were prepared according to the literature following a procedure by Li *et al.*^[165b] and was performed according *chapter 4.5.19.2*.



^1H NMR (300 MHz, CD_3OD): δ [ppm] = 7.92 – 7.89 (m, 2H, 13-H, 12-H), 7.51 – 7.45 (m, 2H, 27-H, 26-H), 7.08 – 7.03 (m, 2H, 25-H), 7.00 – 6.94 (m, 2H, 28-H), 6.57 (s, 2H, 4-H, 3-H), 6.38 – 6.26 (m, 4H, 34-H, 33-H, 30-H, 29-H), 5.98 (s, 2H, 9-H, 8-H), 5.49 – 5.47 (m,

1H, 6-H), 5.02 – 4.99 (m, 1H, 5-H), 4.42 (br s, 1H, 35-H), 4.27 – 4.24 (m, 1H, 33-H), 4.02 – 3.93 (m, 2H, 23-H), 3.74 – 3.66 (m, 4H, 17-H, 16-H), 3.60 (d, $J = 4.3$ Hz, 2H, 18-H), 3.55 (d, $J = 4.7$ Hz, 2H, 19-H), 3.47 (br s, 2H, 20-H), 3.43 (td, $J = 6.1, 3.1$ Hz, 2H, 21-H), 3.33 (td, $J = 3.3, 1.7$ Hz, 8H, 37-H, 35-H), 3.02 – 2.98 (m, 1H, 7-H), 2.95 – 2.90 (m, 1H, 7-H), 1.10 (t, $J = 7.0$ Hz, 12H, 38-H, 36-H).

^{13}C NMR (151 MHz, CD_3OD): δ [ppm] = 167.29, 157.80, 157.69, 156.98, 154.62, 154.30, 147.70, 146.59, 146.16, 144.44, 140.92, 134.29, 133.54, 131.27, 130.79, 130.00, 129.65, 125.24, 124.87, 123.77, 121.44, 112.05, 108.27, 106.65, 99.16, 96.42, 95.69, 78.26, 71.28, 71.12, 70.48, 70.38, 69.91, 69.54, 68.69, 66.38, 50.85, 46.62, 35.55, 26.44, 26.32, 12.38.

IR (Film): ν [cm^{-1}] = 2970 (b), 2900 (b), 2358 (m), 1608 (b), 1514 (m), 1332 (b), 1217 (b), 1078 (b), 1037 (m), 819 (s), 761 (s).

HRMS (ESI) m/z : [M^+] Calc $\text{C}_{59}\text{H}_{63}\text{N}_6\text{O}_{15}$ 1095.4346; found 1095.4330.

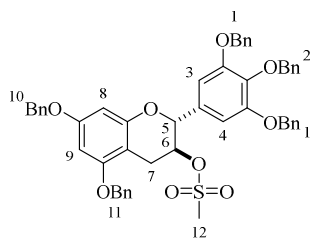
79 (52.7 mg, $4.81 \cdot 10^{-5}$ mol, 87%) was obtained as a pink solid.

TLC = RP 18 (methanol), $R_f = 0.85$.

4.5.20 Synthesis of 3-Azidochromane **85** via Nucleophilic Substitution

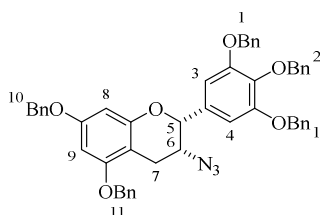
4.5.20.1 (2*R*,3*R*)-3-Azido-5,7-bis(benzyloxy)-2-(3,4,5-tris(benzyloxy)phenyl)-chromane (**85**)

The compound was prepared according to literature following a procedure by Marcotullio *et al.*^[279] A 25-mL, two necked, round-bottomed flask equipped with a magnetic stirring bar was sequentially charged with *trans* **41**(α) (156 mg, 0.206 mmol, 1.00 eq) dissolved in CH_2Cl_2 (10 mL) at rt under N_2 -atmosphere. To this lightly yellow solution triethyl amine (66 μL , 0.474 mmol, 2.30 eq) was added and stirred for 10 min at rt. The mixture was cooled down to 0 °C and methanesulfonic anhydride (54.0 mg, 0.310 mmol, 1.50 eq) was added in one batch to the solution. The resulting mixture was stirred overnight at rt. After TLC (SiO_2 , *n*-hexane/EtOAc, 3:1, $R_f = 0.34$) showed complete consumption of the starting material, the reaction was quenched with water (10 mL), extracted with CH_2Cl_2 (3 x 5mL) and with brine (10 mL), dried (Na_2SO_4), the drying agent was filtered off, and concentrated under reduced pressure. The crude residue (170 mg, 0.204 mmol) was obtained as lightly yellow solid and was used for the next step without further purification.



¹H NMR (300 MHz, CD₃OD): δ [ppm] = 7.31 – 7.18 (m, 25H, 1-H, 2-H, 10-H, 11-H), 6.58 (s, 2H, 3-H, 4-H), 6.17 (d, $J = 2.3$ Hz, 1H, 8-H), 6.11 (d, $J = 2.3$ Hz, 1H, 9-H), 5.14 (s, 1H, 5-H), 4.98 – 4.88 (m, 10H, 1-H, 2-H, 10-H, 11-H), 4.79 – 4.72 (m, 1H, 6-H), 3.01 (dd, $J = 16.8, 5.2$ Hz, 1H, 7-H), 2.84 (td, $J = 16.7, 7.4$ Hz, 1H, 7-H), 2.02 (s, 3H, 12-H).

The compound was prepared according to literature following a procedure by Park.^[280] A 50-mL, round-bottomed flask equipped with a magnetic stirring bar was charged with product **84** (0.585 g, 0.701 mmol, 1.00 eq) dissolved in DMSO (1.00 mL). To this yellow solution (683 mg, 10.5 mmol, 10.0 eq) NaN₃ was added in one batch. This mixture was stirred overnight at 65 °C (TLC = SiO₂, *n*-hexane/EtOAc, 3:1, $R_f = 0.64$). The reaction was hydrolyzed and washed with water (6 x 10mL). The aqueous layer was extracted with EtOAc (6 x 5mL) and the combined organic layers were washed with brine, dried (Na₂SO₄), the drying agent was filtered off and concentrated under reduced pressure. The crude residue was purified by column chromatography (Alox, activity level III, *n*-hexane/EtOAc, 10:1, $R_f = 0.20$) and recrystallization from *n*-hexane provided product **85** (183 mg, 0.234 mmol, 33%) as white solid.



¹H NMR (300 MHz, CDCl₃): δ [ppm] = 7.36 – 7.15 (m, 25H, 1-H, 2-H, 10-H, 11-H), 6.74 (s, 2H, 3-H, 4-H), 6.21 (s, 2H, 8-H, 9-H), 5.19 – 4.94 (m, 10H, 1-H, 2-H, 10-H, 11-H), 4.86 (s, 1H, 5-H), 3.88 (qd, $J = 2.7, 1.8$ Hz, 1H, 6-H), 3.02 (dd, $J = 17.5, 2.7$ Hz, 1H, 7-H), 2.93 (dd, $J = 17.4, 4.7$ Hz, 1H, 7-H).

¹³C NMR (75 MHz, CDCl₃): δ [ppm] = 159.14, 157.91, 155.25, 152.91, 138.61, 137.86, 137.07, 136.87, 136.84, 133.42, 128.64, 128.62, 128.50, 128.19, 128.07, 128.02, 127.90, 127.83, 127.60, 127.57, 127.32, 106.50, 100.21, 94.67, 94.27, 75.29, 71.44, 70.10, 58.31, 25.89.

IR (Film): ν [cm⁻¹] = 3013 (b), 2926 (b), 2869 (b), 2107 (s), 1952 (m), 1876 (m), 1809 (m), 1731 (m), 1615 (s), 1592 (s), 1497 (s), 1434 (s), 1349 (s), 1217 (b), 1147 (s), 1112 (b), 1028 (s), 910 (s), 812 (s), 734 (s), 696 (s).

HRMS (ESI+) m/z : [M+H⁺] Calc C₅₀H₄₄N₃O₆ 782.3225; found 782.3221.

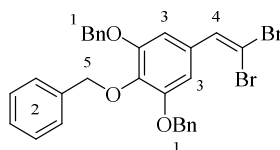
Specific rotation: $[\alpha]_D^{25} = -26.3$ ($c = 2.23$ mol/L, CHCl₃).

Melting point: 123.2 °C.

4.5.21 Synthesis of Ethynyl Benzene Derivative *via* Corey Fuchs Reaction

4.5.21.1 3,4,5-Tris(benzyloxy)-2,2-(dibromovinyl)benzene (**87**)

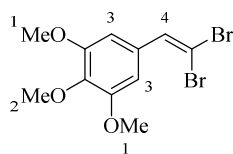
The compound was prepared according to literature following a procedure by Corey and Fuchs *et al.*^[266] A 100-mL, round-bottomed flask equipped with a magnetic stirring bar was sequentially charged with triphenyl phosphine (4.94 g, 18.8 mmol, 4.00 eq) and tetrabromomethane (3.13 g, 9.42 mmol, 2.00 eq) dissolved in CH₂Cl₂ (60 mL) at rt. The lightly yellow solution was cooled to 0 °C. Aldehyde **33b** (2.00 g, 4.72 mmol, 1.00 eq) dissolved in CH₂Cl₂ (10 mL) and was added to the solution. The mixture was allowed to stir for 1 h at 0 °C and for one hour at rt. Pentane (50 mL) was added to the mixture to precipitate the triphenylphosphine oxide. The residue was filtered through a layer of celite. The solvent was removed under reduced pressure to yield a white solid. The solid was purified by flash chromatography on silica gel (*n*-hexane/EtOAc, 10:1, R_f = 0.52) to afford compound **87** (2.30 g, 3.96 mmol, 84%) as white solid.



¹H NMR (300 MHz, CDCl₃): δ [ppm] = 7.46 – 7.27 (m, 16H, 4-H, 2-H, 1-H), 6.83 (s, 2H, 3-H), 5.11 (d, $J = 3.4$ Hz, 6H, 5-H, 1-H).

4.5.21.2 3,4,5-Trimethoxy-2,2-(dibromovinyl)benzene (**86**)

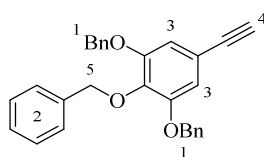
The compound was prepared according to the literature following a procedure by Corey and Fuchs *et al.*^[266] and was performed for the aldehyde **33a** yielding the product **86** in (4.62 g, 13.1 mmol, 86%) as lightly yellow solid.



$^1\text{H NMR}$ (300 MHz, CDCl_3): δ [ppm] = 7.41 (s, 1H, 4-H), 6.80 (s, 2H, 3-H), 3.87 (d, J = 1.5 Hz, 9H, 2-H, 1-H).

4.5.21.3 3,4,5-Tris(benzyloxy)-1-ethynylbenzene (**89**)

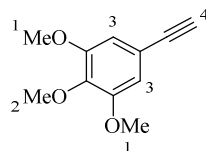
The compound was prepared according to literature following a procedure by Corey and Fuchs *et al.*^[266] A 50-mL, round-bottomed flask equipped with a magnetic stirring bar was sequentially charged with product **87** (2.00 g, 3.45 mmol, 1.00 eq) dissolved in dry THF (25 mL) at rt. The solution was cooled down to $-78\text{ }^\circ\text{C}$ using an acetone-dry ice bath. Then *n*-BuLi (4.31 mL, 1.60 M in *n*-hexane, 2.00 eq) was added dropwise to the solution. Until the *n*-BuLi amount had been completely added, the reaction was stirred for 1 h at $-78\text{ }^\circ\text{C}$, followed by another hour at rt. After TLC (SiO_2 , *n*-hexane/EtOAc, 8:1, R_f = 0.55) showed complete consumption of the starting material, the solution was quenched with sat. NH_4Cl (10 mL) and the organic layer was separated. The aqueous layer was extracted with Et_2O (3 x 25 mL), the combined organic layer was washed with brine (25 mL), dried (MgSO_4), the drying agent was filtered off, and concentrated under reduced pressure to yield a yellow solid. The solid was purified by flash chromatography on silica gel (*n*-hexane/EtOAc, 10:1) to afford **89** (1.09 g, 2.59 mmol, 90%) as lightly yellow solid.



$^1\text{H NMR}$ (300 MHz, CDCl_3): δ [ppm] = 7.51 – 7.29 (m, 17H, 2-H, 1-H), 6.81 (s, 2H, 3-H), 5.07 (d, J = 6.0 Hz, 6H, 5-H, 1-H), 3.00 (s, 1H, 4-H).

4.5.21.4 3,4,5-Trimethoxy-1-ethynylbenzene (**88**)

The compound was prepared according to literature following a procedure by Corey and Fuchs *et al.*^[266] and was performed for **86**, yielding the product **88** (3.44 g, 17.9 mmol, 60%).

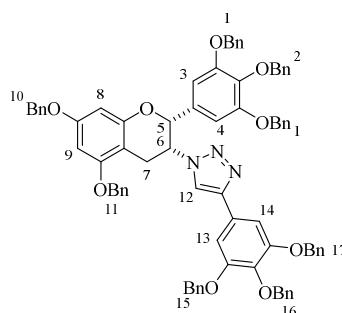


$^1\text{H NMR}$ (300 MHz, CDCl_3): δ [ppm] = 6.73 (s, 2H, 3-H), 3.85 (s, 9H, 2-H, 1-H), 3.03 (s, 1H, 4-H).

4.5.22 Click Reaction of Azido-EGCG **85** and Ethynyl Benzene Derivative **89** to Compound **91**

4.5.22.1 1-((2*R*,3*R*)-5,7-Bis(benzyloxy)-2-(3,4,5-tris(benzyloxy)phenyl)chroman-3-yl)-4-(3,4,5-tris(benzyloxy)phenyl)-1*H*-1,2,3-triazole (**91**)

The compound was prepared according to literature following a procedure by Kolarovic *et al.*^[278] A 25-mL, two necked, round-bottomed flask equipped with a magnetic stirring bar was sequentially charged with copper sulfate pentahydrate (1.7 mg, $6.65 \cdot 10^{-3}$ mmol, 5 mol%), sodium ascorbate (2.64 mg, 0.0133 mmol, 10 mol%) and **89** (72.7 mg, 0.173 mmol, 1.00 eq) in DMSO (1.00 mL). To this yellow mixture a solution of **85** (104 mg, 0.133 mmol, 1.00 eq) in 100 mL was added. The mixture was stirred at 65 °C for 2 h until TLC (SiO_2 , *n*-hexane/EtOAc, 3:1, $R_f = 0.24$) showed complete consumption of starting material. The reaction was hydrolyzed and washed with water (6 x 5mL). The aqueous layer was extracted with EtOAc (6 x 5mL) and the combined organic layers were washed with brine (10 mL), dried (Na_2SO_4), the drying agent was filtered off, and concentrated under reduced pressure. The crude residue was purified by column chromatography (Alox, activity level III, *n*-hexane/EtOAc, 3:1) and recrystallization from *n*-hexane/ CH_2Cl_2 (5:1, v/v) provided product **91** (146.4 mg, 1.21 mmol, 91%) as white solid.



$^1\text{H NMR}$ (300 MHz, CDCl_3): δ [ppm] = 7.46 – 7.21 (m, 41H, 17-H, 16-H, 15-H, 12-H, 11-

H, 10-H, 2-H, 1-H), 7.07 (s, 2H, 14-H, 13-H), 6.42 (d, $J = 2.3$ Hz, 1H, 4-H), 6.39 (d, $J = 2.2$ Hz, 1H, 3-H), 6.26 (s, 2H, 9-H, 8-H), 5.38 (dt, $J = 7.0, 2.4$ Hz, 1H, 6-H), 5.23 (d, $J = 2.1$ Hz, 5-H), 5.12 – 4.95 (m, 14H, 17-H, 16-H, 15-H, 11-H, 10-H, 2-H, 1-H), 4.82 (ABq, $J = 11.6$ Hz, 4H, 17-H, 15-H), 3.43 (dd, $J = 17.8, 6.9$ Hz, 1H, 7-H), 3.14 (dd, $J = 17.7, 2.7$ Hz, 1H, 7-H).

^{13}C NMR (75 MHz, CDCl_3): δ [ppm] = 171.25, 159.50, 157.98, 155.48, 153.42, 153.02, 147.62, 138.83, 137.82, 137.07, 136.93, 136.67, 136.59, 131.63, 128.81, 128.76, 128.71, 128.59, 128.54, 128.52, 128.27, 128.24, 127.97, 127.95, 127.71, 127.53, 127.45, 126.26, 119.25, 105.86, 100.89, 95.16, 75.42, 71.42, 70.42, 60.51, 57.66, 14.33.

IR (Film): ν [cm^{-1}] = 3064 (s), 3031 (s), 2927 (m), 2869 (m), 2333 (s), 1952 (s), 1875 (s), 1810 (s), 1732 (s), 1620 (s), 1590 (s), 1498 (s), 1454 (s), 1373 (s), 1237 (b), 1114 (b), 1028 (b), 910 (s), 821 (m), 735 (b), 696 (s), 620 (s).

HRMS (ESI+) m/z : $[\text{M}+\text{H}^+]$ Calc $\text{C}_{79}\text{H}_{68}\text{N}_3\text{O}_9$ 1202.4950; found 1202.4940.

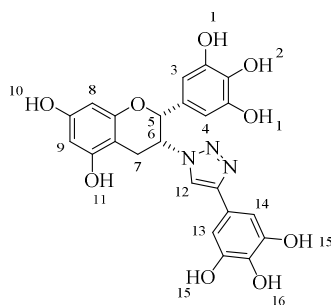
Specific rotation: $[\alpha]_D^{25} = -21.5$ ($c = 1.64$ mol/L, CHCl_3).

Melting point: 150.4 °C.

4.5.23 Catalytic Hydrogenation of Click Derivative **93**

4.5.23.1 1-((2*R*,3*R*)-5,7-Dihydroxy-2-(3,4,5-trihydroxy)phenylchroman-3-yl)-4-(3,4,5-trihydroxy)phenyl)-1*H*-1,2,3-triazole (**93**)

The compounds were prepared according to literature following a procedure by Li *et al.*^[165b] A 25 -mL, two necked, round-bottomed flask equipped with a magnetic stirring bar and three way cock, equipped with a balloon filled with hydrogen, was sequentially charged with protected triazole **91** (52.4 mg, 0.0436 mmol, 1.00 eq) in a mixture of THF/methanol (1.5 mL, 1:1, v/v). The flask was purged with N_2 afterwards one lightly heaped spatula $\text{Pd}(\text{OH})_2$ (20% on carbon) was added in one batch to the solution. The resulting mixture was stirred at rt under H_2 -atmosphere until TLC (RP 18, acetonitrile/ H_2O , 3:2, $R_f = 0.83$) showed complete consumption of the starting material. The black suspension was filtered through a syringe filter (0.45 μm PTFE / 0.20 μm PTFE) and the filtrate was evaporated, the product **93** (12.1 mg, 0.0251 mmol, 55%) was obtained as white solid.



$^1\text{H NMR}$ (300 MHz, CD_3OD): δ [ppm] = 7.44 (s, 1H, 12-H), 6.64 (s, 2H, 14-H, 13-H), 6.22 – 6.16 (m, 2H, 4-H, 3-H), 6.09 – 6.04 (m, 2H, 9-H, 8-H), 5.39 (dt, $J = 6.7$ Hz, 2.1 Hz, 1H, 6-H), 5.24 (br s, 1H, 5-H), 3.41 (dd, $J = 17.7, 6.9$ Hz, 1H, 7-H), 3.01 (dd, $J = 17.6$ Hz, 2.2 Hz, 1H, 7-H).

$^{13}\text{C NMR}$ (75 MHz, CD_3OD): δ [ppm] = 158.70, 158.07, 157.11, 148.99, 147.29, 146.81, 134.72, 133.97, 129.34, 122.50, 120.03, 105.88, 105.79, 99.42, 97.27, 95.93, 78.28, 70.32, 59.72, 28.62, 26.93, 23.08.

IR (Film): ν [cm^{-1}] = 3396 (b), 3124 (b), 2989 (s), 2960 (s), 2920 (s), 2854 (s), 1604 (m), 1519 (s), 1454 (m), 1435 (s), 1311 (s), 1284 (s), 1261 (s), 1242 (s), 1184 (m), 1138 (m), 1082 (s), 1014 (m), 933 (s), 920 (s), 879 (s), 802 (m), 761 (s), 734 (s), 680 (s), 655 (s), 636 (s).

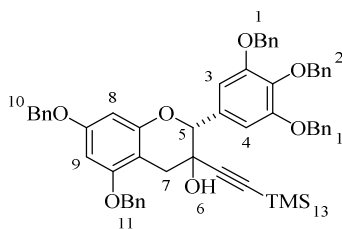
HRMS (ESI+) m/z : $[\text{M}+\text{H}^+]$ Calc $\text{C}_{23}\text{H}_{19}\text{N}_3\text{O}_9$ 482.1194; found 482.1191.

4.5.24 Synthesis of Different EGCG Derivatives

4.5.24.1 (2R)-5,7-Bis(benzyloxy)-3-((trimethylsilyl)ethynyl)-2-(3,4,5-tris(benzyloxy)phenyl)chroman-3-ol (**99**)

The compounds were prepared according to literature following a procedure by Miyazaki *et al.*^[281] A 25-mL, two necked round-bottomed flask equipped with a magnetic stirring bar and three way cock, was charged with LiBr (57.5 mg, 0.662 mmol, 2.00 eq) and was dried under reduced pressure for 30 min dissolved in THF (2 mL). Lithium (trimethylsilyl) acetylide (54.9 μL , 0.464 mmol, 1.40 eq) was added dropwise and cooled to 0 °C. To the mixture *n*-BuLi (269 μL , 1.6 M in hexane, 1.30 eq) was added and stirred for 20 min at 0 °C. This solution was cooled to -78 °C and a solution of ketone **43** (250 mg, 0.331 mmol, 1.00 eq) dissolved in THF (8 mL), was added dropwise. The suspension was stirred for

30 min at $-78\text{ }^{\circ}\text{C}$ and again 2 h at $0\text{ }^{\circ}\text{C}$. The reaction was diluted with EtOAc (10 mL) and washed with sat. NH_4Cl (5 mL). The aqueous layer was extracted with EtOAc (3 x 5 mL) and the combined organic layers were washed with brine (10 mL), dried (Na_2SO_4), the drying agent was filtered off, and concentrated under reduced pressure. The crude residue was purified by column chromatography (Alox, activity level III, *n*-hexane/EtOAc, 3:1) provided product **99** (146.4 mg, 1.21 mmol, 91%) as orange oil.



$^1\text{H NMR}$ (300 MHz, CDCl_3): δ [ppm] = 7.44 – 7.14 (m, 28H, 11-H, 10-H, 2-H, 1-H), 6.87 (dd, $J = 5.3, 1.3$ Hz, 2H, 4-H, 3-H), 6.21 (d, $J = 3.1$ Hz, 2H, 9-H, 8-H), 5.11 – 4.88 (m, 11H, 11-H, 10-H, 5-H, 2-H, 1-H), 3.29 (dd, $J = 16.7, 13.5$ Hz, 1H, 7-H), 2.94 (dd, $J = 42.8, 16.7$ Hz, 1H, 7-H), 2.12 (d, $J = 3.6$ Hz, 1H, 12-H), 0.04 (dd, $J = 9.7, 1.1$ Hz, 9H, 13-H).

$^{13}\text{C NMR}$ (75 MHz, CDCl_3): δ [ppm] = 171.17, 158.98, 158.89, 157.87, 157.70, 155.13, 154.75, 152.46, 152.43, 139.12, 139.03, 137.90, 137.88, 137.05, 136.98, 136.94, 136.92, 136.90, 131.68, 131.24, 128.63, 128.61, 128.57, 128.51, 128.21, 128.14, 128.02, 128.00, 127.97, 127.94, 127.90, 127.86, 127.67, 127.63, 127.56, 127.53, 127.44, 127.12, 108.43, 108.27, 105.74, 105.02, 102.10, 100.59, 94.64, 94.57, 94.27, 94.03, 92.40, 92.10, 82.53, 81.42, 75.33, 75.27, 71.36, 70.15, 70.12, 70.08, 69.89, 67.46, 66.36, 60.44, 35.39, 35.05, 21.07, 14.25, 1.12, 0.01, $-0.06, -0.22$.

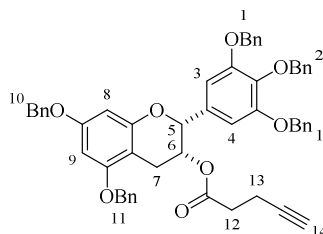
IR (Film): ν [cm^{-1}] = 3553 (b), 3064 (m), 3031 (s), 2956 (m), 2248 (m), 2164 (m), 1951 (s), 1876 (s), 1809 (s), 1732 (s), 1619 (s), 1592 (s), 1499 (8m), 1439 (m), 1375 (m), 1332 (m), 1118 (b), 910 (m), 843 (m), 734 (m), 697 (m).

HRMS (ESI+) m/z : $[\text{M}+\text{H}^+]$ Calc $\text{C}_{55}\text{H}_{53}\text{O}_7\text{Si}^+$ 853.3555; found 853.3555.

Specific rotation: $[\alpha]_D^{25} = -12.1$ ($c = 1.15$ mol/L, CHCl_3).

4.5.24.2 (2*R*,3*R*)-5,7-bis(benzyloxy)-2-(3,4,5-tris(benzyloxy)phenyl)chroman-3-yl-pent-4-ynone (**100**)

The compound was prepared according to literature following a procedure by Khandelwal *et al.*^[215]



¹H NMR (300 MHz, CDCl₃): δ [ppm] = 7.50 – 7.19 (m, 29H, 11-H, 10-H, 2-H, 1-H), 6.76 (s, 2H, 4-H, 3-H), 6.30 – 6.28 (m, 2H, 9-H, 8-H), 5.47 – 5.46 (m, 1H, 6-H), 5.21 – 4.89 (m, 12H, 11-H, 10-H, 5-H, 2-H, 1-H), 3.06 – 2.91 (m, 2H, 7-H), 2.39 – 2.21 (m, 4H, 13-H, 12-H), 1.82 (br s, 1H, 14-H).

¹³C NMR (75 MHz, CDCl₃): δ [ppm] = 171.24, 171.07, 158.91, 158.03, 155.38, 152.92, 138.23, 137.92, 137.17, 136.98, 136.93, 133.34, 128.73, 128.68, 128.61, 128.25, 128.15, 128.06, 128.00, 127.91, 127.67, 127.60, 127.27, 106.28, 100.82, 94.83, 94.10, 82.17, 75.27, 71.43, 70.26, 70.07, 69.31, 68.18, 60.51, 33.34, 26.12, 21.17, 14.39, 14.32.

IR (Film): ν [cm⁻¹] = 3291 (m), 3031 (s), 2926 (b), 1737 (m), 1618 (m), 1592 (m), 1498 (m), 1437 (b), 1374 (b), 1219 (m), 1149 (m), 1116 (m), 1028 (s), 912 (s), 812 (s), 742 (m), 697 (m).

HRMS (ESI+) *m/z*: [M+H⁺] Calc C₅₅H₄₉O₈ 837.3422; found 837.3417.

Specific rotation: [α]_D²⁵ = -18.3 (*c* = 1.75 mol/L, CHCl₃).

100 (49.5 mg, 0.0591 mmol, 90%) was obtained as a lightly yellow oil.

List of Literature

- [1] uncredited, in <http://neurophilosophy.wordpress.com/2006/11/03/100-years-of-alzheimers-disease>, Vol. *Alois_Alzheimer_003.jpg* (300 × 445 Pixel, Dateigröße: 26 KB, MIME-Typ: image/jpeg), **1915**. (downloaded on 01.10.2015)
- [2] J. Bieschke, *Neurotherapeutics* **2013**, *10*, 429-439.
- [3] F. E. Köhler, Vol. *1,424 × 1,725 pixels, file size: 584 KB, MIME type: image/jpeg* (Ed.: C. s.-K. s. Medizinal-Pflanzen-025.jpg), Köhler's Medizinal-Pflanzen - List of Koehler Images, **1897**, pp. Teestrauch. A blühender Zweig, natürl. Grösse; 1 Blüte im Längsschnitt, vergrößert; 2 Staubgefäss, desgl.; 3 Fruchtknoten im Querschnitt, desgl.; 4 Stempel mit Kelch, desgl.; 5 u. 6 reife Frucht von verschiedenen Seiten, mit Samen, natürl. Grösse; 7 Same mit Bindrücken der verkümmerten Samenknospen, desgl.; 8 derselbe zerschnitten, desgl.; 9 Embryo, desgl. (downloaded on 01.04.2016)
- [4] K. Maurer, S. Volk, H. Gerbaldo, *The Lancet* **1997**, *349*, 1546-1549.
- [5] BruceBlaus, Vol. *1,350 × 2,250 pixels, file size: 8.69 MB, MIME type: image/png* (Ed.: F. B. AlzheimersDisease.png), **2013**. (downloaded on 01.09.2014)
- [6] (a) E. Kraepelin, **1910**; (b) E. Kraepelin, *Psychiatry*, Vol. 2, Ambr. Abel., Leipzig, **1908**.
- [7] R. J. Castellani, R. K. Rolston, M. A. Smith, *Dis. Mon.* **2010**, *56*, 484-546.
- [8] C. Haass, D. J. Selkoe, *Nature* **1998**, *391*, 339-340.
- [9] (a) M. Prince, A. Wimo, M. Guerchet, G.-C. Ali, Y.-T. Wu, M. Prina, *Alzheimer's Disease International* **2015**, 1-87; (b) A. Wimo, M. Guerchet, G.-C. Alid, Y.-T. Wue, M. Prina, B. Winblad, L. Jönsson, Z. Liu, M. Prince, *Alzheimer's Dement.* **2017**, *13*, 1-7.
- [10] M. J. Prince, M. M. Guerchet, M. Prina, *WHO* **2015**, pp. 1-4.
- [11] L. E. Hebert, J. Weuve, P. A. Scherr, D. A. Evans, *Neurology* **2013**, *80*, 1778-1783.
- [12] (a) S. Seshadri, P. A. Wolf, A. Beiser, R. Au, K. McNulty, R. White, R. B. D'Agostino, *Neurology* **1997**, *49*, 498-1504; (b) L. E. Hebert, P. A. Scherr, J. J. McCann, L. A. Beckett, D. A. Evans, *Am. J. Epidemiol.* **2001**, *153*, 132-136.
- [13] S. Seshadri, A. Beiser, M. Kelly-Hayes, C. S. Kase, R. Au, W. B. Kannel, P. A. Wolf, *Stroke* **2006**, *37*, 345-350.
- [14] (a) B. L. Plassman, K. M. Langa, G. G. Fisher, S. G. Heeringa, D. R. Weir, M. B. Ofstedal, J. R. Burke, M. D. Hurd, G. G. Potter, W. L. Rodgers, D. C. Steffens, R. J. Willis, R. B. Wallace, *Neuroepidemiology* **2007**, *29*, 125-132; (b) W. A. Kukull, R. Higdon, J. D. Bowen, W. C. McCormick, L. Teri, G. D. Schellenberg, G. van Belle, L. Jolley, E. B. Larson, *Arch. Neurol.* **2002**, *59*, 1737-1746.
- [15] S. L. Murphy, J. Q. Xu, K. D. Kochanek, *Natl. Vital Stat. Rep.* **2013**, *61*, 1-8.
- [16] (a) S. L. Murphy, J. Xu, K. D. Kochanek, S. C. Curtin, E. Arias, *Natl. Cent. Heal. Stat.* **2017**, *66*, 76; (b) J. Gaugler, B. James, T. Johnson, A. Marin, J. Weuve, (Ed.: A. s. Association), **2018**, pp. 1-88.
- [17] (a) M. Ganguli, H. H. Dodge, C. Shen, R. S. Pandav, S. T. DeKosky, *Arch. Neurol.* **2005**, *62*, 779-784; (b) H. Agüero-Torres, L. Fratiglioni, Z. Guo, M. Viitanen, B. Winblad, *J Clin. Epidemiol.* **1999**, *52*, 737-743.
- [18] M. Prince, M. Prina, M. Guerchet, *ADI* **2013**, 2-92.
- [19] B. J. J. Gaugler, T. Johnson, K. Scholz, J. Weuve, *Alzheimer's Dement.* **2014**, *10*, 1-80.

- [20] C.-P. Ferri, M. Prince, C. Brayne, H. Brodaty, L. Fratiglioni, M. Ganguli, K. Hall, K. Hasegawa, H. Hendrine, Y. Huang, A. Jorm, C. Mathers, P.-A. Menezes, E. Rimmer, M. Scazufca, *Lancet* **2005**, *366*, 2112-2117.
- [21] (a) H. Bickel, 2 ed. (Ed.: D. A. G. e. V. S. Demenz), Georg Thieme Verlag, Stuttgart, **2012**, pp. 18-35; (b) A. Kurz, in *Deutsche Alzheimer Gesellschaft, Vol. 23*, Deutsche Alzheimer Gesellschaft e.V. Selbsthilfe Demenz, **2013**, pp. 1-50.
- [22] D. J. Selkoe, *Molecular pathology of Alzheimer's disease: the role of amyloid, Vol. 19*, Boston: Butterworth-Heinemann, **1998**, 257-283 .
- [23] R. H. Edwards, *Molecular analysis of Parkinson's disease*, J. B. Martin, (Ed) ed., New York: Scientific American, **1998**, 1-321.
- [24] M. E. Cudkowicz, R. H. Brown, *Princ. Mol. Med.*, Scientific American, New York, **1998**, 907-911.
- [25] N. W. Kowall, R. J. Ferrante, J. B. Martin, *Trends Neurosci.* **1987**, *10*, 24-29.
- [26] D. J. Selkoe, *Molecular pathology of Alzheimer's disease: the role of amyloid, Vol. 19*, Boston: Butterworth-Heinemann, **1998**, 257-283.
- [27] C. M. Clark, D. Ewbank, V. M. Y. Lee, J. Q. Trojanowski, *Molecular pathology of Alzheimer's disease: neuronal cytoskeletal abnormalities, Vol. 19*, Boston: Buterworth-Heinemann, **1998**, 285-304.
- [28] J. F. Gusella, N. S. Wexler, P. M. Conneally, S. L. Naylor, M. A. Anderson, R. E. Tanzi, P. C. Watkins, K. Ottina, M. R. Wallace, A. Y. Sakaguchi, *Nature* **1983**, *306*, 234-238.
- [29] J. F. Gusella, J. B. Martin, *Princ. neurogenet.*, Scientific American, New York, **1998**, 1-18.
- [30] R. E. Bruke, *Neuroscientist* **1998**, *4*, 301-311.
- [31] H. Braak, E. Braak, D. Yilmazer, R. A. I. de Vos, E. N. H. Jansen, J. Bohl, *J. Neural. Transm.* **1996**, *103*, 455-490.
- [32] (a) A. Baskys, *UCI Medical Center* **2006**, *2*, 327-335; (b) G. L. Wenk, *J. Clin. Psychiatry* **2003**, *64*, 7-10.
- [33] G. G. Ortiz, F. P. Pacheco-Moisés, E. D. González- Renovato, L. Figuera, M. A. Macías-Islas, M. Mireles-Ramírez, L. J. Flores-Alvarado, A. Sánchez-López, D. G. Nuño-Penilla, I. E. Velázquez-Brizuela, J. P. Sánchez-Luna, A. Célis de la Rosa, in *Genetic, Biochemical and Histopathological Aspects of Familial Alzheimer's Disease* (Ed.: I. Zerr), InTech, Chapters published July 01, 2015 under CC BY 3.0 license, **2015**, p. 370.
- [34] (a) L. F. Lue, Y. M. Kuo, A. E. Roher, L. Brachova, Y. Shen, L. Sue, T. Beach, J. H. Kurth, R. E. Rydel, J. Rogers, *Am. J. Pathol.* **1999**, *155*, 853-862; (b) D. M. Walsh, D.-J. Selkoe, *J. Neurochem.* **2007**, *101*, 1172-1184.
- [35] D. Avramopoulos, *Genome Med.* **2009**, *1*, 34.
- [36] K. F. Masuhr, F. Masuhr, M. Neumann, *Neurologie (=Duale Reihe), Vol. 7*, Stuttgart 2007, **2007**.
- [37] H. Bickel, Deutsche Alzheimer Gesellschaft Selbsthilfe Demenz, Psychiatrische Klinik und Poliklinik der Technischen Universität München, **2014**, p. 2.
- [38] G.-L. Wenk, *J. Clin. Psychiatry* **2003**, *64*, 7-10.
- [39] R. J. Castellani, H.-G. Lee, X. Zhu, G. Perry, M. A. Smith, *J. Neuropathol. Exp. Neurol* **2008**, *67*, 523-531.
- [40] (a) C. Pimental, L. Bastista-Nascimento, C. Rodrigues-Pousada, R. A. Menezes, *Oxid. Med. Cell. Longev.* **2012**, 1-10; (b) P.-S. Hauser, R.-O. Ryan, *Curr. Alzheimer Res.* **2013**, *10*, 809-817.
- [41] J. Corey-Bloom, R. Yaari, *Semin. Neurol.* **2007**, *27*, 32-41.

- [42] (a) C. Haass, D.-J. Selkoe, *Cell* **1993**, 75, 1039-1042; (b) S. S. Sisodia, P. H. St. George-Hyslop, *Nat. Rev. Neurosci.* **2002**, 3, 281-290; (c) F. M. LaFerla, K. N. Green, S. Oddo, *Nat. Rev. Neurosci.* **2007**, 8, 499-509.
- [43] (a) C. L. Masters, K. Beyreuther, *Brain Res.* **2006**, 129, 2823-2839; (b) C. Haass, D. J. Selkoe, *Nat. Rev. Mol. Cell Biol.* **2007**, 8, 101-112.
- [44] C. Bouras, P.-R. Hof, P. Giannakopoulos, J.-P. Michel, J.-H. Morrison, *Cereb. Cortex* **1994**, 4, 138-150.
- [45] M.-J. Rowan, I. Klyubin, Q. Wang, N.-W. Hu, R. Anwyl, *Biochem. Soc. Trans.* **2007**, 35, 1219-1223.
- [46] V. P. Prasher, M. J. Farrer, A. M. Kessling, E. M. Fisher, R. J. West, P. C. Barber, A. C. Butler, *Ann. Neurol.* **1998**, 43, 380-383.
- [47] D.-J. Selkoe, *Science* **1997**, 275, 630-631.
- [48] C. Zhang, B. Wu, V. Beglopoulos, M. Wines-Samuels, D. Zhang, I. Dragatsis, T. C. Südhof, J. Shen, *Nature* **2009**, 460, 632-636.
- [49] D. M. Holtzman, A. M. Fagan, B. Mackey, T. Tenkova, L. Sartinus, S. M. Paul, K. Bales, K. H. Ashe, M. C. Irizarry, B. T. Hyman, *Ann. Neurol.* **2000**, 47, 739-747.
- [50] J. L. Cummings, J. J. Wood, *N. Engl. J. Med.* **2004**, 351, 56-67.
- [51] M. Goedert, J.-Q. Trojanowski, V. M.-Y. Lee, *Trends Neurosci.* **1993**, 16, 460-465.
- [52] L. A. Demetrius, P. J. Magistretti, L. Pellerin, *Front. Physiol.* **2015**, 5, 1-18.
- [53] H. W. Querfurth, F. M. LaFerla, *N. Engl. J. Med.* **2010** 362, 329-344.
- [54] J. Hardy, A. Myers, V.-F. Wavrant-De, *Neurodegenerative Dis.* **2004**, 1, 213-217.
- [55] C.-L. Masters, K. Beyreuther, *Brain* **2006**, 129, 2823-2839.
- [56] Y. Chen, B.-L. Tang, *Biochem. Biophys. Res. Commun.* **2006**, 341, 1-5.
- [57] K.-J. Barnham, W.-J. McKinstry, G. Multhaup, D. Galatis, C.-J. Morton, C.-C. Curtain, N.-A. Williamson, A.-R. White, M.-G. Hinds, R.-S. Norton, K. Beyreuther, C.-L. Masters, M.-W. Parker, R. Cappai, *J. Biol. Chem.* **2003**, 278, 17401-17407.
- [58] S. Lammich, E. Kojro, R. Postina, S. Gilbert, R. Pfeiffer, M. Jasionowski, C. Haass, F. Fahrenholz, *Proc. Natl. Acad. Sci. USA* **1999**, 96, 3922-3927.
- [59] N. M. Hooper, A. J. Turner, *Curr. Med. Chem.* **2002**, 9, 1107-1119.
- [60] A. Thathiah, B. De Strooper, *Sci. Signal.* **2009**, 2, 13.
- [61] S. Sinha, I. Lieberburg, *Proc. Natl. Acad. Sci. USA* **1999**, 96, 11049-11053.
- [62] V. M. Chow, M. P. Mattson, P. C. Wong, M. Gleichmann, *Neuromol. Med.* **2010**, 12, 1-12.
- [63] B. De Strooper, W. Annaert, *J. Cell. Sci.* **2000**, 113, 1857-1870.
- [64] J. D. Greene, A. D. Baddeley, J. R. Hodges, *Neuropsychologia* **1996**, 34, 537-551.
- [65] B. H. Price, H. Gurvit, S. Weintraub, C. Geula, E. Leimkuhler, M. Mesulam, *Arch. Neurol.* **1993**, 50, 931-937.
- [66] C. Esteban-Santillan, R. Praditsuwan, H. Ueda, D. S. Geldmacher, *J. Am. Geriatr. Soc.* **1998**, 46, 1266-1269.
- [67] (a) D. Galasko, D. A. Bennett, K. Sano, *Alzheimer Dis. Assoc. Disord.* **1997**, 11, 33-39; (b) M. S. Mega, J. L. Cummings, T. Fiorello, J. Gornbein, *Neurology* **1996**, 46, 130-135.
- [68] H. V. Panglossi, (Ed.: H. V. Pangloss), Nova Science Publishers, **2007**, p. 266.
- [69] F. M. Longo, S. M. Massa, *NeuroRX* **2004**, 1, 117-127.
- [70] C. Lange-Asschenfeldt, *Fortbildungstelegramm Pharmazie* **2009**, 3, 1-17.
- [71] T. E. Golde, *J. Neurochem.* **2006**, 99, 687-707.
- [72] D. Olivares, V. K. Deshpande, Y. Shi, D. K. Lahiri, N. H. Greig, J. T. Rogers, X. Huang, *Curr. Alzheimer. Res.* **2012**, 9, 746-758.

- [73] D. E. Ehrnhoefer, J. Bieschke, A. Boeddrich, M. Herbst, L. Masino, R. Lurz, S. Engemann, A. Pastore, E. E. Wanker, *Nat. Struct. Mol. Biol.* **2008**, *15*, 558-566.
- [74] Z. Y. Wu, P. H. Raven, H. Deyuan, *Flora of China, Vol. 12*, Missouri Botanical Garden Press, St. Louis **2007**, 267-316.
- [75] Y. Hilal, *Untersuchungen über Polyphenole in weißen und grünen Tees*, Dissertation, Cuvillier-Verlag, **2010**, 1-111.
- [76] (a) H. N. Graham, *Prev. Med.* **1992**, *21*, 334-350; (b) H. C. Y. Zuo, Y. Deng *Talanta* **2002**, *57*, 307-316.
- [77] T. Tanaka, I. Kouno, *Food Sci. Techno. Res.* **2003**, *9*, 128-133.
- [78] K. Vasisht, P. D. Sharma, M. Karan, D. D. Rokesh, S. Vyas, S. Sethi, R. Manktala, *Study to Promote the Industrial Exploitation of Green Tea Polyphenols in India*, ICS-UNIDO, AREA Science Park, Padriciano 99, 34012 Trieste, Italy, **2003**, 1-96.
- [79] E. Haslam, Quinone tannin and oxidative polymerization. *In Practical Polyphenolics from Structure to Molecular Recognition and Physiological Action*, Cambridge University Press, UK, **1998**, 138-177.
- [80] R. Schneider, T. Lüdde, S. Töpfer, P. Imming, *Pharmaz. Ztg.* **2008**, *153*, 1429-1436.
- [81] J. Dong, X. Xu, Y. Liang, R. Head, L. Bennett, *Food Funct.* **2011**, *2*, 310-319.
- [82] P. Mulder, H.-G. Korth, D. A. Pratt, G. A. DiLabio, L. Valgimigli, G. F. Pedulli, K. U. Ingold, *J. Phys. Chem. A.* **2005**, *109*, 2647-2655.
- [83] S. Quideau, D. Deffieux, C. Douat-Casassus, P. L., *Angew. Chem. Int. Ed.* **2011**, *50*, 586-621.
- [84] M. Mochizuki, S. Yamazaki, K. Kano, T. Ikeda, *Biochim. Biophys. Acta.* **2002**, *1569*, 35-44.
- [85] N. Yamashita, H. Tanemura, S. Kawanishi, *Mutat. Res.* **1999**, *425*, 107-115.
- [86] Z. Hou, J. D. Lambert, K. V. Chin, C. S. Yang, *Mutat. Res.* **2004**, *555*, 3-19.
- [87] Q. Liang, P. C. Dedon, *Chem. Res. Toxicol.* **2001**, *14*, 416-422.
- [88] K. Freudenberg, K. Weinges, *Fortschr. Chem. Org. Naturstoffe* **1958**, *16*, 1-2.
- [89] J.-J. Macheix, A. Fleuriet, J. Billot, *Fruit Phenolic.* **1990**, *3*, 1-103.
- [90] Y. Cai, S. H. Gaffney, T. H. Lilley, D. Magnolato, R. Martin, C. M. Spencer, E. Haslam, *J. Chem. Soc., Perkin Trans. 2* **1990**, *4*, 2197-2209.
- [91] A. E. Hagerman, M. E. Rice, N. T. Richard, *J. Agric. Food. Chem.* **1998**, *46*, 2590-2595.
- [92] S. Quideau, D. Deffieux, C. Douat-Casassus, L. Pouysegu, *Angew. Chem. Int. Ed.* **2011**, *50*, 586-621.
- [93] L. Mira, M. T. Fernandez, M. Santos, R. Rocha, M. H. Iorêncio, K. R. Jennings, *Free Radical Research* **2009**, *36*, 1199-1208.
- [94] C. A. Rice-Evans, L. Packer, M. Dekker, *Vol. 2*, The Taylor & Francis e-Library, 2005, **1998**, pp. 137-161.
- [95] M. Yoshino, K. Murakami, *Anal. Biochem.* **1998**, *257*, 40-44.
- [96] M. Kumamoto, T. Sonda, K. Nagayama, M. Tabata, *Biosci. Biotechnol. Biochem.* **2001**, *65*, 126-132.
- [97] J. B. Harborne, C. A. Williams, *Photochemistry* **2000**, *55*, 481-504.
- [98] V. Lattanzio, A. Cardinali, C. Ruta, I. M. Fortunato, V. M. T. Lattanzio, V. Linsalata, N. Cicco, *Environ. Exp. Bot.* **2009**, *65*, 54-62.
- [99] I. Morel, G. Lescoat, P. Cogrel, O. Sergent, N. Padeloup, P. Brissot, P. Cillard, J. Cillard, *Biochem. Pharmacol.* **1993**, *45*, 13-19.
- [100] D. Metodieva, A. K. Jaiswal, N. Cenas, E. Dickcacaite, J. Segura-Aguilar, *J. Free Rad. Biol. Med.* **1999**, *26*, 107-126.

- [101] W. Tückmantel, A. P. Kozikowski, L. J. Romanczyk, *J. Am. Chem. Soc.* **1999**, *121*, 12073-12081.
- [102] N. Kakiuchi, M. Hattori, T. Namba, M. Nishizawa, T. Yamagishi, T. Okuda, *J. Nat. Prod.* **1985**, *48*, 614-621.
- [103] (a) A. A. Shahat, S. I. Ismail, F. M. Hammouda, S. A. Azzam, G. Lemièrè, T. De Bruyne, S. De Swaef, L. Pieters, A. Vlietinck, *Phytomedicine* **1998**, *5*, 133; (b) M. Aciram, B. Fuhrman, *Atherosclerosis* **1998**, *137*, 45-50.
- [104] M. Saito, H. Hosoyama, T. Ariga, S. Kataoka, N. Yamaji, *J. Agric. Food Chem.* **1998**, *46*, 1460-1464.
- [105] S. Liao, Y. Umekita, J. Guo, J. M. Kokontis, R. A. Hiipakka, *Cancer Lett.* **1994**, *96*, 239-243.
- [106] J. Jankun, S. H. Selman, R. Swiercz, E. Skrypczak-Jankun, *Nature* **1997**, *387*, 561.
- [107] H. Hibasami, Y. Achiwa, T. Fujikawa, T. Komiya, *Anticancer Res.* **1999**, *16*, 1943-1946.
- [108] M. J. Lee, J. D. Lambert, S. Prabhu, X. Meng, H. Lu, P. Maliakal, C. T. Ho, C. S. C. S. Yang, *Biomarkers. Prev.* **2004**, *13*, 132-137.
- [109] J. Terao, *J. Med. Inv.* **1999**, *46*, 159-168.
- [110] (a) J. V. Higdon, B. Frei, *Crit. Rev. Food Sci. Nutr.* **2003**, *43*, 89-143; (b) C. Manach, A. Scalbert, C. Morand, C. Rémésy, L. Jiménez, *J. Clin. Nutr.* **2004**, *79*, 727-747.
- [111] F. Yang, H. S. Oz, S. Barve, W. J. DeVilliers, C. J. McClain, G. W. Varilek, *Mol. Pharmacol.* **2001**, *60*, 528-533.
- [112] B. A. Warden, L. S. Smith, G. R. Beecher, D. A. Balentine, B. A. Clevidence, *J. Nutr.* **2001**, *131*, 1731-1737.
- [113] A. B. Hodgson, R. K. Randell, A. E. Jeukendrup, *Adv. Nutr.* **2013**, *4*, 129-140.
- [114] I. F. Benzil, Y. T. Szeto, *J. Agric. Food Chem.* **1999**, *47*, 633-636.
- [115] H. N. Graham, *Prev. Med.* **1992**, *21*, 334-350.
- [116] C. A. Rice-Evans, N. J. Miller, G. Paganga, *Free Radic. Biol. Med.* **1996**, *20*, 933-956.
- [117] F. Nanjo, K. Goto, R. Seto, M. Suzuki, M. Sakai, Y. Hara, *Free Radic. Biol. Med.* **1996**, *21*, 895-902.
- [118] I. E. Dreosti, *Nutr. Rev.* **1996**, *54*, 51-58.
- [119] N. J. Miller, C. Castelluccio, L. Tijburg, C. Rice-Evans, *FEBS Lett.* **1996**, *392*, 40-44.
- [120] B. Frei, J. V. Higdon, *J. Nutr.* **2003**, *133*, 3275-3284.
- [121] (a) A. Kazi, Z. Wang, N. Kumar, S. C. Falsetti, T. H. Chan, Q. P. Dou, *Anticancer Res.* **2004**, *24*, 943-954; (b) E. Middleton, C. Kandaswami, T. Theoharides, *Pharmacol. Rev.* **2000**, *52*, 673-751; (c) F. Nanjo, K. Goto, R. Seto, M. Suzuki, M. Sakai, Y. Hara, *Free Radic. Biol. Med.* **1996**, *21*, 895-902.
- [122] J. C. Mak, *Clin. Exp. Pharmacol. Physiol.* **2012**, *39*, 265-273.
- [123] D.-G. Nagle, D. Ferreira, Y.-D. Zhou, *Phytochem.* **2006**, *67*, 1849-1855.
- [124] S. M. Chacko, P. T. Thambi, R. Kuttan, I. Nishigaki, *Chin. Med.* **2010**, *5*, 13-21.
- [125] J. Hong, T. J. Smith, C.-T. Ho, D. A. August, C.-S. Yang, *Biochem. Pharmacol.* **2010**, *62*, 1175-1183.
- [126] (a) Y. Steffen, I. Wiswedel, D. Peter, T. Schewe, H. Sies, *Free Radic. Biol. Med.* **2006**, *41*, 1139-1150; (b) Y. J. Choi, Y. J. Jeong, Y. J. Lee, H. M. Kwon, J. H. Kang, *J. Nutr.* **2005**, *93*, 581-589.
- [127] B. M. Choi, S. M. Kim, T. K. Park, G. Li, S. J. Hong, R. Park, H. T. Chung, B. R. Kim, *J. Nutr. Biochem.* **2007**, *18*, 615-622.

- [128] K. Kawai, N. H. Tsuno, J. Kitayama, Y. Okaji, K. Yazawa, M. Asakage, N. Hori, T. Watanabe, K. Takahashi, H. Nagawa, *J. Allergy Clin. Immunol.* **2003**, *112*, 951-957.
- [129] F. Nanjo, K. Goto, R. Seto, M. Suzuki, M. Sakai, Y. Hara, *Free Radic. Biol. Med.* **1996**, *21*, 895-902.
- [130] (a) S. M. Shenouda, J. A. Vita, *J. Am. Coll. Nutr.* **2007**, *26*, 366-372; (b) V. Stangl, H. Dergler, K. Stangl, M. Lorenz, *Cardiovasc. Res.* **2007**, *73*, 348-358.
- [131] M. S. Westerterp-Plantenga, *Physiol. Behav.* **2010**, *100*, 42-46.
- [132] K. Diepvens, K. R. Westerterp, M. S. Westerterp-Plantenga, *Am. J. Physiol. Regul. Integr. Comp. Physiol.* **2007**, *292*, 77-85.
- [133] (a) N. R. Perron, H. C. Wang, S. N. Deguire, M. Jenkins, M. Lawson, J. L. Brumaghim, *DaltonTrans.* **2010**, *39*, 9982-9987; (b) M. J. Assuncao, M. J. Santos-Marques, F. Carvalho, J. P. Andrade, *Free Radic. Biol. Med.* **2010**, *48*, 831-838.
- [134] Z. X. Zhang, G. C. Román, *Neuroepidemiology* **1993**, *12*, 195-208.
- [135] J. Bieschke, J. Russ, R. P. Friedrich, D. E. Ehrnhoefer, H. Wobst, K. Neugebauer, E. E. Wanker, *Proc. Natl. Acad. Sci. USA* **2010**, *107*, 7710-7715.
- [136] T. Y. Choi, C. H. Jung, S. R. Lee, J. H. Bae, W. K. Baek, M. H. Suh, J. Park, C. W. Park, S. I. Suh, *Life Sci.* **2001**, *70*, 603-614.
- [137] K. Rezai-Zadeh, D. Shytle, N. Sun, T. Mori, H. Hou, D. Jeanniton, J. Ehrhart, K. Townsend, J. Zeng, D. Morgan, J. Hardy, T. Town, J. Tan, *J. Neurosci.* **2005**, *25*, 8807-8814.
- [138] (a) J. W. Fernandez, K. Rezai-Zadeh, D. Obregon, J. Tan, *FEBS Lett.* **2010**, *584*, 4259-4267; (b) J. W. Lee, Y. K. Lee, J. O. Ban, T. Y. Ha, Y. P. Yun, S. B. Han, K. W. Oh, J. H. Hong, *J. Nutr.* **2009**, *139*, 1987-1993.
- [139] S. Y. Jeon, K. Bae, Y. H. Seong, K. S. Song, *Bioorg. Med. Chem. Lett.* **2003**, *13*, 3905-3908.
- [140] A. Mähler, S. Mandel, M. Lorenz, U. Rugg, E. E. Wanker, M. Boschmann, P. Friedemann, *PPPM* **2013**, *4*, 1-17.
- [141] D. G. Nagle, D. Ferreira, Y. D. Zhou, *Photochem.* **2006**, *67*, 1894-1855.
- [142] K. Rezai-Zadeha, G. W. Arendashb, H. Houa, F. Fernandez, M. Jensenb, M. Runfeldtb, R. D. Shytlea, J. Tana, *Brain Res.* **2008**, *1214*, 177-187.
- [143] B. N. Singh, S. Shankar, R. K. Srivastava, *Biochem. Pharmacol.* **2011**, *15*, 1807-1821.
- [144] M. Singh, M. Arseneault, T. Sanderson, V. Murthy, C. Ramasamy, *Food Chem.* **2008**, *56*, 4855-4873.
- [145] C. M. Peters, R. J. Green, E. M. Janle, M. G. Ferruzzi, *Food Res. Int.* **2010**, *43*, 95-102.
- [146] G. Watanabe, K. Ohmori, K. Suzuki, *Chem. Commun.* **2014**, *50*, 14371-14373.
- [147] J. W. Clark-Lewis, L. M. Jackman, T. M. Spotswood, *Aust. J. Chem.* **1964**, *17*, 632-648.
- [148] D. Ferreira, J. P. Steynberg, D. C. Roux, E. V. Brandt, *Tetrahedron Lett.* **1992**, *48*, 1743-1803.
- [149] L. J. Porter, R. Y. Wong, M. Benson, B. G. Chan, V. N. Vishwanadhan, R. D. Gandour, W. L. Mattice, *J. Chem. Res.* **1986**, *830*, 86-87.
- [150] J. Clayden, N. Greeves, S. Warren, *Org. Chem.*, 2 ed., Oxford, **2012**, 1435-1436.
- [151] M. L. F. Ferreyra, S. P. Rius, P. Casati, *Front. Plant Sci.* **2012**, *3*, 1-15.
- [152] J. A. Chemler, L. T. Lock, M. A. G. Koffas, E. S. Tzanakakis, *Appl. Microbiol. Biotechnol.* **2007**, *77*, 797-807.
- [153] M. P. Dewick, *Medicinal Natural Products: a biosynthetic approach*, Second edition ed., University of Nottingham, UK, **2009**, 1-507.

- [154] S. Martens, A. Preuß, U. Matern, *Photochem.* **2010**, *71*, 1040-1049.
- [155] S. Sinha, Z. Du, P. Maiti, F.-G. Klärner, T. Schraber, C. Wang, G. Bitan, *ACS Chem. Neurosci.* **2012**, *3*, 451-458.
- [156] A. Attar, C. Ripoli, E. Riccardi, P. Maiti, T. Liu, M. Jones, F. Yang, C.-H. Tseng, F.-G. Klärner, T. Schrader, S. Frautschy, C. Grassi, G. Bitan, *Alzheimer's Dement.* **2012**, *8*, 259-259.
- [157] S. Sinha, D. H. J. Lopes, Z. Du, E. S. Pang, A. Shanmugam, A. Lomakin, P. Talbiersky, A. Tennstaedt, K. McDaniel, R. Bakshi, P.-Y. Kuo, M. Ehrmann, G. B. Benedek, J. A. Loo, F.-G. Klärner, T. Schrader, C. Wang, G. Bitan, *J. Am. Chem. Soc.* **2011**, *133*, 16958-16969.
- [158] (a) D. A. Zarin, T. Tse, R. J. Williams, R. M. Califf, *N. Engl. J. Med.* **2011**, *364*, 852-860; (b) F. Paul, Charite University, Berlin, Germany, **2017**, p. ClinicalTrials.gov Identifier: NCT00951834
- [159] S. Sinha, D. H. J. Lopes, G. Bitan, *ACS Chem. Neurosci.* **2012**, *3*, 473-481.
- [160] A. Huang, C. M. Stultz, *LoS Comput. Biol.* **2008**, *4*, 1-12.
- [161] J. C. Anderson, C. Headley, P. D. Stapleton, P. W. Taylor, *Tetrahedron* **2005**, *61*, 7703-7711.
- [162] M. Suzuki, M. Sano, R. Yoshida, M. Degawa, T. Miyase, M. Maeda-Yamamoto, *J. Agrc. Food. Chem.* **2003**, *51*, 510-514.
- [163] P. P. Mehta, W. B. Whalley, *J. Chem. Soc.* **1963**, *0*, 5327-5332.
- [164] P. Kiatgrajai, J. D. Wellons, L. Gollob, J. D. White, *J. Org. Chem.* **1982**, *47*, 2910-2912.
- [165] (a) N. T. Zaveri, *Org. Lett.* **2001**, *3*, 843-846; (b) L. Li, T. H. Chan, *Org. Lett.* **2000**, *3*, 739-741.
- [166] H. Tanaka, H. Miyoshi, Y.-C. Chuang, Y. Ando, T. Takahashi, *Angew. Chem. Int. Ed.* **2007**, *46*, 5934-5937.
- [167] T.-J. Ding, X.-L. Wang, X.-P. Cao, *Chin. J. Chem.* **2006**, *24*, 1618-1624.
- [168] J. W. Clark-Lewis, D. C. Skingle, *Aust. J. Chem.* **1967**, *20*, 2169-2190.
- [169] B. Nay, V. Arnaudinaud, J. Vercauteren, *C. R. Chimie* **2002**, *5*, 577-590.
- [170] A. V. Malkov, P. Spoor, V. Vinader, P. Kocovsky, *J. Org. Chem.* **1999**, *64*, 5308-5311.
- [171] B. Nay, M. Collet, M. Lebon, C. Chèze, J. Vercauteren, *Tetrahedron Lett.* **2002**, *43*, 2675-2678.
- [172] M. Kitade, Y. Ohno, H. Tanaka, T. Takahashi, *Synlett* **2006**, *17*, 2827-2829.
- [173] K. Ohmori, T. Yano, K. Suzuki, *Org. Biomol. Chem.* **2010**, *8*, 2693-2696.
- [174] O. Mitsunobu, *Synthesis* **1981**, *1*, 1-28.
- [175] K. B. Sharpless, Y. L. Bennani, G. A. Crispino, J. Hartung, H. J. Jeong, K.-S. Kwong, K. Morikawa, Z.-W. Wang, D. Xu, X.-L. Zhang, *J. Org. Chem.* **1992**, *57*, 2768-2771.
- [176] G. Bartoli, P. E. Todesco, *Acc. Chem. Res.* **1977**, *10*, 125-132.
- [177] T. Durst, M. J. LeBelle, R. Van den Elzen, K.-C. Tin, *Can. J. Chem.* **1974**, *52*, 761-766.
- [178] H. Tanaka, A. Chino, T. Takahashi, *Tetrahedron Lett.* **2012**, *53*, 2493-2495.
- [179] N. M. Green, *Adv. Protein Chem.* **1975**, *29*, 85-133.
- [180] N. M. Green, *Avidin and streptavidin. Methods. Enzymol.* **1990**, *184*, 51-67.
- [181] A. Holmberg, A. Blomstergren, O. Nord, M. Lukacs, J. Lundeberg, M. Uhlén, *Electrophoresis* **2005**, *26*, 501-510.
- [182] H. LeVine, *Anal. Biochem.* **2006**, *356*, 265-272.
- [183] M. Biancalana, S. Koide, *Biochim. Biophys. Acta.* **2010**, *1804*, 1405-1412.
- [184] R. Virchow, *C. R. Acad. Sci.* **1853**, *37*, 860-861.

- [185] P. S. Vassar, C. F. Culling, *Arch. Pathol.* **1959**, *68*, 487-498.
- [186] H. Naiki, K. Higuchi, M. Hosokawa, T. Takeda, *Anal. Biochem.* **1989**, *177*, 244-249.
- [187] M. Groenning, *J. Chem. Biol.* **2009**, *3*, 1-18.
- [188] B.-F. Krippendorff, P. Lienau, A. Reichel, W. Huisinga, *J. Biomol. Screen.* **2007**, *12*, 92-99.
- [189] W. Dzwolak, M. Pecul, *FEBS Lett.* **2005**, *579*, 6601-6603.
- [190] V. I. Stsiapura, A. A. Maskevich, V. A. Kuzmitsky, K. K. Turoverov, I. M. Kuznetsova, *J. Phys. Chem. A* **2007**, *111*, 4829-4835.
- [191] M. Biancalana, K. Makabe, A. Koide, S. Koide, *J. Mol. Biol.* **2008**, *383*, 205-213.
- [192] J. Vogelsang, R. Kasper, C. Steinhäuser, B. Person, M. Heilemann, M. Sauer, P. Tinnefeld, *Angew. Chem. Int. Ed.* **2008**, *47*, 5465-5469.
- [193] A. Yoshida, Y. Hirooka, Y. Sugata, M. Nitta, T. Manabe, S. Ido, K. Murakami, R. K. Saha, T. Suzuki, M. Ohshima, A. Yoshida, K. Itoh, K. Shimizu, N. Oku, T. Furuta, T. Asakawa, T. Wakimotoy, T. Kan, *Chem. Commun.* **2011**, *47*, 1794-1796.
- [194] S. Yamakawa, T. Asai, T. Uchida, M. Matsukawa, T. Akizawa, N. Oku, *Cancer Lett.* **2004**, *210*, 47-55.
- [195] D. W. Han, K. Matsumura, B. Kim, S. H. Hyon, *Bioorg. Med. Chem.* **2008**, *16*, 9652-9659.
- [196] C. J. Gruber, W. Tschugguel, C. Schneeberger, J. C. Huber, *N. Engl. J. Med.* **2002**, *346*, 340-352.
- [197] S. Retana-Márquez, H. Hernández, J.-A. Flores, M. Muñoz-Gutiérrez, G. Duarte, J. Vielma, G. Fitz-Rodríguez, I.-G. Fernández, M. Keller, J.-A. Delgadillo, *Trop. Subtrop. Agroecosyst.* **2012**, *15*, 129-145.
- [198] T. J. Ding, X. L. Wang, X. P. Cao, *Chin. J. Chem.* **2006**, *24*, 1618-1624.
- [199] A. Alam, Y. Fakaguchi, H. Ito, T. Yoshida, S. Tsuboi, *Tetrahedron* **2005**, *61*, 1909-1918.
- [200] H. Kawamoto, F. Nakatsubo, K. Murakami, *Synthetic Commun.* **1996**, *26*, 531-534.
- [201] K. Weinges, D. Seiler, *Liebigs Ann. Chem.* **1968**, *714*, 193-204.
- [202] H. Kawamoto, F. Nakatsubo, K. Murakami, *Mokuzai Gakkaishi* **1992**, *38*, 81-84.
- [203] S. Miura, T. Midorikawa, N. Awata, *Radioisotopes* **1983**, *32*, 225-230.
- [204] W. D. Curtis, J. F. Stoddart, G. H. Jones, *J. Chem. Soc., Perkin Trans. 1*, **1977**, *0*, 785-788.
- [205] Y. Ogino, H. Chen, H.-L. Kwong, K. B. Sharpless, *Tetrahedron Lett.* **1991**, *32*, 3965-3968.
- [206] H. C. Kolb, S. VanNieuwenhze, K. B. Sharpless, *Chem. Rev.* **1994**, *94*, 2483-2547.
- [207] M. Minato, K. Yamamoto, J. Tsuji, *J. Org. Chem.* **1990**, *55*, 766-768.
- [208] E. N. Jacobsen, I. Markd, W. S. Mungall, G. Schrcider, K. B. Sharpless, *J. Am. Chem. Soc.* **1988**, *110*, 1968-1970.
- [209] (a) M. H. Junttila, O. M. O. Hormi, *J. Org. Chem.* **2009**, *74*, 3038-3047; (b) P. O. Norrby, H. C. Kolb, K. B. Sharpless, *J. Am. Chem. Soc.* **1994**, *116*, 8410-8478.
- [210] J. S. Svendsen, I. Marko, E. N. Jacobsen, C. Pulla Rao, S. Bott, K. B. Sharpless, *J. Am. Chem. Soc.* **1989**, *54*, 2263-2264.
- [211] (a) R. Criegee, *Justus Liebigs Ann. Chem* **1936**, *522*, 75-96; (b) J. Böseken, *J. Recl. Trav. Chim* **1922**, *41*, 195-196.
- [212] K. P. M. Vanhessche, K. B. Sharpless, *J. Org. Chem.* **1996**, *61*, 7978-7979.
- [213] M. Zhang, G. E. Jagdmann, M. Van Zandt, P. Beckett, H. Schroeter, *Tetrahedron: Asymmetry* **2013**, *24*, 362-373.
- [214] K. Krohn, I. Ahmed, M. John, *Synthesis* **2009**, *5*, 779-786.
- [215] A. Khandelwal, J. A. Hall, B. S. J. Blagg, *J. Org. Chem.* **2013**, *78*, 7859-7884.

- [216] M. Hesse, H. Meier, B. Zeeh, *Spektroskopische Methoden in der organischen Chemie*, Vol. 7, Thieme, Stuttgart, **2005**, 1-456.
- [217] D. Höfner, S. A. Lesko, G. Binsch, *Org. Magn. Resonance* **1978**, *11*, 179-196.
- [218] R. E. Ireland, L. Liu, *J. Org. Chem.* **1993**, *58*, 2899-2899.
- [219] (a) M. Tsakos, E. S. Schaffert, L. L. Clement, N. L. Villadsen, T. B. Poulsen, *Nat. Prod. Rep.* **2015**, *32*, 605-632; (b) C. A. G. N. Montalbetti, V. Falque, *Tetrahedron* **2005**, *61*, 10827-10852.
- [220] B. Neises, W. Steglich, *Angew. Chem. Int. Ed. Engl.* **1978**, *17*, 522-524.
- [221] K. M. Batzli, B. J. Love, *Adv. Mater. Res.* **2015**, *48*, 359-364.
- [222] E. P. Gillis, K. J. Eastman, M. D. Hill, D. J. Donnelly, N. A. Meanwell, *J. Med. Chem.* **2015**, *58*, 8315-8359.
- [223] F. L. Palhano, J. Lee, N. P. Grimster, J. W. Kelly, *J. Am. Chem. Soc.* **2013**, *135*, 7503-7510.
- [224] B. Nay, V. Arnaudinaud, J. Vercauteren, *Eur. J. Org. Chem.* **2001**, 2379-2384.
- [225] J.-L. Luche, *J. Am. Chem. Soc.* **1978**, *100*, 2226-2227.
- [226] H. Yuan, H. Chen, H. Jin, B. Li, R. Yue, J. Ye, Y. Shen, L. Shan, Q. Sun, W. Zhang, *Tetrahedron Lett.* **2013**, *54*, 2776-2780.
- [227] A. F. Cockerill, G. L. O. Davies, R. C. Harden, D. M. Rackham, *Chem. Rev.* **1973**, *73*, 553-588.
- [228] L. Kürti, B. Czako, *Strategic Applications of Named Reactions in Organic Synthesis*, Elsevier, Burlington, **2005**, 268-269.
- [229] H. Kawamoto, F. Nakatsubo, K. Murakami, *J. Wood Chem. Technol.* **1989**, *9*, 35-52.
- [230] M.-A. Bazin, L. Boderio, C. Tomasoni, B. Rousseau, C. Roussakis, P. Marchand, *Eur. J. Med. Chem.* **2013**, *69*, 823-832.
- [231] C. Huang, Z. Zhang, S. Li, Y. Li, *J. Chem. Research* **1999**, 148.
- [232] N. T. Zaveri, *Org. Lett.* **2001**, *3*, 843-846.
- [233] L. Reus, Heinrich-Heine Universität (Düsseldorf), **2016**.
- [234] M. J. Roberts, M. D. Bentley, J. M. Harris, *Adv. Drug Deliver. Rev.* **2002**, *64*, 116-127.
- [235] A. Merz, R. Manfred, *Synthesis* **1993**, *8*, 797-802.
- [236] B. F. Gisin, *Helv. Chim. Acta* **1973**, *56*, 1477-1482.
- [237] V. Percec, E. Aqad, M. J. Sienkowska, M. A. Ilies, P. A. Heiney, J. Smidrkal, M. Peterca, *J. Am. Chem. Soc.* **2006**, *128*, 3324-3334.
- [238] R. R. Scheline, *Acta Chem. Scand.* **1966**, *20*, 1182-1182.
- [239] D. G. Hall, in *Boronic Acids* (Ed.: D. G. Hall), WILEY-VCH Verlag GmbH & Co. KGaA, Weinheim, **2006**, 1-100.
- [240] J. P. Lorand, J. O. Edwards, *J. Org. Chem.* **1959**, *24*, 769-774.
- [241] V. V. Rostovtsev, L. G. Green, V. V. Fokin, K. B. Sharpless, *Angew. Chem. Int. Ed.* **2002**, *41*, 2596-2599.
- [242] C. W. Tornøe, C. Christensen, M. Meldal, *J. Org. Chem.* **2002**, *67*, 3057-3064.
- [243] V. D. Bock, H. Hiemstra, J. H. van Maarseveen, *Eur. J. Org. Chem.* **2006**, 51-68.
- [244] L. Liang, D. Astruc, *Coord. Chem. Rev.* **2011**, *255*, 2933-2945.
- [245] R. Alvarez, S. Velazquez, A. San-Felix, S. Aquaro, E. De Clercq, C.-F. Perno, A. Karlsson, J. Balzarini, M. J. Carmarasa, *J. Med. Chem.* **1994**, *37*, 4185-4194.
- [246] L. L. Brockunier, E. R. Parmee, H. O. Ok, M. R. Candelore, M. A. Cascieri, L. F. Colwell, L. Deng, W. P. Feeney, M. J. Forrest, G. J. Hom, D. E. MacIntyre, L. Tota, M. J. Wyvratt, M. H. Fisher, A. E. Weber, *Bioorg. Med. Chem. Lett.* **2000**, *10*, 2111-2114.

- [247] M. J. Genin, D. A. Allwine, D. J. Anderson, M. R. Barbachyn, D. E. Emmert, S. A. Garmon, D. R. Graber, K. C. Grega, J. B. Hester, D. K. Hutchinson, J. Morris, R. J. Reischer, C. W. Ford, G. E. Zurenko, J. C. Hamel, R. D. Schaadt, D. Stapert, B. H. Yagi, *J. Med. Chem.* **2000**, *43*, 953-970.
- [248] R. Bhat, A. T. Adam, J. J. Lee, T. J. Gasiewicz, E. C. Henry, D. P. Rotella, *Bioorg. Med. Chem. Lett.* **2014**, *24*, 2263-2266.
- [249] F. Himo, T. Lovell, R. Hilgraf, V. V. Rostovtsev, L. Noodleman, K. B. Sharpless, V. V. Fokin, *J. Am. Chem. Soc.* **2005**, *127*, 210-216.
- [250] V. O. Rodinov, V. V. Fokin, M. G. Finn, *Angew. Chem. Int. Ed.* **2005**, *44*, 2210-2215.
- [251] Y. Urano, M. Kamiya, K. Kanda, T. Ueno, K. Hirose, T. Nagano, *J. Am. Chem. Soc.* **2005**, *127*, 4888-4894.
- [252] V. Hong, I. S. Presolski, C. Ma, M. G. Finn, *Angew. Chem. Int. Ed.* **2009**, *48*, 9879-9883.
- [253] L. Y. Lu, N. Ou, Q.-B. Lu, *Sci. Rep.* **2013**, *3*, 1-11.
- [254] V. Snitsarev, M. N. Young, R. M. S. Miller, D. P. Rotella, *PLOS one* **2013**, *8*, 1-6.
- [255] F. L. Arbeloa, P. R. Ojeda, I. López Arbeloa, *J. Luminesc.* **1989**, *44*, 105-112.
- [256] J. Stichler-Bonaparte, B. Bernet, A. Vasella, *Helv. Chim. Acta* **2002**, *85*, 2235-2257.
- [257] G. V. S. Reddy, G. V. Rao, R. V. K. Subramanyam, D. S. Iyengar, *Synth. Commun.* **2000**, *30*, 2233-2237.
- [258] R. Appel, *Angew. Chem. Int. Ed.* **1975**, *14*, 801-811.
- [259] M. A. Ayedi, Y. Le Bigot, H. Ammar, S. Abid, R. El Gharbi, M. Delmas, *Synth. Commun.* **2013**, *43*, 2127-2133.
- [260] R.-P. Tripathi, S.-S. Verma, J. Pandey, V.-K. Tiwarib, *Curr. Org. Chem.* **2008**, *12*, 1093-1115.
- [261] A. Feher-Voelger, J. Borges-González, R. Carrillo, E. Q. Morales, J. González-Platas, T. Martín, *Chem. Eur. J.* **2014**, *20*, 4007-4022.
- [262] G. Liu, D. A. Cogan, J. A. Ellman, *J. Am. Chem. Soc.* **1997**, *119*, 9913-9914.
- [263] H. M. Peltier, J. A. Ellman, *J. Org. Chem.* **2005**, *70*, 7342-7345.
- [264] R. V. Hoffman, H.-O. Kim, *Tetrahedron* **1992**, *48*, 3007-3020.
- [265] S. Kamble, S. More, C. Rode, *New J. Chem.* **2016**, *40*, 10240-10245.
- [266] E. J. Corey, P. L. Fuchs, *Tetrahedron Lett.* **1972**, *36*, 3769-3772.
- [267] R. Bruckner, *Organic Mechanisms - Reactions, Stereochemistry and Synthesis, Vol. 3*, Spektrum Akademischer Verlag, Springer-Verlag Berlin Heidelberg 2010, **2010**.
- [268] A. P. K. W. Tüeckmantel, L. J. Romanczyk, *J. Am. Chem. Soc.* **1999**, *121*, 12073-12081.
- [269] (a) J. D. Lambert, M. J. Kennett, S. Sang, K. R. Reuhl, J. Ju, C. S. Yang, *Food Chem. Toxicol.* **2010**, *48*, 409-416; (b) G. Mazzanti, F. Menniti-Ippolito, P. A. Moro, F. Cassetti, R. Raschetti, C. Santuccio, S. Mastrangelo, *Eur. J. Clin. Pharmacol.* **2009**, *65*, 331-341.
- [270] K. Iaych, S. Dumarcay, E. Fredon, C. Gérardin, A. Lemor, P. Gérardin, *Appl. Polym. Sci.* **2011**, *120*, 2354-2360.
- [271] E. Haslam, *Biochem. J.* **1974**, *139*, 285-288.
- [272] (a) Y. Lu, A. Bennick, *Arch. Oral. Biol.* **1998**, *256*, 717-728; (b) A. E. Hagerman, L. G. Butler, *J. Biol. Chem.* **1981**, *256*, 4494-4497.
- [273] A. Alam, S. Tsuboi, *Tetrahedron* **2007**, *63*, 10454-10465.
- [274] R. N. Hanson, E. Hua, J. A. Hendricks, D. Labaree, R. B. Hochberg, *Bioorg. Med. Chem.* **2012**, *20*, 3768-3780.
- [275] T. Ueno, Y. Urano, H. Kojima, T. Nagano, *J. Am. Chem. Soc.* **2006**, *128*, 10640-10661.

- [276] F. Fujisaki, M. Oishi, K. Sumoto, *Chem. Pharm. Bull* **2007**, *55*, 124-127.
- [277] G. A. Andrade, A. J. Pistner, G. P. A. Yap, D. A. Lutterman, J. Rosenthal, *ACS Catal.* **2013**, *3*, 1685-1692.
- [278] A. Kolarovic, M. Schnürch, M. D. Mihovilovic, *J Org. Chem* **2011**, *76*, 2613-2618.
- [279] M. C. Marcotullio, V. Campagna, S. Sternativo, F. Costantino, M. Curini, *Synthesis* **2006**, *16*, 2760-2766.
- [280] S. H. Park, *Bull. Korean Chem. Soc.* **2003**, *24*, 253-255.
- [281] T. Miyazaki, S. Yokoshima, S. Simizu, H. Osada, H. Tokuyama, T. Fukuyama, *Org. Lett.* **2007**, *9*, 4737-4740.

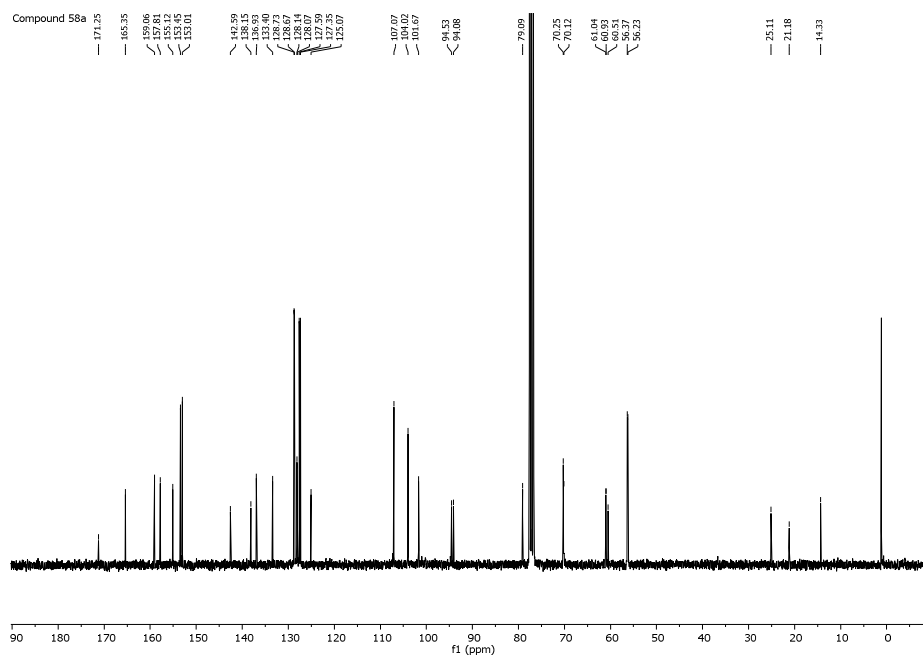
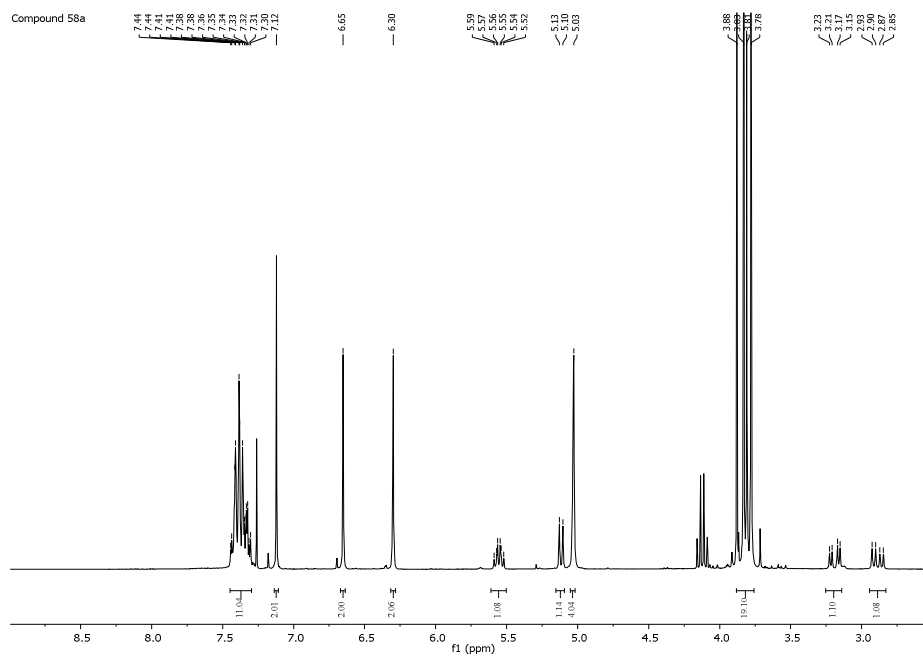
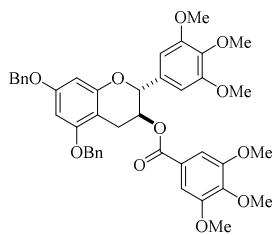
Appendix

The biological results were recorded and evaluated at Max Delbrück Center for Molecular Medicine by C. Secker and Prof. E. Wanker in Berlin.¹⁸ *n*-Propyl ester **52** was made available by L. Reus.^[233] Compound **76** was prepared *via ortho*-ester by R. Steinfort.¹⁹

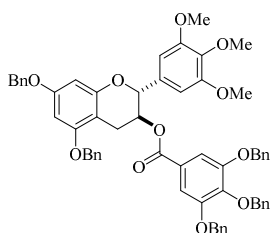
List of all contributors:

1. R. Steinfort (B. Sc.)¹⁹
2. C. Secker and Prof. E. Wanker.¹⁸
3. L. Reus (M. Sc)^[233]

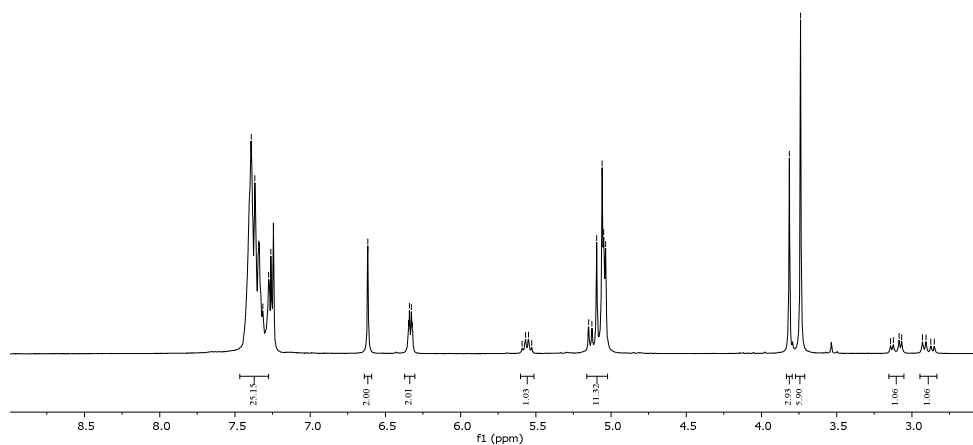
(2*R*,3*S*)-5,7-Bis(benzyloxy)-2-(3,4,5-trimethoxyphenyl)chroman-3-yl-(3,4,5-trimethoxy)benzoate
(**58a**)



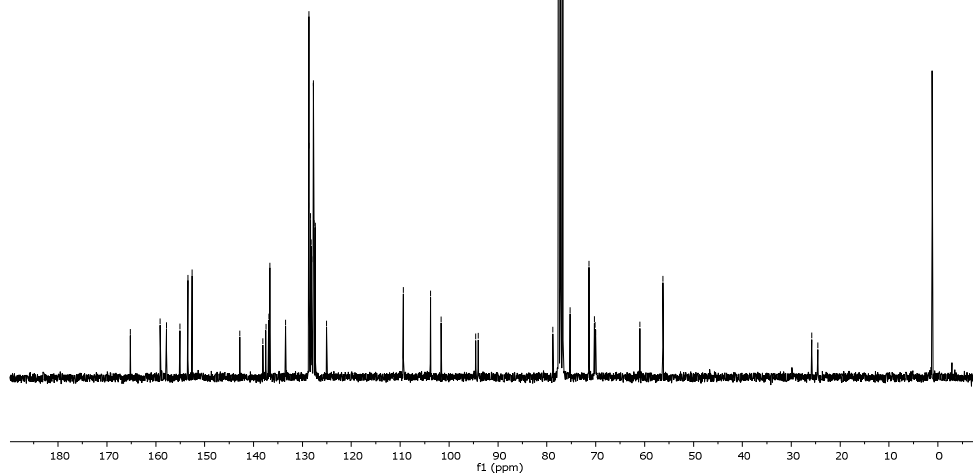
(2R,3S)-5,7-Bis(benzyloxy)-2-(3,4,5-trimethoxyphenyl)chroman-3-yl-(3,4,5-trisbenzyl)benzoate
(**58b**)



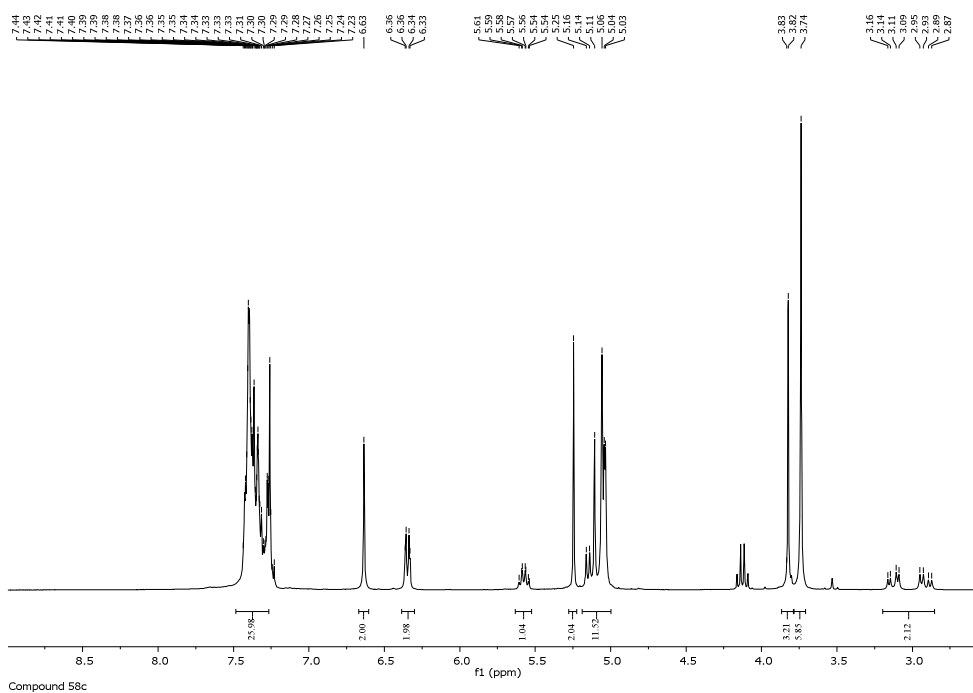
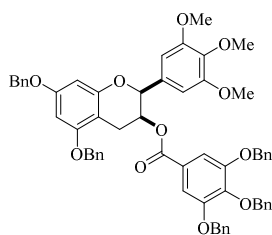
Compound 58b



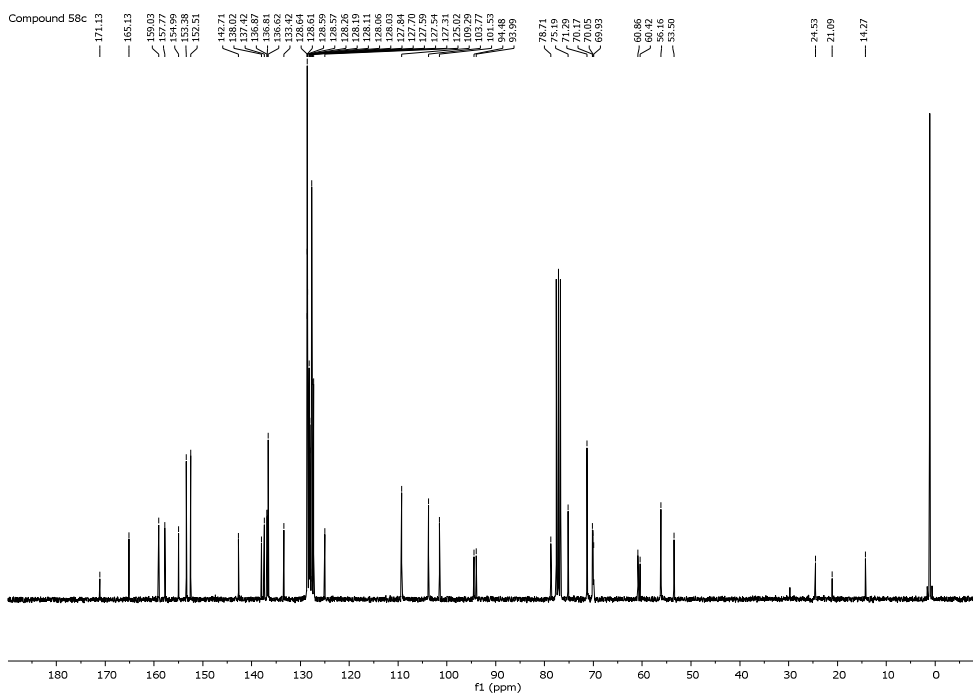
Compound 58b



(2*S*,3*S*)-5,7-Bis(benzyloxy)-2-(3,4,5-trimethoxyphenyl)chroman-3-yl-(3,4,5-trisbenzyloxy)benzoate (**58c**)

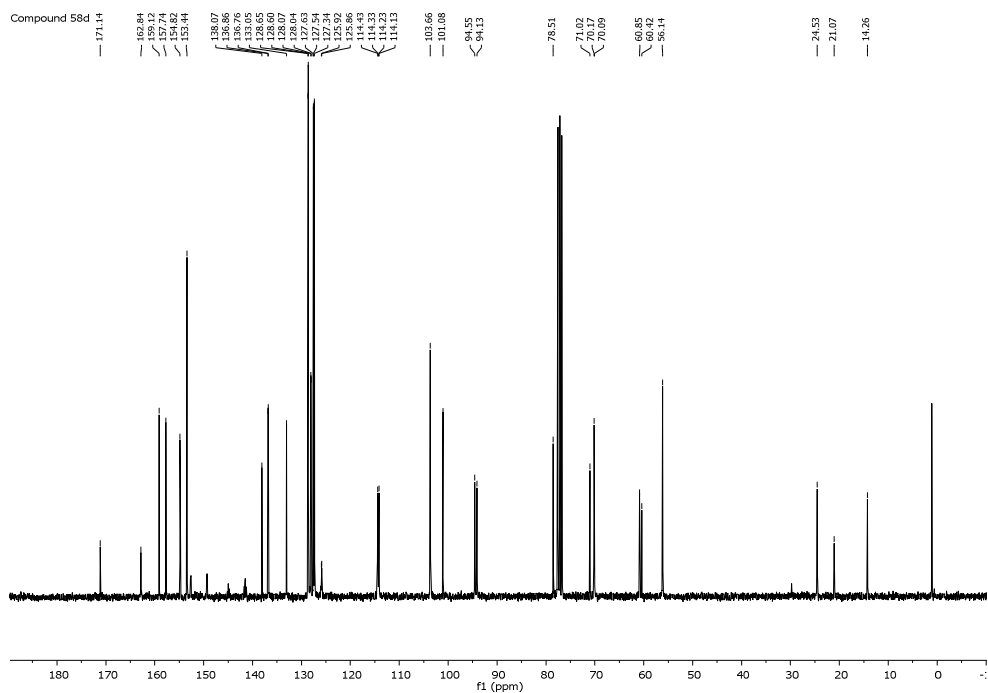
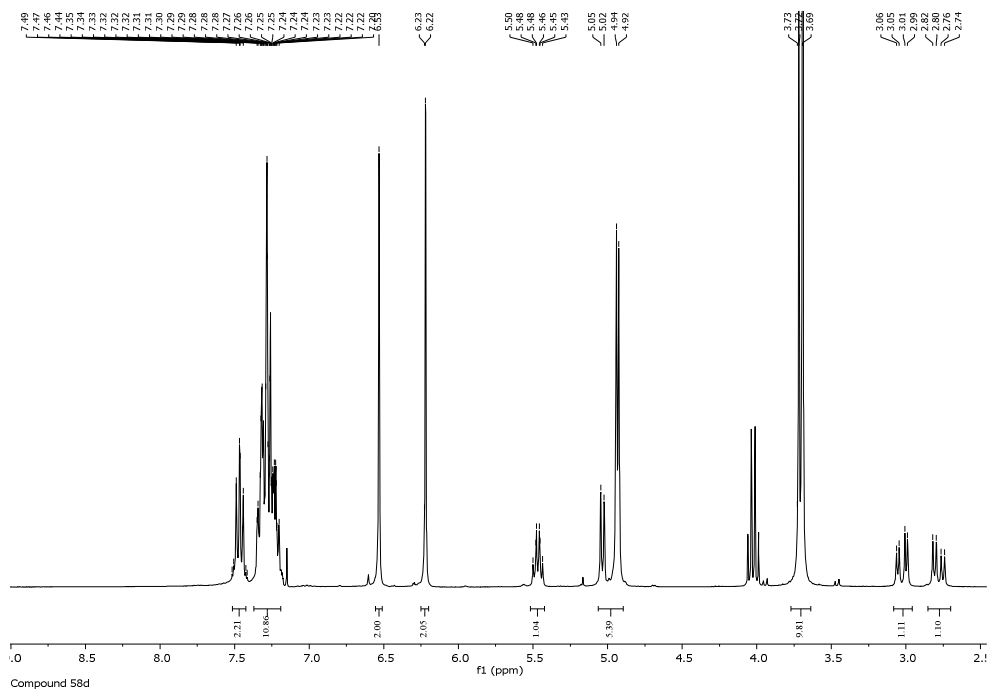
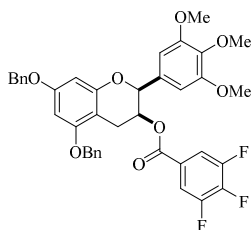


Compound 58c

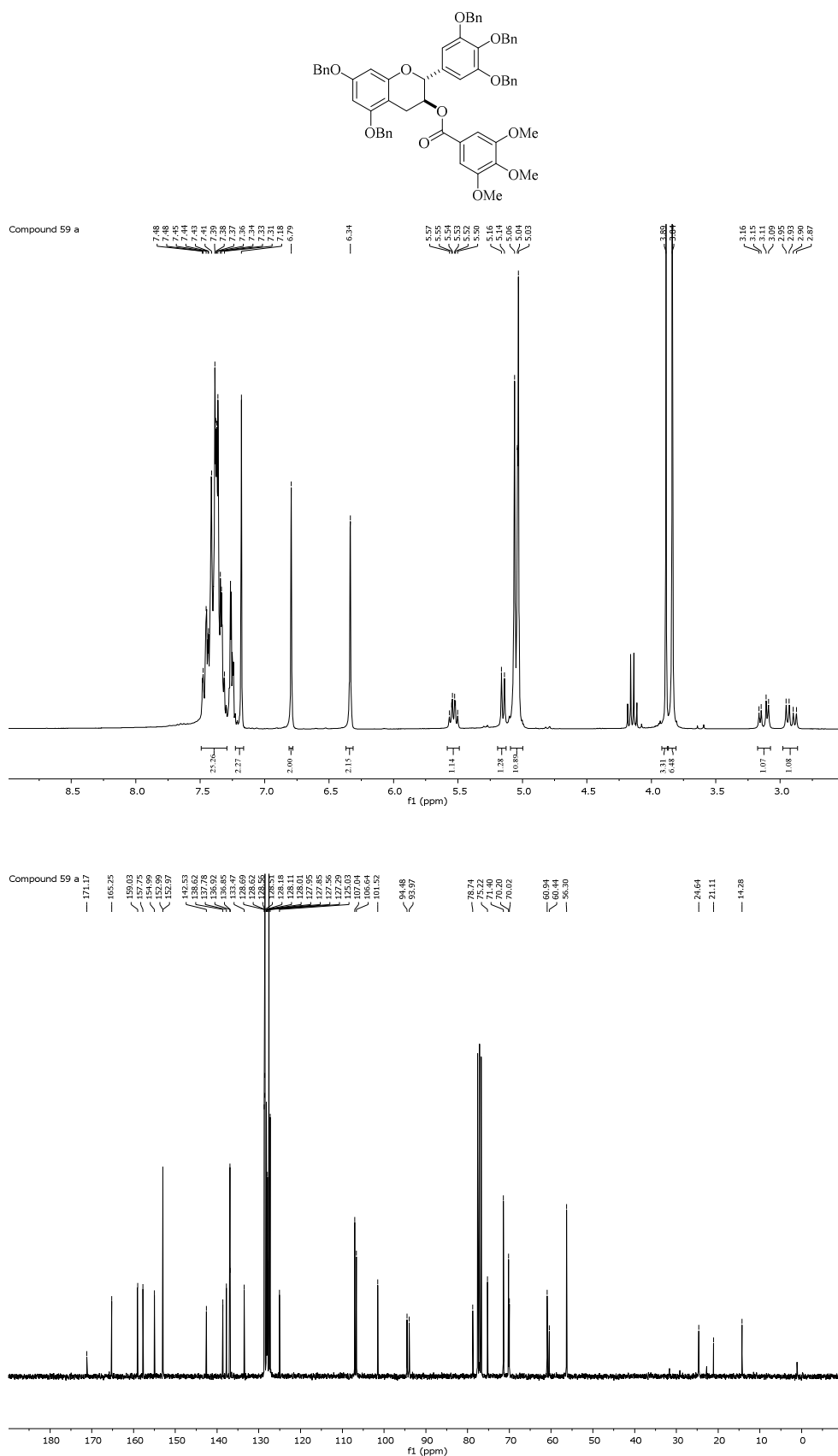


Compound 58c

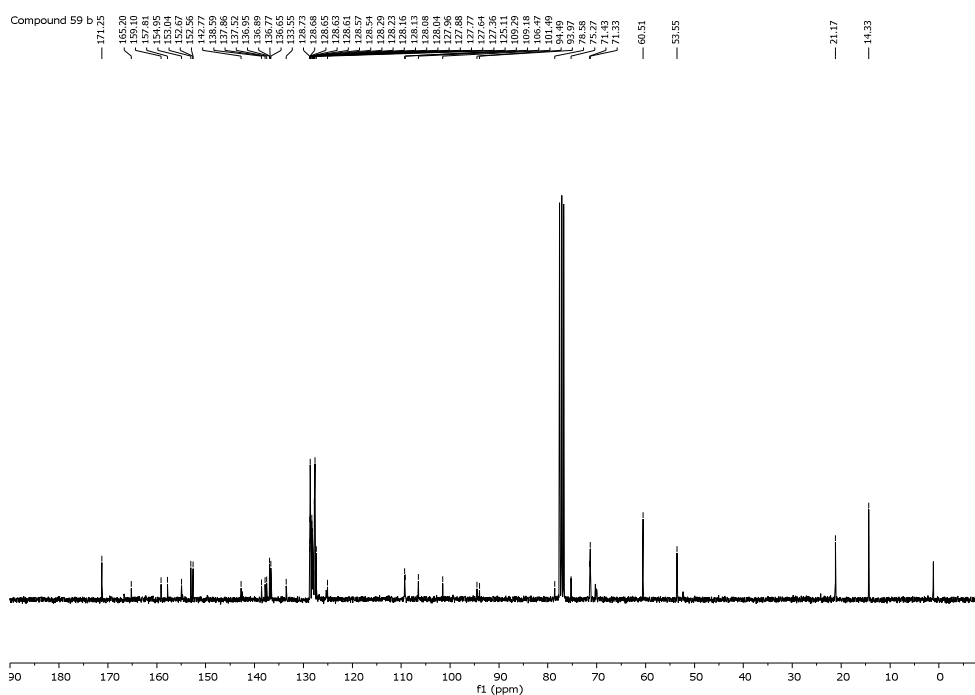
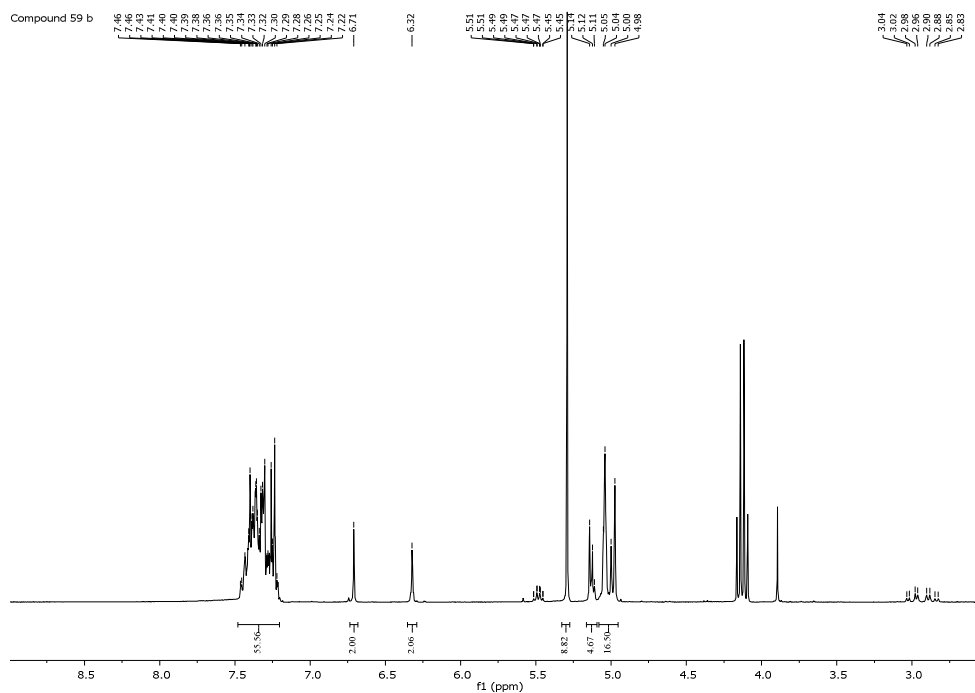
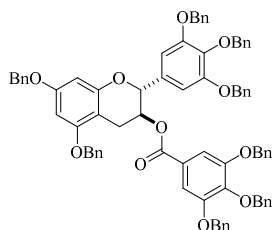
(2*S*,3*S*)-5,7-Bis(benzyloxy)-2-(3,4,5-trimethoxyphenyl)chroman-3-yl-(3,4,5-trifluoro)benzoate
(**58d**)

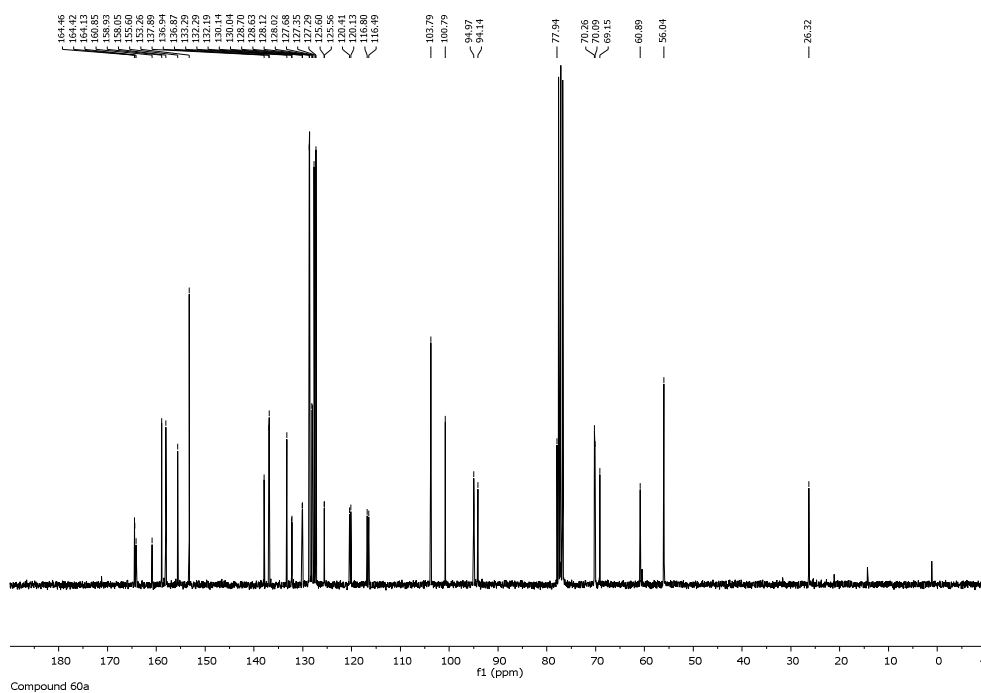
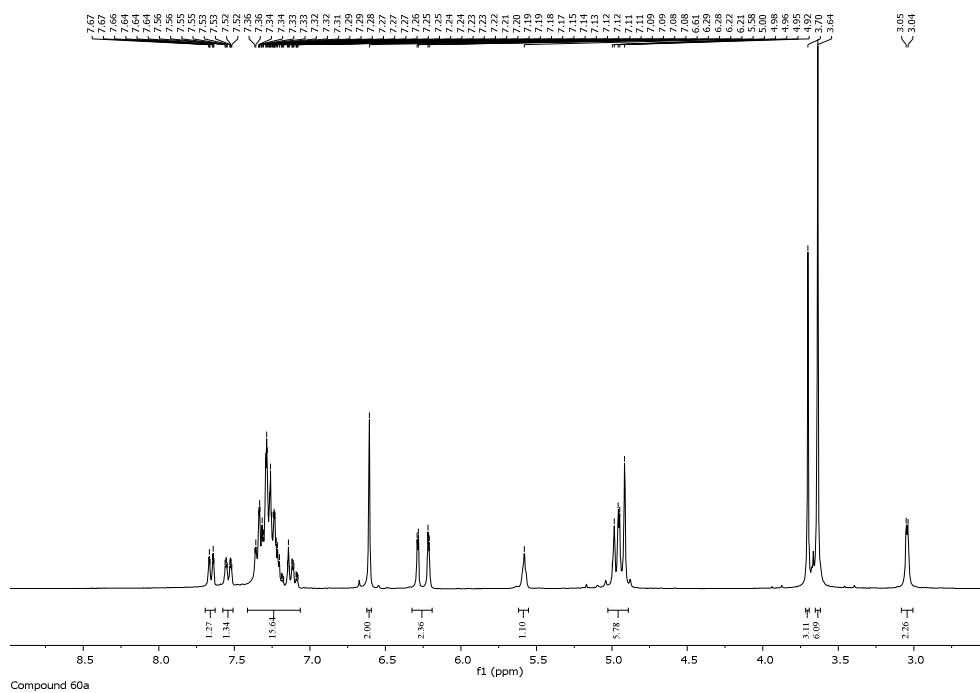
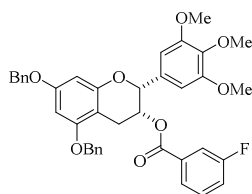


(2*R*,3*S*)-5,7-Bis(benzyloxy)-2-(3,4,5-tribenzyloxyphenyl)chroman-3-yl-(3,4,5-trimethoxy)benzoate
(**59a**)

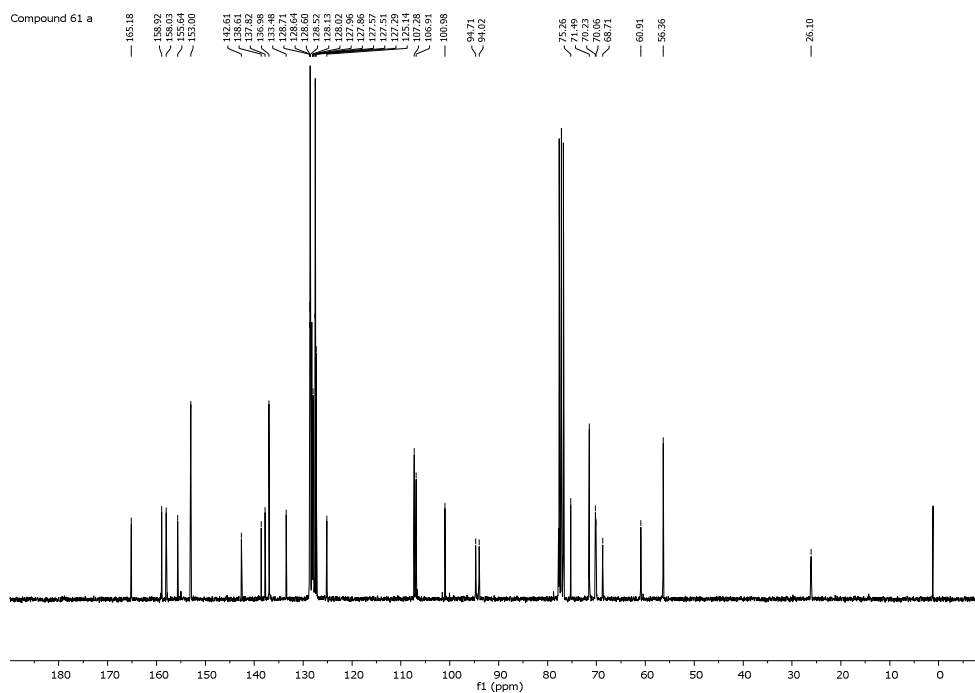
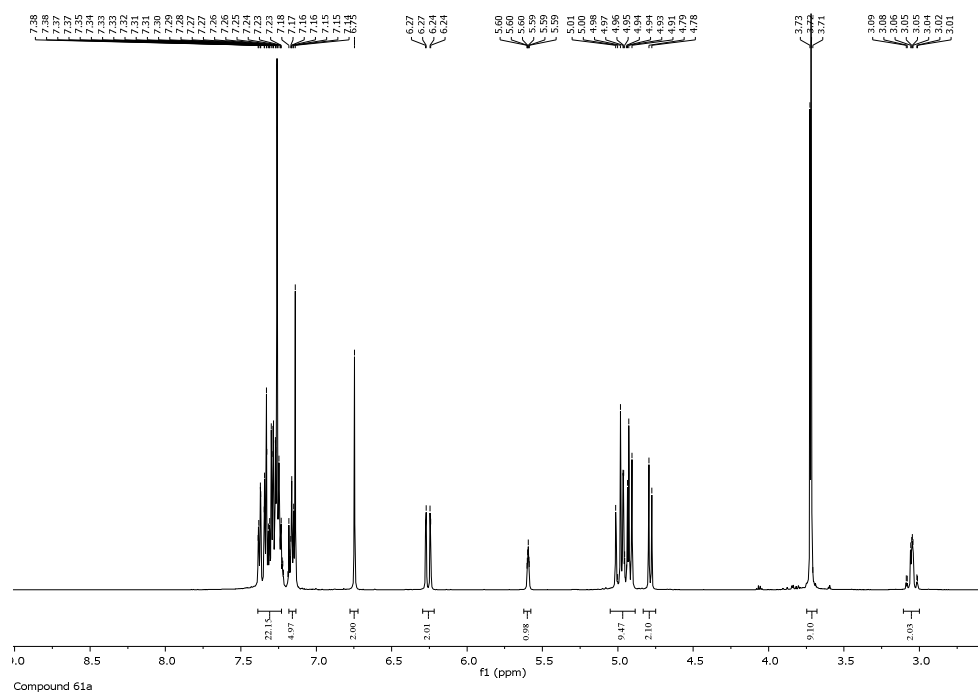
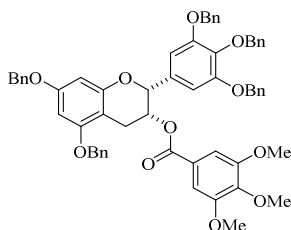


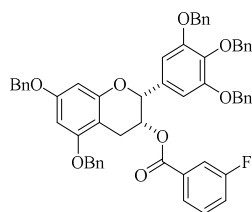
(2*R*,3*S*)-5,7-Bis(benzyloxy)-2-(3,4,5-tribenzyloxyphenyl)chroman-3-yl-(3,4,5-trisbenzyloxy)benzoate
(**59b**)



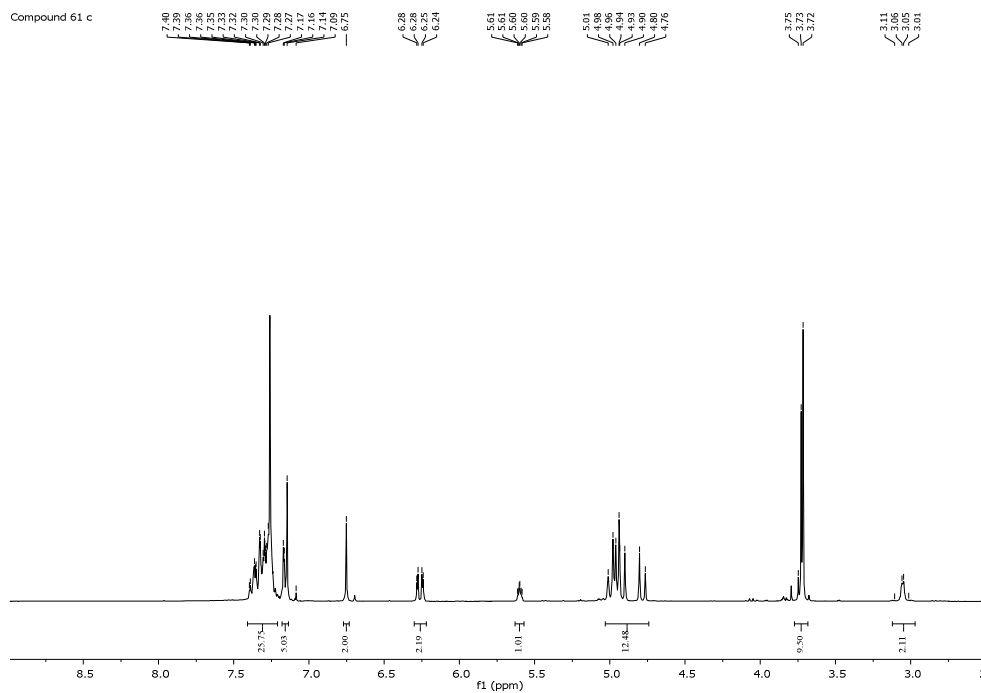
(2*R*,3*R*)-5,7-Bis(benzyloxy)-2-(3,4,5-trimethoxyphenyl)chroman-3-yl-(3-fluoro)benzoate (60a)

(2*R*,3*R*)-5,7-Bis(benzyloxy)-2-(3,4,5-tribenzylphenyl)chroman-3-yl-(3,4,5-trimethoxy)benzoate
(61a)

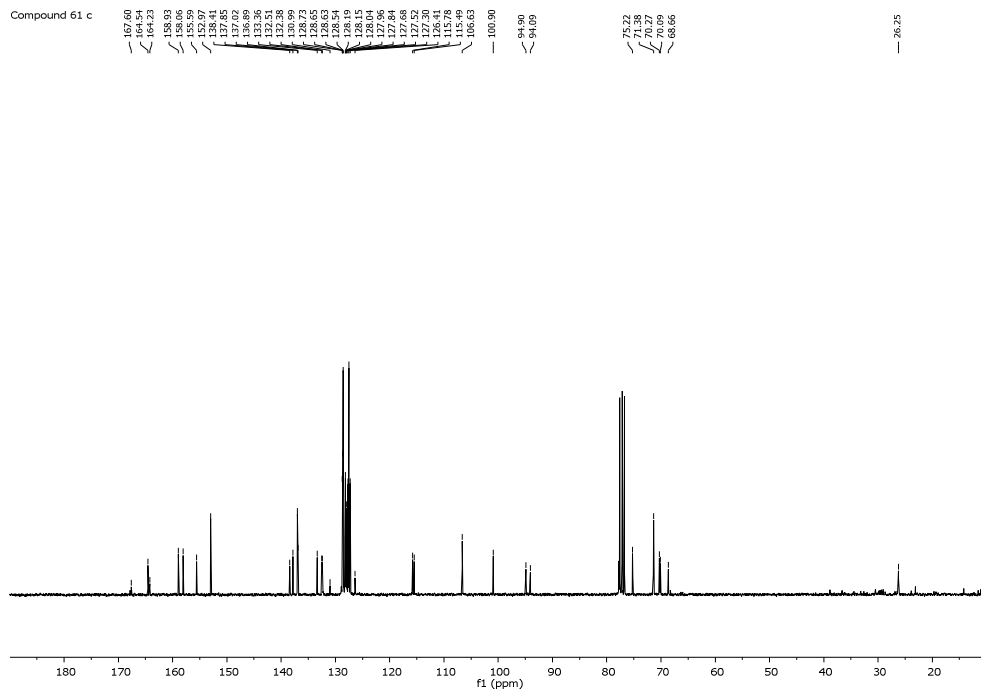


(2*R*,3*R*)-5,7-Bis(benzyloxy)-2-(3,4,5-tribenzyloxyphenyl)chroman-3-yl-(3-fluoro)benzoate (61c)

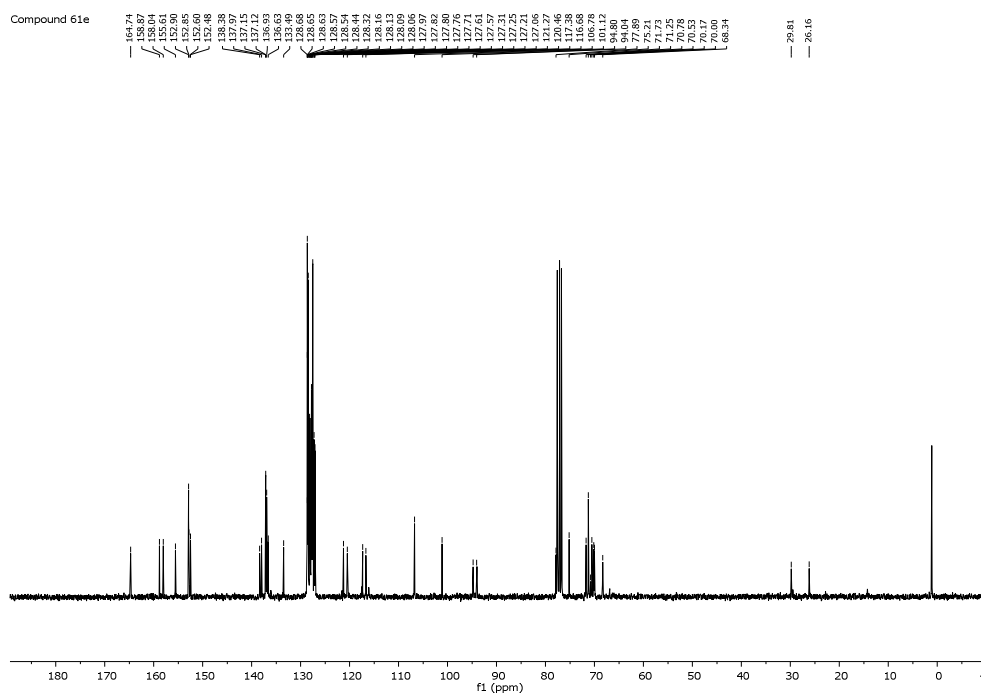
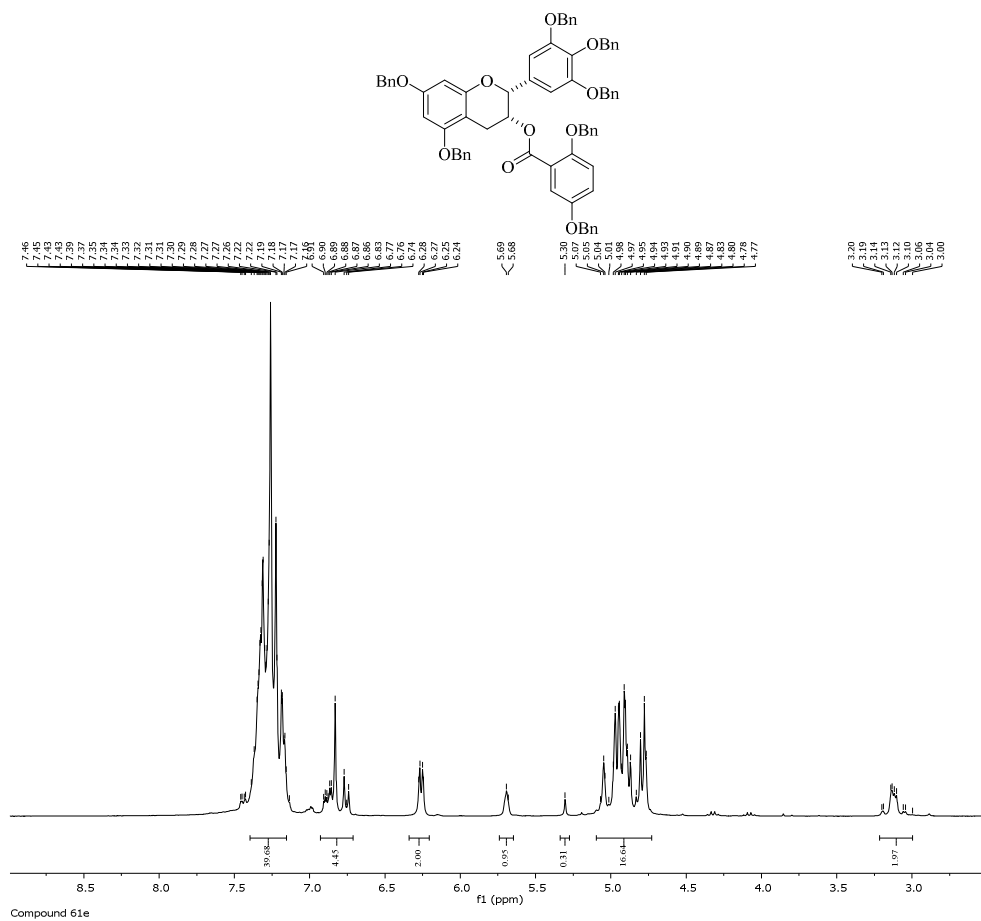
Compound 61 c



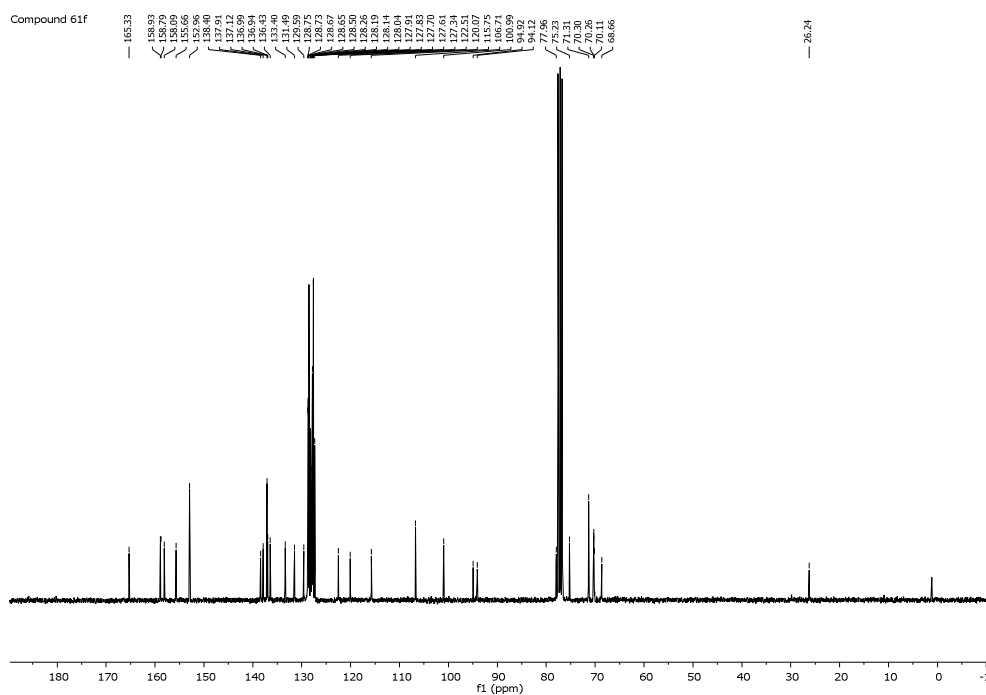
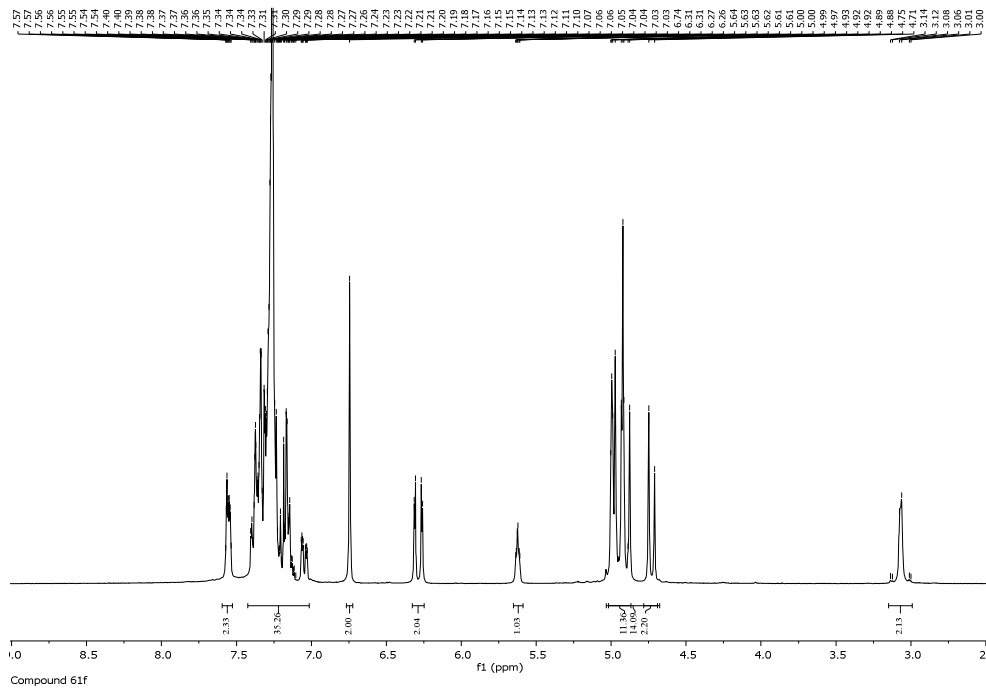
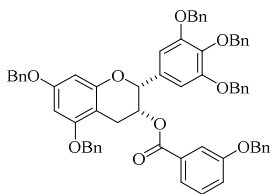
Compound 61 c

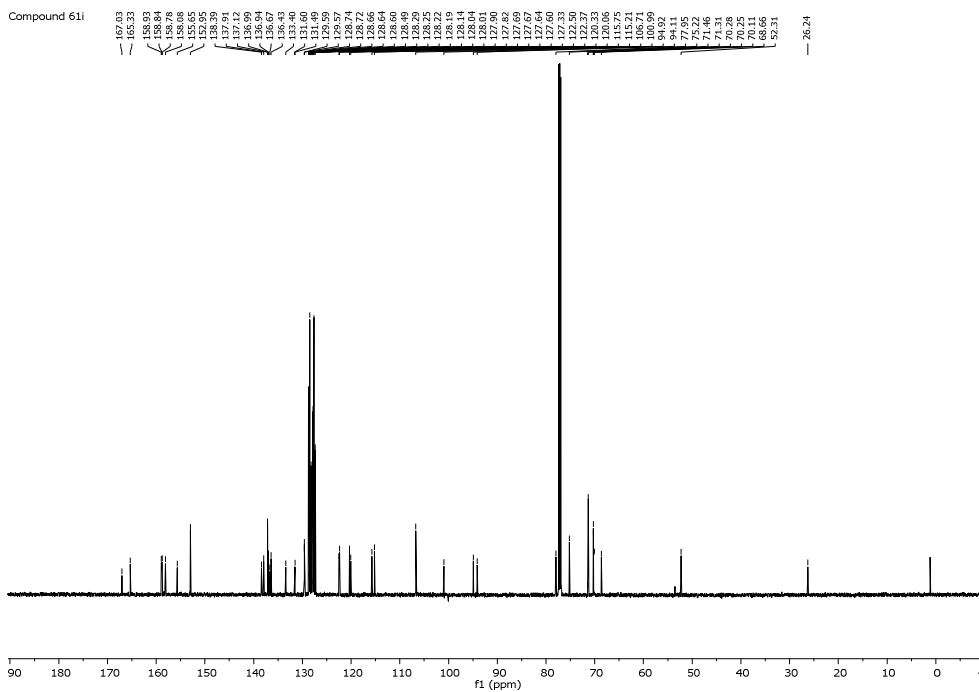
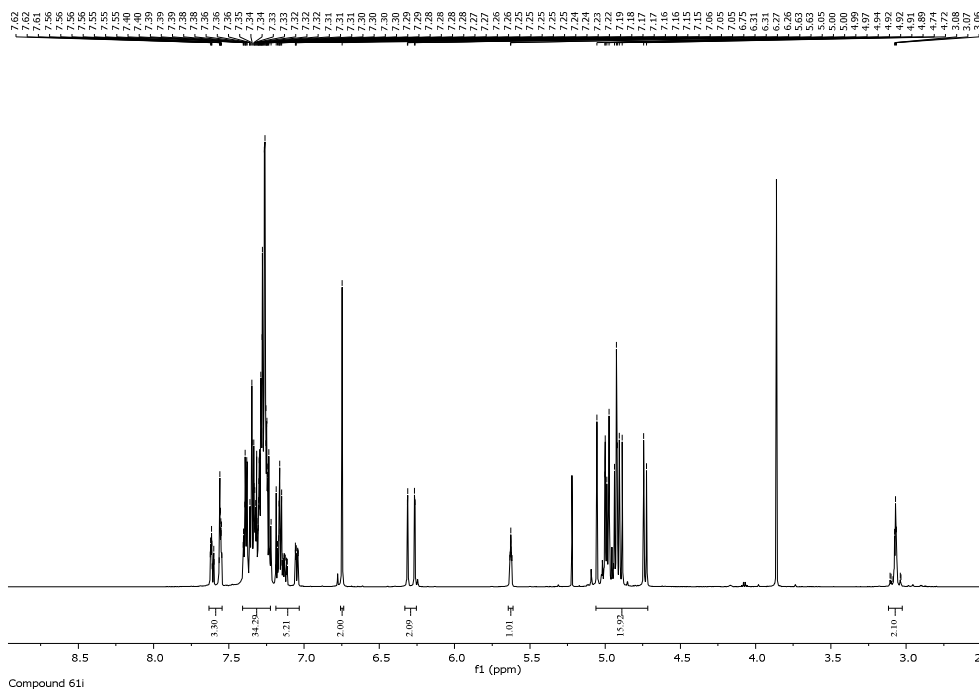
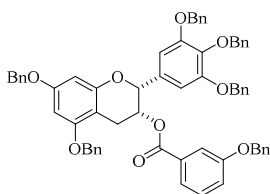


(2*R*,3*R*)-5,7-Bis(benzyloxy)-2-(3,4,5-tribenzylphenyl)chroman-3-yl-(2,5-bis(benzyloxy)benzoate)
(**61e**)

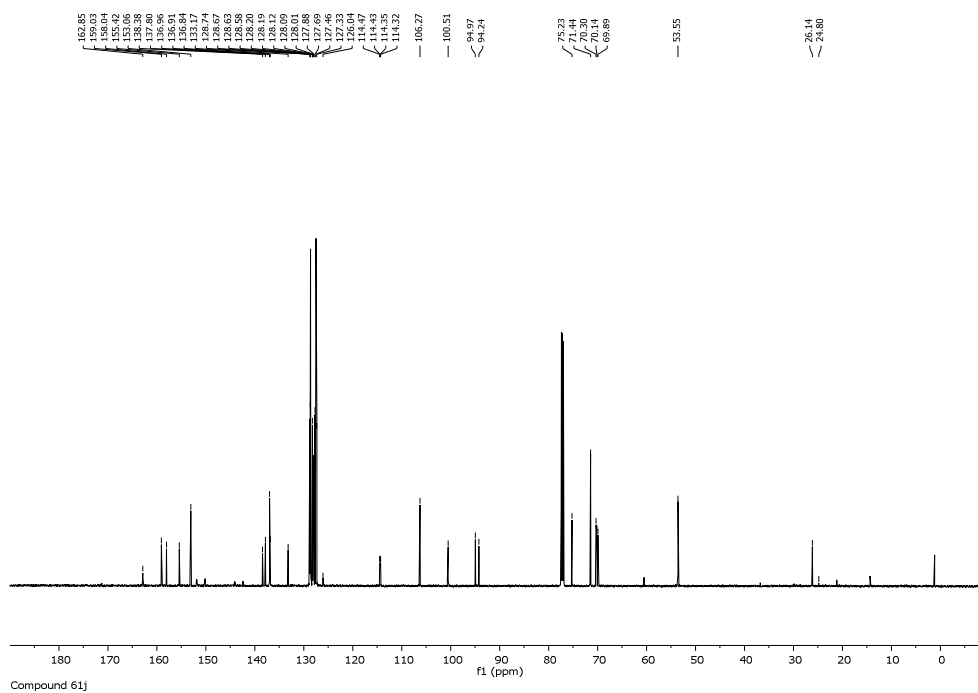
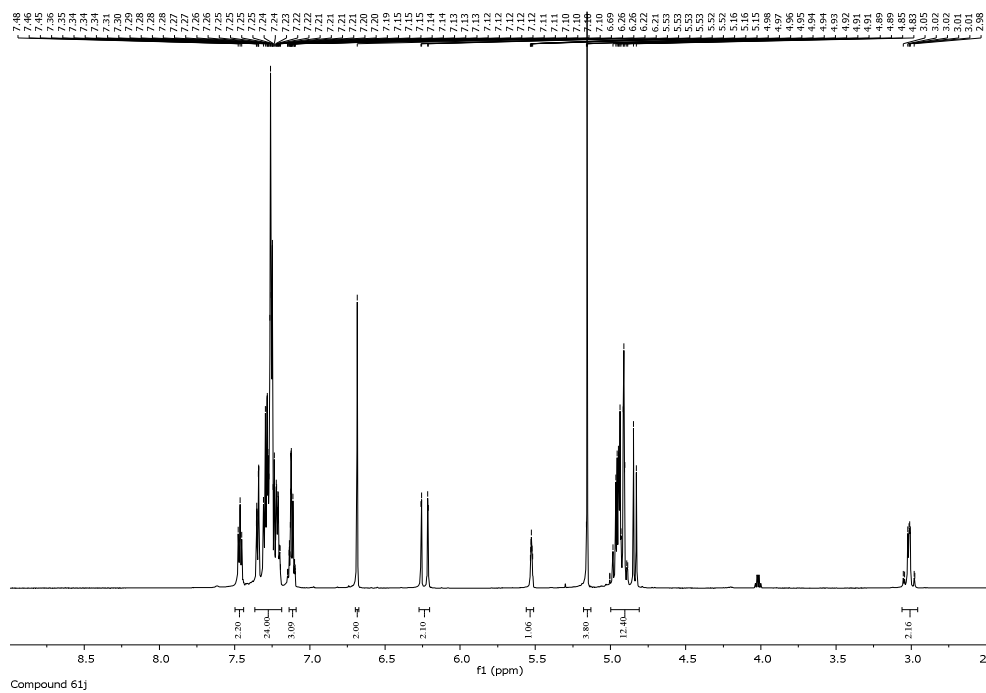
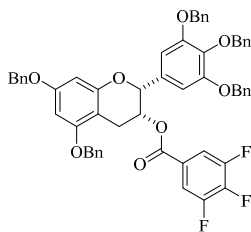


(2*R*,3*R*)-5,7-Bis(benzyloxy)-2-(3,4,5-tribenzylphenyl)chroman-3-yl-(2,4-bis(benzyloxy)benzoate)
(**61f**)

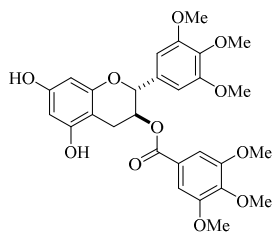


(2*R*,3*R*)-5,7-Bis(benzyloxy)-2-(3,4,5-tribenzylphenyl)chroman-3-yl-(3-benzyloxy)benzoate (**61i**)

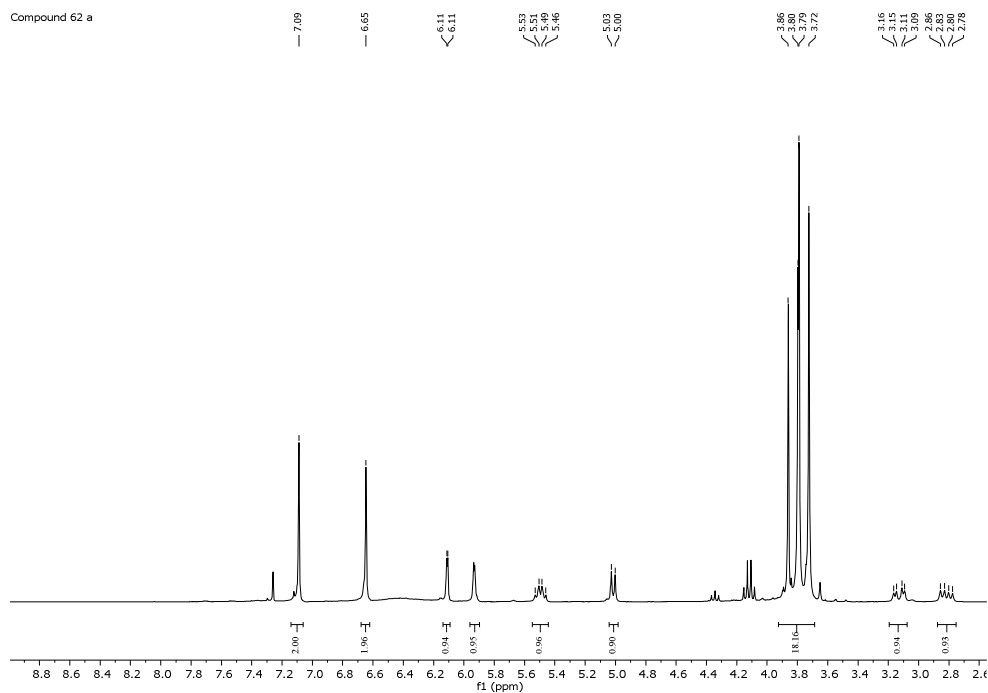
(2*R*,3*R*)-5,7-Bis(benzyloxy)-2-(3,4,5-tribenzyloxyphenyl)chroman-3-yl-(3,4,5-trifluoro)benzoate
(**61j**)



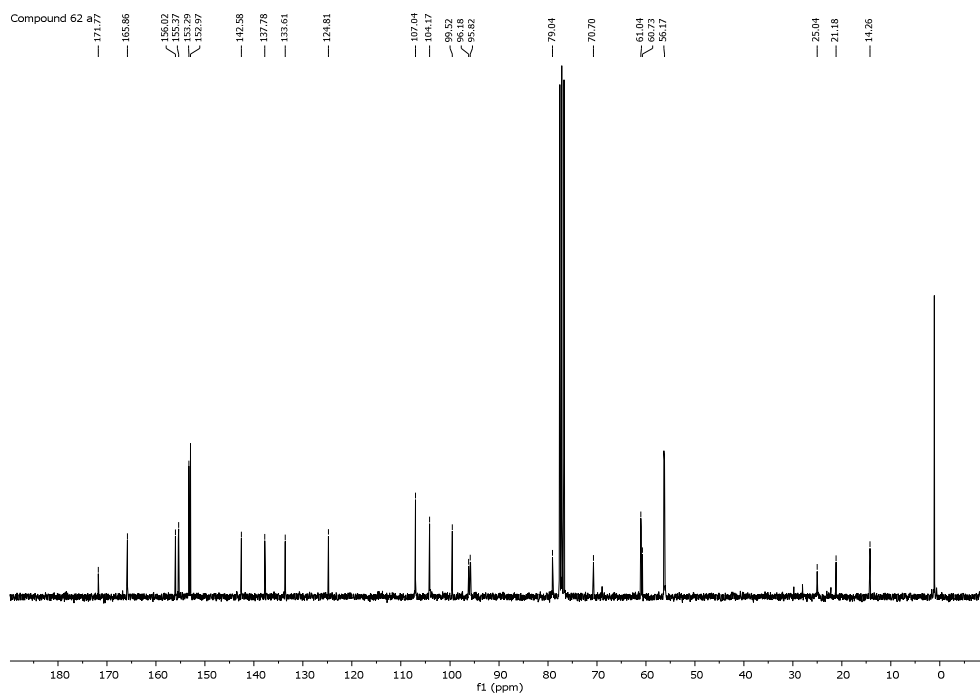
(2*R*,3*S*)-5,7-Dihydroxy-2-(3,4,5-trimethoxyphenyl)chroman-3-yl-(3,4,5-trimethoxy)benzoate
(62a)



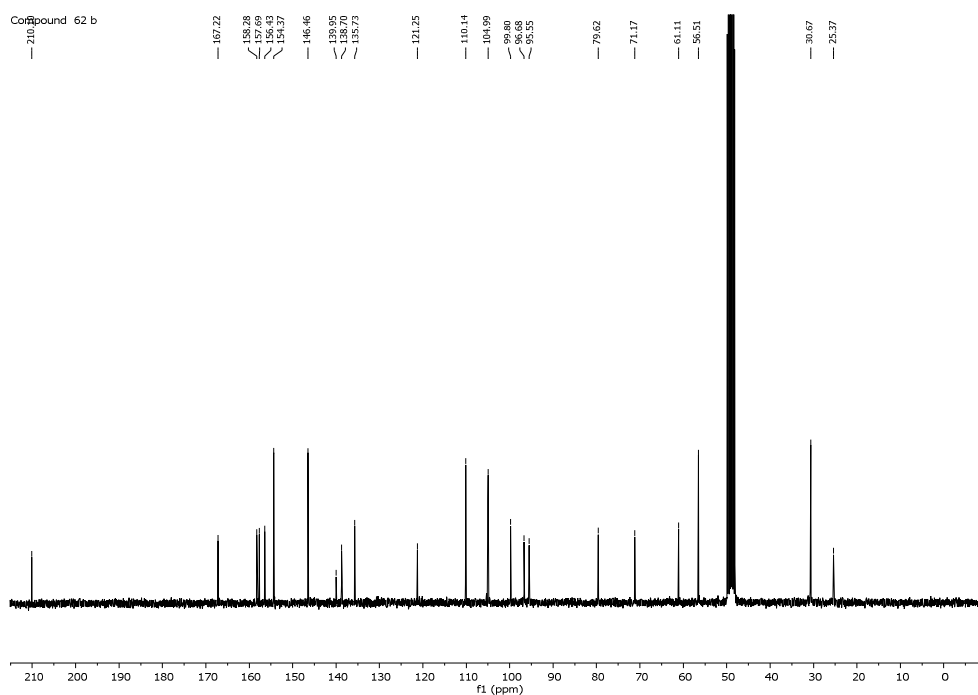
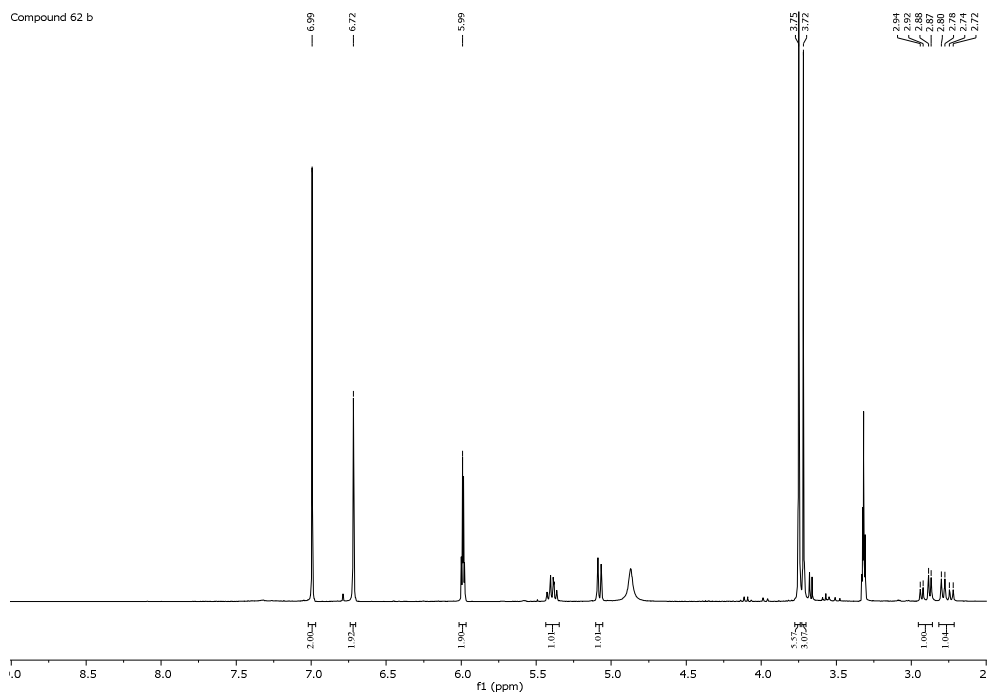
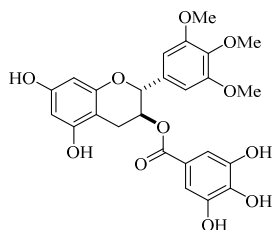
Compound 62 a

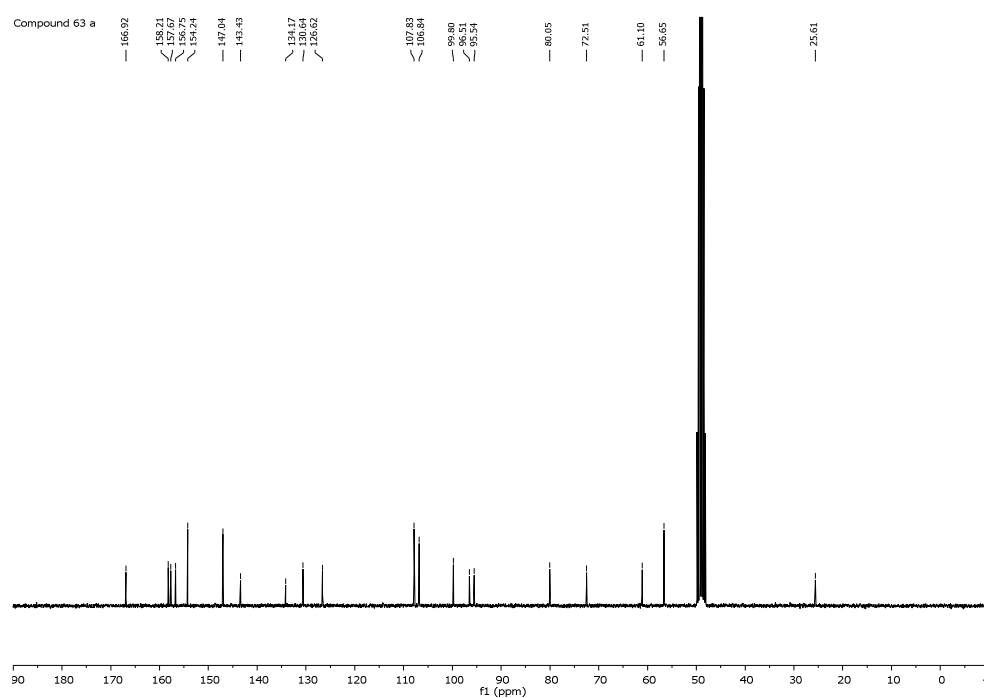
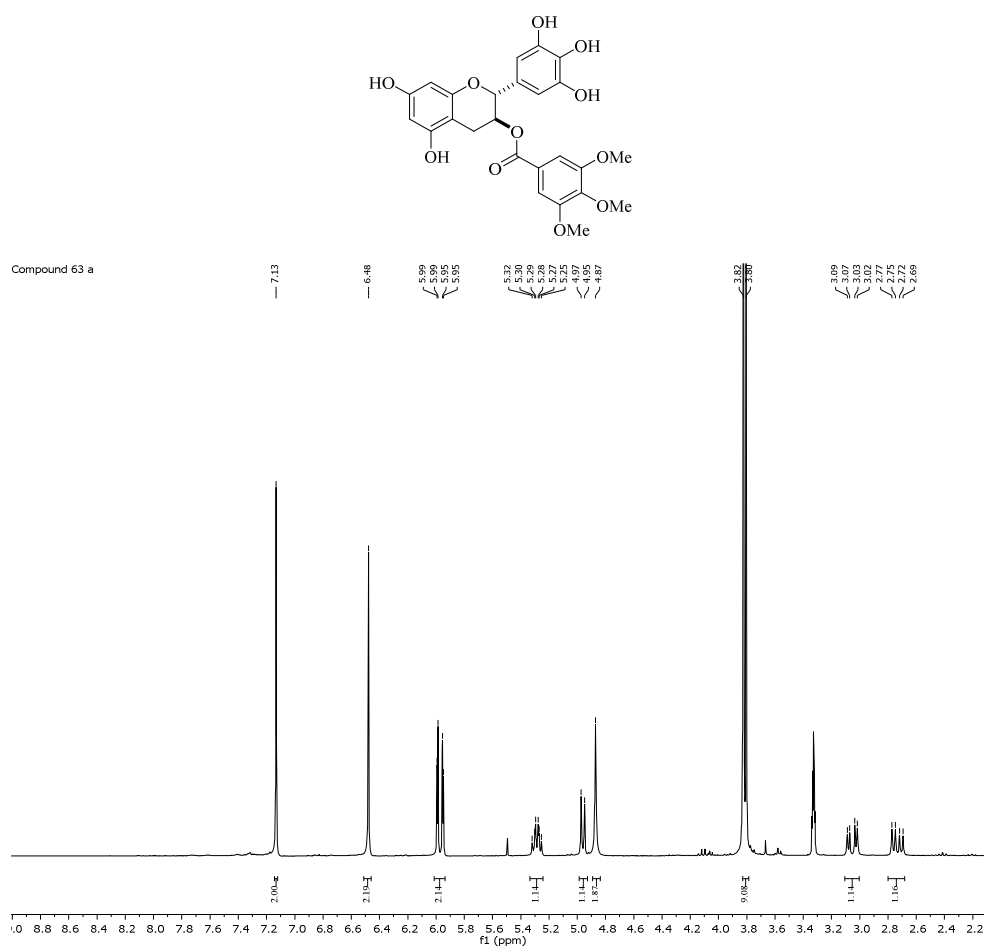


Compound 62 a

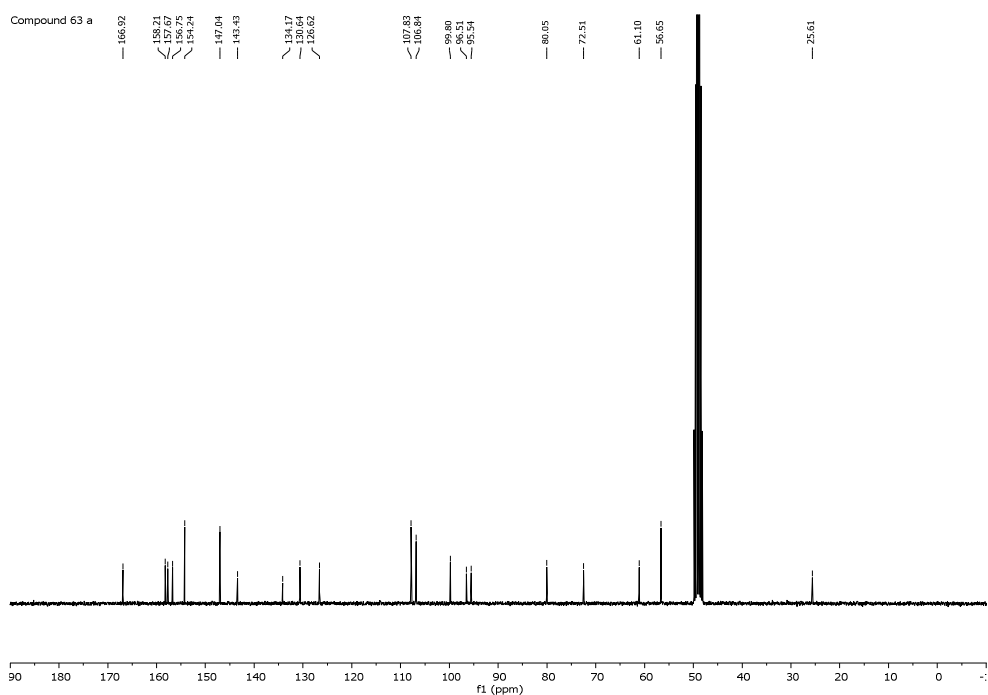
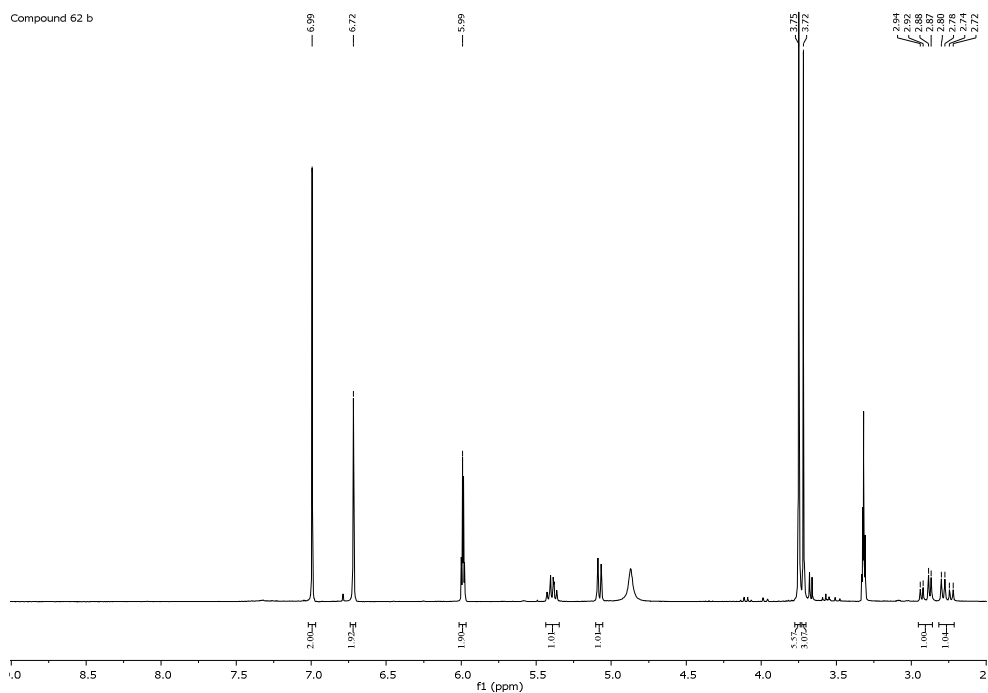
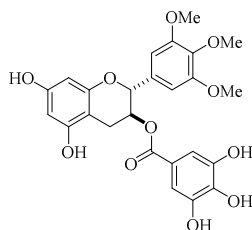


(2*R*,3*S*)-5,7-Dihydroxy-2-(3,4,5-trimethoxyphenyl)chroman-3-yl-(3,4,5-trihydroxy)benzoate
(**62b**)

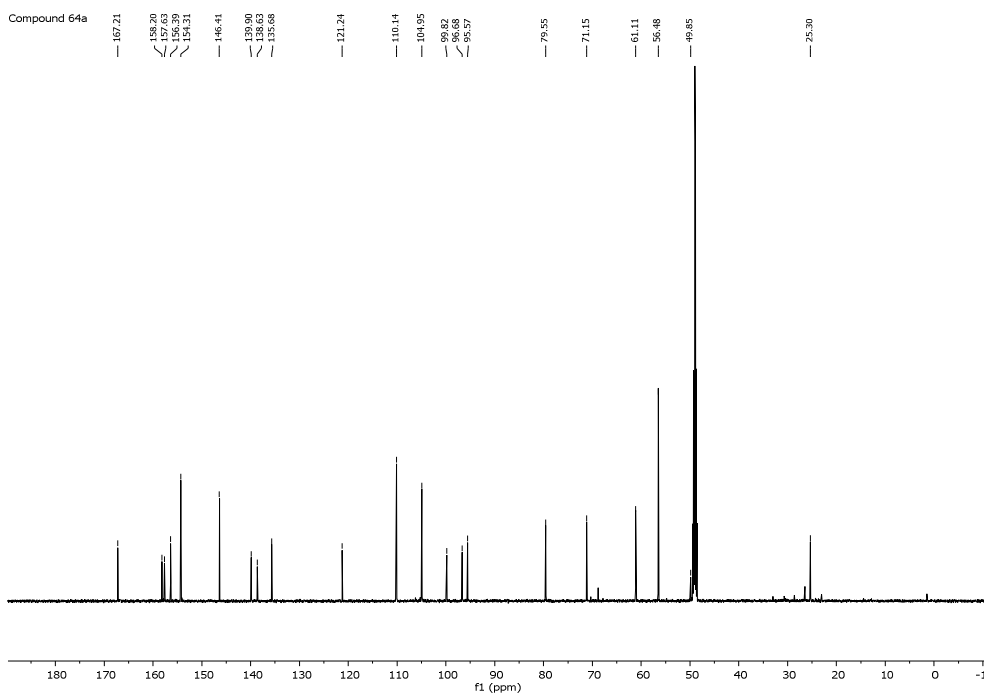
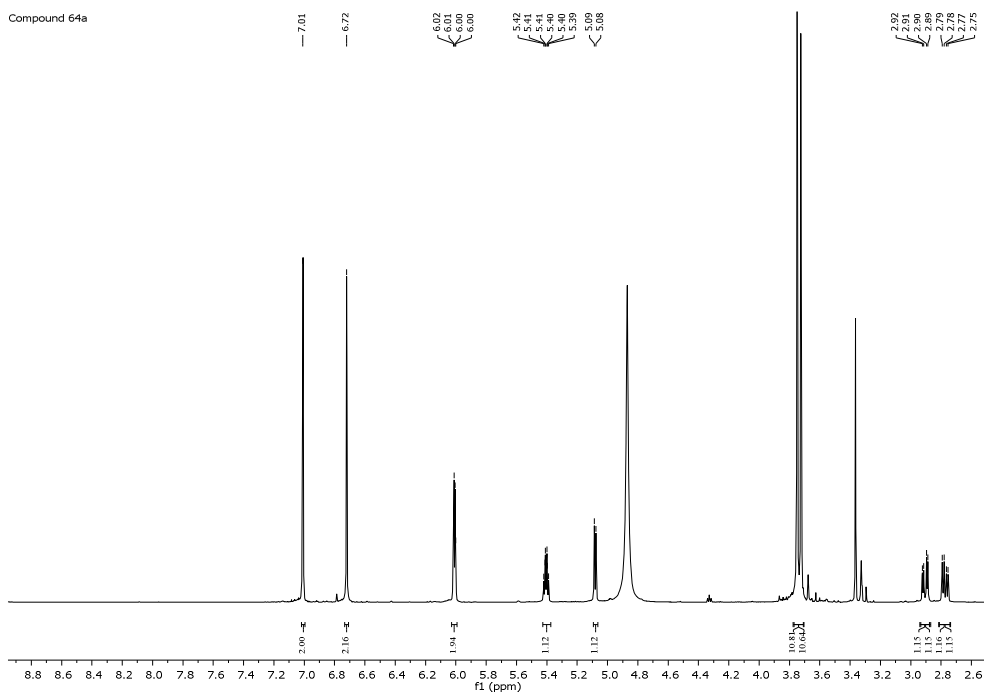
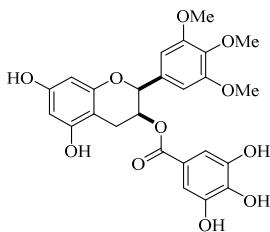


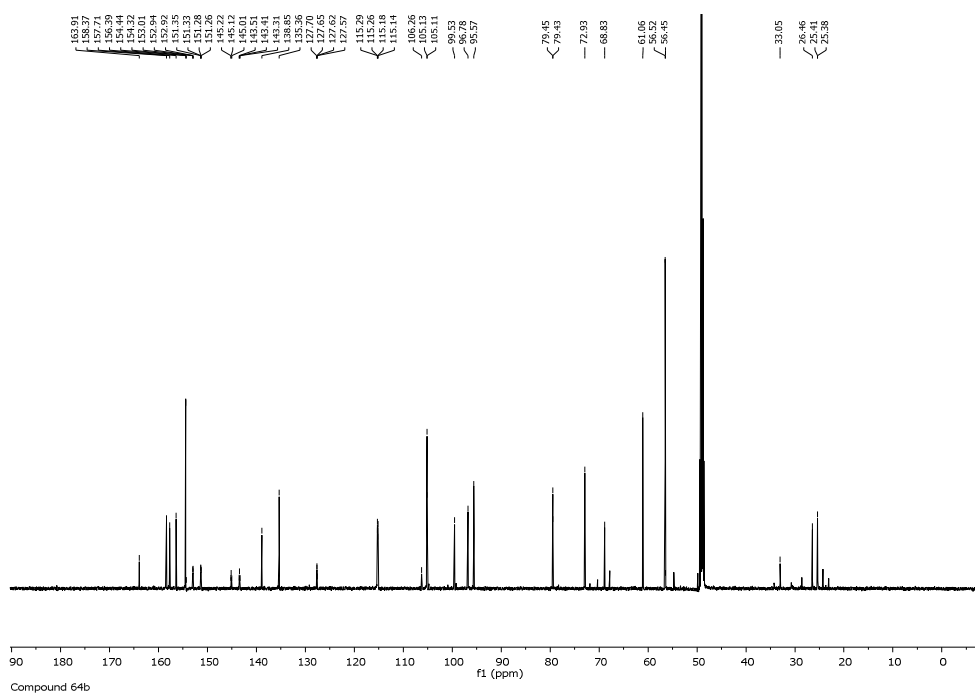
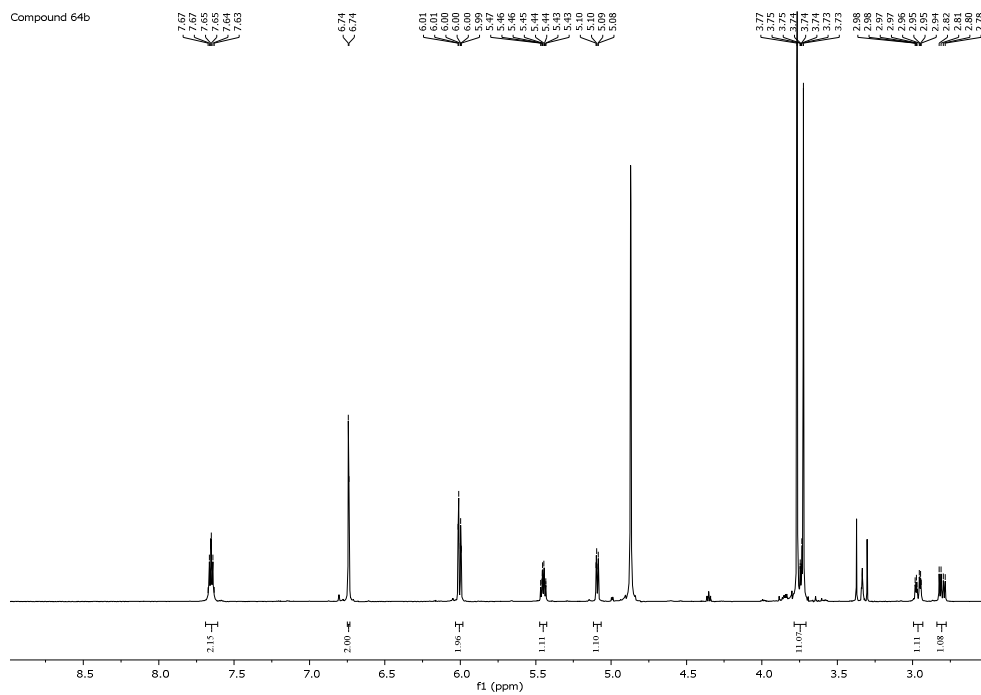
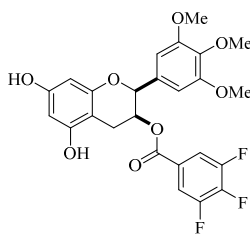
(2*R*,3*S*)-5,7-Dihydroxy-2-(3,4,5-hydroxyphenyl)chroman-3-yl-(3,4,5-trimethoxy)benzoate (63a)

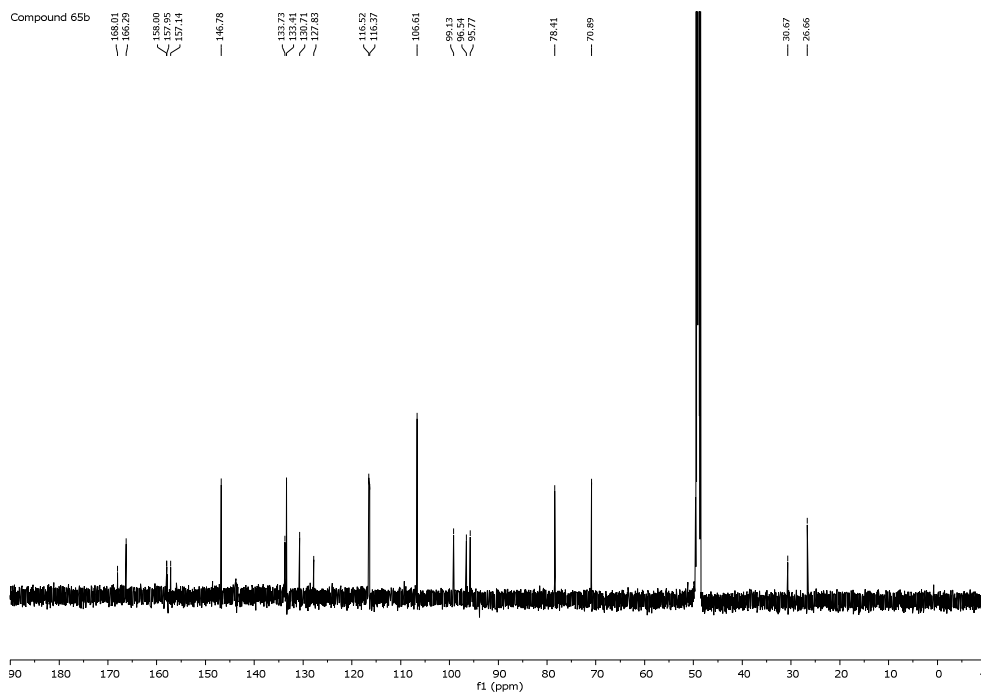
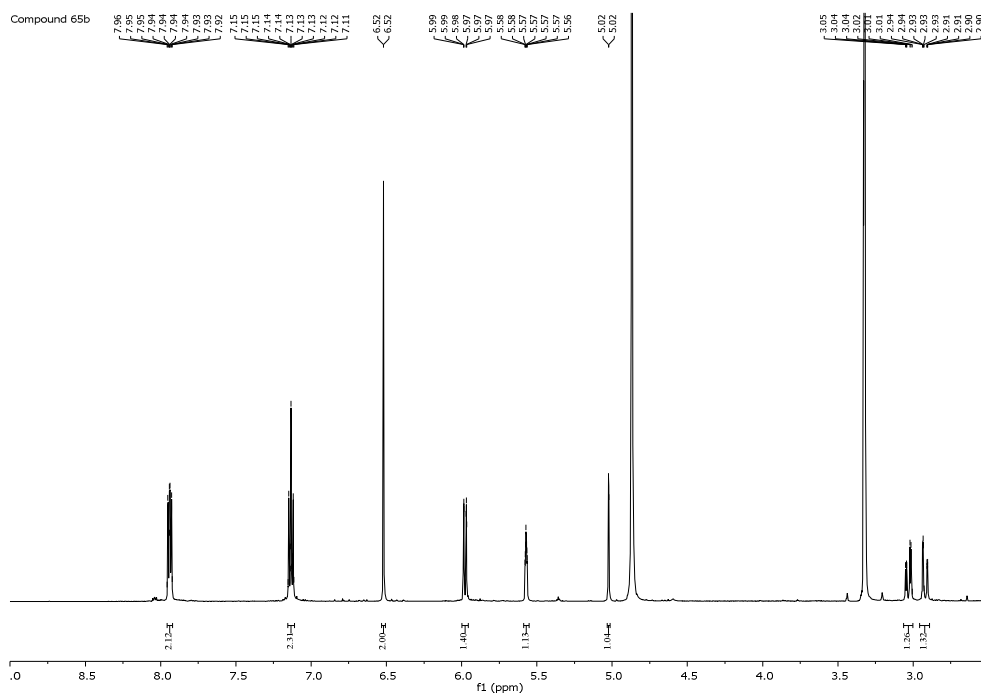
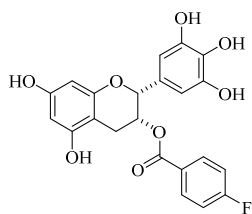
(2*R*,3*S*)-5,7-Dihydroxy-2-(3,4,5-trimethoxyphenyl)chroman-3-yl-(3,4,5-trihydroxy)benzoate
(**62b**)

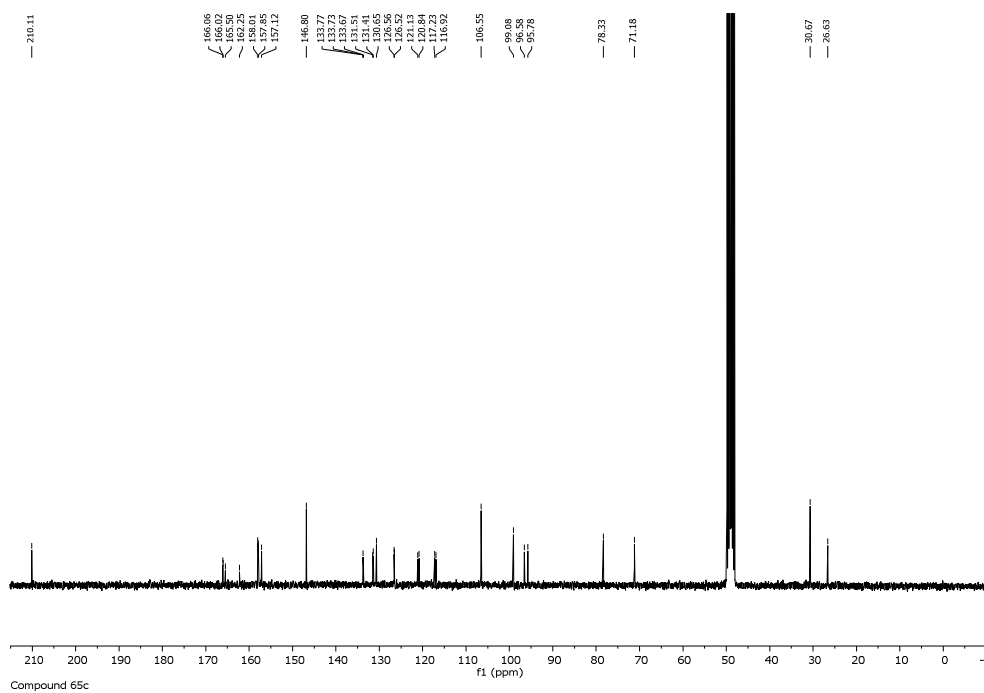
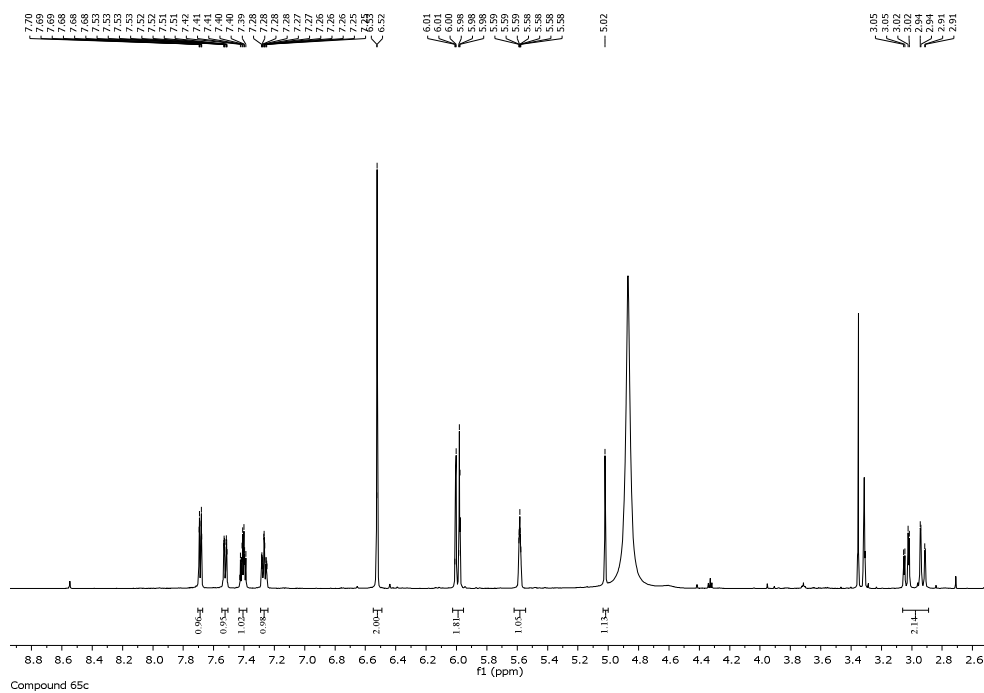
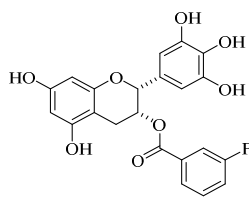


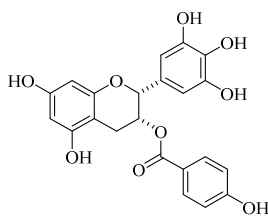
(2*S*,3*S*)-5,7-Dihydroxy-2-(3,4,5-trimethoxyphenyl)chroman-3-yl-(3,4,5-trihydroxy)benzoate
(64a)



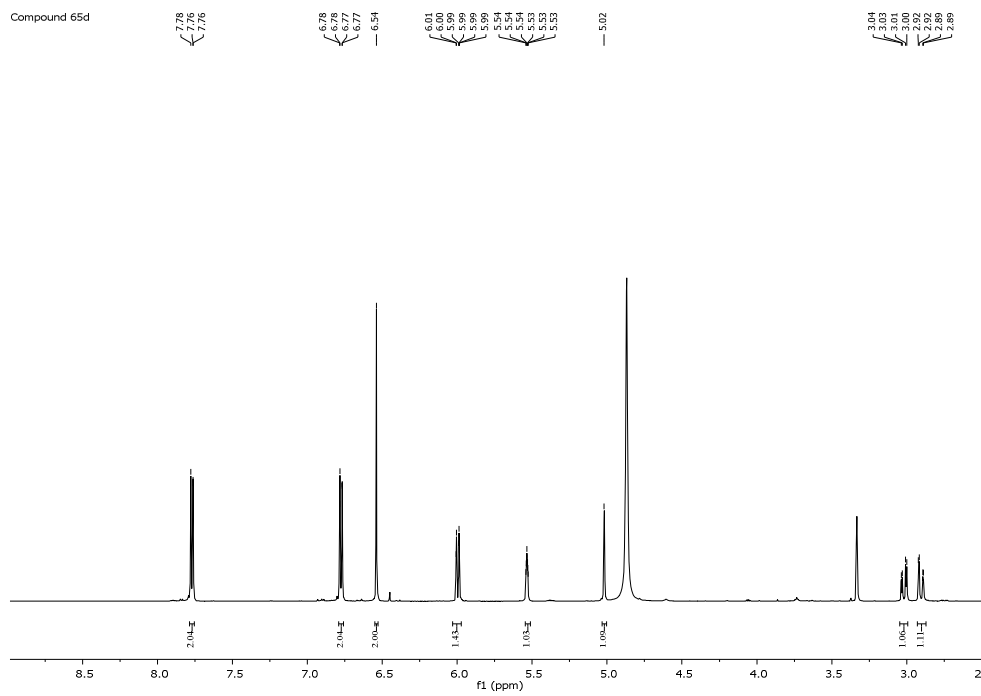
(2*S*,3*S*)-5,7-Dihydroxy-2-(3,4,5-trimethoxyphenyl)chroman-3-yl-(3,4,5-trifluoro)benzoate (64b)

(2*R*,3*R*)-5,7-Dihydroxy-2-(3,4,5-tris(hydroxyl)phenyl)chroman-3-yl-(4-fluoro)benzoate (65b)

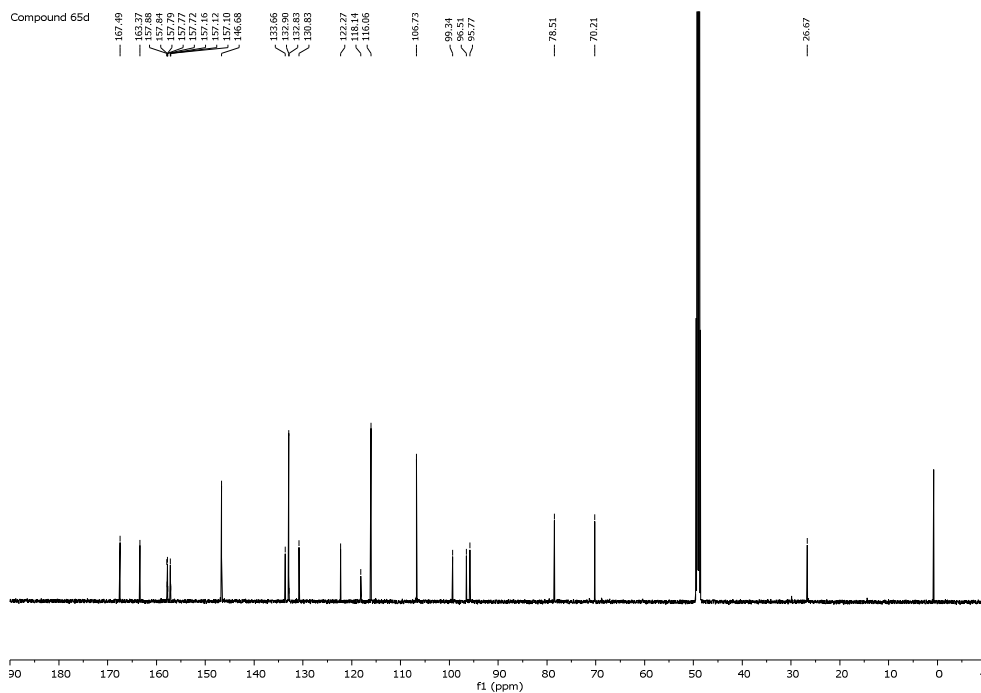
(2*R*,3*R*)-5,7-Dihydroxy-2-(3,4,5-trihydroxyphenyl)chroman-3-yl-(3-fluoro)benzoate (**65c**)

(2*R*,3*R*)-5,7-Dihydroxy-2-(3,4,5-trihydroxyphenyl)chroman-3-yl-(4-hydroxy)benzoate (65d)

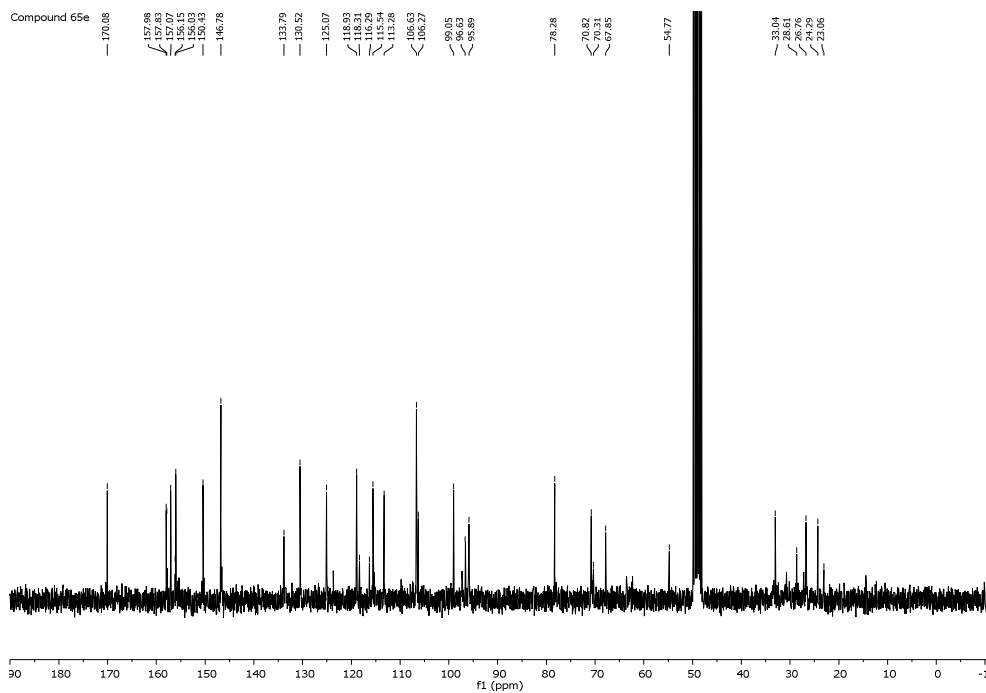
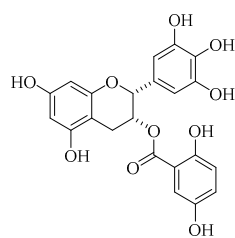
Compound 65d

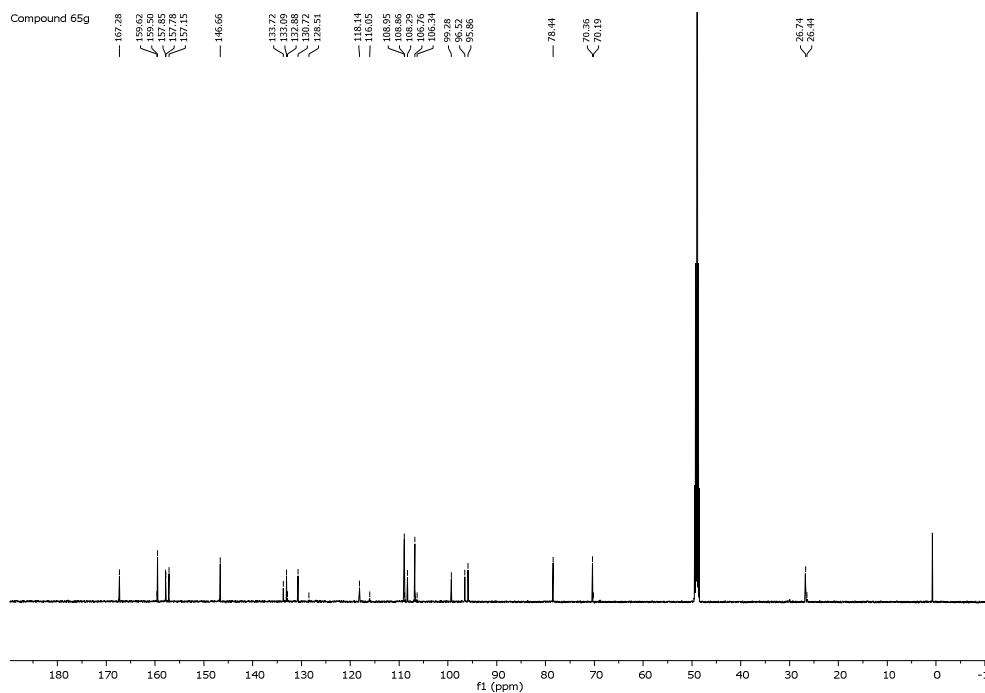
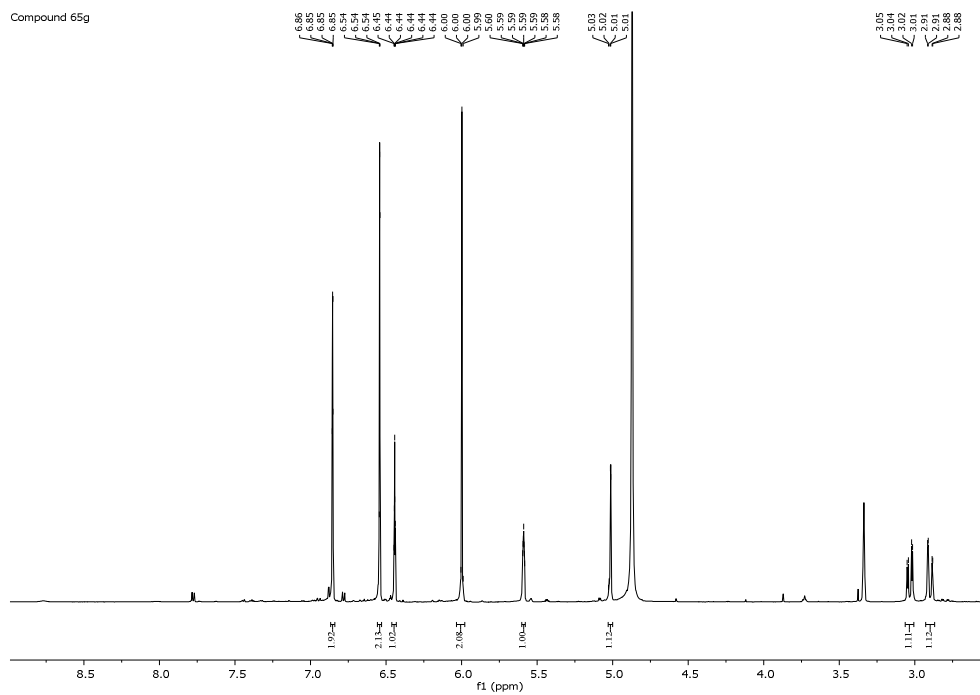
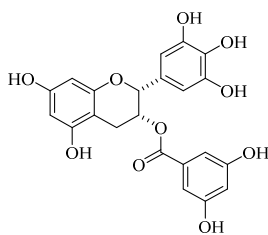


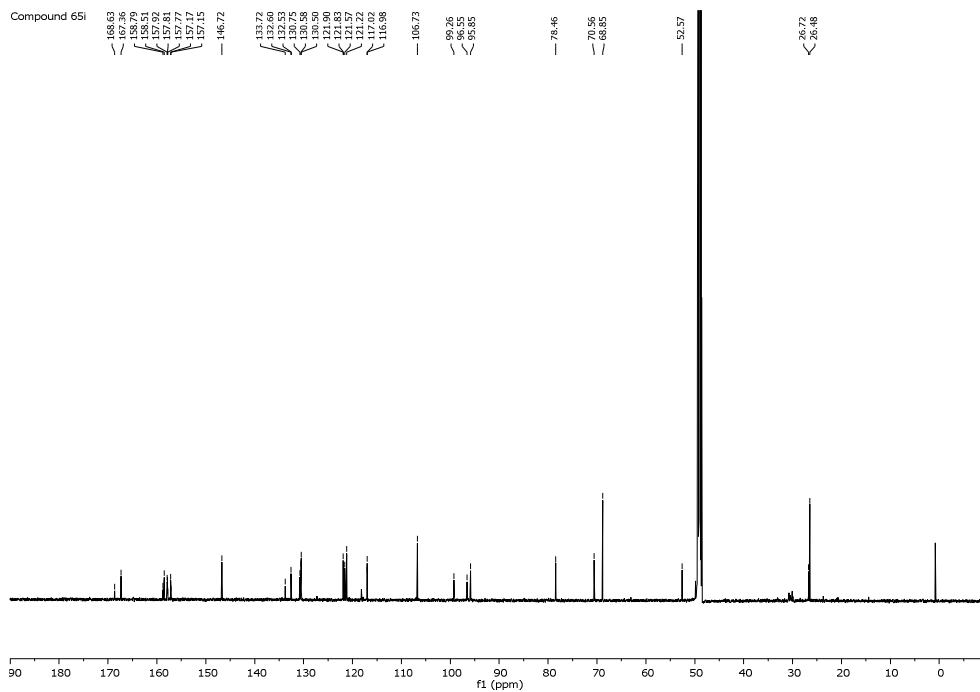
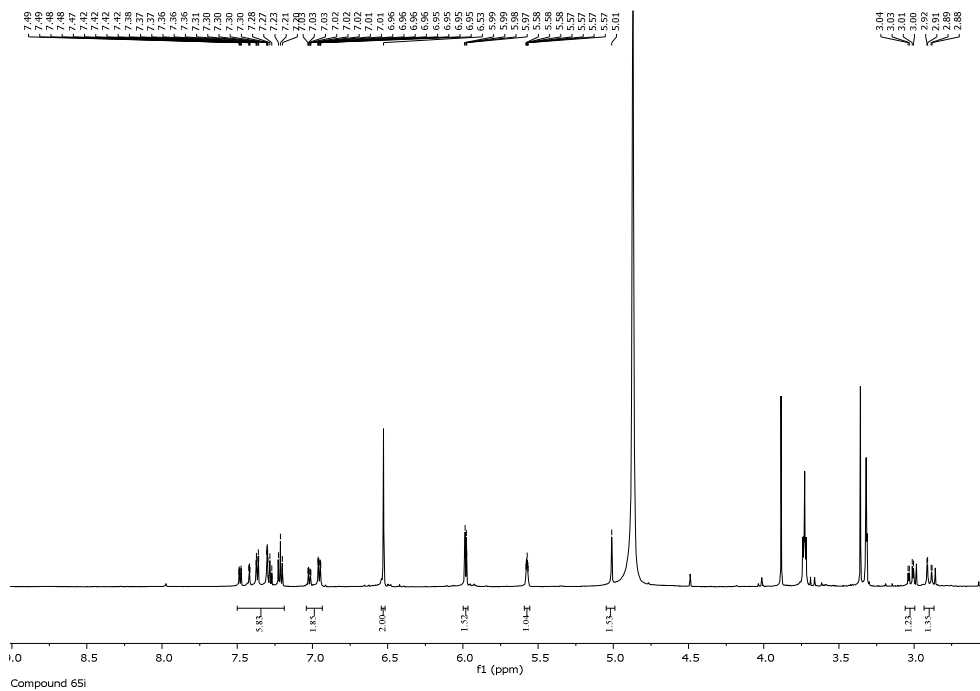
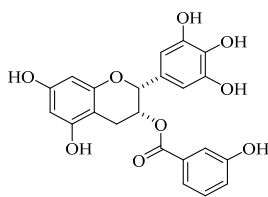
Compound 65d



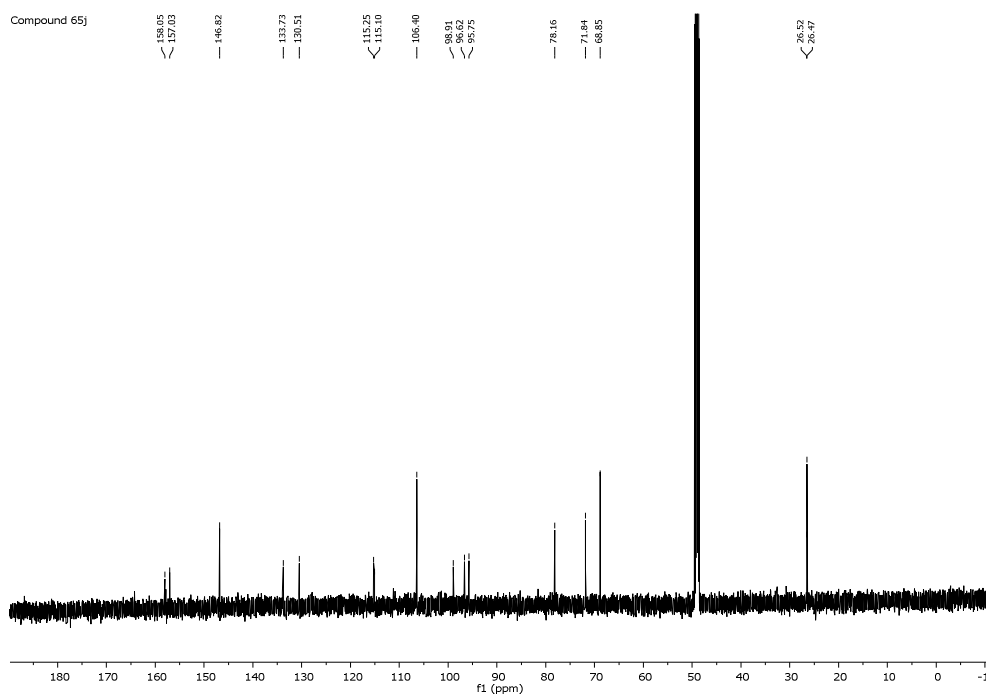
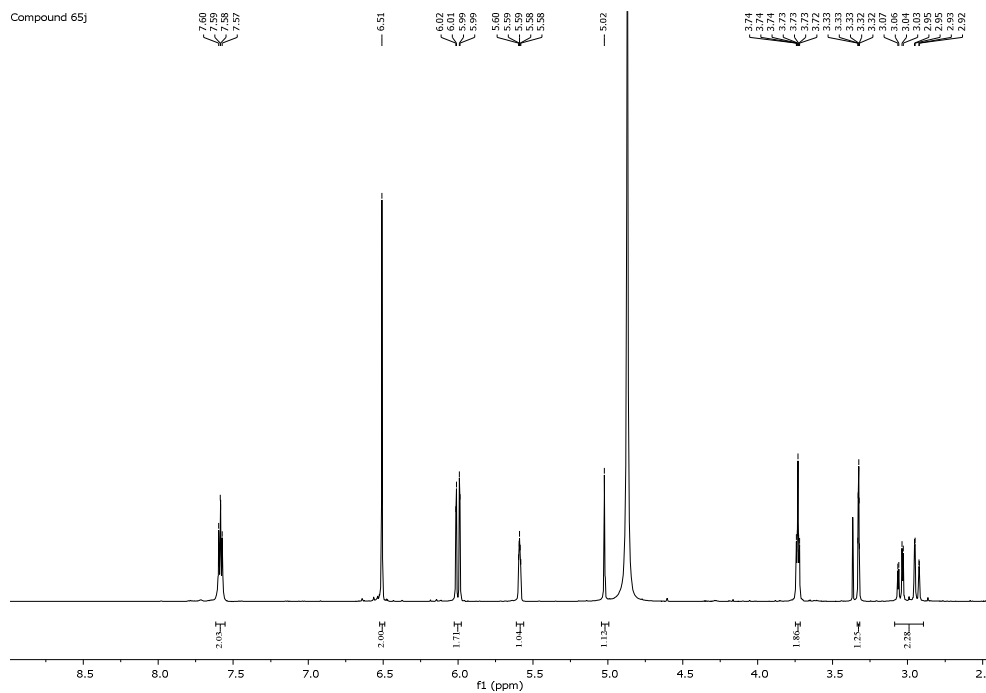
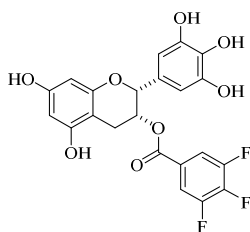
(2*R*,3*R*)-5,7-Dihydroxy-2-(3,4,5-trihydroxyphenyl)chroman-3-yl-(2,5-dihydroxy)benzoate (**65e**)

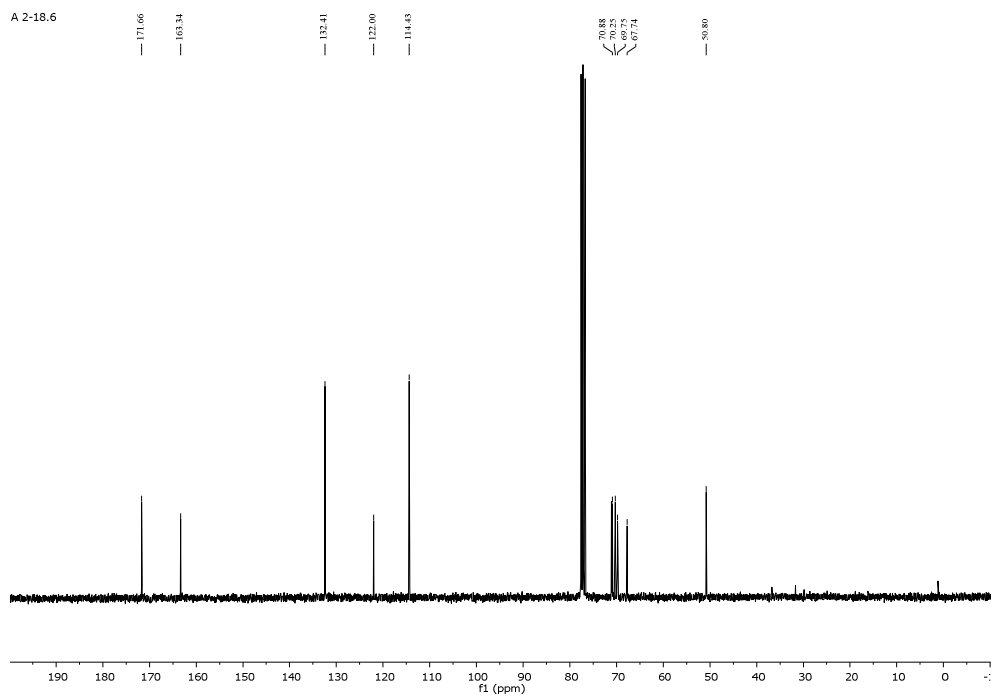
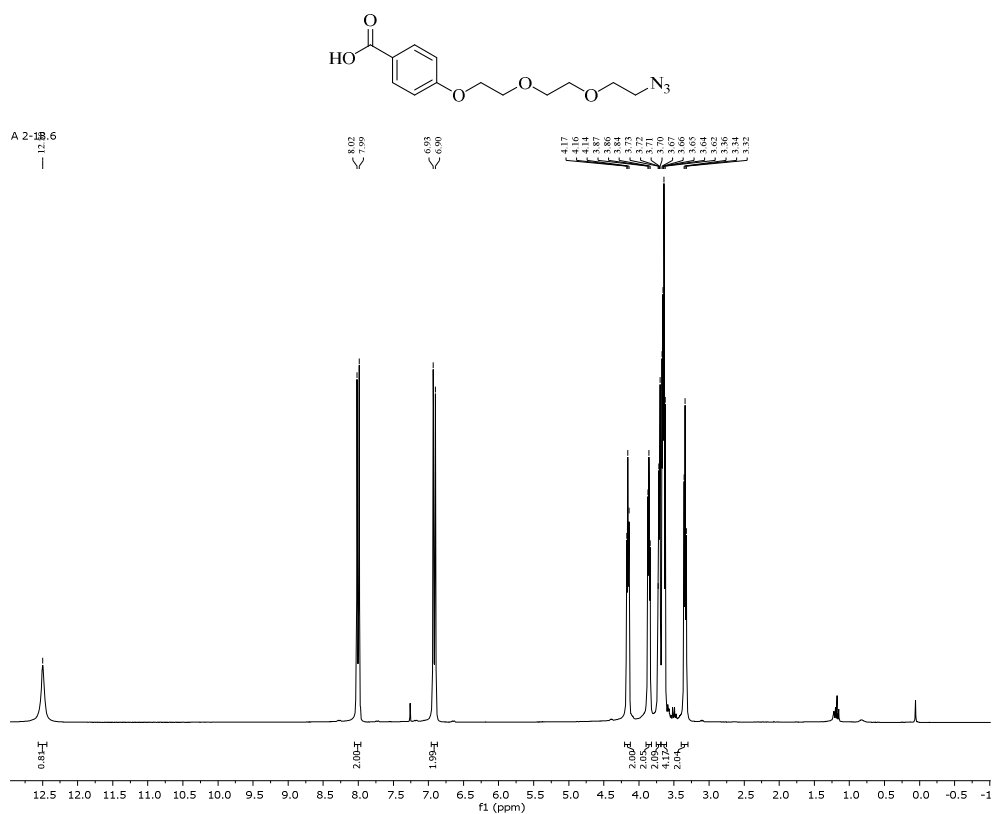


(2R,3R)-5,7-Dihydroxy-2-(3,4,5-trihydroxyphenyl)chroman-3-yl-(3,5-dihydroxy)benzoate (65g)

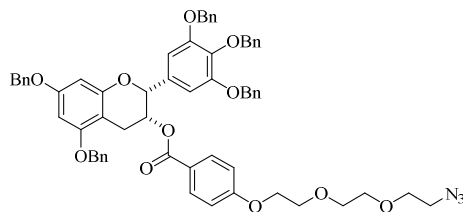
(2*R*,3*R*)-5,7-Dihydroxy-2-(3,4,5-trihydroxyphenyl)chroman-3-yl-(3-hydroxy)benzoate (65i)

(2*R*,3*R*)-5,7-Dihydroxy-2-(3,4,5-trihydroxyphenyl)chroman-3-yl-(3,4,5-trifluoro)benzoate (**65j**)

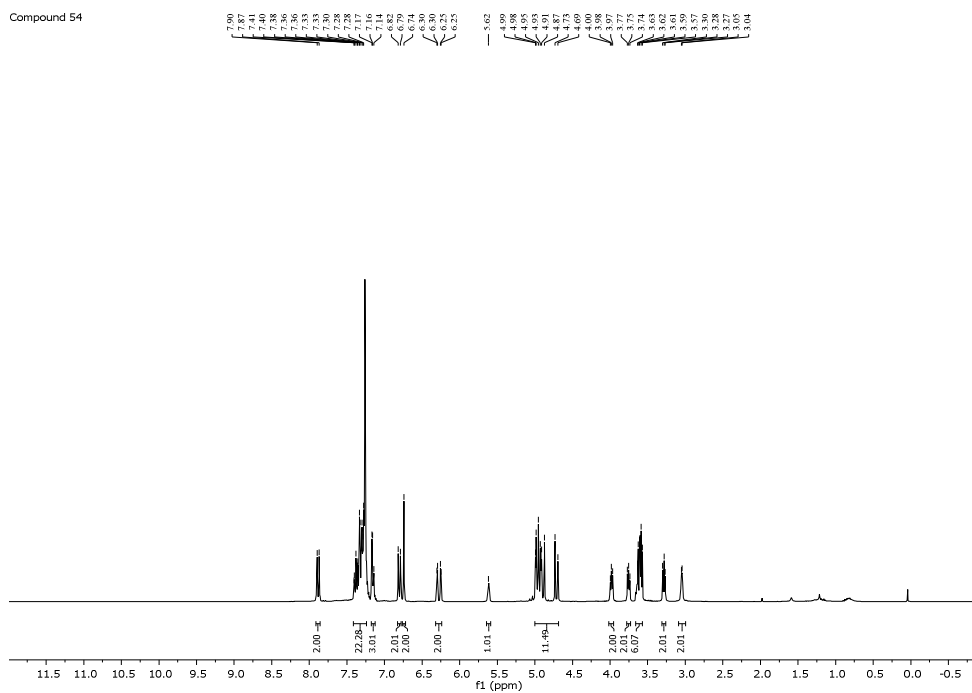


4-(2-(2-(2-azidoethoxy)ethoxy)ethoxy)benzoic acid (**53**)

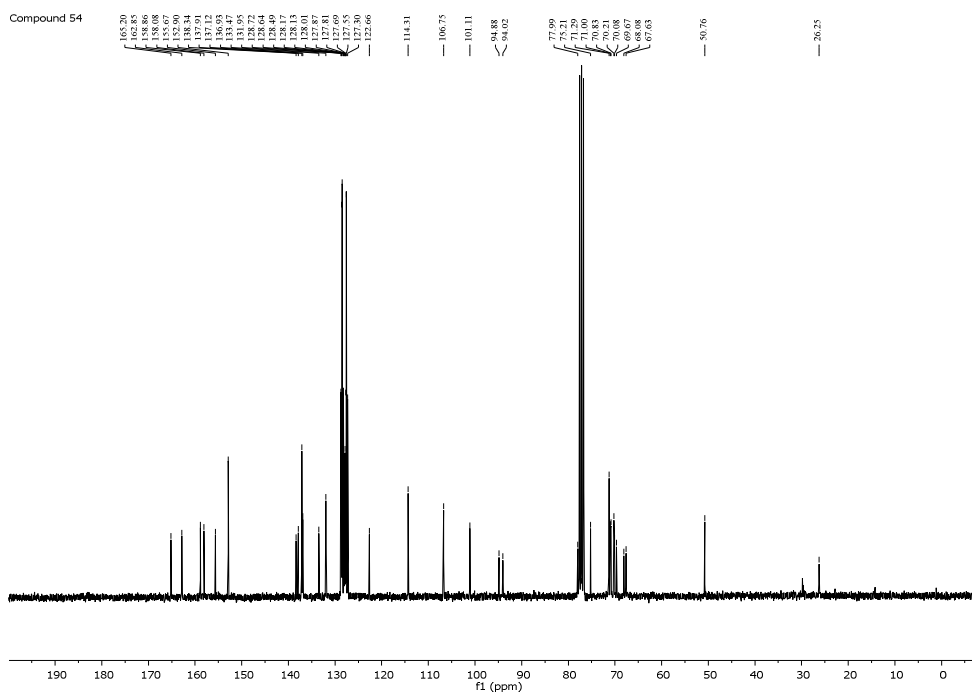
(2*R*,3*R*)-5,7-Bis(benzyloxy)-2-(3,4,5-tris(benzyloxy)phenyl)chroman-3-yl-4-(2-(2-(2-azidoethoxy)ethoxy)ethoxy)benzoate (**54**)



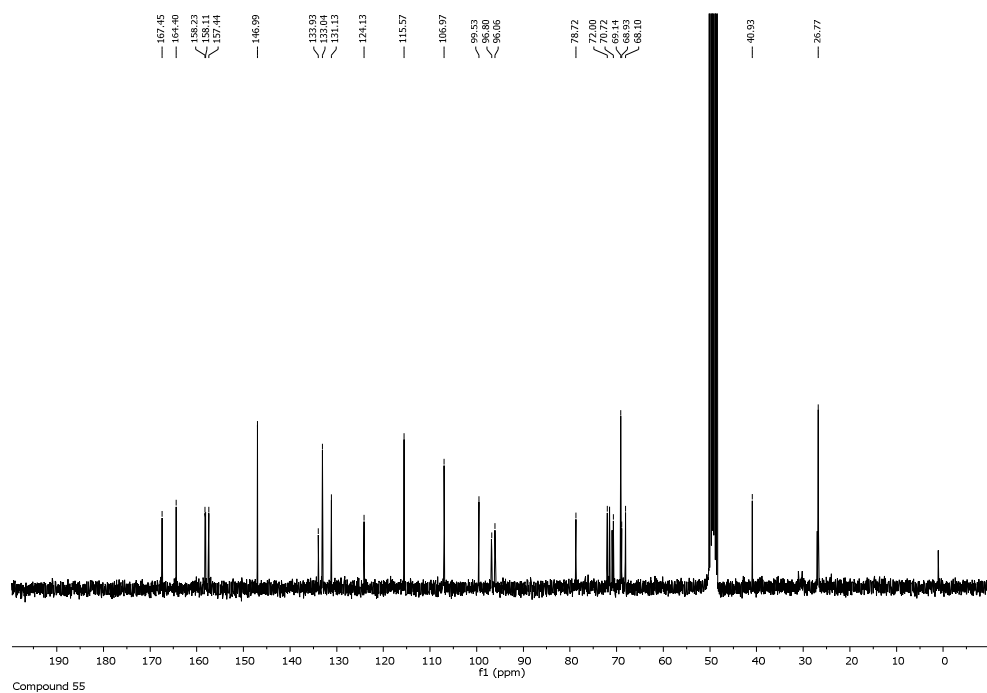
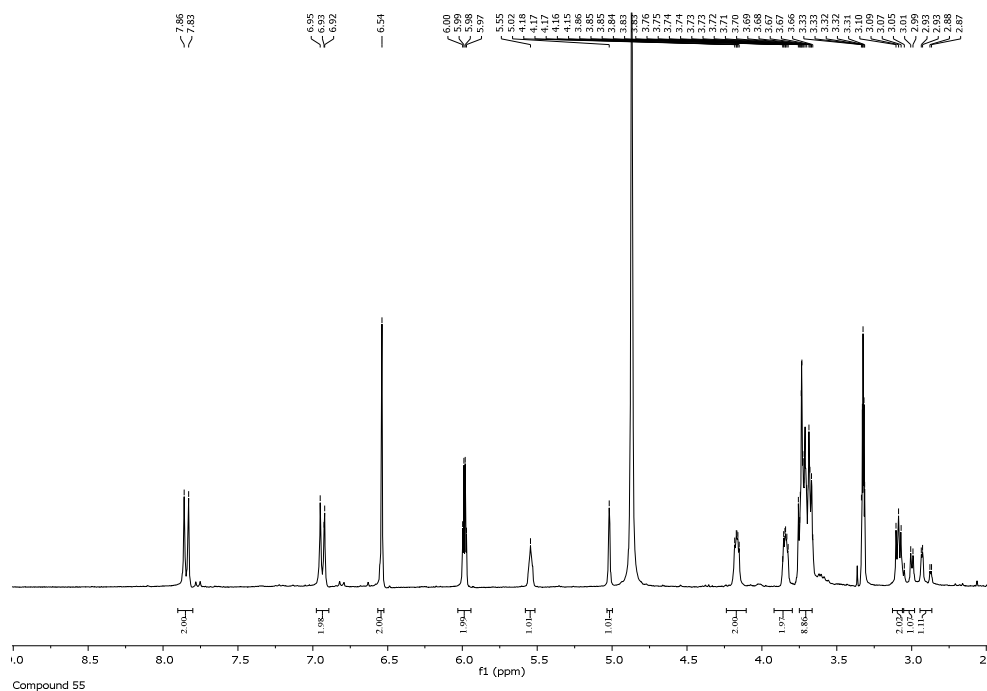
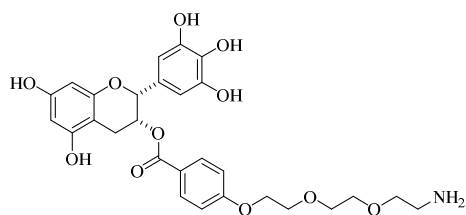
Compound 54



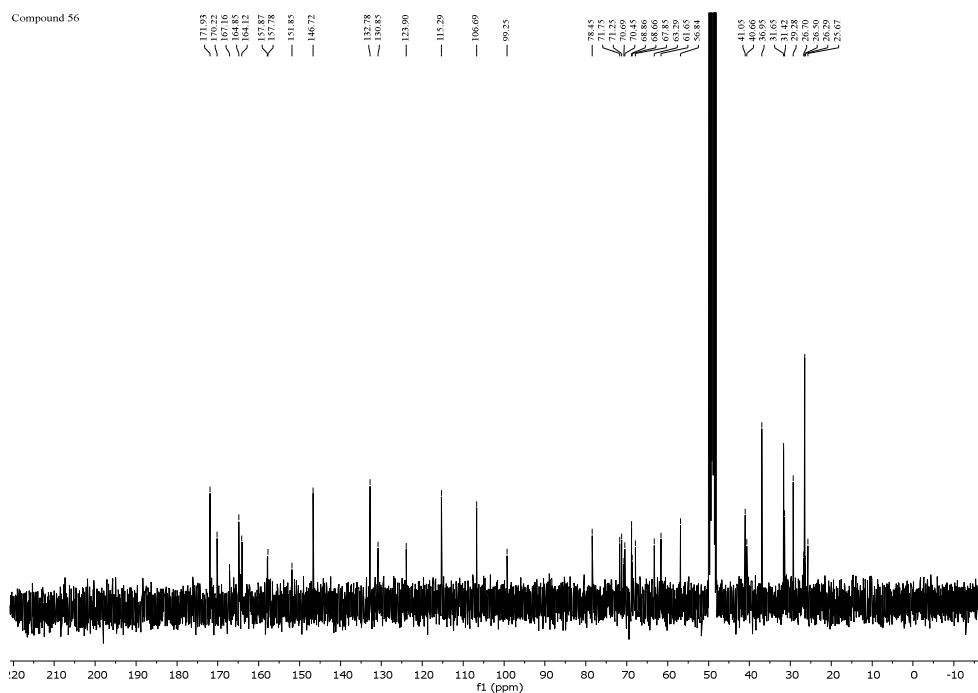
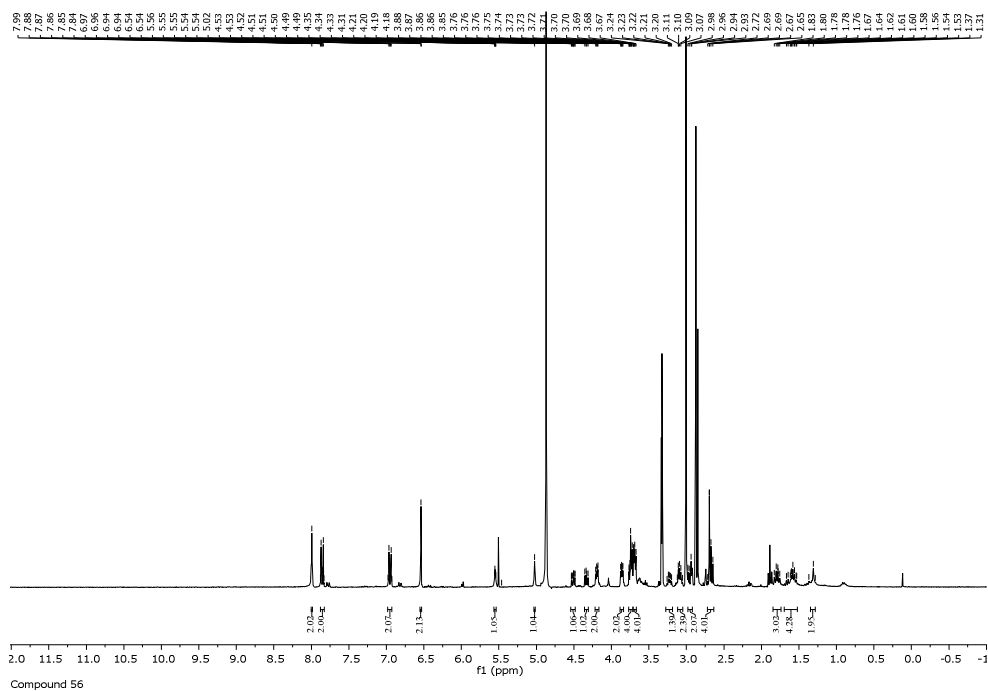
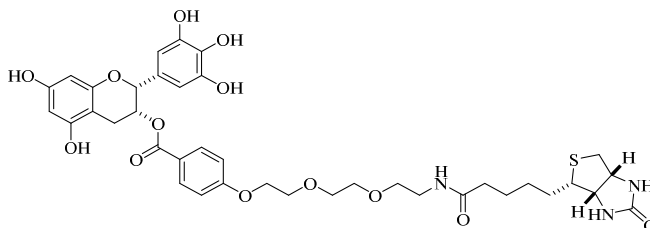
Compound 54



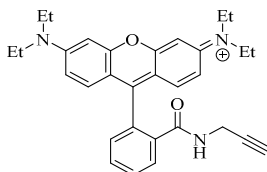
(2*R*,3*R*)-5,7-Dihydroxy-2-(3,4,5-trihydroxyphenyl)chroman-3-yl-4-(2-(2-(2-aminoethoxy)ethoxy)ethoxy)benzoate (**55**)



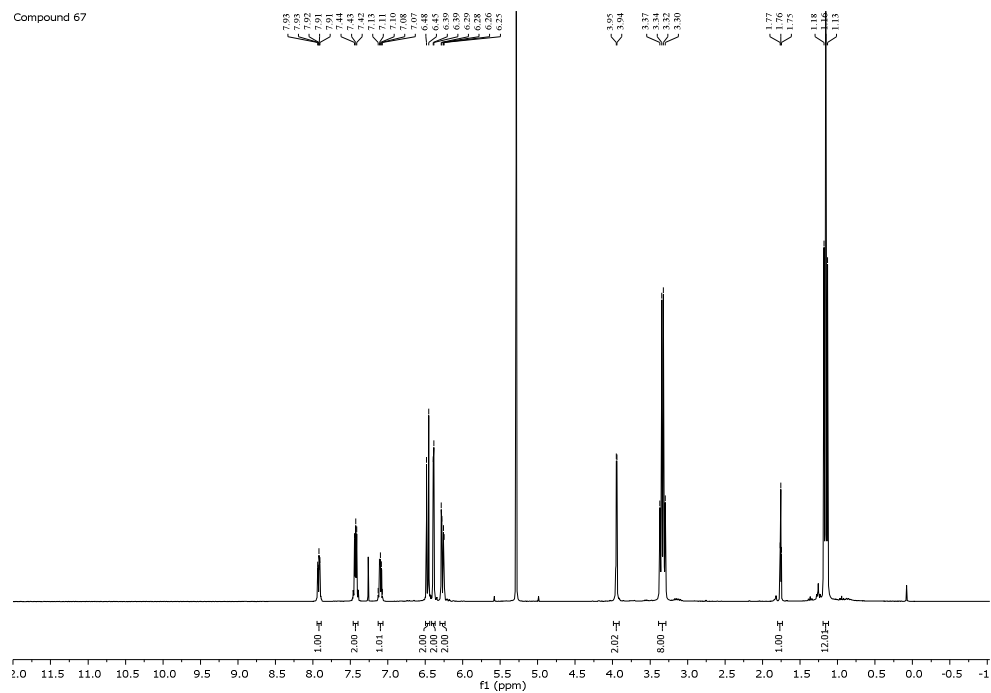
(2*R*,3*R*)-5,7-Dihydroxy-2-(3,4,5-trihydroxyphenyl)chroman-3-yl 4-(2-(2-(2-(5-((3*aS*,4*S*,6*aR*)-2-oxohexahydro-1*H*-thieno[3,4-*d*]imidazol-4-yl)pentanamido)ethoxy)ethoxy)ethoxy)benzoate (**56**)



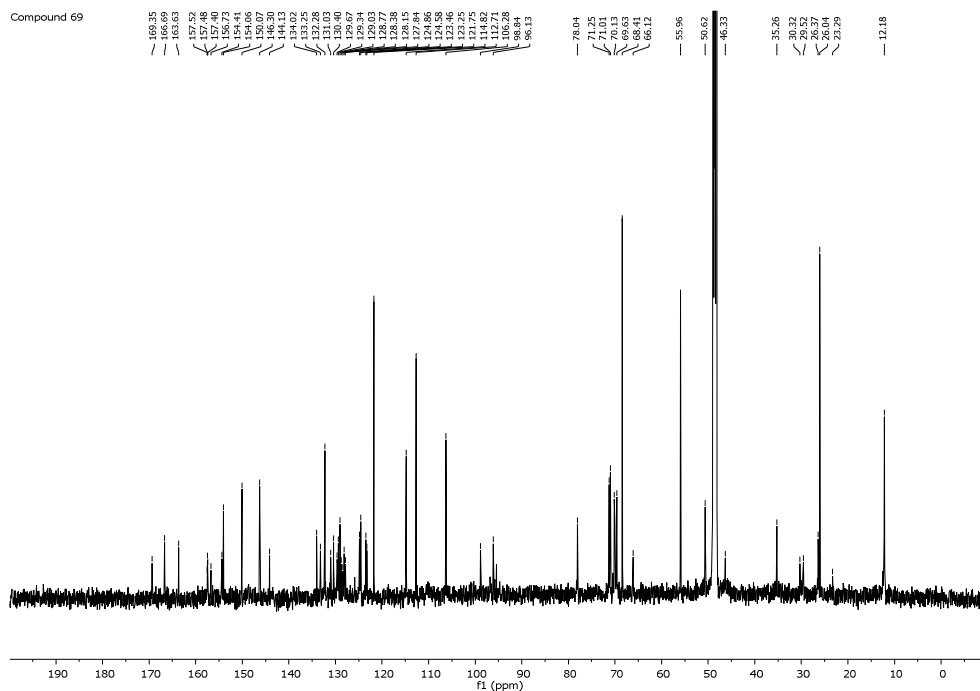
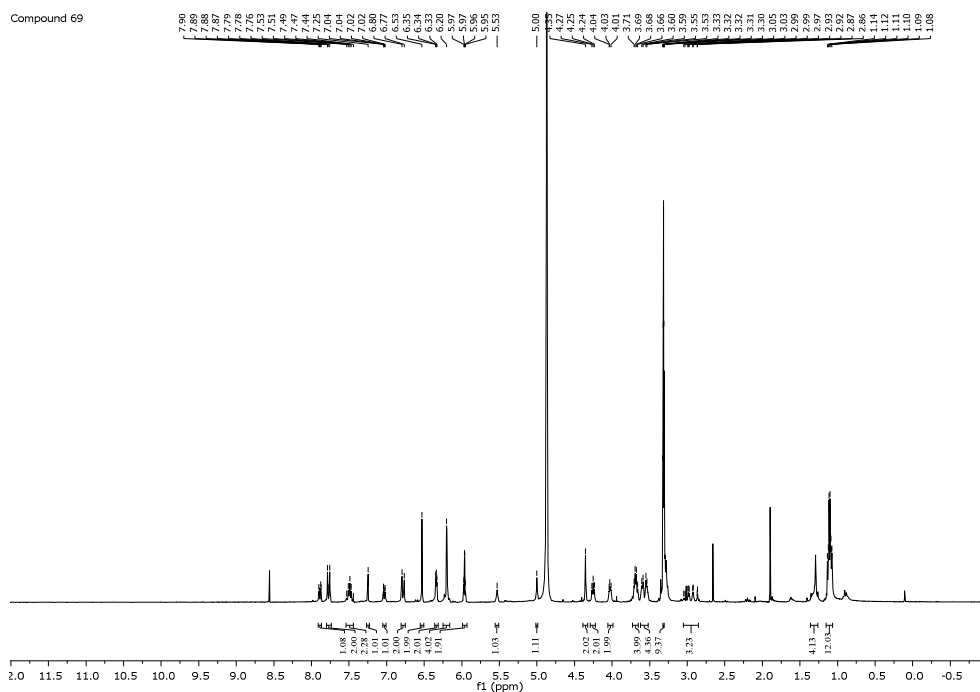
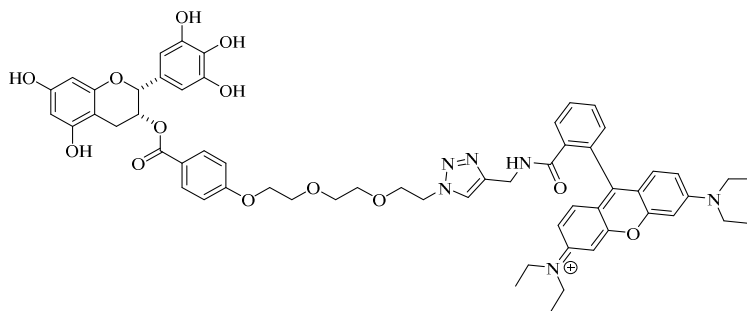
N-(6-(diethylamino)-9-(2-(prop-2-yn-1-ylcarbamoyl)phenyl)-3*H*-xanthen-3-ylidene)-*N*-ethyl ethanaminium (**67**)

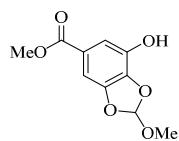


Compound 67

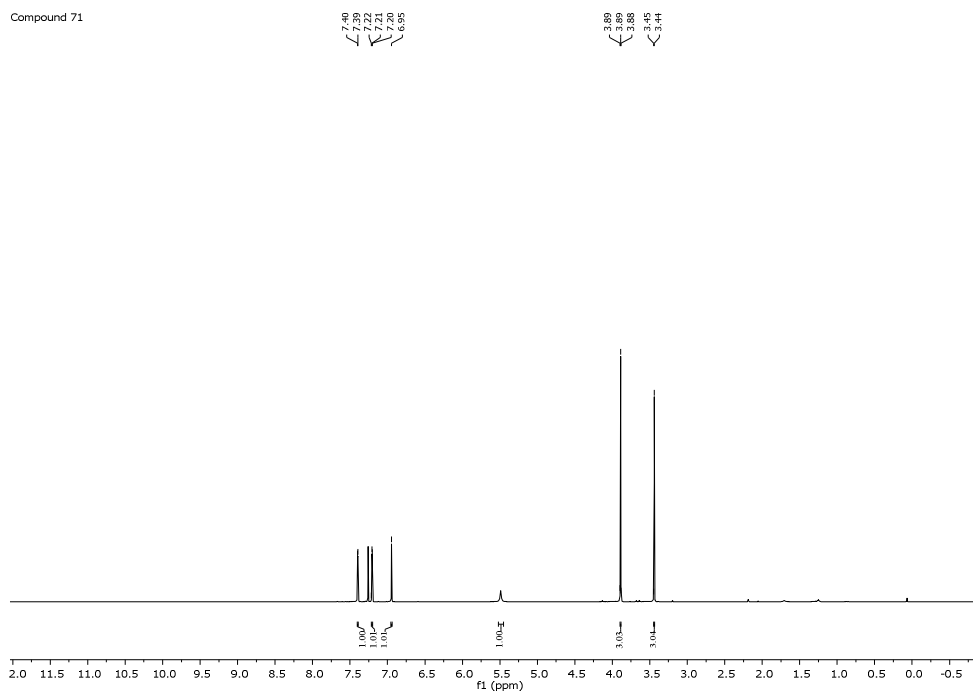


N-(6-(diethylamino)-9-(2-(((1-(2-(2-(2-(4-(((2*R*,3*R*)-5,7-dihydroxy-2-(3,4,5-trihydroxy phenyl) chroman-3-yl)oxy)carbonyl)phenoxy)ethoxy)ethoxy)ethyl)-1*H*-1,2,3-triazol-4-yl)methyl) (69)

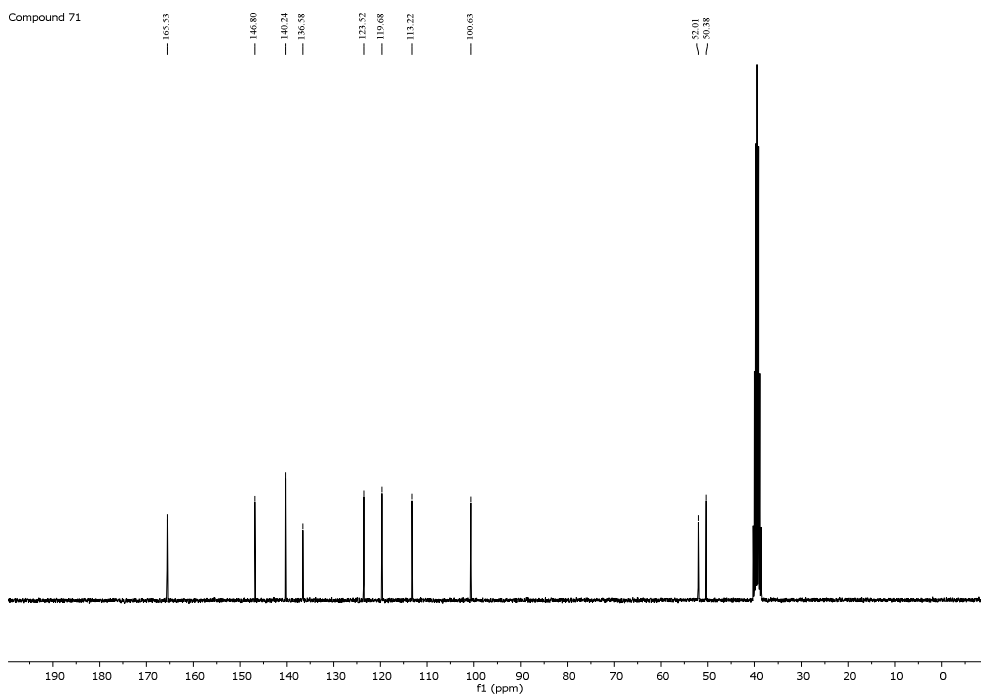


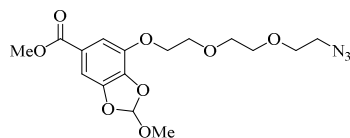
Methyl 7-hydroxy-2-methoxybenzo[d][1,3]dioxole-5-carboxylate (**71**)

Compound 71

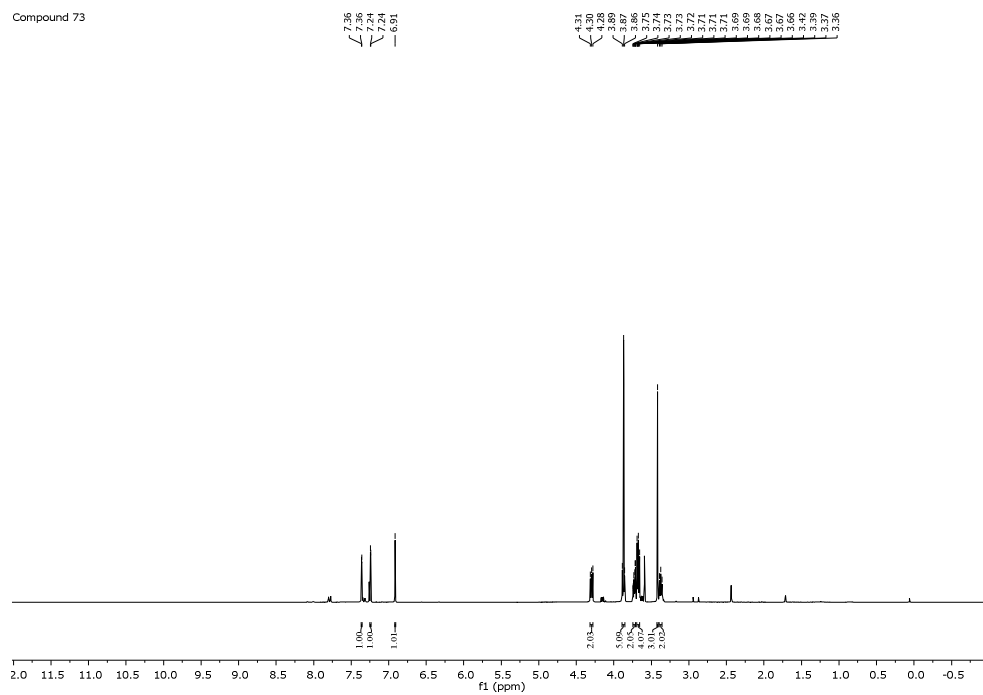


Compound 71

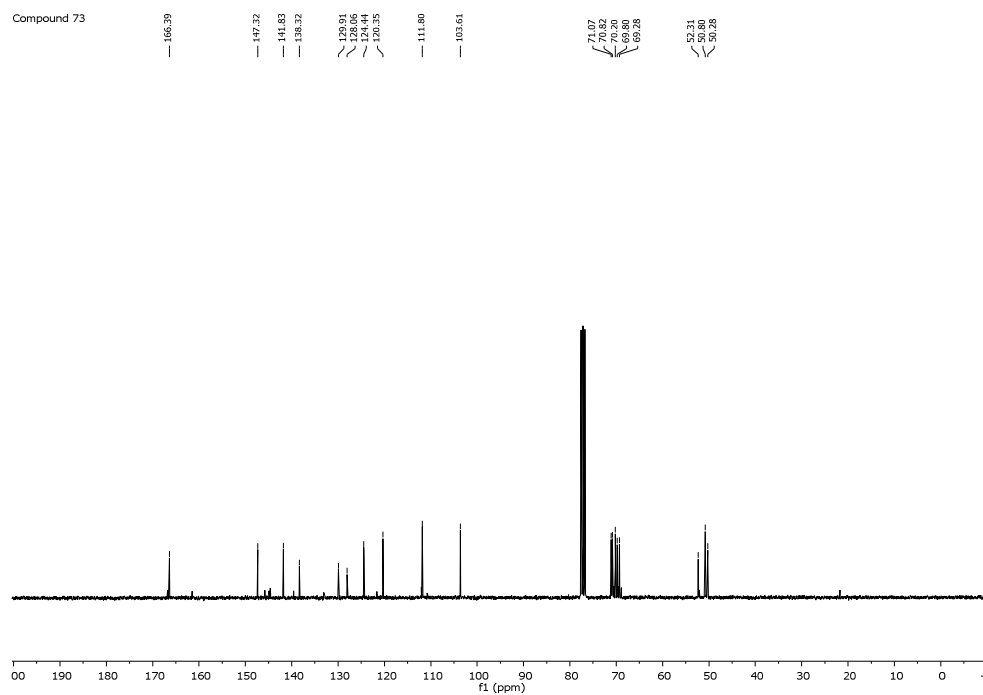


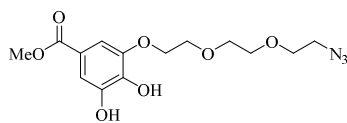
Methyl 7-(2-(2-(2-azidoethoxy)ethoxy)ethoxy)-2-methoxybenzo[*d*][1,3]dioxole-5-carboxylate
(73)

Compound 73

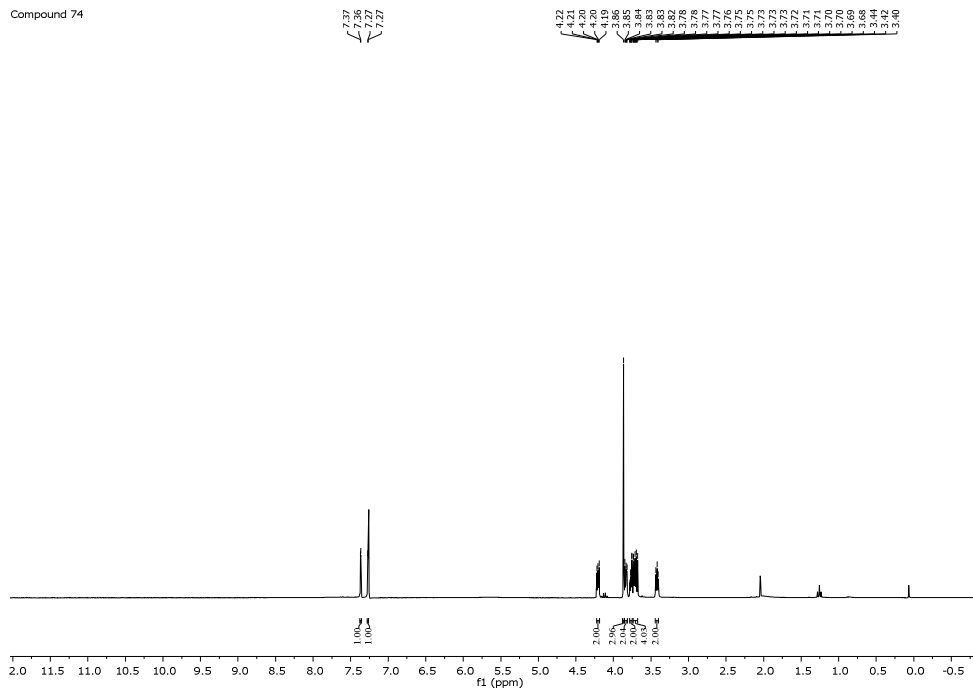


Compound 73

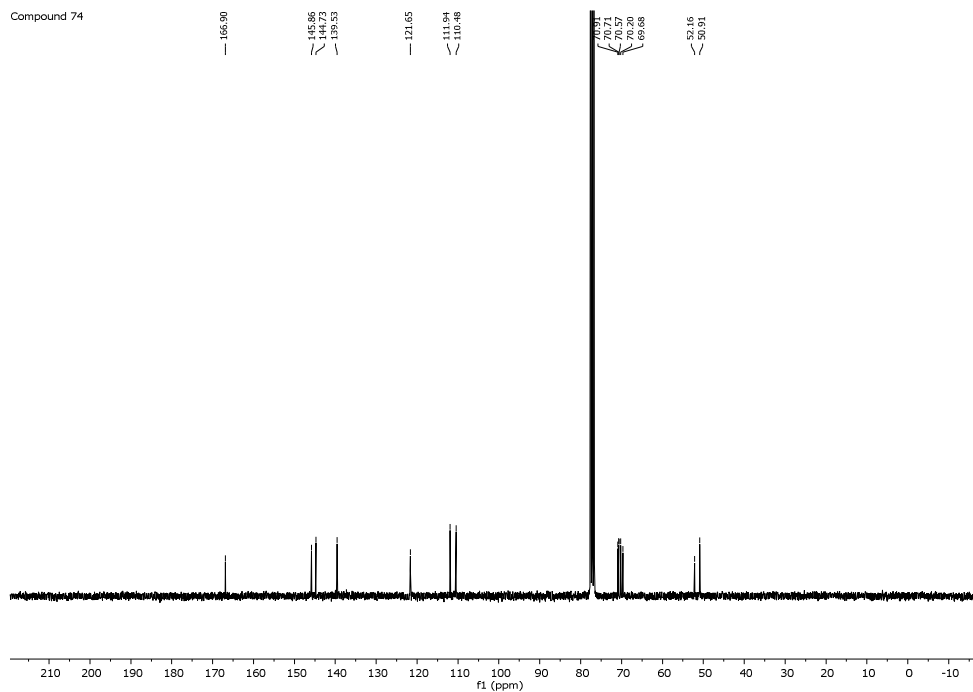


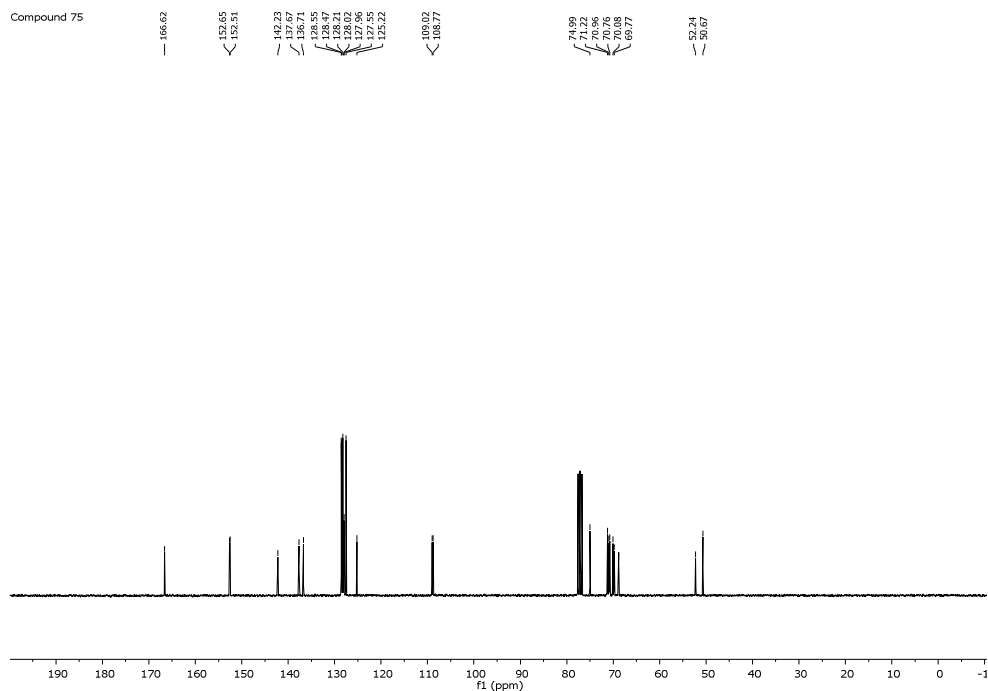
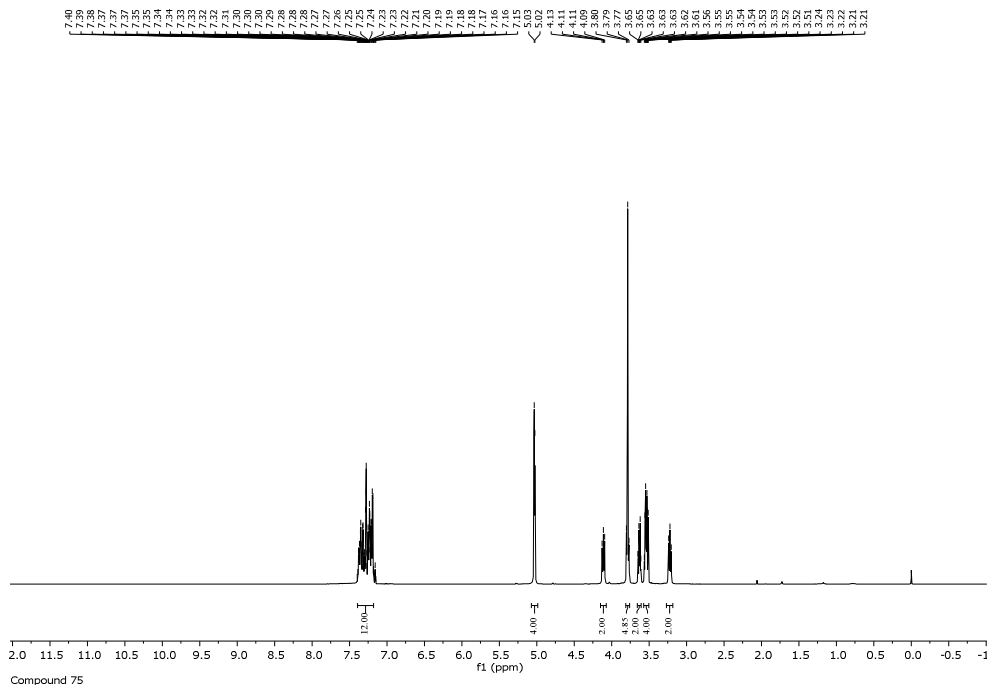
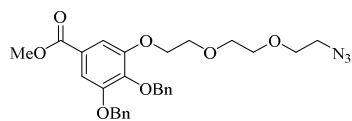
Methyl 3-(2-(2-(2-azidoethoxy)ethoxy)ethoxy)-4,5-dihydroxybenzoate (**74**)

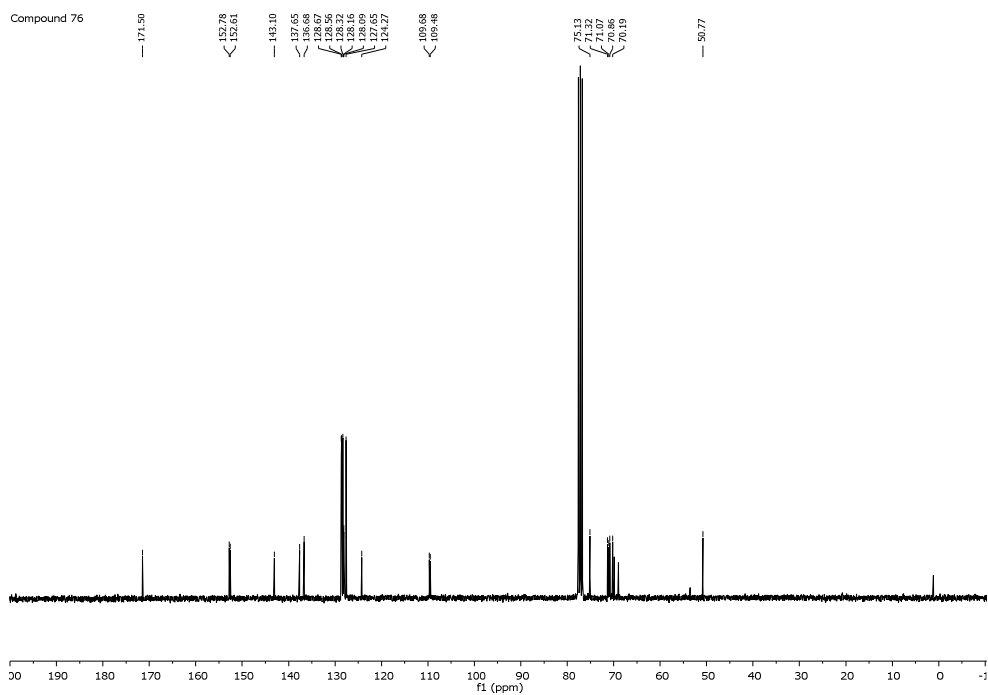
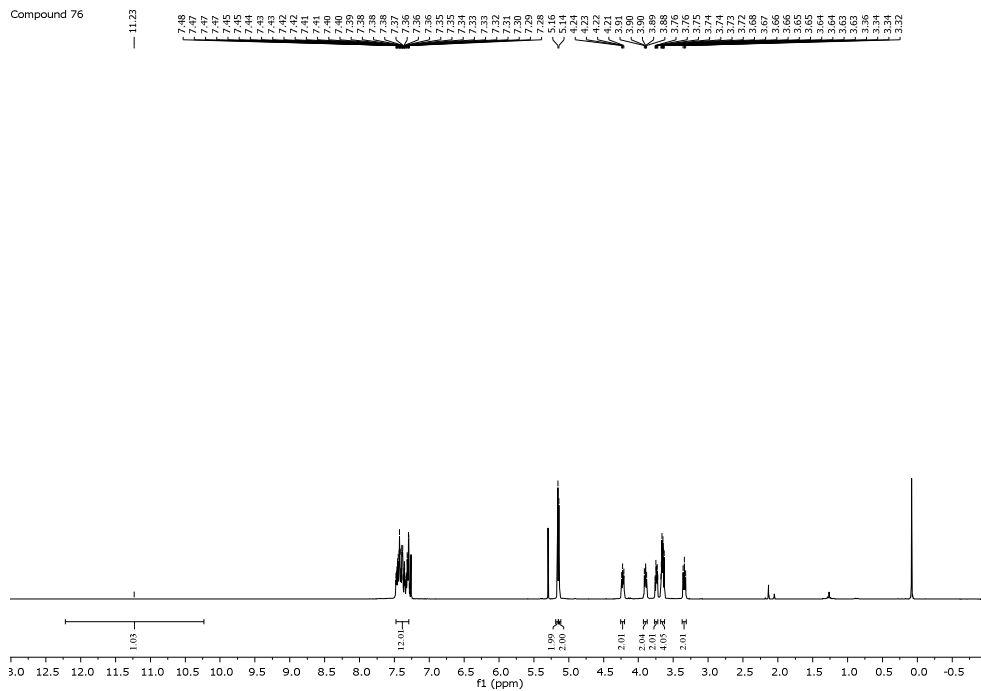
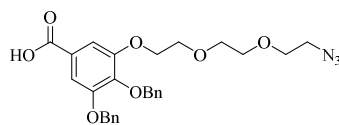
Compound 74



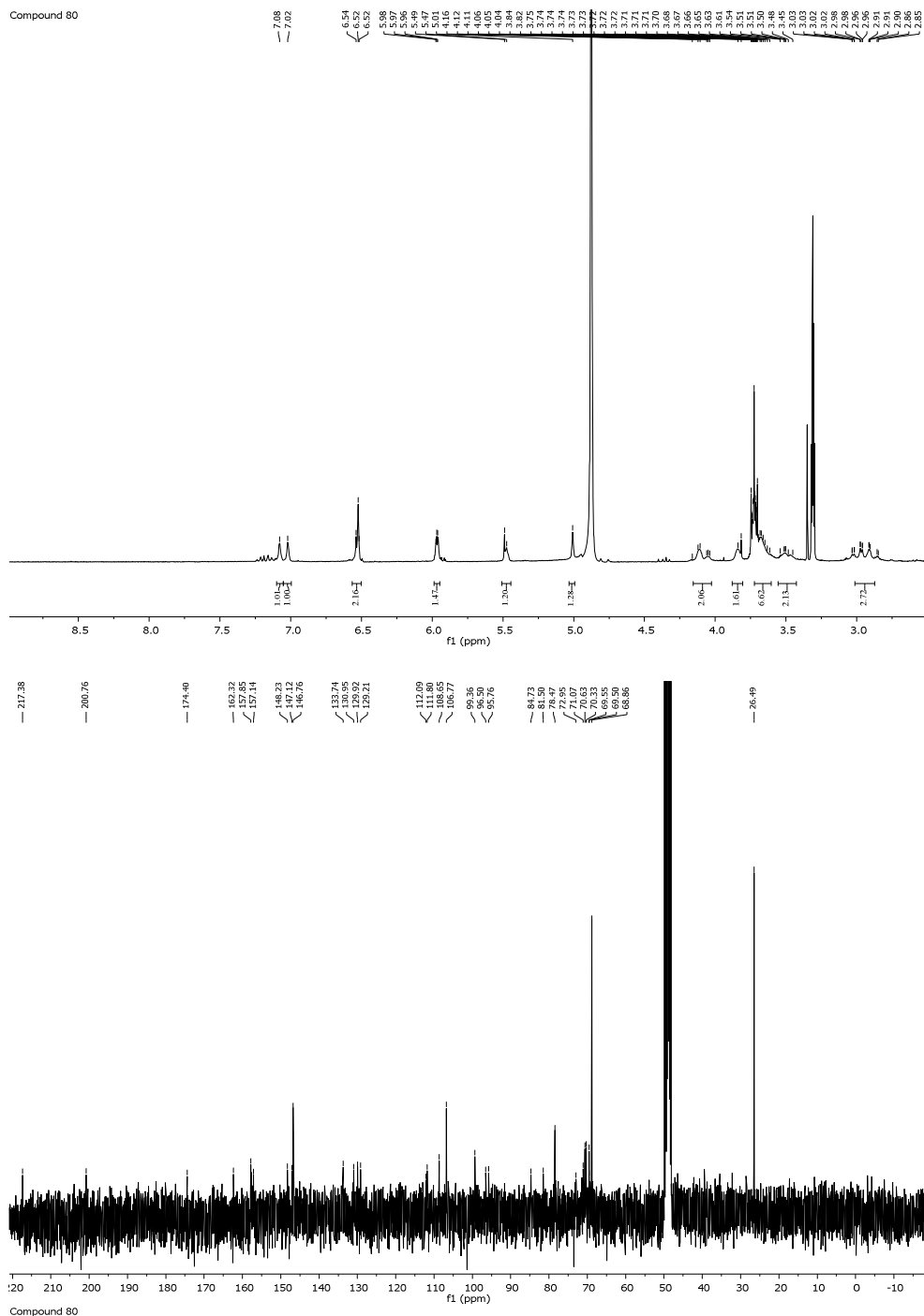
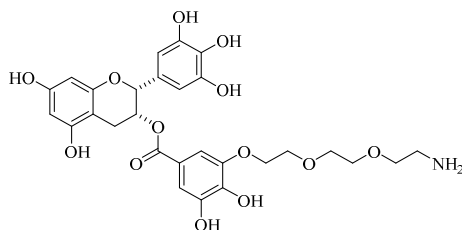
Compound 74



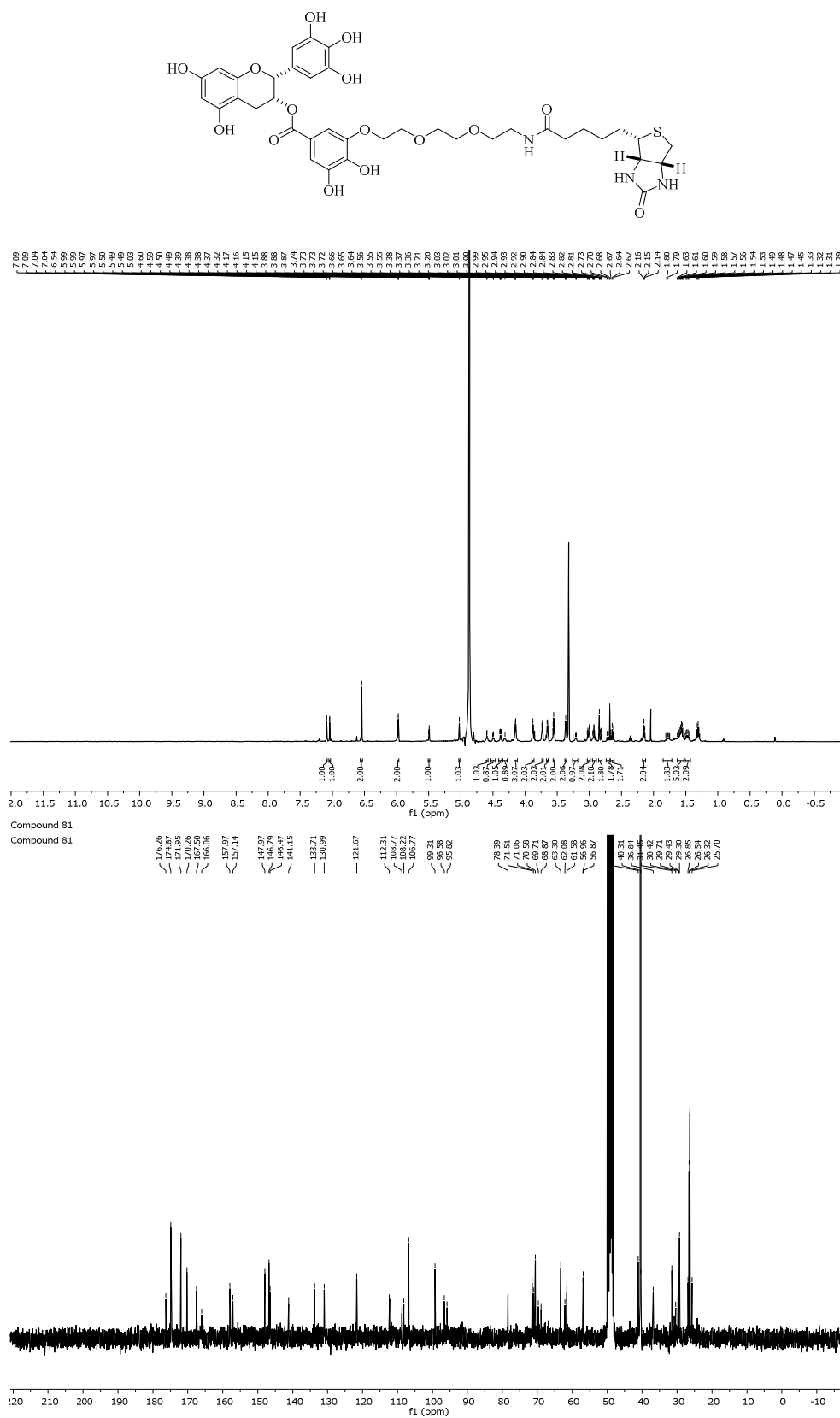
Methyl 3-(2-(2-(2-azidoethoxy)ethoxy)ethoxy)-4,5-dihydroxybenzoate (**75**)

3-(2-(2-(2-azidoethoxy)ethoxy)ethoxy)-4,5-bis(benzyloxy)benzoate (**76**)

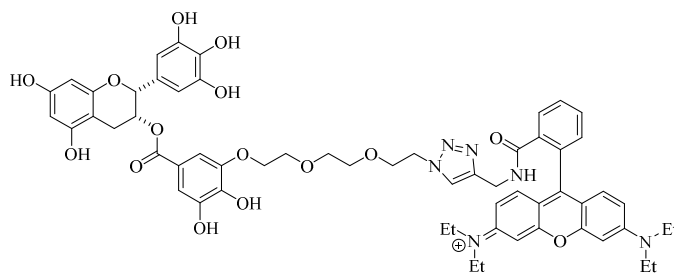
(2*R*,3*R*)-5,7-Dihydroxy-2-(3,4,5-trihydroxyphenyl)chroman-3-yl-3-(2-(2-(2-amino ethoxy)ethoxy)ethoxy)-4,5-dihydroxybenzoate (**80**)



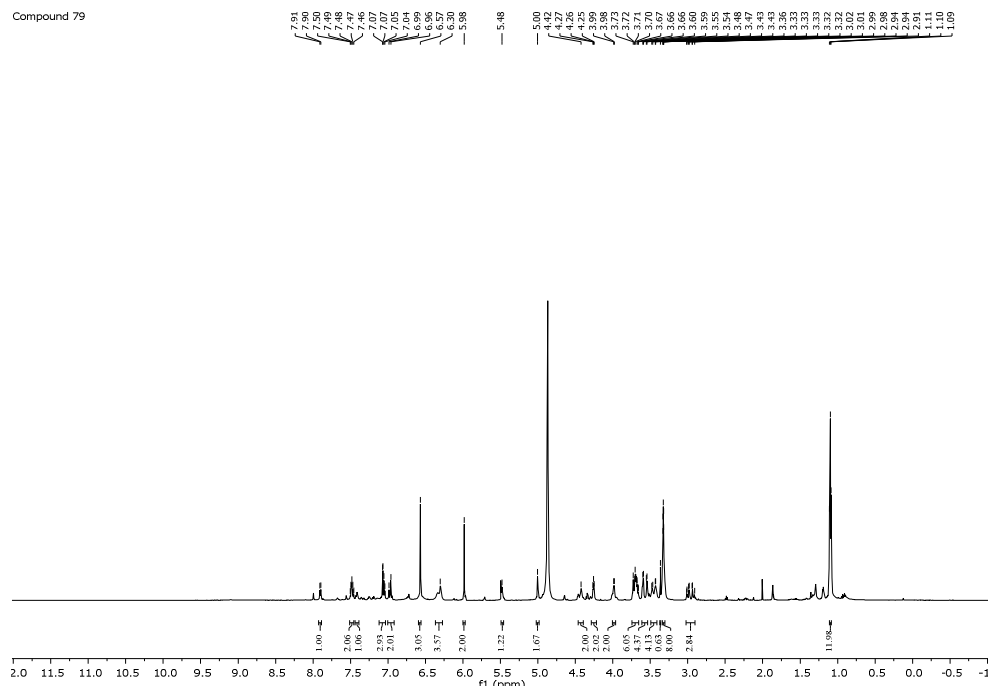
(2*R*,3*R*)-5,7-Dihydroxy-2-(3,4,5-trihydroxyphenyl)chroman-3-yl-3,4-dihydroxy-5-(2-(2-(2-(5-((3*aS*,4*S*,6*aR*)-2-oxohexahydro-1*H*-thieno[3,4-*d*]imidazol-4-yl)pentanamido)ethoxy)ethoxy)ethoxy)benzoate (**81**)



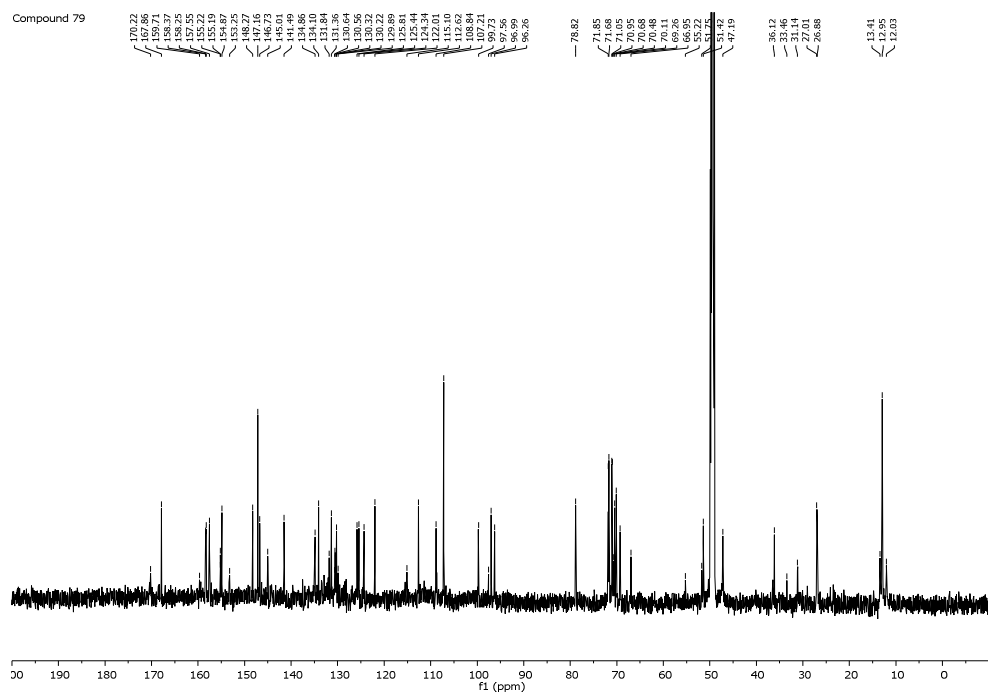
N-(6-(diethylamino)-9-(2-(((1-(2-(2-(2-(5-(((2*R*,3*R*)-5,7-dihydroxy-2-(3,4,5-trihydroxyphenyl)chroman-3-yl)oxy)carbonyl)-2,3-dihydroxyphenoxy)ethoxy)ethoxy)ethyl)-1*H*-1,2,3-triazol-4-yl)methyl)carbamoyl)phenyl)-3*H*-xanthen-3-ylidene)-*N*-ethylethan-aminium (**79**)



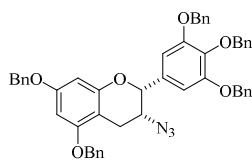
Compound 79



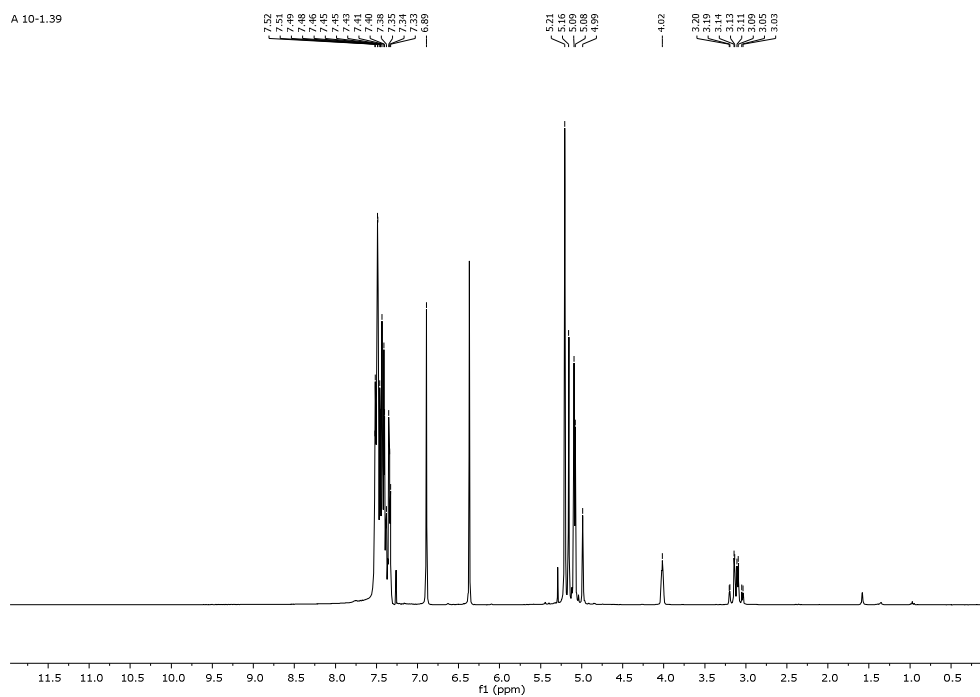
Compound 79



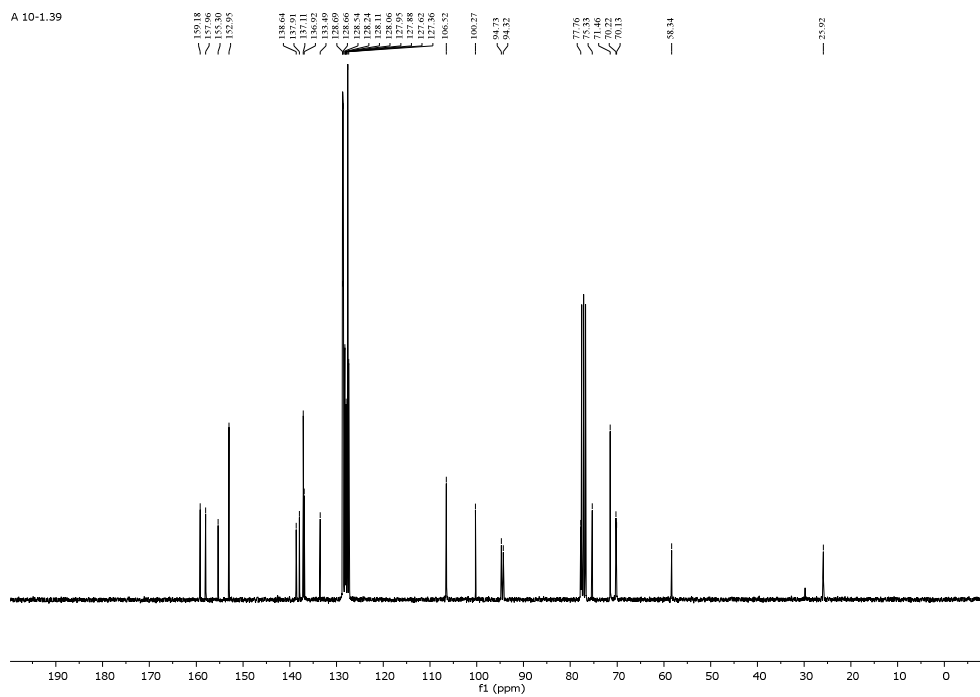
(2*R*,3*R*)-3-Azido-5,7-bis(benzyloxy)-2-(3,4,5-tris(benzyloxy)phenyl)-chromane (**85**)

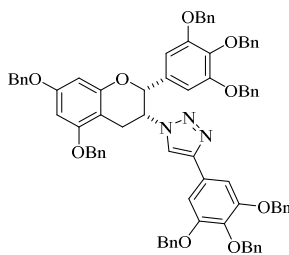


A 10-1.39

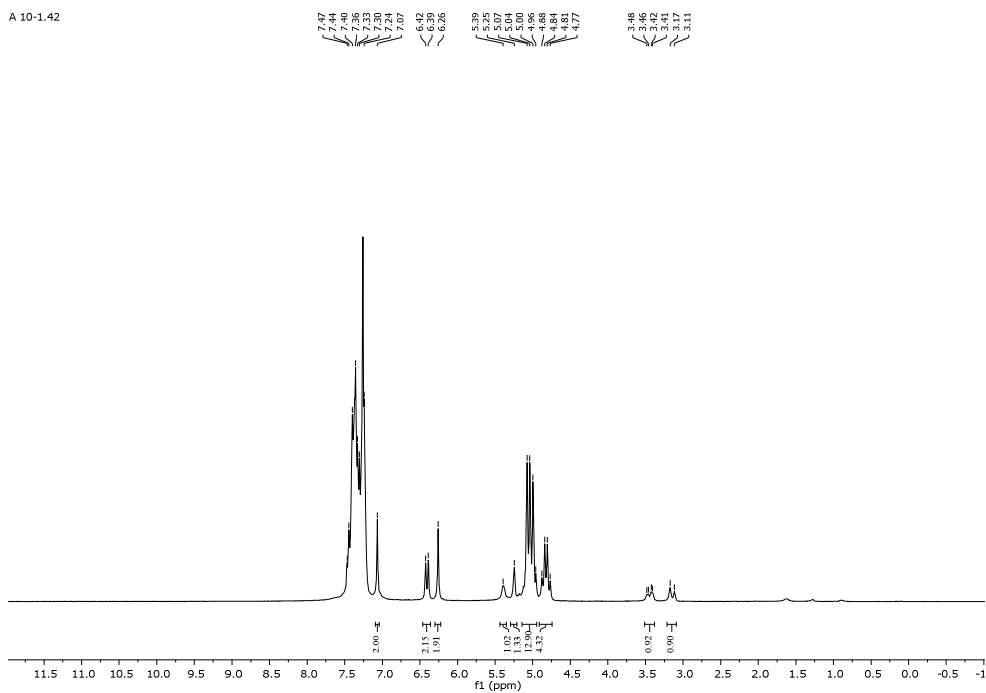


A 10-1.39

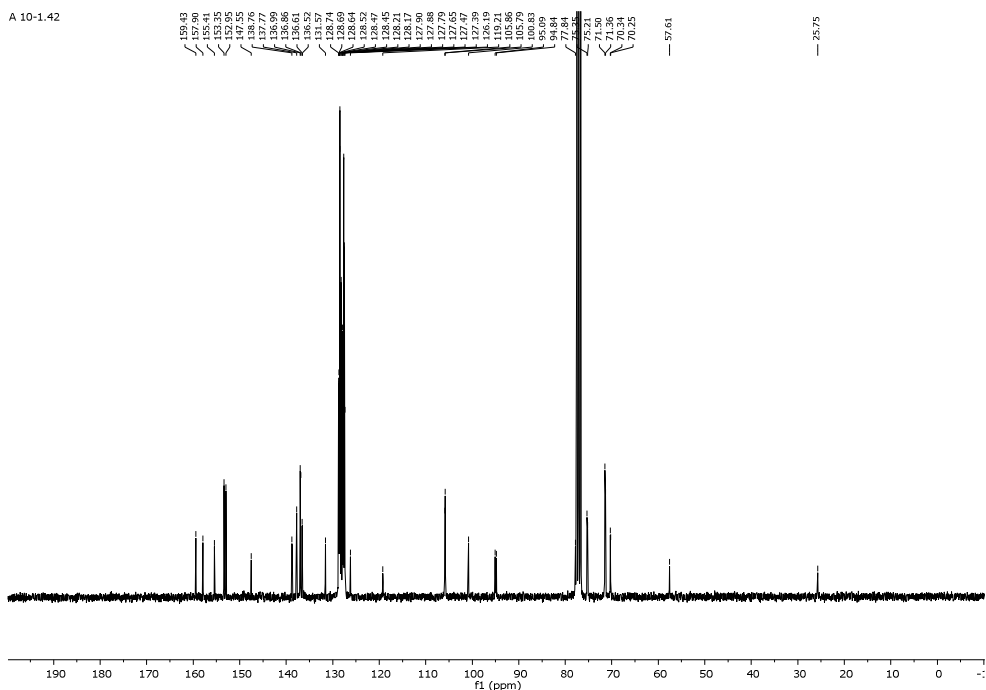


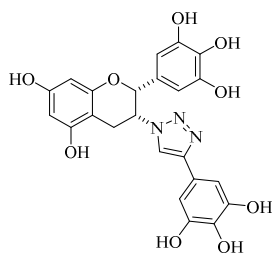
1-((2*R*,3*R*)-5,7-Bis(benzyloxy)-2-(3,4,5-tris(benzyloxy)phenyl)chroman-3-yl)-4-(3,4,5-tris(benzyloxy)phenyl)-1*H*-1,2,3-triazole (**91**)

A 10-1.42

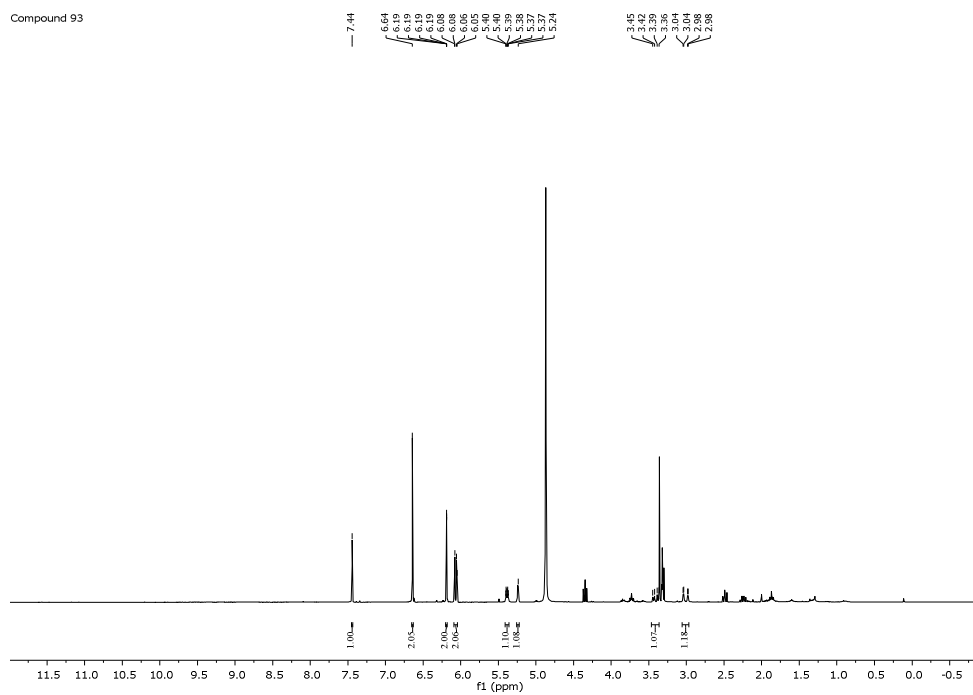


A 10-1.42

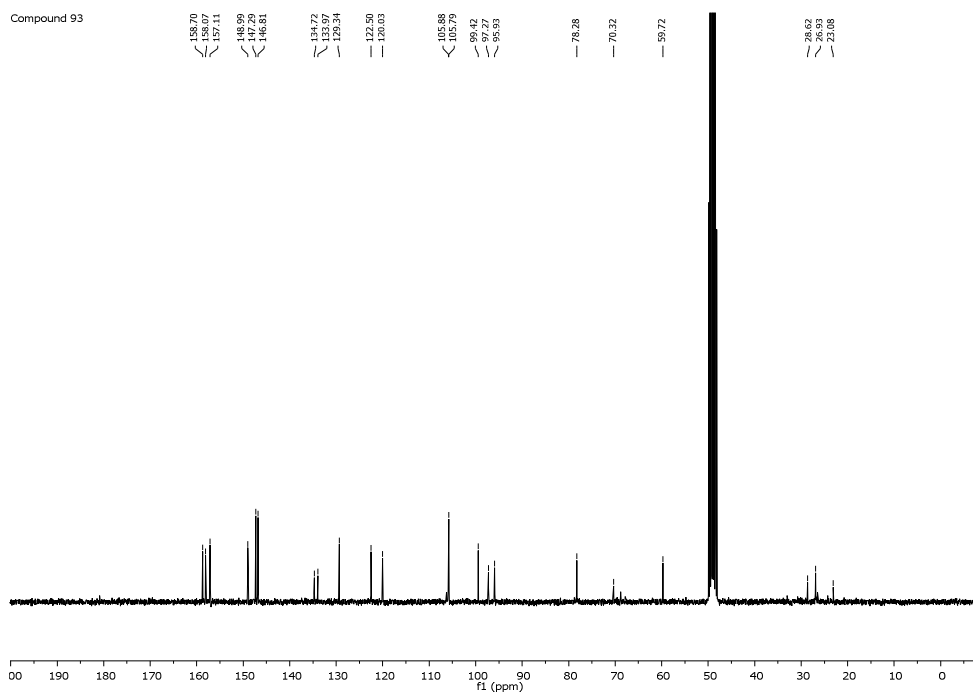


1-((2*R*,3*R*)-5,7-Dihydroxy-2-(3,4,5-trihydroxy)phenylchroman-3-yl)-4-(3,4,5-trihydroxy)phenyl)-1*H*-1,2,3-triazole (**93**)

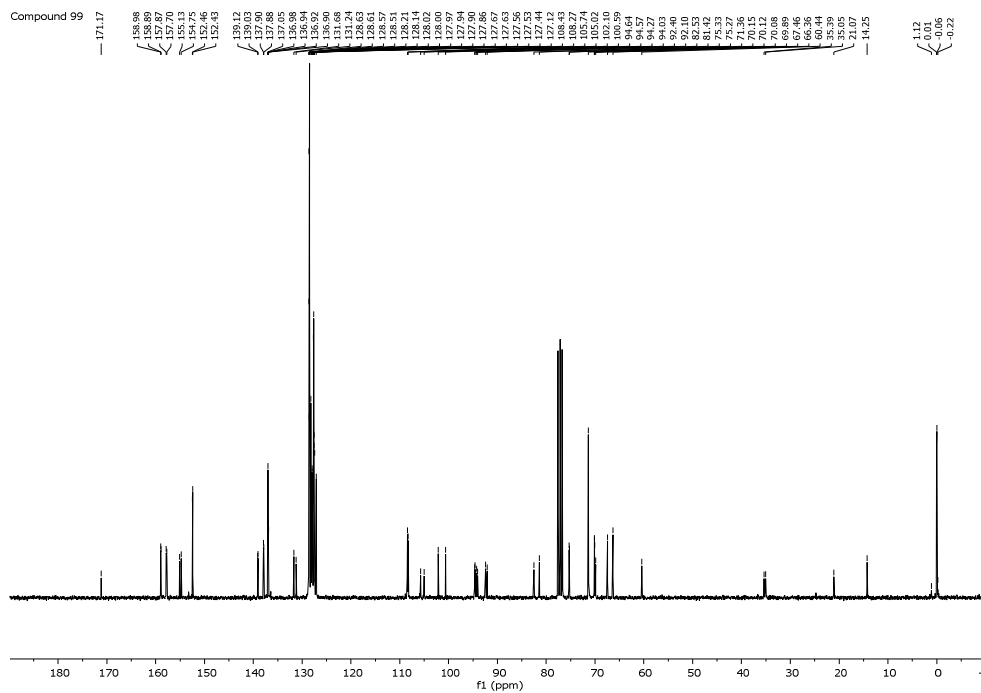
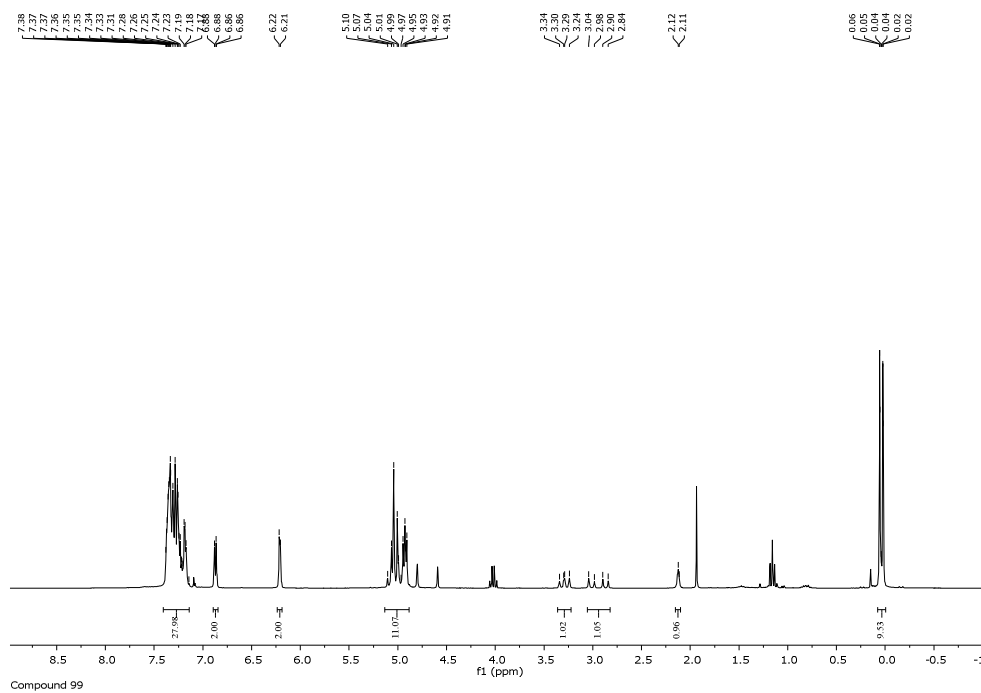
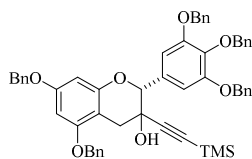
Compound 93



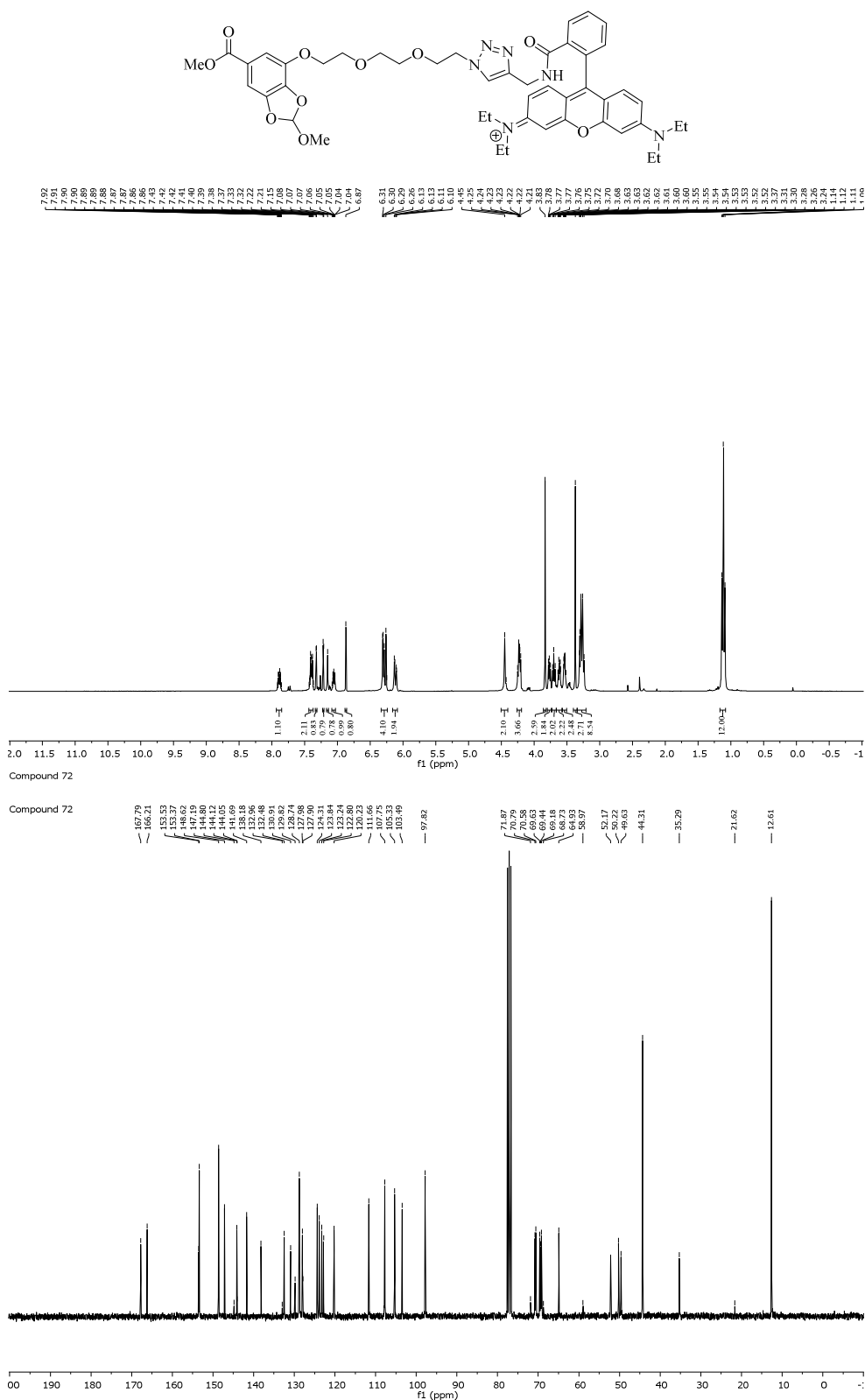
Compound 93

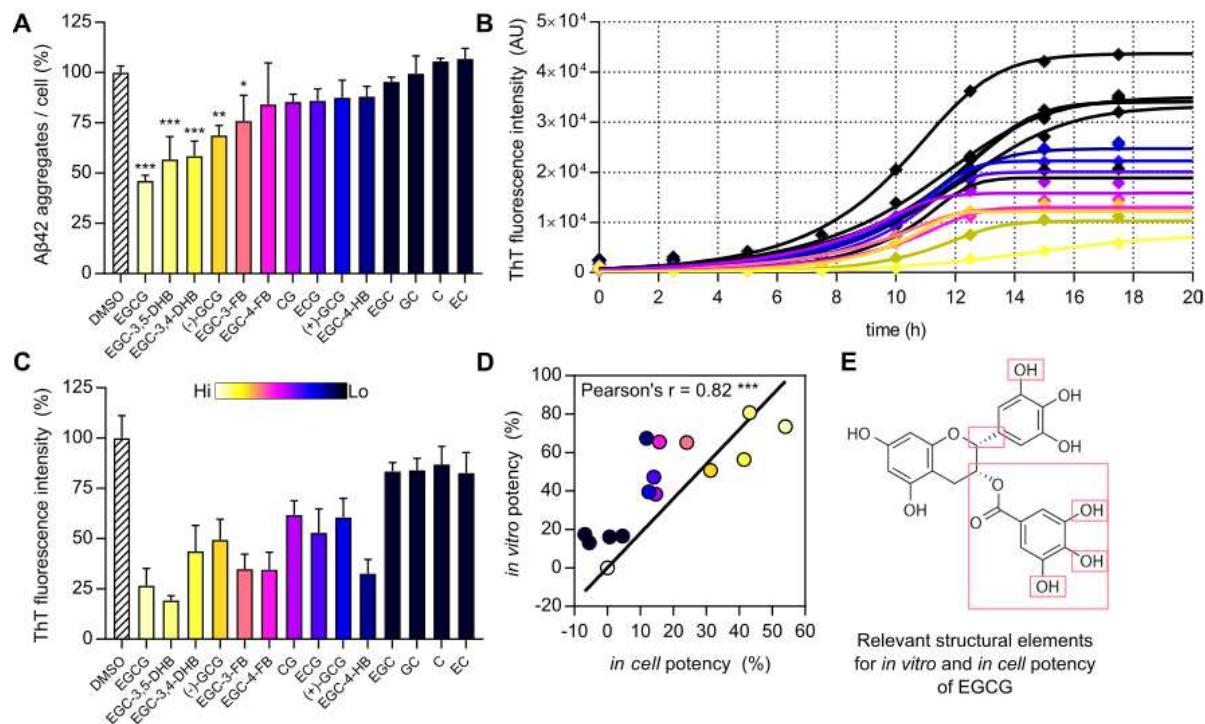


(2*R*)-5,7-Bis(benzyloxy)-3-((trimethylsilyl)ethynyl)-2-(3,4,5-tris(benzyloxy)phenyl)chroman-3-ol (**99**)



N-(6-(diethylamino)-9-(2-(((1-(2-(2-(2-((2-methoxy-6-(methoxycarbonyl)benzo[*d*][1,3]dioxol-4-yl)oxy)ethoxy)ethoxy)ethyl)-1*H*-1,2,3-triazol-4-yl)methyl)carbamoyl)phenyl)-3*H*-xanthen-3-ylidene)-*N*-ethylethanaminium (**72**)



Modulation of A β 42 *in Vitro*

Abbreviation	Derivative name	Systematic name	Inhibition <i>in vitro</i> (%)	Degradation <i>in cells</i> (%) ▼
EGCG	(-)-Epigallocatechin gallate	(2R,3R)-5,7-dihydroxy-2-(3,4,5-trihydroxyphenyl)chroman-3-yl 3,4,5-trihydroxybenzoate	73.4 ± 8.6	54.0 ± 3.0
EGC-3,5-DHB	(-)-Epigallocatechin-3,5-dihydroxybenzoate	(2R,3R)-5,7-dihydroxy-2-(3,4,5-trihydroxyphenyl)chroman-3-yl 3,5-dihydroxybenzoate	80.8 ± 2.4	43.2 ± 11.4
EGC-3,4-DHB	(-)-Epigallocatechin-3,4-dihydroxybenzoate	(2R,3R)-5,7-dihydroxy-2-(3,4,5-trihydroxyphenyl)chroman-3-yl 3,4-dihydroxybenzoate	56.4 ± 13.0	41.5 ± 7.5
(-)-GCG	(-)-Gallocatechin gallate	(2S,3R)-5,7-dihydroxy-2-(3,4,5-trihydroxyphenyl)chroman-3-yl 3,4,5-trihydroxybenzoate	50.6 ± 10.3	31.3 ± 5.0
EGC-3-FB	(-)-Epigallocatechin 3-fluorobenzoate	(2R,3R)-5,7-dihydroxy-2-(3,4,5-trihydroxyphenyl)chroman-3-yl 3-fluorobenzoate	65.2 ± 7.5	24.1 ± 12.8
EGC-4-FB	(-)-Epigallocatechin 4-fluorobenzoate	(2R,3R)-5,7-dihydroxy-2-(3,4,5-trihydroxyphenyl)chroman-3-yl 4-fluorobenzoate	65.5 ± 8.8	15.8 ± 20.6
CG	(-)-Catechin gallate	(2S,3R)-2-(3,4-dihydroxyphenyl)-5,7-dihydroxychroman-3-yl 3,4,5-trihydroxybenzoate	38.3 ± 7.2	14.7 ± 3.9
EGC	(-)-Epicatechin gallate	(2R,3R)-2-(3,4-dihydroxyphenyl)-5,7-dihydroxychroman-3-yl 3,4,5-trihydroxybenzoate	47.1 ± 12.0	14.1 ± 6.0
(+)-GCG	(+)-Gallocatechin gallate	(2R,3S)-5,7-dihydroxy-2-(3,4,5-trihydroxyphenyl)chroman-3-yl 3,4,5-trihydroxybenzoate	39.5 ± 9.6	12.6 ± 8.9
EGC-4-HB	(-)-Epigallocatechin 4-hydroxybenzoate	(2R,3R)-5,7-dihydroxy-2-(3,4,5-trihydroxyphenyl)chroman-3-yl 4-hydroxybenzoate	67.4 ± 7.0	11.9 ± 5.1
EGC	(-)-Epigallocatechin	(2R,3R)-2-(3,4,5-trihydroxyphenyl)-chroman-3,5,7-triol	16.6 ± 4.4	4.6 ± 2.3
GC	(-)-Gallocatechin	(2S,3R)-2-(3,4,5-trihydroxyphenyl)-chroman-3,5,7-triol	16.1 ± 6.0	0.7 ± 8.9
C	(-)-Catechin	(2S,3R)-2-(3,4-dihydroxyphenyl)-chroman-3,5,7-triol	13.1 ± 8.9	-5.5 ± 1.5
EC	(-)-Epicatechin	(2R,3R)-2-(3,4-dihydroxyphenyl)-chroman-3,5,7-triol	17.5 ± 10.4	-6.8 ± 5.3

